Studies of Organomolybdenum Compounds. 2. Synthesis, Structure, and Properties of Dioxodineopentyl(2,2'-bipyridyl)molybdenum(VI) and of Related Compounds

Gerhard N. Schrauzer,* Laura A. Hughes, and Norman Strampach

Department of Chemistry, University of California at San Diego, La Jolla, California 92093

Fred Ross, Dawn Ross, and Elmer O. Schlemper*

Department of Chemistry, University of Missouri, Columbia, Missouri 65211

The synthesis of $Mo(O)_2[CH_2C(CH_3)_3]_2(bpy)$ by the reaction of $Mo(O)_2(Br)_2(bpy)$ with neopentylmagnesium bromide is described. This new dialkyl derivative of dioxomolybdenum(VI) is stable to air up to 182 °C. Thermolysis at higher temperatures is initiated by Mo–C bond homolysis and H abstraction to yield neopentane as the major gas-phase hydrocarbon product. The high thermal stability is primarily due to the absence of hydrogen in β-position relative to molybdenum; higher n-alkyl derivatives of this class of compounds decompose spontaneously by β elimination and cannot be isolated. Decomposition of the dineopentyl complex is slow in neutral protic solvents but occurs on heating in strong alkali, in mineral acids, and with particular ease under reducing conditions. The complex $Mo(O)_2[CH_2C(CH_3)_3]_2(bpy)$ crystallizes from diethyl ether in the monoclinic space group $C2/c$, with a = 24.309 Å, b = 12.635 Å, c = 16.542 Å, and β = 107.68°, with Z = 8. The three-dimensional X-ray data were measured with the θ–2θ scan technique; the structure was resolved by Patterson and Fourier methods. The $Mo(O)_2(bpy)$ moiety is essentially coplanar, the independent Mo–N and Mo–O distances are nearly the same, and the Mo–C bond lengths of 2.236 (5) Å are 0.04 Å longer than in the previously reported dimethyl derivative. Both $C(CH_3)_3$ groups of the two neopentyl residues are positioned above and below the $Mo(O)_2$ group. Two of the CH_3 groups of each neopentyl residue are staggered about one Mo=O bond to minimize the repulsion between the methyl group protons and the oxygen atoms. Repulsive interactions between the oxygen atoms and the neopentyl methyl groups cause a widening of the Mo–C–C angle from normal tetrahedral to 118.9° and a narrowing of the C–Mo–C angle to 145.8°, which is 3.2° smaller than in the dimethyl derivative.

Introduction

The reaction of $(bpy)Mo(O)_2Br_2$ (1) with methylmagnesium bromide has been shown recently[1] to yield the complex $Mo(O)_2(CH_3)_2(bpy)$ (2). Its remarkable stability prompted us to extend our studies to the synthesis of higher dialkyldioxomolybdenum(VI) complexes of this type. While such complexes could not be obtained for reasons to be discussed, we were successful in preparing the dineopentyl derivative $Mo(O)_2[CH_2C(CH_3)_3]_2(bpy)$ (3), whose properties and structure will be described in the following.

The reaction of 1 with neopentylmagnesium bromide has previously been shown[2] to yield the purple complex Mo-

$R_1 = R_2 = Br$ (1)

$R_1 = R_2 = CH_3$ (2)

$R_1 = R_2 = CH_2-C(CH_3)_3$ (3)
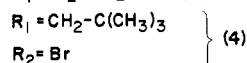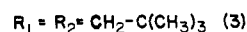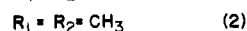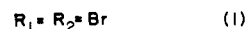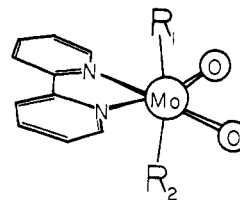
$R_1 = CH_2-C(CH_3)_3$
$R_2 = Br$ (4)

$(O)_2[CH_2C(CH_3)_3](Br)(bpy)$ (4). The colorless alkaline hydrolysis product of 4, the anion $(CH_3)_3CCH_2MoO_3^-$ (5), has also been reported.[2] As other alkyl molybdates it is

(1) Schrauzer, G. N.; Hughes, L. A.; Strampach, N.; Robinson, P.; Schlemper, E. O. *Organometallics* 1982, 1, 44.
(2) Schrauzer, G. N; Hughes, L. A.; Strampach, N. *Z. Naturforsch. B:* 1982, *Anorg. Chem., Org. Chem.* 37B, 380.

<div style="columns:2">

Table I. Summary of Physical Properties of Complexes 2 and 3

physical property		2	3
mp, °C		230 dec	180 dec
IR $\nu_{Mo=O}$,[a] cm^{-1}		934, 905	922, 890
^{1}H NMR,[b] ppm (intensities)	δ_{bpy}	7.5–9.5 (8)	7.5–9.5 (8)
	δ_{CH_2}		1.15 (4)
	δ_{CH_3}	0.58 (6)	0.95 (18)
UV–vis λ_{max},[c] nm (ϵ)		345 (2000)	365 (1900)
		303 (19 600)	304 (18 500)
		293 (17 000)	292 (18 400)
		283s (10 300)	283s (14 300)
		245 (24 900)	250 (25 400)

[a] In KBr. [b] Chemical shifts are relative to Me$_4$Si, measured in CDCl$_3$. [c] Measured in CH$_2$Cl$_2$.

metastable, decomposing into MoO$_4$$^{2-}$ and C(CH$_3$)$_4$; in pH 11 buffered aqueous solution the $t_{1/2}$ is 282 min at 70 °C and ca. 15 days at 23 °C.[2,3] The only other known neopentyl derivatives of oxomolybdate(VI) are the compounds Mo(O)[CH$_2$C(CH$_3$)$_3$]$_3$(Cl) (6) and Mo(O)[CH$_2$C(CH)$_3$]$_4$ (7) described by Osborn and his school.[4]

Experimental Section

Reagents and Chemicals. All reagents and chemicals obtained from commercial sources were of analytical or reagent grade purity and were used without further purification. Tetrahydrofuran (Mallinckrodt) was dried over potassium and distilled immediately prior to use. The argon was of 99.998% purity and was dried by passage over KOH pellets. Complex 1, Mo(O)$_2$Br$_2$(bpy), was prepared according to Hull and Stiddard.[5]

Synthesis of Mo(O)$_2$[CH$_2$C(CH$_3$)$_3$]$_2$(bpy) (3). Neopentyl magnesium chloride was prepared in tetrahydrofuran according to standard methods, usually in batches from 0.5 g of Mg and 1.5 cm^3 of neopentyl chloride in 25 cm^3 of THF, resulting in an approximate 0.5 M solution. A stirred suspension of 2 g of 1 in 100 cm^3 of dry THF was cooled to –10 °C by means of a dry ice/acetone/water bath. Under an atmosphere of argon, 20 cm^3 of a 0.5 M solution of neopentylmagnesium chloride was added dropwise. After 2 h of reaction at –10 °C, the solution was allowed to warm to room temperature and 400 cm^3 of water was added to the reaction solution. The product was extracted into CH$_2$Cl$_2$. Upon evaporation of the dried solvent, bright yellow crystals precipitated. These were collected by vacuum filtration and dried: mp 182 °C dec; yield, 45%, based on 1. Anal. Calcd for C$_{20}$H$_{30}$MoN$_2$O$_2$: C, 56.33; H, 7.09; Mo, 22.50; N, 6.57; O, 7.50; mol. wt. 426.40. Found: C, 56.55; H, 7.60; Mo, 22.62; N, 6.50; O, 6.73; mol. wt. 430 (cryoscopic in benzene).

Physical Properties. Fourier transform ^{1}H NMR spectra were obtained for a solution of 3 in CDCl$_3$ by using a Varian HR-220/Nicolet TT 100 spectrometer. Chemical shifts and intensities of the observed signals of 3 are given in Table I together with the frequencies of important bands in the IR spectra.

Chemical Properties. Thermolysis. Thermolyses of complexes 2 and 3 were performed in argon-filled, serum-capped, Pyrex test tubes of 10-cm length and 11-mm diameter. The tubes were heated to 300 °C for a measured time, typically for 30 s, and gas samples (0.5 cm^3) for hydrocarbon analyses by GLPC were withdrawn. A Hewlett-Packard Model 700 gas chromatograph fitted with an 8 ft × ^{1}/$_8$ in. column packed with phenyl isocyanate on Porasil C operating at 50 °C with an FID detector was used for hydrocarbon detection. The gas phase was also analyzed for H$_2$ by GLPC using a column of 6 ft × ^{1}/$_8$ in., filled with molecular sieves (5 Å), operating at 27 °C, and employing TC detection.

(3) Schrauzer, G. N.; Hughes, L. A.; Strampach, N. Proceedings of the 4th International Conference on Chemistry and Uses of Molybdenum, Aug 9–13, 1982, in press.

(4) Kress, J. R. M.; Russell, M. J. M.; Wesolek, M. G.; Osborn, J. A. *J. Chem. Soc., Chem. Commun.* 1980, 431.

(5) Hull, C. G.; Stiddard, M. H. B. *J. Chem. Soc.* 1966, 1633.

Table II. Initial Hydrocarbon and Hydrogen Formation during the Thermolysis of Complexes 2 and 3 at 300 °C for 30 s

products (% yield)	2		3	
	a	b[a]	a	b[a]
CH$_4$	75.3	91.1	7.7	13.6
C$_2$H$_4$	5.5	4.2	0.9	1.5
C$_3$H$_6$	1.6	1.1		
i-C$_4$H$_8$			9.8	5.7
i-C$_4$H$_{10}$			1.1	3.4
neo-C$_5$H$_{12}$			44.7	75.8
H$_2$	17.7	3.5	35.8	

[a] In Thomas silicone bath oil.

Hydrocarbons were identified by comparison of the retention times and coinjection of authentic samples of hydrocarbons as well as by mass spectrography, employing an LKB 9000 instrument. Results of thermolysis experiments are summarized in Table II.

Photolysis. Solutions of complexes 2 and 3 were exposed to visible and UV light in anhydrous CH$_3$OH as the solvent. Solutions of the complexes were placed into Pyrex or quartz test tubes filled with argon. These were exposed to the light of either a 150-W GE flood light or a 360-W Hg-arc Hanovia UV lamp at a distance of about 12 cm. A stream of cold air was blown over the tubes to maintain the temperature at 50 °C. The gas phase was analyzed for hydrocarbons and H$_2$ by GLPC as described above. After 2 h of exposure to UV light, 2 decomposed quantitatively to yield CH$_4$. Photolysis of 3 under the same conditions was 15% complete and afforded mainly neopentane with traces of methane, ethane, isobutane, and isobutene in the gas phase. After 2 h of exposure of the complexes to the visible light source, 50% of the theoretical yield of CH$_4$ was observed from 2. Under the same conditions, solutions of 3 decomposed only to the extent of about 0.3%, affording neopentane as the only gas-phase hydrocarbon product.

Solvolysis Experiments. Weighed amounts of complexes 2 or 3, usually 2–5 mg, were placed into glass bottles of 38-cm^3 capacity. These were filled with argon and serum capped. Reactions were initiated by injecting a known volume (usually 5 cm^3) of solvent or of the reactant solution. Gas samples were withdrawn at regular intervals and analyzed for hydrocarbons by GLPC as described above.

Structure Analysis. Crystals suitable for X-ray crystallographic analysis were obtained by recrystallizing 3 from diethyl ether. This afforded crystals containing 0.5 molecules of diethyl ether of crystallization per molecule of complex. A crystal of approximate dimensions 0.08 × 10 × 0.30 mm was mounted on an Enraf-Nonius CAD-4 automated diffractometer for data collection. An outline of crystallographic and data collection parameters is given in Table III. The monoclinic (C2/c) unit-cell dimensions were determined by a least-squares fit of 25 reflections obtained by automatic centering on the diffractometer. Intensity data (294 K) were obtained by the θ–2θ step scan technique using Mo Kα radiation ($\lambda = 0.7107$ Å). A total of 5141 reflections were measured out to $2\theta = 45°$. The intensities of three standard reflections measured after each 8000 s of X-ray exposure showed approximately 25% decrease during the data collection, and the data were corrected for this effect. Orientation was checked after every 200 reflections by recentering three reflections. If any of these were significantly off center, all 25 initial reflections were recentered, and a new orientation matrix was obtained. Several psi scans indicated that the transmission varied by less than 2% or so, thus no absorption correction was applied. Averaging of equivalent reflections yielded 2372 independent reflections with $F_o > 2(\sigma(F_o))$; these were used to solve and refine the structure $\sigma^2(F_o{}^2) = \sigma^2_{counting} + (0.05F_o{}^2)^2$ and $\sigma(F_o) = \sigma(F_o{}^2)/2F_o$.

The structure was solved by Patterson and Fourier methods. Least-squares refinement minimizing $\sum w(F_o - F_c)^2$, where $w = 1/\sigma[F_o]^2$, converged with $R = \sum||F_o| - |F_c||/\sum F_o = 0.048$ and $R_w = [\sum w(F_o - F_c)^2/\sum wF_o{}^2]^{1/2} = 0.071$. Hydrogen atoms were located by a combination of difference Fourier methods and chemical reasonability and were held near "ideal" X-ray positions.[6] The

(6) Churchill, M. R. *Inorg. Chem.* 1973, *12*, 1213.

</div>

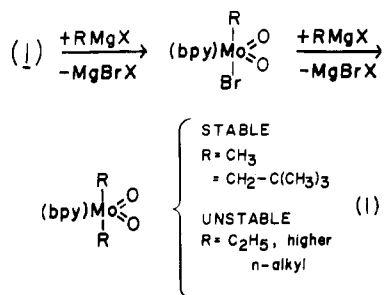## Table III. Crystallographic, Data Collection, and Refinement Parameters

a, Å	24.309 (20)	diffractometer	
b, Å	12.635 (2)	λ, Å (Mo Kα)	
c, Å	16.542 (10)	μ, cm^{-1}	
β, deg	107.68 (4)	abs correctn	not applied
space group	$C2/c$		
ρ_{calcd}, g/cm^3	1.272 (3)		
Z	8		
V, Å	4841 (6)	scan speed	variable, to maintain 3% counting statistics to a max time of 90 s/scan
formula	$MoO_2N_2C_{20}H_{30}\cdot{}^1/_2(C_2H_5)_2O$		
M_r	463.5		
total no. of observns	5141	scan mode	$\theta-2\theta$ (96 steps), 16 background each side and 64 peak
no. of indep reflctns	3174	scan width, deg	(0.50 + 0.35 tan θ)
no. of indep reflectns with $F_o > 2\sigma(F_o)$ used in structure refinement	2372	data limits, 2θ, deg	2–49
		monochromation	graphite monochromator
$R(F_o)$	0.048	largest shift/error on last cycle	0.06
$Rw(F_o)$	0.071		

largest shift on the last cycle was 0.06 times the esd of that parameter, and the error of an observation of unit weight was 1.98. Atomic scattering factors were taken from ref 7 and anomalous scattering factors were included in F_c.

Final atomic positional parameters and thermal parameters are included in Table IV; F_o and F_c values are deposited in the microfilm edition. Selected interatomic distances and angles are given in Tables V and VI.
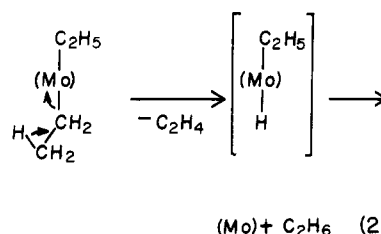
Discussion

Synthesis of 3 and of Related Complexes. The products of the reaction of 1 with stoichiometric amounts of alkylmagnesium bromides are the purple monoalkyl derivatives 4, which have been described elsewhere. Substitution of the remaining bromide ion in 4 according to eq 1 occurs on the reaction with excess organo-

magnesium reagent, but stable dialkyl complexes Mo-(O)$_2$R$_2$(bpy) have thus far been obtained only with R = CH$_3$ and, as is shown herein, with R = CH$_2$C(CH$_3$)$_3$.

In the attempted synthesis of the diethyl derivative, the intermediate purple monoethyl bromide species reacted with a second molecule of the organomagnesium reagent. However, instead of the formation of an isolable diethyl derivative, a spontaneous decomposition reaction took place, accompanied by the evolution of a 1:1 mixture of ethylene and ethane that could not be prevented by lowering the reaction temperature. Attempts to prepare a methyl ethyl complex, either by the reaction of Mo(O)$_2$-(C$_2$H$_5$)(Br)(bpy) with CH$_3$MgBr or in the reverse order of alkylation, likewise failed to produce isolable dialkylated species. Instead, the evolution of a 1:1 mixture of ethylene and methane was observed. The higher di-*n*-alkyl species evidently are inherently unstable, undergoing spontaneous

(7) "International Tables for Crystallography"; Kynoch Press: Birmingham, England, 1974; Vol. IV.

decomposition by way of β elimination and reductive Mo–C bond cleavage in terms of eq 2. The dimethyl and

the dineopentyl derivatives 2 and 3 are obviously stable because the low-energy pathway of decomposition by way of β elimination is not available.

Thermolysis. Although the thermal decomposition of 3 begins at 182 °C, it is slow at this temperature and hence was studied at 300 °C. The rate of thermolysis is relatively slow even at 300 °C, however, and requires ca. 60 s for completion. Thermolysis is further complicated by secondary reactions involving the hydrocarbon thermolysis products, e.g., cracking, disproportionation, hydrogenation/dehydrogenation, carbide formation, etc. To obtain information on the initial decomposition reactions, the thermolyses at 300 °C were typically terminated after short (30 s) and long (2 min) reaction times. The hydrocarbon yields were in the order of 40–60% under all conditions investigated. Neopentane was identified as the first hydrocarbon product in the gas phase under all conditions chosen, but the yields only approach about 50% of theoretical. On continued heating, hydrogen, methane, isobutene, and isobutane appear in the gas phase.

Homolysis of a Mo–C bond appears to be the initial event, which is followed by hydrogen abstraction and other reactions. When the thermolysis of 3 is conducted in a high-boiling solvent containing abstractable hydrogen atoms (e.g., silicone oil), neopentane becomes the nearly exclusive product and hydrogen is no longer formed (see Table II). The neopentyl radicals generated on thermolysis in the absence of a solvent apparently abstract hydrogen atoms from neopentyl residues of neighboring molecules of 3, thus producing new organic radical species which terminate in part by fragmentation, hydrogen abstraction, or loss of hydrogen; hydridomolybdenum as well as (alkylidene)- and (alkylidyne)molybdenum species may be formed as intermediates. Since the formation of an alkylidyne complex, [(CH$_3$)$_3$CCMo(neopentyl)$_2$]$_2$, was ob-

Table IV. Weighed Least-Squares Planes and Final Positional Parameters for 3

atom	x	y	z	dist, Å	esd
		Plane 1[a]			
		Atoms in Plane			
Mo	3.2609	−0.1116	2.2789	0.001	0.001
N(1)	3.0855	0.5028	0.0221	−0.012	0.005
N(2)	5.2887	0.6127	1.4362	0.016	0.005
O(1)	1.5942	−0.4699	2.2356	−0.037	0.005
N(2)	5.2887	0.6127	1.4362	0.016	0.005
C(1)	1.9405	0.4197	−0.6502	−0.019	0.007
C(2)	1.8168	0.7597	−1.9577	−0.017	0.008
C(3)	2.9285	1.2070	−2.6358	0.002	0.009
C(4)	4.1230	1.2964	−1.9807	0.019	0.007
C(5)	4.1993	0.9383	−0.6456	−0.015	0.006
C(6)	5.4183	1.0043	0.1614	0.019	0.006
C(7)	6.6392	1.4682	−0.3486	0.003	0.007
C(8)	7.7218	1.5314	0.5217	−0.039	0.007
C(9)	7.6109	1.1505	1.8162	−0.054	0.008
C(10)	6.3800	0.6839	2.2379	−0.013	0.007
		Other Atoms			
C(11)	4.1696	−1.8819	1.2573	2.139	0.006
C(12)	3.3479	−3.2040	1.2355	3.193	0.007
C(13)	2.8752	−3.5992	2.6105	3.087	0.008
C(14)	2.1296	−3.0692	0.3072	3.034	0.008
C(15)	4.2771	−4.2811	0.6712	4.566	0.009
C(16)	3.2435	2.1143	2.4331	−2.127	0.007
C(17)	2.0356	2.8286	3.0377	−3.236	0.007
C(18)	0.8691	2.6880	2.1157	−3.127	0.009
C(19)	2.3811	4.3080	3.1592	−4.573	0.008
C(20)	1.7005	2.3145	4.3824	−3.191	0.011
		Plane 2[b]			
		Atoms in Plane			
O(1)	1.5942	−0.4699	2.2356	0.057	0.004
N(2)	5.2887	0.6127	1.4362	0.040	0.005
C(11)	4.1692	−1.8819	1.2573	−0.028	0.007
C(12)	3.3479	−3.2040	1.2355	−0.070	0.007
C(15)	4.2771	−4.2811	0.6712	−0.025	0.011
C(16)	3.2435	2.1143	2.4331	−0.018	0.007
C(17)	2.0356	2.8286	3.0377	−0.104	0.007
C(19)	2.3811	4.3080	3.1592	0.008	0.009
		Other Atoms			
Mo	3.2609	−0.1116	2.2789	−0.358	0.001
N(1)	3.0855	0.5028	0.0221	1.939	0.005
O(2)	3.9183	−0.4355	3.8211	−2.053	0.005

x^2 Values

plane no.	x^2
1	205
2	561

Dihedral Angles between Planes 1 and 2: 90.8°

[a] Plane 1: A, 0.2306; B, −0.9357; C, −0.2669; D, 0.2474. [b] Plane 2: A, −0.2708; B, 0.2158; C, −0.9381; D, −2.6872.

Table V. Selected Bond Distances (Å)

Mo–O(1)	1.709 (3)	C(11)–C(12)	1.546 (7)
–O(2)	1.706 (3)	C(16)–C(17)	1.530 (7)
–C(11)	2.237 (5)	C(12)–C(13)	1.507 (8)
–C(16)	2.235 (5)	C(12)–C(14)	1.536 (8)
–N(1)	2.348 (4)	C(12)–C(15)	1.522 (8)
–N(2)	2.317 (4)	C(17)–C(18)	1.491 (8)
		–C(19)	1.526 (8)
C(1)–C(2)	1.354 (8)	–C(20)	1.474 (8)
C(2)–C(3)	1.376 (8)		
C(3)–C(4)	1.369 (8)	C–C(aliphatic)[a]	1.512 (20)
C(4)–C(5)	1.377 (7)	N(1)–C(1)	1.336 (6)
C(6)–C(7)	1.386 (7)	N(1)–C(5)	1.369 (6)
C(7)–C(8)	1.392 (8)	N(2)–C(6)	1.347 (6)
C(8)–C(9)	1.356 (8)	N(2)–C(10)	1.346 (6)
C(9)–C(10)	1.379 (7)	N–C[a]	1.350 (10)
C–C(aromatic)[a]	1.374 (10)	C(5)–C(6)	1.467 (6)

[a] Average value.

is required to afford quantitative yields of neopentane in terms of eq 3. Due to the hydrophobic nature of the

$$(C_5H_{11})_2 Mo(bpy)(O)_2 \xrightarrow[-bpy]{+2OH^-}$$

$$MoO_4^= + 2 (CH_3)_4C \quad (3)$$

complexes, the solvolysis of **3** (and of **2** for comparison) was studied in glycerol solutions. After 1 h at 90 °C, 13% of **2** and only 0.2% of **3** decomposed, as estimated from the yields of methane and neopentane generated. The decomposition of the complexes on heating in 1-thio-glycerol under otherwise identical conditions was essentially quantitative, illustrating the sensitivity of the complexes to reductive Mo–C bond cleavage. Reductive Mo–C bond cleavage with formation of methane and neopentane also occurs on reaction with alkaline $NaBH_4$ or with Zn–HCl. On reaction with concentrated H_2SO_4, **2** yields mainly ethane; a mixture of dineopentyl and neopentane is formed from **3**, the reactions are complete within about 5 min. Both complexes dissolve in, and are relatively resistant to, cold glacial acetic acid; their half-life at 90 °C is about 30 min.

Electronic Spectra and Photolysis. The electronic spectra of **2** and **3** are remarkably similar (see Table I). In addition to the intense absorptions due to the coordinated bpy, a previously unreported low-energy transition appearing at 345 nm (ϵ 2000) in **2** and at 365 nm (ϵ 1900) in **3** is observed and assigned to a transition involving the ϵ MO's of the C–Mo–C moiety. This assignment is supported by the observed light sensitivity of **2** and **3**.

Mo–C bond homolysis is apparently initiated by the transfer of an electron from the weakly bonding or nonbonding filled MO to the σ^* orbital. The estimated energies from the electronic spectra of 347.6 kJ·M^{-1} for the Mo–C bonds in **2** and of 328.3 kJ·M^{-1} of those in **3** is reasonably within the range of stability expected for Mo–C bonds. The Mo–C bonds are significantly more stable than Co–C bonds; values of 83–130 kJ·M^{-1} were observed[9] for neopentylcobalamin and other organocorrins, for example. Compared to **2**, the Mo–C bonds in **3** are labilized by about 20 kJ·M^{-1}, presumably due to steric effects (see below). The fact that **3** undergoes photolysis at slower rates than **2** is not in discord with this conclusion as it may be plausibly attributed to a higher efficiency of recombination.

Structure. The structure of **3** (Figure 1) is of interest because it illustrates, for the first time, the effects of steric

served[8] in the reaction of $Mo(O)Cl_4$ with dineopentyl-magnesium–dioxan, it is possible that related alkylidyne species are formed in the thermolysis of **3**.

In the thermolysis of **2** at 300 °C, CH_4 is the main initial product. In addition, H_2, C_2H_4, and C_3H_6 are formed in lower relative yields that also depend on heating time (see Table II). Thermolysis of **3** in silicone oil further increases the yield of CH_4 at the expense of all other products. Hence, Mo–C bond homolysis is also a major initial event in this case.
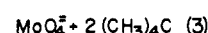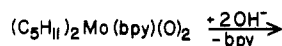
Solvolysis. Solvolysis of the complexes in neutral solvents is generally slow. As with **2**, fusion of **3** with KOH

(8) Clark, D. N.; Schrock, R. R. *J. Am. Chem. Soc.* **1978**, *100*, 6774.

(9) Schrauzer, G. N.; Grate, J. H. *J. Am. Chem. Soc.* **1981**, *103*, 541.

Table VI. Selected Bond Angles (deg)[a]

O(1)-Mo-O(2)	110.0 (2)	Mo-N(1)-C(1)	122.0 (3)
N(1)-Mo-N(2)	68.6 (1)	-N(1)-C(5)	119.5 (3)
C(11)-Mo-C(16)	145.8 (2)	-N(2)-C(6)	121.2 (5)
		-N(2)-C(10)	120.8 (3)
O(1)-Mo-N(1)	87.5 (2)		
O(2)-Mo-N(2)	92.8 (2)	Mo-C(11)-C(12)	118.1 (4)
O(1)-Mo-N(2)	156.1 (2)	Mo-C(16)-C(17)	119.8 (4)
O(2)-Mo-N(1)	161.4 (2)	C-C-C(neopentyl)[b]	109.5 (2.1)
O(1)-Mo-C(11)	102.4 (2)	C-C-C(neopentyl)[c]	107.1 (5)-112.2 (5)
O(1)-Mo-C(16)	101.9 (2)	C-C-C(aromatic)[b]	119.1 (8)
O(2)-Mo-C(11)	96.1 (2)		
O(2)-Mo-C(16)	97.4 (2)	C-N-C(aromatic)[b]	118.2 (3)
O-Mo-C[b]	99.5 (2.7)	N-C-C(aromatic)[b]	122.2 (1.1)
		N-C-C(aromatic)[b]	115.3 (2)
N(1)-Mo-C(11)	78.5 (2)	C(4)-C(5)-C(6)	124.3 (5)
N(1)-Mo-C(16)	78.8 (2)	C(5)-C(6)-C(7)	122.8 (5)
N(2)-Mo-C(11)	74.2 (2)		
N(2)-Mo-C(16)	73.8 (2)		
N-Mo-C[b]	76.3 (2.3)		

[a] For average values the average deviation from the mean is given rather than the least-squares standard deviation. [b] Average value. [c] Range.

Figure 1. Perspective view of Mo(O)₂[CH₂C(CH₃)₃]₂(bpy) with the atoms numbered.

constraints imposed on dioxomolybdenum(VI) by two bulky organic substituents in a relatively simple compound, leading to distortions which may be important factors in heterogeneously catalyzed processes.

Whereas the (bpy)Mo(O)₂ moieties of **2** and **3** are isostructural and the Mo-O and Mo-N bond distances are the same, the Mo-C bonds in **3** are significantly longer [2.236 (5) Å compared with 2.191 (3) Å in **2**], and a significant closing of the C-Mo-C angle from 149.0 (1)° in **2** to 145.8 (2)° in **3** is seen. A larger effect might have been observed had not the Mo-C-C angles opened to 118.9 (9)° at the methylene carbon atom to help reduce repulsion between the alkyl groups and the coordinated oxygen at-

oms. The O-Mo-C and N-Mo-C angles (Table IV) reveal that C(11) and C(16) bend away from N(1) and O(1) relative to N(2) and O(2). Figure 1 also shows that methyl groups (C(13), C(14), C(18), and C(20)) are staggered around O(1) to minimize repulsive effects. Plane 2 (see Table IV), which contains the remaining six neopentyl carbons as well as O(1) and N(2), is remarkably planar (maximum deviation of 0.10(1) Å for C17) and is displaced by 0.36 (1) Å toward N(1) from the Mo atom. Moreover, plane 2 is essentially perpendicular to plane 1.

The highly distorted octahedral coordination geometry of molybdenum in complexes **2** and **3** may be interpreted to suggest that molybdenum(VI) is in a (5s)(6p)³ state of hybridization, giving rise to a tetrahedral coordination geometry of the (alkyl)₂Mo(O)₂ moiety. Its interaction with the bpy ligand is comparatively weak and does not cause a rehybridization to a regular octahedral geometry.

Studies of Molybdenum Compounds. 3. Vinyl Molybdate(VI): Synthesis and Detection in the Molybdothiol-Catalyzed Reduction of Acetylene

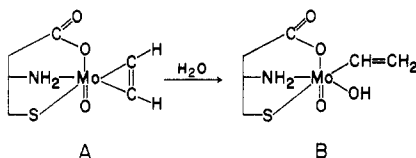Laura A. Hughes, Liu Nan Hui,[1] and Gerhard N. Schrauzer*

Department of Chemistry, University of California at San Diego, Revelle College, La Jolla, California 92093

Received October 12, 1982

Vinyl molybdate(VI), CH_2=$CHMoO_3^-$, generated by alkaline hydrolysis of CH_2=$CHMo(O)_2Br(bpy)$ (bpy = 2,2'-bipyridyl), is a colorless anion undergoing Mo–C bond hydrolysis to molybdate and ethylene with a half-life of 3 h at 23 °C in aqueous solution. In aqueous NaOH, the rate of Mo–C bond hydrolysis exhibits a linear dependence on [OH⁻]. Mo–C bond hydrolysis is also accelerated in strongly acidic solutions; the half-life of vinyl molybdate at pH 1.3 (0.1 M HCl) is 1.3 h. The apparent Arrhenius energies of activation for the hydrolysis of the Mo–C bond of vinyl molybdate are 7 and 3 kcal/mol at pH 11 and 1.3, respectively. Vinyl molybdate species are reactive intermediates in the molybdothiol-catalyzed reduction of acetylene to ethylene and were detected in quenched reaction solutions, employing a chromatographic separation technique. The previously derived mechanism of the molybdothiol-catalyzed reduction of acetylene is extended on the basis of these observations.

Introduction

Previous work[2–4] has suggested that the reduction of acetylene to ethylene in molybdothiol and related model systems of nitrogenase occurs by way of a symmetrically side-on bonded, mononuclear organomolybdenum(VI) intermediate (A), from which ethylene is generated by way of Mo–C bond hydrolysis. Since the hydrolysis of the two Mo–C bonds in A is likely to occur sequentially rather than simultaneously, a vinylmolybdenum(VI) species B should be formed before ethylene is released.

In this paper we report the results of experiments which led us to detect vinyl- and other organomolybdenum species in quenched molybdothiol–acetylene reaction solutions. As intermediate A is expected to be short-lived, we concentrated on detecting vinyl molybdate species related to B, first by studying the properties of the vinyl molybdate anion CH_2=$CHMoO_3^-$, synthesized by the controlled hydrolysis of the complex CH_2=$CHMo(O)_2Br(bpy)$ (bpy = 2,2'-bipyridyl) in analogy to the corresponding alkyl derivatives.[5,6] On the basis of these experiments, it was found that the room-temperature half-life of vinyl molybdate is significantly shorter than that of the known alkyl molybdates.[5,6] However, chromatographic separation of this species from other products in quenched molybdothiol–acetylene reaction solutions was still possible and was employed for its detection.

Table I. Pseudo-First-Order Rates of Mo–C Bond Cleavage in Vinyl Molybdate

no.	conditions buffer	pH	T, °C	10^3k, min⁻¹
1	0.1 M phosphate	14.0	70	21.4
2	0.1 M phosphate	13.0		18.0
3	0.1 M phosphate	11.0		17.5
4	0.1 M phosphate	8.8		16.7
5	0.1 M phosphate	6.2		16.1
6	0.1 M phosphate	3.3		14.4
7	0.1 M HCl	1.0		35.7
8	0.1 M phosphate	11.0	23	3.5
9	0.1 M phosphate	7.0		3.3
10	0.1 M HCl	1.0		21.1
11	0.8 M NaOH	13.9	0	6.1
12	0.1 M NaOH	13.0		1.8
13	0.1 M phosphate	11.0		1.1
14	0.1 M phosphate	7.0		1.3
15	0.1 M HCl	1.0		11.9

Experimental Section

Preparation of Vinyl Molybdate in Solution. Vinyl molybdate was prepared by the alkaline hydrolysis of the complex CH_2=$CHMo(bpy)(O)_2Br$ as described in ref 6. For the preparation of CH_2=$CHMo(bpy)(O)_2Br$, 25 mL of a 1 M solution of vinylmagnesium bromide in THF was added dropwise to a stirred suspension of 4.5 g (10 mmol) of $Mo(O)_2(bpy)Br_2$ in 50 mL of dry THF at 0 °C, while a slow stream of dry argon was passed through the system. The reaction mixture turned slowly dark purple and was allowed to react for an additional 60 min. The purple crystals were collected by filtration through a Schlenk tube. The product was washed with anhydrous diethyl ether and dried at 1 mmHg for 24 h. For analysis, weighed aliquots of the complex were hydrolized in hot 1 M KOH, and the ethylene released was determined by GLPC. On this basis, the crude products isolated were 60–78% pure. For purification, samples were recrystallized from hot THF or CH_2Cl_2. Anal. Calcd for $C_{12}H_{11}N_2O_2BrMo$: Mo, 24.5; CH_2=CH, 6.9. Found: Mo, 23.7; CH=CH_2 (as determined from the amount of C_2H_4 released on alkaline hydrolysis), 6.0.

For the preparation of vinyl molybdate solutions, fresh CH_2=$CHMo(O)_2(bpy)Br$ was always used since the complex undergoes slow irreversible changes on prolonged storage at room temperature. The nature of these changes will be reported elsewhere.

Into a beaker of 250-mL capacity was suspended 1 g of CH_2=$CHMo(O)_2(bpy)Br$ in 100 mL of deionized water. To the slurry was added 1 mL of 6 N NH_4OH solution, and the mixture was magnetically stirred at room temperature for 3 min. The reaction solution was subsequently cooled with ice. Bipyridyl was removed by suction filtration and extraction with CH_2Cl_2. De-
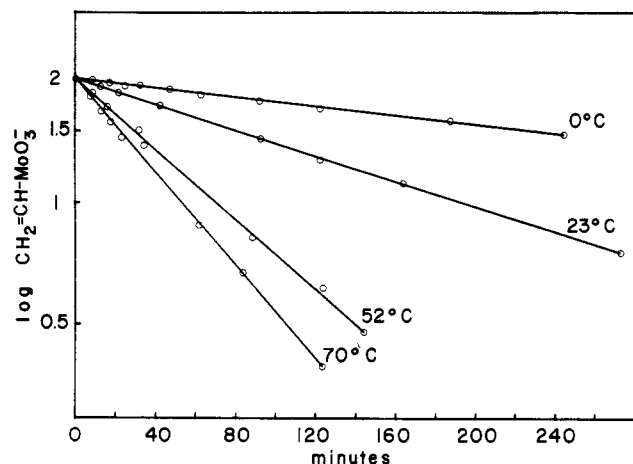
(1) On leave of absence from Lanzhou University, Lanzhou, Gansu, China.

(2) Schrauzer, G. N.; Doemeny, P. A. *J. Chem. Soc.* 1971, *93*, 1608.

(3) Schrauzer, G. N. *Angew. Chem.* 1975, *87*, 579; *Angew. Chem., Int. Ed. Engl.* 1975, *14*, 514 and references cited therein.

(4) Weathers, B. J.; Grate, J. H.; Schrauzer, G. N. *J. Am. Chem. Soc.* 1979, *101*, 917.

(5) Schrauzer, G. N.; Moorehead, E. L.; Grate, J. H.; Hughes, L. *J. Am. Chem. Soc.* 1978, *100*, 4760.

(6) (a) Schrauzer, G. N.; Hughes, L. A.; Strampach, N. *Z. Naturforsch., B: Anorg. Chem., Org. Chem.* 1982, *37B*, 380. (b) Schrauzer, G. N.; Hughes, L. A.; Strampach, N. "Proceedings of the 4th International Conference on Chemistry and Uses of Molybdenum", Climax Molybdenum Co.: Greenwich, CT, 1982, in press.

Figure 1. Rate plot of the decomposition of vinyl molybdate according to $CH_2{=}CHMoO_3^- + OH^- \rightarrow CH_2{=}CH_2 + MoO_4^{2-}$, in pH 11, 0.1 M phosphate buffer at temperatures of 0, 23, 52, and 70 °C.

Table II. Half-Lives and Product Distribution of Aqueous Alkyl (R) Molybdates at 72 °C

	pH 11[a]		pH 1.3[b]	
R	$t_{1/2}$, min	alkane/ alkene	$t_{1/2}$, h	alkane/ alkene
methyl	60	methane	2.7	methane
ethyl	29.3	66.5	0.3	0.08
n-propyl	34.3	24.7	1.9	0.88
isopropyl	40.8	13.2	4.6	0.07
tert-butyl	96.0	1.0	14.0	isobutene
neopentyl	282.0	neopentane	16.2	neopentane
crotyl	16.0	3.4[c]	0.4	1.2[c]
vinyl	39.6	ethylene	0.3	ethylene

[a] In pH 11, 0.1 M phosphate buffer. [b] In 0.1 N HCl. [c] 1-Butene/*trans*-2-butene.

pending on speed of workup, solutions containing 0.1–0.5 μmol/mL vinyl molybdate were obtained as determined from the amount of C_2H_4 generated on alkaline hydrolysis. For ethylene detection, a Hewlett-Packard Model 700 gas chromatograph was used, fitted with an FID detector and an 8 ft × $^1/_8$ in. column packed with phenyl isocyanate on Porasil C, operating at 23 °C.

Hydrolysis Experiments. Hydrolysis of the Mo–C bond of vinyl molybdate was studied in silicone-rubber serum capped bottles of 38-cm³ capacity by measuring the amounts of ethylene released into the gas phase under the conditions indicated in the legends of Table I and Figure 1.

Chromatography of Vinyl Molybdate Solutions. Vinyl molybdate was separated from molybdate by using a 15 × 1 cm silica gel column and 0.6 M HCl/CH_3OH as the eluent. This method was chosen because it allows separation[7] of ReO_4^- from MoO_4^{2-}. Because of the instability of vinyl molybdate, the chromatography and all subsequent operations must be performed as rapidly as possible. The separated fractions were assayed for vinyl molybdate by measuring, with GLPC, the ethylene released into the gas phase on alkaline hydrolysis. This method allows detection of small traces of vinyl molybdate species. Typical elution profiles are shown in Figure 2. Vinyl molybdate appears in fractions immediately preceding molybdate. Molybdate was assayed colorimetrically by using the method described by Sandall.[8]

Detection of Vinyl Molybdate Species in Molybdothiol-Acetylene Reaction Solutions. The conditions used for acetylene reduction with molybdothiol catalysts were modified to allow the detection of organomolybdenum intermediates. The binuclear μ-oxo-bridged L(+)-cysteine complex of Mo(V)

(7) Phipps, A. M. *Anal. Chem.* 1971, *43*, 467.
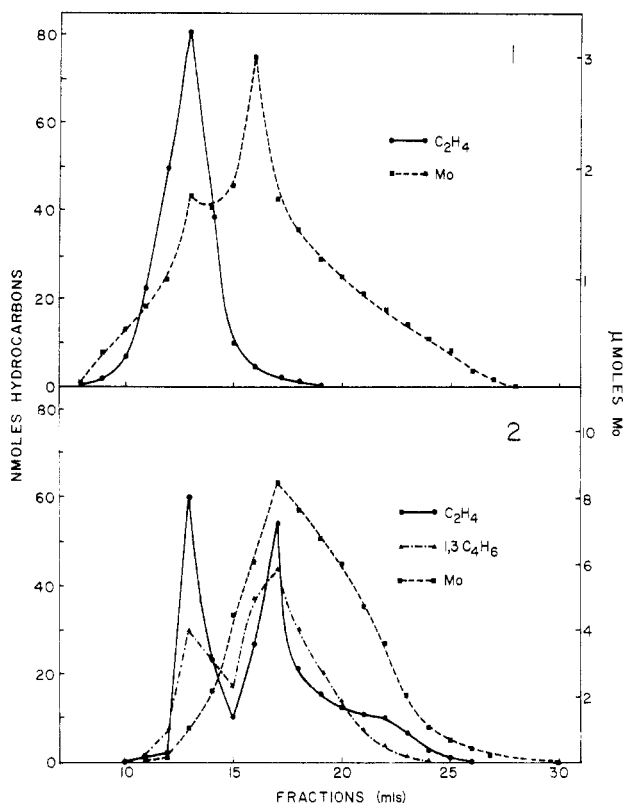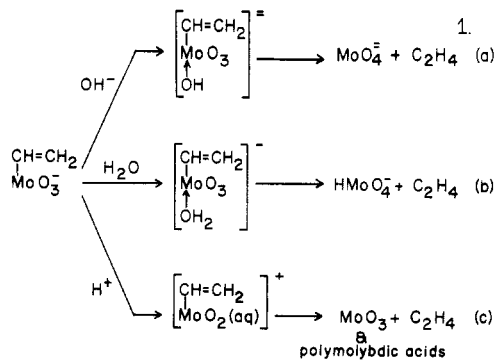(8) Sandall, E. B. "Colorimetric Determination of Traces of Metals", 2nd ed.; Interscience: New York, 1950.

Table III. Relative Rates (%) of Reductive Cleavage of Methyl, Ethyl, and Vinyl Molybdates Using Ferredoxins at 21 °C and 1 h

no.	reactants[a]	methyl	ethyl	vinyl
1	R–Mo	2.9	17.8	22.6
2	R–Mo + $S_2O_4^{2-}$	5.0	27.1	57.9
3	2 + cysteine	2.0	53.0	67.6
4	3 + $Fe_4S_4(S\text{-}n\text{-}C_3H_7)_4]^{2-}$	3.2	58.3	73.7
5	3 + $Fe_4S_4(S\text{-}n\text{-}C_3H_7)_4]^{3-}$	71.3	72.4	78.6
6	3 + $Fe_4S_4(S\text{-}n\text{-}C_3H_7)_4]^{4-}$	83.8	80.2	87.3
7	6 + ATP	100.0[b]	100.0[b]	100.0[b]

[a] Where indicated, reaction solutions contained 0.24 mol of $LiS\text{-}n\text{-}C_3H_7$, 0.06 mol of Li_2S, 0.06 mol of $FeCl_2$ and/or $FeCl_3$, and 0.10 mol of cysteine, all with 5 mmol of alkyl molybdate in a total reaction volume of 10 cm³; solvent, $CH_3OH/0.2$ N, pH 9.6, borate buffer (3:7 by volume). R indicates alkyl group. [b] Yields measured correspond to 15% methyl, 25% ethyl, and 40% vinyl.

Table IV. Percentage of Buta-1,3-diene Relative to Ethylene in Catalytic Acetylene Reduction Experiments with Complex I/NaBH₄ as a Function of pH, after 60 min of Reaction at 23 °C[a]

pH	buffer	% $1,3\text{-}C_4H_6$
11	phosphate	108
9.6	borate	55.6
7.6	borate	7.0
6.5	phosphate	4.5
5.1	phosphate	2.9
3.5	acetate	0
2.0	phosphate	0

[a] Reaction conditions: reaction bottles of 38-mL capacity contained in a total solution volume of 5 mL; complex I, 25 μmol; NaBH₄ (at $t = 0$), 0.133 mmol, in the buffers (0.2 M) as indicated. The acetylene pressure was 1 atm.

("complex I") was employed as the catalyst precursor, with NaBH₄ as the reducing agent. Typically, 0.1 g (159 μmol) of complex I was dissolved in 2 cm³ of H_2O, and the solution was placed into a serum-capped bottle. The solution was purged with argon and allowed to incubate for 2 h. Thereafter, 10 cm³ of acetylene gas were injected, followed by 0.5 cm³ of a freshly prepared 0.3 M NaBH₄ solution. After 30 min, the reaction was quenched by the addition of 50 cm³ of acetone. The acetone served the dual purpose of destroying the excessive NaBH₄ and of precipitating all solutes. These were collected by filtration, redissolved in 0.6 M HCl/CH_3OH and subjected to column chromatography on silica gel as outlined above. As in the experiments with authentic vinyl molybdate, the first fractions that produced ethylene on alkaline hydrolysis appeared immediately prior to the fractions that contained most of the total molybdenum. In addition to ethylene, alkaline hydrolysis of the collected fractions produced variable traces of ethane and buta-1,3-diene, suggesting the presence of other organomolybdate species. The yields of C_2H_6 were invariably very low and are not shown in Figure 2.

The later fractions contained unreacted complex I and other reduced molybdenum species. However, they released hydrocarbons on alkaline hydrolysis and thus presumably contained complexes of L(+)-cysteine of vinyl and other organomolybdates whose separation was not attempted. These fractions also produced varying amounts of acetylene on alkaline hydrolysis, suggesting the existence of molybdenum(V)–acetylene complexes. For elimination of the possibility that the hydrocarbons generated on hydrolysis in any of the fractions were due to the secondary reduction of residual acetylene by disproportionating Mo(V) species,[4] the hydrolysis was run at pH 11, where these secondary disproportionation and reduction reactions do not occur to an appreciable extent. This was confirmed through control experiments with added excess acetylene and complex I.

Reductive Cleavage of Vinyl Molybdate with Ferredoxin Model Compounds. The Mo–C bond cleavage experiments were carried out in serum-capped bottles of 38-cm³ capacity. Details of the experimental conditions are given in the legend of Table

Figure 2. Chromatographic elution profiles from a 100–200 mesh, 15 × 1 cm silica gel column with 0.6 M HCl in CH$_3$OH: (1) authentic vinyl molybdate, generated from CH$_2$=CHMo(O)$_2$Br(bpy); (2) organomolybdates from the solutes of acetone-quenched molybdothiol–acetylene reaction solutions. "Mo" refers to total molybdenum.

III. The preparation of the ions [Fe$_4$S$_4$(SR)$_4$]$^{z-}$ (z = 2–4) was described in ref 9.

Acetylene Reduction Experiments as a Function of pH. The reduction of C$_2$H$_2$ with complex I/NaBH$_4$ as a function of pH was studied under the conditions indicated in the legend of Table IV.

Results and Discussion

Vinyl molybdate, CH$_2$=CHMoO$_3^-$, may be generated in aqueous solutions by the alkaline hydrolysis of CH$_2$=CHMo(O)$_2$(Br)(bpy) (bpy = 2,2′-bipyridyl) in analogy to the reported[6] synthesis of the corresponding alkyl derivatives. The colorless anion undergoes spontaneous Mo–C bond hydrolysis more readily than the previously reported alkyl molybdates(VI), RMoO$_3^-$ (see Tables I and II) and, depending on pH and reaction temperatures, occurs by several mechanisms. In strongly alkaline solutions, Mo–C bond hydrolysis occurs predominantly by the base-dependent mechanism eq 1a, and a linear dependence of the

$$\text{polymolybdic acids}$$
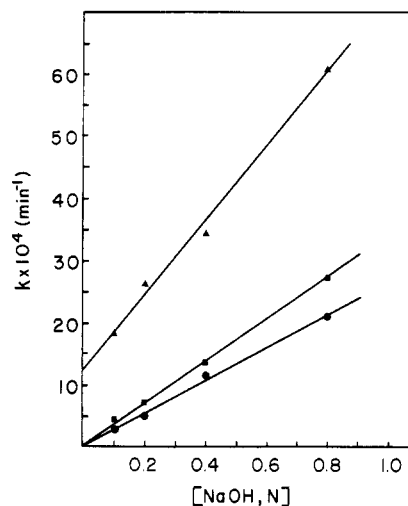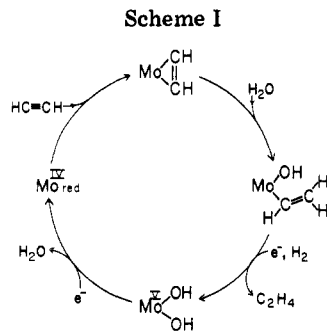
(9) Tano, K.; Schrauzer, G. N. *J. Am. Chem. Soc.* **1975**, *97*, 5404.

Figure 3. Linear dependence of the rates of Mo–C bond cleavage of vinyl (▲), methyl (bsd), and ethyl molybdates (●), on [OH$^-$], at 0 °C. Data for methyl and ethyl molybdates from ref 6a, loc. cit.

hydrolysis rates on [OH$^-$] is observed (see Figure 3). However, the nonzero intercept indicates that Mo–C bond hydrolysis also occurs by a base-independent mechanism formulated in terms of eq 1b, which predominates in neutral solution. Mo–C bond hydrolysis of methyl and ethyl molybdates also exhibits a linear dependence on [OH$^-$], but the slopes and intercepts are smaller, indicating a greater resistance of Mo–alkyl bonds to hydrolysis. The enhanced sensitivity of vinyl molybdate to hydrolysis may be caused by the higher ionic character of the Mo–alkenyl bond. This is presumably also the reason for the lower apparent Arrhenius energies of activation for Mo–C bond hydrolysis of 7 kcal/mol (at pH 11; temperature range, 0–70 °C; experimental data from Figure 1). The Arrhenius energy of activation of Mo–C bond hydrolysis of methyl and ethyl molybdates is 17 kcal/mol under the same conditions.[6] In 0.1 M HCl, the Arrhenius energy of activation for Mo–C bond hydrolysis is 3 kcal/mol, and the half-life of vinyl molybdate at 23 °C is reduced to 1.3 h. Mo–C bond hydrolysis under these conditions presumably occurs via a cationic intermediate as indicated in eq 1c.

Mo–C bond cleavage of vinyl molybdate is accelerated under reducing conditions. Relative rates of reductive cleavage in various systems are given in Table III. As was previously observed with methyl and ethyl molybdates (see ref 6 and Table III), the rates of reductive Mo–C bond cleavage reach a maximum with the "complete" molybdothiol catalyst systems, i.e., in the presence of cysteine, fully reduced ferredoxin model compound (z = 4), a reducing agent (Na$_2$S$_2$O$_4$), and ATP.

Mixtures of L(+)-cysteine with vinyl molybdate also produce active catalysts for the reduction of acetylene. This shows that intermediate vinyl molybdate species formed during reductions of acetylene with molybdothiol catalysts would be short-lived in the presence of excess reductant.

Accordingly, acetone was used to destroy excess NaBH$_4$ and to precipitate the solutes, among which vinyl molybdate species were detected on subsequent column chromatography in 0.6 M HCl in CH$_3$OH. The vinyl molybdate species behaved identically on chromatography to those obtained on similar treatment of authentic vinyl molybdate. These observations permit us to extend the previously derived mechanism of molybdothiol-catalyzed acetylene reduction[2–4] particularly with respect to details

Scheme I

of the release of ethylene from the initially formed side-on bonded organomolybdenum intermediate A. This intermediate is now assumed to undergo Mo–C bond hydrolysis in two steps via vinyl molybdate(VI), from which ethylene is formed in a second step by way of a reductive Mo–C bond cleavage reaction as shown in Scheme I. This modification takes into account that reductive Mo–C bond cleavage of vinyl molybdate is clearly favored over the simple hydrolysis under simulated catalytic conditions (see Table III).

In addition to vinyl molybdate, several other organomolybdenum species appear to be present as judged from the hydrocarbons released on alkaline hydrolysis of the later chromatographic fractions. One of them produces ethane on alkaline hydrolysis and may be a thiol complex of ethyl molybdate(VI), the terminal intermediate of ethane-producing side reactions; it is always formed in much lower yields than vinyl molybdate (yields are not shown in Figure 2), consistent with the generally low yields of ethane in the molybdothiol-catalyzed reduction of acetylene. A species producing ethylene on hydrolysis is the major product. It could be the cysteine complex of vinyl molybdate but has as such not been characterized. Another species that releases buta-1,3-diene on alkaline hydrolysis is observed if the reactions are run under conditions favoring the formation of buta-1,3-diene, i.e., at high concentrations of complex I in the presence of excess acetylene.[4] The early fractions in Figure 2b could contain butadienyl molybdate(VI), $CH_2=CHCH=CHMoO_3^-$, the later fractions cysteine complexes thereof. Butadienyl molybdate could not be obtained by the reaction of vinyl

molybdate with acetylene under conditions of catalytic acetylene reduction. The formation of butadiene in molybdothiol-catalyzed reductions of acetylene presumably occurs by way of C_2H_2 insertion into an organomolybdenum species other than vinyl molybdate, as has been deduced elsewhere.[4] The fact that molybdothiols catalyze the reduction of acetylene to buta-1,3-diene under certain conditions was first emphasized by Corbin et al.[10] and was for some time considered to be a serious shortcoming of these nitrogenase model systems, since nitrogenase reduces acetylene only to ethylene. However, the formation of buta-1,3-diene can be effectively suppressed if the C_2H_2 reductions are carried out at low catalyst concentrations,[11] and we have since found that *reaction pH* is yet another factor controlling the formation of this product. Table IV shows that even at high catalyst concentrations buta-1,3-diene is formed in substantial yields only in the alkaline pH range. Since the active site of functional nitrogenase is likely to be acidic as protons are generated during ATP hydrolysis,[12] the selectivity of the enzymatic C_2H_2 reduction is no longer difficult to rationalize.

Finally, it should be mentioned that, in addition to the hydrocarbons mentioned above, traces of acetylene are released on reaction of the chromatographic fractions with base. This suggests the existence of molybdenum(V)–acetylene complexes whose formation is favored at high concentrations of complex I. These complexes appear to play no role in the catalytic reductions of acetylene, their nature remains to be elucidated.

(10) Corbin, J. L.; Pariyadath, N.; Stiefel, E. I. *J. Am. Chem. Soc.* **1976**, *98*, 7862.
(11) Robinson, P. R.; Moorehead, E. L.; Weathers, B. J.; Ufkes, E. A.; Vickrey, T. M.; Schrauzer, G. N. *J. Am. Chem. Soc.* **1977**, *99*, 3657.
(12) Schrauzer, G. N.; Hughes, L. A.; Palmer, M. R.; Strampach, N.; Grate, J. W. *Z. Naturforsch., B: Anorg. Chem., Org. Chem.* **1980**, *35B*, 1439.

Synthesis, characterization, and reaction chemistry of iridium and rhodium cyclopropyl complexes
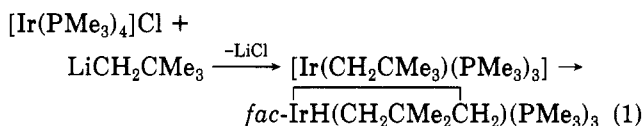
Nancy L. Jones, and James A. Ibers

More About This Article

The permalink http://dx.doi.org/10.1021/om00076a003 provides access to:

- Links to articles and content related to this article
- Copyright permission to reproduce figures and/or text from this article

Synthesis, Characterization, and Reaction Chemistry of Iridium and Rhodium Cyclopropyl Complexes

Nancy L. Jones and James A. Ibers*

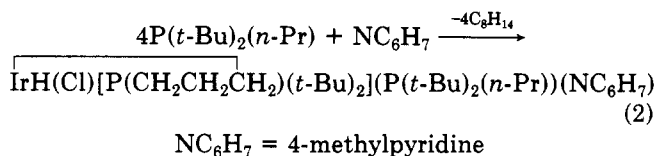*Department of Chemistry, Northwestern University, Evanston, Illinois 60201*

The complexes $MCl_2(COC_3H_5)(PMePh_2)_2$, 1 and 7 (M = Ir, Rh), $IrCl_2(C_3H_5)(CO)(PMePh_2)_2$, 2 and 3, and $IrCl_2(COC_3H_5)(PMePh_2)_3$, 5, have been synthesized in good yield by the reaction of cyclopropylmethanoic chloride (C_3H_5COCl) with the low-valent coordinatively unsaturated metal complexes $[IrCl(C_8H_{14})_2]_2$ or $[RhCl(C_2H_4)_2]_2$ after treatment of the latter with $PMePh_2$. Their structures have been deduced by interpretation of $^{31}P\{^1H\}$ and ^1H NMR and IR spectra. In the five-coordinate acyl complexes 1 and 7, the geometry about the metal is square pyramidal with cis phosphine ligands, cis chloro ligands, and an apical cyclopropylmethanoyl ligand. The six-coordinate octahedral bis(phosphine)iridium complexes 2 and 3 contain cis or trans phosphine ligands, respectively, while the tris(phosphine) complex 5 has meridional phosphine ligands. Abstraction of a chloro ligand from $IrCl_2(COC_3H_5)(PMePh_2)_3$ by NH_4PF_6 affords $[IrCl(C_3H_5)(CO)(PMePh_2)_3][PF_6]$. Reduction of $IrCl_2(C_3H_5)(CO)(PMePh_2)_2$, 3, by K/benzophenone affords *trans*-$Ir(C_3H_5)(CO)(PMePh_2)_2$. No evidence for rearrangement of the cyclopropyl group to a π-allyl group is found.

One popular mechanism for the transition-metal catalyzed isomerization of substituted cyclopropanes is shown in Scheme I.[1] This involves initial insertion of the coordinatively unsaturated metal A into a C–C bond of the three-membered ring to afford a metallacyclobutane complex B. Migration of the β-H atom to the metal yields an allylmetal hydride complex C. When this is followed by migration of the H atom back to the carbon chain (D) and liberation of the olefin, the cycle can become catalytic. Intermediates B and D are well documented for platinum,[2] while intermediate C has been isolated only for iridium.[1] The intermediacy of an iridium metallacycle B has never been reported.
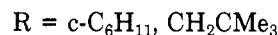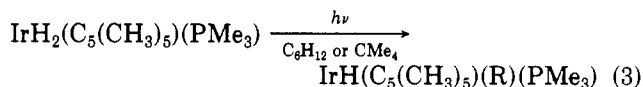
A different mechanism can be envisioned that involves initial oxidative addition of a C–H bond of the cyclopropane to the metal (Scheme I). This results in formation of a cyclopropylmetal hydride complex (E). Cyclopropyl-to-π-allyl rearrangement yields the same allylmetal hydride complex C. Intramolecular activation of C–H bonds (cyclometalation) by iridium is known. Tulip and Thorn report the production of an iridium hydrido-metallacyclobutane by abstraction of the γ-H atom from a coordinated neopentyl ligand (eq 1).[3] Hietkamp et al.[4]

$$[Ir(PMe_3)_4]Cl \ +$$

$$LiCH_2CMe_3 \xrightarrow{-LiCl} [Ir(CH_2CMe_3)(PMe_3)_3] \rightarrow$$

$$fac\text{-}IrH(CH_2CMe_2CH_2)(PMe_3)_3 \quad (1)$$

report cyclometalation involving coordinated tertiary phosphine ligands such as di-*tert*-butyl-*n*-propyl- and di-*tert*-butyl-*n*-butylphosphine (eq 2). Recently Janowicz

$$[IrCl(C_8H_{14})_2]_2 \ +$$

$$4P(t\text{-}Bu)_2(n\text{-}Pr) + NC_6H_7 \xrightarrow{-4C_8H_{14}}$$

$$IrH(Cl)[P(CH_2CH_2CH_2)(t\text{-}Bu)_2](P(t\text{-}Bu)_2(n\text{-}Pr))(NC_6H_7)$$
$$(2)$$

$$NC_6H_7 = 4\text{-methylpyridine}$$

Scheme I

and Bergman reported the intermolecular C–H bond activation of cyclohexane and neopentane by a hydrido-iridium(III) complex (eq 3).[5] To our knowledge no reports

$$IrH_2(C_5(CH_3)_5)(PMe_3) \xrightarrow[C_6H_{12} \text{ or } CMe_4]{h\nu}$$
$$IrH(C_5(CH_3)_5)(R)(PMe_3) \quad (3)$$

$$R = c\text{-}C_6H_{11}, CH_2CMe_3$$

of intermolecular C–H bond activation of cyclopropane by transition-metal complexes have appeared.

The oxidative addition of acid chlorides ($RCOCl$, R = Me, Et, Pr, but not cyclopropyl) to rhodium(I) and iridium(I) tertiary phosphine complexes followed by alkyl migration to the metal has precedent in the literature.[6-18]

(1) Tulip, T. H.; Ibers, J. A. *J. Am. Chem. Soc.* 1979, *101*, 4201-4211 and references therein.

(2) Puddephatt, R. J. *Coord. Chem. Rev.* 1980, *33*, 149-194.

(3) Tulip, T. H.; Thorn, D. L. *J. Am. Chem. Soc.* 1981, *103*, 2448-2450.

(4) Hietkamp, S.; Stufkens, D. J.; Vrieze, K. *J. Organomet. Chem.* 1977, *139*, 189-198.

(5) Janowicz, A. H.; Bergman, R. G. *J. Am. Chem. Soc.* 1982, *104*, 352-354.

(6) Bennett, M. A.; Jeffery, J. C. *Inorg. Chem.* 1980, *19*, 3763-3767.

(7) Bennett, M. A.; Charles, R.; Mitchell, T. R. B. *J. Am. Chem. Soc.* 1978, *100*, 2737-2743.

(8) Egglestone, D. L.; Baird, M. C.; Lock, C. J. L.; Turner, G. *J. Chem. Soc., Dalton Trans.* 1977, 1576-1582.

(9) Lau, K. S. Y.; Becker, Y.; Huang, F.; Baenziger, N.; Stille, J. K. *J. Am. Chem. Soc.* 1977, *99*, 5664-5672.

(10) Egglestone, D.; Baird, M. C. *J. Organomet. Chem.* 1976, *113*, C25-C29.

(11) Dunham, N. A.; Baird, M. C. *J. Chem. Soc., Dalton Trans.* 1975, 774-779.

(12) Stille, J. K.; Regan, M. T. *J. Am. Chem. Soc.* 1974, *96*, 1508-1514.

(13) Stille, J. K.; Fries, R. W. *J. Am. Chem. Soc.* 1974, *96*, 1514-1518.

(14) Stille, J. K.; Huang, F.; Regan, M. T. *J. Am. Chem. Soc.* 1974, *96*, 1518-1522.

(15) Kubota, M.; Blake, D. M.; Smith, S. A. *Inorg. Chem.* 1971, *10*, 1430-1433.

The oxidative addition of cyclopropylmethanoic chloride to rhodium(I) and iridium(I) phosphine complexes appeared to us to be a route to the synthesis and isolation of transition-metal σ-bound cyclopropyl complexes. Once formed the chemistry of the σ-cyclopropyl group could be explored. Our results on the synthetic utility of this method as well as the reaction chemistry of cyclopropyl complexes so generated are presented here.

Experimental Section

All procedures were performed in standard Schlenk-type glassware,[19] in Schlenk-type glassware interfaced to a high vacuum line (10^{-4}–10^{-5} torr), or in an argon-filled glovebox. Argon (prepurified) and dinitrogen (prepurified) were used as obtained from Matheson Gas Co., East Rutherford, NJ. Toluene, diethyl ether, hexane, and tetrahydrofuran (distilled from Na/benzophenone) were condensed and stored over [Ti(C_5H_5)$_2$Cl]$_2$ZnCl$_2$ (toluene, hexane) or [Ti(C_5H_5)$_2$Cl]$_2$ (tetrahydrofuran, diethyl ether)[20] under vacuum in bulbs on the vacuum line. Dichloromethane was distilled from P$_2$O$_5$ and stored over fresh P$_2$O$_5$ on the vacuum line as well. Reagent grade acetone and methanol (Mallinckrodt, Inc.) were deoxygyenated prior to use. Methyldiphenylphosphine (PMePh$_2$) (Strem Chemicals, Inc.) and cyclopropylmethanoic chloride (C$_3$H$_5$COCl) (Aldrich Chemical Co.) were distilled prior to use and stored under dinitrogen. Ethylene (Matheson Gas Co., 99.5%) was used as obtained. Ammonium hexafluorophosphate (NH$_4$PF$_6$) (Alfa Products) was used as obtained. Literature procedures were used to prepare [IrCl(C$_8$H$_{14}$)$_2$]$_2$[21] (C$_8$H$_{14}$ = cyclooctene) and [RhCl(C$_2$H$_4$)$_2$]$_2$.[22]

Elemental analyses were perfomred by Galbraith Laboratories, Inc., Knoxville, TN. The molecular weight of RhCl$_2$-(COC$_3$H$_5$)(PMePh$_2$)$_2$, 7, was determined cryoscopically with the use of apparatus described elsewhere.[19] Infrared spectra were recorded from Nujol mulls on a Perkin-Elmer 283 spectrometer. The ^{31}P{^{1}H} NMR and ^{1}H NMR spectra were obtained on a JEOL FX90Q spectrometer operating at 36.2 and 89.55 MHz, respectively, or on a JEOL FNM-FX270 spectrometer operating at 109.2 and 269.65 MHz, respectively. Positive chemical shifts are reported as downfield from external 85% H$_3$PO$_4$ (^{31}P) or internal Si(CH$_3$)$_4$ (^{1}H). Deuterated toluene (C$_7$D$_8$) and benzene (C$_6$D$_6$) were distilled from Na and degassed by freeze–thaw cycles on a vacuum line before use. Deuterated chloroform (CDCl$_3$) was used without further purification and degassed in a similar manner. Deuterated acetone (CD$_3$COCD$_3$) was dried over and distilled from activated sieves onto fresh activated sieves for storage.

Equilibrium Mixture of IrCl$_2$(COC$_3$H$_5$)(PMePh$_2$)$_2$, 1, and IrCl$_2$(C$_3$H$_5$)(CO)(PMePh$_2$)$_2$, 2. Under a flush of dinitrogen PMePh$_2$ (0.25 mL, 1.35 mmol) was added to a stirred suspension (–78 °C) of [IrCl(C$_8$H$_{14}$)$_2$]$_2$ (0.30 g, 0.34 mmol) in 20 mL of toluene. After being stirred for 10 min, a deep red solution resulted at which time an excess of C$_3$H$_5$COCl (0.25 mL) was syringed into the flask. The reaction mixture was allowed to warm to room temperature, next was refluxed for 10 min, and then was cooled to room temperature. The pale yellow reaction mixture was then filtered to remove any decomposition products that may have formed. The filtrate was concentrated to <2 mL, and diethyl ether was condensed into the flask (–78 °C). The off-white precipitate was isolated by filtration, washed with diethyl ether, and dried in vacuum: yield 90%. IR: 1, ν(C=O) 1680 (m), 1655 (s), 1630 (m)

cm^{-1}; 2, ν(CO) 2025 cm^{-1}, ν(IrCl) 307, 280 cm^{-1}. ^{31}P{^{1}H} NMR (C$_6$D$_6$) 1, δ –11.8 (s); 2, δ –17.6 (d), –26.3 (d, $^2J_{PP}$ = 7 Hz), ratio 1/2 by integrated peak (^{31}P) area = 2. ^{1}H NMR (C$_6$D$_6$): 1, δ 1.46 (d, PMe, $^2J_{PH}$ = 10 Hz), 2.3 (m, CH), 1.25 (m, CH$_2$); 2, δ 2.08 (d, PMe, $^2J_{PH}$ = 10 Hz), 1.71 (d, PMe, $^2J_{PH}$ = 11 Hz), 2.6 (m, CH), 0.73 (m, CH$_2$). Anal. Calcd for C$_{30}$H$_{31}$Cl$_2$OP$_2$Ir: C, 49.19; H, 4.27; Cl, 9.67; P, 8.46. Found: C, 49.28; H, 4.29; Cl, 9.47; P, 8.38.

IrCl$_2$(C$_3$H$_5$)(CO)(PMePh$_2$)$_2$, 3. A mixture of 1 and 2 dissolved in toluene slowly isomerizes at room temperature to 3. After 18 days the ratio fo 1:2:3 was 2.8:1.4:1.0 (by integrated peak (^{31}P) area). Alternatively a reaction mixture, as prepared above, when refluxed for 30 min affords 3 in >90% yield: IR ν(CO) 2025 cm^{-1}, ν(IrCl) 303, 253 cm^{-1}; ^{31}P{^{1}H} NMR (C$_6$D$_6$) δ –19.0 (s); ^{1}H NMR (C$_6$D$_6$) δ 2.39 (t, PMe, $^2J + {}^4J_{PH}$ = 4 Hz), 1.13 (m, CH), 0.16 (d, CH$_2$, J = 8 Hz), –0.30 (d, CH$_2$, J = 6 Hz). Anal. Calcd for C$_{30}$H$_{31}$Cl$_2$OP$_2$Ir: C, 49.19; H, 4.27; Cl, 9.67; P, 8.46. Found: C, 49.45; H, 4.60; Cl, 9.23; P, 8.27.

***trans*-Ir(C$_3$H$_5$)(CO)(PMePh$_2$)$_2$, 4.** A potassium benzophenone ketyl solution (approximately 0.74 M) was prepared by stirring K metal (1 mol) and (C$_6$H$_5$)$_2$CO (1 mol) in THF under dinitrogen until the solution was very dark blue. A solution of 3 (0.33 g, 0.45 mmol) in 20 mL of THF was cooled to 0 °C. Under a flush of dinitrogen, 0.55 mL of K[(C$_6$H$_5$)$_2$CO]/THF solution (0.41 mmol of K, 0.91 equiv) was added dropwise with stirring over a 5-min period to the Ir-containing solution. The reaction mixture went from nearly colorless to orange to yellow-orange. The THF was stripped off at 0 °C after the reaction mixture had been stirred 30 min. The resulting yellow oil was dissolved in cold toluene (15 mL) and filtered cold. The toluene was removed in vacuum at 0 °C. A C$_6$D$_6$ solution was quickly prepared for NMR measurements. In addition to signals from residual starting material 3, signals arising from a new compound, 4, appeared: ^{31}P{^{1}H} NMR (C$_6$D$_6$) δ 10.0 (s); ^{1}H NMR (C$_6$D$_6$) δ 2.71 (m, CH), 1.01 (t, PMe, $^2J + {}^4J_{PH}$ = 6.6 Hz), 0.62 (d, CH$_2$, J = 11 Hz), 0.33 (br, CH$_2$); IR (C$_6$D$_6$ solution) ν(CO) 1935 cm^{-1}. Sodium naphthalide will effect a similar reduction of the iridium(III) complex 3, but several products result. Attempts at separation of the products from the sodium naphthalide reduction were generally unsuccessful although the presence of 4 in the product mixture is inferred from NMR and IR spectroscopic measurements.

***mer*-IrCl$_2$(COC$_3$H$_5$)(PMePh$_2$)$_3$, 5.** In a manner similar to that used in the preparation of 3, an excess of PMePh$_2$ (0.40 mL) was syringed into a stirred suspension of [IrCl(C$_8$H$_{14}$)$_2$]$_2$ (0.30 g, 0.33 mmol) in 20 mL of toluene at –78 °C. An excess of C$_3$H$_5$COCl (0.10 mL) was likewise added and the reaction mixture refluxed for 1 h. After filtration, the pale yellow reaction mixture was concentrated to <2 mL, and diethyl ether or hexane was condensed into the reaction flask (–78 °C). The resulting white precipitate was filtered and washed with diethyl ether or hexane three times: yield 90%; IR ν(CO) 1595 cm^{-1}, ν(IrCl) 285 (br) cm^{-1}; ^{31}P{^{1}H} NMR (CDCl$_3$) δ –31.6 (d), –45.6 (t, $^2J_{PP}$ = 18 Hz); ^{1}H NMR (CDCl$_3$) δ 3.7 (m, CH), 2.28 (t, PMe, $^2J + {}^4J_{PH}$ = 14 Hz), 1.88 (d, PMe, J_{PH} = 9 Hz), 0.60 (m, CH$_2$), 0.01 (m, CH$_2$). Anal. Calcd for C$_{43}$H$_{44}$Cl$_2$OP$_3$Ir: C, 55.36; H, 4.75; Cl, 7.60; P, 9.96. Found: C, 55.82; H, 5.35; Cl, 7.00; P, 9.87.

***mer*-[IrCl(C$_3$H$_5$)(CO)(PMePh$_2$)$_3$][PF$_6$], 6.** An excess of NH$_4$PF$_6$ (0.35 g, 2.1 mmol) in 4 mL of acetone was added to a stirred suspension of *mer*-IrCl$_2$(COC$_3$H$_5$)(PMePh$_2$)$_3$ (0.25 g, 0.27 mmol) in 2 mL of CH$_2$Cl$_2$ and 20 mL of acetone. The reaction mixture was stirred for 1 h, and then the solvents were stripped off. The tan residue was extracted with four 8-mL portions of CH$_2$Cl$_2$. The CH$_2$Cl$_2$ was removed from the extract in vacuum leaving a tan residue that was recrystallized from methanol/diethyl ether: yield 62%; IR ν(CO) 2030 cm^{-1}; ^{31}P{^{1}H} NMR (CDCl$_3$) δ –30.5 (br), –40.8 (t, $^2J_{PP}$ = 11 Hz); ^{1}H NMR (CDCl$_3$) δ 2.36 (t, PMe, $^2J + {}^4J_{PH}$ = 4 Hz), 2.02 (d, PMe, $^2J_{PH}$ = 9 Hz), 0.77 (m, CH), 0.20 (br, CH$_2$), –0.16 (br, CH$_2$). Anal. Calcd for C$_{43}$H$_{44}$ClF$_6$OP$_4$Ir: C, 49.55; H, 4.26; Cl, 3.40; F, 10.94; P, 11.88. Found: C, 48.68; H, 4.53; Cl, 3.54; F, 10.39; P, 12.01.

RhCl$_2$(COC$_3$H$_5$)(PMePh$_2$)$_2$, 7. In a manner similar to that used to prepare 1 and 2, under a flush of dinitrogen PMePh$_2$ (0.95 mL, 5.12 mmol) was syringed into a stirred suspension (–78 °C) of [RhCl(C$_2$H$_4$)$_2$]$_2$ (0.48 g, 1.25 mmol) in 25 mL of toluene. After the suspension was stirred 20 min, an excess of C$_3$H$_5$COCl (0.50 mL) was added to the deep red solution. Stirring was continued at room temperature for 15 min after which a lemon yellow

(16) Ohno, K.; Tsuji, J. *J. Am. Chem. Soc.* **1968**, *90*, 99–107.

(17) The complex IrCl$_2$(COC$_3$H$_5$)(CO)(PPh$_3$)$_2$ is obtained from reaction of IrCl(CO)(PPh$_3$)$_2$ and C$_3$H$_5$COCl. Decarbonylation is not observed. Bruce, M. I.; Iqbal, M. Z.; Stone, F. G. A. *J. Organomet. Chem.* **1969**, *20*, 161–168.

(18) Oxidative addition of C$_3$H$_5$COCl to K[Fe(C$_5$H$_5$)(CO)$_2$] affords Fe(C$_5$H$_5$)(COC$_3$H$_5$)(CO)$_2$ which upon photolysis gives Fe(C$_5$H$_5$)(C$_3$H$_5$)(CO)$_2$. Manganiello, F. J.; Christensen, L. W.; Jones, W. M. *J. Organomet. Chem.* **1982**, *235*, 327–334.

(19) Shriver, D. F. "The Manipulation of Air-Sensitive Compounds"; McGraw-Hill: New York, 1969.

(20) Green, M. L. H.; Lucas, C. R. *J. Chem. Soc., Dalton Trans.* **1972**, 1000–1003.
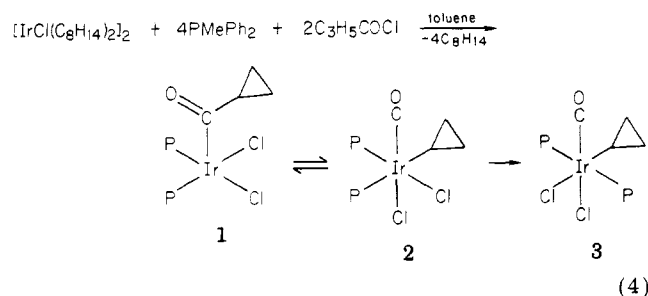
(21) Herde, J. L.; Lambert, J. C.; Senoff, C. V. *Inorg. Synth.* **1974**, *15*, 18–20.

(22) Cramer, R. *Inorg. Synth.* **1974**, *15*, 14–18.

precipitate was observed. Stirring was continued for another 15 min before the toluene was stripped off. After hexane was distilled into the flask, the pale yellow solid was filtered, washed two times with hexane, and dried under vacuum. Isolation of the same product results when excess PMePh$_2$ is used (>9 equiv): yield 96%; IR ν(C=O) 1687, 1660 cm^{-1}, ν(RhCl) 303, 277 cm^{-1}; ^{31}P{^{1}H} NMR (CD$_3$COCD$_3$) δ 29.6 (d, J_{RhP} = 143 Hz); ^{1}H NMR (CD$_3$COCD$_3$) δ 3.8 (m, CH), 1.49 (d, PMe, $^2J_{PH}$ = 10 Hz), 1.3 (m, CH$_2$), 1.1 (m, CH$_2$). Anal. Calcd for C$_{30}$H$_{31}$Cl$_2$OP$_2$Rh: C, 56.01; H, 4.86; Cl, 11.02; P, 9.63; mol wt 643. Found: C, 56.53; H, 4.97; Cl, 10.68; P, 8.72; mol wt (cryoscopic in 1,2-dichloroethane), 588 ($\pm$10%).

Results

IrCl$_2$(C$_3$H$_5$)(CO)(PMePh$_2$)$_2$. Reaction of cyclopropylmethanoic chloride (C$_3$H$_5$COCl) with a solution of [IrCl(C$_8$H$_{14}$)$_2$]$_2$ (1 equiv) and methyldiphenylphosphine (PMePh$_2$, 4 equiv) affords a 90% yield of a 2:1 equilbrium mixture of IrCl$_2$(COC$_3$H$_5$)(PMePh$_2$)$_2$, **1**, and IrCl$_2$(C$_3$H$_5$)(CO)(PMePh$_2$)$_2$, **2** (eq 4). The structures of **1** and **2** were deduced from NMR and IR spectroscopic studies.
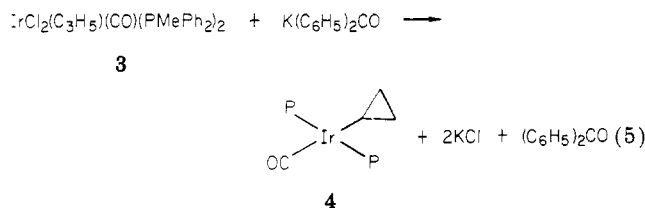

(4)

Compound **1**, IrCl$_2$(COC$_3$H$_5$)(PMePh$_2$)$_2$, displays square-pyramidal geometry about the Ir atom with mutually cis phosphine ligands, cis chloro ligands, and an apical cyclopropylmethanoyl ligand. The ^{31}P{^{1}H} NMR spectrum displays a singlet resonance for the two equivalent phosphine ligands. The ^{1}H NMR spectrum exhibits a doublet P–CH$_3$ resonance (J = 10 Hz) as one would expect for cis phosphine ligands. The position of the Ir–Cl band at 280 cm^{-1} in the IR spectrum is typical for a chloro ligand trans to a phosphine ligand.[23] We have assigned the strong band at 1655 cm^{-1} to ν(C=O). The ^{31}P{^{1}H} NMR spectrum of **2** displays a doublet of doublets attributable to two inequivalent cis phosphine ligands (J_{PP} = 7 Hz). The pair of doublet P–CH$_3$ resonances (J_{PH} = 10, 11 Hz) observed in the ^{1}H NMR spectrum of **2** also confirms the presence of two mutually cis inequivalent phosphine ligands. From the IR spectrum of **2** one can deduce that one chloro ligand lies trans to a phosphine ligand (ν(Ir–Cl) = 280 cm^{-1}) and the other trans to the carbonyl ligand (ν(Ir–Cl) = 307 cm^{-1}).[23] Evidence for alkyl migration from the carbonyl to the iridium center comes from the position in the IR spectrum of the band assignable to a terminal carbonyl ligand (ν(CO) = 2025 cm^{-1}). These assignments are from similar results of Bennett and Jeffery for IrCl$_2$(COR)(L)$_2$ and IrCl$_2$(R)(CO)(L)$_2$ (L = PMePh$_2$, R = Me, Et, n-Pr).[6] Compounds **1** and **2** exist as an equilibrium mixture in solution. The equilibrium constant K for **1** $\rightleftharpoons$ **2** in C$_6$D$_6$ solution at 25 °C is 0.5 (by ^{31}P{^{1}H} NMR spectroscopy).

The complexes **1** and **2** isomerize slowly in solution at room temperature but rapidly in refluxing toluene to **3** (eq 4). The appearance of a new signal in the ^{31}P{^{1}H} NMR spectrum and disappearance of those assigned to **1** and **2** are evidence for the isomerization. We assign the new singlet to equivalent phosphine ligands. The data obtained from ^{1}H NMR spectroscopic measurements support a trans

arrangement of the phosphine ligands, namely the assignment of the virtual triplet resonance to the P–Me groups (^2J + $^4J_{PH}$ = 4 Hz). The geometry of the chloro ligands can be determined by the position of the two Ir–Cl bands in the IR spectrum of **3**. One chloro ligand lies trans to the cyclopropyl group (ν(IrCl) = 253 cm^{-1}), the other trans to the terminal carbonyl (ν(IrCl) = 303 cm^{-1}, ν(CO) = 2025 cm^{-1}). The ^{1}H NMR chemical shifts of the cyclopropyl protons of **3** lie to higher field than the corresponding protons of **1** and **2**. Similar behavior has been reported for analogous Ir–PPh$_3$ and Ir–PMePh$_2$ complexes.[6,7] This shift upfield is attributed to shielding of the alkyl protons of complex **3** by the aromatic groups on the phosphine ligands. The corresponding protons of **1** and **2** are not constrained to lie within the aromatic shielding zone of the cis phosphine ligands.[6]
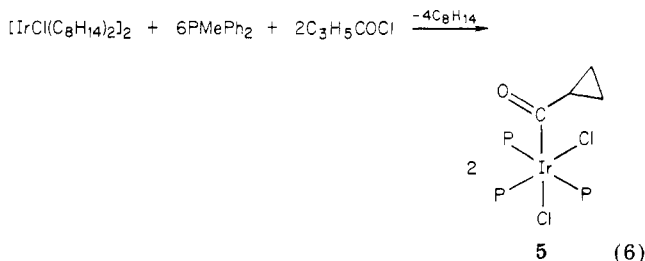
Complexes **1**–**3** are white or off-white, air-stable solids. Complex **3** is very stable thermally. It may be heated in refluxing toluene for several hours after which no decomposition or isomerization of the cyclopropyl group is observed.

Reduction of **3** with potassium benzophenone ketyl in tetrahydrofuran results in isolation of a mixture of the Ir(III) starting material **3** and a bright yellow complex, **4** (eq 5).[24] Repeated attempts to isolate **4** in analytically

pure form have been thwarted by the extreme solubility of the complex in organic solvents. We propose complex **4** to be *trans*-Ir(C$_3$H$_5$)(CO)(PMePh$_2$)$_2$ from NMR and IR spectroscopic studies. The ^{31}P{^{1}H} NMR spectrum displays a singlet; this implies equivalent phosphine ligands. A band in the IR spectrum at 1935 cm^{-1} we assign to ν(CO); this value is typical of ν(CO) for Ir(R)(CO)(PR$_3$)$_2$-type complexes.[25,26] Resonances attributable to cyclopropyl protons are observed in the ^{1}H NMR spectrum. We do not observe any resonances that we can attribute to allylic protons. Thus the cyclopropyl group does not rearrange to a π-allyl group.

mer-IrCl$_2$(COC$_3$H$_5$)(PMePh$_2$)$_3$. When an excess of PMePh$_2$, instead of 4 equiv is allowed to react with [IrCl(C$_8$H$_{14}$)$_2$]$_2$, an air-stable six-coordinate iridium(III) acyl complex **5** is isolated in 90% yield (eq 6). The disposition

(6)

of the ligands about the iridium center was deduced from

(23) Deeming, A. J.; Shaw, B. L. *J. Chem. Soc. A* **1969**, 1128–1134.

(24) The complex Pt(C$_3$H$_5$)$_2$(PMe$_2$Ph)$_2$ has been prepared by the reaction of cyclopropyllithium with PtCl$_2$(PMe$_2$Ph)$_2$ (Phillips, R. L.; Puddephatt, R. J. *J. Chem. Soc., Dalton Trans.* **1978**, 1732–1735). We have been unable to synthesize iridium(I) σ-cyclopropyl complexes by this method.
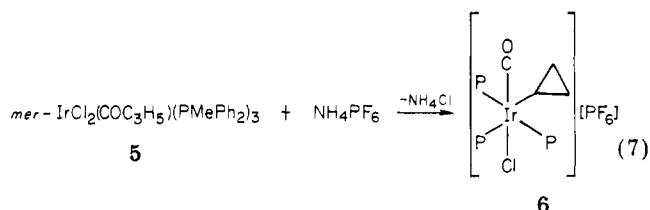
(25) Mirzaei, F.; Dahlenburg, L. *J. Organomet. Chem.* **1979**, *173*, 325–333.

(26) Dahlenburg, L.; Nast, R. *J. Organomet. Chem.* **1976**, *110*, 395–406.

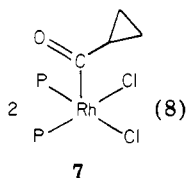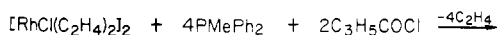NMR and IR spectroscopic measurements. The $^{31}P\{^1H\}$-NMR spectrum appears as a first-order AX_2 pattern. The ^1H NMR resonance patterns consist of a triplet assigned to two mutually trans P–Me groups ($^2J + {}^4J_{PH} = 14$ Hz) and a doublet assigned to another P–Me group. Resonances assigned to the cyclopropyl protons appear downfield of those for 1–3. The IR spectrum of 5 displays a strong band at 1595 cm^{-1} that we assign to the acyl carbonyl group and a broad band at 285 cm^{-1} that we assign as ν(IrCl) for the chloro ligand trans to a phosphine ligand.

Treatment of *mer*-IrCl$_2$(COC$_3$H$_5$)(PMePh$_2$)$_3$, 5, with an excess of NH$_4$PF$_6$ affords complex 6, *mer*-[IrCl(C$_3$H$_5$)-(CO)(PMePh$_2$)$_3$][PF$_6$] (eq 7). The band assigned to ν-

$$mer\text{-}IrCl_2(COC_3H_5)(PMePh_2)_3 \ + \ NH_4PF_6 \ \xrightarrow{-NH_4Cl} \ \underset{\textbf{6}}{\left[\begin{array}{c} \end{array}\right][PF_6]} \quad (7)$$
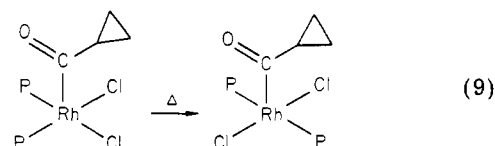
5

(C=O) in the IR spectrum of 5 has disappeared, and a band that we assign to a terminal carbonyl ligand (2030 cm^{-1}) has appeared. The *mer* arrangement of the three phosphine ligands is confirmed by the presence of an AX_2 pattern of resonances in the $^{31}P\{^1H\}$ NMR spectrum, similar to that of the starting material 5, and by the presence of doublet and triplet resonances in the ^1H NMR spectrum assignable to the P–Me groups.[27] The cyclopropyl proton resonances are shifted upfield from those of the starting acyl complex 5.

RhCl$_2$(COC$_3$H$_5$)(PMePh$_2$)$_2$. The addition of C$_3$H$_5$CO-Cl to a solution of [RhCl(C$_2$H$_4$)$_2$]$_2$ (1 equiv) and PMePh$_2$ (4 equiv) results in the isolation of the five-coordinate square-pyramidal rhodium acyl complex 7, (eq 8). The

$$[RhCl(C_2H_4)_2]_2 \ + \ 4PMePh_2 \ + \ 2C_3H_5COCl \ \xrightarrow{-4C_2H_4}$$

$$2 \quad \left[\begin{array}{c} \end{array} \right] \quad (8)$$

7

pale yellow air-stable solid was isolated in 96% yield. A doublet resonance is observed in the $^{31}P\{^1H\}$ NMR spectrum that we assign to equivalent phosphine ligands (J_{RhP} = 143 Hz). Assignment of the phosphines as cis is from the magnitude of the coupling constant J_{RhP}. For complexes RhCl$_2$(COR)(PR$_3$)$_2$ a coupling constant, J_{RhP}, of approximately 140 Hz is expected for cis phosphine ligands, while that of about 108 Hz is expected for trans phosphine ligands.[28] Bands in the IR spectrum of 7 assignable to ν(C=O) are observed at 1687 and 1660 cm^{-1} and to ν(RhCl) at 303 and 277 cm^{-1}. The existence of complex 7 as a monomer was confirmed by cryoscopic molecular weight measurements in 1,2-dichloroethane. Complex 7 is very stable thermally. Only a very small amount of the isomer of RhCl$_2$(COC$_3$H$_5$)(PMePh$_2$)$_2$ with trans phosphine ligands (J_{RhP} = 108 Hz) contaminates 7 (with cis phosphines) after 4 days in refluxing toluene (eq 9).
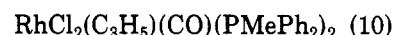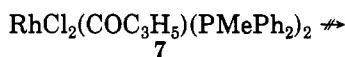
Attempts to prepare a six-coordinate rhodium(III) acyl complex analogous to 5 with the use of an excess of PMePh$_2$ were unsuccessful and afforded the five-coordi-

$$\left[\begin{array}{c} \end{array} \right] \ \xrightarrow{\Delta} \ \left[\begin{array}{c} \end{array} \right] \quad (9)$$

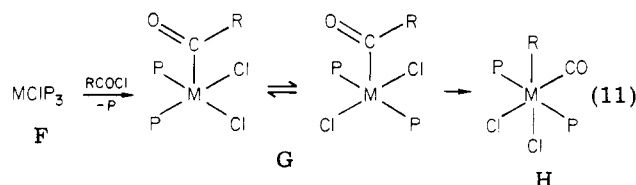nate complex RhCl$_2$(COC$_3$H$_5$)(PMePh$_2$)$_2$, 7, exclusively.

Discussion

Our search for methods for synthesizing transition-metal σ-cyclopropyl complexes has led to the study of the oxidative addition of cyclopropylmethanoic chloride to rhodium(I) and iridium(I) tertiary phosphine complexes. Oxidative addition of cyclopropylmethanoic chloride to a mixture of [IrCl(C$_8$H$_{14}$)$_2$]$_2$ and 4 equiv of PMePh$_2$ affords an equilibrium mixture of IrCl$_2$(COC$_3$H$_5$)(PMePh$_2$)$_2$, 1 and IrCl$_2$(C$_3$H$_5$)(CO)(PMePh$_2$)$_2$, 2 (eq 4), while with a mixture of 4 or more equiv of PMePh$_2$ and [RhCl(C$_2$H$_4$)$_2$]$_2$ one obtains only RhCl$_2$(COC$_3$H$_5$)(PMePh$_2$)$_2$, 7 (eq 8). Complex 7 undergoes isomerization (eq 9) only under forcing conditions. Cyclopropyl migration is not observed (eq 10).

$$\underset{\textbf{7}}{RhCl_2(COC_3H_5)(PMePh_2)_2} \ \nrightarrow$$

$$RhCl_2(C_3H_5)(CO)(PMePh_2)_2 \quad (10)$$

Abstraction of a chloro ligand of 7 by AgBF$_4$ leaves the acyl group intact, as determined by IR spectroscopy. In contrast, cyclopropyl migration to iridium is effected when a chloro ligand of 5 is abstracted by NH$_4$PF$_6$ (eq 3).

This contrast between iridium(III) and rhodium(III) acyl complexes in their propensity to undergo alkyl migration has been noted previously.[7,28-30] When M = Ir and P = PPh$_3$ or PMePh$_2$ (eq 11), the five-coordinate acyl complex

$$MClP_3 \ \xrightarrow[-P]{RCOCl} \ \underset{\textbf{G}}{\rightleftharpoons} \ \underset{\textbf{H}}{\longrightarrow} \quad (11)$$

F

undergoes alkyl migration readily and cleanly to afford the isolable six-coordinate alkyl complex H (R = Me, Et, n-Pr).[7] When M = Rh and P$_2$ = Ph$_2$P(CH$_2$)$_3$PPh$_2$, reaction stops at G.[28,31] This difference in reactivity has been attributed to the greater tendency of Rh(III) relative to Ir(III) to form five-coordinate complexes in preference to six-coordinate complexes and to a lower Rh–alkyl bond strength as compared with that of an Ir–alkyl bond.[32]

The cyclopropyl group σ bound to an iridium center has proved to be a sturdy entity. There is no evidence for the rearrangement of the cyclopropyl group to an allyl group in any of the complexes 1, 2, 3, or 4. The presence of open coordination sites at the metal center, although necessary, is not sufficient for the rearrangement. For example, Ir-(C$_3$H$_5$)(CO)(PMePh$_2$)$_2$, 4 does not undergo cyclopropyl-to-allyl rearrangement. Given the stability of the σ-bound cyclopropyl group, the intermediacy of a cyclopropylmetal hydride complex, E, shown in Scheme I, lacks the credibility the allylmetal hydride intermediate has earned. One

(27) Mann, B. E.; Masters, C.; Shaw, B. L. *J. Chem. Soc., Dalton Trans.* **1972**, 704–708.

(28) Slack, D. A.; Egglestone, D. L.; Baird, M. C. *J. Organomet. Chem.* **1978**, *146*, 71–76.

(29) Bennett, M. A.; Jeffery, J. C.; Robertson, G. B. *Inorg. Chem.* **1981**, *20*, 323–330.

(30) Kubota, M.; Blake, D. M. *J. Am. Chem. Soc.* **1971**, *93*, 1368–1373.

(31) McGuiggan, M. F.; Doughty, D. H.; Pignolet, L. H. *J. Organomet. Chem.* **1980**, *185*, 241–249.

(32) Baird, M. C.; Mague, J. T.; Osborn, J. A.; Wilkinson, G. *J. Chem. Soc. A* **1967**, 1347–1360.

wonders what transformations at the metal center would be necessary to induce rearrangement of the σ-bound three-membered ring.

Synthesis and Characterization of the Bridged Diiodide Complexes [η⁵-C₅H₅Fe(CO)I]₂[(PhO)₂PC₂H₄P(OPh)₂] and Me₂Si[η⁵-C₅H₄Fe(CO)(L)I]₂ (L = PPh₃ and P(OPh)₃). Molecular and Crystal Structures of Me₂Si[η⁵-C₅H₄Fe(CO)₂I]₂ and d,l-[η⁵-C₅H₄Fe(CO)I]₂[(PhO)₂PC₂H₄P(OPh)₂]

Victor W. Day* and Michael R. Thompson

Chemistry Department, University of Nebraska, Lincoln, Nebraska 68588

Gregory O. Nelson* and Michael E. Wright

Chemistry Department, University of Arizona, Tucson, Arizona 85721

Reaction of (PhO)₂PC₂H₄P(OPh)₂ with [η⁵-C₅H₅Fe(CO)₂]₂ in refluxing benzene leads to the formation of [η⁵-C₅H₅Fe(CO)]₂[(PhO)₂PC₂H₄P(OPh)₂] (2) in 35% yield. Treatment of 2 with 3 mol equiv of iodine in chloroform gives quantitative yield of the diiodide [η⁵-C₅H₅Fe(CO)i]₂[(PhO)₂PC₂H₄P(OPh)₂] (3) as a mixture of diastereoisomers. These isomers are readily separated on the basis of solubility differences in benzene. The cyclopentadienyl-bridged complexes Me₂Si[η⁵-C₅H₄Fe(CO)(L)I]₂ (4, L = PPh₃; 5, L = P(OPh)₃) are prepared in >80% yields by irradiation of Me₂Si[η⁵-C₅H₄Fe(CO)₂I]₂ (1) in the presence of the appropriate phosphine or phosphite ligand. In the case of L = PPh₃ the diastereoisomers are efficiently separated by solubility differences in CH₂Cl₂. These diiodides are characterized by ¹H, ¹³C, and ³¹P NMR and IR spectroscopy and analytical methods. The molecular structures of 1 and d,l-[η⁵-C₅H₅Fe(CO)I]₂-[(PhO)₂PC₂H₄P(OPh)₂] (3b) are determined by X-ray diffraction. Complex 1 crystallizes in the space group $P2_1/n$ with $a = 7.731$ (2) Å, $b = 22.386$ (7) Å, $c = 12.273$ (3) Å, $\alpha = 90.00°$, $\beta = 97.60$ (2)°, and $\gamma = 90.00°$ with $Z = 4$. The structure was refined to $R_1 = 0.049$ and $R_2 = 0.060$ for 3614 independent reflections having $I > 3.0\sigma(I)$. Compound 3b crystallizes in the space group $P\bar{1}$ with $a = 11.066$ (4) Å, $b = 11.751$ (7) Å, $c = 18.784$ (13) Å, $\alpha = 99.04$ (5)°, $\beta = 98.34$ (4)°, and $\gamma = 114.06$ (4)° with $Z = 2$. The structure is refined to $R_1 = 0.066$ and $R_2 = 0.087$ for 4916 independent reflections having $I > 3.0\sigma(I)$. The overall geometry of both structures show the iron centers to be in a transoid relationship about the bridging ligand. Interpretation of ¹H and ¹³C NMR data along with information from a M-3 macromolecule manipulation system suggests these complexes have intramolecular steric interactions limiting their rotational freedom.

Introduction

A variety of mechanically linked binuclear iron complexes have been prepared and characterized in recent years.[1] These types of systems are well suited for study of the interactions between two metal reaction sites since the link inherently retains the metals in close proximity. With this purpose in mind we have prepared several bridged diiodides, namely, Me₂Si[η⁵-C₅H₄Fe(CO)(L)I]₂ (1, L = CO; 4, L = PPh₃; 5, L = P(OPh)₃) and [η⁵-C₅H₅Fe-(CO)I]₂[(PhO)₂PC₂H₄P(OPh)₂] (3), and explored their structure by both spectroscopic means and X-ray analysis. It is our intent to examine the conformational and stereochemical aspects of these complexes in order to aid in an understanding of their reactivities that are presently being explored. These bridged binuclear diiodides were chosen because they are easily prepared in high yields (>80%) and present a large variety of electronic and steric properties around each metal site. Furthermore, related mononuclear systems such as η⁵-C₅H₅Fe(CO)(L)I, L = CO, PPh₃, are P(OPh)₃, are extensively studied and their reactivity patterns well understood.[2]

We report here full details on the preparation of the Fe–Fe bonded species 2 and the diiodide complexes 3–5. The ¹H, ¹³C, and ³¹P NMR and IR spectra of these compounds and molecular and crystal structures of complexes Me₂Si[η⁵-C₅H₄Fe(CO)₂I]₂ (1) and d,l-[η⁵-C₅H₅Fe(CO)I]₂-[(PhO)₂PC₂H₄P(OPh)₂] (3b) by X-ray diffraction are presented. On the basis of these data conformational preference of these systems is discussed. In addition, we describe the separation of the diastereoisomers formed in the preparation of compounds 3 and 4.

*Address correspondence as follows: V.W.D., University of Nebraska; G.O.N., Research Laboratories, Tennessee Eastman, Co., P.O. Box 511, Kingston, TN 37662.

(1) Weaver, J.; Woodward, P. *J. Chem. Soc., Dalton Trans.* **1973**, 1439. Wegner, P. A.; Uski, V. A.; Kiester, R. P.; Dabestani, S.; Day, V. W. *J. Am. Chem. Soc.* **1977**, 99, 4846. Poilblanc, R. *Inorg. Chim. Acta* **1982**, 62, 75.
(2) Reger, D. L.; Coleman, C. J.; McElligot, P. J. *J. Organomet. Chem.* **1979**, 171, 73–84. Reger, D. L.; Coleman, C. J. *Inorg. Chem.* **1979**, 11, 3155.

wonders what transformations at the metal center would be necessary to induce rearrangement of the σ-bound three-membered ring.

Synthesis and Characterization of the Bridged Diiodide Complexes [η5-C$_5$H$_5$Fe(CO)I]$_2$[(PhO)$_2$PC$_2$H$_4$P(OPh)$_2$] and Me$_2$Si[η5-C$_5$H$_4$Fe(CO)(L)I]$_2$ (L = PPh$_3$ and P(OPh)$_3$). Molecular and Crystal Structures of Me$_2$Si[η5-C$_5$H$_4$Fe(CO)$_2$I]$_2$ and d,l-[η5-C$_5$H$_4$Fe(CO)I]$_2$[(PhO)$_2$PC$_2$H$_4$P(OPh)$_2$]

Victor W. Day* and Michael R. Thompson

Chemistry Department, University of Nebraska, Lincoln, Nebraska 68588

Gregory O. Nelson* and Michael E. Wright

Chemistry Department, University of Arizona, Tucson, Arizona 85721

Reaction of (PhO)$_2$PC$_2$H$_4$P(OPh)$_2$ with [η5-C$_5$H$_5$Fe(CO)$_2$]$_2$ in refluxing benzene leads to the formation of [η5-C$_5$H$_5$Fe(CO)]$_2$[(PhO)$_2$PC$_2$H$_4$P(OPh)$_2$] (2) in 35% yield. Treatment of 2 with 3 mol equiv of iodine in chloroform gives quantitative yield of the diiodide [η5-C$_5$H$_5$Fe(CO)i]$_2$[(PhO)$_2$PC$_2$H$_4$P(OPh)$_2$] (3) as a mixture of diastereoisomers. These isomers are readily separated on the basis of solubility differences in benzene. The cyclopentadienyl-bridged complexes Me$_2$Si[η5-C$_5$H$_4$Fe(CO)(L)I]$_2$ (4, L = PPh$_3$; 5, L = P(OPh)$_3$) are prepared in >80% yields by irradiation of Me$_2$Si[η5-C$_5$H$_4$Fe(CO)$_2$I]$_2$ (1) in the presence of the appropriate phosphine or phosphite ligand. In the case of L = PPh$_3$ the diastereoisomers are efficiently separated by solubility differences in CH$_2$Cl$_2$. These diiodides are characterized by ¹H, ¹³C, and ³¹P NMR and IR spectroscopy and analytical methods. The molecular structures of 1 and d,l-[η5-C$_5$H$_5$Fe(CO)I]$_2$-[(PhO)$_2$PC$_2$H$_4$P(OPh)$_2$] (3b) are determined by X-ray diffraction. Complex 1 crystallizes in the space group P2$_1$/n with a = 7.731 (2) Å, b = 22.386 (7) Å, c = 12.273 (3) Å, α = 90.00°, β = 97.60 (2)°, and γ = 90.00° with Z = 4. The structure was refined to R$_1$ = 0.049 and R$_2$ = 0.060 for 3614 independent reflections having I > 3.0σ(I). Compound 3b crystallizes in the space group PĪ with a = 11.066 (4) Å, b = 11.751 (7) Å, c = 18.784 (13) Å, α = 99.04 (5)°, β = 98.34 (4)°, and γ = 114.06 (4)° with Z = 2. The structure is refined to R$_1$ = 0.066 and R$_2$ = 0.087 for 4916 independent reflections having I > 3.0σ(I). The overall geometry of both structures show the iron centers to be in a transoid relationship about the bridging ligand. Interpretation of ¹H and ¹³C NMR data along with information from a M-3 macromolecule manipulation system suggests these complexes have intramolecular steric interactions limiting their rotational freedom.

Introduction

A variety of mechanically linked binuclear iron complexes have been prepared and characterized in recent years.[1] These types of systems are well suited for study of the interactions between two metal reaction sites since the link inherently retains the metals in close proximity. With this purpose in mind we have prepared several bridged diodides, namely, Me$_2$Si[η5-C$_5$H$_4$Fe(CO)(L)I]$_2$ (1, L = CO; 4, L = PPh$_3$; 5, L = P(OPh)$_3$) and [η5-C$_5$H$_5$Fe-(CO)I]$_2$[(PhO)$_2$PC$_2$H$_4$P(OPh)$_2$] (3), and explored their structure by both spectroscopic means and X-ray analysis. It is our intent to examine the conformational and stereochemical aspects of these complexes in order to aid in an understanding of their reactivities that are presently being explored. These bridged binuclear diiodides were chosen because they are easily prepared in high yields (>80%) and present a large variety of electronic and steric

properties around each metal site. Furthermore, related mononuclear systems such as η5-C$_5$H$_5$Fe(CO)(L)I, L = CO, PPh$_3$, are P(OPh)$_3$, are extensively studied and their reactivity patterns well understood.[2]

We report here full details on the preparation of the Fe–Fe bonded species 2 and the diiodide complexes 3–5. The ¹H, ¹³C, and ³¹P NMR and IR spectra of these compounds and molecular and crystal structures of complexes Me$_2$Si[η5-C$_5$H$_4$Fe(CO)$_2$I]$_2$ (1) and d,l-[η5-C$_5$H$_5$Fe(CO)I]$_2$-[(PhO)$_2$PC$_2$H$_4$P(OPh)$_2$] (3b) by X-ray diffraction are presented. On the basis of these data conformational preference of these systems is discussed. In addition, we describe the separation of the diastereoisomers formed in the preparation of compounds 3 and 4.

---

(1) Weaver, J.; Woodward, P. *J. Chem. Soc., Dalton Trans.* 1973, 1439. Wegner, P. A.; Uski, V. A.; Kiester, R. P.; Dabestani, S.; Day, V. W. *J. Am. Chem. Soc.* 1977, 99, 4846. Poilblanc, R. *Inorg. Chim. Acta* 1982, 62, 75.

(2) Reger, D. L.; Coleman, C. J.; McElligot, P. J. *J. Organomet. Chem.* 1979, 171, 73–84. Reger, D. L.; Coleman, C. J. *Inorg. Chem.* 1979, 11, 3155.
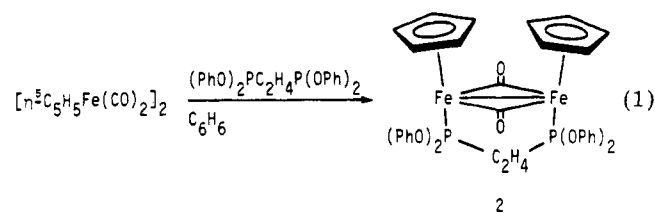
Table I. Crystallographic Parameters

parameter	1	3b
space group	$P2_1/n$	$P\bar{1}$
a, Å	7.731 (2)	11.066 (4)
b, Å	22.386 (7)	11.751 (7)
c, Å	12.273 (3)	18.784 (13)
α, deg	90.00	99.04 (5)
β, deg	97.60 (2)	98.34 (4)
γ, deg	90.00	114.06 (4)
V, Å^3	2106 (1)	2141 (2)
d_{calcd}, g/cm^3	2.09	1.57
Z	4	2
fw	663.9	1014.1
cryst size, mm	0.50 × 0.50 × 0.38	0.35 × 0.10 × 0.20
μ(Mo Kα), cm^{-1}	43.5	11.1
diffractometer	Nicolet four-circle	Syntex P2$_1$
monochromator	graphite	graphite
method	ω scan technique	θ-2θ scan technique
scan speed, deg/min	0-43, 4.0; 43.0-58.7, 3.0	2.0-29.3(variable)
bkgd time	half the scan time	same as scan time
stds	6 every 300 reflections	3 every 100 reflections
2θ limits	0.0-58.7	4.0-50.0
no. of unique data	5707	7554
no. of data with $|F_o^2| > 3\sigma|F_o^2|$	3614	4916
R_1	0.049	0.066
R_2	0.060	0.087
no. of variables	282	283
largest shift	0.16	0.07
goodness of fit	1.3	3.2

Results and Discussion

Preparation and Characterization of [η^5-C$_5$H$_5$Fe-(CO)]$_2$[(PhO)$_2$PC$_2$H$_4$P(OPh)$_2$] (2) and [η^5-C$_5$H$_5$Fe-(CO)I]$_2$[(PhO)$_2$PC$_2$H$_4$P(OPh)$_2$] (3). The bis(phosphite) ligand (PhO)$_2$PC$_2$H$_4$P(OPh)$_2$ is readily obtained in 80% yield from the reaction of 1,2-bis(dichlorophosphino)ethane with 4 equiv of phenol and triethylamine. Reaction of [η^5-C$_5$H$_5$Fe(CO)$_2$]$_2$ with the bis(phosphite) in refluxing benzene for 8 h affords complex 2 in 32-40% yield (eq 1).

$$[\eta^5 C_5H_5Fe(CO)_2]_2 \xrightarrow[\text{C}_6\text{H}_6]{\text{(PhO)}_2\text{PC}_2\text{H}_4\text{P(OPh)}_2} \quad (1)$$

2

In these preparations it is necessary to remove byproducts by a combination of CH$_3$CN washes and column chromatography (alumina III, benzene). In pure form complex 2 exists as blue, air-stable crystals. By analogy with the NMR and IR characteristics of a similar bis(phosphine)-linked complex reported by Haines and Duprees,[3] [η^5-C$_5$H$_5$Fe(CO)]$_2$[Ph$_2$PC$_2$H$_4$PPh$_2$], the structure of compound 2 is assigned that shown in eq 1.

Reaction of 2 with iodine occurs instantaneously and quantitatively in chloroform solution (eq 2), giving rise to a mixture of diastereomers in a ratio of 5:4 for 3a/3b, respectively. Recognizing that isomer 3b is very soluble in benzene but 3a is only sparingly soluble allows separation of the two diastereoisomers by solubility differences. One diastereoisomer, 3b, is characterized by a single-crystal X-ray diffraction study. Both isomers exhibit a single ^{31}P

(3) Haines, R. J.; DuPreez, A. L. *J. Organomet. Chem.* **1970**, *21*, 181-193.

[η^5-C$_5$H$_5$Fe(CO)]$_2$[(PhO)$_2$PC$_2$H$_4$P(OPh)$_2$]

$$\downarrow I_2, \text{CHCl}_3 \qquad (2)$$

3a   **3b**

resonance at δ 228.5 and a IR ν(CO) absorption at 1977 cm^{-1}; however, 3a and 3b do show differences in their ^{13}C and ^{1}H NMR spectra. For example, the ^{1}H and ^{13}C NMR resonances for the η^5-C$_5$H$_5$ group in 3a appear at δ 4.22 and 81.50, respectively, whereas in 3b they are at δ 4.33 and 81.39.

The formation of diastereoisomers in the reaction of 2 with iodine is not surprising considering that two asymmetric metal centers are generated. Since both isomers are formed, the addition of iodine to complex 2 can be designated as a nonstereoselective reaction. It is interesting to note that in the related system [η^5-C$_5$H$_5$Fe-(CO)I]$_2$[Ph$_2$PC$_2$H$_4$PPh$_2$], also containing two asymmetric centers, that diastereomeric products are not recognized.[4] We have recently prepared the related complex [C$_5$H$_5$Fe(CO)I]$_2$[Ph$_2$PCH$_2$PPh$_2$] and have found that indeed diastereoisomers analogous to 3a and 3b are formed.[5] It is perhaps also noteworthy that if mild conditions are not employed in the synthesis of 3, that one diastereoisomer can be decomposed. Thus, after several hours of reaction of a mixture of 3a and 3b in refluxing CHCl$_3$ only one isomer, namely, 3b, is isolated along with variable amounts of η^5-C$_5$H$_5$Fe(CO)$_2$I.

Preparation and Characterization of Me$_2$Si[η^5-C$_5$H$_4$Fe(CO)(L)I]$_2$, L = PPh$_3$ and P(OPh)$_3$. The diiodide derivatives Me$_2$Si[η^5-C$_5$H$_4$Fe(CO)(PPh$_3$)I]$_2$ (4) and Me$_2$Si[η^5-C$_5$H$_4$Fe(CO)[P(OPh)$_3$]I]$_2$ (5) are obtained by irradiation of a benzene solution for 3 h containing Me$_2$Si[η^5-C$_5$H$_4$Fe(CO)$_2$I]$_2$ (1) and the appropriate phosphine or phosphite ligand (eq 3). Complex 4 is obtained

$$\text{Me}_2\text{Si}[(\eta^5\text{-C}_5\text{H}_4)\text{Fe(CO)}_2\text{I}]_2 \xrightarrow{L, h\nu} \quad (3)$$

4, L = PPh$_3$
5, L = P(OPh)$_3$
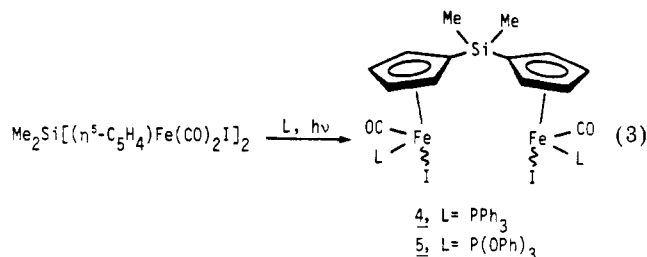
in pure form as a green, air-stable powder by precipitation from the crude photolysis mixture (after removal of solvent) with CH$_3$CN. Analytically pure 5 is obtained as a golden brown oil, soluble in benzene and CH$_2$Cl$_2$, as well as other polar solvents, and is also stable to air.

(4) Haines, R. J.; DuPreez, A. L. *Inorg. Chem.* **1972**, *11*, 330.

(5) Photolysis of 2 equiv of CpFe(CO)$_2$I in the presence of Ph$_2$PCH$_2$PPh$_2$ (dppm) yields [CpFe(CO)I]$_2$[dppm] as a mixture of diastereoisomers that are separatable by medium-pressure chromatography (alumina III, benzene). The isomers display identical IR ν(CO) bands; however, their ^{1}H and ^{13}C NMR spectra show significant differences. Details to be published elsewhere, G. O. Nelson and C. P. Eck.
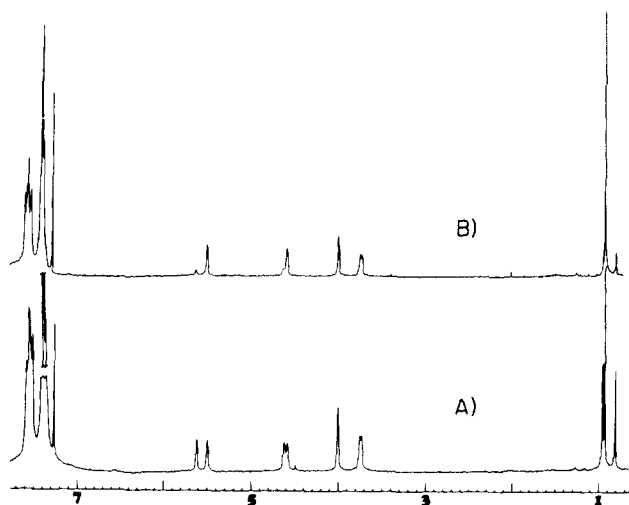
Figure 1. Proton NMR (250-MHz) spectra of (A) a $CDCl_3$ solution containing equal amounts of the diastereoisomers for $Me_2Si[\eta^5\text{-}C_5H_4Fe(CO)(PPh_3)I]_2$ (4) and (B) a $CDCl_3$ solution containing enrichment of the CH_2Cl_2-insoluble isomer **4b**.

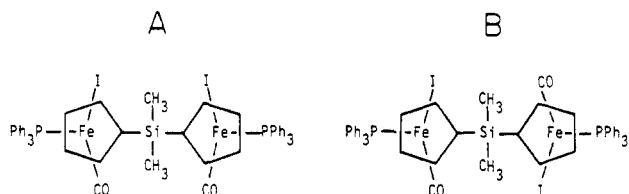**Figure 2.** Illustrations of two of the three possible stereoisomers for $Me_2Si[\eta^5\text{-}C_5H_4Fe(CO)(PPh_3)I]_2$ (4). Configuration A and its mirror image are assigned to **4b** and B is assigned to isomer **4a** on the basis of ^1H and ^{13}C NMR data.

Figure 3. A perspective ORTEP drawing of $Me_2Si[\eta^5\text{-}C_5H_4Fe(CO)_2I]_2$ (1) with non-hydrogen atoms represented by thermal vibration ellipsoids drawn to encompass 50% of the electron density. Hydrogen atoms are represented by arbitrarily small spheres that are in no way representative of their true thermal motion.

As in the preparation of **3**, a mixture of diastereoisomers is found in the synthesis of both **4** and **5**. We have successfully separated the two isomers of **4**; however, separation of the isomers of complex **5** is not yet possible. Treatment of **4** with CH_2Cl_2 gives a CH_2Cl_2-soluble compound that identifies as **4a** and a CH_2Cl_2-insoluble substance, **4b**. The 250-MHz ^1H NMR spectrum of the reaction product shows by relative peak integrals that they are formed in approximately equal amounts (Figure 1A). By enrichment of the mixture with **4b** (insoluble isomer) in the ^1H NMR spectrum (Figure 1B) the four resonances at δ 5.49, 4.58, 4.00, and 3.73 are assigned to the cyclopentadienyl (Cp) ring and the single resonance at δ 0.93 is assigned to the silyl methyls of **4b**. By difference the remaining resonances at δ 5.61, 4.61, 4.00, and 3.73 are assigned to the Cp ring and the resonances at δ 0.96 and 0.81 to the silyl methyls of **4a**. In the absence of a single-crystal X-ray study for either **4a** or **4b** we can tentatively assign their structures on the basis of ^1H and ^{13}C data. Two of the three possible stereoisomers of **4** are depicted in Figure 2 viewing down the Cp–Fe bond. Configuration "B" represents one of the *d,l* isomers, which possesses symmetry such that the silyl methyls can be in equivalent environments. In contrast, "A" shows that the two methyl groups are in different environments regardless of rotation about either the Cp–Fe or Si–Cp bonds. Since **4b** displays a single resonance at δ 0.93 for the silyl methyls, we assign to **4b** configuration "B". It follows that configuration "A" is representative of isomer **4a**.

Perhaps the most striking feature in the ^1H and ^{13}C NMR spectra of complexes **4** and **5** is found in the large spread of the Cp resonances. The four ^1H NMR resonances of the Cp moiety are expected since the protons are nonequivalent. However, the relative positions, as well
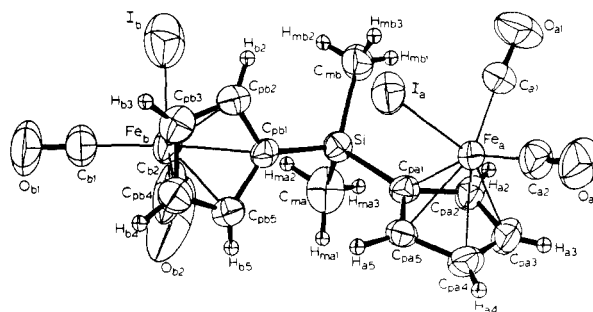
as the magnitude of the chemical shift differences, are not quite as clear-cut. In comparison to the proton resonance of the related mononuclear complexes $\eta^5\text{-}C_5H_5Fe(CO)(L)I$, $L = PPh_3$[6] and $P(OPh)_3$[7] (δ 4.48 and 4.20, respectively), **4** and **5** exhibit resonances both significantly upfield and downfield. From the comparison it is apparent that certain Cp protons are deshielded while others are shielded. This could be due to the effect of the different ligand environments about the iron or perhaps the effects of a phenyl ring on the PPh_3 and $P(OPh)_3$ ligands. This latter effect is suggestive of **4** and **5** having strong conformational preferences (for each diastereomer). The conformational preference of these complexes is also supported by an analysis of intramolecular steric interactions (discussed below).

A preliminary study of the reactivity of these complexes has already appeared.[8] One of the key points noted in the study is that **4** can be monoalkylated with BuLi to produce $Me_2Si[\eta^5\text{-}C_5H_4Fe(CO)(PPh_3)I][\eta^5\text{-}C_5H_4Fe(CO)(PPh_3)(\eta^1\text{-}C_4H_9)]$, indicating that different organic groups can be placed on the metal centers. Since mixtures of diastereomers are used, the important question of whether each diastereomer behaves differently under the reaction conditions explored is not addressed. Work on this point and others is continuing.

Crystal and Molecular Structures of 1 and 3b. Graphic Display Study. Complete details of the X-ray analysis for **1** and **3b** are given in Tables A and B, respectively. The final atomic coordinates for non-hydrogen and nongroup atoms from the X-ray study of **1** and **3b** are given in Tables II and III, respectively. Refined anisotropic thermal parameters for non-hydrogen and nongroup atoms are presented for **1** and **3b** in Tables C and D, respectively. The final atomic coordinates and isotropic thermal parameters for group atoms in **3b** are listed in Table IV. Final atomic positions for the hydrogen atoms and isotropic thermal parameters of **1** are set out in Table J. Perspective views of the structures which illustrate the numbering scheme are shown for **1** and **3b** in Figures 3 and 4, respectively.

Relevant bond lengths and angles for **1** and **3b** are set out in Tables V and VI. The $(\eta^5\text{-}C_5H_4)Fe(CO)_2I$ moieties (not crystallographically equivalent) in complex **1** have typical coordination geometries[9] and are identical with one

(6) Treichel, P. M.; Shubkin, R. L.; Barnett, K. W.; Reichard, D. *Inorg. Chem.* **1966**, *5*, 1177.

(7) Brown, D. A.; Lyons, H. J.; Manning, A. R.; Rowley, J. M. *Inorg. Chim. Acta* **1969**, *3*, 346.

(8) Nelson, G. O.; Wright, M. E. *Organometallics* **1982**, *1*, 565–568.

(9) Cotton, F. A.; Frenz, B. A.; White, A. J. *J. Organomet. Chem.* **1973**, *60*, 147.

Table II. Atomic Coordinates for Non-Hydrogen Atoms in Crystalline Me$_2$Si[η^5-C$_5$H$_4$Fe(CO)$_2$I]$_2$ (1)^a

atom^b type	fractional coordinates		
	x	y	z
I$_a$	0.27647 (7)	0.31485 (2)	0.25527 (5)
I$_b$	0.69189 (12)	0.05762 (3)	0.15612 (8)
Fe$_a$	0.54763 (13)	0.37091 (4)	0.35489 (8)
Fe$_b$	0.56429 (15)	0.07990 (5)	0.33693 (10)
Si	0.7524 (3)	0.2266 (1)	0.3397 (2)
O$_{a1}$	0.6640 (12)	0.4033 (4)	0.1467 (6)
O$_{a2}$	0.3497 (11)	0.4814 (3)	0.3671 (7)
O$_{b1}$	0.4366 (14)	−0.0418 (3)	0.3413 (8)
O$_{b2}$	0.8919 (17)	0.0478 (4)	0.4648 (14)
C$_{a1}$	0.6162 (12)	0.3896 (4)	0.2272 (7)
C$_{a2}$	0.4237 (12)	0.4382 (4)	0.3609 (7)
C$_{b1}$	0.4864 (14)	0.0053 (4)	0.3375 (8)
C$_{b2}$	0.7635 (18)	0.0603 (4)	0.4173 (14)
C$_{pa1}$	0.7047 (9)	0.2968 (3)	0.4122 (5)
C$_{pa2}$	0.8045 (10)	0.3517 (3)	0.4183 (7)
C$_{pa3}$	0.7339 (13)	0.3924 (4)	0.4879 (7)
C$_{pa4}$	0.5904 (13)	0.3646 (4)	0.5269 (7)
C$_{pa5}$	0.5714 (11)	0.3062 (3)	0.4820 (6)
C$_{pb1}$	0.5664 (9)	0.1742 (3)	0.3503 (5)
C$_{pb2}$	0.4350 (10)	0.1568 (3)	0.2627 (6)
C$_{pb3}$	0.3146 (11)	0.1176 (4)	0.3035 (7)
C$_{pb4}$	0.3651 (12)	0.1126 (4)	0.4183 (7)
C$_{pb5}$	0.5172 (12)	0.1466 (4)	0.4471 (7)
C$_{ma}$	0.9601 (12)	0.1967 (5)	0.4155 (11)
C$_{mb}$	0.7721 (16)	0.2415 (5)	0.1945 (8)

^{a} The numbers in parentheses are the estimated standard deviations in the last significant digit. ^{b} Atoms are labeled in agreement with Figure 3.

Table III. Atomic Coordinates for Non-Hydrogen and Nongroup Atoms in Crystalline [η^5-C$_5$H$_5$Fe(CO)I]$_2$[(PhO)$_2$PC$_2$H$_4$P(OPh)$_2$] (3b)^a

atom^b type	fractional coordinates		
	x	y	z
I$_a$'	0.60178 (8)	−0.28863 (10)	0.11529 (5)
I$_b$'	0.57878 (9)	0.17586 (10)	0.43178 (5)
Fe$_a$'	0.34798 (15)	−0.35609 (16)	0.12253 (8)
Fe$_b$'	0.80784 (14)	0.16097 (13)	0.43643 (8)
P$_a$'	0.40914 (25)	−0.29793 (24)	0.24177 (15)
P$_b$'	0.74993 (23)	0.09581 (23)	0.31779 (13)
C$_a$'	0.3524 (11)	−0.2068 (14)	0.1137 (6)
O$_a$'	0.3439 (9)	−0.1195 (10)	0.1085 (4)
C$_{pa1}$'	0.1868 (25)	−0.5289 (18)	0.1236 (10)
C$_{pa2}$'	0.1395 (15)	−0.4634 (20)	0.0840 (14)
C$_{pa3}$'	0.1988 (24)	−0.4478 (20)	0.0217 (11)
C$_{pa4}$'	0.2831 (23)	−0.4973 (26)	0.0230 (14)
C$_{pa5}$'	0.2919 (23)	−0.4498 (17)	0.0834 (21)
O$_{pa1}$'	0.4129 (8)	−0.4155 (7)	0.2748 (4)
O$_{pa2}$'	0.3148 (6)	−0.2519 (6)	0.2859 (4)
C$_b$'	0.8980 (13)	0.3240 (13)	0.4289 (6)
O$_b$'	0.9554 (11)	0.4212 (9)	0.4238 (5)
C$_1$'	0.5720 (10)	−0.1628 (9)	0.2939 (5)
C$_2$'	0.5867 (9)	−0.0409 (9)	0.2666 (5)
O$_{pb1}$'	0.8459 (6)	0.0452 (6)	0.2781 (4)
O$_{pb2}$'	0.7475 (6)	0.2095 (6)	0.2804 (3)
C$_{pb1}$'	0.8598 (14)	0.0112 (12)	0.4489 (7)
C$_{pb2}$'	0.9769 (12)	0.1340 (13)	0.4800 (8)
C$_{pb3}$'	0.9398 (14)	0.2016 (13)	0.5397 (7)
C$_{pb4}$'	0.8070 (13)	0.1230 (13)	0.5438 (6)
C$_{pb5}$'	0.7536 (13)	0.0042 (13)	0.4884 (7)

^{a} The numbers in parentheses are the estimated standard deviations in the last significant digit. ^{b} Atoms are labeled in agreement with Figure 4.

Table IV. Atomic Coordinates and Isotropic Thermal Parameters for Group Atoms in Crystalline [η^5-C$_5$H$_5$Fe(CO)I]$_2$[(PhO)$_2$PC$_2$H$_4$P(OPh)$_2$] (3b)^a

atom^b type	fractional coordinates			B, Å^2
	x	y	z	
C$_{1a1}$'	0.5048 (7)	−0.4098 (7)	0.3341 (3)	3.5 (2)
C$_{1a2}$'	0.5011 (7)	−0.3675 (8)	0.4064 (4)	4.6 (2)
C$_{2a3}$'	0.5883 (9)	−0.3740 (9)	0.4646 (3)	5.9 (3)
C$_{1a4}$'	0.6792 (8)	−0.4229 (9)	0.4505 (4)	6.0 (3)
C$_{1a5}$'	0.6830 (8)	−0.4652 (9)	0.3782 (5)	6.5 (3)
C$_{1a6}$'	0.5958 (8)	−0.4587 (8)	0.3200 (3)	5.2 (3)
C$_{2a1}$'	0.1736 (5)	−0.3045 (7)	0.2640 (4)	3.5 (2)
C$_{2a2}$'	0.0938 (8)	−0.4140 (7)	0.2846 (4)	4.8 (3)
C$_{2a3}$'	−0.0464 (7)	−0.4671 (7)	0.2620 (5)	6.3 (3)
C$_{2a4}$'	−0.1068 (6)	−0.4107 (9)	0.2189 (5)	6.5 (3)
C$_{2a5}$'	−0.0270 (8)	−0.3012 (9)	0.1984 (5)	6.7 (3)
C$_{2a6}$'	0.1132 (8)	−0.2481 (6)	0.2209 (4)	5.0 (3)
C$_{1b1}$'	0.9870 (5)	0.1076 (7)	0.2946 (4)	3.2 (2)
C$_{1b2}$'	1.0571 (7)	0.2364 (7)	0.2962 (4)	4.6 (2)
C$_{1b3}$'	1.1977 (7)	0.2939 (6)	0.3111 (5)	6.0 (3)
C$_{1b4}$'	1.2682 (5)	0.2226 (8)	0.3244 (5)	5.4 (3)
C$_{1b5}$'	1.1981 (7)	0.0939 (8)	0.3228 (5)	5.6 (3)
C$_{1b6}$'	1.0575 (7)	0.0364 (8)	0.3080 (4)	5.2 (3)
C$_{2b1}$'	0.6763 (8)	0.1951 (8)	0.2104 (4)	4.0 (2)
C$_{2b2}$'	0.7172 (9)	0.1579 (10)	0.1483 (5)	7.1 (4)
C$_{2b3}$'	0.6509 (12)	0.1533 (11)	0.0788 (4)	9.7 (5)
C$_{2b4}$'	0.5437 (11)	0.1859 (12)	0.0715 (4)	8.7 (4)
C$_{2b5}$'	0.5028 (9)	0.2231 (11)	0.1336 (6)	8.3 (4)
C$_{2b6}$'	0.5691 (9)	0.2277 (9)	0.2031 (5)	6.1 (3)

^{a} The numbers in parentheses are the estimated standard deviations in the last significant digit. ^{b} Atoms are labeled in agreement with Figure 4.
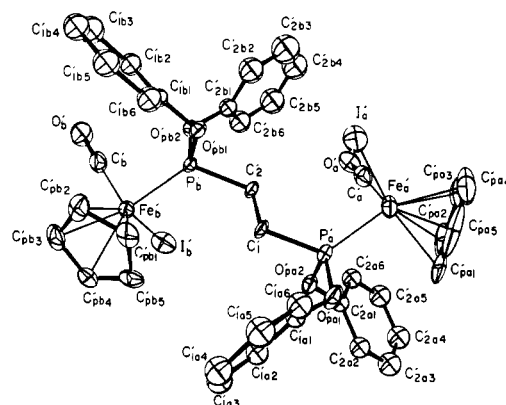

Figure 4. A perspective ORTEP drawing of [η^5-C$_5$H$_5$Fe(CO)I]$_2$-[(PhO)$_2$PC$_2$H$_4$P(OPh)$_2$] (3b) with non-hydrogen atoms represented by thermal vibration ellipsoids drawn to encompass 50% of the electron density. Group atoms are represented by thermal vibration spheres drawn to encompass 30% of the electron density.

bond lengths shows no significant differences.

The relationship of the two iron centers in these dinuclear complexes is of interest. It appears that the overall structure of these diiodiodes is largely determined by intramolecular nonbonded repulsions. In each complex the (η^5-C$_5$H$_5$)Fe(CO)I groups are oriented in a transoid fashion presumably to minimize steric interactions.

With the hopes of gaining some information on the steric interactions within complexes 1 and 3b, the X-ray coordinates are fed into a M-3 macromolecule manipulation system. With a 1-Å C–H bond length and idealized sp^2 and sp^3 hybridization, the coordinates for all hydrogen atoms in 3b are calculated and entered into the file. A graphics display for complex 1 is shown in Figure 5.

The M-3 system has the ability to allow one to manually rotate the graphics display around single bonds (up to six at one time). A false center is placed in the Cp rings to allow rotation around the Fe–Cp linkage. A van der Waals

another within experimental errors. In contrast the (η^5-C$_5$H$_5$)Fe(CO)(P)I groups in 3b show significant differences in geometry about the two iron centers. For instance, I$_a$'Fe$_a$'P$_a$' (90.3 (2)°) is 2.0° larger than its counterpart I$_b$'Fe$_b$'P$_b$' (88.3 (3)°) and P$_a$'Fe$_a$'C$_a$' (93.6 (5)°) is 3.3° greater than P$_b$'Fe$_b$'C$_b$' (90.3 (6)°). However, comparison of the

Table V. Selected Bond Lengths (Å) Involving Non-Hydrogen and Nongroup Atoms in Crystalline
$Me_2Si[\eta^5\text{-}C_5H_4Fe(CO)_2I]_2$ (1) and $[\eta^5\text{-}C_5H_5Fe(CO)I]_2[(PhO)_2PC_2H_4P(OPh)_2]$ (3b)[a]

atom[b] type	length		atom[b] type	length	
	1	3b		1	3b
$Fe_a\text{-}I_a$	2.605 (1)	2.620 (2)	$Fe_b\text{-}I_b$	2.593 (2)	2.601 (2)
$Fe_a\text{-}C_{a1}$[c]	1.770 (8)	1.769 (18)	$Fe_b\text{-}C_{b1}$	1.776 (10)	1.803 (14)
$Fe_a\text{-}C_{a2}$	1.793 (9)		$Fe_b\text{-}C_{b2}$	1.771 (15)	
$Fe_a\text{-}P_a$		2.155 (4)	$Fe_b\text{-}P_b$		2.148 (3)
$Fe_a\text{-}C_{pa1}$	2.121 (7)	2.092 (19)	$Fe_b\text{-}C_{pb1}$	2.117 (6)	2.097 (17)
$Fe_a\text{-}C_{pa2}$	2.080 (8)	2.072 (14)	$Fe_b\text{-}C_{pb2}$	2.134 (8)	2.095 (16)
$Fe_a\text{-}C_{pa3}$	2.085 (9)	2.115 (19)	$Fe_b\text{-}C_{pb3}$	2.097 (8)	2.107 (13)
$Fe_a\text{-}C_{pa4}$	2.097 (8)	2.104 (24)	$Fe_b\text{-}C_{pb4}$	2.076 (8)	2.132 (13)
$Fe_a\text{-}C_{pa5}$	2.119 (7)	2.077 (20)	$Fe_b\text{-}C_{pb5}$	2.078 (8)	2.131 (15)
$Fe_a\text{-}C_{ga}$[d]	1.716	1.720	$Fe_b\text{-}C_{gb}$[d]	1.718	1.719

[a] The numbers in parentheses are the estimated standard deviations in the last significant digit. [b] Atoms are labeled in agreement with Figures 3 and 4. Note for simplification 3b's atoms are not labeled with primes (') in this table. [c] In the case of 3b C_{a1} is equivalent to C_a and C_{b1} to C_b. [d] The symbols C_{ga} and C_{gb} are used to denote the centers of gravity for the five-membered rings whose atoms carry the subscript a and b, respectively.

Table VI. Selected Bond Angles (deg) in Crystalline
$Me_2Si[\eta^5\text{-}C_5H_4Fe(CO)_2I]_2$ (1) and
$[\eta^5\text{-}C_5H_5Fe(CO)I]_2[(PhO)_2PC_2H_4P(OPh)_2]$ (3b)[a]

$I_a Fe_a C_{a1}$[b]	90.0 (3)	$I_b Fe_b C_{b1}$	89.5 (3)
$I_a Fe_a C_{a2}$	91.3 (3)	$I_b Fe_b C_{b2}$	91.6 (5)
$I_a Fe_a C_{ga}$[c]	123.6	$I_b Fe_b C_{gb}$[c]	123.9
$C_{a1} Fe_a C_{a2}$	93.6 (4)	$C_{b1} Fe_b C_{b2}$	92.0 (6)
$C_{a1} Fe_a C_{ga}$	124.7	$C_{b1} Fe_b C_{gb}$	123.9
$C_{a2} Fe_a C_{ga}$	123.3	$C_{b2} Fe_b C_{gb}$	125.8
$I_a' Fe_a' C_a'$	94.3 (5)	$I_b' Fe_b' C_b'$	93.4 (7)
$I_a' Fe_a' P_a'$	90.3 (2)	$I_b' Fe_b' P_b'$	88.3 (3)
$I_a' Fe_a' C_{ga}'$[c]	120.7	$I_b' Fe_b' C_{gb}'$[c]	121.8
$P_a' Fe_a' C_a'$	93.6 (5)	$P_b' Fe_b' C_b'$	90.3 (6)
$C_a' Fe_a' C_{ga}'$	120.6	$C_b' Fe_b' C_{gb}'$	124.1
$P_a' Fe_a' C_{ga}'$	128.6	$P_b' Fe_b' C_{gb}'$	128.5

[a] The numbers in parentheses are the estimated standard deviations in the last significant digit. [b] Atoms are labeled in agreement with Figure 4. [c] The symbols C_{ga} and C_{gb} are used to denote the centers of gravity for the five-membered rings whose atoms carry the subscripts a and b, respectively.
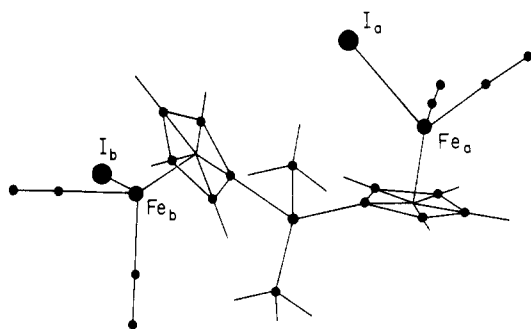

Figure 6. Graphics display of $Me_2Si[\eta^5\text{-}C_5H_4Fe(CO)_2I]_2$ (1) after rotation about the $Fe\text{-}(\eta^5\text{-}C_5H_4)$ axis. The dashed line represents steric interactions when a minimum contact distance of 2.4 Å is employed.

(depending on the direction of rotation) and the methyl hydrogens. This is illustrated in Figure 6. Overall steric interaction within complex 3b is more difficult to assess due to the greater number of possible rotations. Rotation about most of the bonds produces a steric interaction, indicating that this is a fairly "tight" molecule. However, as pointed out earlier, this complex appears to be "looser" than the cyclopentadienyl-bridged system at least as far as the two iron centers are concerned.

Summary

In this work we prepare and characterize several new bridged diiodide complexes. In each complex diastereoisomers are formed and in the cases of 3 and 4 they are easily separated by solubility differences. The ability to separate these isomers will enable us to study each diastereomer's reactivity by using a systematic approach. In addition, these bridged diiodides appear from NMR data and analysis by graphic display to have limited rotational freedom, especially in the cyclopentadienyl-bridged complexes 4 and 5. We are presently trying to obtain more detail about this limited rotational freedom through the synthesis and structural study of other substituted derivatives of 1. Reactivity of these complexes is a subject also under current investigation.

Experimental Section

General Data. All manipulations of complexes and solvents are carried out by using standard Schlenk techniques. Solvents are degassed and purified by distillation under nitrogen from standard drying agents.[10] Spectroscopic measurements utilize

Figure 5. Graphics display of $Me_2Si[\eta^5\text{-}C_5H_4Fe(CO)_2I]_2$ (1) utilizing the atomic coordinates from the molecular structure determination.

interaction between atoms through space is indicated by the appearance of a dashed line in the display. Such a dashed line in the display of these dinuclear complexes could indicate reasonable barriers to rotation around the appropriate single bonds.

The most significant result obtained from this exercise is that rotation about the Si–Cp and Fe–Cp linkages in complex 1 appears to be hindered. For instance with a minimum contact distance of 2.4-Å active, rotation about the Si–Cp bond results in the interaction between the hydrogens on the Cp ring and the hydrogens on the nearest methyl group attached to the silane. When one rotates around the Cp–Fe connection, there is an immediate "bumping" between the carbonyl oxygen or the iodide
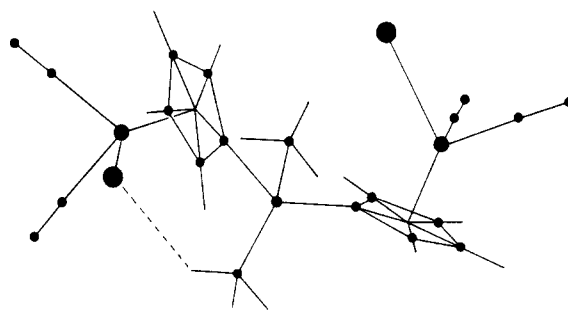
(10) Gordon, A. J.; Ford, R. A. "The Chemist's Companion"; Wiley: New York, 1972.

the following instrumentation: ^{1}H NMR, Varian EM360, Bruker 250FT (at 250 MHz); ^{13}C NMR, Bruker 250FT (at 62.9 MHz); ^{31}P NMR, Bruker 250FT (at 101.3 MHz); IR, Perkin-Elmer 281B. NMR chemical shifts are reported in δ vs. Me$_4$Si assigning the CDCl$_3$ resonance in ^{13}C spectra to be at 77.00 ppm, and in ^{31}P spectra an external reference of H$_3$PO$_4$ is assigned 0.00 ppm. Carbon-13 spectra are run with ^{1}H decoupling and resonances may be assumed to be singlets unless multiplicity is specified. The phenyl carbon resonances of complexes **2**, **3**, and **5** are assigned following Stewart et al.[11] The Me$_2$Si[η^5-C$_5$H$_4$Fe(CO)$_2$I]$_2$ is prepared by the method of Wegner et al.[12] The Cl$_2$PCH$_2$C-H$_2$PCl$_2$ and cyclopentadienyliron dicarbonyl dimer are purchased from Strem Chemical and used as received.

1,2-Bis(diphenyl phosphito)ethane. To a chilled (0 °C) benzene (200 mL) solution containing C$_6$H$_5$OH (16.2 g, 172 mmol) and Et$_3$N (17.4 g, 172 mmol) is added dropwise a solution of Cl$_2$PCH$_2$CH$_2$PCl$_2$ (10.0 g, 43 mmol) and benzene (50 mL). The resulting slurry is warmed to room temperature and stirred for an additional hour. This mixture is then filtered to remove the precipitated Et$_3$N·HCl. The filtrate is concentrated to 75 mL and placed on a chromatography column (alumina III, 3 × 10 cm). Elution with benzene collecting the initial 300 mL followed by evaporation of solvent yields white crystals (16.0 g, 80%): ^{1}H NMR (CDCl$_3$) δ 7.20 (20, m, C$_6$H$_5$), 2.18 (4, t, J = 8.0 Hz, C$_2$H$_4$); ^{13}C NMR (CDCl$_3$) δ 155.46 (O-bound phenyl carbons), 129.65 (meta phenyl carbons), 120.02 (ortho phenyl carbons), 26.92 (t, J = 30 Hz, C$_2$H$_4$); ^{31}P NMR (CDCl$_3$) δ 179.88.

[η^5-C$_5$H$_5$Fe(CO)]$_2$[(PhO)$_2$PC$_2$H$_4$P(OPh)$_2$] (2). A benzene (50 mL) solution containing (PhO)$_2$PC$_2$H$_4$P(OPh)$_2$ (1.00 g, 2.2 mmol) and [η^5-C$_5$H$_5$Fe(CO)$_2$]$_2$ (0.80 g, 2.2 mmol) is refluxed for 8 h. The solvent is then removed and the residue treated with 25 mL of CH$_3$CN and vigorously agitated. This mixture is filtered and the precipitate extracted with benzene (15 mL) and placed on a chromatography column (alumina III, 3 × 20 cm). Elution with benzene developes an initial blue-green band that separates far ahead of a red-brown band (not isolated) that remained on the top portion of the column. The solvent is evaporated from the blue-green band to yield blue crystals (0.60 g, 36%): ^{1}H NMR (CDCl$_3$) δ 7.40 (20, m, C$_6$H$_5$), 4.27 (10, s, C$_5$H$_5$), 1.60 (4, d, J = 8 Hz, C$_2$H$_4$). IR (cm^{-1} in CH$_2$Cl$_2$) ν(CO) 1703; ^{13}C NMR (CDCl$_3$) δ 136.98 (d, J = 39.8 Hz, O-bound phenyl carbons), 132.74 (meta phenyl carbons), 129.41 (para phenyl carbons), 128.12 (d, J = 18.6 Hz, ortho phenyl carbons), 86.33 (C$_5$H$_5$), 22.37 (d, J = 26.6 Hz, C$_2$H$_4$); ^{31}P NMR (CDCl$_3$) δ 223.03. Anal. Calcd for C$_{38}$H$_{34}$Fe$_2$O$_6$P$_2$: C, 60.03; H, 4.51. Found: C, 59.89; H, 4.59.

[η^5-C$_5$H$_5$Fe(CO)I]$_2$[(PhO)$_2$PC$_2$H$_4$P(OPh)$_2$] (3). A CHCl$_3$ (25 mL) solution of [η^5-C$_5$H$_5$Fe(CO)]$_2$[(PhO)$_2$PC$_2$H$_4$P(OPh)$_2$] (0.50 g, 0.7 mmol) and iodine (0.50 g, 2.0 mmol) is stirred for 10 min. The CHCl$_3$ solution is first washed with 10% aqueous sodium thiosulfate (25 mL) and then dried over anhydrous magnesium sulfate. The solution is filtered and the solvent evaporated to yield a mixture of two diastereoisomers (0.68 g, 100%): ^{1}H NMR (CDCl$_3$) δ 7.33 (20, m, C$_6$H$_5$), 4.33 (**3b**), 4.22 (**3a**), (s, s, 10, C$_5$H$_5$), 3.00 (b s, 4, C$_2$H$_4$); IR (cm^{-1} in CH$_2$Cl$_2$) ν(CO) 1977; ^{13}C NMR (CDCl$_3$) δ 218.15 (**3b**) (t, J = 18 Hz, CO), 153.10 (d, J = 30 Hz, O-bound phenyl carbons), 129.84 (d, J = 8.7 Hz, meta phenyl carbons), 124.89 (d, J = 17.4 Hz, para phenyl carbons), 121.34 (d, J = 24.0 Hz, ortho phenyl carbons), 81.50 (**3a**), 81.39 (**3b**) (C$_5$H$_5$), 33.69 (**3b**), 33.11 (**3a**) (t, t, J = 18 Hz, C$_2$H$_4$); ^{31}P NMR (acetone-d_6) δ 228.46. Anal. Calcd for C$_{38}$H$_{34}$Fe$_2$I$_2$O$_6$P$_2$: C, 45.01; H, 3.38; I, 25.03. Found: C, 44.90; C, 3.41; I, 25.09.

Separation of Diastereoisomers 3a and 3b. A mixture of **3a** and **3b** (0.68 g, 0.7 mmol) is stirred in benzene (5 mL) for 15 min. The solution is filtered and the light green precipitate washed with benzene (2 mL). The solvent is then evaporated from the filtrate to yield brown crystals (0.30 g, 44%) that are later recrystallized and found by a X-ray diffraction study to be the *d,l* isomer **3b**. The light green precipitate is identified as the meso isomer **3a** by spectroscopic means.

Me$_2$Si[η^5-C$_5$H$_4$Fe(CO)(PPh$_3$)I]$_2$ (4). A brown benzene (50 mL) solution containing Me$_2$Si[η^5-C$_5$H$_4$Fe(CO)$_2$I]$_2$ (1) (1.00 g, 1.5

mmol) and PPh$_3$ (1.00 g, 3.7 mmol) is irradiated (450-W medium-pressure Hg lamp) in a Pyrex Schlenk flask for 3 h. The resulting green solution is filtered and the solvent evaporated from the filtrate to give a dark green oil. The oil is then dissolved in CH$_3$CN (30 mL) and placed at -25 °C for 2 h. The light green precipitate that forms is collected, washed with CH$_3$CN (2 × 15 mL), and air-dried (1.40 g, 82%). The filtrate is concentrated and then filtered and the solid washed with CH$_3$CN to afford an additional 0.15 g (91% combined yield): IR (cm^{-1} in CH$_2$Cl$_2$) ν(CO) 1952. The diastereoisomers **4a** and **4b** are separated by solubility differences involving repeated extractions and filtrations with CH$_2$Cl$_2$. **4a:** ^{1}H NMR (CDCl$_3$) δ 7.39 (m, 30, C$_6$H$_5$), 5.61 (m, 2, C$_5$H$_4$), 4.61 (m, 2, C$_5$H$_4$), 4.00 (s, 2, C$_5$H$_4$), 3.73 (m, 2, C$_5$H$_4$), 0.81 (s, s, 6, SiCH$_3$). **4b:** ^{1}H NMR (CDCl$_3$) δ 7.39 (m, 30, C$_6$H$_5$), 5.49 (m, 2, C$_5$H$_4$), 4.58 (m, 2, C$_5$H$_4$), 4.00 (s, 2, C$_5$H$_4$), 3.73 (m, 2, C$_5$H$_4$), 0.93 (s, 6, SiCH$_3$). **4a:** ^{13}C NMR (CDCl$_3$) δ 221.40 (d, J = 33 Hz, CO), 136.45–128.07 (C$_6$H$_5$), 103.78, 87.93, 84.22, 79.91 (C$_5$H$_4$), -0.13, -1.13 (SiCH$_3$). **4b:** ^{13}C NMR (CDCl$_3$) δ 221.56 (d, J = 33 Hz, CO), 136.45–128.07 (C$_6$H$_5$), 103.78, 87.93, 84.30, 79.80 (C$_5$H$_4$), -0.74 (SiCH$_3$). ^{31}P NMR (CDCl$_3$): δ 69.57. Anal. Calcd for C$_{50}$H$_{44}$Fe$_2$I$_2$O$_2$P$_2$Si: C, 53.13; H, 3.92; I, 22.45. Found: C, 52.97; H, 3.97; I, 22.39.

Me$_2$Si[C$_5$H$_4$Fe(CO)[P(OPh)$_3$]I]$_2$ (5). Me$_2$Si[(η^5-C$_5$H$_4$)Fe(CO)$_2$I]$_2$ (1) (1.00 g, 1.5 mmol), P(OPh)$_3$ (0.94 g, 3.0 mmol), and benzene (50 mL) are placed in a Schlenk tube and irradiated for 3 h. The resulting brown solution is filtered and the solvent removed to yield a brown oil (1.70 g, 92%). Medium-pressure chromatography on silica gel (LiChroprep Si 60) with benzene gives a single brown band. The band is collected and the solvent removed to afford analytically pure **5** as a mixture of diastereoisomers: ^{1}H NMR (CDCl$_3$) δ 7.36 (m, 30, C$_6$H$_5$), 5.04, 5.00 (s, s, 2, C$_5$H$_4$), 4.35 (s, 2, C$_5$H$_4$), 3.98 (s, 2, C$_5$H$_4$), 3.14, 3.12 (s, s, 2, C$_5$H$_4$), 0.64, 0.62, 0.58 (s, s, s, 6, SiCH$_3$); ^{13}C NMR (CDCl$_3$) δ 218.64, 218.53, 217.91, 217.80 (CO), 151.48 (d, J = 9.1 Hz, O-bound phenyl carbons), 129.65 (meta phenyl carbons), 121.52 (d, J = 3.5 Hz, ortho phenyl carbons), 99.61, 83.77, 81.86, 81.57, 79.31, 79.01 (C$_5$H$_5$), -1.05, -1.52, -1.76 (SiCH$_3$); ^{31}P NMR (CDCl$_3$) δ 151.35, 151.39. Anal. Calcd for C$_{50}$H$_{44}$Fe$_2$I$_2$O$_8$P$_2$Si: C, 48.89; H, 3.61; I, 20.66. Found: C, 49.01; H, 3.65; I, 20.53.

Crystallographic Summary for [η^5-C$_5$H$_5$Fe(CO)I]$_2$-[(PhO)$_2$PC$_2$H$_4$P(OPh)$_2$] (3b). Single crystals of **3b** are obtained by slow diffusion of petroleum ether (30–60) into a CHCl$_3$ solution. Pertinent crystal data and all the details of data collection are listed in Table I.[13] Accurate cell parameters are obtained by a least-squares analysis of 25 carefully centered reflections chosen from diverse regions of reciprocal space.

Intensity data are collected with use of the 2θ–θ scan method on a Syntex P2$_1$ diffractometer using Mo K$\bar\alpha$ radiation (λ = 0.710 73 Å). Intensity data are reduced to relative squared amplitudes, $|F_0{}^2|$, by means of standard Lorentz and polarization corrections. No correction for absorption is deemed necessary because of the modest size of the crystal and the small linear absorption coefficient. Of the 7554 reflections collected 4916 are considered observed by applying the rejection criterion $I < 3\sigma(I)$ where $\sigma(I)$ is the standard deviation in intensity computed from $\sigma^2(I) = C_t + B/k^2$ where C_t is the total count for scanning, k is the ratio of scanning time to total background time (in this case k = 1.0), and B is the total background count. The three standard reflections monitored every 100 reflections collected show no significant changes in intensity throughout the course of data collection.

The positions of the heaviest atoms (I, Fe, P) are found with the aid of the program MULTAN utilizing the most probable set. The positions of all but two non-hydrogen atoms are located from a three-dimensional electron density difference map. The remaining two non-hydrogen atoms are placed in their calculated positions and then refined. The structure is initially refined by

(11) Stewart, R. P.; Isbrandt, L. R.; Benedict, J. J.; Palmer, J. G. *J. Am. Chem. Soc.* **1976**, *98*, 3245.

(12) Wegner, P. A.; Kiester, R. P.; Speckman, D.; Sterling, G. Pacicfic Conference on Chemistry and Spectroscopy, Anaheim, CA, Oct 1977.

(13) All calculations were preformed on a CDC CYBER-175 computer at the University of Arizona computer center. The programs employed in the structure determination were FORDAP (Fourier summation program, A. Zalkin), Iber's NUCLS (Structure factor calculations and full-matrix least-squares refinement, itself a modification of ORFLS by W. R. Busing, K. O. Martin, and H. A. Levy), ORFEE (locally modified, calculations of bond distances, angles, and least-squares planes with standard deviations by Busing, Martin, and Levy), and ORTEP (thermal ellipsoid drawing program, C. K. Johnson).

full-matrix least-squares techniques with isotropic thermal parameters for all non-hydrogen atoms. The four phenyl rings are then defined as rigid groups, and the model is blocked into two molecular fragments. Each fragment is refined by counter-weighted full-matrix least-squares methods with anomalous dispersion corrections (I, Fe, P), anisotropic thermal parameters for nongroup and non-hydrogen atoms and isotropic thermal parameters for group atoms to give final values of $R_1 = 0.066$ and $R_2 = 0.087$, where $R_1 = \sum ||F_o| - |F_c||/\sum |F_o|$ and $R_2 = [\sum w(|F_o| - |F_c|)^2/\sum w|F_o|^2]^{1/2}$.

Crystallographic Summary for $Me_2I[\eta^5\text{-}C_5H_4Fe(CO)_2I]_2$ (1). X-ray quality crystals of 1 are obtained by slow diffusion of petroleum ether (30–60) into a CHCl$_3$ solution containing 1. Pertinent crystal data and all the details of data collection are listed in Table I.[14] Least-squares refinement of the cell dimensions are based on 15 computer-centered reflections. Intensity data are collected with use of the ω scans on a computer-controlled four-circle Nicolet autodiffractometer using Mo K$\bar{\alpha}$ radiation (λ = 0.710 73 Å). The intensity data are corrected empirically for absorption effects by using psi scans for five reflections having 2θ between 10.35° and 30.37° and are then reduced to relative squared amplitudes, $|F_o|^2$, by means of standard Lorentz and polarization corrections. Of the 5707 relfections collected 3614 are considered observed by applying the same rejection criterion as for 3b (see above). Six standard reflections monitored every 300 reflections collected show no significant variation in intensity during the course of data collection.

The atomic positions of all non-hydrogen atoms are located by use of direct methods program MULTAN. The hydrogen atomic positions are found by standard difference Fourier techniques or generated by using idealized sp^2 or sp^3 hybridization and a C–H bond length of 0.95 Å. The structure is initially refined by full-matrix least-squares procedures with minimization of the function $\sum w(|F_o| - |F_c|)^2$ (where $w = 1/\sigma_F{}^2$). The final cycles of unit-weighted full-matrix least-squares refinement, which employ anisotropic thermal parameters for non-hydrogen atoms, isotropic thermal parameters for hydrogen atoms, and anomalous dispersion corrections (I, Fe, Si) converge to final values of 0.049 and 0.060 for R_1 and R_2, respectively.

Supplementary Material Available: Tables of crystallographic reports, thermal parameters, hydrogen atomic coordinates, complete bond legnths and angles, and structure factors for 1 and 3b (64 pages). Ordering information is given on any current masthead page.

---

(14) All calculations with the absorption-corrected intensity data were preformed on a Data General Eclipse S-200 computer utilizing versions of the Nicolet E-XTL interactive crystallographic software package as modified at Crystalytics Co.

Organotransition-Metal Metallacarboranes. 1. Iron Complexes Derived from $C_8H_8{}^{2-}$. Structure of $(\eta^6\text{-}C_8H_{10})Fe[2,3\text{-}(CH_3)_2C_2B_4H_4]$[1]

Richard B. Maynard, Robert G. Swisher, and Russell N. Grimes*

Department of Chemistry, University of Virginia, Charlottesville, Virginia 22901

The reaction of the $C_8H_8{}^{2-}$ (cyclooctatetraenide) dianion with FeCl$_2$ and the $(C_2H_5)_2C_2B_4H_5{}^-$ carborane ion in THF produces a 1,3,5-cyclooctatriene complex, $(\eta^6\text{-}C_8H_{10})Fe[(C_2H_5)_2C_2B_4H_4]$ (I), in 50% yield as a red, air-stable solid, together with two minor products, $(\eta^6\text{-}C_6H_6)Fe(C_2H_5)_2C_2B_4H_4$ and $(C_{16}H_{18})Fe(C_2H_5)_2C_2B_4H_4$. Compound I has been characterized from IR and mass spectra, ^{11}B, ^{1}H, and ^{13}C high-resolution FT NMR, and an X-ray diffraction study of its C,C'-dimethyl homologue and contains a 1,3,5-cyclooctatriene ligand. Compound I is the first metallacarborane complex of a C$_8$-ring ligand to be structurally characterized by X-ray diffraction and is apparently only the third η^6-cyclooctatriene–transition-metal complex whose crystal structure has been determined. The metallacarborane portion of the molecule consists of a seven-vertex FeC$_2$B$_4$ pentagonal-bipyramidal cage similar to previously reported MC$_2$B$_4$ systems. The geometry of the η^6-1,3,5-C$_8$H$_{10}$ ligand closely resembles that of the previously reported complexes $(\eta^6\text{-}C_8H_{10})Fe(\eta^4\text{-}C_8H_{10})$ and $(\eta^6\text{-}C_8H_{10})Cr(CO)_3$; the six metal-coordinated carbon atoms are nearly, but not quite, coplanar, and the two noncoordinated (methylene) ring carbons are bent well out of the plane, away from the metal. The NMR data are consistent with a nonfluxional structure. Crystal data: $(C_8H_{10})Fe[(CH_3)_2C_2B_4H_4]$, $M_r = 264$, space group $C2/c$, $Z = 8$, $a = 31.403$ (7) Å, $b = 7.098$ (3) Å, $c = 12.348$ (7) Å, $\beta = 100.61$ (3)°, $V = 2706$ Å^3, $R = 0.048$ for 1805 reflections having $F_o{}^2 > 3\sigma(F_o{}^2)$.

Introduction

Metallacarboranes bearing exopolyhedral hydrocarbon ligands form a large family of well-characterized compounds,[2] but the hydrocarbon in nearly all cases is cyclo-pentadienide, $C_5H_5{}^-$. Its role is usually passive, in that it serves as a "capping" ligand, completing the valence coordination of the metal and stabilizing the complex. The relative inertness and bulk of the tightly coordinated $C_5H_5{}^-$

---

(1) Reported in part at the 182nd National Meeting of the American Chemical Society, New York, Aug 1981; American Chemical Society: Washington, DC, 1981; Abstract INOR-11.

(2) Grimes, R. N. In "Comprehensive Organometallic Chemistry"; Wilkinson, G., Stone, F. G. A., Abel, E., Eds.; Pergamon Press: Oxford, 1982; Volume 1, Chapter 5.5, pp 459–542.

full-matrix least-squares techniques with isotropic thermal parameters for all non-hydrogen atoms. The four phenyl rings are then defined as rigid groups, and the model is blocked into two molecular fragments. Each fragment is refined by counter-weighted full-matrix least-squares methods with anomalous dispersion corrections (I, Fe, P), anisotropic thermal parameters for nongroup and non-hydrogen atoms and isotropic thermal parameters for group atoms to give final values of $R_1 = 0.066$ and $R_2 = 0.087$, where $R_1 = \sum ||F_o| - |F_c||/\sum |F_o|$ and $R_2 = [\sum w(|F_o| - |F_c|)^2/\sum w|F_o|^2]^{1/2}$.

Crystallographic Summary for $Me_2I[\eta^5\text{-}C_5H_4Fe(CO)_2I]_2$ (1). X-ray quality crystals of 1 are obtained by slow diffusion of petroleum ether (30–60) into a $CHCl_3$ solution containing 1. Pertinent crystal data and all the details of data collection are listed in Table I.[14] Least-squares refinement of the cell dimensions are based on 15 computer-centered reflections. Intensity data are collected with use of the ω scans on a computer-controlled four-circle Nicolet autodiffractometer using Mo K$\bar{\alpha}$ radiation (λ = 0.710 73 Å). The intensity data are corrected empirically for absorption effects by using psi scans for five reflections having 2θ between 10.35° and 30.37° and are then reduced to relative squared amplitudes, $|F_o|^2$, by means of standard Lorentz and polarization corrections. Of the 5707 relfections collected 3614 are considered observed by applying the same rejection criterion as for **3b** (see above). Six standard reflections monitored every 300 reflections collected show no significant variation in intensity during the course of data collection.

The atomic positions of all non-hydrogen atoms are located by use of direct methods program MULTAN. The hydrogen atomic positions are found by standard difference Fourier techniques or generated by using idealized sp^2 or sp^3 hybridization and a C–H bond length of 0.95 Å. The structure is initially refined by full-matrix least-squares procedures with minimization of the function $\sum w(|F_o| - |F_c|)^2$ (where $w = 1/\sigma_F^2$). The final cycles of unit-weighted full-matrix least-squares refinement, which employ anisotropic thermal parameters for non-hydrogen atoms, isotropic thermal parameters for hydrogen atoms, and anomalous dispersion corrections (I, Fe, Si) converge to final values of 0.049 and 0.060 for R_1 and R_2, respectively.

Registry No. 1, 42830-83-1; 2, 84521-28-8; **3a**, 84521-29-9; **3b**, 84581-03-3; **4a**, 84581-04-4; **4b**, 84581-05-5; 5 (isomer 1), 84581-06-6; 5 (isomer 2), 84581-07-7; $(PhO)_2PC_2H_4P(OPh)_2$, 78819-34-8; $[\eta^5\text{-}C_5H_5Fe(CO)_2]_2$, 38117-54-3; PPh_3, 603-35-0; $P(OPh)_3$, 101-02-0; C_6H_5OH, 108-95-2; $Cl_2PCH_2CH_2PCl_2$, 28240-69-9; iodine, 7553-56-2.

Supplementary Material Available: Tables of crystallographic reports, thermal parameters, hydrogen atomic coordinates, complete bond legnths and angles, and structure factors for 1 and **3b** (64 pages). Ordering information is given on any current masthead page.

(14) All calculations with the absorption-corrected intensity data were preformed on a Data General Eclipse S-200 computer utilizing versions of the Nicolet E-XTL interactive crystallographic software package as modified at Crystalytics Co.

Organotransition-Metal Metallacarboranes. 1. Iron Complexes Derived from $C_8H_8^{2-}$. Structure of $(\eta^6\text{-}C_8H_{10})Fe[2,3\text{-}(CH_3)_2C_2B_4H_4]^1$

Richard B. Maynard, Robert G. Swisher, and Russell N. Grimes*

Department of Chemistry, University of Virginia, Charlottesville, Virginia 22901

The reaction of the $C_8H_8^{2-}$ (cyclooctatetraenide) dianion with $FeCl_2$ and the $(C_2H_5)_2C_2B_4H_5^-$ carborane ion in THF produces a 1,3,5-cyclooctatriene complex, $(\eta^6\text{-}C_8H_{10})Fe[(C_2H_5)_2C_2B_4H_4]$ (I), in 50% yield as a red, air-stable solid, together with two minor products, $(\eta^6\text{-}C_6H_6)Fe(C_2H_5)_2C_2B_4H_4$ and $(C_{16}H_{18})Fe(C_2\text{-}H_5)_2C_2B_4H_4$. Compound I has been characterized from IR and mass spectra, ^{11}B, ^1H, and ^{13}C high-resolution FT NMR, and an X-ray diffraction study of its C,C'-dimethyl homologue and contains a 1,3,5-cyclooctatriene ligand. Compound I is the first metallacarborane complex of a C_8-ring ligand to be structurally characterized by X-ray diffraction and is apparently only the third η^6-cyclooctatriene–transition-metal complex whose crystal structure has been determined. The metallacarborane portion of the molecule consists of a seven-vertex FeC_2B_4 pentagonal-bipyramidal cage similar to previously reported MC_2B_4 systems. The geometry of the $\eta^6\text{-}1,3,5\text{-}C_8H_{10}$ ligand closely resembles that of the previously reported complexes $(\eta^6\text{-}C_8H_{10})Fe(\eta^4\text{-}C_8H_{10})$ and $(\eta^6\text{-}C_8H_{10})Cr(CO)_3$; the six metal-coordinated carbon atoms are nearly, but not quite, coplanar, and the two noncoordinated (methylene) ring carbons are bent well out of the plane, away from the metal. The NMR data are consistent with a nonfluxional structure. Crystal data: $(C_8H_{10})Fe[(CH_3)_2C_2B_4H_4]$, M_r = 264, space group $C2/c$, Z = 8, a = 31.403 (7) Å, b = 7.098 (3) Å, c = 12.348 (7) Å, β = 100.61 (3)°, V = 2706 Å^3, R = 0.048 for 1805 reflections having $F_o^2 > 3\sigma(F_o^2)$.

Introduction

Metallacarboranes bearing exopolyhedral hydrocarbon ligands form a large family of well-characterized compounds,[2] but the hydrocarbon in nearly all cases is cyclo-

pentadienide, $C_5H_5^-$. Its role is usually passive, in that it serves as a "capping" ligand, completing the valence coordination of the metal and stabilizing the complex. The relative inertness and bulk of the tightly coordinated $C_5H_5^-$

(1) Reported in part at the 182nd National Meeting of the American Chemical Society, New York, Aug 1981; American Chemical Society: Washington, DC, 1981; Abstract INOR-11.

(2) Grimes, R. N. In "Comprehensive Organometallic Chemistry"; Wilkinson, G., Stone, F. G. A., Abel, E., Eds.; Pergamon Press: Oxford, 1982; Volume 1, Chapter 5.5, pp 459–542.

Table I. 360-MHz ¹H FT NMR Data (C_6D_6 Solution)

compd	δ relative to $Si(CH_3)_4$,[b]	relative area
$(\eta^6\text{-}C_8H_{10})Fe[(C_2H_5)_2C_2B_4H_4]$ (I)[a]	5.56 m [H(3,4)], 5.16 dd [H(2,5)], 4.68 m [H(1,6)], 1.95 m (CH_2), 1.72 m (CH_2), 1.68 m [H(7,8), endo], 1.06 t (CH_3), -0.20 m [H(7,8), exo]	2, 2, 2, 2, 2, 2, 6, 2
$(\eta^6\text{-}C_6H_6)Fe[(C_2H_5)_2C_2B_4H_4]$ (II)	5.92 s (C_6H_6), 3.10 m (CH_2), 2.76 m (CH_2), 1.62 t (CH_3)	6, 2, 2, 6
$(C_{16}H_{18})Fe[(C_2H_5)_2C_2B_4H_4]$ (III)	6.10 d, 5.22 t, 5.07 m, 4.67 q, 4.01 m, 2.78 m, 2.02 m (C_2H_5), 1.83 m (C_2H_5), 1.68 m (C_2H_5), 1.22 q, 1.07 m (C_2H_5), 0.90 m, 0.27 m, -2.87 m	1, 1, 2, 2, 1, 1, 1, 2, 1, 2, 6, 2, 1, 1

[a] Acetone-d_6 solution.   [b] Legend: m = multiplet, d = doublet, t = triplet, q = quadruplet, dd = doublet of doublets.

Table II. ¹³C FT NMR Data (C_6D_6 Solution)[a]

compd	δ [relative to $Si(CH_3)_4$]
$(\eta^6\text{-}C_8H_{10})Fe[(C_2H_5)_2C_2B_4H_4]$ (I)	100.37 d [C(3,4)], 91.59 d [C(2,5)], 86.40 d [C(1,6)], 32.91 t [C(7,8)], 22.81 t [C_2H_5], 14.76 q [C_2H_5]
$(\eta^6\text{-}C_6H_6)Fe[(C_2H_5)_2C_2B_4H_4]$ (II)	93 [carborane C],[b] 83.91 d [C_6H_6], 24.82 t [CH_2], 15.24 q [CH_3]
$(C_{16}H_{18})Fe[(C_2H_5)_2C_2B_4H_4]$ (III)	105.79 d, 95.98 d, 93.22 d, 88.90 d, 87.75 d, 84.10 d, 77.54 d, 59.81 d, 26.61 t

[a] Obtained at 90.80 MHz.   [b] Broad, weak singlet.

group tend to protect the metal from attack, so that such complexes are usually poor candidates for homogenous catalysts or catalyst precursors. Consequently, efforts to develop metallacarborane catalysts have centered on complexes with more easily displaceable ligands such as phosphines.[2,3]

Since arene and larger cyclic hydrocarbon ligands in transition-metal complexes are often more labile than $C_5H_5^-$, we have begun a systematic examination of the synthesis and chemistry of (C_nH_m)metal(carborane) complexes where $n \geq 6$, with the objective of preparing species having displaceable hydrocarbon ligands and relatively active metal centers. Our chosen carborane ligand, pyramidal $R_2C_2B_4H_4^{2-}$, is readily accessible[2,4] and tightly binds to metal ions, forming stable seven-vertex MC_2B_4 polyhedral cages on which metal-centered reactions can be conducted without disruption of the cage framework.

Several metallacarboranes having six- or eight-membered cyclic hydrocarbon ligands have been reported previously, in which the organic group is $C_8H_8^{2-}$ (cyclooctatetraenide),[5] 1,5-C_8H_{12} (cyclooctadiene),[6] C_6H_6,[7] 1,3,5-$C_6(CH_3)_3H_3$,[7b] $CH_3C_6H_5$,[7] $C_6(CH_3)_6$,[7b] xylene,[7a] or $C_{10}H_8$ (naphthalene).[7a,8] Of these, X-ray structure determinations have been reported only for $[C_6(CH_3)_3H_3]$-$Fe(C_2B_9H_{11})$,[7b] ($C_6H_5CH_3$)$Fe[(CH_3)_2C_2B_9H_9]$,[7a] and (C_6-H_5CH_3)$Fe[(C_2H_5)_2C_2B_9H_4]$.[9] In this article we report the reaction of the $C_8H_8^{2-}$ ion with $(C_2H_5)_2C_2B_4H_5^-$ and $FeCl_2$ and the structural characterization of a (1,3,5-cyclooctatriene)iron carborane complex $(\eta^6\text{-}C_8H_{10})Fe$-$[(C_2H_5)_2C_2B_4H_4]$. The following paper[10] describes the

conversion of the latter species to several (arene)iron(carborane) complexes and X-ray crystallographic studies on three prototype compounds.

Results

Reaction of $FeCl_2$, $(C_2H_5)_2C_2B_4H_5^-$, and $C_8H_8^{2-}$. In a procedure designed to minimize formation of the bis-(carborane)iron complex[11] and promote the desired mixed-ligand species, the three reagents are combined in a ~1:1:1 mole ratio in cold THF and subsequently warmed to room temperature. Chromatography on silica gel in air gives one major characterizable product, red (η^6-C_8H_{10})-$Fe[(C_2H_5)_2C_2B_4H_4]$ (I) that can be isolated as an air-stable crystalline solid in 50% yield. Compound I has been fully characterized from its high-resolution ¹H, ¹³C, and ¹¹B FT NMR spectra, IR and mass spectra, and an X-ray diffraction study of its C,C'-dimethyl homologue, (η^6-C_8H_{10})$Fe[(CH_3)_2C_2B_4H_4]$ (IA).

A minor product, isolated only in trace amount, has been identified as an η^6-benzene complex, (C_6H_6)$Fe[(C_2H_5)_2$-$C_2B_4H_4]$ (II). This compound has subsequently been produced in much higher yield via displacement of the C_8H_{10} ligand in I by benzene over $AlCl_3$ and has been structurally characterized from spectroscopic and X-ray data (see following paper).[10] The formation of II in the $C_8H_8^{2-}/FeCl_2$/carborane reaction appeared to us unlikely, and we at first assumed that this compound formed during chromatography of the product mixture, in which benzene was employed as an eluent. Remarkably, however, it was discovered that II is obtained even when benzene is entirely excluded from the reaction and workup. Moreover, addition of benzene to the reaction mixture does not increase the yield of II.

Table III. 115.5-MHz ¹¹B FT NMR Data

compd	solvent	δ (J, Hz)[a]	rel area
I	$CDCl_3$	10.65 (141), 6.22 (160), 3.10 (149)	1, 1, 2
II	C_6D_6	12.47,[b] 6.61 (140), 3.53[b]	1, 1, 2
II	$(CD_3)_2CO$	6.21 (158), 4.62 (158), 1.14 (134)	1, 1, 2
III	C_6D_6	12.54,[b] 6.56,[b] 3.23[b]	1, 1, 2

[a] $BF_3 \cdot O(C_2H_5)_2$ shift is 0; positive shifts downfield.   [b] J not measurable.

(3) (a) Paxson, T. E.; Hawthorne, M. F. *J. Am. Chem. Soc.* **1974**, *96*, 4674. (b) Delaney, M. S.; Knobler, C. B.; Hawthorne, M. F. *Inorg. Chem.* **1981**, *20*, 1341 and references therein. (c) Grimes, R. N. In "Metal Interactions with Boron Clusters", Grimes, R. N., Ed.; Plenum Press: New York, 1982, Chapter 7, and references therein.

(4) (a) Maynard, R. B.; Borodinsky, L.; Grimes, R. N. *Inorg. Synth.*, in press. (b) Hosmane, N. S.; Grimes, R. N. *Inorg. Chem.* **1979**, *18*, 3294.

(5) Salentine, C. G.; Hawthorne, M. F. *Inorg. Chem.* **1976**, *15*, 2872.

(6) Green, M.; Spencer, J. L.; Stone, F. G. A.; Welch, A. J. *J. Chem. Soc., Dalton Trans.* **1975**, 179.

(7) (a) Garcia, M. P.; Green, M.; Stone, F. G. A.; Somerville, R. G.; Welch, A. J. *J. Chem. Soc., Chem. Commun.* **1981**, 871. (b) Hanusa, T. P.; Huffman, J. C.; Todd, L. J. *Polyhedron* **1982**, *1*, 77.

(8) Salentine, C. G.; Hawthorne, M. F. *J. Am. Chem. Soc.* **1975**, *97*, 6382.

(9) Sneddon, L. G., Workshop on Main-Group Chemistry, Keystone, Colorado, June, 1982; Sneddon, L. G., private communication. Micciche, R. P.; Sneddon, L. G. *Organometallics*, in press.

(10) Swisher, R. G.; Sinn, E.; Grimes, R. N., following article in this issue.

(11) Maxwell, W. M.; Miller, V. R.; Grimes, R. N. *Inorg. Chem.* **1976**, *15*, 1343.

Table IV. Infrared Absorptions (cm⁻¹)ᵃ

I[b]   3035 w, 3005 w, 2980 s, 2945 s, 2890 m, 2850 m, 2560 s, 2530 vs, 1504 w, 1452 s, 1440 m, 1410 w, 1380 m,
        1347 m, 1308 m, 1290 m, 1240 w, 1220 w, 1190 w, 1160 w, 1065 m, 1035 w, 980 w, 950 w, 930 w, 901 w,
        888 m, 872 m, 852 m, 836 m, 810 w, 798 w, 735 m, 720 m, 618 m, 490 w, 465 m, 408 m
II[b]   3090 w, 2980 vs, 2940 s, 2890 m, 2530 vvs, 1650 w, 1450 vs, 1370 m, 1270 w, 1155 w, 1100 w, 1065 w,
        1015 w, 985 w, 965 w, 895 sh, 878 s, 820 s, 735 m, 700 m, 670 w, 605 m, br, 490 m, 420 s
III[c] 3020 w, 3010 s, 2978 vs, 2940 vs, 2880 m, 2650 w, 1450 s, 1380 m, 1345 w, 1270 m, 1220 m, 1200 m,
        1065 m, 965 m, 915 m, 875 s, 840 m, 825 m, 800 w, br, 660 m

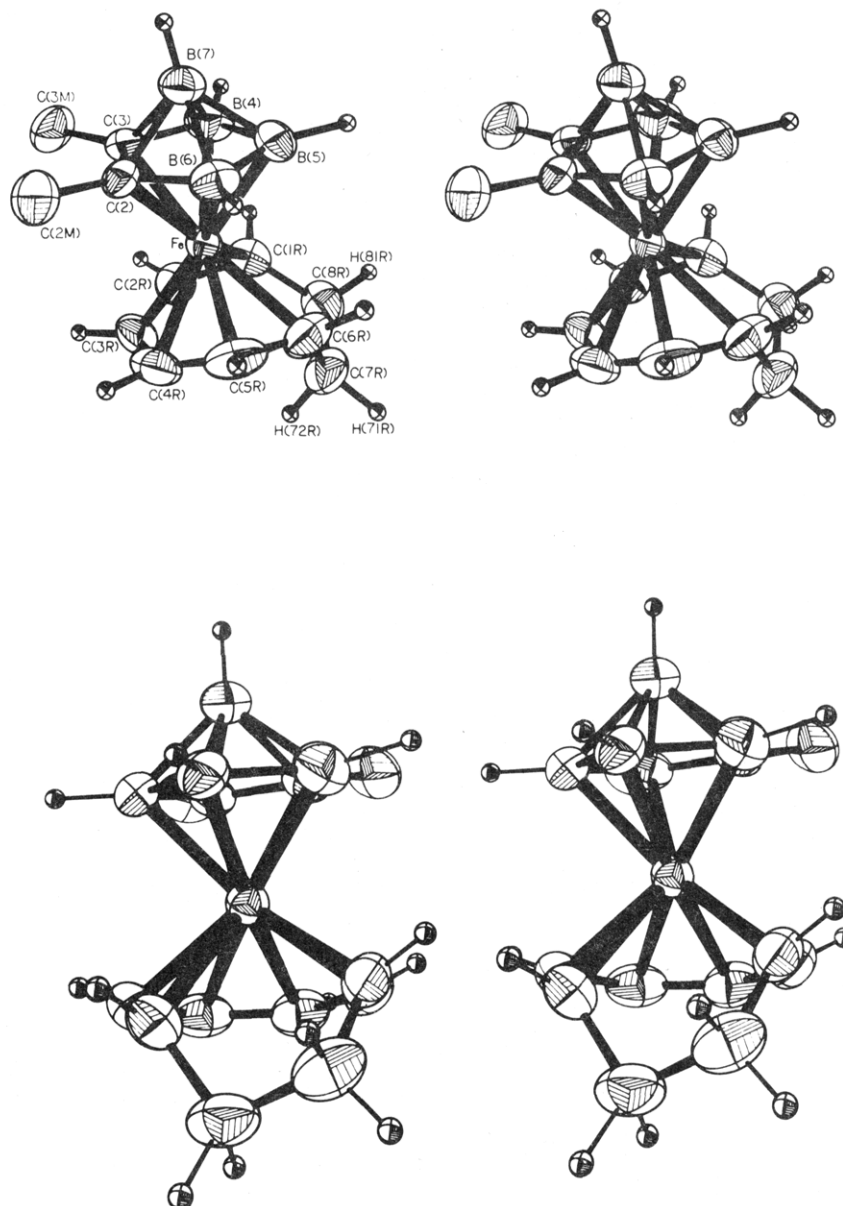ᵃ Key: vs = very strong, s = strong, m = medium, w = weak, sh = shoulder. ᵇ KBr pellet. ᶜ CHCl₃ solution vs. CHCl₃.

Figure 1. Stereoviews of the molecular structure of $(\eta^6\text{-}C_8H_{10})Fe[(CH_3)_2C_2B_4H_4]$

A second minor product has been identified as $(C_{16}H_{18})Fe[(C_2H_5)_2C_2B_4H_4]$ (III), but no structure has been assigned; NMR and other spectroscopic data are reported below. At present we cannot account for the formation of II and III, and while their origin poses intriguing questions, these are presently outside the scope of this research and have not been pursued.

Spectroscopic Characterization of $(\eta^6\text{-}C_8H_{10})Fe\text{-}(R_2C_2B_4H_4)$ (I, R = C₂H₅; IA, R = CH₃). The ¹H, ¹³C, and ¹¹B FT NMR spectra of I (Tables I–III) and infrared absorptions (Table IV) are all consistent with a structure consisting of an iron atom η^5 coordinated to an $R_2C_2B_4H_4{}^{2-}$ pyramidal ligand and η^6 bonded to a 1,3,5-cyclooctatriene

ring; this geometry has been established by an X-ray investigation described below. There is no evidence of fluxionality in solution at room temperature or below, all of the spectral data pointing to a single ligand conformation. The ¹¹B NMR spectrum is typical of seven-vertex *closo*-metallacarboranes, and the ¹H and ¹³C NMR spectra closely resemble those reported for other $(\eta^6\text{-}1,3,5\text{-cyclo-octadiene})$metal complexes, e.g., $(\eta^6\text{-}C_8H_{10})M(\eta^4\text{-}C_8H_{12})$ (M = Fe,[12] Ru,[12,13] Ir[14]) and $(\eta^6\text{-}C_8H_{10})M(CO)_3$ (M = Cr, Mo).[15]

(12) Fischer, E. O.; Müller, J. *Chem. Ber.* **1963**, *96*, 3217.
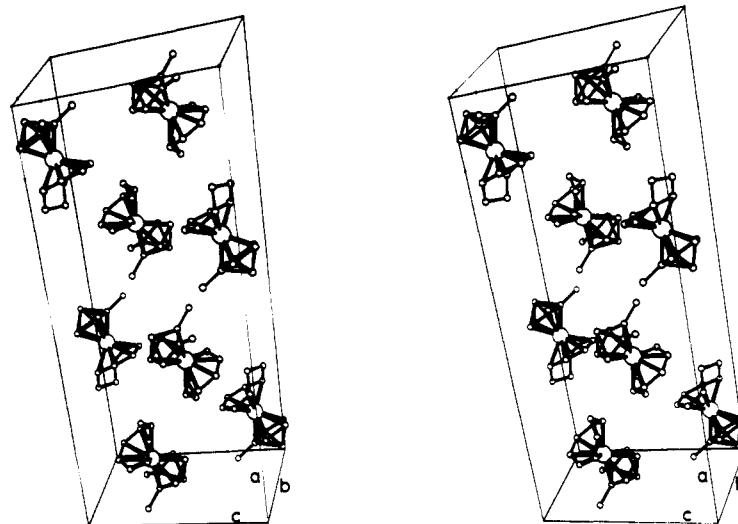(13) Pertici, P.; Vitulli, G.; Paci, M.; Porri, L. *J. Chem. Soc., Dalton Trans.* **1961**, 1980.

Figure 2. Stereoview of contents of a unit cell.

Table V.   Experimental Parameters and Crystal Data[a]

M_r	287	trans coeff (max)	0.9476
space group	$C2/c$	trans coeff (min)	0.7077
a, Å	31.403 (7)	2θ range, deg	50
b, Å	7.098 (3)	reflctns obsd	1956
c, Å	12.348 (7)	reflctns refined	1805
β, deg	100.61 (3)	R	0.048
V, Å^3	2706	R_w	0.057
μ, cm^{-1}	11.195	esd unit wt	2.1
D(calcd), g cm^{-3}	1.41	Z	8
A	0.60		
B	0.35		

[a] Crystal dimensions (mm from centroid): 100 (0.105), $\bar{1}$00 (0.105), 010 (0.25), 0$\bar{1}$0 (0.25), 00$\bar{1}$ (0.28), 001 (0.28).

The assignments for I in Tables I–III have been facilitated by these similarities.

X-ray Structure Determination on (η^6-C$_8$H$_{10}$)Fe-[(CH$_3$)$_2$C$_2$B$_4$H$_4$] (IA). The molecular geometry of IA is depicted in Figure 1, and Tables V–VIII list the experimental parameters and crystal data, positional parameters, bond distances, and bond angles. The iron atom completes a seven-vertex pentagonal-bipyramidal MC$_2$B$_4$ metallacarborane cage that is closely similar to other seven-vertex metallacarboranes of first-row transition elements.[16] Thus, the metal is approximately centered over the C$_2$B$_3$ face and is 1.648 Å above it. The short cage carbon–carbon [C-(2)–C(3)] distance [1.440 (3) Å] reflects some multiple-bond character, an effect that has been consistently noted in 1,2,3-MC$_2$B$_4$ *closo*-metallacarboranes.[16a,17] The methyl carbons are deflected slightly out of the C$_2$B$_3$ plane (~0.18 Å) in a direction away from the C$_8$H$_{10}$ ligand, probably owing to steric interaction with the hydrocarbon ring.

Our primary interest in this structure is in the C$_8$H$_{10}$ group. To our knowledge, only two crystal structures of η^6-cyclooctatriene–transition-metal complexes have been reported prior to this work (vide infra). The iron atom in I is bound to six of the eight carbons, with Fe–C bond distances of 2.053–2.164 Å. Carbons C(1R) through C(5R)

(14) Müller, J.; Menig, H.; Huttner, G.; Frank, A. *J. Organomet. Chem.* **1980**, *185*, 251.

(15) Kreiter, C. G.; Lang, M.; Strack, H. *Chem. Ber.* **1975**, *108*, 1502.

(16) (a) Borodinsky, L.; Sinn, E.; Grimes, R. N. *Inorg. Chem.* **1982**, *21*, 1928. (b) Weiss, R.; Bryan, R. F. *Acta Crystallogr., Sect. B* **1977**, *B33*, 589. (c) Pipal, J. R.; Maxwell, W. M.; Grimes, R. N. *Inorg. Chem.* **1978**, *17*, 1447. (d) Pipal, J. R.; Grimes, R. N. *Ibid.* **1979**, *18*, 263.

(17) Pipal, J. R.; Grimes, R. N. *Inorg. Chem.* **1978**, *17*, 10 and references therein.

are nearly coplanar (largest deviation 0.06 Å); the remaining coordinated carbon atom C(6R) is 0.39 Å out of this plane, away from the iron atom. The C(1R)–C(5R) plane is 1.235 Å from Fe and is not quite parallel to the C$_2$B$_3$ carborane face (dihedral angle 12°). The C–C distances in the C(1R)–C(6R) group are almost identical, averaging 1.409 (1) Å, and there is little indication of alternating long and short bonds. The two noncoordinated (methylene) carbon atoms C(7R) and C(8R) are bent out of the C$_6$ plane away from the iron at nonbonding distances from it and exhibit normal tetrahedral valence angles.

The Fe–C$_8$H$_{10}$ portion of the molecule bears a close resemblance to the structure of (η^6-C$_8$H$_{10}$)Fe(η^4-C$_8$H$_{10}$)[18] that contains two different cyclooctatriene ligands, one of which is η^6-1,3,5-cyclooctatriene as in I. The corresponding C–C distances and angles in the two molecules are virtually the same; however, the iron atom is slightly closer to the η^6-C$_8$H$_{10}$ ring in (C$_8$H$_{10}$)$_2$Fe than in I [average Fe–C value 2.101 (4) vs. 2.117 (1) Å]. This effect appears contrary to the normal expectation of *shorter* Fe–C distances in I owing to the formal oxidation state of +2 in that molecule compared to zero in (C$_8$H$_{10}$)$_2$Fe; this observation may, in fact, signal that the actual charge distributions in these compounds are substantially different from those implied by the formal oxidation states.

The only other published structure of an η^6-1,3,5-cyclooctatriene–transition-metal complex is that of (η^6-C$_8$H$_{10}$)Cr(CO)$_3$,[19] where again the hydrocarbon ligand geometry closely resembles that in I (mean distance between metal-coordinated carbon atoms is 1.42 (1) Å). The metal–C$_8$H$_{10}$ ligand distance [average Cr–C value 2.27 (1) Å] is substantially larger than in I and (C$_8$H$_{10}$)$_2$Fe.

Discussion

The formation of an η^6-1,3,5-cyclooctatriene complex directly from C$_8$H$_8$$^{2-}$ ion is unusual but not unprecedented, having been observed, for example, in the synthesis of (η^6-C$_8$H$_{10}$)M(η^4-C$_8$H$_{12}$) (M = Ru, Os) from C$_8$H$_8$$^{2-}$ and (C$_8$H$_{12}$MCl$_2$)$_n$, and of (η^6-C$_8$H$_{10}$)Ru(NBD) from C$_8$H$_8$$^{2-}$ and [(NBD)RuCl$_2$]$_n$ (NBD = norbornadiene).[20] However, most known complexes of 1,3,5-C$_8$H$_{10}$ have been prepared directly from the free cycloalkene.[21] In our work, the

(18) Huttner, G.; Bejenke, V. *Chem. Ber.* **1974**, *107*, 156.

(19) Armstrong, V. S.; Prout, C. K. *J. Chem. Soc.* **1962**, 3770.

(20) Schrock, R. R.; Lewis, J. *J. Am. Chem. Soc.* **1973**, *95*, 4102.

(21) Fray, G. I.; Saxton, R. G. "The Chemistry of Cyclo-Octatetraene and its Derivatives"; Cambridge University Press: New York, 1978.
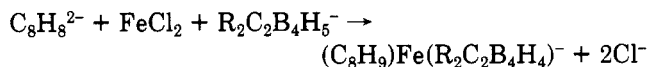
Table VI. Positional Parameters for $(C_8H_{10})Fe(CH_3)_2C_2B_4H_6$

	x	y	z		x	y	z
Fe	0.13871 (1)	0.20087 (6)	0.11982 (3)	H(4R)	0.156 (1)	0.351 (7)	0.341 (3)
C(1R)	0.1754 (1)	−0.0477 (5)	0.0957 (3)	H(5R)	0.177 (1)	0.501 (5)	0.200 (3)
C(2R)	0.1601 (1)	−0.0508 (5)	0.1963 (3)	H(6R)	0.205 (1)	0.394 (6)	0.047 (3)
C(3R)	0.1603 (1)	0.0859 (6)	0.2800 (3)	H(71R)	0.260 (1)	0.202 (6)	0.141 (4)
C(4R)	0.1679 (1)	0.2807 (6)	0.2821 (3)	H(72R)	0.244 (1)	0.143 (6)	0.223 (3)
C(5R)	0.1825 (1)	0.3918 (5)	0.2004 (3)	H(81R)	0.220 (1)	0.029 (5)	−0.001 (3)
C(6R)	0.2027 (1)	0.3135 (5)	0.1199 (3)	H(82R)	0.239 (1)	−0.118 (6)	0.094 (3)
C(7R)	0.2368 (1)	0.1619 (6)	0.1440 (3)	H(31M)	0.038 (2)	0.055 (7)	0.214 (4)
C(8R)	0.2203 (1)	−0.0069 (6)	0.0776 (3)	H(32M)	0.054 (1)	−0.099 (6)	0.148 (3)
C(3)	0.0727 (1)	0.1311 (5)	0.0863 (3)	H(33M)	0.018 (1)	−0.032 (6)	0.100 (3)
C(2)	0.0785 (1)	0.3246 (5)	0.1208 (3)	H(21M)	0.071 (1)	0.543 (7)	0.235 (3)
C(3M)	0.0444 (1)	−0.0005 (7)	0.1383 (3)	H(22M)	0.029 (2)	0.422 (6)	0.195 (4)
C(2M)	0.0564 (1)	0.4114 (7)	0.2075 (3)	H(23M)	0.056 (2)	0.323 (7)	0.272 (4)
B(4)	0.0934 (1)	0.0853 (6)	−0.0161 (3)	H(4)	0.008 (1)	−0.079 (6)	−0.072 (3)
B(5)	0.1151 (1)	0.2894 (6)	−0.0482 (3)	H(5)	0.130 (1)	0.312 (5)	−0.127 (3)
B(6)	0.1042 (1)	0.4414 (6)	0.0448 (3)	H(6)	0.111 (1)	0.597 (6)	0.053 (3)
B(7)	0.0619 (1)	0.2964 (6)	−0.0241 (3)	H(7)	0.030 (1)	0.328 (5)	−0.070 (3)
H(1R)	0.160 (1)	−0.143 (5)	0.044 (3)				
H(2R)	0.141 (1)	−0.138 (6)	0.206 (3)				
H(3R)	0.142 (1)	0.038 (5)	0.335 (2)				

Table VII. Bond Distances (Å) in $(\eta^6\text{-}C_8H_{10})Fe[(CH_3)_2C_2B_4H_4]$

Carborane Ligand

Fe–C(2)	2.086 (2)	C(3)–B(4)	1.559 (3)
Fe–C(3)	2.098 (2)	C(3)–B(7)	1.783 (3)
Fe–B(4)	2.153 (2)	C(3)–C(3M)	1.512 (3)
Fe–B(5)	2.164 (2)	B(4)–B(5)	1.680 (3)
Fe–B(6)	2.139 (2)	B(4)–B(7)	1.788 (3)
C(2)–C(3)	1.440 (3)	B(5)–B(6)	1.657 (3)
C(2)–B(6)	1.581 (3)	B(5)–B(7)	1.751 (3)
C(2)–B(7)	1.781 (3)	B(6)–B(7)	1.769 (3)
C(2)–C(2M)	1.510 (3)	⟨B–H⟩	1.18 (2)
		⟨C(methyl)–H⟩	0.94 (2)

C_8H_{10} Ligand

Fe–C(1R)	2.158 (2)	C(2R)–C(3R)	1.417 (3)
Fe–C(2R)	2.074 (2)	C(3R)–C(4R)	1.403 (3)
Fe–C(3R)	2.132 (2)	C(4R)–C(5R)	1.422 (3)
Fe–C(4R)	2.121 (2)	C(5R)–C(6R)	1.391 (3)
Fe–C(5R)	2.053 (2)	C(6R)–C(7R)	1.509 (3)
Fe–C(6R)	2.164 (2)	C(7R)–C(8R)	1.490 (3)
C(1R)–C(2R)	1.412 (3)	C(8R)–C(1R)	1.496 (3)
		⟨C–H⟩	0.98 (2)

Nonbonded Distances

Fe–C(7R)	3.054 (2)	C(1R)–C(6R)	2.703 (3)
Fe–C(8R)	3.083 (2)	Fe–B(7)	2.802 (2)

$R_2C_2B_4H_5^-$ carborane ligand is a proton donor via the acidic B–H–B bridge as in the proposed reaction

$$C_8H_8^{2-} + FeCl_2 + R_2C_2B_4H_5^- \rightarrow$$
$$(C_8H_9)Fe(R_2C_2B_4H_4)^- + 2Cl^-$$

The anionic complex, however, has not been observed; at some stage, most likely during workup in air,[22] it is protonated to give neutral $(C_8H_{10})Fe(R_2C_2B_4H_4)$ (I). Protonation of free C_8H_8 and $C_8H_8^{2-}$, and of their metal complexes, has been extensively studied,[21] and a variety of $C_8H_9^+$ complexes has been found; the stereochemistry is often complex, involving a number of bonding modes that in most cases have been proposed from NMR data and are not established by crystallographic studies. In the present work, the observation of a single major isolable product, I, is accountable in terms of a strong thermodynamic drive to achieve a filled-shell $(2n + 2)$-electron FeC$_2$B$_4$ *closo*-

carborane cage[2] and a full 18-electron configuration on the metal. This is accomplished via six-electron contributions to Fe^{2+} from the $R_2C_2B_4H_4^{2-}$ and C_8H_{10} ligands, requiring in the latter case η^6 (tridentate) coordination to the metal. It is to be expected, however, that reactions of $C_8H_8^{2-}$ and $R_2C_2B_4H_5^-$ with other transition metals may be more complicated; indeed, we have found that the interaction with CoCl$_2$ produces *three* isomeric $(C_8H_9)Co^{III}$ $(R_2C_2B_4H_4)$ products that differ in the conformation of the $C_8H_9^-$ ligand.[1] In this case there appear to be several competing ligand structures of similar energy, unlike the iron system where only one C_8H_{10} isomer is observed. A full report on the cobalt species awaits X-ray structural analyses.

As noted in the Introduction, we anticipated that C_8H_x metallacarborane complexes would exhibit some lability of the hydrocarbon ligand, a potentially useful property in synthesis. This has proved to be the case, in that C_8H_{10} is readily displaced from II by arenes to give $(\eta^6$-arene)-Fe(R$_2$C$_2$B$_4$H$_4$) complexes as described in the following article.[10]

Experimental Section

---

(22) Protonation in solution, prior to exposure to air, could occur only via interaction of the anion with a second equivalent of $R_2C_2B_4H_5^-$ (there being no other available proton donor), but such a process is inconsistent with the observed stoichiometry. Moreover, *uncomplexed* $R_2C_2B_4H_5^-$ is an extremely poor Brønsted acid.[23]

(23) Onak, T.; Dunks, G. B. *Inorg. Chem.* **1966**, *5*, 439.

(24) (a) Hosmane, N. S.; Grimes, R. N. *Inorg. Chem.* **1979**, *18*, 3294. (b) Maynard, R. B.; Borodinsky, L.; Grimes, R. N. *Inorg. Synth.*, in press.

(25) Streitweiser, A.; Müller-Westerhoff, U.; Sonnichsen, G.; Mares, F.; Morrell, D. G.; Hodgson, K. O.; Harmon, C. A. *J. Am. Chem. Soc.* **1973**, *95*, 8644.

Table VIII. Selected Bond Angles (deg)

C(3)-C(2)-B(6)	112.03 (16)	B(4)-C(3)-C(3M)	125.56 (20)	C(3R)-C(4R)-C(5R)	127.54 (20)
Fe-C(7)-B(7)	92.54 (11)	C(3)-B(4)-B(5)	105.07 (17)	C(4R)-C(5R)-C(6R)	122.38 (20)
C(3)-C(2)-C(2M)	123.33 (18)	B(4)-B(5)-B(6)	104.66 (17)	C(5R)-C(6R)-C(7R)	123.07 (21)
B(6)-C(2)-C(2M)	123.95 (19)	B(5)-B(6)-C(2)	105.29 (17)	C(6R)-C(7R)-C(8R)	107.62 (18)
C(2)-C(3)-B(4)	112.95 (16)	C(2R)-C(1R)-C(8R)	128.08 (18)	C(7R)-C(8R)-C(1R)	108.43 (17)
Fe-C(3)-B(7)	92.10 (11)	C(1R)-C(2R)-C(3R)	132.49 (19)	C(1R)-Fe-C(6R)	77.42 (8)
C(2)-C(3)-C(3M)	121.08 (18)	C(2R)-C(3R)-C(4R)	131.79 (18)		

Reaction of $Na^+(C_2H_5)_2C_2B_4H_5^-$, $FeCl_2$, and $K_2C_8H_8$. A THF solution of $K_2C_8H_8$ was prepared[25] from 0.850 g (21.8 mmol) of potassium metal and 0.969 g (9.32 mmol) of cyclooctatetraene in 25 mL of dry THF at -30 °C. This solution was filtered in vacuo onto 1.186 g (9.36 mmol) of anhydrous $FeCl_2$ in a 100-mL round-bottom flask that was cooled in liquid nitrogen. A THF solution of $Na^+(C_2H_5)_2C_2B_4H_5^-$ was prepared from 1.149 g (8.77 mmol) of $2,3\text{-}(C_2H_5)_2C_2B_4H_8$ and 0.240 g (9.98 mmol) of NaH in 25 mL of THF. The $Na^+(C_2H_5)_2C_2B_4H_5^-$ solution was filtered in vacuo into the reaction flask containing $FeCl_2$ and $K_2C_8H_8$ at liquid N_2 temperature. The reactor was placed in an ice–salt water bath and stirred for 1 h, after which the bath was removed and the mixture was stirred at room temperature for 4 h. The solvent was removed in vacuo, dry nitrogen was introduced into the reactor, and 10 mL of dry toluene was added to the dark brown residue. Stirring was continued for 1 h, after which the mixture was filtered through 2 cm of silica gel onto a sintered glass frit. The silica gel was washed with methylene chloride until the effluent became colorless. The volume of the orange-brown filtrate was reduced to 50 mL by rotary evaporation, and this solution was placed on a 4.5 × 25 cm column of silica gel that had been charged with *n*-hexane. Elution with 50% toluene in *n*-hexane produced a large orange-brown fraction, which was evaporated to dryness and dissolved in a minimum amount of methylene chloride. Refrigeration at 0 °C overnight produced 1.265 g (4.35 mmol, 49.6% yield based on carborane employed) of $[(C_2H_5)_2\text{-}C_2B_4H_4]Fe(C_8H_{10})$ (I) as large red crystals: mp 88–89 °C; exact mass determination, calcd for $^{56}Fe^{12}C_{14}^{11}B_4^1H_{24}$ 292.1600, found 292.1600.

Further elution of the column with 100% toluene gave a small yellow fraction. Following removal of solvent, the residue was dissolved in a minimum amount of methylene chloride. This solution was placed on a silica gel TLC plate and developed with 25% methylene chloride in *n*-hexane, producing 11 mg (0.042 mmol, 0.48% yield) of $[(C_2H_5)_2C_2B_4H_4]Fe(C_6H_6)$ (II) (R_f 0.33) as a golden solid and 7 mg (0.018 mmol, 0.20%) of $[(C_2H_5)_2C_2B_4\text{-}H_4]Fe(C_{16}H_{18})$ (III) (R_f 0.19) as a red-brown solid. Exact mass determinations: calcd for $^{56}Fe^{12}C_{12}^{11}B_4^1H_{20}$ (II) 264.1286, found 264.1294; calcd for $^{56}Fe^{12}C_{22}^{11}B_4^1H_{32}$ (III) 396.2233, found 396.2229. The mass spectrum of III exhibits intense peaks corresponding to fragments with high-mass cutoffs at m/e 318 (representing loss of C_6H_6) and m/e 264 (loss of $C_{10}H_{12}$); the m/e 264 fragment is in composition identical with compound II (observed mass 264.1286, corresponding to $^{56}Fe^{12}C_{12}^{11}B_4^1H_{20}$).

Two additional products (R_f 0.23 and 0.43) were isolated in yields of < 5 mg but were not characterized.

X-ray Structure Determination on $[(CH_3)_2C_2B_4H_4]Fe(\text{-}C_8H_{10})$ (IA). Single crystals of IA (prepared from $(CH_3)_2C_2B_4H_5^-$ in a procedure analogous to the synthesis of I, described above) were grown from a methylene chloride/*n*-hexane solution by slow evaporation at ~+10 °C. A selected crystal, mounted on a glass fiber, was examined by precession photography and found acceptable. Relevant parameters for the data collection and structure determination are given in Table V. The procedures followed in data collection and processing have been described elsewhere.[26]

The space group $C2/c$ was chosen on the basis of chemical and spectroscopic information taken together with systematic absences.

The intensities of four standard reflections, monitored at regular intervals, showed no greater fluctuations during the data collection than those expected from Poisson statistics. The raw intensity data were corrected for Lorentz–polarization effects and then for absorption. Only those reflections for which $F_o^2 > 3\sigma(F_o^2)$, where $\sigma(F_o^2)$ was estimated from counting statistics ($p = 0.03$),[27] were used in the final refinement of the structural parameters, after averaging for equivalent reflections.

Solution and Refinement of the Structure. Full-matrix least-squares refinement was based on F, and the function minimized was $w(|F_o| - |F_c|)^2$. The weights w were taken as $[2F_o/\sigma(F_o^2)]^2$, where $|F_o|$ and $|F_c|$ are the observed and calculated structure factor amplitudes. The atomic scattering factors for non-hydrogen atoms were taken from Cromer and Waber[28] and those for hydrogen from Stewart et al.[29] The effects of anomolous dispersion for all non-hydrogen atoms were included in F by using the values of Cromer and Ibers[30] for $\Delta f'$ and $\Delta f''$.

The iron atom was located from a three-dimensional Patterson difference map calculated from all intensity data. Subsequent Fourier difference maps revealed the positions of all other non-hydrogen atoms. After anisotropic thermal parameters were introduced for all non-hydrogen atoms, additional Fourier syntheses located most of the hydrogen atoms. Several of the ethyl hydrogens were inserted into calculated positions and included in subsequent refinement. All hydrogen positions were held fixed in the final least-squares cycles. The model converged to the final R and R_w values given in Table V, where $R = \sum||F_o| - |F_c||$ and $R_w = (\sum w(|F_o| - |F_c|)^2/\sum w|F_o|^2)^{1/2}$. Tables of observed and calculated structure factors and thermal parameters are available (see paragraph at end of paper on supplementary material). The computing system and programs are described elsewhere.[31]

Supplementary Material Available: Listings of observed and calculated structure factors and anisotropic thermal parameters (10 pages). Ordering information is given on any current masthead page.

(26) Finster, D. C.; Grimes, R. N. *J. Am. Chem. Soc.* **1981**, *103*, 2675.

(27) Corfield, P. W. R.; Doedens, R. J.; Ibers, J. A., *Inorg. Chem.* **1967**, *6*, 197.
(28) Cromer, D. T.; Waber, J. T. "International Tables for X-ray Crystallography"; Kynoch Press: Birmingham, England, 1974; Vol. IV.
(29) Stewart, R. F.; Davidson, E. R.; Simpson, W. T. *J. Chem. Phys.* **1965**, *42*, 3175.
(30) Cromer, D. T.; Ibers, J. A., in ref 28.
(31) Freyberg, D. P.; Mockler, G. M.; Sinn, E., *J. Chem. Soc., Dalton Trans.* **1976**, 447.

Organotransition-Metal Metallacarboranes. 2. Synthesis and Structures of (η^6-Arene)Fe[(C$_2$H$_5$)$_2$C$_2$B$_4$H$_4$] Complexes

Robert G. Swisher, Ekk Sinn, and Russell N. Grimes*

Department of Chemistry, University of Virginia, Charlottesville, Virginia 22901

Reactions of the (1,3,5-cyclooctatriene)ferracarborane complex (η^6-C$_8$H$_{10}$)Fe(R$_2$C$_2$B$_4$H$_4$) (R = C$_2$H$_5$) with benzene or other arenes over AlCl$_3$ form the corresponding (η^6-arene)Fe(R$_2$C$_2$B$_4$H$_4$) species, as air-stable crystalline solids. Complexes in which the arene is benzene, 1,3,5-trimethylbenzene (mesitylene), and hexamethylbenzene have been characterized via ^{13}C, ^{1}H, and ^{11}B FT NMR, IR, and mass spectroscopy and X-ray crystal structure determinations. In all cases the arene ring is planar, centered over the metal, and nearly parallel to the C$_2$B$_3$ ring of the carborane ligand. The benzene complex crystallizes with two molecules in the asymmetric unit, one of which is eclipsed with respect to the C(2)-C(3) bond of the carborane ligand while the other is staggered. The mesitylene and hexamethylbenzene complexes are approximately staggered and eclipsed, respectively. The reaction of (η^6-C$_8$H$_{10}$)Fe[(C$_2$H$_5$)$_2$C$_2$B$_4$H$_4$] with *N,N,N',N'*-tetramethyl-1,2-diaminoethane results in extraction of the apex boron and forms (η^6-C$_8$H$_{10}$)Fe-[(C$_2$H$_5$)$_2$C$_2$B$_3$H$_5$], characterized from spectroscopic data as a sandwich complex containing a planar carborane ligand. Crystal data: (η^6-C$_6$H$_6$)Fe[(C$_2$H$_5$)$_2$C$_2$B$_4$H$_4$], M_r = 264, space group *Pbca*, Z = 8 (two molecules/asymmetric unit), a = 14.187 (5) Å, b = 15.796 (6) Å, c = 24.714 (10) Å, V = 5538 Å^3, R = 0.069 for 3124 reflections having $F_0^2 > 3\sigma(F_0^2)$; [η^6-C$_6$(CH$_3$)$_3$H$_3$]Fe[(C$_2$H$_5$)$_2$C$_2$B$_4$H$_4$], M_r 306, space group *P2$_1$/n*, Z = 4, a = 7.610 (2) Å, b = 14.646 (4) Å, c = 15.348 (7) Å, β = 95.95 (4)°, V = 1701 Å^3, R = 0.063 for 2105 reflections having $F_0^2 > 3\sigma(F_0^2)$; [η^6-C$_6$(CH$_3$)$_6$]Fe[(C$_2$H$_5$)$_2$C$_2$B$_4$H$_4$], M_r = 348, space group *P2$_1$/n*, Z = 4, a = 8.892 (1) Å, b = 13.250 (1) Å, c = 16.547 (4) Å, β = 98.51 (2)°, V = 1928 Å^3, R = 0.047 for 2424 reflections having $F_0^2 > 3\sigma(F_0^2)$.
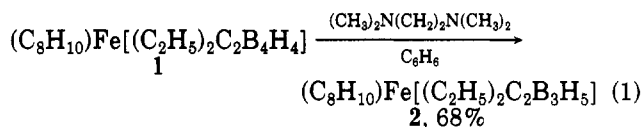
Introduction

Transition-metal sandwich complexes containing mixed arene and carborane ligands are of interest both in terms of their electronic and molecular structures, the study of which has only recently begun,[1-3] and also their potential utility as synthetic agents.[4] Metal ions typically form robust π-bonded complexes with *nido*-carborane ligands such as C$_2$B$_9$H$_{11}$$^{2-}$, C$_2B_4H_6$$^{2-}$, and their derivatives;[5] hence (η^6-arene)metal(η^5-carborane) complexes in principle allow one to explore the chemistry of the coordinated arene groups while the metal is tightly held in a stable borane cage matrix. If the arene ligands are relatively labile, such complexes should open a synthetic gateway to a host of other organotransition-metal carborane species.

Few examples of (π-arene)metallacarboranes are currently known. Recently, Todd and co-workers[2] prepared several (η^6-arene)M(C$_2$B$_9$H$_{11}$) complexes incorporating C$_6$H$_6$, 1,3,5-C$_6$(CH$_3$)$_3$H$_3$ (mesitylene), or C$_6$(CH$_3$)$_6$ by reaction of Tl$^+$[3,1,2-TlC$_2$B$_9$H$_{11}$]$^-$ with bis(arene)iron(II) salts in THF and determined the crystal structure of [η^6-C$_6$-(CH$_3$)$_3$H$_3$]Fe(C$_2$B$_9$H$_{11}$). Stone et al.[1] obtained several (arene)Fe[(CH$_3$)$_2$C$_2$B$_9$H$_9$] complexes via treatment of neutral (CH$_3$)$_2$C$_2$B$_9$H$_9$ with (1,5-C$_8$H$_{12}$)Fe(C$_5$H$_5$) in benzene, toluene, *o*-xylene, or naphthalene/petroleum mixtures and reported the X-ray crystallographic characterization of (η^6-C$_6$H$_5$CH$_3$)Fe[(CH$_3$)$_2$C$_2$B$_9$H$_9$]. Sneddon[3] has prepared (η^6-C$_6$H$_5$CH$_3$)Fe[(CH$_3$)$_2$C$_2$B$_4$H$_4$] from the reaction of (C-H$_3$)$_2$C$_2$B$_4$H$_6$, toluene, and iron vapor and determined the

molecular structure by X-ray diffraction. In our work, the availability of the complex (η^6-C$_8$H$_{10}$)Fe[(C$_2$H$_5$)$_2$C$_2$B$_4$H$_4$], described in the preceding paper,[6a] led to a new general route to (η^6-arene)Fe(R$_2$C$_2$B$_4$H$_4$) species that we now describe together with full structural characterizations of three of the products.

Results

Properties of (η^6-C$_8$H$_{10}$)Fe[(C$_2$H$_5$)$_2$C$_2$B$_4$H$_4$] (1). The 1,3,5-cyclooctatriene complex 1, obtained in 50% yield as red-orange crystals from the reaction of C$_8$H$_8$$^{2-}$ with (C$_2$-H$_5$)$_2$C$_2$B$_4$H$_5$$^-$ ion and FeCl$_2$ in THF,[6a] is air-stable in the solid state and does not decompose appreciably on heating at 180 °C. Treatment of 1 with *N,N,N',N'*-tetramethyl-1,2-diaminoethane in benzene removes the apex BH unit to give the *nido*-carborane analogue 2 (eq 1 and Figure 1).

$$(C_8H_{10})Fe[(C_2H_5)_2C_2B_4H_4] \xrightarrow[\substack{C_6H_6}]{(CH_3)_2N(CH_2)_2N(CH_3)_2} $$
$$\mathbf{1}$$
$$(C_8H_{10})Fe[(C_2H_5)_2C_2B_3H_5] \quad (1)$$
$$\mathbf{2}, 68\%$$

From NMR and mass spectroscopic data, 2 is proposed to have a six-vertex FeC$_2$B$_3$ pyramidal cage structure with two B-H-B bridging groups on the basal plane, analogous to a number of previously described metallacarboranes of this class, including several structurally established species[7] such as 1-(CO)$_3$FeC$_2$B$_3$H$_7$. (One can also describe these compounds as sandwich complexes containing planar R$_2$C$_2$B$_3$H$_5$$^{2-}$ carborane ligands.)

Compound 1 is unaffected by prolonged refluxing in benzene, nor does it react with benzene in the presence of FeCl$_3$ or H$_2$. Irradiation of a benzene solution of 1 under ultraviolet light generates a small amount of a substance

(1) Garcia, M. P.; Green, M.; Stone, F. G. A.; Somerville, R. G.; Welch, A. J. *J. Chem. Soc., Chem. Commun.* **1981**, 871.

(2) Hanusa, T. P.; Huffman, J. C.; Todd, L. J. *Polyhedron* **1982**, *1*, 77.

(3) Sneddon, L. G., Workshop on Main-Group Chemistry, Keystone, Colorado, June 1982; Sneddon, L. G., private communication. Micciche, R. P.; Sneddon, L. G. *Organometallics*, in press.

(4) Arene-transition-metal complexes are widely employed in organic synthesis; for a review see: Jaouen, G. In "Transition Metal Organometallics in Organic Synthesis"; Alper, H., Ed.; Academic Press: New York, 1978; Vol. II, Chapter 2, pp 65-120.

(5) Grimes, R. N. In "Comprehensive Organometallic Chemistry"; Wilkinson, G., Stone, F. G. A., Abel, E., Eds.; Permagon Press: Oxford, 1982; Vol. 1, Chapter 5.5, pp 459-542.

(6) (a) Maynard, R. B.; Swisher, R. G.; Grimes, R. N., preceding article in this issue. (b) See ref 16 in ref 6a.

(7) (a) Brennan, J. P.; Grimes, R. N.; Schaeffer, R.; Sneddon, L. G. *Inorg. Chem.* **1973**, *12*, 2266. (b) Pipal, J. R.; Maxwell, W. M.; Grimes, R. N. *Ibid.* **1978**, *17*, 1447. (c) Borodinsky, L.; Sinn, E.; Grimes, R. N. *Ibid.* **1982**, *21*, 1928.

Table I. 360-MHz ^{1}H FT NMR Data

compd	δ [rel to Si(CH$_3$)$_4$]^a	rel area
(η^6-C$_8$H$_{10}$)Fe[(C$_2$H$_5$)$_2$C$_2$B$_3$H$_5$) (2)^b	5.37 m (C$_8$H$_{10}$), 5.27 m (C$_8$H$_{10}$), 1.92 m (C$_8$H$_{10}$), 1.76 m (CH$_2$), 1.66 m (CH$_2$), 1.54 s,^{b} 0.96 t (CH$_3$), 0.38 m (C$_8$H$_{10}$), −5.53 s, br (B–H–B)	4, 2, 2, 2, 2, 2, 6, 2, 2
(η^6-C$_6$H$_6$)Fe[(C$_2$H$_5$)$_2$C$_2$B$_4$H$_4$] (4)^d	5.92 s (C$_6$H$_6$), 3.10 m (CH$_2$), 2.76 m (CH$_2$), 1.62 t (CH$_3$)	6, 2, 2, 6
[η^6-C$_6$(CH$_3$)$_3$H$_3$[Fe[(C$_2$H$_5$)$_2$C$_2$B$_4$H$_4$]^d (5)	5.21 s (ring CH), 2.66 m (CH$_2$), 2.34 m (CH$_2$), 2.23 (ring CH$_3$), 1.16 t (ethyl CH$_3$)	3, 2, 2, 9, 6
[η^6-C$_6$(CH$_3$)$_6$]Fe[(C$_2$H$_5$)$_2$C$_2$B$_4$H$_4$]^d (6)	2.48 m (CH$_2$), 2.26 m^e (CH$_2$), 2.24 s (ring CH$_3$), 1.06 t (ethyl CH$_3$)	2, 2,^{e} 18, 6

^{a} Legend: m = multiplet, d = doublet, t = triplet, q = quadruplet. ^{b} CDCl$_3$ solution. ^{c} Unidentified impurity. ^{d} Acetone-d_6 solution. ^{e} Partially obscured by neighboring signal.
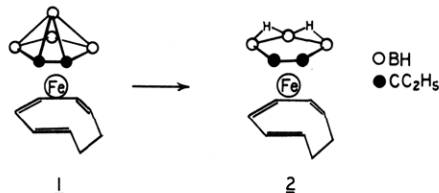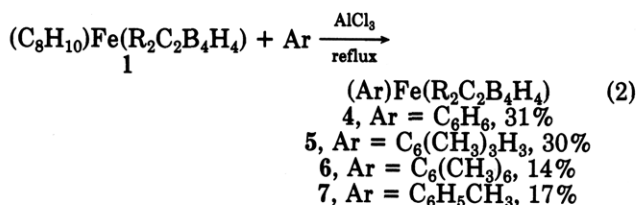

Figure 1. Base-promoted conversion of (η^6-C$_8$H$_{10}$)Fe[(C$_2$H$_5$)$_2$C$_2$B$_4$H$_4$] (1) to (η^6-C$_8$H$_{10}$)Fe[(C$_2$H$_5$)$_2$C$_2$B$_3$H$_5$] (2).

whose mass spectrum corresponds to (C$_8$H$_8$)Fe[(C$_2$H$_5$)$_2$-C$_2$B$_4$H$_4$] (3); this compound has not been characterized further. The most significant chemistry we have observed thus far for 1 involves displacement of the 1,3,5-cyclooctatriene ligand by arenes, as described in the following section.

Synthesis of (η^6-Arene)Fe[(C$_2$H$_5$)$_2$C$_2$B$_4$H$_4$] Complexes. In contrast to the unreactivity of 1 toward arenes under the conditions noted above, we found that treatment with arene solvents over AlCl$_3$ gave moderate yields of the desired complexes via eq 2. Inasmuch as the cyclooctatriene complex 1 is readily available,^{6a} reaction 2 represents a general route to workable quantities of the arene species.

$$(C_8H_{10})Fe(R_2C_2B_4H_4) + Ar \xrightarrow[\text{reflux}]{AlCl_3}$$
$$\text{1}$$
$$(Ar)Fe(R_2C_2B_4H_4) \quad (2)$$
$$\text{4, Ar = C}_6\text{H}_6,\ 31\%$$
$$\text{5, Ar = C}_6(\text{CH}_3)_3\text{H}_3,\ 30\%$$
$$\text{6, Ar = C}_6(\text{CH}_3)_6,\ 14\%$$
$$\text{7, Ar = C}_6\text{H}_5\text{CH}_3,\ 17\%$$

Compounds 4–7 have been isolated as yellow to orange solids that are stable to air over prolonged periods. Characterization of complexes 4–6 via ^{1}H, ^{13}C, and ^{11}B FT NMR, IR, and mass spectroscopy was straightforward, and
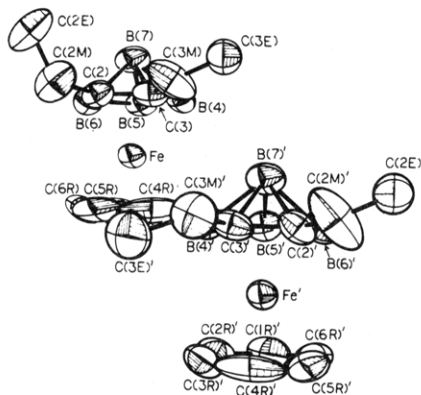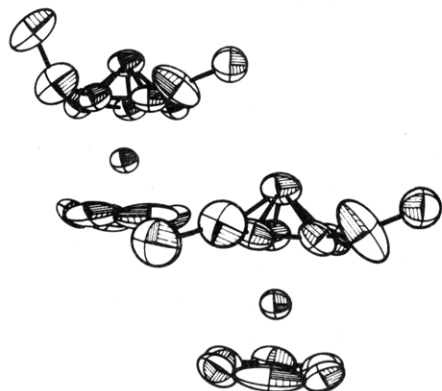
Table II. 90-MHz ^{13}C FT NMR Data (C$_6$D$_6$ Solution)

compd	δ [rel to Si(CH$_3$)$_4$]
(η^6-C$_6$H$_6$)Fe[(C$_2$H$_5$)$_2$C$_2$B$_4$H$_4$] (4)	93 (carborane C),^{a} 83.91 d (C$_6$H$_6$), 24.82 t (C$_2$H$_5$), 15.24 q (C$_2$H$_5$)
[η^6-C$_6$(CH$_3$)$_3$H$_3$]Fe[(C$_2$H$_5$)$_2$C$_2$B$_4$H$_4$] (5)	96.00 (carborane C), 84.68 d (ring C), 23.82 t (CH$_2$), 20.44 q (ring CH$_3$), 15.54 q (ethyl CH$_3$)
[η^6-C$_6$(CH$_3$)$_6$]Fe[(C$_2$H$_5$)$_2$C$_2$B$_4$H$_4$] (6)	93.41 (ring C), 22.83 t (CH$_2$), 16.91 q (ring CH$_3$),^{b} 15.73 q (ethyl CH$_3$)^b

^{a} Broad, weak singlet. ^{b} Tentative assignment.

Table III. 115.5-MHz ^{11}B FT NMR Data

compd	solvent	δ (J, Hz)^a	rel area
2	CH$_2$Cl$_2$	3.52 (130)	
4	C$_6$D$_6$	12.47,^{b} 6.61 (140), 3.53^b	1, 1, 2
	(CD$_3$)$_2$CO	6.21 (158), 4.62 (158), 1.14 (134)	1, 1, 2
5	CH$_2$Cl$_2$	6.86 (134), 2.95 (152), 1.70 (146)	1, 1, 2
6	CH$_2$Cl$_2$	8.71 (135), 2.43 (158), 0.81 (179)	1, 2, 1

^{a} BF$_3$·O(C$_2$H$_5$)$_2$ shift is 0; positive shifts downfield. ^{b} J not measurable.

the data are given in Tables I–III and the Experimental Section. The η^6-benzene complex 4 is identical with a minor product (II) obtained in the reaction of C$_8$H$_8^{2-}$ with FeCl$_2$ and (C$_2$H$_5$)$_2$C$_2$B$_4$H$_5^-$ as described in the preceding

Figure 2. Stereoview of the molecular structure of (η^6-C$_6$H$_6$)Fe[(C$_2$H$_5$)$_2$C$_2$B$_4$H$_4$] (4) showing the two crystallographically independent molecules (A, unprimed labels, B, primed labels). An ethyl carbon atom in each molecule [C(3E) and C(3E)'] is disordered; only one arbitrarily selected position is depicted. All hydrogen atoms are omitted for clarity.
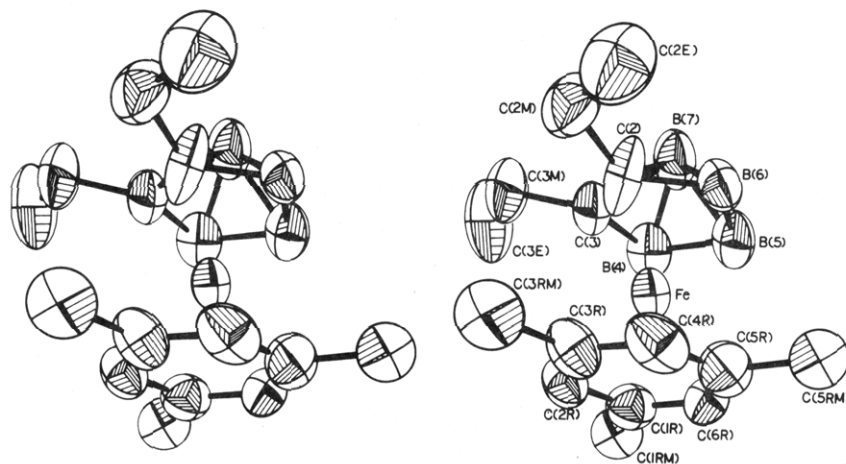
Figure 3. Molecular structure of $[\eta^6\text{-}C_6(CH_3)_3H_3]Fe[(C_2H_5)_2C_2B_4H_4]$ (**5**).
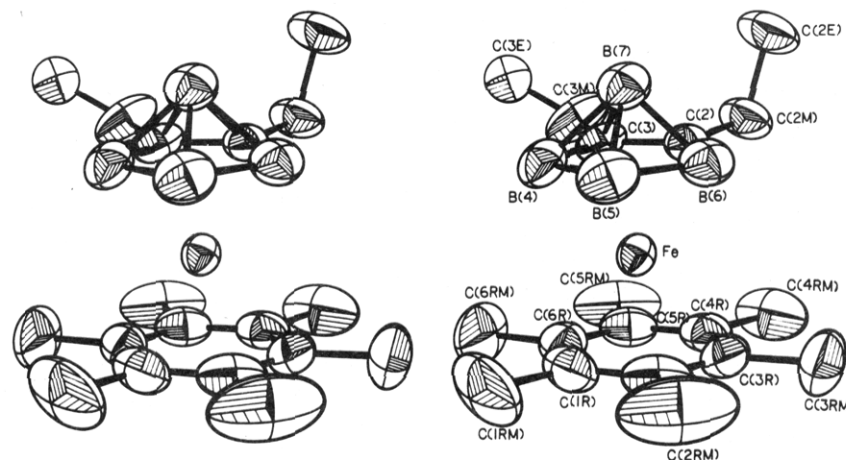
Figure 4. Molecular structure of $[\eta^6\text{-}C_6(CH_3)_6]Fe[(C_2H_5)_2C_2B_4H_4]$ (**6**). Only one of three disordered positions for C(3E) is shown.
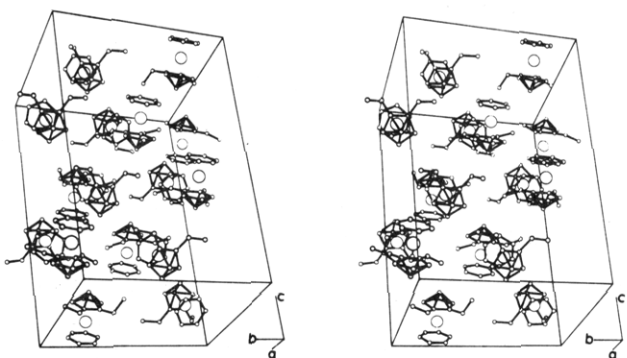
Figure 5. Unit cell packing in **4**.
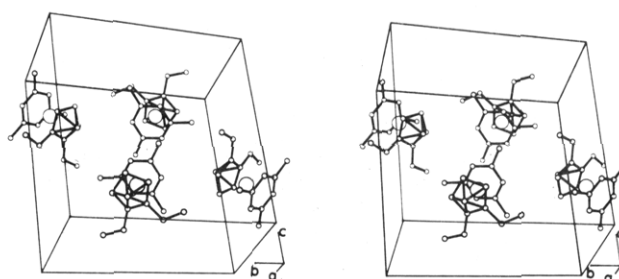
Figure 6. Unit cell packing in **5**.
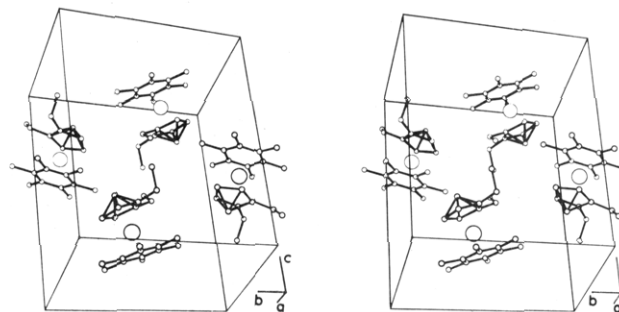
Figure 7. Unit cell packing in **6**.

paper.[6a] In order to more precisely establish the details of molecular structure in these prototype complexes, we conducted X-ray crystallographic studies on **4–6**.

X-ray Structure Determinations on $(\eta^6\text{-}C_6H_6)Fe$-$[(C_2H_5)_2C_2B_4H_4]$ (**4**), $[\eta^6\text{-}C_6(CH_3)_3H_3]Fe[(C_2H_5)_2C_2B_4H_4]$ (**5**), **and** $[\eta^6\text{-}C_6(CH_3)_6]Fe[(C_2H_5)_2C_2B_4H_4]$ (**6**). Stereo drawings of the molecular structures and crystal packing are presented in Figures 2–7, and relevant crystallographic data are given in Tables IV–XII. As it happens, the benzene complex **4** crystallizes with two independent molecules in the asymmetric unit (see below), so that the three compounds in fact provide four different molecular structures for comparison. Each species incorporates a seven-vertex FeC_2B_4 closo polyhedron (pentagonal bipyramid) with iron in one apex, analogous in major respects to the structures of **1**[6a] and other previously reported MC_2B_4 closo systems in which M is a first-row transition metal.[5,6b] In all four molecules in the present study, the ethyl groups attached to the cage carbon atoms are deflected out of the C_2B_3 (equatorial) plane in a direction away from the metal; the methylene carbons are, on the average, ~0.2 Å (~7°) from this plane, with the methyl carbons bent still further out (see Figures 2–4). Steric interactions between the C_2H_5 groups and the arene ligands

Table IV. Experimental Parameters and Crystal Data

	4	5	6
M_r	264[a]	306	348
space group	Pbca	$P2_1/n$	$P2_1/n$
a, Å	14.187 (5)	7.610 (2)	8.892 (1)
b, Å	15.796 (6)	14.646 (4)	13.250 (1)
c, Å	24.714 (10)	15.348 (7)	16.547 (4)
β, deg		95.95 (4)	98.51 (2)
V, Å³	5538	1701	1928
μ, cm⁻¹	10.9	8.9	8.0
D(calcd), g/cm³	1.26	1.19	1.20
A^b	0.60		
B^b	0.30		
max trans coeff[c]	0.873		
min trans coeff	0.704		
2θ range, deg	1.5–50	1–52	1–52
reflctns obsd.	4284	2888	3193
reflctns refined	3124	2105	2424
R	0.069	0.063	0.047
R_w	0.071	0.072	0.052
esd unit wt	2.3	2.2	1.7
Z	8	4	4

[a] Two molecules/asymmetric unit. [b] For explanation see ref 11. [c] Crystal dimensions (mm from centroid): 100 (0.115), $\bar{1}$00 (0.115), 010 (0.35), 0$\bar{1}$0 (0.35), 01$\bar{1}$ (0.46), 0$\bar{1}$1 (0.46), 011 (0.52), 0$\bar{1}\bar{1}$ (0.52).

may be a factor in this bending, but electronic effects are also likely to be important, as suggested by several recent theoretical treatments of out-of-plane C–H bending in transition metal–cyclic hydrocarbon π complexes.[8]

Our primary interest in the structures of **4–6** is centered on the arene rings and their steric relationship to the metal and carborane ligand. First, we offer several general observations. As expected, the C_6 rings are planar within experimental error in all cases (maximum deviation 0.025 Å), and except for two anomalously low values in one of the independent molecules of **4** (<1.3 Å) the ring C–C and Fe–ring C distances are normal and show no large or systematic variations. With the iron approximately centered over the ring in each species and ~1.55 Å from the C_6 plane (see Table XII for exact values), all of these compounds are true (η^6-arene)metal sandwich complexes. In the 1,3,5-trimethylbenzene compound **5**, the methyl carbon atoms are bent out-of-plane by an average 0.035 Å (1.3°) *toward* the metal; this observation is roughly in accord with theoretical predictions of C–H bending in (benzene) metal complexes[8] if we assume that such findings can be extrapolated to include methyl-substituted benzenes. However, in the hexamethylbenzene species **6**, the average deviation of methyl carbons is only 0.012 Å (toward iron) and one of the methyls [C(5RM)] is actually bent *away* from the metal by 0.036 Å. The small size of these effects and the possibility that crystal packing forces may be significant here preclude further discussion on this point.

The most interesting features of these structures, in our view, are the orientations of the C_6 rings with respect to the carborane ligands. Discussion of the ring conformations must be in an approximate rather than an exact sense because of the large thermal motions of the rings (especially in **4**) that are typical of arene and $C_5H_5^-$ ligands in metal π complexes. Nevertheless, the orientations are sufficiently well-defined to reveal some clear patterns. In Figure 8 the arene and carborane rings in each molecule are projected onto a common plane. The two crystallographically independent molecules of the benzene complex

---

(8) Jemmis, E. D.; Schleyer, P. v. R. *J. Am. Chem. Soc.* **1982**, *104*, 4781 and references cited therein.

Table V. Positional Parameters for $(C_6H_6)Fe[(C_2H_5)_2C_2B_4H_4]$

atom	x	y	z
Fe	0.11513 (8)	0.23990 (8)	−0.06989 (4)
Fe'	0.18914 (8)	−0.01266 (7)	0.17588 (4)
C(1R)	0.0907 (9)	0.2901 (9)	0.0053 (4)
C(2R)	0.0985 (8)	0.1981 (11)	0.0089 (4)
C(3R)	0.0418 (9)	0.1529 (8)	−0.0253 (5)
C(4R)	−0.0163 (7)	0.1893 (10)	−0.0561 (4)
C(5R)	−0.0230 (8)	0.2683 (11)	−0.0604 (4)
C(6R)	0.0281 (10)	0.3232 (8)	−0.0330 (5)
C(1R)'	0.0464 (7)	−0.209 (7)	0.1789 (4)
C(2R)'	0.0700 (7)	0.0582 (7)	0.1943 (4)
C(3R)'	0.1354 (8)	0.0698 (6)	0.2347 (4)
C(4R)'	0.1759 (8)	−0.0028 (10)	0.2600 (3)
C(5R)'	0.1441 (9)	−0.0851 (7)	0.2408 (4)
C(6R)'	0.0800 (9)	−0.0911 (7)	0.2002 (4)
C(2)	0.2476 (7)	0.1987 (6)	−0.0867 (3)
C(2M)	0.3230 (8)	0.1521 (8)	−0.0537 (5)
C(3)	0.2425 (6)	0.2909 (6)	−0.0870 (3)
C(3M)	0.3109 (8)	0.3467 (8)	−0.0564 (4)
C(3E)	0.3861 (8)	0.3864 (8)	−0.0884 (5)
C(2)'	0.3179 (6)	−0.0647 (6)	0.1591 (3)
C(2M)'	0.3881 (9)	−0.1191 (8)	0.1889 (4)
C(3)'	0.3236 (5)	0.0283 (6)	0.1613 (3)
C(3M)'	0.3978 (7)	0.0738 (7)	0.1945 (4)
C(3E)'	0.3778 (8)	0.1627 (7)	0.2093 (5)
C(2E)[a]	0.329 (2)	0.068 (1)	−0.0579 (9)
C(2F)[b]	0.390 (2)	0.104 (2)	−0.0828 (13)
C(2G)[c]	0.378 (4)	0.067 (3)	−0.0701 (21)
C(2E)'[d]	0.421 (2)	−0.195 (2)	0.1747 (10)
C(2F)'[e]	0.377 (2)	−0.209 (2)	0.1807 (12)
C(2G)'[f]	0.465 (2)	−0.157 (2)	0.1667 (13)
B(4)	0.1703 (9)	0.3253 (7)	−0.1280 (4)
B(5)	0.1257 (8)	0.2392 (8)	−0.1569 (3)
B(6)	0.1791 (9)	0.1587 (7)	−0.1284 (4)
B(7)	0.2432 (8)	0.2443 (9)	−0.1521 (4)
B(4)'	0.2553 (8)	0.0716 (6)	0.1198 (4)
B(5)'	0.2006 (7)	−0.0092 (7)	0.0884 (3)
B(6)'	0.2450 (7)	−0.0962 (7)	0.1164 (4)
B(7)'	0.3199 (8)	−0.0137 (8)	0.0946 (4)
H(1R)	0.139 (6)	0.317 (6)	0.024 (4)
H(2R)	0.138 (6)	0.164 (5)	0.028 (3)
H(3R)	0.046 (7)	0.081 (6)	−0.028 (4)
H(4R)	−0.063 (6)	0.158 (5)	−0.080 (3)
H(5R)	−0.065 (6)	0.307 (5)	−0.082 (3)
H(6R)	0.040 (7)	0.396 (6)	−0.028 (4)
H(1R)'	−0.000 (6)	−0.032 (5)	0.152 (3)
H(2R)'	0.040 (5)	0.107 (5)	0.174 (3)
H(3R)'	0.157 (5)	0.126 (4)	0.245 (3)
H(4R)'	0.233 (7)	0.013 (6)	0.284 (3)
H(5R)'	0.180 (6)	−0.137 (5)	0.258 (3)
H(6R)'	0.067 (6)	−0.153 (5)	0.190 (3)
H(4)	0.165 (5)	0.401 (4)	−0.134 (3)
H(5)	0.073 (5)	0.238 (5)	−0.187 (3)
H(6)	0.182 (5)	0.084 (5)	−0.130 (3)
H(7)	0.299 (5)	0.251 (5)	−0.176 (3)
H(4)'	0.249 (5)	0.138 (4)	0.109 (3)
H(5)'	0.141 (5)	−0.003 (5)	0.057 (3)
H(6)'	0.231 (5)	−0.168 (4)	0.109 (3)
H(7)'	0.397 (5)	−0.011 (4)	0.064 (3)
H(31M)	0.276 (6)	0.394 (5)	−0.045 (3)
H(32M)	0.334 (5)	0.317 (5)	−0.030 (3)
H(21M)'	0.392 (5)	−0.105 (5)	0.220 (3)
H(31M)'	0.409 (6)	0.035 (5)	0.223 (3)
H(32M)'	0.460 (5)	0.070 (5)	0.177 (3)
H(31E)'	0.318 (6)	0.171 (5)	0.229 (3)
H(32E)'	0.434 (6)	0.187 (5)	0.237 (3)
H(33E)'	0.370 (7)	0.210 (6)	0.179 (4)

[a] Mult = 0.43. [b] Mult = 0.37. [c] Mult = 0.20. [d] Mult = 0.40. [e] Mult = 0.30. [f] Mult = 0.30.

4 (labeled A and B) are seen to differ in their ring carborane conformations: in molecule B, the benzene is "staggered" with respect to the carbon–carbon edge [C-(2)–C(3)], while in molecule A the benzene is "eclipsed" in the sense that one of the C–C edges in the C_6 ring is

Table VI. Positional Parameters for
$[C_6(CH_3)_3H_3]Fe[(C_2H_5)_2C_2B_4H_4]$

atom	x	y	z
Fe	0.10253 (8)	0.09630 (4)	0.22154 (5)
C(1R)	−0.0989 (7)	0.1295 (4)	0.1235 (4)
C(2R)	−0.1641 (7)	0.0678 (4)	0.1832 (4)
C(3R)	−0.0783 (7)	−0.0141 (3)	0.2080 (4)
C(4R)	0.0763 (8)	−0.0349 (4)	0.1698 (4)
C(5R)	0.1516 (8)	0.0227 (4)	0.1109 (4)
C(6R)	0.0571 (8)	0.1054 (4)	0.0871 (4)
C(1RM)	−0.1916 (9)	0.2177 (5)	0.1020 (4)
C(3RM)	−0.1486 (10)	−0.0762 (4)	0.2722 (6)
C(2)	0.2022 (8)	0.0833 (3)	0.3423 (4)
C(2M)	0.2161 (9)	0.0117 (5)	0.4193 (4)
C(2E)	0.3407 (11)	−0.0675 (5)	0.4162 (5)
C(3)	0.0945 (7)	0.1581 (4)	0.3418 (4)
C(3M)	−0.0441 (8)	0.1642 (4)	0.4070 (4)
C(3E)	−0.1530 (11)	0.2435 (6)	0.4037 (6)
C(5RM)	0.3169 (11)	−0.0005 (6)	0.0735 (5)
B(4)	0.1353 (9)	0.2301 (4)	0.2714 (5)
B(5)	0.3164 (8)	0.1912 (4)	0.2317 (5)
B(6)	0.3655 (7)	0.0953 (5)	0.2832 (4)
B(7)	0.3143 (9)	0.1919 (5)	0.3430 (5)
H(4)	0.066 (7)	0.291 (4)	0.269 (3)
H(5)	0.392 (7)	0.223 (4)	0.179 (3)
H(6)	0.462 (7)	0.046 (4)	0.285 (3)
H(7)	0.372 (8)	0.213 (4)	0.397 (4)
H(1R1)	−0.247 (8)	0.236 (4)	0.148 (4)
H(1R2)	−0.279 (8)	0.206 (4)	0.053 (4)
H(1R3)	−0.111 (8)	0.260 (4)	0.084 (4)
H(2R)	−0.260 (7)	0.083 (4)	0.212 (3)
H(3R1)	−0.035 (8)	−0.108 (4)	0.308 (4)
H(3R2)	−0.205 (8)	−0.040 (4)	0.314 (4)
H(3R3)	−0.223 (9)	−0.108 (5)	0.249 (4)
H(4R)	0.138 (7)	−0.087 (4)	0.184 (3)
H(5R1)	0.381 (6)	0.048 (3)	0.072 (3)
H(5R2)	0.303 (7)	0.020 (4)	0.033 (3)
H(5R3)	0.358 (6)	−0.032 (3)	0.106 (3)
H(6R)	0.095 (7)	0.144 (4)	0.049 (3)
H(2M1)	0.101 (7)	−0.009 (4)	0.419 (3)
H(2M2)	0.242 (7)	0.042 (4)	0.471 (4)
H(2E1)	0.450 (7)	−0.043 (4)	0.405 (4)
H(2E2)	0.289 (8)	−0.104 (4)	0.364 (4)
H(2E3)	0.345 (8)	−0.102 (4)	0.465 (4)
H(3M1)	0.010 (8)	0.161 (4)	0.468 (4)
H(3M2)	−0.110 (6)	0.105 (4)	0.397 (3)
H(3E1)	−0.073 (7)	0.298 (4)	0.404 (4)
H(3E2)	−0.218 (9)	0.246 (5)	0.451 (4)
H(3E3)	−0.206 (8)	0.239 (4)	0.354 (4)

Table VII. Positional Parameters for
$[C_6(CH_3)_6]Fe[(C_2H_5)_2C_2B_4H_4]$

atom	x	y	z
Fe	0.04291 (7)	0.13290 (5)	0.32014 (4)
C(1R)	−0.1098 (6)	0.1588 (4)	0.4012 (3)
C(2R)	0.0349 (7)	0.1982 (4)	0.4337 (3)
C(3R)	0.1645 (6)	0.1353 (5)	0.4381 (3)
C(4R)	0.1493 (6)	0.0347 (4)	0.4118 (3)
C(5R)	0.0059 (7)	−0.0038 (4)	0.3812 (3)
C(6R)	−0.1223 (6)	0.0573 (4)	0.3754 (3)
C(1RM)	−0.2459 (8)	0.2284 (7)	0.3939 (5)
C(2RM)	0.0535 (13)	0.3060 (5)	0.4613 (4)
C(3RM)	0.3190 (8)	0.1804 (8)	0.4713 (4)
C(4RM)	0.2850 (9)	−0.0345 (6)	0.4168 (4)
C(5RM)	−0.0085 (12)	−0.1133 (5)	0.3549 (4)
C(6RM)	−0.2767 (8)	0.0173 (7)	0.3402 (5)
C(2)	0.1785 (5)	0.1179 (4)	0.2303 (3)
C(2M)	0.3098 (6)	0.0505 (5)	0.2185 (3)
C(2E)	0.3837 (7)	0.0795 (6)	0.1451 (4)
C(3)	0.0191 (6)	0.0914 (4)	0.1983 (3)
C(3M)	−0.0198 (9)	−0.0073 (5)	0.1525 (3)
C(3E)[a]	−0.142 (2)	0.008 (1)	0.076 (1)
C(3F)[b]	−0.175 (2)	−0.009 (2)	0.109 (1)
C(3G)[c]	−0.058 (2)	−0.014 (2)	0.069 (1)
B(4)	−0.0927 (7)	0.1793 (5)	0.2093 (4)
B(5)	0.0172 (8)	0.2724 (5)	0.2519 (4)
B(6)	0.1903 (7)	0.2275 (5)	0.2651 (4)
B(7)	0.0757 (8)	0.2119 (5)	0.1695 (4)
H(4)	−0.225 (5)	0.169 (4)	0.192 (3)
H(5)	−0.032 (5)	0.352 (4)	0.267 (3)
H(6)	0.325 (5)	0.247 (4)	0.286 (3)
H(7)	0.096 (5)	0.225 (4)	0.106 (3)
H(2M1)	0.270 (5)	−0.034 (4)	0.215 (3)
H(2M2)	0.389 (5)	0.045 (4)	0.266 (3)
H(2E1)	0.297 (5)	0.087 (4)	0.089 (3)
H(2E2)	0.463 (5)	0.037 (4)	0.141 (3)
H(2E3)	0.428 (5)	0.145 (4)	0.148 (3)
H(1R1)	−0.315 (6)	0.172 (4)	0.383 (3)
H(1R2)	−0.270 (6)	0.272 (4)	0.348 (3)
H(1R3)	−0.268 (6)	0.260 (4)	0.438 (3)
H(2R1)	0.098 (6)	0.310 (4)	0.516 (3)
H(2R2)	−0.048 (6)	0.339 (5)	0.452 (3)
H(2R3)	0.120 (6)	0.345 (4)	0.429 (3)
H(3R1)	0.337 (5)	0.245 (4)	0.431 (3)
H(3R2)	0.395 (6)	0.134 (4)	0.466 (3)
H(3R3)	0.332 (6)	0.195 (4)	0.527 (3)
H(4R1)	0.297 (6)	−0.079 (4)	0.450 (3)
H(4R2)	0.371 (6)	0.009 (4)	0.427 (3)
H(4R3)	0.282 (6)	−0.071 (4)	0.360 (3)
H(5R1)	−0.033 (6)	−0.165 (4)	0.394 (3)
H(5R2)	0.082 (6)	−0.133 (4)	0.334 (3)
H(5R3)	−0.085 (6)	−0.120 (4)	0.307 (3)
H(6R1)	−0.358 (5)	0.010 (4)	0.376 (3)
H(6R2)	−0.261 (6)	−0.053 (4)	0.319 (3)
H(6R3)	−0.311 (6)	0.053 (4)	0.293 (3)

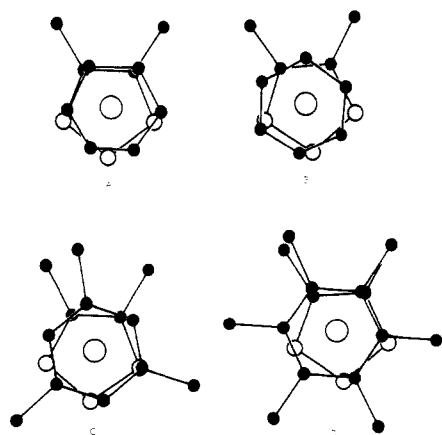[a] Mult = 0.40. [b] Mult = 0.31. [c] Mult = 0.29.

Figure 8. Projections of arene rings onto carborane C_2B_3 equatorial planes in 4, 5, and 6. Carbon atoms are shown as solid circles and boron atoms as open circles. A and B depict the independent molecules (A and B, respectively) in 4; C and D represent 5 and 6, respectively. Ethyl carbons C(2E) and C(3E) are omitted in each case.

nearly parallel to C(2)–C(3).[9] This clear difference accounts for the unexpected observation of two molecules

in the asymmetric unit. In the trimethylbenzene complex 5, the conformation is staggered with respect to C(2)–C(3), though not symmetric in that the nearest arene carbon [C(3R)] is closer to C(2) than to C(3). The hexamethylbenzene species 6 displays a nearly eclipsed arrangement, the C(4R)–C(5R) and C(2)–C(3) edges being close to parallel (Figure 8D).

It is possible to account for these findings in a qualitative way by invoking symmetry arguments, if it is assumed that in each case the most favorable conformation will have an approximate plane of symmetry. In the benzene complex, such a plane can be achieved in both the eclipsed and staggered arrangements; the fact that both forms are equally present in the crystal suggests that they are closely

(9) The terms "eclipsed" and "staggered" as used here are defined in terms of the C(2)–C(3) edge, a unique geometric feature of the equatorial carborane ring.

Table VIII. Bond Distances (A) in $(\eta^6\text{-arene})\text{Fe}[(C_2H_5)_2C_2B_4H_4]$

	4 (arene = C_6H_6)		5	6
	molecule A[a]	molecule B[b]	(arene = $C_6(CH_3)_3H_3$)	(arene = $C_6(CH_3)_6$)
	Hydrocarbon Ligand			
Fe-C(1R)	2.050 (5)	2.031 (5)	2.091 (3)	2.074 (3)
Fe-C(2R)	2.069 (6)	2.078 (5)	2.095 (3)	2.079 (3)
Fe-C(3R)	2.046 (6)	2.096 (5)	2.120 (3)	2.087 (3)
Fe-C(4R)	2.058 (7)	2.093 (4)	2.082 (3)	2.113 (3)
Fe-C(5R)	2.024 (8)	2.072 (5)	2.077 (3)	2.124 (3)
Fe-C(6R)	2.022 (7)	2.073 (6)	2.061 (3)	2.096 (3)
⟨Fe-C⟩	2.045	2.074	2.088	2.096
C(1R)-C(2R)	1.461 (12)	1.347 (7)	1.413 (4)	1.418 (5)
C(1R)-C(6R)	1.398 (13)	1.317 (8)	1.408 (4)	1.411 (6)
C(2R)-C(3R)	1.367 (12)	1.376 (7)	1.399 (4)	1.415 (5)
C(3R)-C(4R)	1.260 (11)	1.426 (9)	1.402 (5)	1.402 (6)
C(4R)-C(5R)	1.257 (11)	1.456 (9)	1.402 (5)	1.397 (5)
C(5R)-C(6R)	1.318 (13)	1.357 (9)	1.436 (5)	1.390 (5)
⟨C-C$_{ring}$⟩	1.344	1.380	1.410	1.406
C(1R)-C(1RM)			1.492 (5)	1.511 (6)
C(2R)-C(2RM)				1.502 (6)
C(3R)-C(3RM)			1.482 (5)	1.525 (5)
C(4R)-C(4RM)				1.509 (5)
C(5R)-C(5RM)			1.475 (6)	1.514 (5)
C(6R)-C(6RM)				1.507 (5)
⟨C$_{ring}$-H⟩		1.02	0.90	
⟨C$_{alkyl}$-H⟩		0.96	0.91	0.98
	Ferracarborane Cage			
Fe-C(2)	2.031 (5)	2.046 (4)	1.938 (4)	2.057 (3)
Fe-C(3)	2.023 (4)	2.047 (4)	2.062 (3)	2.079 (3)
Fe-B(4)	2.119 (5)	2.139 (5)	2.109 (3)	2.132 (4)
Fe-B(5)	2.155 (4)	2.169 (4)	2.134 (3)	2.160 (4)
Fe-B(6)	2.136 (5)	2.128 (5)	2.123 (3)	2.115 (4)
C(2)-C(2M)	1.533 (7)	1.508 (6)	1.575 (5)	1.505 (5)
C(2M)-C(2E)	1.338 (14)	1.332 (14)	1.502 (5)	1.514 (5)
C(2M)-C(2F)	1.418 (19)	1.449 (17)		
C(2M)-C(2G)	1.603 (33)	1.354 (17)		
C(2)-C(3)	1.459 (6)	1.472 (6)	1.367 (4)	1.480 (4)
C(2)-B(6)	1.551 (7)	1.559 (6)	1.622 (4)	1.561 (5)
C(2)-B(7)	1.770 (6)	1.785 (6)	1.804 (5)	1.769 (5)
C(3)-C(3M)	1.514 (6)	1.514 (6)	1.530 (4)	1.526 (5)
C(3M)-C(3E)	1.468 (7)	1.479 (8)	1.425 (6)	1.554 (14)
C(3M)-C(3F)				1.463 (15)
C(3M)-C(3G)				1.382 (16)
C(3)-B(4)	1.540 (7)	1.569 (6)	1.564 (5)	1.559 (5)
C(3)-B(7)	1.770 (6)	1.778 (6)	1.743 (5)	1.761 (5)
B(4)-B(5)	1.661 (8)	1.684 (7)	1.663 (5)	1.664 (6)
B(4)-B(7)	1.750 (9)	1.745 (8)	1.751 (6)	1.776 (6)
B(5)-B(6)	1.639 (8)	1.662 (7)	1.637 (6)	1.634 (6)
B(5)-B(7)	1.673 (8)	1.702 (7)	1.710 (6)	1.727 (6)
B(6)-B(7)	1.731 (8)	1.766 (8)	1.752 (6)	1.764 (6)
⟨B-H⟩		1.14	1.04	1.17

[a] Atom labels unprimed. [b] Atom labels primed.

comparable in energy. Significantly, the only symmetric arrangement possible in the trimethylbenzene complex is the staggered one; despite the deviation from ideal mirror symmetry, which can be attributed to crystal packing, the observed conformation (Figure 8) is much closer to the staggered than to the eclipsed arrangement.

In the hexamethylbenzene species 6, mirror symmetry could be achieved in either eclipsed or staggered geometries, but only the (nearly) eclipsed form is observed, in contrast to the benzene complex. In 6, however, the difference in energy between eclipsed and staggered forms is likely to be larger than in the benzene species owing to steric interactions between the six methyl substituents and the ethyl groups in the former. Hence it appears that the eclipsed conformation in 6 is favored. A simple rationale for this finding rests on the fact that, in the eclipsed form, there are two "close" interactions between the carboranyl ethyl groups and the $C_6(CH_3)_6$ methyls, whereas in the staggered arrangement there would be four (each C_2H_5 unit lying relatively near two CH_3 groups). In this event, the

eclipsed arrangement offers a means of minimizing the energy of interaction.

This discussion of ring conformations in the (arene)-iron(carborane) complexes is necessarily limited to the solid state; in solution, free rotation of the arene ligands is assumed but NMR data are inconclusive on this point, as discussed elsewhere.[10] Certainly, the arene–carborane distances are sufficiently large that rotational energy barriers caused by steric contacts would be quite small and unlikely to be significant in solution.

Experimental Section

Materials and Instrumentation. $(\eta^6\text{-1,3,5-Cyclo-octatriene})\text{iron(diethyldicarbahexaborane)}$, $(C_8H_{10})\text{Fe}[(C_2H_5)_2\text{-}C_2B_4H_4]$, was prepared as described in the preceding article.[6a]

(10) Boron-11 and proton NMR spectra of metallacarboranes involving $R_2C_2B_4H_4{}^{2-}$ ligands usually do not distinguish between different rotamers; see: Borodinsky, L.; Grimes, R. N. *Inorg. Chem.* **1982**, *21*, 1921. Hosmane, N. S.; Grimes, R. N. *Ibid.* **1980**, *19*, 3482.

Table IX. Bond Angles (deg) for $(C_6H_6)Fe[(C_2H_5)_2C_2B_4H_4]$[a]

C(2R)	C(1R)	C(6R)	117.5 (7)	Fe	B(4)	B(7)	89.1 (2)
C(1R)	C(2R)	C(3R)	115.9 (7)	C(3)	B(4)	B(5)	104.4 (4)
C(2R)	C(3R)	C(4R)	121.3 (9)	Fe	B(5)	B(7)	89.9 (2)
C(3R)	C(4R)	C(5R)	123.6 (9)	B(4)	B(5)	B(6)	105.9 (4)
C(4R)	C(5R)	C(6R)	124.7 (9)	Fe	B(6)	B(7)	89.0 (2)
C(1R)	C(6R)	C(5R)	116.8 (8)	C(2)	B(6)	B(5)	105.0 (4)
C(2R)'	C(1R)'	C(6R)'	125.3 (6)	Fe'	C(2)'	C(2M)'	136.0 (2)
C(1R)'	C(2R)'	C(3R)'	119.7 (5)	Fe'	C(2)'	B(7)'	90.8 (2)
C(2R)'	C(3R)'	C(4R)'	118.8 (5)	C(2M)'	C(2)'	C(3)'	121.0 (4)
C(3R)'	C(4R)'	C(5R)'	116.8 (5)	C(2M)'	C(2)'	B(6)'	125.9 (4)
C(4R)'	C(5R)'	C(6R)'	120.7 (6)	C(2M)'	C(2)'	B(7)'	133.1 (4)
C(1R)'	C(6R)'	C(5R)'	118.6 (6)	C(3)'	C(2)'	B(6)'	112.4 (4)
Fe	C(2)	C(2M)	133.7 (2)	C(2)'	C(2M)'	C(2E)'	128.0 (8)
Fe	C(2)	B(7)	91.4 (2)	C(2)'	C(2M)'	C(2F)'	115.0 (8)
C(2M)	C(2)	C(3)	121.1 (5)	C(2)'	C(2M)'	C(2G)'	125.6 (9)
C(2M)	C(2)	B(6)	126.5 (5)	Fe'	C(3)'	C(3M)'	134.6 (2)
C(2M)	C(2)	B(7)	134.8 (4)	Fe	C(3)'	B(7)'	91.0 (2)
C(3)	C(2)	B(6)	111.9 (4)	C(2)'	C(3)'	C(3M)'	122.2 (4)
C(2)	C(2M)	C(2E)	118.8 (8)	C(2)'	C(3)'	B(4)'	112.1 (4)
C(2)	C(2M)	C(2F)	117.4 (9)	C(3M)'	C(3)'	B(4)'	125.1 (4)
C(2)	C(2M)	C(2G)	127.3 (3)	C(3M)'	C(3)'	B(7)'	134.3 (4)
Fe	C(3)	C(3M)	134.5 (2)	C(3)'	C(3M)'	C(3E)'	116.8 (5)
Fe	C(3)	B(7)	91.7 (2)	Fe'	B(4)'	B(7)'	88.9 (2)
C(2)	C(3)	C(3M)	123.2 (5)	C(3)'	B(4)'	B(5)'	104.8 (4)
C(2)	C(3)	B(4)	112.8 (4)	Fe'	B(5)'	B(7)'	89.0 (2)
C(3M)	C(3)	B(4)	123.4 (5)	B(4)'	B(5)'	B(6)'	105.1 (4)
C(3M)	C(3)	B(7)	133.9 (4)	Fe'	B(6)'	B(7)'	88.7 (2)
C(3)	C(3M)	C(3E)	116.4 (5)	C(2)'	B(6)'	B(5)'	105.6 (4)

[a] Molecule A, unprimed labels; molecule B, primed labels.

Table X. Bond Angles (deg) for $[C_6(CH_3)_3H_3]Fe[(C_2H_5)_2C_2B_4H_4]$

Fe	C(1R)	C(1RM)	131.0 (3)	C(2M)	C(2)	B(6)	119.7 (3)
C(2R)	C(1R)	C(6R)	117.6 (3)	C(2M)	C(2)	B(7)	126.0 (4)
C(2R)	C(1R)	C(1RM)	120.5 (3)	C(3)	C(2)	B(6)	113.8 (3)
C(6R)	C(1R)	C(1RM)	121.9 (3)	C(2)	C(2M)	C(2E)	118.9 (3)
C(1R)	C(2R)	C(3R)	122.7 (3)	Fe	C(3)	C(3M)	134.2 (2)
Fe	C(3R)	C(3RM)	132.7 (3)	Fe	C(3)	B(7)	91.0 (2)
C(2R)	C(3R)	C(4R)	117.4 (3)	C(2)	C(3)	C(3M)	119.8 (3)
C(2R)	C(3R)	C(3RM)	121.2 (3)	C(2)	C(3)	B(4)	112.5 (3)
C(4R)	C(3R)	C(3RM)	121.4 (3)	C(3M)	C(3)	B(4)	127.8 (3)
C(3R)	C(4R)	C(5R)	123.7 (3)	C(3M)	C(3)	B(7)	134.6 (3)
Fe	C(5R)	C(5RM)	132.1 (3)	C(3)	C(3M)	C(3E)	117.5 (3)
C(4R)	C(5R)	C(6R)	116.4 (3)	Fe	B(4)	B(7)	89.2 (2)
C(4R)	C(5R)	C(5RM)	122.3 (4)	C(3)	B(4)	B(5)	104.7 (3)
C(6R)	C(5R)	C(5RM)	121.3 (4)	Fe	B(5)	B(7)	89.4 (2)
C(1R)	C(6R)	C(5R)	122.1 (3)	B(4)	B(5)	B(6)	105.8 (3)
Fe	C(2)	C(2M)	140.5 (3)	Fe	B(6)	B(7)	88.7 (2)
Fe	C(2)	B(7)	93.3 (2)	C(2)	B(6)	B(5)	102.3 (3)
C(2M)	C(2)	C(3)	122.1 (3)				

Table XI. Bond Angles (deg) for $[C_6(CH_3)_6]Fe[(C_2H_5)_2C_2B_4H_4]$

Fe	C(1R)	C(1RM)	129.9 (3)	C(5R)	C(6R)	C(6RM)	120.8 (5)
C(2R)	C(1R)	C(6R)	119.4 (3)	Fe	C(2)	C(2M)	134.4 (2)
C(2R)	C(1R)	C(1RM)	118.5 (5)	Fe	C(2)	B(7)	92.0 (2)
C(6R)	C(1R)	C(1RM)	122.1 (5)	C(2M)	C(2)	C(3)	122.2 (3)
Fe	C(2R)	C(2RM)	130.8 (3)	C(2M)	C(2)	B(6)	126.0 (3)
C(1R)	C(2R)	C(3R)	119.3 (3)	C(2M)	C(2)	B(7)	133.5 (3)
C(1R)	C(2R)	C(2RM)	121.2 (5)	C(3)	C(2)	B(6)	111.2 (3)
C(3R)	C(2R)	C(2RM)	119.5 (5)	C(2)	C(2M)	C(2E)	113.0 (3)
Fe	C(3R)	C(3RM)	131.1 (3)	Fe	C(3)	C(3M)	134.0 (2)
C(2R)	C(3R)	C(4R)	120.2 (3)	Fe	C(3)	B(7)	91.8 (2)
C(2R)	C(3R)	C(3RM)	118.2 (5)	C(2)	C(3)	C(3M)	121.0 (4)
C(4R)	C(3R)	C(3RM)	121.6 (5)	C(2)	C(3)	B(4)	112.0 (3)
Fe	C(4R)	C(4RM)	133.1 (3)	C(3M)	C(3)	B(4)	126.7 (3)
C(3R)	C(4R)	C(5R)	120.1 (3)	C(3M)	C(3)	B(7)	134.1 (3)
C(3R)	C(4R)	C(4RM)	121.4 (4)	C(3)	C(3M)	C(3E)	111.7 (6)
C(5R)	C(4R)	C(4RM)	118.5 (4)	C(3)	C(3M)	C(3F)	112.6 (7)
Fe	C(5R)	C(5RM)	133.9 (3)	C(3)	C(3M)	C(3G)	123.7 (8)
C(4R)	C(5R)	C(6R)	120.4 (3)	Fe	B(4)	B(7)	89.4 (2)
C(4R)	C(5R)	C(5RM)	119.2 (5)	C(3)	B(4)	B(5)	105.0 (3)
C(6R)	C(5R)	C(5RM)	120.3 (5)	Fe	B(5)	B(7)	89.7 (2)
Fe	C(6R)	C(6RM)	131.0 (3)	B(4)	B(5)	B(6)	105.7 (3)
C(1R)	C(6R)	C(5R)	120.5 (3)	Fe	B(6)	B(7)	90.2 (2)
C(1R)	C(6R)	C(6RM)	118.6 (5)	C(2)	B(6)	B(5)	106.1 (3)

Table XII. Selected Mean Planes

atom	dev, A	atom	dev, A

Planes in $(C_6H_6)Fe[(C_2H_5)_2C_2B_4H_4]$ (4)

Plane 1: Benzene Ring (Molecule A)

$-0.7063x + 0.0013y - 0.7060z = 0.8399$

C(1R)	−0.019	C(5R)	−0.008
C(2R)	−0.004	C(6R)	0.025
C(3R)	0.024	Fe	1.541
C(4R)	−0.019		

Plane 2: C_2B_3 Ring (Molecule A)

$0.7137x + 0.0357y - 0.6995z = 4.1208$

C(2)	−0.003	B(6)	0.002
C(3)	0.002	Fe	−1.611
B(4)	−0.001	C(2M)	0.165
B(5)	−0.001	C(3M)	0.198

Plane 3: Benzene Ring (Molecule B)

$0.7370x - 0.0010y - 0.6759z = -2.5088$

C(1R)'	0.005	C(5R)'	−0.006
C(2R)'	−0.007	C(6R)'	0.002
C(3R)'	0.002	Fe'	1.548
C(4R)'	0.004		

Plane 4: C_2B_3 Ring (Molecule B)

$0.7201x - 0.0164y - 0.6937x = 0.5349$

C(2)'	0.003	B(6)'	−0.002
C(3)'	−0.002	Fe'	−1.615
B(4)'	0.000	C(2M)'	0.223
B(5)'	0.001	C(3M)'	0.176

Planes in $[C_6(CH_3)_3H_3]Fe[(C_2H_5)_2C_2B_4H_4]$ (5)

Plane 5: Benzene Ring

$0.4591x + 0.4676y + 0.7554z = 1.8715$

C(1R)	−0.004	C(6R)	0.009
C(2R)	0.002	Fe	−1.539
C(3R)	−0.005	C(1RM)	−0.051
C(4R)	0.010	C(3RM)	−0.028
C(5R)	−0.012	C(5RM)	−0.027

Plane 6: C_2B_3 Ring

$0.4977x + 0.4752y + 0.7256z = 4.9237$

C(2)	0.057	B(6)	−0.037
C(3)	−0.050	Fe	1.587
B(4)	0.019	C(2M)	−0.289
B(5)	0.011	C(3M)	−0.238

Planes in $[C_6(CH_3)_6]Fe[(C_2H_5)_2C_2B_4H_4]$ (6)

Plane 7: Benzene Ring

$0.2728x + 0.2815y - 0.9200z = -5.9875$

C(1R)	0.005	C(1RM)	0.050
C(2R)	−0.007	C(2RM)	0.006
C(3R)	0.003	C(3RM)	0.024
C(4R)	0.004	C(4RM)	−0.002
C(5R)	−0.006	C(5RM)	−0.036
C(6R)	0.002	C(6RM)	0.032
Fe	1.554		

Plane 8: C_2B_3 Ring

$0.2559x + 0.3468y - 0.9024z = -2.5968$

C(2)	−0.001	B(6)	−0.006
C(3)	0.008	Fe	−1.623
B(4)	−0.011	C(2M)	0.170
B(5)	0.010	C(3M)	0.171

Dihedral Angles between Planes

planes	angle, deg	planes	angle, deg
1, 2	2.08	5, 6	2.83
3, 4	1.66	7, 8	2.08

Other reagents and solvents were reagent grade and used as received. NMR, IR, and mass spectra were obtained on instruments listed elsewhere.[6a]

Reaction of $(C_8H_{10})Fe[(C_2H_5)_2C_2B_4H_4]$ (1) with $(CH_3)_4$-$N_2C_2H_4$. A 25-mL round-bottom flask was charged with 47 mg (0.16 mmol) of $(C_8H_{10})Fe[(C_2H_5)_2C_2B_4H_4]$ (1) in 10 mL of benzene

and 1 mL of N,N,N',N'-tetramethyl-1,2-diaminoethane (99%, Aldrich Chemical Co.) was added. The flask was stoppered and stirred at room temperature for 4 days, during which a small amount of white precipitate formed in the orange solution. The reaction mixture was filtered and the filtrate taken to dryness by rotary evaporation. The orange residue was dissolved in 1 mL of methylene chloride and placed on a silica gel TLC plate. Development with 25% methylene chloride in n-hexane produced two orange bands (R_f 0.43 and 0.74). One compound (R_f 0.43) was identified as unreacted 1, while the product (R_f 0.74) was characterized as $(C_8H_{10})Fe[(C_2H_5)_2C_2B_3H_5]$ (2) from its mass spectrum, which exhibits a strong parent grouping consistent with the indicated formula, and its ^{1}H and ^{11}B NMR spectra (Tables I and III). The presence of B–H–B bridges on the open C_2B_3 ring is indicated by a broad, high-field resonance in the ^{1}H NMR spectrum. The yield of 2, a red oil, was 31 mg (68%).

Synthesis of $(\eta^6\text{-}C_6H_6)Fe[(C_2H_5)_2C_2B_4H_4]$ (4) from 1. Dry benzene (100 mL), aluminum powder (0.11 g, 4.1 mmol), and $(C_8H_{10})Fe[(C_2H_5)_2C_2B_4H_4]$ (1, 0.373 g, 1.28 mmol) were placed in a 200-mL round-bottom flask and 0.38 g (2.9 mmol) of $AlCl_3$ was added with stirring. The mixture was refluxed with stirring for 3 h. After the mixture was cooled to room temperature, the benzene was removed by rotary evaporation. The dark residue was extracted with acetone and filtered through 1 cm of silica gel on a sintered glass frit. After the mixture was washed with acetone, the volume of the filtrate was reduced by rotary evaporation to 2 mL. This solution was placed on a silica gel TLC plate and developed with 50% benzene in n-hexane, yielding 0.103 g (0.391 mmol, 30.5%) of $(\eta^6\text{-}C_6H_6)Fe[(C_2H_5)_2C_2B_4H_4]$ (4) as a golden yellow solid: mp 156–157 °C; R_f 0.65. This product is identical with compound II described in the preceding paper, which reports IR and mass spectroscopic data.[6a] No unreacted 1 was detected.

Synthesis of $[\eta^6\text{-}C_6(CH_3)_3H_3]Fe[(C_2H_5)_2C_2B_4H_4]$ (5) from 1. 1,3,5-Trimethylbenzene (5 mL), 0.050 g (1.9 mmol) of aluminum powder, and 0.051 g (0.17 mmol) of 1 were placed in a 25-mL round-bottom flask, and 50 mg (0.38 mmol) of $AlCl_3$ was added with stirring. The reaction mixture was heated in an oil bath at 80 °C for 3 hrs and then cooled to room temperature. Unreacted 1,3,5-trimethylbenzene was removed by rotary evaporation. After 2 mL of methylene chloride was added, the residue was placed on a silica gel TLC plate and developed with 25% methylene chloride in n-hexane to produce pure 5 as a yellow solid: mp 110–112 °C; R_f 0.32; yield 16 mg (0.052 mmol, 30%); IR (KBr pellet) 2980 (s), 2940 (s), 2880 (w), 2850 (w), 2750 (w), 2540 (vvs), 2380 (w), 1830 (w, br), 1650 (w, br), 1540 (m), 1458 (s), 1388 (s), 1330 (w), 1310 (w), 1040 (m), 1015 (m), 970 (w), 925 (w), 880 (s), 820 (m), 800 (m), 735 (m), 703 (m), 615 (w), 590 (sh), 505 (m), 412 (m) cm^{-1}; mass spectrum exhibits a strong parent envelope with a cutoff at m/e 307 corresponding to $^{13}C^{12}C_{14}{}^{56}Fe^{11}B_4{}^1H_{26}{}^+$.

Synthesis of $[\eta^6\text{-}C_6(CH_3)_6]Fe[(C_2H_5)_2C_2B_4H_4]$ (6) from 1. Hexamethylbenzene (0.74 g, 4.6 mmol), cyclohexane (20 mL), 0.10 g (3.7 mmol) of aluminum powder, and 0.180 g (0.618 mmol) of 1 were placed in a 100-mL round-bottom flask, and 0.10 g (0.75 mmol) of $AlCl_3$ was added with stirring. After this mixture was refluxed for 3.5 h and cooled to room temperature, the solution was rotary evaporated to dryness and the residue extracted with 50 mL of acetone. The acetone extract was filtered through 1 cm of silica gel on a sintered glass frit, yielding a yellow solution. The silica gel was washed with acetone until the effluent was colorless, after which the combined filtrates were reduced to a volume of 2 mL by rotary evaporation. Development on a silica gel TLC plate with acetone removed the excess hexamethylbenzene from the crude product. Further development with 25% methylene chloride in n-hexane produced an orange-brown band that was removed and placed on another TLC plate. Development with acetone gave the product as a bright orange solid: mp 204–205 °C; R_f 0.32; yield 0.031 g (0.089 mmol, 14%); IR (KBr pellet) 2980 (s), 2940 (s), 2880 (w), 2530 (sh), 2512 (vvs), 2880 (w), 1630 (w, br), 1455 (s), 1390 (s), 1070 (m), 1018 (m), 960 (w), 918 (w), 884 (s), 825 (w), 800 (w), 730 (m), 675 (w), 612 (w), 515 (w), 450 (w) cm^{-1}; the mass spectrum contains a strong parent envelope with a high-mass cutoff at m/e 349 corresponding to $^{13}C^{12}C_{17}{}^{56}Fe^{11}B_4{}^1H_{32}{}^+$.

Synthesis of $(\eta^6\text{-}C_6H_5CH_3)Fe[(C_2H_5)_2C_2B_4H_4]$ (7) from 1. A 50-mL round-bottom flask was charged with 5 mL of toluene,

50 mg (1.8 mmol) of aluminum powder, and 45 mg (0.15 mmol) of **1**, and 50 mg (0.38 mmol) of $AlCl_3$ was added with stirring. The mixture was heated in an oil bath to 80 °C for 3 h. After the mixture was cooled to room temperature, the toluene was removed by rotary evaporation. The residue was extracted with 2 mL of methylene chloride and developed on a silica gel TLC plate with 50% methylene chloride in *n*-hexane. The product was separated as a yellow solid (R_f 0.54; mp 91–92 °C; yield 7 mg (0.025 mmol, 17%)). Identification was via the mass spectrum and the crystallographic unit cell and space group, which matched data obtained by Sneddon.[3]

X-ray Structure Determinations on $(\eta^6\text{-}C_6H_6)Fe$-$[(C_2H_5)_2C_2B_4H_4]$ (4), $[\eta^6\text{-}C_6(CH_3)_3H_3]Fe[(C_2H_5)_2C_2B_4H_4]$ (5), and $[\eta^6\text{-}C_6(CH_3)_6]Fe[(C_2H_5)_2C_2B_4H_4$ (6). Single crystals of **4** were grown from *n*-pentane solution and of **5** and **6** from acetone solution, by slow evaporation. In each case, selected crystals mounted on glass fibers were examined by precession photography and found acceptable.

Relevant parameters for the data collection and structure determination are given in Table IV. The procedures followed in data collection and processing have been described elsewhere.[11] The space groups indicated were chosen on the basis of systematic absences and chemical and spectroscopic information.

The intensities of three standard reflections, monitored at regular intervals, showed no greater fluctuations during the data collection than those expected from Poisson statistics. The raw intensity data were corrected for Lorentz–polarization effects and in the case of **4** for absorption; the crystals of **5** and **6** were irregular and absorption corrections were not possible. For all three compounds, only those reflections for which $F_o^2 > 3\sigma(F_o^2)$, where $\sigma(F_o^2)$ was estimated from counting statistics ($p = 0.03$)[12] were used in the final refinement of the structural parameters, after averaging for equivalent reflections.

Solution and Refinement of the Structure. Full-matrix least-squares refinement was based on F, and in each case the function minimized was $w(|F_o| - |F_c|)^2$. The weights w were taken as $[2F_o/\sigma(F_o^2)]^2$, where $|F_o|$ and $|F_c|$ are the observed and calculated structure factor amplitudes. The atomic scattering factors for non-hydrogen atoms were taken from Cromer and Waber[13] and those for hydrogen from Stewart et al.[14] The effects of anomolous dispersion for all non-hydrogen atoms were included in F by using

the values of Cromer and Ibers[15] for $\Delta f'$ and $\Delta f''$.

In each structure, the iron atom was located from a three-dimensional Patterson difference map calculated from all intensity data. In the case of **4**, two iron positions were found, and the asymmetric unit contains two crystallographically independent $(C_6H_6)Fe[(C_2H_5)_2C_2B_4H_4]$ molecules; as discussed above, these molecules differ significantly in the orientation of the C_6H_6 ring relative to the carborane ligand. For each structure, subsequent Fourier difference maps revealed the positions of all other non-hydrogen atoms. In complex **4**, both molecules exhibited disordered positions for the terminal CH_3 carbon atom of one (and only one) ethyl group attached to the carborane cage; the same disorder was observed in **6**, but not in **5**. In the refinement of the structures of **4** and **6**, the three highest occupancy positions for this disordered ethyl carbon atom were included in the calculation. In structure **4** these positions are labeled C(2E), C(2F), and C(2G) on one molecule and C(2E)', C(2F)', and C(2G)' on the other; in **6** the disordered carbon positions are labeled C(3E), C(3F), and C(3G). In Figures 2–7 only one arbitrarily selected position is depicted in each case.

Following the introduction of anisotropic thermal parameters for all non-hydrogen atoms (except for the disordered carbons), additional Fourier syntheses located all of the hydrogen atoms; these were included in the refinement for several cycles and thereafter held fixed. The model converged to the final R and R_w values given in Table IV, where $R = \sum||F_o| - |F_c||/\sum|F_o|$ and $R_w = (\sum w(|F_o| - |F_c|)^2/\sum w|F_o|^2)^{1/2}$. Tables of observed and calculated structure factors and thermal parameters are available (see paragraph at end of paper on supplementary material.) The computing system and programs are described elsewhere.[16]

(11) Finster, D. C.; Grimes, R. N. *J. Am. Chem. Soc.* **1981**, *103*, 2675.
(12) Corfield, P. W. R.; Doedens, R. J.; Ibers, J. A. *Inorg. Chem.* **1967**, *6*, 197.
(13) Cromer, D. T.; Waber, J. T. "International Tables for X-ray Crystallography"; Kynoch Press: Birmingham, England, 1974; Vol. IV.
(14) Stewart, R. F.; Davidson, E. R.; Simpson, W. T. *J. Chem. Phys.* **1965**, *42*, 3175.

(15) Cromer, D. T.; Ibers, J. A., in ref 13.
(16) Freyberg, D. P.; Mockler, G. M.; Sinn, E. *J. Chem. Soc., Dalton Trans.* **1976**, 447.

Crystal and Molecular Structure and Substitution Reactivity of (μ-Hydrido)(μ-pyridyl)dirhenium Octacarbonyl, (μ-H)Re₂(CO)₈(μ-NC₅H₄). Crystal and Molecular Structure of (μ-Hydrido)(μ-pyridyl)(trimethylamine *N*-oxide)dirhenium Heptacarbonyl, (μ-H)Re₂(CO)₇(μ-NC₅H₄)(Me₃NO)[1]

Philip O. Nubel, Scott R. Wilson, and Theodore L. Brown*

School of Chemical Sciences, University of Illinois, Urbana, Illinois 61801

Received October 13, 1982

An X-ray crystal structure determination of $(\mu\text{-H})\text{Re}_2(\text{CO})_8(\mu\text{-NC}_5\text{H}_4)$, I, has been performed. The compound crystallizes in the triclinic space group $P\bar{1}$, with $a = 13.864$ (5) Å, $b = 14.927$ (5) Å, $c = 8.855$ (2) Å, $\alpha = 99.00$ (3)°, $\beta = 92.68$ (3)°, $\gamma = 65.66$ (2)°, $V = 1648.8$ (9) Å³, and $Z = 4$. Two independent but structurally similar molecules were observed per asymmetric unit of the unit cell. The hydride of each was located in a bridging position opposite the μ-pyridyl ligand. The Re–Re distances, 3.2088 (4) and 3.1956 (5) Å, are consistent with a H-bridged Re–Re single bond. This compound reacts with Me₃NO to yield $(\mu\text{-H})\text{Re}_2(\text{CO})_7(\mu\text{-NC}_5\text{H}_4)(\text{NMe}_3)$, which undergoes reaction with excess Me₃NO to produce $(\mu\text{-H})\text{Re}_2(\text{CO})_7(\mu\text{-NC}_5\text{H}_4)(\text{Me}_3\text{NO})$, III. The structure of III has been determined by X-ray crystallography. III crystallizes in the orthorhombic space group *Pbca*, with $a = 14.662$ (4) Å, $b = 26.300$ (6) Å, $c = 10.201$ (2) Å, $V = 3934$ (2) Å³, and $Z = 8$. The amine oxide ligand of III is coordinated to the same Re as the μ-pyridyl nitrogen. CO substitution of I by other ligands has been attained via three methods: (1) reaction with Me₃NO in the presence of excess L (pyridine, PPh₃), (2) thermal reaction with L (refluxing benzene; L = pyridine, PPh₃, CH₃CN), or (3) 366-nm photolysis (L = pyridine, PPh₃, P(OPh)₃, 1-octene). The μ-hydrido, μ-pyridyl structure is maintained in the products. Monosubstituted products are proposed to be isostructural with III on the basis of IR data. Disubstitution has been achieved by all three methods for L = pyridine and PPh₃. Isomeric disubstituted products were observed; structures are proposed for some of these based upon IR data. Trisubstituted products (L = pyridine, PPh₃) have been obtained only through photolysis.

Introduction

A variety of oxidative addition reactions involving polynuclear metal carbonyl systems has emerged over the past several years.[2] In particular C–H oxidative addition has been observed for a large number of functionalized organic molecules, including alkenes, alkynes, and aromatics. By far the most studied polynuclear systems have been the osmium and ruthenium trinuclear clusters. Gard and Brown have observed the formation of $(\mu\text{-H})\text{Re}_2(\text{CO})_8(\mu\text{-NC}_5\text{H}_4)$, I, in the thermal reaction of 1,2-*eq*,*eq*-Re₂(CO)₈(pyridine)₂.[3] This type of intramolecular oxi-

I

$$1,2\text{-}eq,eq\text{-Re}_2(\text{CO})_8(\text{py})_2 \xrightarrow[\text{C}_6\text{H}_6]{80\ °\text{C}} \text{I} + \text{py}$$
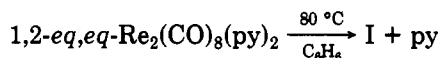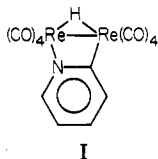
dative addition had not been observed previously for group 7 dinuclear carbonyl compounds, although a triosmium analogue of I, $(\mu\text{-H})\text{Os}_3(\text{CO})_{10}(\mu\text{-NC}_5\text{H}_4)$, is known.[4,5] We report here some results of an investigation of the chemistry of I, including thermal, photochemical, and Me₃NO-induced reactions of I with a variety of ligands. The results of X-ray crystal and molecular structure determinations of I and a substitution product, $(\mu\text{-H})\text{Re}_2(\text{CO})_7(\mu\text{-NC}_5\text{H}_4)(\text{Me}_3\text{NO})$, III, are also presented.

Experimental Section

General Data. Dirhenium decacarbonyl was purchased from Pressure Chemical Co. and used without further purification. Anhydrous trimethylamine *N*-oxide, Me₃NO, was prepared by vacuum sublimation of the dihydrate, Me₃NO·2H₂O (Aldrich, 98%). CP grade CO was purchased from Linde and used directly. Triphenylphosphine was recrystallized twice from ethanol. Triphenyl phosphite (Aldrich) was degassed prior to use. Benzene and toluene were treated with concentrated H₂SO₄, rinsed with aqueous NaHCO₃, dried over MgSO₄, and distilled from CaH₂ under an argon atmosphere. Tetrahydrofuran was distilled from CaH₂ under argon. Acetonitrile was stirred over CaH₂, followed by distillation from P₂O₅ under argon. Pyridine was predried over KOH, distilled under argon, and stored over 3A molecular sieves (Linde). 1-Octene was predried over MgSO₄ and distilled from CaH₂ under argon.

Reagent grade solvents (hexane, benzene, CH₂Cl₂) were used without purification for chromatography and recrystallization. Silica gel (70–230 mesh, EM Reagents) was employed for column chromatography. Preparative TLC plates (20 × 20 cm, 2.0 mm silica with UV₂₅₄ fluorescent indicator) were obtained from Brinkmann Instruments, Inc.

Infrared spectra were obtained by using a Beckman IR-4240 spectrophotometer. Electronic spectra were recorded on a Cary-219 Spectrophotometer using matched 1.0-cm quartz cells. Field desorption mass spectra (FDMS) were obtained with a Varian MAT 731 spectrometer equipped with a field desorption source. ¹H NMR spectra were recorded at ambient temperature by using a 90-MHz Varian EM-390 or 360-MHz Nicolet NT-360 instrument. Elemental analyses were performed by the University of Illinois Microanalytical Laboratory.

Preparation of (μ-H)Re₂(CO)₈(μ-NC₅H₄), I. This compound was prepared by the method reported by Gard and Brown,[3] modified to obtain higher yields.

1,2-*eq*,*eq*-Re₂(CO)₈(py)₂ (py = pyridine; 3.5 g, 4.6 mmol), as prepared by the method of Koelle,[6] was dissolved in 600 mL of benzene. The solution was refluxed under argon for 28 h, at which point conversion to $(\mu\text{-H})\text{Re}_2(\text{CO})_7(\mu\text{-NC}_5\text{H}_4)(\text{py})$, IV, appeared

(1) This research was sponsored by the National Science Foundation through Research Grant NSF CHE 81-19525.
(2) Deeming, A. J. "Transition Metal Clusters"; Johnson, B. F. G., Ed.; Wiley: New York, 1980; p 391.
(3) Gard, D. R.; Brown, T. L. *Organometallics* **1982**, *1*, 1143.
(4) Yin, C. C.; Deeming, A. J. *J. Chem. Soc., Dalton Trans.* **1975**, 2091.
(5) Tachikawa, M.; Shapley, J. R. *J. Organomet. Chem.* **1977**, *124*, C19.

(6) Koelle, U. *J. Organomet. Chem.* **1978**, *155*, 53.

complete by IR analysis. The solution was cooled to room temperature, and solvent was removed under vacuum, leaving a brown oil. Extraction of IV from this oil was achieved by column chromatography with 4:1 hexane/CH_2Cl_2. Colorless needles of IV (1.85 g, 55%) were obtained after several recrystallizations from hexane/CH_2Cl_2 (slow evaporation). Anal. Calcd for $C_{17}H_{10}N_2O_7Re_2$: C, 28.10; H, 1.39; N, 3.86. Found: C, 28.32; H, 1.45; N, 4.04. IR (toluene) 2090 (w), 2025 (s), 1995 (s), 1977 (s), 1942 (ms), 1919 (sh), 1913 (ms) cm^{-1}.

IV (310 mg, 0.43 mmol) was loaded into a 250-mL pressure bottle (Parr Instrument Co.) and dissolved in 110 mL of benzene. After the solution was vacuum degassed, the bottle was pressurized with CO to 60 psig and immersed in an oil bath at 75 °C for 25 hours. IR analysis after this time indicated complete conversion to I. The solution was cooled and solvent removed under vacuum, leaving a white solid. Recrystallization from CH_2Cl_2/hexane afforded 279 mg (97%) of I. IR (toluene) 2114 (vw), 2086 (w), 2015 (s), 2004 (sh), 1993 (m), 1977 (vw), 1955 (ms, br) cm^{-1}. Anal. Calcd for $C_{13}H_5NO_8Re_2$: C, 23.11; H, 0.75; N, 2.07. Found: C, 23.46; H, 0.80; N, 2.10.

Preparation of $(\mu\text{-H})Re_2(CO)_7(\mu\text{-NC}_5H_4)(Me_3NO)$, III. I (50 mg, 0.074 mmol) was dissolved in 1 mL of CH_2Cl_2 (reagent grade). To this was added $Me_3NO\cdot2H_2O$ (40 mg, 0.36 mmol), and the solution was stirred vigorously at room temperature for 10 h. The solution was then filtered and the filtrate washed several times with small quantities of H_2O to remove excess Me_3NO. Hexane was added to the CH_2Cl_2 solution, and slow evaporation afforded 45 mg (84%) of III. Anal. Calcd for $C_{15}H_{14}N_2O_8Re_2$: C, 24.93; H, 1.95; N, 3.88. Found: C, 24.91; H, 1.89; N, 3.90. See Table VIII for IR, ^{1}H NMR, and FDMS data.

Crystallographic Analyses of I and III. Colorless, transparent, prismatic crystals of each compound were obtained by slow evaporation of a CH_2Cl_2/hexane solution. Both data sets were collected on a Syntex P2$_1$ diffractometer at 25 °C by using graphite-monochromated Mo Kα (0.710 69 Å) radiation. Details are given in Table I.

Both structures were solved by direct methods (SHELX 76)[7] and a combination of difference-Fourier and least-squares techniques. Data were corrected for absorption and for Lorentz and polarization effects. Atomic scattering factors and anomalous scattering terms ($\Delta f'$ and $\Delta f''$) were obtained from ref 8.

Me_3NO Reactions. Except where noted, all reactions employing Me_3NO were run at room temperature (25 °C), with reagent grade CH_2Cl_2 as solvent. The reactions were insensitive to the presence of air or moisture and thus were not generally performed under inert atmosphere. The concentration of the reactant dirhenium complex was typically (0.5–1.0) × 10^{-2} M. The reactions were conducted by adding Me_3NO to a solution of rhenium carbonyl compound and ligand (if employed). Anhydrous Me_3NO was added as a methylene chloride solution; the dihydrate was used in solid form. Vigorous stirring was employed in reactions involving the dihydrate, due to its low solubility.

Thermal Reactions. Reactions at elevated temperature (~80 °C) were performed under an argon atmosphere using purified solvents and reagents. The concentration of the reactant rhenium compound was typically (0.5–1.0) × 10^{-2} M. Exclusion of room

(7) Sheldrick, G. M. SHELX 76, a program for crystal structure determination, University of Cambridge, England, 1976.
(8) "International Tables for X-Ray Crystallography"; Kynoch Press: Birmingham, England, 1974; Vol. 4: (a) pp 99–101; (b) pp 149–150.
(9) (a) Space group was distinguished from $P1$ by the probability distribution of the normalized structure factors. (b) The smallest available sample was used, but there was still a severe absorption problem. Before the numerical correction for absorption, refinement of the anisotropic thermal coefficients led to imaginary tensors for a number of atoms and despite this compensation, F_o was systematically less than F_c for low sin θ. Following the correction, the thermal parameters refined to reasonable values and the systematic error with respect to sin θ was greatly reduced. This was taken as evidence that the considerable increase in precision made possible by the absorption correction (the uncorrected data refined to an unweighted R factor of 0.145) reflected a corresponding improvement in the accuracy of the proposed model. To determine the accuracy of the positional parameters, the lengths of chemically similar bonds from the two independent molecules were compared. The weighted root mean square difference (not including hydrogen atoms) was 0.014 (10) Å, indicating that the estimated standard deviations were slightly, but not severely underestimated.
(10) Zachariasen, W. H. *Acta Crystallogr., Sect. A* **1968**, *24*, 212.

Figure 1. ORTEP drawing of molecule A, $(\mu\text{-H})Re_2(CO)_8(\mu\text{-NC}_5H_4)$, I, showing 30% electron-density probability ellipsoids. Thermal parameters for the hydrogen atoms have been artificially reduced.
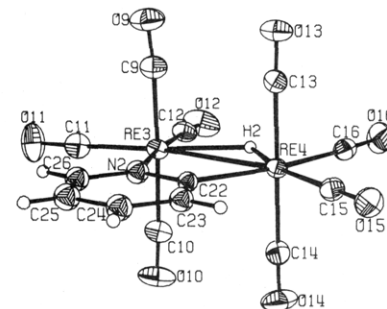
Figure 2. ORTEP drawing of molecule B, $(\mu\text{-H})Re_2(CO)_8(\mu\text{-NC}_5H_4)$, I, showing 30% electron-density probability ellipsoids. Thermal parameters for the hydrogen atoms have been artificially reduced.

light had no effect upon any of the reactions studied.

Photochemical Reactions. Photochemical reactions were performed under an argon atmosphere using purified toluene as solvent. The irradiation source was a General Electric 275-W sunlamp.[11] Reaction vessels (25–50-mL Pyrex Schlenk flasks) were placed ~10 cm from the lamp. The Pyrex-filtered radiation consists primarily of 366-nm wavelength;[12] significant emission is also observed at 313, 334, 406, and 436 nm. Solutions were maintained at room temperature (25 °C) during photolysis by air cooling the reaction vessels. The concentration of reactant rhenium compound was typically (3–5) × 10^{-3} M (0.04–0.08 mmol in 10–25 mL of toluene). Argon-purging was accomplished (where indicated) by bubbling a stream of Ar through the reaction solution via a syringe needle inserted through a silicone septum. A separate needle, attached to a mineral oil bubbler, was inserted through the septum to allow escape of purge gases.

Results

Crystallographic Analysis and UV–Visible Spectrum of I. Two crystallographically independent molecules of I, A and B, are present in the asymmetric unit of the unit cell. These are pictured in Figures 1 and 2, respectively. Final atomic coordinates for both molecules are given in Table II. Bond distances and angles are contained in Tables III and IV.

The UV–visible spectrum of I in THF solution shows an absorption maximum at 291 nm (1.0 × 10^4 M^{-1} cm^{-1}) with a weak shoulder at ~345 nm (~1100 M^{-1} cm^{-1}).

Reaction of I with Me_3NO. Treatment of a CH_2Cl_2 solution of I with 1 equiv of anhydrous Me_3NO at 25 °C resulted in 80% yield (by ^{1}H NMR) of an air-stable, colorless new compound, $(\mu\text{-H})Re_2(CO)_7(\mu\text{-NC}_5H_4)(NMe_3)$, II. Although reaction had ceased within several minutes, 10% of I remained and a second product, III, was obtained in 10% yield. II has been characterized spectroscopically (see Table VIII) but not isolated because it decomposes

(11) General Electric Lighting Business Group, "RS Sunlamp Report", Nela Park, Cleveland, OH.
(12) Gard, D. R.; Brown, T. L. *J. Am. Chem. Soc.* **1982**, *104*, 6340.

Table I. Crystallographic Data for X-ray Diffraction Studies

	$(\mu\text{-}H)Re_2(CO)_8(\mu\text{-}NC_5H_4)$	$(\mu\text{-}H)Re_2(CO)_7(\mu\text{-}NC_5H_4)(Me_3NO)$
(a) Crystal Parameters		
crystal class	triclinic	orthorhombic
space group	$P\bar{1}$ (see ref 9a)	*Pbca*
a, Å	13.864 (5)	14.662 (4)
b, Å	14.927 (5)	26.300 (6)
c, Å	8.855 (2)	10.201 (2)
α, deg	99.00 (3)°	
β, deg	92.68 (3)°	
γ, deg	65.66 (2)°	
V, Å³	1648.8 (9)	3934 (2)
d(calcd), g/cm³	2.72	2.44
approx dimens, mm	0.22 × 0.28 × 0.72	0.12 × 0.18 × 0.72
Z	4	8
(b) Data Measurement and Treatment		
2θ range, deg	3.5–55.0	3.5–55.0
reflctns measd	$\pm h, \pm k, +l$	$+h, +k, +l$
no. of measd reflctns	8410	5267
no. of independent reflctns	7611	4545
internal consistency index (R)	0.020	0.019
μ, cm⁻¹	149.0	125.1
max and min transmission factors	0.12 and 0.02 (see ref 9b)	0.24 and 0.11
abs correctn method	numerical	numerical
empirical isotropic extinction correctn coeff[10]	3.6×10^{-8}	no correctn applied
R	0.0310	0.0321
R_w	0.0395	0.0402

on silica or alumina chromatographic supports. Treatment of a solution of **II** with excess pyridine (20 equiv) resulted within several hours in quantitative formation of $(\mu\text{-}H)\text{-}Re_2(CO)_7(\mu\text{-}NC_5H_4)(py)$, **IV**, a compound originally prepared by Gard and Brown.[3] Production of free NMe_3 was observed by ¹H NMR spectroscopy.

When a solution of **I** was stirred at 25 °C with excess Me_3NO (dihydrate form, 5–10 equiv), the initial product observed was **II**. Over the course of several hours, however, the solution turned light yellow and **II** was converted in essentially quantitative yield (by NMR) to $(\mu\text{-}H)Re_2\text{-}(CO)_7(\mu\text{-}NC_5H_4)(Me_3NO)$, **III**. Production of free NMe_3 was observed. **III** was characterized spectroscopically (Table VIII) and purified as outlined in the Experimental Section. In the absence of excess Me_3NO, it does not react with excess pyridine over several hours at temperatures up to 50 °C (C_6H_6 solvent).

Crystallographic Analysis of III. The structure determined for **III** is shown in Figure 3. Final atomic coordinates, bond distances, and bond angles are given in Tables V, VI, and VII, respectively.

Reactions of I with Me₃NO in the Presence of Another Ligand. (A) Pyridine. The species initially produced when a solution of **I** is treated with Me_3NO (5–10 equiv, dihydrate form) in the presence of pyridine (100 equiv) was the monosubstituted compound **IV**. **I** completely reacts within several minutes, and no **II** or **III** is detected in the ¹H NMR. Within an hour, however, two additional reaction products are observed by NMR. Both of these species were produced when a solution of **IV** was similarly reacted with Me_3NO/pyridine and were subsequently isolated and identified as isomers of a disubstituted complex, $(\mu\text{-}H)Re_2(CO)_6(\mu\text{-}NC_5H_4)(py)_2$, **IXa,b**. Complete reaction of **IV** required approximately 1 day, after which the CH_2Cl_2 solution was washed several times with H_2O to remove excess Me_3NO. Physical separation of the two isomers was achieved by column chromatography (2:1 benzene/CH_2Cl_2 eluent). The major isomer produced in the reaction, **IXa**, was the first to elute. Both compounds were colorless and were crystallizable from CH_2Cl_2/hexane. Spectroscopic data are listed in Table VIII.
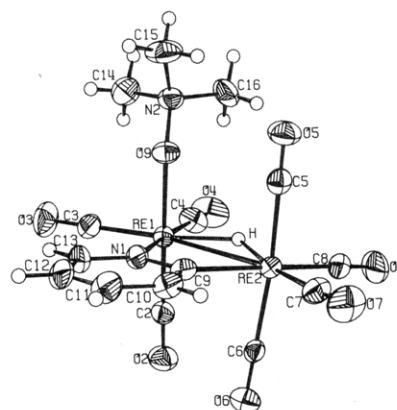
Figure 3. ORTEP drawing of $(\mu\text{-}H)Re_2(CO)_7(\mu\text{-}NC_5H_4)(Me_3NO)$, **III**, showing 35% electron-density probability ellipsoids. Thermal parameters for the hydrogen atoms have been artificially reduced.

The initial isomer distribution of the reaction of **IV** with Me_3NO/py, as measured by NMR within the first 30 min of reaction, was determined to be 80–85% **IXa** and 15–20% **IXb**. Isolated **IXb** was observed to isomerize to **IXa** in solution at room temperature in the dark with a half-life of about 1.5 days.

The overall conversion of **I** to **IXa** and **IXb** by Me_3NO/py was determined by IR and NMR spectroscopy to be nearly quantitative (>90%). The rate of reaction of **I** was estimated to be at least 10 times greater than that of the monosubstituted complex **IV**. The disubstituted compounds did not undergo detectable further substitution, even after 24 h in refluxing CH_2Cl_2 solution in the presence of excess Me_3NO and pyridine.

(B) Triphenylphosphine. The reaction of **I** with Me_3NO/PPh_3 also resulted in mono and disubstitution of CO. A 1-h reaction period with 5 equiv $Me_3NO\cdot2H_2O$ and 20 equiv of PPh_3 generated $(\mu\text{-}H)Re_2(CO)_7(\mu\text{-}NC_5H_4)\text{-}(PPh_3)$, **V**, as the major product. This species could be isolated by preparative TLC (mobile phase, hexane) and crystallized from CH_2Cl_2/hexane (slow evaporation). Additional reaction time (24 h) resulted in quantitative production of a single isomer of $(\mu\text{-}H)Re_2(CO)_6(\mu\text{-}$

Table II. Final Atomic Coordinates for the Two
(μ-H)Re$_2$(CO)$_8$(μ-NC$_5$H$_4$) Molecules[a]

atom	x/a	y/b	z/c
Re(1)	-0.20422 (3)	0.34849 (2)	-0.04616 (4)
Re(2)	-0.31130 (3)	0.51757 (2)	-0.25982 (4)
Re(3)	0.30832 (3)	0.02346 (2)	0.19509 (4)
Re(4)	0.16791 (3)	0.10895 (2)	0.50299 (4)
O(1)	-0.2711 (6)	0.5149 (5)	0.2366 (9)
O(2)	-0.1405 (6)	0.1829 (5)	-0.3314 (8)
O(3)	-0.0339 (7)	0.2116 (6)	0.1478 (9)
O(4)	-0.3669 (7)	0.2745 (6)	0.0508 (10)
O(5)	-0.3815 (7)	0.6749 (5)	0.0361 (9)
O(6)	-0.2259 (6)	0.3557 (5)	-0.5502 (8)
O(7)	-0.3260 (8)	0.6823 (6)	-0.4408 (12)
O(8)	-0.5423 (6)	0.5435 (6)	-0.3240 (10)
O(9)	0.1435 (7)	-0.0498 (6)	0.0339 (10)
O(10)	0.4869 (7)	0.0697 (7)	0.3695 (10)
O(11)	0.4729 (7)	-0.1166 (6)	-0.0528 (10)
O(12)	0.2478 (7)	0.1998 (6)	0.0156 (11)
O(13)	-0.0079 (6)	0.0470 (5)	0.3466 (8)
O(14)	0.3411 (7)	0.1694 (7)	0.6725 (9)
O(15)	0.0829 (6)	0.1185 (5)	0.8222 (8)
O(16)	0.0170 (7)	0.3259 (5)	0.4742 (9)
N(1)	-0.0975 (6)	0.4055 (5)	-0.1278 (8)
N(2)	0.3356 (6)	-0.0845 (5)	0.3505 (8)
C(1)	-0.2471 (7)	0.4556 (7)	0.1326 (10)
C(2)	-0.1625 (7)	0.2428 (6)	-0.2282 (10)
C(3)	-0.0962 (8)	0.2634 (6)	0.0722 (11)
C(4)	-0.3052 (9)	0.3035 (6)	0.0160 (11)
C(5)	-0.3554 (8)	0.6194 (7)	-0.0726 (12)
C(6)	-0.2577 (7)	0.4148 (6)	-0.4445 (11)
C(7)	-0.3225 (8)	0.6216 (7)	-0.3745 (13)
C(8)	-0.4594 (8)	0.5370 (7)	-0.3007 (12)
C(9)	0.2009 (8)	-0.0186 (7)	0.0928 (11)
C(10)	0.4222 (8)	0.0564 (7)	0.3061 (11)
C(11)	0.4130 (8)	-0.0675 (7)	0.0424 (12)
C(12)	0.2717 (7)	0.1332 (6)	0.0775 (11)
C(13)	0.0576 (7)	0.0674 (6)	0.4025 (10)
C(14)	0.2791 (8)	0.1488 (6)	0.6078 (11)
C(15)	0.1154 (7)	0.1139 (6)	0.7027 (10)
C(16)	0.0706 (8)	0.2481 (6)	0.4901 (11)
C(17)	-0.1449 (6)	0.4819 (5)	-0.2116 (9)
C(18)	-0.0831 (8)	0.5222 (6)	-0.2679 (11)
C(19)	0.0234 (8)	0.4880 (6)	-0.2460 (11)
C(20)	0.0704 (8)	0.4098 (6)	-0.1655 (10)
C(21)	0.0089 (7)	0.3720 (6)	-0.1076 (10)
C(22)	0.2786 (6)	-0.0485 (5)	0.4808 (9)
C(23)	0.2907 (7)	-0.1086 (6)	0.5880 (10)
C(24)	0.3618 (8)	-0.2080 (6)	0.5650 (11)
C(25)	0.4205 (8)	-0.2441 (7)	0.4320 (12)
C(26)	0.4078 (7)	-0.1843 (6)	0.3246 (11)
H(1)	-0.3126 (84)	0.4155 (70)	-0.1874 (121)
H(2)	0.1874 (88)	0.1365 (71)	0.3361 (122)
H(18)	-0.1161	0.5759	-0.3241
H(19)	0.0640	0.5174	-0.2856
H(20)	0.1447	0.3827	-0.1504
H(21)	0.0419	0.3190	-0.0498
H(23)	0.2496	-0.0819	0.6801
H(24)	0.3693	-0.2497	0.6396
H(25)	0.4707	-0.3114	0.4145
H(26)	0.4479	-0.2104	0.2316

[a] The aromatic hydrogen atoms were fixed in calculated positions; positions for the two bridging hydrogen atoms were allowed to vary during least squares.

NC$_5$H$_4$)(PPh$_3$)$_2$, X. After the solution was washed with H$_2$O to remove excess Me$_3$NO, this compound was crystallized as above. Data for V and X are contained in Table VIII.

As is the case when pyridine is ligand, reaction of V was slower than I. X did not undergo reaction with excess Me$_3$NO/PPh$_3$.

(C) 1-Octene. Reaction of I with 1 equiv of Me$_3$NO in the presence of a large excess of 1-octene yielded only II, which did not undergo further reaction at room temperature.

Table III. Interatomic Distances (Å) for the Two
(μ-H)Re$_2$(CO)$_8$(μ-NC$_5$H$_4$) Molecules

molecule A		molecule B	
Re-Re, Re-H, and Pyridyl Distances			
Re(1)-Re(2)	3.2088 (4)	Re(3)-Re(4)	3.1956 (5)
Re(1)-H(1)	1.9 (1)	Re(3)-H(2)	2.1 (1)
Re(2)-H(1)	1.75 (9)	Re(4)-H(2)	1.7 (1)
Re(1)-N(1)	2.184 (7)	Re(3)-N(2)	2.185 (7)
Re(2)-C(17)	2.181 (8)	Re(4)-C(22)	2.197 (7)
N(1)-C(17)	1.372 (9)	N(2)-C(22)	1.34 (1)
C(17)-C(18)	1.38 (1)	C(22)-C(23)	1.36 (1)
C(18)-C(19)	1.36 (1)	C(23)-C(24)	1.39 (1)
C(19)-C(20)	1.37 (1)	C(24)-C(25)	1.37 (1)
C(20)-C(21)	1.36 (1)	C(25)-C(26)	1.36 (1)
C(21)-N(1)	1.36 (1)	C(26)-N(2)	1.40 (1)
Re-Carbonyl Carbon Distances			
Re(1)-C(1)	1.981 (9)	Re(3)-C(9)	1.97 (1)
Re(1)-C(2)	1.990 (9)	Re(3)-C(10)	2.01 (1)
Re(1)-C(3)	1.912 (10)	Re(3)-C(11)	1.940 (10)
Re(1)-C(4)	1.918 (10)	Re(3)-C(12)	1.956 (9)
Re(2)-C(5)	1.993 (10)	Re(4)-C(13)	2.000 (9)
Re(2)-C(6)	1.992 (9)	Re(4)-C(14)	2.010 (10)
Re(2)-C(7)	1.935 (10)	Re(4)-C(15)	1.923 (9)
Re(2)-C(8)	1.98 (1)	Re(4)-C(16)	1.974 (8)
Carbonyl C-O Distances			
C(1)-O(1)	1.13 (1)	C(9)-O(9)	1.15 (1)
C(2)-O(2)	1.13 (1)	C(10)-O(10)	1.11 (1)
C(3)-O(3)	1.16 (1)	C(11)-O(11)	1.14 (1)
C(4)-O(4)	1.18 (1)	C(12)-O(12)	1.13 (1)
C(5)-O(5)	1.13 (1)	C(13)-O(13)	1.14 (1)
C(6)-O(6)	1.14 (1)	C(14)-O(14)	1.13 (1)
C(7)-O(7)	1.14 (1)	C(15)-O(15)	1.15 (1)
C(8)-O(8)	1.12 (1)	C(16)-O(16)	1.12 (1)

Thermal Reactions of I with Ligands. (A) Pyridine.
I did not react with pyridine at room temperature. In refluxing benzene, complete reaction of I in the presence of 100 equiv of pyridine required about 24 h, at which point the major product was IV. Eventual conversion to IXa was quantitative, as judged by IR and NMR spectroscopy, but slower by an order of magnitude. No reaction of IXa was detected over several days under these conditions.

(B) Triphenylphosphine. No reaction of I with PPh$_3$ is observed at 25 °C. In refluxing benzene solution in the presence of 5 equiv of PPh$_3$, I reacts over 15–20 h to yield the monosubstituted compound V and (more slowly) disubstituted species. The major disubstituted product was X, the product of the Me$_3$NO/PPh$_3$ reaction. An additional minor product, which could not be separated from X chromatographically, was characterized by NMR spectroscopy. The hydride resonance appeared at δ -11.70 (dd, 1 H, $J_{\text{H-P(1)}}$ = 11.0 Hz, $J_{\text{H-P(2)}}$ = 9.5 Hz) in CD$_2$Cl$_2$ (360 MHz). Aromatic protons could not be distinguished from those of X except for a resonance at δ 6.31 (td, 1 H, μ-py$_{\beta \text{ or } \gamma}$, J = 7 and 1 Hz). The amount of this product, which is judged to be an isomer of X, was 5–10% of X.

(C) CH$_3$CN and CO. (μ-H)Re$_2$(CO)$_7$(μ-NC$_5$H$_4$)-(CH$_3$CN), VI, was obtained in essentially quantitative yield by refluxing an acetonitrile solution of I for 10–15 hours. No evidence of disubstitution was observed. In the absence of excess CH$_3$CN, VI was found to decompose slowly in solution in the presence of air. Successful recrystallization was achieved by slow evaporation of a benzene/heptane-/CH$_3$CN (2/3/1 by volume) solution. Table VIII contains spectroscopic data for VI.

A toluene solution of I under 60 psig of CO showed no apparent reaction after 1 day at 80 °C.

Photochemical Reactions of I with Ligands. (A) Pyridine. Photolysis of a toluene solution of I in the presence of 100 equiv of pyridine resulted in CO substi-

Table IV. Bond Angles (deg) for the Two (μ-H)Re₂(CO)₈(μ-NC₅H₄) Molecules

Angles about Re(1) and Re(3)

molecule A		molecule B	
Re(2)-Re(1)-N(1)	65.1 (2)	Re(4)-Re(3)-N(2)	65.1 (2)
Re(2)-Re(1)-C(1)	87.9 (3)	Re(4)-Re(3)-C(9)	90.9 (3)
Re(2)-Re(1)-C(2)	91.0 (2)	Re(4)-Re(3)-C(10)	88.7 (3)
Re(2)-Re(1)-C(3)	157.3 (3)	Re(4)-Re(3)-C(11)	160.7 (3)
Re(2)-Re(1)-C(4)	111.0 (3)	Re(4)-Re(3)-C(12)	107.3 (3)
Re(2)-Re(1)-H(1)	28 (3)	Re(4)-Re(3)-H(2)	28 (3)
N(1)-Re(1)-C(1)	90.8 (3)	N(2)-Re(3)-C(9)	88.6 (3)
N(1)-Re(1)-C(2)	88.8 (3)	N(2)-Re(3)-C(10)	87.3 (3)
N(1)-Re(1)-C(3)	92.4 (3)	N(2)-Re(3)-C(11)	95.7 (3)
N(1)-Re(1)-C(4)	176.0 (3)	N(2)-Re(3)-C(12)	172.4 (3)
N(1)-Re(1)-H(1)	91 (3)	N(2)-Re(3)-H(2)	93 (3)
C(1)-Re(1)-C(2)	178.9 (4)	C(9)-Re(3)-C(10)	175.6 (4)
C(1)-Re(1)-C(3)	89.9 (4)	C(9)-Re(3)-C(11)	89.8 (4)
C(1)-Re(1)-C(4)	89.7 (4)	C(9)-Re(3)-C(12)	92.5 (4)
C(1)-Re(1)-H(1)	99 (3)	C(9)-Re(3)-H(2)	89 (3)
C(2)-Re(1)-C(3)	91.1 (4)	C(10)-Re(3)-C(11)	89.2 (4)
C(2)-Re(1)-C(4)	90.6 (4)	C(10)-Re(3)-C(12)	91.9 (4)
C(2)-Re(1)-H(1)	80 (3)	C(10)-Re(3)-H(2)	93 (3)
C(3)-Re(1)-C(4)	91.5 (4)	C(11)-Re(3)-C(12)	91.9 (4)
C(3)-Re(1)-H(1)	171 (3)	C(11)-Re(3)-H(2)	171 (3)
C(4)-Re(1)-H(1)	85 (3)	C(12)-Re(3)-H(2)	80 (3)

Angles about Re(2) and Re(4)

molecule A		molecule B	
Re(1)-Re(2)-C(17)	65.1 (2)	Re(3)-Re(4)-C(22)	64.7 (2)
Re(1)-Re(2)-C(5)	89.1 (3)	Re(3)-Re(4)-C(13)	90.1 (2)
Re(1)-Re(2)-C(6)	89.8 (3)	Re(3)-Re(4)-C(14)	90.6 (3)
Re(1)-Re(2)-C(7)	157.4 (3)	Re(3)-Re(4)-C(15)	159.6 (3)
Re(1)-Re(2)-C(8)	110.0 (3)	Re(3)-Re(4)-C(16)	107.4 (3)
Re(1)-Re(2)-H(1)	32 (3)	Re(3)-Re(4)-H(2)	36 (3)
C(17)-Re(2)-C(5)	90.8 (3)	C(22)-Re(4)-C(13)	89.0 (3)
C(17)-Re(2)-C(6)	85.5 (3)	C(22)-Re(4)-C(14)	90.3 (3)
C(17)-Re(2)-C(7)	92.5 (3)	C(22)-Re(4)-C(15)	95.0 (3)
C(17)-Re(2)-C(8)	174.6 (3)	C(22)-Re(4)-C(16)	171.6 (3)
C(17)-Re(2)-H(1)	95 (3)	C(22)-Re(4)-H(2)	101 (3)
C(5)-Re(2)-C(6)	176.3 (4)	C(13)-Re(4)-C(14)	178.7 (4)
C(5)-Re(2)-C(7)	88.4 (4)	C(13)-Re(4)-C(15)	91.3 (4)
C(5)-Re(2)-C(8)	91.5 (4)	C(13)-Re(4)-C(16)	88.2 (4)
C(5)-Re(2)-H(1)	100 (3)	C(13)-Re(4)-H(2)	88 (4)
C(6)-Re(2)-C(7)	91.3 (4)	C(14)-Re(4)-C(15)	87.6 (4)
C(6)-Re(2)-C(8)	92.2 (4)	C(14)-Re(4)-C(16)	92.7 (4)
C(6)-Re(2)-H(1)	81 (3)	C(14)-Re(4)-H(2)	94 (4)
C(7)-Re(2)-C(8)	92.5 (4)	C(15)-Re(4)-C(16)	92.9 (4)
C(7)-Re(2)-H(1)	169 (3)	C(15)-Re(4)-H(2)	164 (3)
C(8)-Re(2)-H(1)	80 (3)	C(16)-Re(4)-H(2)	71 (3)

Angles about Hydride and Pyridyl Atoms

molecule A		molecule B	
Re(1)-H(1)-Re(2)	120 (6)	Re(3)-H(2)-Re(4)	116 (5)
Re(1)-N(1)-C(21)	127.2 (5)	Re(3)-N(2)-C(26)	125.3 (6)
Re(1)-N(1)-C(17)	114.8 (5)	Re(3)-N(2)-C(22)	115.1 (5)
Re(2)-C(17)-N(1)	114.9 (5)	Re(4)-C(22)-N(2)	115.1 (5)
Re(2)-C(17)-C(18)	126.3 (6)	Re(4)-C(22)-C(23)	124.6 (6)
N(1)-C(17)-C(18)	118.6 (7)	N(2)-C(22)-C(23)	120.2 (7)
C(17)-C(18)-C(19)	122.7 (8)	C(22)-C(23)-C(24)	121.3 (8)
C(18)-C(19)-C(20)	118.2 (9)	C(23)-C(24)-C(25)	118.1 (8)
C(19)-C(20)-C(21)	118.8 (9)	C(24)-C(25)-C(26)	120.5 (9)
C(20)-C(21)-N(1)	123.7 (7)	C(25)-C(26)-N(2)	120.2 (8)
C(21)-N(1)-C(17)	118.0 (7)	C(26)-N(2)-C(22)	119.6 (7)

Angles about Carbonyl Carbons

molecule A		molecule B	
Re(1)-C(1)-O(1)	178.3 (8)	Re(3)-C(9)-O(9)	175.1 (8)
Re(1)-C(2)-O(2)	178.8 (8)	Re(3)-C(10)-O(10)	176.3 (9)
Re(1)-C(3)-O(3)	177.1 (9)	Re(3)-C(11)-O(11)	175.9 (9)
Re(1)-C(4)-O(4)	178.4 (8)	Re(3)-C(12)-O(12)	176.6 (9)
Re(2)-C(5)-O(5)	177.4 (9)	Re(4)-C(13)-O(13)	177.6 (7)
Re(2)-C(6)-O(6)	179.4 (8)	Re(4)-C(14)-O(14)	176.8 (9)
Re(2)-C(7)-O(7)	178.0 (9)	Re(4)-C(15)-O(15)	178.9 (8)
Re(2)-C(8)-O(8)	176.8 (8)	Re(4)-C(16)-O(16)	176.0 (9)

Torsion Angles

molecule A		molecule B	
C(1)-Re(1)-Re(2)-C(5)	-1.9 (4)	C(9)-Re(3)-Re(4)-C(13)	-0.1 (4)
C(2)-Re(1)-Re(2)-C(6)	-5.4 (4)	C(10)-Re(3)-Re(4)-C(14)	3.2 (4)
C(3)-Re(1)-Re(2)-C(7)	-2.9 (11)	C(11)-Re(3)-Re(4)-C(15)	2.2 (12)
C(4)-Re(1)-Re(2)-C(8)	-4.3 (4)	C(12)-Re(3)-Re(4)-C(16)	4.7 (4)
Re(1)-N(1)-C(17)-Re(2)	-5.5 (7)	Re(3)-N(2)-C(22)-Re(4)	1.9 (7)
H(1)-Re(1)-N(1)-C(17)	15.0 (30)	H(2)-Re(3)-N(2)-C(22)	-4.1 (29)
H(1)-Re(2)-C(17)-N(1)	-7.8 (34)	H(2)-Re(4)-C(22)-N(2)	1.9 (37)

Table V. Final Atomic Coordinates for
$(\mu\text{-H})\text{Re}_2(\text{CO})_7(\mu\text{-NC}_5\text{H}_4)(\text{Me}_3\text{NO})^a$

atom	x/a	y/b	z/c
Re(1)	0.27153 (2)	0.40771 (1)	0.09180 (4)
Re(2)	0.16235 (2)	0.36025 (1)	0.33839 (4)
O(2)	0.4201 (5)	0.4470 (3)	0.2746 (8)
O(3)	0.4015 (6)	0.4173 (3)	−0.1417 (9)
O(4)	0.2217 (7)	0.5205 (3)	0.0633 (10)
O(5)	−0.0010 (5)	0.3235 (3)	0.1654 (8)
O(6)	0.3375 (5)	0.3763 (3)	0.5053 (8)
O(7)	0.0943 (7)	0.2824 (3)	0.5419 (9)
O(8)	0.0629 (6)	0.4525 (3)	0.4645 (9)
O(9)	0.1669 (4)	0.3710 (2)	−0.0213 (7)
N(1)	0.2969 (5)	0.3279 (3)	0.1287 (7)
N(2)	0.1092 (6)	0.3927 (3)	−0.1164 (8)
C(2)	0.3643 (7)	0.4315 (4)	0.2047 (10)
C(3)	0.3534 (8)	0.4138 (4)	−0.0541 (11)
C(4)	0.2393 (7)	0.4786 (4)	0.0725 (11)
C(5)	0.0578 (7)	0.3384 (3)	0.2260 (10)
C(6)	0.2733 (7)	0.3729 (3)	0.4419 (8)
C(7)	0.1212 (8)	0.3113 (4)	0.4663 (11)
C(8)	0.0960 (7)	0.4170 (4)	0.4203 (10)
C(9)	0.2487 (6)	0.3082 (3)	0.2323 (9)
C(10)	0.2645 (7)	0.2563 (4)	0.2612 (10)
C(11)	0.3238 (9)	0.2275 (4)	0.1888 (12)
C(12)	0.3702 (8)	0.2482 (5)	0.0871 (11)
C(13)	0.3547 (7)	0.2978 (4)	0.0593 (11)
C(14)	0.1617 (9)	0.4172 (6)	−0.2225 (12)
C(15)	0.0570 (9)	0.3486 (5)	−0.1727 (14)
C(16)	0.0455 (7)	0.4302 (5)	−0.0593 (13)
H	0.1834	0.4045	0.2191
H(10)	0.2331	0.2411	0.3326
H(11)	0.3325	0.1926	0.2101
H(12)	0.4120	0.2286	0.0370
H(13)	0.3862	0.3124	−0.0128
H(141)	0.1169	0.4308	−0.2799
H(142)	0.1938	0.3907	−0.2656
H(143)	0.2032	0.4433	−0.1981
H(151)	0.0200	0.3679	−0.2309
H(152)	0.0207	0.3365	−0.1021
H(153)	0.0826	0.3205	−0.2184
H(161)	−0.0008	0.4421	−0.1167
H(162)	0.0840	0.4577	−0.0351
H(163)	0.0182	0.4161	0.0169

^{a} The aromatic hydrogen atoms were fixed in calculated positions; the position for the bridging hydrogen atom was derived from a difference Fourier map and fixed for least squares. The methyl hydrogen atoms were varied as a fixed group for each methyl carbon atom.

Table VI. Interatomic Distances (Å) for
$(\mu\text{-H})\text{Re}_2(\text{CO})_7(\mu\text{-NC}_5\text{H}_4)(\text{Me}_3\text{NO})$

Re–Re, Re–H, Pyridyl, and Me$_3$NO Distances

Re(1)–Re(2)	3.2324 (5)	C(11)–C(12)	1.35 (2)
Re(1)–H	1.8 (2)	C(12)–C(13)	1.35 (2)
Re(2)–H	1.7 (3)	C(13)–N(1)	1.36 (1)
Re(1)–N(1)	2.165 (7)	Re(1)–O(9)	2.148 (6)
Re(2)–C(9)	2.156 (9)	O(9)–N(2)	1.41 (1)
N(1)–C(9)	1.37 (1)	N(2)–C(14)	1.47 (2)
C(9)–C(10)	1.42 (1)	N(2)–C(15)	1.50 (2)
C(10)–C(11)	1.37 (2)	N(2)–C(16)	1.48 (1)

Re–Carbonyl Carbon Distances

Re(1)–C(2)	1.89 (1)	Re(2)–C(5)	2.00 (1)
Re(1)–C(3)	1.92 (1)	Re(2)–C(6)	1.968 (9)
Re(1)–C(4)	1.93 (1)	Re(2)–C(7)	1.93 (1)
		Re(2)–C(8)	1.97 (1)

Carbonyl C–O Distances

C(2)–O(2)	1.16 (1)	C(6)–O(6)	1.15 (1)
C(3)–O(3)	1.14 (1)	C(7)–O(7)	1.15 (1)
C(4)–O(4)	1.14 (1)	C(8)–O(8)	1.15 (1)
C(5)–O(5)	1.13 (1)		

tution. Complete reaction of I required 1–2 h, at which point the major product was IV. The only disubstituted species produced was IXa; conversion of IV to IXa was estimated to be 5–10 times slower than monosubstitution. Overall conversion of I and IXa was quantitative after 10–15 h. A pure sample of IXb, obtained from the reaction of I with Me$_3$NO/py, was found to isomerize rapidly in solution to IXa under photolysis.

A more highly substituted product was slowly produced when the solution was purged with Ar during photolysis. IXa (50 mg in 25 mL of toluene), photolyzed in this manner for 10–15 h in the presence of excess pyridine, was converted in 20% isolated yield to the trisubstituted complex $(\mu\text{-H})\text{Re}_2(\text{CO})_5(\mu\text{-NC}_5\text{H}_4)(\text{py})_3$, XI. This compound was isolated as a yellow solid by TLC (1:1 CH$_2$Cl$_2$/benzene) and characterized spectroscopically (see Table VIII).

(B) Triphenylphosphine. Photolysis of a solution of I in the presence of a five fold excess of PPh$_3$ resulted in mono- and disubstitution on a similar time scale as the reaction with pyridine. The monosubstituted species V could be separated from the more polar disubstituted products by TLC with a 2:1 hexane/benzene mobile phase. In contrast to the Me$_3$NO-promoted and thermal reactions, photolysis generated three disubstituted products (X plus two isomers). These could not be separated by TLC or column chromatography. The two major species, produced in approximately equal amounts, were X and an isomer of X characterized by NMR (360 MHz, CD$_2$Cl$_2$): δ −11.81 (dd, 1 H, μ-H, $J_{\text{H-P(1)}}$ = 9 Hz, $J_{\text{H-P(2)}}$ = 11 Hz), 8.30 (dd, 1 H, μ-py$_\alpha$), 7.5–7.1 (complex m, 2 PPh$_3$ + μ-py$_{\beta'}$), 6.82 (td, 1 H, μ-py$_{\beta \text{ or } \gamma}$), 6.60 (td, 1 H, μ-py$_{\gamma \text{ or } \beta}$); $J_{\alpha\beta}$, $J_{\beta\gamma}$, $J_{\beta'\gamma}$ = 6–7 Hz, $J_{\alpha\gamma}$, $J_{\beta\beta'}$ = 1–2 Hz. A minor amount of another isomer, the same as observed in the thermal reaction with PPh$_3$, was also present.

Low isolated yields (10–20%) of a trisubstituted complex, $(\mu\text{-H})\text{Re}_2(\text{CO})_5(\mu\text{-NC}_5\text{H}_4)(\text{PPh}_3)_3$, XII, were obtained by using extended photolysis of a solution purged with Ar. The product was isolated as a pale yellow solid by TLC (2:1 hexane/benzene) and characterized spectroscopically (Table VIII).

(C) Triphenyl Phosphite. $(\mu\text{-H})\text{Re}_2(\text{CO})_7(\mu\text{-}$ NC$_5$H$_4$)[P(OPh)$_3$], VII, was generated by photolysis of I in the presence of 1 equiv of P(OPh)$_3$ for about 1 h. Only a small amount of disubstitution occurred under these conditions. The crude product was isolated as a colorless oil by TLC (4:1 hexane/benzene) and subsequent solvent evaporation. Spectroscopic data for VII is contained in Table VIII.

(D) 1-Octene. Photolysis of an argon-purged solution of I containing 100 equiv of 1-octene resulted in formation of $(\mu\text{-H})\text{Re}_2(\text{CO})_7(\mu\text{-NC}_5\text{H}_4)(\eta^2\text{-1-octene})$, VIII, within an hour. Yields estimated by IR and NMR exceeded 50%. Although stable in the absence of excess 1-octene (removed by vacuum), VIII decomposed rapidly when exposed to air. It was thus characterized by IR and ^{1}H NMR only (Table VIII). The hydride and vinyl proton resonances observed in the NMR are probably broadened due to olefin rotation about the Re–olefin bond.[13] VIII reacted with CO (1 atm, benzene solution) at room temperature within a few minutes to yield equimolar amounts of I and free 1-octene, as observed by NMR spectroscopy. VIII showed no tendency to isomerize excess 1-octene to internal octenes at 25 °C and decomposed to IV plus insoluble species upon heating to 70 °C in benzene.

Discussion

Solid-State Structure of I. The two crystallographically independent molecules of I are structurally very

---

(13) Herberhold, M. "Metal π-Complexes"; Elsevier Scientific: New York, 1974; Vol. II, Part 2, pp 59–66.

Table VII. Bond Angles (deg) for (μ-H)Re₂(CO)₇(μ-NC₅H₄)(Me₃NO)

Angles about Re Atoms

Re(2)-Re(1)-N(1)	64.9 (2)	O(9)-Re(1)-H	82 (7)	C(9)-Re(2)-C(6)	83.7 (4)
Re(2)-Re(1)-O(9)	83.7 (2)	C(2)-Re(1)-C(3)	89.7 (4)	C(9)-Re(2)-C(7)	95.7 (4)
Re(2)-Re(1)-C(2)	90.6 (3)	C(2)-Re(1)-C(4)	85.3 (4)	C(9)-Re(2)-C(8)	170.1 (4)
Re(2)-Re(1)-C(3)	161.0 (3)	C(2)-Re(1)-H	95 (6)	C(9)-Re(2)-H	88 (9)
Re(3)-Re(1)-C(4)	109.3 (3)	C(3)-Re(1)-C(4)	89.6 (5)	C(5)-Re(2)-C(6)	172.1 (4)
Re(2)-Re(1)-H	23 (10)	C(3)-Re(1)-H	174 (6)	C(5)-Re(2)-C(7)	87.5 (4)
N(1)-Re(1)-O(9)	77.3 (3)	C(4)-Re(1)-H	87 (11)	C(5)-Re(2)-C(8)	94.7 (4)
N(1)-Re(1)-C(2)	95.3 (4)	Re(1)-Re(2)-C(9)	64.1 (2)	C(5)-Re(2)-H	86 (7)
N(1)-Re(1)-C(3)	96.2 (4)	Re(1)-Re(2)-C(5)	92.5 (3)	C(6)-Re(2)-C(7)	90.5 (4)
N(1)-Re(1)-C(4)	174.1 (4)	Re(1)-Re(2)-C(6)	86.7 (3)	C(6)-Re(2)-C(8)	93.1 (4)
N(1)-Re(1)-H	87 (11)	Re(1)-Re(2)-C(7)	159.8 (3)	C(6)-Re(2)-H	97 (7)
O(9)-Re(1)-C(2)	172.1 (3)	Re(1)-Re(2)-C(8)	106.4 (3)	C(7)-Re(2)-C(8)	93.7 (4)
O(9)-Re(1)-C(3)	93.9 (4)	Re(1)-Re(2)-H	25 (8)	C(7)-Re(2)-H	172 (6)
O(9)-Re(1)-C(4)	101.8 (4)	C(9)-Re(2)-C(5)	88.9 (4)	C(8)-Re(2)-H	83 (9)

Angles about Hydride and Pyridyl Atoms

Re(1)-H-Re(2)	131 (17)	Re(2)-C(9)-C(10)	127.1 (7)	C(11)-C(12)-C(13)	118 (1)
Re(1)-N(1)-C(13)	125.6 (6)	N(1)-C(9)-C(10)	116.1 (8)	C(12)-C(13)-N(1)	123.8 (10)
Re(1)-N(1)-C(9)	114.3 (6)	C(9)-C(10)-C(11)	121.7 (10)	C(13)-N(1)-C(9)	120.2 (8)
Re(2)-C(9)-N(1)	116.7 (6)	C(10)-C(11)-C(12)	121 (1)		

Angles about Me₃NO Atoms

Re(1)-O(9)-N(2)	128.1 (5)	O(9)-N(2)-C(15)	104.9 (8)	O(9)-N(2)-C(16)	112.2 (8)
O(9)-N(2)-C(14)	111.6 (8)				

Angles about Carbonyl Carbons

Re(1)-C(2)-O(2)	178.6 (9)	Re(2)-C(5)-O(5)	176.3 (9)	Re(2)-C(7)-O(7)	178 (1)
Re(1)-C(3)-O(3)	179.4 (10)	Re(2)-C(6)-O(6)	174.6 (8)	Re(2)-C(8)-O(8)	174.5 (9)
Re(1)-C(4)-O(4)	178 (1)				

Torsion Angles

O(9)-Re(1)-Re(2)-C(5)	-9.3 (3)	C(4)-Re(1)-Re(2)-C(8)	-4.7 (5)
C(2)-Re(1)-Re(2)-C(6)	-11.7 (4)	Re(1)-N(1)-C(9)-Re(2)	-1.6 (8)
C(3)-Re(1)-Re(2)-C(7)	-3.3 (14)		

similar, with small differences attributable to crystal packing forces. The geometry about each rhenium is best described as distorted octahedral. When viewed down the Re–Re bond, the C–Re–Re–C torsion angles are less than 6°. The eclipsed geometry, which contrasts with the staggered (D_{4d}) geometry of Re₂(CO)₁₀,[14] presumably originates in the geometrical requirements of the bridging pyridyl ligand.

The Re–Re bond distances of 3.2088 (4) and 3.1956 (5) Å are longer than that of Re₂(CO)₁₀ (3.0413 (11) Å)[15] but are consistent with values reported for other hydride-bridged Re–Re single bonds.[16] The symmetrical hydride bridge is located opposite the pyridyl bridge between the C(4) and C(8) carbonyls in molecule A and between the C(12) and C(16) carbonyls in B. Molecules A and B differ with respect to the hydride position, but the differences are not great relative to the estimated error. Assignment of the position of the hydride is supported by the relatively large Re–Re–C(4) (C(12)) and Re–Re–C(8) (C(16)) bond angles, 107–111°. The Re–N(py) bond lengths, 2.184 (7) and 2.185 (7) Å, are comparable to the Re–N values reported for [ReCl₄(NO)(py)]⁻ (2.218 (6) Å)[17] and H₃Re₃(CO)₁₀(py)₂ (mean 2.22 Å).[18] The Re–C(pyridyl) bond distances, 2.181 (8) and 2.197 (7) Å, are only slightly shorter than the 2.22-Å value calculated for an Re–C(sp²) single

bond[19] and significantly longer than those observed in Re(η¹-Ph)₃(PEt₂Ph)₂ (average Re–C distance is 2.027 (3) Å).[19] The pyridyl bridge system appears to be essentially free of strain, as the Re-pyridyl bond angles (Re(1)–N-(1)–C(21), Re(1)–N(1)–C(17), Re(2)–C(17)–N(1), and Re-(2)–C(17)–C(18) in A; Re(3)–N(2)–C(26), Re(3)–N(2)–C-(22), Re(4)–C(22)–N(2), and Re(4)–C(22)–C(23) in B) are within a 4–8° range of 120°. The absence of substantial ring strain is reflected in the stability of the pyridyl bridge, which does not undergo elimination at 80 °C in the presence of CO, PPh₃, or other ligands.

The average of the Re–C bond lengths for carbonyl groups trans to another CO (A, 1.99 (1) Å; B, 2.00 (2) Å)[20] is significantly longer than the average for the carbonyl groups that lack a trans CO (A, 1.94 (3) Å; B, 1.95 (2) Å). This phenomenon has been noted frequently in structural studies of substituted metal carbonyl complexes and is probably due to competition for dπ-electron density between mutually trans carbonyls.[21] The effect is also observed in Re₂(CO)₁₀, where the average Re–CO(equatorial) distance, 1.987 (15) Å, is longer than the Re–CO(axial) bond length, 1.929 (7) Å.[15] There appears to be no significant difference between the two rheniums in I in terms of the Re–C bond lengths of the mutually trans carbonyls. Among the carbonyl ligands that lack a trans CO, the longest Re–C distance in A is Re(2)–C(8) (Re(4)–C(16) in B), trans to the bond to pyridyl carbon.

UV–Visible Spectrum of I. The UV–visible spectrum of I is markedly different from that of Re₂(CO)₁₀,[22] eq-

(14) Dahl, L. F.; Ishishi, E.; Rundle, R. E. *J. Chem. Phys.* 1957, *26*, 1750.

(15) Churchill, M. R.; Amoh, K. N.; Wasserman, H. J. *Inorg. Chem.* 1981, *20*, 1609.

(16) (a) Huie, B. T.; Kirtley, S. W.; Knobler, C. B.; Kaesz, H. D. *J. Organomet. Chem.* 1981, *213*, 45. (b) Wei, C.; Garlaschelli, L.; Bau, R.; Koetzle, T. F. *Ibid.* 1981, *213*, 63. (c) Churchill, M. R. *Adv. Chem. Ser.* 1978, *No. 167*, 36.

(17) Ciani, G.; Giusto, D.; Manassero, M.; Sansoni, M. *J. Chem. Soc., Dalton Trans.* 1978, 798.

(18) Ciani, G.; D'Alfonso, G.; Freni, M.; Romiti, P.; Sironi, A. *J. Organomet. Chem.* 1980, *186*, 353.

(19) Carroll, W. E.; Bau, R. *J. Chem. Soc., Chem. Commun.* 1978, 825.

(20) Esd's of average distances were calculated via the scattter formula [σ]² = [∑ₙ(dᵢ − d̄)²]/(N − 1).

(21) (a) Atwood, J. L.; Darensbourg, D. J. *Inorg. Chem.* 1977, *16*, 2314. (b) Cotton, F. A.; Darensbourg, D. J.; Klein, S.; Kolthammer, B. W. S. *Ibid.* 1982, *21*, 1651. (c) Cotton, F. A.; Darensbourg, D. J.; Klein, S.; Kolthammer, B. W. S. *Ibid.* 1982, *21*, 2661.

Table VIII. Spectroscopic Data for the Substitution Products of I

compd[a]	^{1}H NMR,[b,c] δ	ν_{CO},[d] cm^{-1}	FDMS,[e] m/e
(a)	$(\mu\text{-H})\text{Re}_2(\text{CO})_7(\mu\text{-NC}_5\text{H}_4)\text{L}$		
II (L = NMe$_3$)[f]	8.42 (dd, 1 H, μ-py$_\alpha$), 7.66 (dd, 1 H, μ-py$_{\beta'}$),[g] 7.26 (td, 1 H, μ-py$_{\beta or \gamma}$), 6.89 (td, 1 H, μ-py$_{\gamma or \beta}$), 2.67 (s, 9 H, NMe$_3$), $-$10.74 (s, 1 H, μ-H); $J_{\alpha\beta'}$, $J_{\beta\gamma}$, $J_{\gamma\beta'}$ = 6-7 Hz; $J_{\alpha\gamma}$, $J_{\beta\beta'}$ = 1-2 Hz[h]	2088 (w), 2023 (s), 1996 (s), 1970 (ms), 1948 (ms), 1916 (sh), 1910 (ms)	M$^+$ 706
III (L = Me$_3$NO)[i]	8.38 (dd, 1 H, μ-py$_\alpha$), 7.66 (dd, 1 H, μ-py$_{\beta'}$), 7.21 (td, 1 H, μpy$_{\beta or \gamma}$), 6.80 (td, 1 H, μ-py$_{\gamma or \beta}$), 3.11 (s, 9 H, Me$_3$NO), $-$11.00 (s, 1 H, μ-H)	2088 (w), 2015 (s), 1988 (s), 1978 (sh), 1936 (ms), 1907 (m), 1889 (m)	M$^+$ 722
V (L = PPh$_3$)[i]	7.52 (dd, 1 H, μ-py$_\alpha$), 7.45-7.30 (m, PPh$_3$ + μ-py$_{\beta'}$), 7.04 (td, 1 H, μ-py$_{\beta or \gamma}$), 6.37 (td, 1 H, μ-py$_{\gamma or \beta}$), $-$12.65 (d, 1 H, μ-H); $J_{(\mu\text{-H})\text{-P}}$ = 12.6 Hz	2088 (w), 2029 (ms), 1992 (m), 1978 (m), 1949 (s), 1942 (w), 1920 (m)	M$^+$ 909
VI (L = CH$_3$CN)[i]	8.39 (dd, 1 H, μ-py$_\alpha$), 7.63 (dd, 1 H, μ-py$_{\beta'}$), 7.24 (td, 1 H, μ-py$_{\beta or \gamma}$), 6.83 (td, 1 H, μ-py$_{\gamma or \beta}$), 2.20 (s, 3 H, CH$_3$CN), $-$12.66 (s, 1 H, μ-H)	2090 (w), 2031 (s), 1996 (s), 1972 (s), 1943 (ms), 1930 (sh), 1920 (ms)	M$^+$ 688
VII (L = P(OPh)$_3$)	8.03 (dd, 1 H, μ-py$_\alpha$), 7.53 (dd, 1 H, μ-py$_{\beta'}$), 7.3-7.0 (m, P(OPh)$_3$ + μ-py$_{\beta or \gamma}$), 6.60 (td, 1 H, μ-py$_{\gamma or \beta}$), $-$13.70 (d, 1 H, μ-H); $J_{(\mu\text{-H})\text{-P}}$ = 17 Hz	2091 (w), 2042 (s), 1993 (s), 1986 (sh), 1961 (m), 1948 (s), 1936 (m)	M$^+$ 957
VIII (L = 1-octene)	7.67 (dd, 1 H, μ-py$_\alpha$), 7.33 (dd, 1 H, μ-py$_{\beta'}$), 6.47 (td, 1 H, μ-py$_{\beta or \gamma}$), 6.02 (td, 1 H, μ-py$_{\gamma or \beta}$), 4.8-3.7 (br m, 1 H, vinyl H), 2.9-1.5 (br m, 2 H, 2 vinyl H), 1.17 (br s, -(CH$_2$)$_5$-), 0.87 (t, 3 H, CH$_3$), $-$13.70 (br s, half-width ~9 Hz, 1 H, μ-H)	2088 (w), 2035 (m), 1993 (s), 1978 (s), 1945 (s), 1928 (m)	
(b)	$(\mu\text{-H})\text{Re}_2(\text{CO})_6(\mu\text{-NC}_5\text{H}_4)\text{L}_2$		
IXa (L = py)[i]	8.7-8.4 (m, 5 H, 4 py$_\alpha$ + μ-py$_\alpha$), 7.92 (dd, 1 H, μ-py$_{\beta'}$), 7.8-7.6 (m, 2 H, 2 py$_\gamma$), 7.41 (td, 1 H, μ-py$_{\beta or \gamma}$), 7.3-7.05 (m, 4 H, 4 py$_\beta$), 6.97 (td, 1 H, μ-py$_{\gamma or \beta}$), $-$7.68 (s, 1 H, μ-H)	2022 (w), 2002 (m), 1909 (s, br), ~1894 (sh)	M$^+$ 777
IXb (L = py)	8.56 (dd, 1 H, μ-py$_\alpha$), 8.31 (dd, 2 H, 2 py$_\alpha$), 8.0-7.9 (m, 3 H, 2 py$_\alpha$ + μ-py$_{\beta'}$), 7.5-7.3 (m, 3 H, 2 py$_\gamma$ + μ-py$_{\beta or \gamma}$), 6.98 (td, 1 H, μ-py$_{\gamma or \beta}$), 6.72 (td, 4 H, 4 py$_\beta$), $-$7.34 (s, 1 H, μ-H)	2028 (m), 2002 (m), 1930 (m), 1904 (m, br), 1899 (m, br)	M$^+$ 777
X (L = PPh$_3$)[i]	7.79 (dd, 1 H, μ-py$_\alpha$), 7.29 (dd, 1 H, μ-py$_{\beta'}$), 6.92 (td, 1 H, μpy$_{\beta or \gamma}$), 6.44 (td, 1 H, μ-py$_{\gamma or \beta}$), 8.0-6.8 (br s, 2 PPh$_3$), $-$11.99 (t, 1 H, μ-H); $J_{(\mu\text{-H})\text{-P}}$ = 8.6 Hz	2027 (w), 2011 (s), 1932 (s), 1924 (sh), 1909 (ms, br)	[M $-$ PPh$_3$]$^+$ 881
(c)	$(\mu\text{-H})\text{Re}_2(\text{CO})_5(\mu\text{-NC}_5\text{H}_4)\text{L}_3$		
XI (L = py)[i]	9.00 (dd, 1 H, μ-py$_\alpha$), 8.80 (dd, 2 H, 2 py$_\alpha$), 8.30 (dd, 2 H, 2 py$_\alpha$), 8.20 (dd, 2 H, 2 py$_\alpha$), 7.93 (dd, 1 H, μ-py$_{\beta'}$), 7.6-6.9 (m, 7 H, 3 py$_\gamma$ + 2 py$_\beta$ + 2 μ-py), 6.68 (td, 2 H, 2 py$_\beta$), 6.42 (td, 2 H, 2 py$_\beta$), $-$5.62 (s, 1 H, μ-H)	2000 (m), 1900 (s, br), ~1887 (sh), 1825 (m)	M$^+$ 828
XII (L = PPh$_3$)[k]	5.56 (td, 1 H, μ-py$_{\beta or \gamma}$), 7.9-6.5 (complex m, 3 PPh$_3$ + μ-py$_\alpha$ + μ-py$_{\beta'}$ + μ-py$_{\gamma or \beta}$), $-$11.33 (q, 1 H, μ-H); $J_{(\mu\text{-H})\text{-P}}$ = 7.0 Hz	2030 (w), 1924 (s), 1896 (m), 1850 (m)	[M $-$ PPh$_3$]$^+$ 1115

[a] Colorless, except where noted. [b] CD$_2$Cl$_2$ solution for all except VIII (C$_6$D$_6$). [c] 90 MHz for II, III, VI-IX, and XI; 360 MHz for V, X, and XII. [d] Toluene solution for II, III, VI, and VIII-XII; hexane solution for V and VII. [e] Re$_2$ = 372. [f] Sample contains ~10% I and ~10% II. [g] β' is defined as the μ-pyridyl proton ortho to the Re-C(pyridyl) bond. [h] The same values of these five coupling constants were observed for all compounds in the table. [i] Satisfactory elemental analysis (±0.4%) obtained for C, H, and N. [j] Yellow compound. [k] Pale yellow compound.

Re$_2$(CO)$_9$(py),[3] or 1,2-*eq,eq*-Re$_2$(CO)$_8$(py)$_2$,[3] which show strong absorptions in THF (25 °C) at 310 (13 900), 337 (13 600), and 355 nm (13 800 M^{-1} cm^{-1}), respectively. These are assigned to the σ-σ* transition[23] of the dinuclear complex. The 291-nm band of I is less intense than these and is significantly higher in energy. Because the Re-Re bond of I is longer than in Re$_2$(CO)$_{10}$, one might expect a σ-σ* transition to occur at lower energy. Thus, on the basis of both energy and intensity, the 291-nm band does not appear to be a σ-σ* transition.

The absorption may be due to a metal-ligand charge transfer to either CO or pyridyl. The spectrum of Re$_2$(C-

O)$_{10}$ (in 3-PIP, 77 K) exhibits M $\rightarrow$ CO charge-transfer bands at 278 (18 000) and 262 nm (12 500 M^{-1} cm^{-1}),[22] an absorption at 295 nm (8000 M^{-1} cm^{-1}) in *fac*-ReCl(CO)$_3$-(py)$_2$ (in CH$_2$Cl$_2$, 298 K) has been assigned as an Re $\rightarrow$ py charge-transfer transition.[24] The 291-nm band of I is comparable to these in energy and intensity.

The 345-nm band of I may be attributable to a ligand field transition[25] on the basis of its relatively low intensity ($\epsilon \approx 1100$ M^{-1} cm^{-1}).

Reaction of I with Me$_3$NO. Solid-State Structure of III. Me$_3$NO has been employed frequently in the past few years in the preparation of substituted metal carbonyl

(22) Levenson, R. A.; Gray, H. B. *J. Am. Chem. Soc.* **1975**, *97*, 6042.
(23) Geoffroy, G. L.; Wrighton, M. S. "Organometallic Photochemistry"; Academic Press: New York, 1979; p 107.
(24) Giordano, P. J.; Wrighton, M. S. *J. Am. Chem. Soc.* **1979**, *101*, 2888.
(25) Reference 23; pp 12-15.

Table IX. IR Data for $(\mu\text{-}H)Re_2(CO)_7(\mu\text{-}NC_5H_4)L$ Compounds

compd	ν_{CO},[c] cm^{-1}
II (L = NMe$_3$)[a]	2088 (w), 2023 (s),* 1996 (s), 1970 (ms), 1948 (ms), 1916 (sh),* 1910 (ms)*
IV (L = py)[a]	2090 (w), 2025 (s),* 1995 (s), 1977 (s), 1942 (ms), 1919 (sh),* 1913 (ms)*
VI (L = CH$_3$CN)[a]	2090 (w), 2031 (s),* 1996 (s), 1972 (s), 1943 (ms), 1930 (sh),* 1920 (ms)*
V (L = PPh$_3$)[b]	2088 (w), 2029 (ms),* 1992 (m), 1978 (m), 1949 (s), 1942 (w),* 1920 (m)*
VII (L = P(OPh)$_3$)[b]	2091 (w), 2042 (s),* 1993 (s), 1986 (sh), 1948 (s), 1961 (m),* 1936 (m)*
III (L = Me$_3$NO)[a]	2088 (w), 2015 (s),* 1988 (s), 1978 (sh), 1936 (ms), 1907 (m),* 1889 (m)*

[a] Toluene solution. [b] Hexane solution. [c] See text for reference to starred and unstarred bands.

compounds.[26] The reaction is believed to proceed via nucleophilic attack of Me$_3$NO at a carbonyl carbon, followed by evolution of CO$_2$ and coordination of a donor ligand. In the absence of L, a few trimethylamine complexes have been prepared in this manner.[26b,27] The formation of $(\mu\text{-}H)Re_2(CO)_7(\mu\text{-}NC_5H_4)(NMe_3)$, II, in the present study is another example of such a reaction. The trimethylamine ligand of II is relatively labile, as facile substitution by pyridine occurs at 25 °C. The size of the Me$_3$N ligand may be largely responsible for its lability.

In the presence of excess Me$_3$NO, II does not undergo a second CO substitution to give a bis NMe$_3$ complex. Instead, the Me$_3$N ligand is substituted by trimethylamine N-oxide, yielding III. This phenomenon has not been observed previously in reactions of R$_3$NO with metal carbonyls. Further, III is apparently the first example of an organometallic compound containing a trialkylamine N-oxide ligand, although pyridine N-oxide complexes are known (Mo(CO)$_3$(C$_5$H$_5$NO)$_3$, Re(CO)$_3$(C$_5$H$_5$NO)$_2$X[28]). The compound is surprisingly robust; III does not react with pyridine at temperatures below 50 °C. IR studies indicate that the Me$_3$NO ligand is a strong donor (vide infra).

The solid-state molecular structure of III is closely similar to that of I, with the C(1) (molecule A) or C(9) (molecule B) carbonyl substituted by an O-bound Me$_3$NO ligand. The Re(1)-O(9)-N(2) bond angle, 128.1 (5)°, is typical for coordinated N-oxide ligands.[29,30] The O(9)-N(2) bond distance, 1.41 (1) Å, is very close to that reported for uncoordinated Me$_3$NO (1.388 (5) Å).[31] The bulky Me$_3$NO group apparently causes a large distortion from octahedral symmetry about Re(1) ($\angle$N(1)-Re(1)-O(9) = 77.3 (3)°, $\angle$O(9)-Re(1)-C(4) = 101.8 (4)°). The eclipsed structure of I is maintained in III, except that the O(9)-Re(1)-Re(2)-C(5) and C(2)-Re(1)-Re(2)-C(6) torsion angles (9.3 (3) and 11.7 (4)°, respectively) are larger than the analogous angles in I. This could result from the steric requirements of the Me$_3$NO ligand, which may also be responsible for the ~0.03 Å longer Re-Re bond in III.

The presence of the bridging hydride, located as in I, is manifested by large and approximately equal Re(2)-Re(1)-C(4) and Re(1)-Re(2)-C(8) angles. The Re-N(py) bond length is very similar to that of I. The Re-C(pyridyl) distance is slightly shorter than in I, but probably indicates a Re-C single bond with little or no π bonding. The M-CO bond length for the carbonyl trans to Me$_3$NO (1.89 (1) Å) is significantly shorter than the analogous bond length in

I (1.990 (9) Å in A and 2.01 (1) Å in B). Substitution of CO by nitrogen[32] or phosphorus[33] ligands in octahedral complexes has been observed to shorten the trans M-CO bond. As in I (A and B), the longest M-CO distance among the carbonyls that are not trans to a CO is that of the carbonyl trans to the C-bound pyridyl ring.

Monosubstitution of I. Substitution of one carbonyl ligand of I can be readily achieved via a thermal or photochemical reaction or by use of Me$_3$NO. A variety of substituting ligands has been employed in this study. In all cases, only one isomer of $(\mu\text{-}H)Re_2(CO)_7(\mu\text{-}NC_5H_4)L$ is observed. The olefin complex VIII (L = 1-octene) can be prepared only by the photochemical technique. In contrast, all three methods are suitable for L = py or PPh$_3$, and all yield the same isomer of IV or V, respectively. In reactions with Me$_3$NO, formation of III is prevented by a large excess of L.

The IR spectra in the carbonyl region of II–VIII are very similar. Thus it is likely that these compounds are isostructural.

On the basis of the X-ray crystal structure of III, we conclude that L is coordinated to the same Re as the bridging pyridyl nitrogen and occupies a position trans to CO.
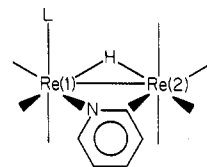
It is possible that substitution at the nitrogen-bound rhenium has its origins in a cis-labilizing effect.[34] Pyridine is found to be a much better cis-labilizing ligand than hyride, SnPh$_3^-$, or GePh$_3^-$. It is reasonable to suppose that an aryl group bound to rhenium should be more weakly labilizing than pyridine. If Me$_3$NO reactions proceed through a transition state that is similarly stabilized by a cis-labilizing ligand, then Me$_3$NO-induced monosubstitution at Re(1) is also reasonable. The photosubstitution behavior of I is more difficult to explain. As discussed earlier, the 345-nm band in the UV–visible spectrum of I may be a ligand field transition. Irradiation of such a transition in metal carbonyl compounds is generally observed to result in CO dissociation.[25] It is not clear, however, why monosubstitution occurs exclusively at Re(1). One possibility is that regardless of where CO loss occurs, the unsaturated intermediate undergoes rapid intramolecular rearrangement via carbonyl migration such that the vacant site ends up at the metal center where coordinative unsaturation is most favored energetically, i.e., at Re(1). Such a mechanism has been proposed for the substitution

(26) (a) Shvo, Y.; Hazum, E. *J. Chem. Soc., Chem. Commun.* **1976**, *829.* (b) Koelle, U. *J. Organomet. Chem.* **1977**, *133*, 53. (c) Blumer, D. J.; Barnett, K. W.; Brown, T. L. *Ibid.* **1979**, *173*, 71. (d) Shapley, J. R.; Pearson, G. A.; Tachikawa, M.; Schmidt, G. E.; Churchill, M. R.; Hollander, F. J. *J. Am. Chem. Soc.* **1977**, *99*, 8064.

(27) Elzinga, J.; Hogeveen, H. *J. Chem. Soc., Chem. Commun.* **1977**, 705.

(28) Sartorelli, U.; Canziani, F.; Zingales, F. *Inorg. Chem.* **1966**, *5*, 2233.

(29) Kai, Y.; Yasuoka, N.; Kasai, N.; Kakudo, M. *Bull. Chem. Soc. Jpn.* **1972**, *45*, 3388.

(30) Karayannis, N. M.; Pytlewski, L. L.; Mikulski, C. M. *Coord. Chem. Rev.* **1973**, *11*, 93.

(31) Caron, A.; Donohue, J. *Acta Crystallogr.* **1962**, *15*, 1052.

(32) (a) Cotton, F. A.; Richardson, D. C. *Inorg. Chem.* **1966**, *5*, 1851. (b) Hitchcock, P. B.; Lappert, M. F.; Pye, P. L. *J. Chem. Soc., Dalton Trans.* **1977**, 2160.

(33) (a) Cheung, K. K.; Lai, T. F.; Mok, K. S. *J. Chem. Soc. A* **1971**, 1644. (b) Plastas, H. J.; Stewart, J. M.; Grim, S. O. *Inorg. Chem.* **1973**, *12*, 265.

(34) Atwood, J. D.; Brown, T. L. *J. Am. Chem. Soc.* **1976**, *98*, 3160.

Table X. Hydride NMR Chemical Shifts[a]

compd	δ	compd	δ
$(\mu\text{-H})Re_2(CO)_8(\mu\text{-NC}_5H_4)$	−14.52 (s)	$(\mu\text{-H})Re_2(CO)_{8-n}(\mu\text{-NC}_5H_4)(py)_n$	
		$n = 1$	−11.36 (s)
$(\mu\text{-H})Re_2(CO)_7(\mu\text{-NC}_5H_4)L$		$n = 2$[b]	−7.34 (s), −7.68 (s)
L = P(OPh)$_3$	−13.70 (d)	$n = 3$	−5.62 (s)
L = CH$_3$CN	−12.66 (s)		
L = PPh$_3$	−12.65 (d)	$(\mu\text{-H})Re_2(CO)_{8-n}(\mu\text{-NC}_5H_4)(PPh_3)_n$	
L = py	−11.36 (s)	$n = 1$	−12.65 (d)
L = Me$_3$NO	−11.00 (s)	$n = 2$[c]	−11.99 (t), −11.81 (dd), −11.70 (dd)
L = NMe$_3$	−10.74 (s)	$n = 3$	−11.33 (q)

[a] CD$_2$Cl$_2$ solution. [b] Two isomers. [c] Three isomers.

of Mn$_2$(CO)$_{10}$ and Ru$_3$(CO)$_{12}$ by PPh$_3$.[34]

The IR spectra in the carbonyl region of II–VIII can be interpreted roughly in terms of a local symmetry analysis, i.e., consideration of each metal carbonyl unit as independent and without influence on the CO stretching modes of the other. The three carbonyls about Re(1) in II–VIII are in a facial ("C_{3v}") arrangement. Appropriate mononuclear analogs are fac-L$_2$L'M(CO)$_3$ complexes, which generally show three strong carbonyl bands.[35] Examples include Re(CO)$_3$(py)$_2$I (2041, 1934, and 1891 cm^{-1} in CHCl$_3$) and Re(CO)$_3$(PPh$_3$)$_2$I (2049, 1996, and 1904 cm^{-1} in CHCl$_3$).[36] The four carbonyls about Re(2) are in a "C_{2v}"-type arrangement, for which a reasonable analogy is cis-M(CO)$_4$L$_2$. These compounds display four IR bands: a weak, high-frequency band and three of lower frequency that range from medium to strong in intensity.[37] Re-(CO)$_4$(phen)$^+$ is representative: 2123 (w), 2032 (vs), 2010 (m), 1967 (m) cm^{-1} in acetone.[38] IR spectral data for II–VII are summarized in Table IX. The starred bands are believed to be the stretching modes of the Re(1) tricarbonyl unit. These assignments are made on the basis of two observations: the intensities of the three bands for each complex are comparable (medium-strong, with the one exception of the 1942- cm^{-1} band for L = PPh$_3$) and these bands are the most strongly affected by the electronic nature of L. Among the nitrogen ligand compounds (II, IV, and VI), the starred bands clearly show the expected trend based upon the donor strength of L, i.e., an increase in frequency upon substitution of Me$_3$N or pyridine by CH$_3$CN. A similar effect is noted on changing L from PPh$_3$ to P(OPh)$_3$. The four unstarred bands of each complex are consistent with the general frequency and intensity pattern expected for the Re(2) "C_{2v}" tetracarbonyl unit. Although these bands are somewhat affected by the nature of L, their frequencies shift considerably less than the starred bands. (It should be noted that the 1948–49 cm^{-1} band for L = PPh$_3$ and P(OPh)$_3$ is intense in both complexes and is thus distinguished from the two nearby, less intense Re(1) tricarbonyl bands.)

Comparison of the IR spectrum of III (L = Me$_3$NO) with those of the nitrogen ligand complexes (II, IV, and VI) clearly indicates that the Me$_3$NO group is a strong donor. The spectrum in general is noticeably lower in frequency than II or IV (L = Me$_3$N, py). The starred bands, which are likely the stretching modes of the Re(1) carbonyls, are most strongly shifted.

Higher Substitution. Disubstitution of I by pyridine or PPh$_3$ can be effected by thermal, photochemical, or Me$_3$NO means. Reaction with a second equivalent of ligand, however, proceeds more slowly than the first in all

three reaction types. In addition, more than one isomer of the disubstituted complex is often produced.

Disubstitution of I by pyridine via Me$_3$NO initially generates two isomers of $(\mu\text{-H})Re_2(CO)_6(\mu\text{-NC}_5H_4)(py)_2$, IXa (80–85%) and IXb (15–20%). Since these species are the products of substitution of IV, a logical question that arises is whether the second substitution occurs at Re(1) or Re(2). If substitution took place at Re(1), then the "C_{2v}"-type tetracarbonyl geometry about Re(2) would remain intact. The disubstituted complex would be expected to show the four-band IR pattern associated with Re(2) as observed in the spectrum of IV (see Table IX, unstarred bands), although the pattern might be slightly perturbed. The IR spectra of both IXa and IXb, however, clearly do not show these bands. Most noticeably, the high-frequency band (2090 cm^{-1}) of IV is absent from the spectra of IXa,b. It therefore appears that substitution of the second pyridine occurs at Re(2). This result is understandable in terms of a ground-state picture of IV. Re(1) is more electron-rich than Re(2), so Me$_3$NO attack preferentially occurs at a carbonyl bound to Re(2). Making the reasonable assumption that the pyridine ligand prefers to occupy a site trans to a CO, the two possible structures of IX are
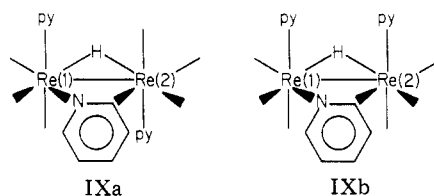
This assignment is consistent with the fact that IXb is a more polar species than IXa, as observed in chromatographic separation. Second, the thermal isomerization of IXb to IXa is likely a consequence of unfavorable steric interaction between the two adjacent pyridines in IXb. Isomerization to IXa clearly reduces interligand steric interaction.

The mechanism of the formation of these two isomers is not completely understood. One possibility is that Me$_3$NO can attack either of the mutually trans Re(2) carbonyls in IV. Immediate trapping of the resulting unsaturated intermediates by pyridine would give IXa,b. Another possibility is Me$_3$NO attack at only one carbonyl, followed by rapid fluxional rearrangement of the intermediate and coordination of pyridine at either of the two sites. Whatever the mechanism, the low yield of IXb relative to IXa is likely due to the steric effect of the nonbridging pyridine ligand in IV.

The thermal (80 °C) reaction of IV with pyridine yields only IXa, which is reasonable based on the thermal instability of IXb with respect to isomerization. The ground-state electronic picture of IV is consistent with CO loss from Re(2). The photochemical reaction likewise yields only IXa. That no IXb is observed is understandable in view of the fact that IXb undergoes rapid isom-

(35) Braterman, P. S. "Metal Carbonyl Spectra"; Academic Press: New York, 1975; pp 44–49.

(36) Abel, E. W.; Wilkinson, G. *J. Chem. Soc.* **1959**, 1501.

(37) Reference 35; pp 255–256.

(38) Kruck, Th.; Noack, M. *Chem. Ber.* **1964**, 97, 1693.

erizatioin to IXa under photolysis.

Disubstitution of I by PPh$_3$ via Me$_3$NO generates only one isomer of (μ-H)Re$_2$(CO)$_6$(μ-NC$_5$H$_4$)(PPh$_3$)$_2$, X. The structure of this complex is probably analogous to IXa. Formation of a IXb-type isomer is likely precluded by the severe steric repulsion of two adjacent PPh$_3$ ligands. In contrast to pyridine, thermal and photochemical reactions with PPh$_3$ produce more than one disubstituted isomer. The reason for this is not readily apparent but may involve the much greater π acidity of PPh$_3$. It is possible that, under the thermal or photochemical conditions, stable complexes can be formed in which PPh$_3$ ligands occupy sites that are not trans to a carbonyl. Unfortunately, the inability to physically separate the isomers for IR or X-ray analysis precludes structural determination.

Trisubstitution of I by pyridine or PPh$_3$ cannot be achieved by thermal (80 °C) or Me$_3$NO (up to 40 °C) means. The photochemical route yields a single isomer of (μ-H)Re$_2$(CO)$_5$(μ-NC$_5$H$_4$)L$_3$. The ligand arrangement in these compounds cannot be deduced from the spectroscopic data at hand. An interesting feature of the IR spectra is the band at very low frequency, particularly in the case where L = pyridine (1825 cm^{-1}, Table VIII). These low frequencies are probably due to buildup of electron density on the metals and are not indicative of bridging carbonyls.

It is noteworthy that the bridging pyridyl ligand of I and its derivatives is exceptionally stable. As an example, no reaction of I is observed at 80 °C under several atmo-spheres CO (toluene solution) after an entire day. In all the thermal, photochemical, and Me$_3$NO reactions with ligands, CO substitution is the only process observed; the μ-pyridyl, μ-hydrido structure is maintained.

Hydride NMR Chemical Shifts. Gard and Brown[3] originally postulated that the hydrides of I and IV were bridging on the basis of a high-field chemical shift in the NMR spectra. This hypothesis is confirmed by the X-ray crystallographic results for I and III. It is likely that the hydrides of all the substituted derivatives of I are bridging as well.

An interesting trend is noted in the hydride chemical shifts of these compounds (Table X). Substitution of CO by ligands that are stronger σ donors and weaker π acceptors results in a general downfield shift of the hydride resonance. The trend is most clearly evident among the (μ-H)Re$_2$(CO)$_{8-n}$(μ-NC$_5$H$_4$)(py)$_n$ species, n = 1–3.

Novel (η⁶-6-Alkenylfulvene)tricarbonylchromium(0) Complexes Resulting from the Reactions of Na[(η⁵-C₅H₄R')Cr(CO)₃] (R' = H or Me) with Some Allyl Chlorides

Allen D. Hunter and Peter Legzdins*

Department of Chemistry, The University of British Columbia, Vancouver, British Columbia, Canada V6T 1Y6

The principal organometallic products resulting from the reactions of Na[(η⁵-C₅H₄R')Cr(CO)₃] (R' = H or Me) with the allyl chlorides H$_2$C=C(R)C(R)HCl (R = H or Me) in THF are the green, dimeric [(η⁵-C₅H₄R')Cr(CO)₃]$_2$ complexes that can be isolated in yields of 51–67%. The organometallic byproducts usually formed during these conversions are novel (η⁶-6-alkenylfulvene)Cr(CO)$_3$ complexes that can be separated from the dried final reaction mixtures by extraction with hexanes and are isolable in yields of 5–8%. These alkenylfulvene-containing compounds are bright red, low-melting solids or liquids that have been characterized completely by conventional spectroscopic methods. A plausible reaction sequence that accounts for the formation of both types of organometallic products is proposed.

Introduction

During some of our investigations a few years ago, we had occasion to require [(η⁵-C₅H₅)Cr(CO)₃]$_2$.[1] This dimeric compound may be prepared by methods such as eq 1 and 2, but the generally accepted procedure for synthesizing the complex in bulk quantities involves the treatment of Na[(η⁵-C₅H₅)Cr(CO)₃] with various organic halides such as tropylium bromide, allyl bromide, or allyl chloride,[4] i.e.,

$$(\eta^5\text{-}C_5H_5)_2Cr + CO \xrightarrow[150\text{-}170\ ^\circ C]{100\ atm} [(\eta^5\text{-}C_5H_5)Cr(CO)_3]_2 \quad (1)^2$$

$$2(\eta^5\text{-}C_5H_5)Cr(CO)_3H \xrightarrow[\text{reflux}]{THF} [(\eta^5\text{-}C_5H_5)Cr(CO)_3]_2 + H_2 \quad (2)^3$$

$$2Na[(\eta^5\text{-}C_5H_5)Cr(CO)_3] + 2RX \xrightarrow{\text{diglyme}}$$
$$[(\eta^5\text{-}C_5H_5)Cr(CO)_3]_2 + 2NaX + R\text{-}R \quad (3)$$

where R = C$_7$H$_7$ or C$_3$H$_5$ and X = Br or Cl. Not surprisingly, therefore, we found during our earlier work[1] that reaction 3 proceeded as described[4] with RX = C$_3$H$_5$Br even when THF was employed as the solvent in place of di-

---

(1) Kolthammer, B. W. S.; Legzdins, P.; Malito, J. T. *Inorg. Chem.* 1977, *16*, 3173.

(2) Fischer, E. O.; Hafner, W. *Z. Naturforsch. B.* 1955, *102*, 140.
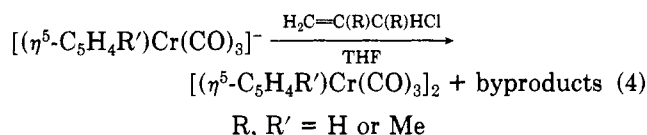(3) Keppie, S. A.; Lappert, M. F. *J. Chem. Soc. A.* 1971, 3216.
(4) King, R. B.; Stone, F. G. A. *Inorg. Synth.* 1963, *7*, 104.

erizatioin to IXa under photolysis.

Disubstitution of I by PPh_3 via Me_3NO generates only one isomer of $(\mu\text{-H})Re_2(CO)_6(\mu\text{-NC}_5H_4)(PPh_3)_2$, X. The structure of this complex is probably analogous to IXa. Formation of a IXb-type isomer is likely precluded by the severe steric repulsion of two adjacent PPh_3 ligands. In contrast to pyridine, thermal and photochemical reactions with PPh_3 produce more than one disubstituted isomer. The reason for this is not readily apparent but may involve the much greater π acidity of PPh_3. It is possible that, under the thermal or photochemical conditions, stable complexes can be formed in which PPh_3 ligands occupy sites that are not trans to a carbonyl. Unfortunately, the inability to physically separate the isomers for IR or X-ray analysis precludes structural determination.

Trisubstitution of I by pyridine or PPh_3 cannot be achieved by thermal (80 °C) or Me_3NO (up to 40 °C) means. The photochemical route yields a single isomer of $(\mu\text{-H})Re_2(CO)_5(\mu\text{-NC}_5H_4)L_3$. The ligand arrangement in these compounds cannot be deduced from the spectroscopic data at hand. An interesting feature of the IR spectra is the band at very low frequency, particularly in the case where L = pyridine (1825 cm^{-1}, Table VIII). These low frequencies are probably due to buildup of electron density on the metals and are not indicative of bridging carbonyls.

It is noteworthy that the bridging pyridyl ligand of I and its derivatives is exceptionally stable. As an example, no reaction of I is observed at 80 °C under several atmo-spheres CO (toluene solution) after an entire day. In all the thermal, photochemical, and Me_3NO reactions with ligands, CO substitution is the only process observed; the μ-pyridyl, μ-hydrido structure is maintained.

Hydride NMR Chemical Shifts. Gard and Brown[3] originally postulated that the hydrides of I and IV were bridging on the basis of a high-field chemical shift in the NMR spectra. This hypothesis is confirmed by the X-ray crystallographic results for I and III. It is likely that the hydrides of all the substituted derivatives of I are bridging as well.

An interesting trend is noted in the hydride chemical shifts of these compounds (Table X). Substitution of CO by ligands that are stronger σ donors and weaker π acceptors results in a general downfield shift of the hydride resonance. The trend is most clearly evident among the $(\mu\text{-H})Re_2(CO)_{8-n}(\mu\text{-NC}_5H_4)(py)_n$ species, $n = 1$–3.

Novel (η^6-6-Alkenylfulvene)tricarbonylchromium(0) Complexes Resulting from the Reactions of Na[$(\eta^5\text{-C}_5H_4R')$Cr(CO)$_3$] (R′ = H or Me) with Some Allyl Chlorides

Allen D. Hunter and Peter Legzdins*

Department of Chemistry, The University of British Columbia, Vancouver, British Columbia, Canada V6T 1Y6

The principal organometallic products resulting from the reactions of Na[$(\eta^5\text{-C}_5H_4R')$Cr(CO)$_3$] (R′ = H or Me) with the allyl chlorides H_2C=C(R)C(R)HCl (R = H or Me) in THF are the green, dimeric [$(\eta^5\text{-C}_5H_4R')$Cr(CO)$_3$]$_2$ complexes that can be isolated in yields of 51–67%. The organometallic byproducts usually formed during these conversions are novel (η^6-6-alkenylfulvene)Cr(CO)$_3$ complexes that can be separated from the dried final reaction mixtures by extraction with hexanes and are isolable in yields of 5–8%. These alkenylfulvene-containing compounds are bright red, low-melting solids or liquids that have been characterized completely by conventional spectroscopic methods. A plausible reaction sequence that accounts for the formation of both types of organometallic products is proposed.

Introduction

During some of our investigations a few years ago, we had occasion to require [$(\eta^5\text{-C}_5H_5)$Cr(CO)$_3$]$_2$.[1] This dimeric compound may be prepared by methods such as eq 1 and 2, but the generally accepted procedure for synthesizing the complex in bulk quantities involves the treatment of Na[$(\eta^5\text{-C}_5H_5)$Cr(CO)$_3$] with various organic halides such as tropylium bromide, allyl bromide, or allyl chloride,[4] i.e.,
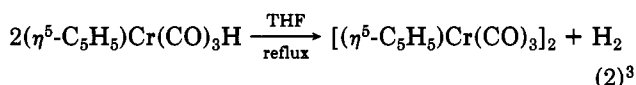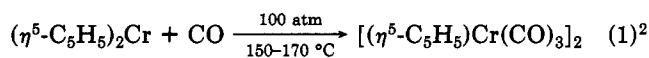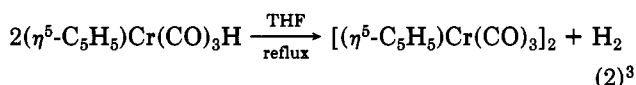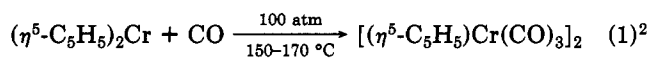
$$(\eta^5\text{-C}_5H_5)_2Cr + CO \xrightarrow[150-170\ °C]{100\ atm} [(\eta^5\text{-C}_5H_5)Cr(CO)_3]_2 \quad (1)^2$$

$$2(\eta^5\text{-C}_5H_5)Cr(CO)_3H \xrightarrow[reflux]{THF} [(\eta^5\text{-C}_5H_5)Cr(CO)_3]_2 + H_2 \quad (2)^3$$

$$2Na[(\eta^5\text{-C}_5H_5)Cr(CO)_3] + 2RX \xrightarrow{diglyme}$$
$$[(\eta^5\text{-C}_5H_5)Cr(CO)_3]_2 + 2NaX + R\text{–}R \quad (3)$$

where R = C_7H_7 or C_3H_5 and X = Br or Cl. Not surprisingly, therefore, we found during our earlier work[1] that reaction 3 proceeded as described[4] with RX = C_3H_5Br even when THF was employed as the solvent in place of di-

(1) Kolthammer, B. W. S.; Legzdins, P.; Malito, J. T. *Inorg. Chem.* **1977**, *16*, 3173.

(2) Fischer, E. O.; Hafner, W. *Z. Naturforsch. B* **1955**, *10²*, 140.
(3) Keppie, S. A.; Lappert, M. F. *J. Chem. Soc. A* **1971**, 3216.
(4) King, R. B.; Stone, F. G. A. *Inorg. Synth.* **1963**, *7*, 104.

glyme. We subsequently observed, however, that when allyl *chloride* in THF was used, the published workup procedure afforded markedly inferior yields of [(η^5-C_5H_5)Cr(CO)$_3$]$_2$. Furthermore, infrared spectral monitoring of the progress of the latter reaction indicated the formation of other carbonyl-containing products in addition to the desired dimer. Intrigued by these observations, we decided to examine more closely the reactions of Na-[(η^5-C_5H_5)Cr(CO)$_3$] and its methylcyclopentadienyl analogue in THF with some allyl chlorides. In this paper, we present the results of these studies.

Results and Discussion

When effected in THF, the reactions between Na[(η^5-C_5H_4R')Cr(CO)$_3$] (R' = H or Me) and allyl chlorides exhibit several characteristics that are different from those observed when diglyme is employed as the solvent (cf. eq 3). First, the transformations occur at a much slower rate. Consequently, greater than equimolar amounts of the allyl chlorides are required to consume completely the anionic reactants within reasonable periods of time. Typically, initial 1:3 mixtures of anion–chloride reach completion after 3–7 days at ambient temperatures. The rates of reaction are enhanced by refluxing the reaction mixture, but the final distribution of products is unaltered by doing so. Second, the use of THF as the solvent permits the more convenient separation of the organometallic products formed during these reactions. In particular, previously unknown (η^6-6-alkenylfulvene)tricarbonylchromium(0) complexes can be readily isolated from the final reaction mixtures.

The principal organometallic products formed during these conversions in THF (just as in diglyme) are the dimeric [(η^5-C_5H_4R')Cr(CO)$_3$]$_2$ (R' = H or Me) species, i.e., eq 4. The dimers are most conveniently separated by

$$[(\eta^5\text{-}C_5H_4R')Cr(CO)_3]^- \xrightarrow[\text{THF}]{H_2C=C(R)C(R)HCl} [(\eta^5\text{-}C_5H_4R')Cr(CO)_3]_2 + \text{byproducts} \quad (4)$$

$$R, R' = H \text{ or } Me$$

benzene extraction of the residues remaining after hexanes extraction of the dried final reaction mixtures. Removal of solvent from the benzene extracts in vacuo affords the dimeric complexes suitable for most purposes in yields of 51–67%. Analytically pure samples may be obtained by recrystallization of these materials from benzene–hexanes or hot hexanes.

The physical properties of [(η^5-C_5H_5)Cr(CO)$_3$]$_2$, including its solid-state molecular structure, have been amply described previously[4-6] and do not deserve further comment here. To the best of our knowledge, however, the properties or [(η^5-C_5H_4Me)Cr(CO)$_3$]$_2$ have not been reported[7] and hence merit brief delineation. The methylcyclopentadienyl dimer is a dark green, air-sensitive solid (mp 70 °C dec) that is freely soluble in common organic solvents but less so in paraffin hydrocarbons at ambient temperatures. Its IR [(CH_2Cl_2) ν_{CO} 2000 (m), 1941 (s), 1915 (s) cm^{-1}] and ^1H NMR spectra [($CDCl_3$) δ 5.64 (2 H, $\Delta\omega_{1/2} \simeq$ 15 Hz), 5.49 (2 H, $\Delta\omega_{1/2} \simeq$ 15 Hz), 3.51 (3 H, $\Delta\omega_{1/2}$ = 14 Hz)] are consistent with it being isostructural with its C_5H_5 analogue and displaying similar behavior in solution.[5] Its 70-eV mass spectrum (probe temperature 60 °C) exhibits
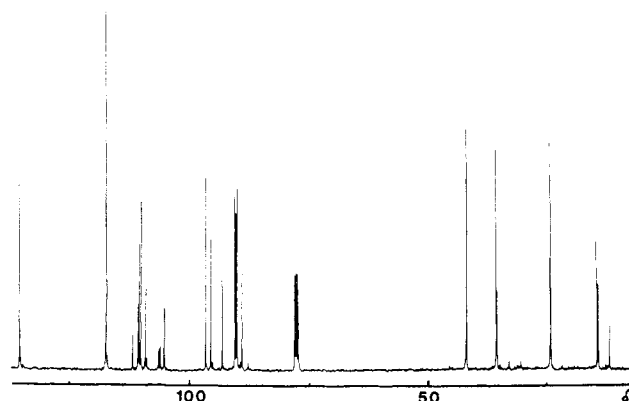
Figure 1. The 100.6-MHz $^{13}C\{^1H\}$ FT NMR spectrum in the hydrocarbon ligand region of (η^6-$C_{13}H_{18}$)Cr(CO)$_3$ (3) in CDCl$_3$.

no signals due to ions containing two chromium atoms. The principal spectral features are peaks due to the ions (C_5H_4Me)Cr(CO)$_n^+$ (n = 3, 2, 1, or 0) that indicate the weakness of the Cr–Cr linkage in the dimer.[6]

The organometallic byproducts usually formed during the conversions represented by eq 4 are novel (η^6-6-alkenylfulvene)Cr(CO)$_3$ complexes.[8] They can be separated from the dried final reaction mixtures by hexanes extraction and are isolabile in yields of 5–8% by subsequent chromatography on Florisil and sublimation in vacuo onto a water-cooled probe. They are bright red, low-melting solids or liquids at room temperature which can be handled in air for short periods of time without the occurrence of noticeable decomposition. They are freely soluble in common organic solvents to produce bright red solutions. Their spectral properties indicate that the complexes possess the molecular structures 1–3 in which the chro-
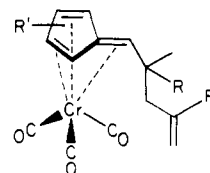
1, R' = R = H
2, R' = H, R = Me
3, R' = Me, R = H

mium atoms attain the favored 18-electron configuration by η^6 coordination to the substituted alkenylfulvenes as shown. The monomeric natures of the compounds are suggested by their mass spectra, all of which display prominent peaks due to the parent ions and ions resulting from the successive loss of CO groups from them. IR spectra of solutions of the complexes exhibit three strong carbonyl absorptions, indicative of a Cr(CO)$_3$ grouping, in the region previously reported for other (η^6-fulvene)Cr-(CO)$_3$ species.[9] The ^1H and $^{13}C\{^1H\}$ NMR data for these complexes (Table I) are consistent. In particular, the spectra of compound 3 in CDCl$_3$ (Table I and Figure 1)

(5) Adams, R. D.; Collins, D. E.; Cotton, F. A. *J. Am. Chem. Soc.* **1974**, *96*, 749.

(6) King, R. B. *J. Am. Chem. Soc.* **1966**, *88*, 2075.

(7) [(η^5-C_5H_4Me)Cr(CO)$_3$]$_2$ has been used to prepare [(η^5-C_5H_4Me)-Cr(CO)$_2$]$_2$; see: Hackett, P.; O'Neill, P. S.; Manning, A. R. *J. Chem. Soc., Dalton Trans.* **1974**, 1625.

(8) The reaction between Na[(η^5-C_5H_5)Cr(CO)$_3$] and 3-chloro-1-butene does not produce detectable amounts of a substituted fulvene-containing complex. Also, the (η^6-$C_{14}H_{20}$)Cr(CO)$_3$ byproduct from the reaction of Na[(η^5-C_5H_4Me)Cr(CO)$_3$] with 3-chloro-2-methylpropene may only be detected spectroscopically [IR (hexanes) ν_{CO} 1990 (s), 1928 (s), 1907 (s) cm^{-1}] as it has insufficient thermal stability to permit its isolation in a pure state at ambient temperature.

(9) For representative examples see: (a) Cooper, R. L.; Fischer, E. O.; Semmlinger, W. *J. Organomet. Chem.* **1967**, *9*, 333. (b) Andrianov, V. G.; Struchkov, Y. T.; Setkina, V. N.; Zdanovich, V. I.; Zhakaeva, A. Z.; Kursanov, D. N. *J. Chem. Soc., Chem. Commun.* **1975**, 117. (c) Edelmann, F.; Behrens, U. *J. Organomet. Chem.* **1977**, *134*, 31. (d) Edelmann, F.; Wormsbächer, D.; Behrens, U. *Chem. Ber.* **1978**, *111*, 817. (e) Koch, O.; Edelmann, F.; Behrens, U. *Ibid.* **1982**, *115*, 1313.

Table I. ^{1}H and ^{13}C $\{^1$H$\}$ NMR Data (δ scale) for the Isolated $(\eta^6$-6-Alkenylfulvene$)Cr(CO)_3$ Complexes in CDCl$_3$

assignt[b]	^{1}H NMR complex			assign	^{13}C$\{^1$H$\}$ NMR[a] complex		
	1	2	3		1	2	3
H(1,4)	4.79 (m)	4.76 (s), 4.87 (s)	4.74 (m), 4.81 (m)	C(1,2,3,4)	89.78 (d) 90.03 (d) 92.27 (d) 93.54 (d)	90.30 (d) 91.34 (d) 91.65 (d) 93.97 (d)	88.29 (d), 89.30 (d), 89.34 (d), 89.52 (d), 89.77 (d), 89.81 (d), 92.44 (d), 94.93 (d), 95.88 (d)
H(2,3)	5.31 (s), 5.35 (s)	5.29 (s), 5.32 (s)	5.31 (m)				
				C(5)	105.29 (s)	103.97 (s)	104.65 (s), 104.67 (s), 105.49 (s), 105.79 (s)
H(6)	4.21 (s)	4.03 (s)	4.14 (s), 4.21 (s)	C(6)	109.96 (d)	120.51 (d)	108.49 (d), 109.50 (d), 109.88 (d), 110.08 (d), 111.20 (s)
H(7)	2.03 (br)	$\cdots$	2.07 (m)	C(7)	35.81 (d)	39.83 (s)	35.13 (d), 35.18 (d), 35.23 (d), 35.39 (d), 35.44 (d)
H(8)	1.21 (d, J_{8-7} = 7 Hz)	1.20 (s)	1.24 (m)	C(8)	24.05 (q)	25.00 (q)	23.74 (q), 23.89 (q)
H(9)	2.23 (m), 2.55 (br)	2.32 (s)	2.26 (m), 2.58 (br)	C(9)	41.80 (t)	53.02 (t)	41.54 (t), 41.60 (5), 41.65 (t)
H(10)	5.88 (m)	$\cdots$	5.84 (br)	C(10)	135.40 (d)	142.54 (s)	135.22 (d), 135.27 (d)
H(11)	5.11 (d, J_{11a-10} = 10 Hz), 5.14 (d, J_{11b-10} = 16 Hz)	4.96 (s), 5.03 (s)	5.17 (t)	C(11)	117.29 (t)	116.00 (t)	116.85 (t), 116.88 (t)
H(12)	$\cdots$	1.31 (s)[c]	$\cdots$	C(12)	$\cdots$	26.10 (q)[c]	$\cdots$
H(13)	$\cdots$	1.85 (s)[d]	$\cdots$	C(13)	$\cdots$	30.07 (q)[d]	$\cdots$
H(14)	$\cdots$	$\cdots$	1.72 (s), 2.08 (s), 2.14 (s)[e]	C(14)	$\cdots$		11.37 (q), 13.70 (q), 13.99 (q)[e]
				CO	f	238.71 (s)	237.44 (s)

[a] The indicated multiplicities were derived from single frequency off-resonance decoupling (SFORD) of protons at δ −2. [b] These assignments are in accord with observed signal intensities and have been confirmed by homonuclear decoupling experiments. [c] For R = CH$_3$ at C(7). [d] For R = CH$_3$ at C(10). [e] For R' = CH$_3$ at C(1)-C(4) or C(6). [f] Not observable under the conditions employed for complexes 2 and 3.

clearly indicate the presence of the five isomers having R' = Me at any one of the ternary fulvene carbons (i.e., C-(1)–C(4) and C(6)) in approximately equal amounts. Regrettably, we have not as yet succeeded in growing suitable crystals of 1 (the only solid complex) for X-ray diffraction studies so that precise intramolecular dimensions can be determined for a representative compound of this type.[10]

The substituted fulvene complexes are somewhat thermally unstable, the isolated compounds decomposing partially to green oils when stored under an N$_2$ atmosphere at −6 °C for several months. The rate of decomposition is enhanced when the compounds are heated in vacuo at 60 °C, significant amounts of the green products being present after several days. We have isolated a small amount of the green complex resulting from the thermal decomposition of 1 by chromatography on Florisil with hexanes as eluant. Its low-resolution mass spectrum (probe temperature 100 °C) exhibits signals due to the ions L$_2$Cr$_2$(CO)$_n^+$ (where L$_2 \simeq$ C$_{22}$H$_{30}$ and n = 3, 2, 1, or 0), and its IR spectrum [(hexanes) ν_{CO} 1900 (s), 1880 (s) cm^{-1}] is indicative of Cr(CO)$_2$ groupings [cf. ν_{CO} for [(η^5-C$_5$H$_4$Me)Cr(C(CO)$_2$]$_2$ in hexanes at 1901 (s) and 1883 (s) cm^{-1}].[7] It thus appears that thermal decomposition involves a dimerization of the original complex with concomitant loss of CO. An analogous mode of decomposition has been reported recently for (η^6-diethylfulvene)Cr(CO)$_3$.[9e]

The exact mechanism by which the (η^6-6-alkenylfulvene)Cr(CO)$_3$ complexes originate during the reactions summarized by eq 4 remains to be ascertained. Nevertheless, the following observations are pertinent. The principal products of eq 4, i.e., the [(η^5-C$_5$H$_4$R')Cr(CO)$_3$]$_2$ dimers, do not react with allyl chlorides in THF at ambient temperatures.[11] Hence, the alkenylfulvene-containing byproducts must arise from the direct reactions of the [(η^5-C$_5$H$_4$R')Cr(CO)$_3$]$^-$ anions with the various H$_2$C=CRCH$_2$Cl (R = H or Me) reactants. Furthermore, the addition of a few milligrams of 2,2'-azobis(2-methylpropionitrile) to the reaction mixtures at room temperature has no apparent effect on the rates of reaction, thereby suggesting that free radicals are not involved in the rate-determining step of the mechanism. One plausible reaction sequence that accounts for the formation of both the [(η^5-C$_5$H$_4$R')Cr(CO)$_3$]$_2$ and (η^6-6-alkenylfulvene)Cr(CO)$_3$ products under ambient conditions is shown in Scheme I.

Initial electrophilic attack on the metal centers in the anionic reactants would result in the formation of η^1-allyl complexes. These complexes may convert directly to the [(η^5-C$_5$H$_4$R')Cr(CO)$_3$]$_2$ dimers (the predominant path a)

(10) The solid state molecular structures of two simpler (η^6-fulvene)-Cr(CO)$_3$ complexes, namely, (η^6-C$_5$H$_4$CPh$_2$)Cr(CO)$_3$[9b] and (η^6-C$_5$H$_4$CH$_2$)Cr(CO)$_3$,[9e] have been determined.

(11) [(η^5-C$_5$H$_5$)Cr(CO)$_3$]$_2$ does react with CH$_2$CHCH$_2$Cl in refluxing THF to produce 1 as the only carbonyl-containing product. This may well reflect the formation in situ of significant amounts of [(η^5-C$_5$H$_5$)-Cr(CO)$_3$]$^-$ under these conditions (cf. ref 7). It has previously been reported [Fischer, E. O.; Ulm, K.; Kuzel, P. Z. Anorg. Allg. Chem. 1963, 319, 253] that the dimer is converted to (η^5-C$_5$H$_5$)CrX$_2$·THF by CH$_2$CHCH$_2$X (X = Br or I) in the presence of THF.

Scheme I

$H_2C=C-CH_2Cl$

$-Cl^-$

Cr = Cr(CO)$_3$
R,R' = H or Me

(a)

(b)

(c)

$-[CH_2-C=CH_2]_2$

$-H_2$

or may transfer the allyl groups to the cyclopentadienyl rings in an endo fashion (step b). The latter complexes would probably have the structures indicated, the chromium atoms attaining 18-electron configurations. These diene–olefin complexes could then undergo condensation reactions with their respective η^1-allyl precursors, processes which result in the formation of the requisite carbon skeleton. The dinuclear condensation products could then rearrange to give the final, isolable (η^6-alkenylfulvene)-Cr(CO)$_3$ products via nontrivial rearrangements that may involve metal-assisted migrations of various substituents. [The (η^5-C$_5$H$_4$R')Cr(CO)$_3$H products resulting from the last step would slowly convert to [(η^5-C$_5$H$_4$R')Cr(CO)$_3$]$_2$ at ambient temperature.][12] Even though the postulated steps b[13] and c[14] have precedents in the literature of organometallic chemistry, it is obvious that this proposed reaction sequence must next be subjected to experimental scrutiny.

Experimental Section

General procedures routinely employed in these laboratories have been described previously.[15] Carbon-13 NMR spectra were recorded on Bruker WP-80 or WH-400 spectrometers with reference to the solvent used, but all ^{13}C chemical shifts are reported in parts per million downfield from Me$_4$Si. Mrs. M. Austria and Ms. M. A. Heldman assisted in obtaining these data.

Reaction of Na[(η^5-C$_5$H$_5$)Cr(CO)$_3$] with 3-Chloropropene. To a stirred, bright yellow solution of Na[(η^5-C$_5$H$_5$)Cr(CO)$_3$][16] (5.00 g, 22.3 mmol) in THF (150 mL) was added freshly distilled 3-chloropropene (5.5 mL, 67 mmol), and the progress of the reaction was monitored by IR spectroscopy. The characteristic, strong carbonyl absorptions of the anionic reactant at ca. 1895, 1790, and 1740 cm^{-1} gradually diminished in intensity, and the reaction mixture developed a green coloration. The carbonyl anion was

consumed after 3 days, the final mixture consisting of a brown precipitate and a dark green solution whose IR spectrum displayed absorptions at ca. 2005 (m), 1985 (m), 1940 (s), 1915 (s), and 1895 (s) cm^{-1}. The precipitate was removed by filtration through a medium porosity frit, and the filtrate was taken to dryness in vacuo. The resulting dark green tar was then extracted with hexanes (4 × 30 mL). The red extracts were concentrated under reduced pressure to a volume of ca. 5 mL, at which point an IR spectrum exhibited bands at 2020 (w), 1999 (s), 1950 (m), 1934 (s), 1915 (s), and 1890 (w) cm^{-1}. The concentrated extracts were transferred by syringe to the top of a Florisil column (3 × 6 cm) made up in hexanes. Elution of the column with hexanes developed a red band which was collected and taken to dryness in vacuo. Sublimation of the residue at ambient temperature and <0.005 mm onto a water-cooled probe afforded 0.32 g (5.1% yield based on Cr) of (η^6-C$_{11}$H$_{14}$)Cr(CO)$_3$ (1) as an analytically pure red solid: IR (hexanes) ν_{CO} 1999 (s), 1934 (s), 1915 (s) cm^{-1}; mass spectrum (probe temperature 120 °C), most intense parent ion m/z 282; mp (in air) 55–56 °C. Anal. Calcd for C$_{14}$H$_{14}$CrO$_3$: C, 59.57; H, 5.00; Cr, 18.42. Found: C, 59.45; H, 4.95; Cr, 18.37.

The insoluble green solid remaining after the extraction with hexanes was then extracted with benzene (4 × 50 mL). Solvent was removed from the extracts under reduced pressure to obtain 3.01 g (67% yield based on Cr) of spectroscopically pure [(η^5-C$_5$H$_5$)Cr(CO)$_3$]$_2$ as a green, microcrystalline solid. Analytically pure samples of the compound were obtained by recrystallization from benzene–hexanes: IR (CH$_2$Cl$_2$) ν_{CO} 2007 (m), 1945 (s), 1919 (s) cm^{-1}; ^{1}H NMR (CDCl$_3$) δ 6.45 ($\Delta\omega_{1/2}$ = 20 Hz). Anal. Calcd for C$_{16}$H$_{10}$Cr$_2$O$_6$: C, 47.78; H, 2.51. Found: C, 47.76; H, 2.38.

Reaction of Na[(η^5-C$_5$H$_4$Me)Cr(CO)$_3$][16] with 3-Chloropropene. This reaction was effected in a manner identical with that described in the preceding section. In this case, however, the conversion was complete in only 2 days. The final reaction mixture was worked up in the customary fashion with the exception that the red hexanes extracts were chromatographed thrice rather than once to obtain 0.42 g (6.6% yield based on Cr) of (η^6-C$_{12}$H$_{16}$)Cr(CO)$_3$ (3) as an analytically pure, viscous red liquid: IR (hexanes) ν_{CO} 1993 (s), 1927 (s), 1910 (s) cm^{-1}; mass spectrum (probe temperature 25 °C), most intense parent ion m/z 296. Anal. Calcd for C$_{15}$H$_{16}$CrO$_3$: C, 60.81; H, 5.44. Found: C, 60.69; H, 5.73.

The usual workup also resulted in the isolation of 2.5 g (54% yield based on Cr) of [(η^5-C$_5$H$_4$Me)Cr(CO)$_3$]$_2$ as a green solid. The isolated material was further purified by crystallization from hexanes to obtain 1.5 g of dark green crystals: IR (CH$_2$Cl$_2$) ν_{CO} 2000 (m), 1941 (s), 1915 (s) cm^{-1}; ^{1}H NMR (CDCl$_3$) δ 5.64 (2 H, $\Delta\omega_{1/2}$ = 15 Hz), 5.49 (2 H, $\Delta\omega_{1/2}$ = 15 Hz), 3.51 (3 H, $\Delta\omega_{1/2}$ = 14 Hz); mass spectrum (probe temperature 60 °C), highest m/z ion 215; mp 70 °C dec. Anal. Calcd for C$_{18}$H$_{14}$Cr$_2$O$_6$: C, 50.24; H,

(12) Fischer, E. O. *Inorg. Synth.* **1963**, *7*, 136.

(13) Attack on the metal by an electrophile followed by endo migration to the cyclopentadienyl ring has been invoked for reactions of (η^5-C$_5$H$_5$)Mn(CO)$_3$ and related complexes: Balem, M. P.; Le Plouzennec, M.; Louër, M. *Inorg. Chem.* **1982**, *21*, 2573 and references contained therein.

(14) Carbon–carbon bond formation by condensation of (η^5-C$_5$H$_5$)Fe-(CO)$_2$(η^1-allyl) complexes with (η^5-C$_5$H$_5$)Fe(CO)$_2$(η^2-olefin) cations has been demonstrated by Rosenblum and co-workers: Lennon, P. J.; Rosan, A.; Rosenblum, M.; Tancrede, J.; Waterman, P. *J. Am. Chem. Soc.* **1980**, *102*, 7033.

(15) Hames, B. W.; Legzdins, P. *Organometallics* **1982**, *1*, 116.

(16) Hoyano, J. K.; Legzdins, P.; Malito, J. T. *Inorg. Synth.* **1978**, *18*, 126.

3.28. Found: C, 50.03; H, 3.40.

Reactions of Na[(η⁵-C₅H₅)Cr(CO)₃] with 3-Chloro-2-methylpropene. (a) In THF at Ambient Temperature. To a stirred yellow solution of Na[(η⁵-C₅H₅)Cr(CO)₃] (3.00 g, 13.4 mmol) in THF (100 mL) was added freshly distilled 3-chloro-2-methylpropene (6 mL, 61 mmol). The reaction mixture became green very slowly, 7 days being required for the anionic reactant to be consumed completely. Workup of the final reaction mixture (a green solution and a brown precipitate) in the manner described above afforded 1.42 g (52.7% yield based on Cr) of green [(η⁵-C₅H₅)Cr(CO)₃]₂ and 0.33 g (7.9% yield based on Cr) of (η⁶-C₁₃H₁₈)Cr(CO)₃ (2) as a viscous, bright red liquid: IR (hexanes) ν_CO 1994 (s), 1932 (s), 1910 (s) cm⁻¹; mass spectrum (probe temperature 120 °C), most intense parent ion m/z 310. Anal. Calcd for C₁₆H₁₈CrO₃: C, 61.93; H, 5.85. Found: C, 61.48; H. 5.77.

In a separate experiment, it was found that the addition of a few mg of 2,2′-azobis(2-methylpropionitrile) to the original reaction mixture had no effect on the rate of the reaction or on the isolated yields of the products indicated above. However, the free radical initiator did facilitate the formation in trace amounts of other carbonyl-containing products (IR (hexanes) ν_CO 2005 (m), 1950 (s), 1895 (m) cm⁻¹), but these products were not characterized further.

(b) In Refluxing THF. The reaction between Na[(η⁵-C₅H₅)Cr(CO)₃] (0.50 g, 2.2 mmol) and 3-chloro-2-methylpropene (1 mL, 10 mmol) in refluxing THF (40 mL) was complete in 5h, as judged by the attendant IR spectral changes. IR spectroscopy also indicated that the product (η⁶-C₁₃H₁₈)Cr(CO)₃ (2) and [(η⁵-C₅H₅)Cr(CO)₃]₂ complexes were formed in yields comparable to those observed when the conversions were effected at room temperature (vide supra).

Reaction of Na[(η⁵-C₅H₅)Cr(CO)₃] with 3-Chloro-1-butene. This reaction was performed in a manner identical with that described previously for 3-chloropropene. However, in this instance, 10 days were required for the conversion to go to completion, and extraction with hexanes of the final reaction residue did not produce any substituted fulvene-containing organometallic complex. The customary workup afforded a 51% yield (based on Cr) of [(η⁵-C₅H₅)Cr(CO)₃]₂.

Reaction of [(η⁵-C₅H₅)Cr(CO)₃]₂ with 3-Chloropropene. Freshly distilled 3-chloropropene (0.6 mL, 7.4 mmol) was added to a green THF solution (40 mL) of [(η⁵-C₅H₅)Cr(CO)₃]₂ (0.40 g, 1.0 mmol). The resulting solution was stirred at room temperature for 18 h with no apparent change occurring in its IR spectrum. The solution was then refluxed for 22h, whereupon it darkened to a mauve color. An IR spectrum of the final solution revealed that the only carbonyl-containing complex in solution was (η⁶-C₁₁H₁₄)Cr(CO)₃ (1) that was isolated in 25% yield by using the standard procedures.

Ground-State and Excited-State Properties of Adducts Derived from Tris(η⁵-cyclopentadienyl)ytterbium(III)

Connie J. Schlesener and Arthur B. Ellis*

Department of Chemistry, University of Wisconsin—Madison, Madison, Wisconsin 53706

Received September 20, 1982

Electronic spectra of several adducts of tris(η⁵-cyclopentadienyl)ytterbium(III), Cp₃Yb, have been investigated in benzene solution. When added to solutions of this Lewis acid, bases such as triethylphosphine, pyrrolidine, tetrahydrofuran, and tetrahydrothiophene cause significant changes in the Cp₃Yb absorption spectrum. Titrations reveal that these changes are consistent with the formation of 1:1 adducts whose formation constants, log K_f, range from ∼3.4 to 5.0. Correlations of the magnitude of K_f with the position of a visible absorption band, previously assigned as a ligand-to-metal charge-transfer (LMCT) transition, and with the gas-phase basicities of the bases employed are discussed. Luminescence is observed in the near-IR (∼1000–1100 nm), f–f spectral region from Cp₃Yb and its adducts upon excitation into their LMCT bands. Spectral changes accompanying base addition are consistent with 1:1 adduct formation with apparent excited-state adduct formation constants, log K^*_{app}, equal to the corresponding log K_f values within experimental error. The extent to which K^*_{app} reflects the establishment of excited-state equilibrium is discussed.

Introduction

In recent studies we have examined the effects of adduct formation on photoreactive Lewis base substrates. Specifically, we were able to demonstrate that adduct formation can significantly perturb the excited-state manifold and reactivity of Lewis bases by examining adducts derived from *all-trans*-retinal and (η⁶-acetophenone)tricarbonylchromium(0).[1,2] The Lewis acid employed in both of these studies was the β-diketonate complex tris(6,6,7,7,8,8,8-

heptafluoro-2,2-dimethyl-3,5-octanedionato)europium(III), Eu(fod)₃. Perturbation of the excited-state properties of Eu(fod)₃ in these adducts was not investigated but has been amply demonstrated for many lanthanide β-diketonate complexes: titrations with a variety of Lewis bases were reported to significantly perturb f–f emission spectra, concomitantly providing adduct stoichiometries and formation constants.[3]

The coordinative unsaturation of Eu(fod)₃ exploited in its selection as an adduct partner is a characteristic of

(1) Ellis, A. B.; Schreiner, R.; Ulkus, R. A. *Proc. Natl. Acad. Sci., U.S.A.* **1981**, *78*, 3993.

(2) Schreiner, R.; Ellis, A. B. *J. Am. Chem. Soc.* **1982**, *104*, 3374.

(3) See, for example: (a) Brittain, H. G. *Inorg. Chem.* **1980**, *19*, 640. (b) Brittain, H. G. *J. Chem. Soc., Dalton Trans.* **1979**, 1187. (c) Brittain, H. G.; Richardson, F. S. *J. Am. Chem. Soc.* **1976**, *98*, 5858.

3.28. Found: C, 50.03; H, 3.40.

Reactions of Na[(η⁵-C₅H₅)Cr(CO)₃] with 3-Chloro-2-methylpropene. (a) In THF at Ambient Temperature. To a stirred yellow solution of Na[(η⁵-C₅H₅)Cr(CO)₃] (3.00 g, 13.4 mmol) in THF (100 mL) was added freshly distilled 3-chloro-2-methylpropene (6 mL, 61 mmol). The reaction mixture became green very slowly, 7 days being required for the anionic reactant to be consumed completely. Workup of the final reaction mixture (a green solution and a brown precipitate) in the manner described above afforded 1.42 g (52.7% yield based on Cr) of green [(η⁵-C₅H₅)Cr(CO)₃]₂ and 0.33 g (7.9% yield based on Cr) of (η⁶-C₁₃H₁₈)Cr(CO)₃ (2) as a viscous, bright red liquid: IR (hexanes) ν_{CO} 1994 (s), 1932 (s), 1910 (s) cm⁻¹; mass spectrum (probe temperature 120 °C), most intense parent ion m/z 310. Anal. Calcd for C₁₆H₁₈CrO₃: C, 61.93; H, 5.85. Found: C, 61.48; H. 5.77.

In a separate experiment, it was found that the addition of a few mg of 2,2′-azobis(2-methylpropionitrile) to the original reaction mixture had no effect on the rate of the reaction or on the isolated yields of the products indicated above. However, the free radical initiator did facilitate the formation in trace amounts of other carbonyl-containing products (IR (hexanes) ν_{CO} 2005 (m), 1950 (s), 1895 (m) cm⁻¹), but these products were not characterized further.

(b) In Refluxing THF. The reaction between Na[(η⁵-C₅H₅)Cr(CO)₃] (0.50 g, 2.2 mmol) and 3-chloro-2-methylpropene (1 mL, 10 mmol) in refluxing THF (40 mL) was complete in 5h, as judged by the attendant IR spectral changes. IR spectroscopy also indicated that the product (η⁶-C₁₃H₁₈)Cr(CO)₃ (2) and [(η⁵-C₅H₅)Cr(CO)₃]₂ complexes were formed in yields comparable to those observed when the conversions were effected at room temperature (vide supra).

Reaction of Na[(η⁵-C₅H₅)Cr(CO)₃] with 3-Chloro-1-butene. This reaction was performed in a manner identical with that described previously for 3-chloropropene. However, in this instance, 10 days were required for the conversion to go to completion, and extraction with hexanes of the final reaction residue did not produce any substituted fulvene-containing organometallic complex. The customary workup afforded a 51% yield (based on Cr) of [(η⁵-C₅H₅)Cr(CO)₃]₂.

Reaction of [(η⁵-C₅H₅)Cr(CO)₃]₂ with 3-Chloropropene. Freshly distilled 3-chloropropene (0.6 mL, 7.4 mmol) was added to a green THF solution (40 mL) of [(η⁵-C₅H₅)Cr(CO)₃]₂ (0.40 g, 1.0 mmol). The resulting solution was stirred at room temperature for 18 h with no apparent change occurring in its IR spectrum. The solution was then refluxed for 22h, whereupon it darkened to a mauve color. An IR spectrum of the final solution revealed that the only carbonyl-containing complex in solution was (η⁶-C₁₁H₁₄)Cr(CO)₃ (1) that was isolated in 25% yield by using the standard procedures.

Ground-State and Excited-State Properties of Adducts Derived from Tris(η⁵-cyclopentadienyl)ytterbium(III)

Connie J. Schlesener and Arthur B. Ellis*

Department of Chemistry, University of Wisconsin—Madison, Madison, Wisconsin 53706

Received September 20, 1982

Electronic spectra of several adducts of tris(η⁵-cyclopentadienyl)ytterbium(III), Cp₃Yb, have been investigated in benzene solution. When added to solutions of this Lewis acid, bases such as triethylphosphine, pyrrolidine, tetrahydrofuran, and tetrahydrothiophene cause significant changes in the Cp₃Yb absorption spectrum. Titrations reveal that these changes are consistent with the formation of 1:1 adducts whose formation constants, log K_f, range from ∼3.4 to 5.0. Correlations of the magnitude of K_f with the position of a visible absorption band, previously assigned as a ligand-to-metal charge-transfer (LMCT) transition, and with the gas-phase basicities of the bases employed are discussed. Luminescence is observed in the near-IR (∼1000–1100 nm), f–f spectral region from Cp₃Yb and its adducts upon excitation into their LMCT bands. Spectral changes accompanying base addition are consistent with 1:1 adduct formation with apparent excited-state adduct formation constants, log K^*_{app}, equal to the corresponding log K_f values within experimental error. The extent to which K^*_{app} reflects the establishment of excited-state equilibrium is discussed.

Introduction

In recent studies we have examined the effects of adduct formation on photoreactive Lewis base substrates. Specifically, we were able to demonstrate that adduct formation can significantly perturb the excited-state manifold and reactivity of Lewis bases by examining adducts derived from *all-trans*-retinal and (η⁶-acetophenone)tricarbonyl-chromium(0).[1,2] The Lewis acid employed in both of these studies was the β-diketonate complex tris(6,6,7,7,8,8,8-

heptafluoro-2,2-dimethyl-3,5-octanedionato)europium(III), Eu(fod)₃. Perturbation of the excited-state properties of Eu(fod)₃ in these adducts was not investigated but has been amply demonstrated for many lanthanide β-diketonate complexes: titrations with a variety of Lewis bases were reported to significantly perturb f–f emission spectra, concomitantly providing adduct stoichiometries and formation constants.[3]

The coordinative unsaturation of Eu(fod)₃ exploited in its selection as an adduct partner is a characteristic of

(1) Ellis, A. B.; Schreiner, R.; Ulkus, R. A. *Proc. Natl. Acad. Sci., U.S.A.* **1981**, *78*, 3993.
(2) Schreiner, R.; Ellis, A. B. *J. Am. Chem. Soc.* **1982**, *104*, 3374.

(3) See, for example: (a) Brittain, H. G. *Inorg. Chem.* **1980**, *19*, 640. (b) Brittain, H. G. *J. Chem. Soc., Dalton Trans.* **1979**, 1187. (c) Brittain, H. G.; Richardson, F. S. *J. Am. Chem. Soc.* **1976**, *98*, 5858.

Table I. Electronic Spectral Properties of Adducts of Cp$_3$Yb[a]

complex	λ, nm (ε, M^{-1} cm^{-1})			emissn[e] λ, nm
	I[b]	II[c]	III[d]	
Cp$_3$Yb	1030 (38)	879 (70)	616 (53) sh	1034
	1061 (24)	916 (30)	655 (60)	1065
		940 (13)		1085 sh
		961 (8)		
pyrrolidine adduct	1007 (38)	895 (22)	625 (89)	1011 sh
	1020 (180)	920 (25) sh		1021
	1035 (25)	929 (68)		1036
		939 (27)		1090
triethylphosphine adduct	1009 (32) sh	896 (18)	629 (95)	1011 sh
	1021 (150)	924 (53)		1022
		939 (15)		1035 sh
				1095
tetrahydrothiophene adduct	1015 (39)	901 (30)	636 (96)	1017 sh
	1026 (140)	913 (66)		1027
	1041 (30) sh	925 (26)		1042 sh
		946 (14)		1112
tetrahydrofuran adduct	1019 (38)	906 (29)	647 (72)	1022 sh
	1033 (99)	922 (56)		1036
	1047 (26) sh	925 (30)		1050 sh
		950 (10)		1110

[a] Spectral features observed in benzene solution at room temperature; sh denotes shoulder. Absorptivities were determined from spectrophotometric titrations (changes in absorbance from addition of known quantities of base) assuming that any impurities present (see text) did not compete for the base. Absorptivities obtained in this manner exceeded values obtained gravimetrically, although the two values were generally within 15% of one another. [b] Absorption band maxima observed from 1000 to 1100 nm ($^2F_{7/2} \rightarrow {}^2F_{5/2}$). [c] Absorption band maxima observed from 870 to 1000 nm ($^2F_{7/2} \rightarrow {}^2F_{5/2}$). [d] LMCT absorption band maxima. [e] Uncorrected emission band maxima obtained from dye laser excitation into the LMCT band. Excitation wavelengths are given in Figure 4.

many lanthanide complexes originating from the large size and coordination numbers of the lanthanide ions.[4] Lanthanide complexes with η^5-cyclopentadienyl ligands represent another class of compounds that could potentially be used to study effects of adduct formation on the excited-state properties of the adduct partners. A comparatively well-studied member of this class is tris(η^5-cyclopentadienyl)ytterbium(III), Cp$_3$Yb. Crystallographic evidence for adduct formation involving Cp$_3$Yb has been obtained from its pyrazine-bridged dimer;[5] formation in solution of adducts derived from Cp$_3$Yb has been inferred from both electronic and NMR spectral changes resulting from the addition of various Lewis bases having N-, O-, P-, and S-donor atoms.[6-10] These observations prompted us to investigate the excited-state properties of Cp$_3$Yb and its adducts.

In this paper we present what we believe to be the first quantitative studies of adduct formation involving Cp$_3$Yb and the first description of the emissive properties of the Lewis acid and its adducts. In particular, we show that adduct formation is reflected in both electronic absorption and emission spectra; spectrophotometric and luminescence titrations support the presence of 1:1 adducts whose formation constants with various Lewis bases span several orders of magnitude. These data not only provide insight into the steric and electronic factors affecting adduct formation but also permit assessment of adduct formation and dissociation as excited-state reactions.

(4) For reviews, see, for example: (a) Marks, T. J. *Prog. Inorg. Chem.* **1978**, *24*, 51. (b) Baker, E. C.; Halstead, G. W.; Raymond, K. N. *Struct. Bonding (Berlin)* **1976**, *25*, 23.

(5) Baker, E. C.; Raymond, K. N. *Inorg. Chem.* **1977**, *16*, 2710.

(6) Fischer, R. D.; Fischer, H. *J. Organomet. Chem.* **1965**, *4*, 412.

(7) Marks, T. J.; Porter, R.; Kristoff, J. S.; Shriver, D. F. In "Nuclear Magnetic Resonance Shift Reagents"; Sievers, R. E., Ed.; Academic Press: New York, 1973; p 247.

(8) Bielang, G.; Fischer, R. D. *J. Organomet. Chem.* **1978**, *161*, 335.

(9) Pappalardo, R.; Jørgensen, C. K. *J. Chem. Phys.* **1967**, *46*, 632.

(10) Calderazzo, F.; Pappalardo, R.; Losi, S. *J. Inorg. Nucl. Chem.* **1966**, *28*, 987.

Results and Discussion

Adduct formation was investigated in deoxygenated benzene solution with the following Lewis bases: tetrahydrofuran (THF), tetrahydrothiophene (THT), pyrrolidine (pl), triethylphosphine (PEt$_3$), triethylamine (NEt$_3$), and triphenylphosphine (PPh$_3$). In sections below we describe the electronic absorption and emission spectral features of mixtures of these bases with Cp$_3$Yb.

Electronic Absorption Spectra of Cp$_3$Yb/Lewis Base Mixtures. Benzene solutions of Cp$_3$Yb, lime green in color, are characterized by numerous absorption bands between 500 and 1100 nm. These features, illustrated in the bottom panel of Figure 1, are very similar to those reported for solid Cp$_3$Yb.[9,10] Previous assignments for the Cp$_3$Yb transitions have characterized the bands at ~650 nm as ligand-to-metal charge transfer (LMCT) and those above 750 nm as f-f in nature ($^2F_{7/2} \rightarrow {}^2F_{5/2}$) with vibronic contributions.[9,10]

As reported previously, both LMCT and f-f bands undergo significant changes when Lewis bases are permitted to coordinate to Cp$_3$Yb.[6,8-10] Figure 1 depicts the spectral changes observed in benzene solutions of Cp$_3$Yb upon addition of stoichiometric excesses of PEt$_3$, pl, THT, and THF; prominent spectral features of these solutions are compiled in Table I. Among the noteworthy common features resulting from base addition are (1) a blue shift of the maximum of the lowest energy LMCT band, (2) a diminution of absorbance features between ~720 and 870 nm, and (3) significant changes in band patterns from 870 to 1100 nm, highlighted by the disappearance and appearance of relatively strong bands at 879 and 1020–1035 nm, respectively. The band patterns exhibited by the adducts between 870 and 1100 nm are quite similar to one another and suggest a common origin in changes in the crystal field experienced by Yb upon adduct formation.

With respect to the LMCT band, the observed changes support that assignment; increased electron density at the metal in the adduct should oppose the shifts in electron density anticipated for a π Cp → Yb transition. From this

Table II. Formation Constants for Adducts of Cp₃Yb and Comparisons with Other Measures of Basicity

Lewis base	$\log K_f{}^a$	$\log K_{app}*{}^b$	LMCT band λ_{max},^{c} nm	GB^d
pyrrolidine	5.0 ± 0.4	4.6 ± 0.5	625	216.1
triethylphosphine	4.9 ± 0.5	4.2 ± 0.5	629	223.9
tetrahydrothiophene	3.6 ± 0.1	3.4 ± 0.2	636	198.3 (Et₂S)^e
tetrahydrofuran	3.4 ± 0.2	3.5 ± 0.2	647	192.3

^{a} Formation constants for adducts of Cp₃Yb prepared with the indicated bases; a 1:1 adduct stoichiometry (eq 1) has been assumed. Data were obtained from spectrophotometric titrations as described in the text and Experimental Section and assume no interference from impurities. Error bars represent the range over which the fitted curve comes within one standard deviation of the data points. ^{b} Apparent excited-state formation constants obtained from luminescence titrations conducted in benzene solution with Cp₃Yb and the indicated bases; a 1:1 adduct stoichiometry has been assumed. Excitation at an isosbestic point in the LMCT band was employed as described in the text and Experimental Section. Error bars represent the range over which the fitted curve comes within one standard deviation of the data points. ^{c} Maximum of the adduct's LMCT band in benzene solution. ^{d} Gas-phase basicities for the various Lewis bases from ref 11a. GB of a base, A, is defined as $-\Delta G°$ for the gas-phase reaction $A + H^+ \rightleftharpoons AH^+$. ^{e} We were unable to obtain a GB value for tetrahydrothiophene and list instead the GB value of diethyl sulfide.
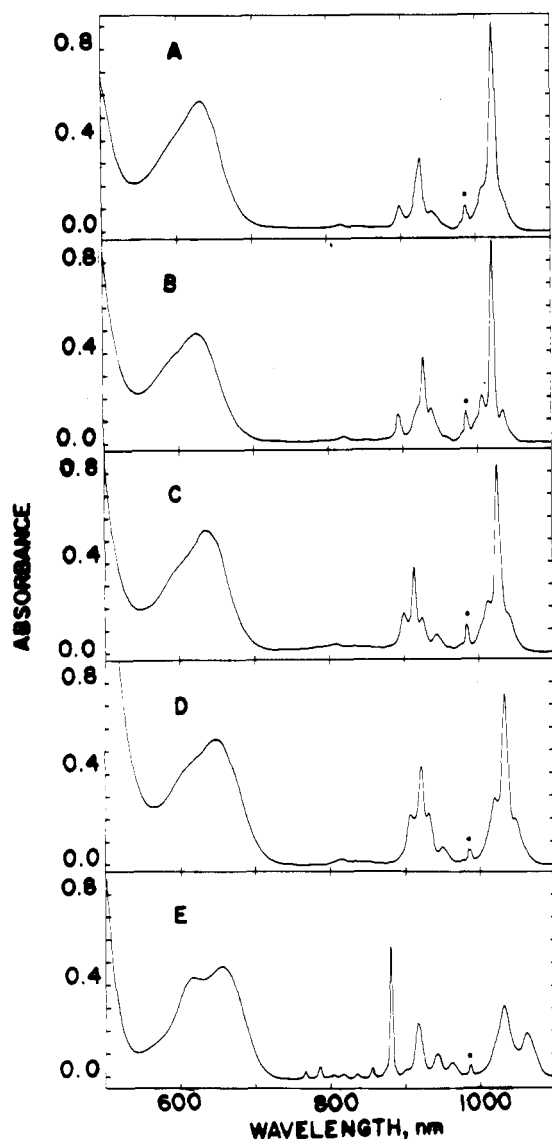
Figure 1. Absorption spectra of Cp₃Yb and several of its adducts in benzene solution at room temperature: A = Cp₃Yb·PEt₃; B = Cp₃Yb·pl; C = Cp₃Yb·THT; D = Cp₃Yb·THF; and E = Cp₃Yb. The concentration of Cp₃Yb was ∼5–8 mM in all cases, and adduct solutions contained enough equivalents of base to saturate spectral changes, typically ∼2–8 equiv. The peak labeled with an asterisk is due to decomposition.

logic, the magnitude of the blue shift in the LMCT band would be expected to increase with the electron-donating ability of the ligand. Using the shift in λ_{max} values as a rough measure of the electronic component of ligand

basicity, Table II shows that the spectral shifts do crudely correlate with gas-phase basicities (GBs)^{11a} of the Lewis base; the trend is best expressed by the bases with similar structures—pl, THF, and THT.

The spectral changes pictured in Figure 1 evolve smoothly with incremental additions of Lewis base. Figure 2 illustrates such a titration of Cp₃Yb with pl. Although isosbestic points are generally seen at the outset of a titration, they are rarely maintained throughout it owing to some decomposition. A band at 986 nm, labeled with an asterisk in Figures 1 and 2, provides a probe for the extent of decomposition; its absorbance increases slightly during titrations and dominates the spectra of solutions that are exposed to air. Because solutions of Cp₃Yb invariably had some absorbance at 986 nm, we were concerned that the unidentified species responsible for the band might influence the course of the titrations. We saw no evidence for this in titrations conducted with THF at various initial impurity:Cp₃Yb ratios (see Figures 1 and 2 for typical ratios) and assume that the impurity's role in titrations is negligible.

Titrations like that pictured in Figure 2 permit the determination of ground-state adduct stoichiometries and formation constants, K_f. The decline in Cp₃Yb absorbance at 879 nm is a particularly convenient probe for monitoring adduct formation. Representative data are illustrated in Figure 3 for the spectrophotometric titration of Cp₃Yb with THT; a reasonable fit to the data is obtained with a curve drawn for a 1:1 stoichiometry and a K_f value of (∼4 ± 1) × 10³ M⁻¹. Titration data for all of the bases employed were well fit by assuming that the observed spectral changes reflect formation of 1:1 adducts, eq 1. Treatment
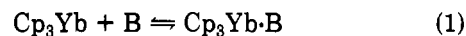
$$Cp_3Yb + B \rightleftharpoons Cp_3Yb·B \qquad (1)$$

of the spectral changes as being due to formation of a 1:2 (Cp₃Yb:B) adduct, another possibility, is inconsistent with the cessation of spectral changes observed for the pl and PEt₃ systems before the addition of 2 equiv of base and provides additional support for the 1:1 stoichiometry.

As shown in Table II, the log K_f values corresponding to 1:1 adducts range from ∼3.4 to 5.0. The trend in log K_f values indicates an ordering of basicities similar to those obtained from LMCT spectral shifts and GB values. This point is noteworthy, since inversions in the "intrinsic" ordering of basicity based on GB values often occur in

(11) (a) Aue, D. H.; Bowers, M. T. In "Gas Phase Ion Chemistry", Bowers, M. T., Ed.; Academic Press: New York, 1979; Vol. 2, p 2. (b) Brown, H. C. *Record Chem. Prog.* 1953, *14*, 83. (c) Ahrland, S. In "The Chemistry of Nonaqueous Solvents"; Lagowski, J. J., Ed.; Academic Press: New York, 1978; Vol. VA, p 1. (d) Jensen, W. B. "The Lewis Acid-Base Concepts: An Overview"; Interscience: New York, 1980; Chapter 7.
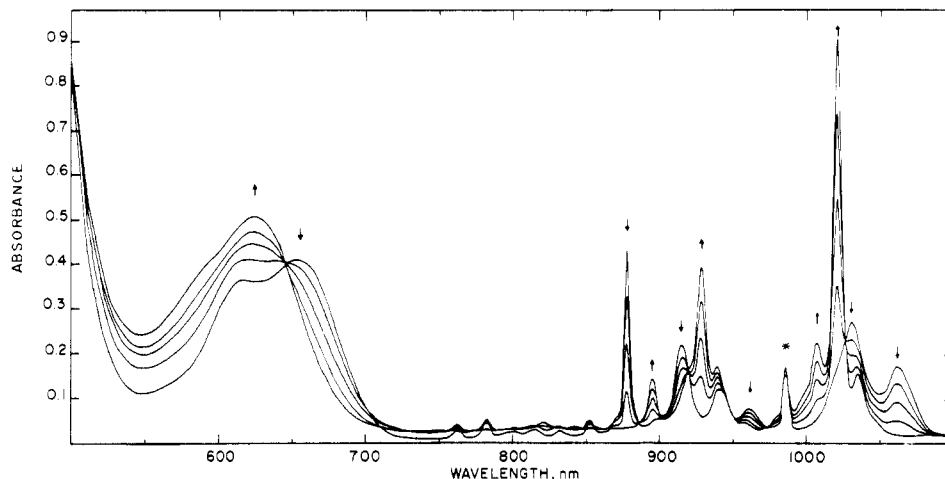
Figure 2. Spectrophotometric titration of Cp_3Yb with pl in benzene solution. The initial concentration of Cp_3Yb is 5.5 mM. Arrows indicate the direction in which the bands are changing with addition of 0.27, 0.55, 0.82, and 1.23 equiv of the base. The peak labeled with an asterisk is due to decomposition.
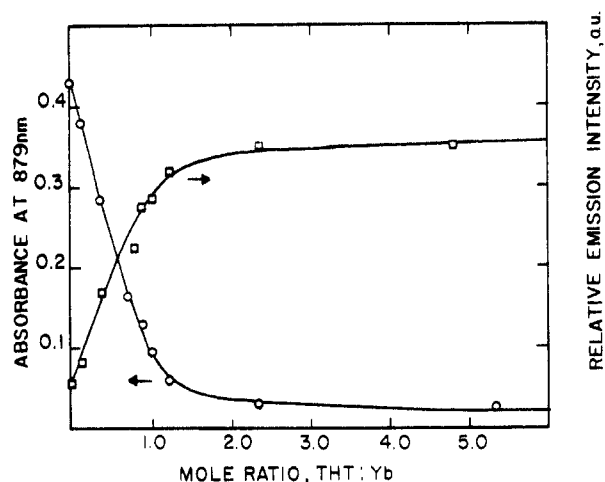
Figure 3. Curves for the spectrophotometric and emission titrations of Cp_3Yb with THT in benzene solution. Circles represent the solution absorbance at 879 nm as a function of the THT:Yb mole ratio; squares represent the relative emission intensity at 1027 nm (615-nm excitation) as a function of this ratio. Solid lines are the best least-squares fit to the data points on the basis of 1:1 adduct formation.

condensed systems through solvation effects and with the use of different Lewis acids through steric and/or electronic effects.[11] A base that was at variance with GB predictions, presumably for steric reasons,[11b] was NEt_3: in a titration of Cp_3Yb, no spectroscopic evidence for adduct formation was obtained despite the fact that NEt_3 has a GB value roughly that of PEt_3. Steric effects may also contribute to the low formation constant (≤ 100 M^{-1}) obtained for PPh_3.

We examined ground-state adduct lability by successively adding ~ 2 equiv each of THF, THT, PEt_3 and pl to a solution of Cp_3Yb. Spectral changes consistent with data in Figure 1 and Table I were immediately evident after each addition and confirmed the relative ordering of K_f values. Although this experiment only demonstrates exchange on a scale of seconds, NMR studies of Yb-$(thd)_3$·pinacolone (thd is 2,2,6,6-tetramethyl-3,5-heptanedionate) yielded a first-order dissociation rate constant of $\sim 10^7$ s^{-1}, suggesting that exchange may be quite rapid.[12]

Emission Spectra of Cp_3Yb/Lewis Base Mixtures. Weak luminescence in the f–f, near-IR region is observed when Cp_3Yb and its adducts are excited in their LMCT

bands at 295 K in benzene solution. Figure 4 presents uncorrected emission spectra obtained for Cp_3Yb and its adducts with the Lewis bases of Figure 1; band maxima are given in Table I. As is the case for absorption spectra, base-dependent changes in emission spectra accompany adduct formation, permitting their use as adduct "fingerprints". The structured emission typically consists of up to four bands between 1000 and 1130 nm (some appearing as shoulders) that are likely transitions from the lowest crystal field level of the $^2F_{5/2}$ excited state to the crystal-field levels of the $^2F_{7/2}$ ground state; for any symmetry below cubic, the $^2F_{7/2}$ state is split into four levels and the $^2F_{5/2}$ into three.[13] Supporting this tentative assignment is a match in energy with absorption bands for all but the lowest energy emission band (cf. Table I); the corresponding transitions in absorption would originate from the lowest three $^2F_{7/2}$ crystal field levels that, lying within ~ 250 cm^{-1} of one another, can be thermally populated at 295 K. A higher energy emission band is often seen at 986 nm, Figure 4, but it appears to be impurity related: whereas the other bands maintain their relative intensities for different excitation wavelengths, the relative 986-nm band intensity varies with this parameter, becoming fairly intense for wavelengths ≤ 500 nm. That the impurity is the same as that inferred from absorption spectra (vide supra) is suggested by the match in transition energy and by the enhanced emission intensity at 986 nm accompanying deliberate decomposition of Cp_3Yb. By exciting into the LMCT transition of Cp_3Yb and its adducts, we were able to minimize the emission at 986 nm.

Paralleling our absorption studies, we conducted luminescence titrations, exciting in the isosbestic region of the LMCT bands to preserve optical penetration depth. Figure 5 illustrates such a titration for the Cp_3Yb/pl system and reveals isoemissive "regions" at ~ 1050 and 1080 nm, indicative of a smooth conversion between emissive species. The incremental changes in emission intensity resulting from added aliquots of titrant yield luminescence titration curves from which apparent excited-state formation constants, K^*_{app}, could be culled, assuming a 1:1 adduct stoichiometry. Because of the overlap in absorption and emission spectra, changes in emission intensity at several wavelengths were used in K^*_{app} calculations to demonstrate that self-absorption effects on the titration data were minimal. Figure 3 includes a plot

(12) Lenkinski, R. E.; Reuben, J. *J. Magn. Reson.* **1976**, *21*, 47.

(13) Hüfner, S. "Optical Spectra of Transparent Rare Earth Compounds"; Academic Press: New York, 1978; Chapter 3.10.
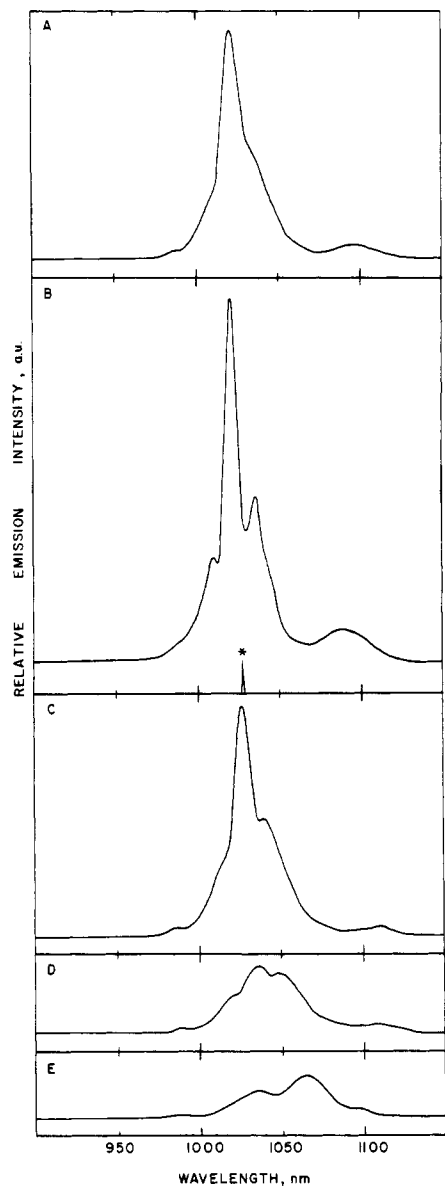
Figure 4. Uncorrected emission spectra of Cp₃Yb and several of its adducts in benzene solution at room temperature: A = Cp₃Yb·PEt₃; B = Cp₃Yb·pl; C = Cp₃Yb·THT; D = Cp₃Yb·THF; E = Cp₃Yb. Sufficient equivalents of the bases to saturate spectral changes were present (typically ~2–8 equiv) and excitation wavelengths of 640, 640, 615, 605, and 605 nm were employed for panels A–E, respectively. The peak marked with an asterisk in panel B is a calibration line at 1029 nm (overtone of the 514.5-nm line of an Ar ion laser).

of emissive changes during the THT titration that are well fit by 1:1 adduct formation with a log K^*_{app} value of 3.4 ± 0.3. Table II summarizes the log K^*_{app} values for several adducts, all of which gave titration data consistent with a 1:1 stoichiometry.

What is particularly striking about the K^*_{app} values is the similarity to their K_f counterparts—within experimental error the two are identical. The significance of these results can be viewed in the framework of Scheme I which summarizes the species and processes of relevance with A, B, and AB representing Cp₃Yb, Lewis base, and adduct, respectively; A* and AB* are the excited Cp₃Yb and adduct species; and τ_{A^*} and τ_{AB^*} are their corresponding lifetimes. Of particular interest is whether the excited-state equilibrium represented by K_f^* can be established for adducts of Cp₃Yb. This, in turn, is contingent upon the rates of adduct formation and dissociation in the excited state being competitive with the rates for return
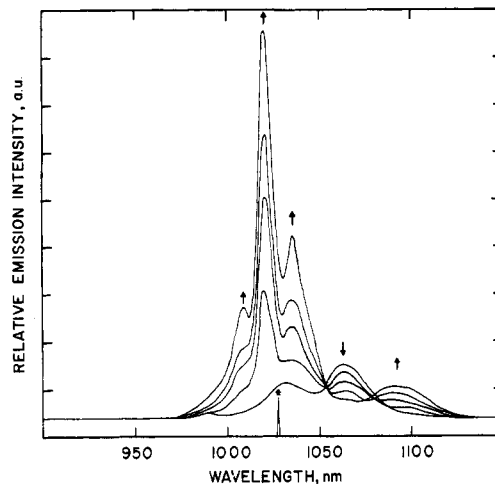
Figure 5. Emission titration of Cp₃Yb with pl in benzene solution. This titration was conducted on the sample described in Figure 2, and intermediate curves match those of that figure in terms of base equivalents added; excitation at 640 nm was employed. The peak labeled with an asterisk is a calibration line at 1029 nm.

Scheme I
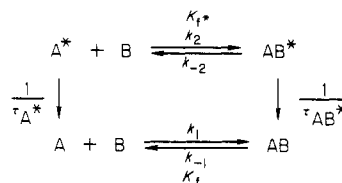
of A* and AB* to their ground states, respectively.[14]

For the system at hand, Scheme I is a simplification in the sense that several excited states are involved. If emission occurred from the LMCT excited state and equilibrium were established for this state, K_f would be expected to exceed K_f^* on the basis of the blue-shift in absorption spectra with adduct formation. This is equivalent to saying that in its LMCT excited state Cp₃Yb is a poorer Lewis acid than in its ground state. On the other hand, establishment of equilibrium in the emissive $^2F_{5/2}$ excited state may not yield differences in K_f and K_f^*, since the f orbitals from which the state derives are relatively shielded from the ligand environment. A crude analogy for these different expectations for the LMCT and $^2F_{5/2}$ excited states might be to the pK_a and pK_a^* values of organic molecules: the pK_a^* value of a triplet excited state is often similar to the ground-state pK_a value, whereas pK_a^* for the singlet excited state of the same molecule can be quite disparate from pK_a.[14a] Because the similarity in K_f and K^*_{app} could reasonably be expected for the emissive $^2F_{5/2}$ state of Cp₃Yb and its adducts, it is important to determine whether, in fact, excited-state equilibrium has been established. Although we were unable to definitively answer this question for the Cp₃Yb-based system, the methodology we employed should eventually provide such information and is described below.

On the basis of the interconversion of A* and AB* shown in Scheme I, there are two limiting scenarios for interpreting the coincidence in measured K_f and K^*_{app} values: either (1) no interconversion occurs and our data merely reflect the ground-state composition that has been excited or (2) excited-state equilibrium is fully established at K_f^* ≃ K_f. Of course, interconversion at insufficient rates to establish equilibrium can also occur.

(14) (a) Ireland, J. F.; Wyatt, P. A. H. *Adv. Phys. Org. Chem.* **1976**, *12*, 131. (b) Weller, A. In "Progress in Reaction Kinetics"; Porter, G., Ed.; Pergamon Press: New York, 1961; Vol. 1, p 187.

Distinguishing among these scenarios is most convincingly accomplished by selective-excitation experiments. For example, the excited-state reactions of Scheme I can be demonstrated if excitation of Cp_3Yb yields adduct emission and adduct excitation yields Cp_3Yb emission. And if the emission is independent of the species excited, evidence for the establishment of excited-state equilibrium has been obtained. In order to examine excited-state kinetics, we focused our attention on the Cp_3Yb/pl system for which the largest emissive changes were observed with adduct formation. Inspection of Figure 2 indicates that selective-excitation experiments would be optimized at 879 and 895 nm where Cp_3Yb and $Cp_3Yb\cdot pl$ can be almost exclusively excited, respectively. Lacking optical sources of sufficient intensity at these wavelengths, however, we tried as an alternative to excite within the LMCT band; the ratio of Cp_3Yb to $Cp_3Yb\cdot pl$ absorptivities varies from ~0.5 to 1.0 between 570 and 640 nm. Excitation at 637, 582, and 566 nm of a 1:10 pl/Cp_3Yb mixture did yield similar emission spectra, but the differences from spectra calculated by assuming no exchange were within experimental error and did not permit a conclusion to be drawn regarding excited-state exchange. Excitation at the aforementioned near-IR wavelengths coupled with time-resolved measurements should provide a more definitive assessment of the extent to which excited-state equilibrium is established for this system.

Experimental Section

Materials. Benzene and toluene were dried by distillation from lithium aluminum hydride (LAH) under nitrogen that had been prepurified by sequential passage through reduced BASF-R311 catalyst and 4-Å molecular sieves. Benzene was stored over LAH and degassed prior to its use in spectroscopic studies; a blanket of Ar was placed over it after degassing. All transfers of benzene were made under vacuum ($\sim 10^{-3}$ torr). Anhydrous $YbCl_3$ (ROC/RIC) was used as received. Synthesis of Cp_3Yb was accomplished via a literature method from anhydrous $YbCl_3$ and sodium cyclopentadienide in toluene.[10] An elemental analysis was obtained for Cp_3Yb from Schwarzkopf Laboratories: Calcd for $C_{15}H_{15}Yb$: C, 48.92; H, 4.10; Yb, 46.98. Found: C, 48.76; H, 4.21; Yb, 47.30. Triethylamine, tetrahydrofuran, tetrahydrothiophene, and pyrrolidine were all obtained from Aldrich; triethylphosphine was acquired from Alfa. The bases were all purified by distillation under N_2 onto 4-Å molecular sieves that had been activated by heating under vacuum with a Bunsen flame for ~5 min; prior to use, the bases were degassed via three freeze–pump–thaw cycles and stored under a blanket of Ar. Triphenylphosphine was obtained from Alfa and used as received.

Sample Preparation. All manipulations were performed on a Schlenk line or in a Vacuum Atmospheres HE-43 glovebox equipped with a HE-493 Dri-train. Benzene solutions of Cp_3Yb having concentrations of ~5 mM were prepared in the glovebox by adding the organolanthanide, weighed in the glovebox on a Cahn Model 7500 DTL electrobalance, to a round-bottom flask containing ~30 mL of the degassed solvent. A syringe was then used to transfer ~3.0–5.0 mL of the solution to the cell with which spectroscopic studies were conducted. The cell is constructed around a 10-mm i.d. × 80-mm Pyrex tube whose bottom was closed off and whose top was fused to a Teflon stopcock; the side arm of the stopcock terminates in a 10/30 joint that can be attached to a Schlenk line. A 1.0-cm quartz emission cuvette is attached to the test tube via a graded seal and forms roughly an "h"-shape with it; the cuvette, which lies beneath the joint, is fused to the test tube ~6 cm above the tube's base and extends ~3 cm beneath it. The cell is filled with solution by removing the Teflon stopcock.

Electronic Spectra. Visible and near-IR absorption spectra were recorded on a Cary 17D spectrophotometer using the cell described above and a conventional 1.0-cm matched quartz cuvette filled with benzene as a reference cell. The resolution in the near-IR was normally set at 1.0 nm at 1100 nm. Uncorrected emission spectra were obtained with a spectrometer constructed around a McPherson Model 270, 0.35-m monochromator equipped with a grating blazed at 1000 nm. The monochromator was interfaced to an EMI Model 9684B PMT (S-1 response) cooled with dry ice/methanol. Signals from the PMT were amplified by a Keithley Model 414S picoammeter and displayed on a Houston Model 2000 x-y recorder. Excitation sources included a Coherent Radiation Model CR-12 argon ion laser and a Coherent Radiation Model CR-590-03 tunable dye laser equipped with Rhodamine 6G dye and pumped by the CR-12 argon ion laser. Laser excitation was filtered by placing a solution (ethanolic solution of the precipitate obtained by mixing NaSCN and Fe-$(NO_3)_3\cdot 9H_2O$ in a 6:1 mole ratio in water) in front of the monochromator. Emission was observed at ~90° to the excitation source. A monochromator slitwidth of 1.0 mm was used which corresponded to an emission resolution of ~5 nm at 1030 nm.

Titrations. Absorption and emission spectra of Cp_3Yb benzene solutions, prepared as described above, were initially recorded. Prior to the addition of base, the solution was transferred from the cuvette to the test-tube portion of the cell, and the cell was attached to a Schlenk line. The Teflon stopcock was removed under a N_2 purge and the base added without dilution in sub-microliter aliquots by using a Hamilton 1.0-μL syringe; the base was injected directly into the solution. After replacement of the stopcock, absorption and emission spectra were run from 1100 to 500 nm and from 900 to 1100 nm, respectively. Emission titrations employed excitation wavelengths at or near isosbestic points. Changes in absorbance and emission intensity as a function of the mole ratio of base to lanthanide complex were used to determine formation constants through the use of a BASIC computer program;[2] a 1:1 adduct stoichiometry was assumed.

535

Intermediates in the Associative Phosphine Substitution Reaction of (η^5-C$_5$H$_5$)Re(CO)$_3$

Charles P. Casey,* Joseph M. O'Connor, William D. Jones, and Kenneth J. Haller

Department of Chemistry, University of Wisconsin, Madison, Wisconsin 53706

The reaction of (η^5-C$_5$H$_5$)Re(CO)$_3$, 11, with P(CH$_3$)$_3$ produces *fac*-(η^1-C$_5$H$_5$)Re(CO)$_3$[P(CH$_3$)$_3$]$_2$, 12. The reaction is reversible with K_{eq} = 19 M^{-2} at 51 °C in benzene. At longer reaction times, the equilibrium mixture of 11 and 12 is converted to (η^5-C$_5$H$_5$)Re(CO)$_2$[P(CH$_3$)$_3$], 13. The structure of 12 was determined by X-ray crystallography: monoclinic space group $P2_1/n$, with unit-cell constants a = 8.011 (5) Å, b = 14.042 (3) Å, c = 16.349 (3) Å, β = 92.08 (2)°, and Z = 4.

In 1965, Basolo and Schuster-Woldan noted that the rate of reaction between P(C$_6$H$_5$)$_3$ and the coordinatively saturated (η^5-C$_5$H$_5$)Rh(CO)$_2$ to give (η^5-C$_5$H$_5$)Rh(CO)[P(C$_6$H$_5$)$_3$] was unusually fast and depended on the concentration of both the rhodium complex and phosphine.[1] To explain this associative substitution at a formally coordinatively saturated metal center, they proposed that slippage of the cyclopentadiene ring occurs as phosphine attacks to produce the intermediate shown.

Recently we found structural evidence for cyclopentadiene ring slippage during phosphine substitution reactions at coordinatively saturated metal centers. The reactions of (η^5-C$_5$H$_5$)Re(NO)(CO)(CH$_3$), 1, with 2 equiv of P(CH$_3$)$_3$ at 25 °C yields the bis(phosphine) adduct (η^1-C$_5$H$_5$)Re(NO)(CO)(CH$_3$)[P(CH$_3$)$_3$]$_2$, 2, in which the η^5-C$_5$H$_5$ ring has slipped all the way to an η^1-C$_5$H$_5$ configuration.[2] Upon heating to 90 °C, 1 and 2 equilibrate and are converted to a mixture of phosphine-substituted methyl compound 3 and the phosphine-substituted acetyl compound 4. The rate of formation of 2 depends on the concentration of both 1 and P(CH$_3$)$_3$ and thus requires a mono(phosphine) adduct 5 as an intermediate. Two possible 18-electron structures for such an intermediate are an η^3-C$_5$H$_5$ linear nitrosyl compound or an η^5-C$_5$H$_5$ bent nitrosyl compound.

able at room temperature and decompose to starting material and η^5-C$_5$H$_5$ mono(phosphine) adducts. The reactions of 6 and 7 with P(CH$_3$)$_3$ also show second-order kinetics and require a mono(phosphine) intermediate 10. Since both 6 and 7 contain a nitrosyl ligand, there are again two possible 18-electron formulations for intermediate 10: an η^3-C$_5$H$_5$ linear nitrosyl compound and an η^5-C$_5$H$_5$ bent nitrosyl compound.

To determine whether a nitrosyl ligand is required for formation of η^1-cyclopentadienyl bis(phosphine) adducts, we have studied the reaction of P(CH$_3$)$_3$ with the non-nitrosyl-containing compound (η^5-C$_5$H$_5$)Re(CO)$_3$, 11. Here we report that 11 reacts with P(CH$_3$)$_3$ to give a very stable η^1-C$_5$H$_5$ bis(phosphine) adduct (η^1-C$_5$H$_5$)Re(CO)$_3$[P(CH$_3$)$_3$]$_2$, 12, which we have characterized by spectroscopy and by X-ray crystallography. 11 and 12 were found to equilibrate more rapidly than they were converted to (η^5-C$_5$H$_5$)Re(CO)$_2$[P(CH$_3$)$_3$], 13.

Results

Synthesis of *fac*-(η^1-C$_5$H$_5$)Re(CO)$_3$[P(CH$_3$)$_3$]$_2$. Reaction of (η^5-C$_5$H$_5$)Re(CO)$_3$, 11, with 3.3 M P(CH$_3$)$_3$ for 2.5 days in hexane at 64 °C led to the precipitation of light yellow crystals of *fac*-(η^1-C$_5$H$_5$)Re(CO)$_3$[P(CH$_3$)$_3$]$_2$, 12, in 85% yield. The hexane solution contained only unreacted 11 and none of the phosphine substitution product (η^5-C$_5$H$_5$)Re(CO)$_2$[P(CH$_3$)$_3$], 13. Elemental analysis, NMR, and IR data established that 12 was an η^1-C$_5$H$_5$ bis-(phosphine) adduct and X-ray analysis defined the cis geometry of the phosphine ligands.

The reactions of (η^5-C$_5$H$_5$)Mo(CO)$_2$(NO), 6, and (η^5-C$_5$H$_5$)W(CO)$_2$(NO), 7, with P(CH$_3$)$_3$ at -60 °C also give observable bis(phosphine) η^1-cyclopentadienyl compounds (η^1-C$_5$H$_5$)Mo(CO)$_2$(NO)[P(CH$_3$)$_3$]$_2$, 8, and (η^1-C$_5$H$_5$)W-(CO)$_2$(NO)[P(CH$_3$)$_3$]$_2$, 9.[3] Compounds 8 and 9 are unst-
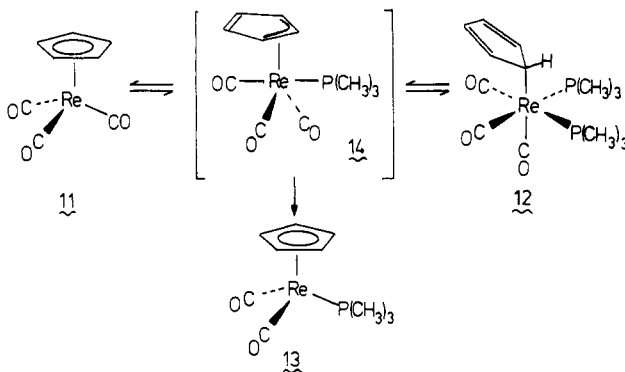
The ^{1}H NMR of 12 in benzene-d_6 consists of a triplet at δ 6.15 (J_{PH} = 1.5 Hz, 5 H) and a multiplet at δ 1.04 (18 H). The triplet is assigned to the fluxional η^1-C$_5$H$_5$ group of 12; we have been unable to freeze out the fluxionality of the η^1-C$_5$H$_5$ group of 12 even at -87 °C in acetone-d_6.

(1) Schuster-Woldan, H. G.; Basolo, F. *J. Am. Chem. Soc.* 1966, *88*, 1657–1663.

(2) Casey, C. P.; Jones, W. D. *J. Am. Chem. Soc.* 1980, *102*, 6154–6156, and references therein. See also: Werner, H.; Kühn, A.; Burschka, C. *Chem. Ber.* 1980, *113*, 2291–2307. Goel, A. B.; Goel, S.; Van Derveer, D.; Clark, H. C. *Inorg. Chim. Acta* 1981, *53*, L117–L118.

(3) Casey, C. P.; Jones, W. D.; Harsy, S. G. *J. Organomet. Chem.* 1981, *206*, C38–C42.

Table I. Interatomic Distances (Å) and Angles (deg) for 12[a]

Distances

Re–P(1)	2.480 (3)	P(1)–C(5)	1.826 (13)	C(3)–O(3)	1.134 (13)
Re–P(2)	2.460 (3)	P(1)–C(6)	1.820 (12)	C(10)–C(11)	1.475 (16)
Re–C(1)	1.910 (13)	P(2)–C(7)	1.814 (12)	C(10)–C(14)	1.448 (14)
Re–C(2)	1.944 (14)	P(2)–C(8)	1.772 (13)	C(11)–C(12)	1.333 (17)
Re–C(3)	1.956 (13)	P(2)–C(9)	1.798 (14)	C(12)–C(13)	1.429 (17)
Re–C(10)	2.360 (10)	C(1)–O(1)	1.157 (13)	C(13)–C(14)	1.363 (16)
P(1)–C(4)	1.812 (13)	C(2)–O(2)	1.154 (13)		

Angles

P(1),Re,P(2)	93.54 (10)	P(2),Re,C(10)	89.49 (27)	Re,P(2),C(9)	120.6 (4)
P(1),Re,C(1)	90.90 (37)	C(1),Re,C(2)	90.82 (49)	C(8),P(2),C(9)	100.0 (8)
P(1),Re,C(2)	176.9 (3)	C(1),Re,C(3)	90.76 (48)	Re,C(10),C(11)	108.5 (7)
P(1),Re,C(3)	87.46 (35)	C(1),Re,C(10)	176.7 (4)	Re,C(10),C(14)	110.8 (8)
P(1),Re,C(10)	87.12 (29)	C(2),Re,C(3)	89.95 (46)	C(11),C(10),C(14)	103.5 (9)
P(2),Re,C(1)	88.08 (32)	C(2),Re,C(10)	91.28 (43)	C(10),C(11),C(12)	109.9 (10)
P(2),Re,C(2)	89.08 (33)	C(3),Re,C(10)	91.70 (45)	C(12),C(13),C(14)	109.2 (10)
P(2),Re,C(3)	178.5 (4)	Re,P(2),C(8)	112.8 (5)		

[a] The estimated standard deviation of the least significant digit is given in parentheses.
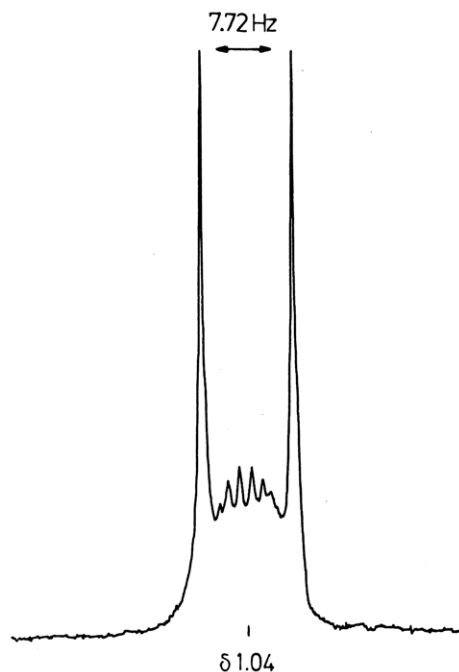
Figure 1. Signals due to cis $P(CH_3)_3$ ligands in the 270–MHz ^1H NMR spectrum of *fac*-$(\eta^1$-$C_5H_5)Re(CO)_3[P(CH_3)_3]_2$, **12**.

Figure 2. ORTEP diagram of *fac*-$(\eta^1$-$C_5H_5)Re(CO)_3[P(CH_3)_3]_2$, **12**.

Similarly, the η^1-C_5H_5 groups of **2**, **8**, and **9** are fluxional at low temperature. The $AX_9A'X'_9$ multiplet at δ 1.04 (Figure 1) is assigned to the equivalent cis $P(CH_3)_3$ ligands of **12**. Analysis[4] of the spectrum indicates $J_{PH} + J_{PH'} = 7.7$ Hz ($J_{PH} = 6.6$ Hz, $J_{PH'} = 1.1$ Hz) and $J_{PP} = -13 \pm 2$ Hz. The magnitude of J_{PP} is consistent with the cis orientation of the $P(CH_3)_3$ ligands but does not require this geometry since there is great variability in the magnitude of trans P–M–P coupling constants.[4] For comparison, $|J_{PP}| = 20$ Hz for the cis $P(CH_3)_3$ ligands of **2**. In the ^{13}C NMR of **12**, the fluxional η^1-C_5H_5 group gives rise to a singlet at δ 110.8.

Three strong carbonyl bands are seen in the IR spectrum of **12** in CH_2Cl_2 at 2007, 1936, and 1890 cm^{-1}. This spectrum is consistent with the facial structural assignment of **12** but does not allow exclusion of a meridinal structure.

X-ray Structure of *fac*-$(\eta^1$-$C_5H_5)Re(CO)_3[P(CH_3)_3]_2$. The facial configuration of **12** was demonstrated by X-ray crystallographic analysis (Figure 2, Table I). Only minor

deviations from octahedral geometry were observed; the largest deviation is associated with a wider 93.5 (1)° angle between the bulky $P(CH_3)_3$ ligands. The η^1-C_5H_5 ring is nearly planar; the maximum deviation of carbon from the mean plane of the ring is 0.036 Å. The η^1-C_5H_5 ring is oriented over the cis CO ligands and away from the bulky $P(CH_3)_3$ ligands. The angle between rhenium, C(10) of cyclopentadiene ring, and the center of gravity of the C_5H_5 ring is 120.48°.

Formation of $(\eta^5$-$C_5H_5)Re(CO)_2[P(CH_3)_3]$. In the course of studying the rate of formation of **12** in aromatic solvents and its equilibration with **11**, we observed a side reaction leading to the phosphine substitution product $(\eta^5$-$C_5H_5)Re(CO)_2[P(CH_3)_3]$, **13**. For example, reaction of **11** (0.44 M) and $P(CH_3)_3$ (2.31 M) in benzene-d_6 at 100 °C initially gave 50% starting material **11** and 50% bis(phosphine) adduct **12** after 1.5 h. However, after 4.5 h, 2.7% of a new compound identified below as $(\eta^5$-$C_5H_5)$-$Re(CO)_2[P(CH_3)_3]$, **13**, was observed in addition to 38% **11** and 58% **12**. After prolonged heating for 90 h, the only identifiable material in solution was **13**, formed in 63% yield (determined with 1,4-bis(trimethylsilyl)benzene as an internal NMR standard).

Pure substitution product **13** was obtained as a white crystalline solid in 57% isolated yield from reaction of $(\eta^5$-$C_5H_5)Re(CO)_3$ with 2.5 M $P(CH_3)_3$ at 102 °C for 43 h in toluene. The ^1H NMR of **13** consists of a doublet ($J = 0.6$ Hz) at δ 4.56 for the η^5-C_5H_5 unit and a doublet ($J = 9.4$ Hz) at δ 1.20 for the $P(CH_3)_3$ ligand and thus allows its detection in the presence of both **11** and **12**. Attempted

(4) Bertrand, R. D.; Ogilvie, F. B.; Verkade, J. G. *J. Am. Chem. Soc.* **1970**, *92*, 1908–1915.

preparation of 13 by prolonged photolysis (366 nm) of 11 and $P(CH_3)_3$ in benzene-d_6 at 40 °C gave only 32% 13 in addition to 28% 11 after 15 days.

Equilibration of 11 and 12. The reversibility of the formation of 12 was demonstrated by heating a dilute solution of 12 (0.073 M) in benzene-d_6 at 85 °C in a sealed NMR tube in the probe of a Bruker 270-MHz NMR spectrometer. 12 was completely converted to $(\eta^5\text{-}C_5H_5)$-$Re(CO)_3$, 11, and $P(CH_3)_3$ upon heating at 85 °C for 3 h; none (<1%) of the phosphine substitution product 13 was detected by NMR. Greater than 95% of the $P(CH_3)_3$ enters the gas phase above the solution and drives the reaction to completion. The time for 50% reaction was 30 min.

To measure the equilibrium constant between 11 and 12, a solution of 11 (0.2 M) and $P(CH_3)_3$ (0.5 M) in benzene-d_6 was heated to 50.9 ± 0.2 °C and the concentrations of 11, 12, and $P(CH_3)_3$ were monitored by ^1H NMR spectroscopy. Equilibrium was established slowly over the course of 40 days, and none of the substitution product 13 was observed. The equilibrium constant, K = $[12]/[11][P(CH_3)_3]^2$, was found to be 19 M^{-2}. For comparison, $(\eta^5\text{-}C_5H_5)Re(CO)(NO)(CH_3)$, 1, reacts with $P(C\text{-}H_3)_3$ to form the substantially more thermodynamically stable $\eta^1\text{-}C_5H_5$ bis(phosphine) adduct 2 (K = 74 M^{-2} in benzene-d_6 at 51 ± 1 °C).

Rate Studies. The $P(CH_3)_3$ concentration dependence of the rate of reaction of 11 and 12 in benzene-d_6 was measured by ^1H NMR spectroscopy. Two nearly identical NMR tubes, one containing 0.194 M 11 and 1.37 M $P(C\text{-}H_3)_3$ and the other containing 0.160 M 11 and 3.52 M $P(CH_3)_3$, were totally submerged in an 88.3 ± 0.2 °C constant temperature bath. The tubes were periodically monitored by ^1H NMR spectroscopy over the first 30% reaction.[5] The observed pseudo-first-order rate constants for disappearance of 11 were found to be 2.8 × 10^{-5} and 5.9 × 10^{-5} s^{-1}, respectively. While the absolute $P(CH_3)_3$ concentrations at 88 °C were not determined, the relative concentrations are proportional to the total amount of $P(CH_3)_3$ present. The 2.1-fold faster rate in the tube containing 2.5 times more phosphine is in reasonable agreement with a first-order dependence on $[P(CH_3)_3]$. Previously, we have shown[2] that the rate of formation of 2 and 1 and $P(CH_3)_3$ also has a first-order dependence on $[P(CH_3)_3]$.

Discussion

Our recent finding,[2] that the rate of reaction of $P(CH_3)_3$ with $(\eta^5\text{-}C_5H_5)Re(CO)(NO)(CH_3)$, 1, to produce the $\eta^1\text{-}C_5H_5$ bis(phosphine) complex 2 depends on the concentration of 1 and $P(CH_3)_3$, requires an intermediate whose stoichiometry is $(C_5H_5)Re(CO)(NO)(CH_3)[P(CH_3)_3]$, 5. There are two possible 18-electron formulations for this intermediate: an $\eta^3\text{-}C_5H_5$ linear nitrosyl complex 5A and an $\eta^5\text{-}C_5H_5$ bent nitrosyl complex 5B. The only other $\eta^5\text{-}C_5H_5$
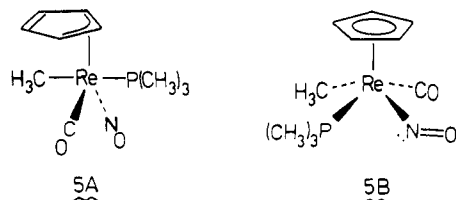
compounds that we have previously observed to undergo

conversion to bis(phosphine) $\eta^1\text{-}C_5H_5$ derivatives are the molybdenum and tungsten compounds 6 and 7 that also contain nitrosyl ligands. The observation reported here that the rate of reaction of $(\eta^5\text{-}C_5H_5)Re(CO)_3$, 11, with $P(CH_3)_3$ to give $\eta^1\text{-}C_5H_5$ bis(phosphine) adduct 12 depends on 11 and $P(CH_3)_3$ requires an intermediate mono(phosphine) adduct. Since 11 possesses no nitrosyl ligands, the only reasonable 18-electron formulation for the intermediate is the $\eta^3\text{-}C_5H_5$ complex 14. This demonstrates that nitrosyl ligands are not a requirement for formation of bis(phosphine) $\eta^1\text{-}C_5H_5$ compounds. However, it should be pointed out that the formation of a bis(phosphine) $\eta^1\text{-}C_5H_5$ compound from 11 is substantially slower than from the nitrosyl-containing compounds 1, 6, and 7. Nevertheless, we favor $\eta^3\text{-}C_5H_5$ intermediates in the reactions of 1, 6, and 7 because of the similarity with reactions of 11 and because this pathway provides a smooth transition from η^5- to η^3- to $\eta^1\text{-}C_5H_5$ derivatives.

The rate of formation of $\eta^1\text{-}C_5H_5$ bis(phosphine) adducts, the rate of reversal of the $\eta^1\text{-}C_5H_5$ bis(phosphine) adducts back to $\eta^5\text{-}C_5H_5$ compounds and free $P(CH_3)_3$, and the rate of formation of mono(phosphine)-substituted $\eta^5\text{-}C_5H_5$ compounds all follow the same sequence: molybdenum compound 6 > tungsten compound 7 > rhenium nitrosyl methyl compound 1 > rhenium carbonyl compound 11.[6] The similarity of all these relative rate sequences is readily explained since all three reactions are proposed to proceed via the same $\eta^3\text{-}C_5H_5$ mono(phosphine) intermediate. The rate sequence is therefore providing information about the ease of formation of the $\eta^3\text{-}C_5H_5$ intermediate in the various systems.

In spite of the fact that $(\eta^1\text{-}C_5H_5)Re(CO)(NO)(CH_3)[P(CH_3)_3]_2$, 2, reverts to $(\eta^5\text{-}C_5H_5)Re(CO)(NO)(CH_3)$, 1, much more rapidly than $(\eta^1\text{-}C_5H_5)Re(CO)_3[P(CH_3)_3]_2$, 12, reverts to 11[7] the equilibrium constant for formation of 2 at 50 °C (74 M^{-2}) is somewhat larger than the equilibrium constant for formation of 12 (19 M^{-2}) at the same temperature. No direct comparison of equilibrium constants for the molybdenum and tungsten compounds 6 and 7 is possible since their $\eta^1\text{-}C_5H_5$ bis(phosphine) adducts are kinetically stable only at low temperatures. However, the fact that 8 and 9 were observable only at high $P(CH_3)_3$ concentrations and at low temperature where adduct formation should be more favorable entropically suggests that the formation of adducts 8 and 9 is less thermodynamically favorable than formation of rhenium adducts 2 and 12.

Experimental Section

General Data. All reactions were carried out under an atmosphere of dry nitrogen using degassed solvents. NMR spectra were recorded on JEOL FX-200 (^{13}C, ^{31}P) or Brucker WH-270 (^1H) spectrometers. Infrared spectra were recorded on a Beckman 4230 infrared spectrometer. Mass spectra were recorded on an AEI-MS-902 spectrometer at 26 eV.

fac-$(\eta^1\text{-}C_5H_5)Re(CO)_3[P(CH_3)_3]_2$, 12. On a high vacuum line, $P(CH_3)_3$[8] (9.8 mmol) was condensed into a tube containing 11[9] (657 mg, 1.96 mmol) and 3 mL of hexane. The tube was sealed under vacuum at liquid-nitrogen temperature and then heated at 70 °C for 56 h. Large light yellow crystals, which formed in

---

(5) Beyond 30% reaction, the 1.37 M $P(CH_3)_3$ reaction slowly approached equilibrium with the formation of 13 apparent at long reaction times.

(6) For example, the temperatures at which these compounds react with $P(CH_3)_3$ to from bis(phosphine) $\eta^1\text{-}C_5H_5$ derivatives are −60 °C for 6, −60 °C for 7 (5.7 times slower than 6), 25 °C for 1, and 64 °C for 11.

(7) For 2 → 1, $t_{1/2}$ = 3.1 × 10^{-4} s^{-1} at 25.0 °C, whereas 12 is stable for weeks at 25.0 °C.

(8) Markham, R. T.; Dietz, E. A.; Martin, D. R. *Inorg. Synth.* **1976**, *16*, 153. Wolfsberger, W.; Schmidbaur, H. *Synth. React. Inorg. Met.-Org. Chem.* **1974**, *4*, 149.

(9) Casey, C. P.; Andrews, M. A.; McAlister, D. R.; Rinz, J. E. *J. Am. Chem. Soc.* **1980**, *102*, 1927–1933.

the hot hexane as the reaction progressed, were collected by filtration in an inert-atmosphere box and washed with hexane to give analytically pure 12 (809 mg, 85%): mp (sealed capillary) 133 °C dec; ^{1}H NMR (benzene-d_6) δ 6.15, (t, J_{PH} = 1.47 Hz, 5 H), 1.04 (m, AX$_9$A'X'$_9$, J_{PP} = -13 $\pm$ 2 Hz, J_{PH} = 6.6 Hz, $J_{PH'}$ = 1.1 Hz, 18 H); ^{13}C NMR (THF-d_8, 0.09 M Cr(acac)$_3$, -30 °C) δ 194.4 (br, COs trans to P(CH$_3$)$_3$), 192.7 (br, CO trans to C$_5$H$_5$), 110.8 (s, C$_5$H$_5$), 18.5 (t, J_{PC} = 14.6 Hz, P(CH$_3$)$_3$); ^{31}P NMR (acetone-d_6) δ -42.65 (s) relative to external H$_3$PO$_4$; IR (CH$_2$Cl$_2$) 2007 (s), 1936 (s), 1890 (s) cm^{-1}.

Anal. Calcd for C$_{14}$H$_{23}$O$_3$P$_2$Re: C, 34.49; H, 4.76. Found: C, 34.74; H, 4.80. Significant high mass peaks retaining both P(CH$_3$)$_3$ ligands: 423 (M - C$_5$H$_5$) and 395 (M - C$_5$H$_5$ - CO); exact mass calcd for ^{187}ReC$_{14}$H$_{23}$P$_2$O$_3$ 488.0677, found 488.0653.

(η^5-C$_5$H$_5$)Re(CO)$_2$[P(CH$_3$)$_3$], 13. On a high vacuum line, P(CH$_3$)$_3$ (7.7 mmol) was condensed into a tube fitted with a Teflon needle valve and containing 11 (496 mg, 1.48 mmol) and 3 mL of toluene. The tube was closed off under vacuum at liquid-nitrogen temperatures and then heated at 102 °C for 43 h. The solvent and excess P(CH$_3$)$_3$ were pumped off, and the residue was thin layer chromatographed (silica gel–toluene) under a nitrogen atmosphere to give analytically pure 13 (R_f = 0.6) as a white crystalline solid (325 mg, 57%): mp (sealed capillary) 99–100 °C dec; ^{1}H NMR (benzene-d_6, 270 MHz) δ 4.56 (d, J = 0.6 Hz, 5 H), 1.20 (d, J = 9.4 Hz, 9 H); ^{13}C NMR (acetone-d_6, 0.09 M Cr(acac)$_3$) δ 202.8 (br, CO), 82.76 (s, C$_5$H$_5$), 23.96 (d, J_{PC} = 36.7 Hz, P(CH$_3$)$_3$); ^{31}P NMR (acetone-d_6, 0.09 M Cr(acac)$_3$) δ -25.02 (s) relative to external H$_3$PO$_4$; IR (THF) 1929 (s), 1859 (s) cm^{-1}.

Anal. Calcd for C$_{10}$H$_{14}$O$_2$PRe: C, 31.33; H, 3.68. Found: C, 31.25; H, 3.71.

Conversion of 12 to 11. On a high vacuum line, benzene-d_6 (0.28 mL) was condensed into an NMR tube containing 12 (10 mg, 0.02 mmol) and 1,4-bis(trimethylsilyl)benzene (5 mg, 0.02 mmol). The tube was sealed under vacuum at liquid-nitrogen temperatures and placed in the probe of a Bruker WH-270 spectrometer maintained at 85 °C. The quantitative conversion of 12 to 11 was then monitored by ^{1}H NMR spectroscopy. See Results section.

Equilibration of 11 and 12. On a high vacuum line, P(CH$_3$)$_3$ (0.22 mmol) and benzene-d_6 were condensed into an NMR tube containing 11 (30 mg, 0.089 mmol) to give a total volume of 0.44 mL at 51 $\pm$ 1 °C. The tube was then sealed under vacuum at liquid-nitrogen temperature and placed in a constant temperature bath at 50.9 $\pm$ 0.2 °C. The concentrations of 11 and 12 were periodically monitored by ^{1}H NMR with equilibration occurring after 41 days. The tube was then placed in the probe of the Bruker WH 270 maintained at 51 $\pm$ 1 °C, and the concentrations of 11, 12, and P(CH$_3$)$_3$ were determined to be 0.101, 0.099, and 0.224 M respectively, giving K = [12]/[11][P(CH$_3$)$_3$]^2 = 19.5 M^{-2}.

Equilibration of 1 and 2. A sealed NMR tube containing 1 (12.3 mg, 0.038 mmol) and P(CH$_3$) (0.076 mmol) in benzene-d_6 (total volume 0.38 mL at 51 $\pm$ 1 °C) was placed in the probe of a Bruker WH-270 NMR spectrometer maintained at 51 $\pm$ 1 °C. Equilibration was achieved within 30 min. The concentrations of 1, 2, and P(CH$_3$)$_3$ were found to be 0.058, 0.041, and 0.098 M by ^{1}H NMR, giving K = [2]/[1][P(CH$_3$)$_3$]^2 = 73.6 M^{-2}.

X-ray Data Collection. Single crystals of *fac*-(η^1-C$_5$H$_5$)Re-(CO)$_3$[P(CH$_3$)$_3$]$_2$, 12, suitable for X-ray diffraction studies were obtained by evaporation of THF. A single crystal of approximate dimensions 0.12 $\times$ 0.15 $\times$ 0.55 mm was mounted on a Syntex-Nicolet P$\bar{1}$ four-circle diffractometer. Preliminary examination of the crystal showed it to be monoclinic. The systematic absences of h0l, h + l = 2n + 1, and 0k0, k = 2n + 1, uniquely determine

the space group to be $P2_1/n$ (No. 14). The unit-cell parameters (at 19 $\pm$ 1 °C; λ (Mo K$\bar{\alpha}$) = 0.710 73 Å) are a = 8.011 (5) Å, b = 14.042 (3) Å, c = 16.349 (3) Å, and β = 92.08 (2)°. These parameters were determined from a least-squares refinement utilizing the setting angles of 62 accurately centered reflections from diverse regions of reciprocal space collected at $\pm 2\theta$ ($|2\theta| \approx 35°$). The unit cell volume of 1837.9 Å^3 led to a calculated density of 1.62 g/cm^3 for four formula units of ReP$_2$O$_3$C$_{14}$H$_{23}$ per unit cell.

A total of 4206 unique intensity data with (sin θ)/λ $\leq$ 0.649 Å^{-1} were collected by using a θ–2θ step-scan technique with a scan range of 0.65° below 2θ(Mo Kα_1) to 0.65° above 2θ(Mo Kα_2) and a variable scan rate (2.0–24.0°/min). Throughout data collection four standard reflections from diverse regions of reciprocal space were monitored every 50 reflections. There were no systematic variations of the intensities of the standard reflections during the time required to collect the data. The intensity data were reduced and standard deviations calculated using methods similar to those described previously.[10] Absorption corrections were applied to the data by using an empirical psi curve method (μ = 64.9 cm^{-1}).

Structure Solution and Refinement. The structure was solved by the standard heavy-atom method from the Patterson map. The rest of the non-hydrogen atoms were located from a series of electron density difference maps. The full-matrix least-squares refinement of the model was based on F_o and used the 2712 data with F_o > 3σ(F_o). Atomic form factors for the non-hydrogen atoms were taken from Cromer and Waber[11] and that for hydrogen from Stewart, Davidson, and Simpson.[12] An electron density difference map calculated after isotropic refinement of the non-hydrogen atoms had converged revealed reasonable positions for most of the hydrogen atoms. All hydrogen atoms were included in the remaining cycles of refinement as fixed contributors in idealized positions (d_{CH} = 0.95 Å; B_H = B_C + 1.0). In the final cycles of refinement all non-hydrogen atoms were assumed to vibrate anisotropically. At convergence the discrepancy indices were R_1 = $\sum ||F_o| - |F_c||/\sum |F_o|$ = 0.045 and R_2 = $[\sum w(|F_o| - |F_c|)^2/\sum w(F_o)^2]^{1/2}$ = 0.054. The estimated standard deviation of an observation of unit weight was 1.45 with a final data/variable ratio of 15.0. The final electron density difference map had one high peak (about 33% of a typical carbon atom peak) associated with the Re atom. Final atomic coordinates (Table II), a table of the anisotropic thermal parameters (Table III), a table of the fixed hydrogen atom parameters (Table IV), and a listing of observed and calculated structure factors ($\times$10) are available as supplementary material.

(10) Haller, K. J.; Enemark, J. H. *Inorg. Chem.* **1978**, *17*, 3552–3558.
(11) Cromer, D. T.; Waber, J. T. "International Tables for X-ray Crystallography"; Kynoch Press: Birmingham, England, 1974; Vol. 4, pp 99–101, Table 2.2B.
(12) Stewart, R. F.; Davidson, E. R.; Simpson, W. T. *J. Chem. Phys.* **1965**, *42*, 3175–3187.

Electron-Rich Cations: Preparation and Hydride Reductions of the Cations {(η^5-C₅H₅)Ru[MeC(CH₂PPh₂)₃]}⁺ and {(η^5-C₅H₅)Ru[PhP(CH₂CH₂PPh₂)₂]}⁺

Stephen G. Davies* and Stephen J. Simpson

The Dyson Perrins Laboratory, Oxford, OX1 3QY, England

Hugh Felkin and Tauqir Fillebeen-Khan

Institut de Chimie des Substances Naturelles, CNRS, 91190 Gif-sur-Yvette, France

The cations {(η^5-C₅H₅)Ru[MeC(CH₂PPh₂)₃]}⁺ and {(η^5-C₅H₅)Ru[PhP(CH₂CH₂PPh₂)₂]}⁺ are reduced regioselectively by lithium aluminum hydride to give the corresponding cyclopentadiene complexes. The mechanism of these reductions involves direct attack of hydride exo onto the cyclopentadienyl ligand.

The cyclopentadienyl ligand is the least susceptible of the common hydrocarbon ligands toward nucleophilic attack.[1,2] Nucleophilic addition to cyclopentadienyliron tris(triphenyl phosphite) cation 1, however, has been shown to occur onto the cyclopentadienyl ring to give the corresponding cyclopentadiene complex 2;[3] in this 18-electron cation no alternative position is available. Direct attack onto the metal atom of 18-electron cations can occur only in cases where a 2-electron ligand readily dissociates, thereby generating a 16-electron intermediate.[1] For example, nucleophilic addition to the cyclopentadienyliron tripod [MeC(CH₂PPh₂)₃] and triphos [PhP(CH₂CH₂PPh₂)₂] cations 3 and 4 gives the corresponding iron hydrides by direct attack on the metal. These latter reactions proceed via an S_N1 mechanism with prior dissociation of a phosphine ligand and nucleophilic attack onto the thus formed coordinatively unsaturated metal atom.[4,5] Ligand loss in cations 3 and 4, but not in cation 1, is presumably encouraged by steric and strain factors associated with the tris(phosphine) ligands bonding to the relatively small iron atom.[5,6]

We describe here the preparation and reactivity toward hydride of the cations [(η^5-C₅H₅)Ru(tripod)]PF₆ (5) and [(η^5-C₅H₅)Ru(triphos)]PF₆ (6). On going from iron to the larger ruthenium atom steric and strain effects would be expected to lessen and hence the tendency for ligand dissociation to decrease. It was of interest to us to determine whether the reactivity of cations 5 and 6 resembled that of the iron cation 1 or the iron cations 3 and 4. Part of this work has been the subject of a preliminary communication.[5]

Results and Discussion

The ruthenium cations 5 and 6 were prepared by treatment of the chloride 7[7] with tripod and triphos in refluxing decalin.[8] Phosphine exchange and displacement of chloride gives, after anion exchange, cations 5 and 6, respectively.

Reduction of the tripod cation 5 with lithium aluminum hydride in tetrahydrofuran gives the corresponding cyclopentadiene complex 8. In the ¹H NMR spectrum of 8 H_{exo} and H_{endo} could be unambiguously assigned by the fact that only one of them shows coupling to the three equivalent phosphorus atoms. Only H_{exo} would be expected to show long-range coupling to phosphorus. Such couplings occur over four bonds between nuclei in a "W" arrangement.[9] H_{endo} unlike H_{exo} cannot achieve such an arrangement with the phosphorus atoms. Consistent with this assignment is the fact that coupling to the olefinic protons, identified by selective decoupling experiments, are only observed for H_{endo} and not for H_{exo}. This is what is anticipated from consideration of the expected bond angles.[10] The ³¹P NMR spectrum confirms that all three phosphorus atoms are bound to ruthenium.

Reduction of the tripod cation 5 with lithium aluminum deuteride in tetrahydrofuran gives the cyclopentadiene complex 9 with deuterium in the exo position. The absorption assigned to H_{exo} in the ¹H NMR spectrum of 8 is completely absent in that of 9; the rest of the spectrum remaining essentially unchanged. The characteristic IR absorption of cyclopentadiene H_{exo}[11] at 2715 cm⁻¹ was present in the spectrum of 8. This absorption was absent, however, from the spectrum of 9 and had been replaced by D_{exo} absorptions at 2050, 2020, and 1995 cm⁻¹.

1

2

3 P₃ = tripod
4 P₃ = triphos
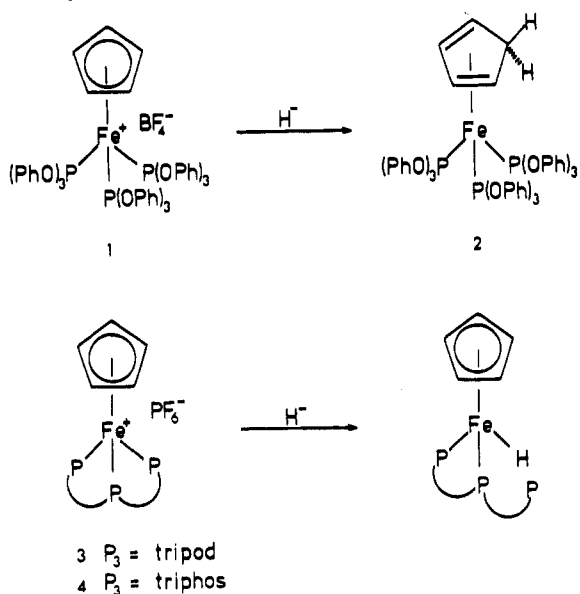
(1) Davies, S. G.; Green, M. L. H.; Mingos, D. M. P. *Tetrahedron* **1978**, *34*, 3047.
(2) Efraty, A.; Maitlis, P. M. *J. Am. Chem. Soc.* **1967**, *89*, 3744. Maitlis, P. M. *Chem. Soc. Rev.* **1981**, *10*, 1.
(3) Green, M. L. H.; Whiteley, R. N. *J. Chem. Soc. A* **1971**, 1943.
(4) Davies, S. G.; Felkin, H.; Watts, O. *J. Chem. Soc., Chem. Commun.* **1980**, 159.
(5) Davies, S. G.; Felkin, H.; Fillebeen-Khan, T.; Tadj, F.; Watts, O. *J. Chem. Soc., Chem. Commun.* **1981**, 341.
(6) Davies, S. G.; Simpson, S. J.; Felkin, H.; Tadj, F.; Watts, O.; submitted for publication.
(7) Bruce, M. I.; Windsor, N. *J. Aust. J. Chem.* **1977**, *30*, 1601.
(8) Ashby, G. S.; Bruce, M. I.; Tomkins, I. B.; Wallis, R. C. *Aust. J. Chem.* **1979**, *32*, 1003.
(9) Meinwald, J.; Meinwald, Y. C. *J. Am. Chem. Soc.* **1963**, *85*, 2514.
(10) Gunther, H. "NMR Spectroscopy"; Wiley: New York, 1980.
(11) White, D. A. *Organomet. Chem. Rev. A* **1968**, *3*, 497.

Table I. Chemical Shifts of H_{exo} and H_{endo} (δ)

	ref	H_{exo}	H_{endo}	J_{HH}, Hz
$(C_5H_6)Fe[P(OPh)_3]_3$ (2)	3	3.00	2.40	
$(C_5H_6)Fe(CO)_3$	17	1.92	2.37	12
$[(1-CO_2Me)C_5H_5]Co(C_5H_4CO_2Me)$	18	1.78	2.68	15
$(C_5H_6)Co(C_5H_5)$	19	1.95	2.60	12.7
$(C_5H_6)Rh(C_5H_5)$	19	2.92	3.34	11.2
$(C_5H_6)Ru(tripod)$ (8)		4.01	3.54	9.0
$(C_5H_6)Ru(triphos)$ (10)		3.57	2.58	10.3
$(C_5H_6)Fe(CO)(Ph_2PCH_2CH_2PPh_2)$	20	2.75	3.03	10.0
$[(C_5H_6)Mo(C_5H_5)(Ph_2PCH_2CH_2PPh_2)]PF_6$	24	3.58	2.51	12
$(C_5H_6)Fe(CO)_2(PPh_3)$	20	2.24	2.78	10.5

Reduction of the triphos cation 6 similarly gives the corresponding cyclopentadiene complex 10. Once again H_{exo} could be assigned in the ^1H NMR spectrum on the basis of the observed long-range couplings to two equivalent and a third phosphorus atoms. Selective decoupling of the phosphorus atoms clearly demonstrates the phosphorus–hydrogen coupling in the ^1H NMR spectrum. As before only H_{endo} showed coupling to olefinic protons. Lithium aluminum deuteride reduction of 6 gives the cyclopentadiene complex 11 with deuterium in the exo position. The signal assigned to H_{exo} was completely absent from the ^1H NMR spectrum of 11. The H_{exo} IR absorption in 10 at 2750 cm^{-1} had been replaced in 11 by D_{exo} absorptions at 2045 and 2015 cm^{-1}. The ^{31}P NMR spectrum of 10 confirmed that all three phosphorus atoms, two of which are equivalent, were bound to ruthenium. The ^{31}P NMR spectrum of 10 was broad at 302 K due to exchange between rotational isomers.[12] At 332 K, however, exchange was sufficiently rapid for the expected sharp triplet and doublet to be observed.

There has been some controversy in the literature about the validity of assigning the IR absorption at 2750 ± 50 cm^{-1} in the spectra of cyclopentadiene and cycloheptatriene complexes to the presence or absence of an exo hydrogen.[13] The unambiguous assignment here of H_{exo} and H_{endo} for the cyclopentadiene compounds 8 and 10 is based on three further criteria: (1) the ^1H NMR and IR spectra of the corresponding deuterides 9 and 11; (2) the observation of long-range coupling between H_{exo} and phosphorus that is not exhibited by H_{endo}; (3) the absence of observable vicinal

coupling to H_{exo}, whereas that to H_{endo} is clearly observable for 8 and 10. These combined criteria enable us to confirm our confidence in the use of the IR criterion, at least for cyclopentadiene ligands. It is noteworthy that in the four examples known of a cyclopentadiene ligand bearing an exo hydrogen and an endo substituent the exo hydrogen IR absorption at ca. 2750 cm^{-1} is indeed present.[15] It should be pointed out here that two other common criteria are not always reliable: trityl tetrafluoroborate will not selectively remove H_{exo} in preference to H_{endo}[14] and the chemical shift of H_{endo} is not always at lower field than that of H_{exo} (see Table I). A similar situation exists for cycloheptatrienyl compounds.[13,18]

Hydride attack occurs regioselectively onto the cyclopentadienyl ring in the ruthenium tripod and triphos cations 5 and 6, respectively, and in the iron tris(triphenyl phosphite) cation 1.[3] In contrast the analogous iron tripod and triphos cations 3 and 4, respectively, undergo hydride addition to the metal. These differences in regioselectivity can be attributed to strain present in the iron cations 3 and 4 that promotes dissociation of a phosphine ligand to generate a 16-electron species prior to nucleophilic attack.

Experimental Section

Compound 5, $\{(\eta^5-C_5H_5)Ru[MeC(CH_2PPh_2)_3]\}PF_6$. This was prepared by a modification of the method of Bruce et al.[8] A

(12) Ungermann, C. B.; Caulton, K. G. *J. Organomet. Chem.* **1975**, *94*, C9.

(13) Faller, J. W. *Inorg. Chem.* **1980**, *19*, 2857.

(14) Nesmeyanov, A. N.; Vol'Kenau, N. A.; Shilovtieva, L. S.; Petrakova, V. A. *J. Organomet. Chem.* **1975**, *85*, 365.

(15) Fachinetti, G.; Floriani, C. *J. Chem. Soc., Chem. Commun.* **1974**, 516. Benfield, F. W. S.; Green, M. L. H. *J. Chem. Soc., Dalton Trans.* **1974**, 1324.

(16) Winstein, S.; Kaesz, H. D.; Kreiter, C. G.; Friedrich, E. C. *J. Am. Chem. Soc.* **1965**, *87*, 3267. Brown, J. M.; Coles, D. G. *J. Organomet. Chem.* **1973**, *60*, C31.

(17) Whitesides, T. H.; Shelly, J. *J. Organomet. Chem.* **1975**, *92*, 215.

(18) Rosenblum, M.; North, B.; Wells, D.; Giering, W. P. *J. Am. Chem. Soc.* **1972**, *94*, 1239.

(19) Green, M. L. H.; Pratt, L.; Wilkinson, G. *J. Chem. Soc.* **1959**, 3753.

(20) Davies, S. G.; Hibberd, J.; Simpson, S. J., to be submitted for publication.

(21) Shriver, D. F. "The Manipulation of Air-Sensitive Compounds"; McGraw-Hill: New York, 1969.

(22) Dubois, D. L.; Meyers, W. H.; Meek, D. W. *J. Chem. Soc., Dalton Trans.* **1975**, 1011.

(23) Hewertson, W.; Watson, H. R. *J. Chem. Soc.* **1962**, 1490.

(24) Aviles, T.; Green, M. L. H.; Dias, A. R.; Romao, C. *J. Chem. Soc., Dalton Trans.* **1979**, 1367.

mixture of $(\eta^5\text{-}C_5H_5)Ru(PPh_3)_2Cl$ (7, 1.8 g, 2.47 mmol), tripod (1.6 g, 2.60 mmol), and NH_4PF_6 (0.5 g, 3.07 mmol) was heated in decalin (60 mL) under reflux for 4 h. The cooled solution was filtered and the solid triturated with toluene (2 × 40 mL) and dried in vacuo. The dried solid was stirred with NH_4PF_6 (0.5 g, 3.07 mmol) in wet acetone (70 mL) for 30 min, and then the solvent was removed under reduced pressure. The residue was extracted with dichloromethane (2 × 50 mL), and the filtered extracts were concentrated to 20 mL. Slow addition of diethyl ether gave pale yellow needles of **5** containing 1 mol of dichloromethane of crystallization: 1.7 g, 73%; ^1H NMR ($CDCl_3$) δ 7.30–6.70 (m, 30 H, PPh), 5.32 (s, 5 H, C_5H_5), 2.55–2.30 (m, 6 H, CH_2P), 1.63 (m, 3 H, Me); $^{31}P\{^1H\}$ NMR (CH_2Cl_2) δ 38.5 (s). Anal. Calcd for $C_{47}H_{46}Cl_2F_6P_4Ru$: C, 55.35; H, 4.51; P, 12.16. Found: C, 55.70; H, 4.59; P, 12.34.

Compound 6, $\{(\eta^5\text{-}C_5H_5)Ru[PhP(CH_2CH_2PPh_2)_2]\}PF_6$. A mixture of 7 (2.0 g, 2.76 mmol), triphos (1.6 g, 3.00 mmol), and NH_4PF_6 (0.6 g, 3.68 mmol) was heated in decalin (75 mL) under reflux for 3 h. The cooled solution was filtered and the resulting yellow mass triturated with toluene (2 × 20 mL) and dried in vacuo. The solid was stirred with NH_4PF_6 (0.6 g, 3.68 mmol) in wet acetone (50 mL) for 30 min and the solvent removed under reduced pressure. The crude product was recrystallized from dichloromethane/diethyl ether as pale yellow needles containing 0.25 mol of dichloromethane of crystallization: 1.8 g, 77%; ^1H NMR (CD_2Cl_2) δ 7.25–6.70 (m, 25 H, PPh), 5.20 (s, 5 H, C_5H_5), 2.55–1.30 (m, 8 H, CH_2P); $^{31}P\{^1H\}$ NMR (CH_2Cl_2) δ 98.6 (t, 1 P, J_{PP} = 26 Hz), 80.4 (d, 2 P, J_{PP} = 26 Hz). Anal. Calcd for $C_{39.25}H_{38.5}Cl_{0.5}F_6P_4Ru$: C, 54.38; H, 4.45; P, 14.31. Found: C, 54.24; H, 4.48; P, 14.52.

Compound 8, $(\eta^4\text{-}C_5H_6)Ru[MeC(CH_2PPh_2)_3]$. LiAlH$_4$ (0.2 g, 5.26 mmol) was added to a stirred solution of cation **5** (1.6 g, 1.71 mmol) in tetrahydrofuran (75 mL). After being stirred at room temperature for 14 h, the mixture was cooled (0 °C) and carefully hydrolyzed (H_2O, 0.5 mL). Solvent was removed under reduced pressure and the solid residue extracted with diethyl ether (3 × 50 mL). The yellow extract was concentrated (15 mL) and cooled (−30 °C). The pale yellow needles were washed with ice-cold petroleum ether and dried in vacuo: 0.9 g, 67%; IR

$\nu_{max}(C\text{-}H_{exo})$ 2715 cm^{-1}; ^1H NMR (C_6D_6) δ 7.15–6.81 (m, 30 H, PPh), 5.85 (m, 2 H, $H_{2,3}$), 4.01 (dq, 1 H, H_{exo}, J_{HH} = 9.0, J_{PH} = 14.2 Hz), 3.54 (m, 1 H, H_{endo} [$W_{1/2}$ = 13 Hz]), 2.59 (m, 2 H, $H_{1,4}$), 2.19 (m, 6 H, CH_2P), 1.23 (m, 3 H, Me); $^{31}P\{^1H\}$ NMR (toluene) δ 35.3 (s). Anal. Calcd for $C_{46}H_{45}P_3Ru$: C, 69.78; H, 5.68; P, 11.75. Found: C, 69.63; H, 5.80; P, 11.49.

Compound 9, $(\eta^4\text{-}C_5H_5D_{exo})Ru[MeC(CH_2PPh_2)_3]$. This was prepared as for **8** above by using LiAlD$_4$ in place of LiAlH$_4$: yield 70%; IR $\nu_{max}(C\text{-}D_{exo})$ 2050 (m), 2020 (m), 1995 (w) cm^{-1}.

Compound 10, $(\eta^4\text{-}C_5H_6)Ru[PhP(CH_2CH_2PPh_2)_2]$. LiAlH$_4$ (0.2 g, 5.26 mmol) was added to a stirred suspension of cation **6** (1.2 g, 1.42 mmol) in tetrahydrofuran (50 mL). The mixture was stirred at room temperature for 16 h, then cooled (0 °C), and carefully hydrolyzed (H_2O, 0.5 mL). Solvent was removed under reduced pressure and the dry solid extracted with diethyl ether (3 × 40 mL). The pale yellow extract was concentrated (20 mL) and cooled (−30 °C). The pale yellow blocks obtained were washed with ice-cold petroleum ether and dried in vacuo: 0.6 g, 60%; IR $\nu_{max}(C\text{-}H_{exo})$ 2750 cm^{-1}; ^1H NMR (C_6D_6) δ 7.80–6.85 (m, 25 H, PPh), 5.36 (m, 2 H, $H_{2,3}$), 3.57 (ddt, 1 H, H_{exo}, J_{HH} = 10.3, J_{PH} = 8.1, 18.8 Hz), 2.90 (m, 2 H, $H_{1,4}$), 2.58 (m, 1 H, H_{endo} [$W_{1/2}$ = 17 Hz]), 2.15–1.10 (m, 8 H, CH_2P); $^{31}P\{^1H\}$ NMR (toluene, 332 K) δ 91.1 (t, 1 P, J_{PP} = 10 Hz), 79.85 (d, 2 P, J_{PP} = 10 Hz). Anal. Calcd for $C_{39}H_{39}P_3Ru$: C, 66.76; H, 5.56; P, 13.26. Found: C, 66.48; H, 5.60; P, 12.97.

Compound 11, $(\eta^4\text{-}C_5H_5D_{exo})Ru[PhP(CH_2CH_2PPh_2)_2]$. This was prepared as for **1** above by using LiAlD$_4$ in place of LiAlH$_4$: yield 65%; IR $\nu_{max}(C\text{-}D_{exo})$ 2045 (m), 2015 (m) cm^{-1}.

Registry No. 5, 71397-19-8; 6, 79019-68-4; 7, 32993-05-8; 8, 79019-70-8; 9, 84174-44-7; 10, 79019-69-5; 11, 84174-45-8; LiAlD$_4$, 14128-54-2.

Stereochemical Aspects of the Formation and Trifluoroacetolysis of Some Allylic Bis(trimethylsilyl)cyclohexenes

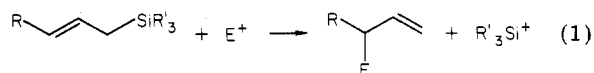Geoffrey Wickham and William Kitching*

Department of Chemistry, University of Queensland, Brisbane 4067, Australia

Received September 16, 1982

The stereochemistry of the 3,4-bis(trimethylsilyl)cyclohexene resulting from disilylation of 1,3-cyclohexadiene is concluded to be cis on the basis of ^1H and ^{13}C nuclear magnetic resonance spectra and hydrogenation to *cis*-1,2-bis(trimethylsilyl)cyclohexane. The higher boiling *cis*- and *trans*-3,6-bis(trimethylsilyl)cyclohexenes could be separated from the above 3,4-isomer but not from each other by careful spinning band distillation. However, the cis,trans compositions of various fractions were established by ^{13}C NMR spectra and chromatographic characteristics. Trifluoroacetolysis (CF_3COOD in chloroform) of the cis 3,4-isomer proceeds to yield cyclohexene-d_2 as the final product, and analysis of ^2H NMR spectra and intermediates demonstrates the importance of a facile 1,2-trimethylsilyl shift in the presumed intermediate ion. Trifluoroacetolysis of the mixtures of the 3,6-disilyl isomers proceeds regiospecifically to yield cyclohex-3-enyltrimethylsilane. A preferred anti mode of attack by the electrophile is indicated for the cis isomer, but syn and anti modes are about equally preferred in the trans isomer. This is attributed to steric congestion by the trimethylsilyl group in the γ-carbon region, hindering anti approach by the electrophile.

## Introduction

The regiospecific γ cleavage of allylic derivatives of silicon by electrophiles confers considerable potential on these compounds as allylation reagents, and their use in carbon–carbon bond formation has been described (eq 1).[1,2]

$$R\diagdown\diagup\diagdown\diagup SiR'_3 + E^+ \longrightarrow R\diagdown\diagup\diagdown + R'_3Si^+ \quad (1)$$

Full exploitation of these silanes as allylation agents will require an appreciation of the factors regulating the ste-

mixture of (η^5-C$_5$H$_5$)Ru(PPh$_3$)$_2$Cl (7, 1.8 g, 2.47 mmol), tripod (1.6 g, 2.60 mmol), and NH$_4$PF$_6$ (0.5 g, 3.07 mmol) was heated in decalin (60 mL) under reflux for 4 h. The cooled solution was filtered and the solid triturated with toluene (2 × 40 mL) and dried in vacuo. The dried solid was stirred with NH$_4$PF$_6$ (0.5 g, 3.07 mmol) in wet acetone (70 mL) for 30 min, and then the solvent was removed under reduced pressure. The residue was extracted with dichloromethane (2 × 50 mL), and the filtered extracts were concentrated to 20 mL. Slow addition of diethyl ether gave pale yellow needles of **5** containing 1 mol of dichloromethane of crystallization: 1.7 g, 73%; ^{1}H NMR (CDCl$_3$) δ 7.30–6.70 (m, 30 H, PPh), 5.32 (s, 5 H, C$_5$H$_5$), 2.55–2.30 (m, 6 H, CH$_2$P), 1.63 (m, 3 H, Me); ^{31}P{^{1}H} NMR (CH$_2$Cl$_2$) δ 38.5 (s). Anal. Calcd for C$_{47}$H$_{46}$Cl$_2$F$_6$P$_4$Ru: C, 55.35; H, 4.51; P, 12.16. Found: C, 55.70; H, 4.59; P, 12.34.

Compound 6, {(η^5-C$_5$H$_5$)Ru[PhP(CH$_2$CH$_2$PPh$_2$)$_2$]}PF$_6$. A mixture of **7** (2.0 g, 2.76 mmol), triphos (1.6 g, 3.00 mmol), and NH$_4$PF$_6$ (0.6 g, 3.68 mmol) was heated in decalin (75 mL) under reflux for 3 h. The cooled solution was filtered and the resulting yellow mass triturated with toluene (2 × 20 mL) and dried in vacuo. The solid was stirred with NH$_4$PF$_6$ (0.6 g, 3.68 mmol) in wet acetone (50 mL) for 30 min and the solvent removed under reduced pressure. The crude product was recrystallized from dichloromethane/diethyl ether as pale yellow needles containing 0.25 mol of dichloromethane of crystallization: 1.8 g, 77%; ^{1}H NMR (CD$_2$Cl$_2$) δ 7.25–6.70 (m, 25 H, PPh), 5.20 (s, 5 H, C$_5$H$_5$), 2.55–1.30 (m, 8 H, CH$_2$P); ^{31}P{^{1}H} NMR (CH$_2$Cl$_2$) δ 98.6 (t, 1 P, J_{PP} = 26 Hz), 80.4 (d, 2 P, J_{PP} = 26 Hz). Anal. Calcd for C$_{39.25}$H$_{38.5}$Cl$_{0.5}$F$_6$P$_4$Ru: C, 54.38; H, 4.45; P, 14.31. Found: C, 54.24; H, 4.48; P, 14.52.

Compound 8, (η^4-C$_5$H$_6$)Ru[MeC(CH$_2$PPh$_2$)$_3$]. LiAlH$_4$ (0.2 g, 5.26 mmol) was added to a stirred solution of cation **5** (1.6 g, 1.71 mmol) in tetrahydrofuran (75 mL). After being stirred at room temperature for 14 h, the mixture was cooled (0 °C) and carefully hydrolyzed (H$_2$O, 0.5 mL). Solvent was removed under reduced pressure and the solid residue extracted with diethyl ether (3 × 50 mL). The yellow extract was concentrated (15 mL) and cooled (−30 °C). The pale yellow needles were washed with ice-cold petroleum ether and dried in vacuo: 0.9 g, 67%; IR

ν_{max}(C–H$_{exo}$) 2715 cm^{-1}; ^{1}H NMR (C$_6$D$_6$) δ 7.15–6.81 (m, 30 H, PPh), 5.85 (m, 2 H, H$_{2,3}$), 4.01 (dq, 1 H, H$_{exo}$, J_{HH} = 9.0, J_{PH} = 14.2 Hz), 3.54 (m, 1 H, H$_{endo}$ [$W_{1/2}$ = 13 Hz]), 2.59 (m, 2 H, H$_{1,4}$), 2.19 (m, 6 H, CH$_2$P), 1.23 (m, 3 H, Me); ^{31}P{^{1}H} NMR (toluene) δ 35.3 (s). Anal. Calcd for C$_{46}$H$_{45}$P$_3$Ru: C, 69.78; H, 5.68; P, 11.75. Found: C, 69.63; H, 5.80; P, 11.49.

Compound 9, (η^4-C$_5$H$_5$D$_{exo}$)Ru[MeC(CH$_2$PPh$_2$)$_3$]. This was prepared as for **8** above by using LiAlD$_4$ in place of LiAlH$_4$: yield 70%; IR ν_{max}(C–D$_{exo}$) 2050 (m), 2020 (m), 1995 (w) cm^{-1}.

Compound 10, (η^4-C$_5$H$_6$)Ru[PhP(CH$_2$CH$_2$PPh$_2$)$_2$]. LiAlH$_4$ (0.2 g, 5.26 mmol) was added to a stirred suspension of cation **6** (1.2 g, 1.42 mmol) in tetrahydrofuran (50 mL). The mixture was stirred at room temperature for 16 h, then cooled (0 °C), and carefully hydrolyzed (H$_2$O, 0.5 mL). Solvent was removed under reduced pressure and the dry solid extracted with diethyl ether (3 × 40 mL). The pale yellow extract was concentrated (20 mL) and cooled (−30 °C). The pale yellow blocks obtained were washed with ice-cold petroleum ether and dried in vacuo: 0.6 g, 60%; IR ν_{max}(C–H$_{exo}$) 2750 cm^{-1}; ^{1}H NMR (C$_6$D$_6$) δ 7.80–6.85 (m, 25 H, PPh), 5.36 (m, 2 H, H$_{2,3}$), 3.57 (ddt, 1 H, H$_{exo}$, J_{HH} = 10.3, J_{PH} = 8.1, 18.8 Hz), 2.90 (m, 2 H, H$_{1,4}$), 2.58 (m, 1 H, H$_{endo}$ [$W_{1/2}$ = 17 Hz]), 2.15–1.10 (m, 8 H, CH$_2$P); ^{31}P{^{1}H} NMR (toluene, 332 K) δ 91.1 (t, 1 P, J_{PP} = 10 Hz), 79.85 (d, 2 P, J_{PP} = 10 Hz). Anal. Calcd for C$_{39}$H$_{39}$P$_3$Ru: C, 66.76; H, 5.56; P, 13.26. Found: C, 66.48; H, 5.60; P, 12.97.

Compound 11, (η^4-C$_5$H$_5$D$_{exo}$)Ru[PhP(CH$_2$CH$_2$PPh$_2$)$_2$]. This was prepared as for **1** above by using LiAlD$_4$ in place of LiAlH$_4$: yield 65%; IR ν_{max}(C–D$_{exo}$) 2045 (m), 2015 (m) cm^{-1}.

Registry No. 5, 71397-19-8; 6, 79019-68-4; 7, 32993-05-8; 8, 79019-70-8; 9, 84174-44-7; 10, 79019-69-5; 11, 84174-45-8; LiAlD$_4$, 14128-54-2.

Stereochemical Aspects of the Formation and Trifluoroacetolysis of Some Allylic Bis(trimethylsilyl)cyclohexenes

Geoffrey Wickham and William Kitching*

Department of Chemistry, University of Queensland, Brisbane 4067, Australia

Received September 16, 1982

The stereochemistry of the 3,4-bis(trimethylsilyl)cyclohexene resulting from disilylation of 1,3-cyclohexadiene is concluded to be cis on the basis of ^{1}H and ^{13}C nuclear magnetic resonance spectra and hydrogenation to *cis*-1,2-bis(trimethylsilyl)cyclohexane. The higher boiling *cis*- and *trans*-3,6-bis(trimethylsilyl)cyclohexenes could be separated from the above 3,4-isomer but not from each other by careful spinning band distillation. However, the cis,trans compositions of various fractions were established by ^{13}C NMR spectra and chromatographic characteristics. Trifluoroacetolysis (CF$_3$COOD in chloroform) of the cis 3,4-isomer proceeds to yield cyclohexene-d_2 as the final product, and analysis of ^{2}H NMR spectra and intermediates demonstrates the importance of a facile 1,2-trimethylsilyl shift in the presumed intermediate ion. Trifluoroacetolysis of the mixtures of the 3,6-disilyl isomers proceeds regiospecifically to yield cyclohex-3-enyltrimethylsilane. A preferred anti mode of attack by the electrophile is indicated for the cis isomer, but syn and anti modes are about equally preferred in the trans isomer. This is attributed to steric congestion by the trimethylsilyl group in the γ-carbon region, hindering anti approach by the electrophile.

Introduction

The regiospecific γ cleavage of allylic derivatives of silicon by electrophiles confers considerable potential on these compounds as allylation reagents, and their use in carbon–carbon bond formation has been described (eq 1).[1,2]

$$R\text{---}SiR'_3 + E^+ \longrightarrow R\text{---}E + R'_3Si^+ \quad (1)$$

Full exploitation of these silanes as allylation agents will require an appreciation of the factors regulating the ste-

reospecificity of these electrophilic γ cleavages, and in this connection we noted recently that the syn or anti transition states for S_E' reactions seemed to be of comparable energy.[2] In particular we demonstrated a highly preferred anti mode for trifluoroacetolysis of *cis*- and *trans*-5-methyl-cyclohex-2-enyl systems[2] (below) although there were indications[3] from other systems that steric congestion in the γ-carbon region or changing electrophiles, could promote syn approach (eq 2). In an effort to learn more of the

(2)
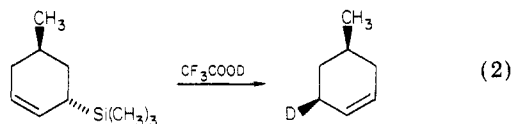
factors regulating the stereochemical aspects of these regiospecific electrophilic γ cleavages of allylsilanes, we have extended our studies to a group of allylic cyclohexenyltrimethylsilanes formed by reductive silylation of 1,3-cyclohexadiene.

Results and Discussion

Our interest was drawn initially to the report of Dunogues and Calas[4] that described the synthesis of 3,6-bis(trimethylsilyl)cyclohexenes, which are, of course, 4-substituted cyclohex-2-enyltrimethylsilanes, careful study of which could provide interesting insights into stereochemical aspects of electrophilic γ cleavage (S_E'). The route employed is shown in eq 3. The essential absence
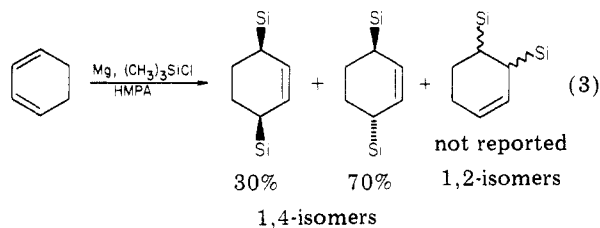
(CH$_3$)$_3$Si is represented as Si

of the 3,4-isomer was argued[4] on the basis of the appearance of the ^{1}H vinyl resonance (δ 5.57) that was quite narrow as expected for the 3,6-isomers. (In the 3,4-isomers, a cis [1]H–[1]H coupling between the vinylic protons of ca. 7–10 Hz would be anticipated). In addition, the nonallylic >C(H)Si would resonate at ~0.7 ppm in the 1,2 compounds. Subsequently, it was stated[5] that some 1,2 compound had been formed in the above disilyation, but the stereochemistry was not established.

Reductive trimethylsilylation of 1,3-cyclohexadiene was conducted to produce a mixture of disilyl isomers, capillary VPC examination of which showed three peaks (32%, 36%, 32%). Careful spinning band distillation was conducted, and the largest fraction collected (~30%; fraction no. 2) was a pure compound, corresponding to the first peak in the gas chromatogram of the total product. Fractions 10–18 contained none of this isomer but varying amounts of the two higher boiling components, e.g., no. 10 was a 62/38 mixture while no. 17 was a 40/60 mixture.

Treatment of fraction no. 2 with 1 equiv of CF$_3$COOH produced a compound exhibiting ^{13}C NMR signals iden-

tical with those of cyclohex-2-enyltrimethylsilane.[6] Addition of a further equivalent of acid produced cyclohexene, so that fraction no. 2 is a 3,4-disilyl compound (eq 4).

(4)
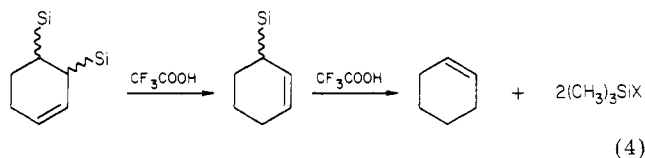
However, treatment of fractions 10 or 17 with excess CF$_3$COOH produced cyclohex-3-enyltrimethylsilane by comparison of its ^{13}C NMR spectrum with that of an authentic sample.[7] Thus those fractions contain only the 1,4-disilyl isomers, with the nonallylic cyclohex-3-enyltrimethylsilane being relatively stable to the excess acid (eq 5). Having established the nature of the regioisomers formed, it was necessary to determine their stereochemistries for the trifluoroacetolyses.

(5)
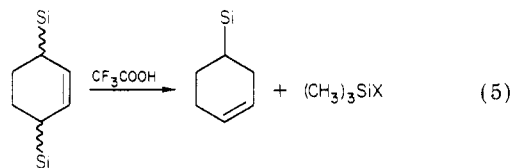
3,4-Bis(trimethylsilyl)cyclohexene. There are several features that emerge from a comparison of the ^{13}C NMR shifts (in δ) of the 3,4-isomer with those of cyclohex-2-enyl-[6] and cyclohexyltrimethylsilanes,[8] as shown in A–C. Al-

though only one ^{13}C signal for the Si(CH$_3$)$_3$ groups was observed, two [29]Si signals (+2.79 and +3.60 ppm relative to (CH$_3$)$_4$Si) were in evidence. Comparing the 25.05-ppm signal of B with the analogous 23.63-ppm signal of A, the high-field shift of ca. 1.4 ppm would require the nonallylic Si(CH$_3$)$_3$ to have some axial character, as the γ effect of equatorial Si(CH$_3$)$_3$ is small but positive.[8] As the trans isomer would have these groups predominantly equatorial and quasi-equatorial, this suggests the 1,2-isomer is cis. Rapid conformational interconversion is indicated with K determined primarily by the stabilizing C–Si π interaction when Si(CH$_3$)$_3$ is quasi-axial. (a 1,3-diaxial (CH$_3$)$_3$Si–H interaction operates in each conformer but would be more severe in D).
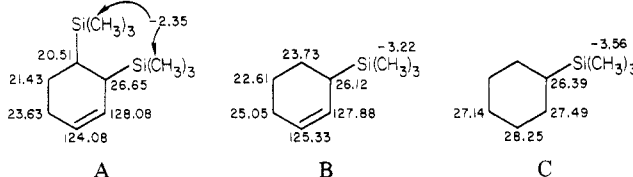
(6)
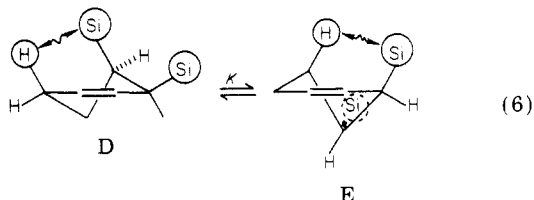
Thus comparable populations of the conformations (slight excess of E) would rationalize the Si(CH$_3$)$_3$ shift (−2.35 ppm) and other features of the spectrum. The more

(1) See, for example: Chan, T. H.; Fleming, I. *Synthesis* **1979**, 761. Sakurai, H. *Pure Appl. Chem.* **1982**, *54*, 1.

(2) (a) Wickham, G. Ph.D. Thesis, University of Queensland, 1983. (b) Wickham, G.; Kitching, W. *J. Org. Chem.*, in press.

(3) Young, D.; Kitching, W. *J. Org. Chem.*, in press.

(4) Dunogues, J.; Calas, R.; Dedier, J.; Pisciotti, F. *J. Organomet. Chem.* **1970**, *25*, 51.

(5) Laguerre, M.; Dunogues, J.; Calas, R. *Tetrahedron* **1978**, *34*, 1823. Dunogues, J., private communication, May, 1980.

(6) Wickham, G.; Young, D.; Kitching, W. *J. Org. Chem.* **1982**, *47*, 4884.

(7) A copy of this ^{13}C NMR spectrum was kindly provided by Professor Robert Benkeser, Purdue University.

(8) (a) Kitching, W.; Marriott, M.; Adcock, W.; Doddrell, D. *J. Org. Chem.* **1976**, *41*, 1671. (b) Kitching, W.; Olszowy, H. A.; Drew, G. M.; Adcock, W. *Ibid.*, in press.

shielded nature of the γ-carbon in A (124.08 ppm) compared with 125.13 ppm (in B) is also consistent as σ–π interaction leads to such γ-carbon shielding. However in B, the quasi-axial orientation of $Si(CH_3)_3$ promoting σ–π interaction, is countered by the 1,3-diaxial $Si(CH_3)_3$–H interaction. This also explains the ^{13}C shift of $Si(CH_3)_3$ (-3.22 ppm) in B, a value close to that for equatorial Si-$(CH_3)_3$ in C (-3.56 ppm). (The conformational A value of $Si(CH_3)_3$ is ca. 2.5 kcal/mol).[8]

Although the ^{13}C NMR data were inconsistent with the trans arrangement, we sought confirmation from the 300-MHz ^1H NMR spectrum, that was fully assigned by extensive spin-decoupling experiments.[2a] There were no large (ca. 10–13 Hz) couplings appropriate for *vic*-diaxial protons, as would be present in the trans 3,4-isomer, with *equatorial* and *quasi-equatorial* $Si(CH_3)_3$ groups. Interpretation of the spectrum is possible in terms of averaging of proton couplings by the rapid D $\rightleftharpoons$ E interconversion. Full details are reported elsewhere.[2a]

Hydrogenation of this *cis*-3,4-disilylcyclohexene (5% rhodium/carbon) produced in high yield a pure isomer of 1,2-bis(trimethylsilyl)cyclohexane. Thus, the ^{13}C spectrum (shifts given in δ; four signals including $Si(CH_3)_3$ at -0.66 ppm) was consistent with a cis relationship of the $Si(CH_3)_3$ groups, as the significant shielding of γ-carbons has occurred (below), when compared with the data for cyclohexyltrimethylsilane (C above).
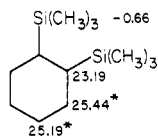
Further, Eaborn[9] has described the synthesis of the cis and trans isomers by reduction (lithium/ethylamine) of 1,2-bis(trimethylsilyl)benzene and he showed that for one isomer, two $Si(CH_3)_3$ ^1H NMR signals (in δ) were resolved at -80 °C. This would be the case for the cis isomer, for which the >$CH$$Si(CH_3)_3$ signal was at δ 0.9 but at δ 0.2 for the other (trans) isomer. In our case, the important ^1H

NMR feature was the triplet at δ 0.99 (2 H, $J \approx 3.7$ Hz) ascribable to >$CH$$Si(CH_3)_3$ with the small *vic* ^1H–^1H coupling being inconsistent with the conformationally "fixed" trans isomer. We conclude therefore that the original allylic silane is the cis 3,4-isomer which is unchanged by hydrogenation, an outcome which is regrettably not general (see below).
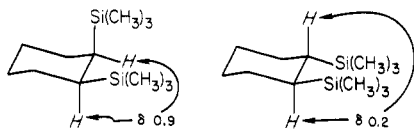
3,6-Bis(trimethylsilyl)cyclohexene. Hydrogenation of two mixtures (40/60 and 60/40) of the 3,6-disilylisomers provided in high yield the same mixture of cis and trans (75/25) 1,4-bis(trimethylsilyl)cyclohexanes, which have been fully characterized elsewhere.[8b] Not surprisingly, mobility of an allylic hydrogen has permitted isomerization, a process obviously less favorable in the 3,4-disilyl case. Examination of the 300-MHz ^1H spectra were not definitive as to isomer composition, and ^{29}Si shifts are not sensitive enough or adequately understood to be used for stereochemical assignments.

However, we have noted a useful generalization that the ^{13}C NMR shift of $(CH_3)_3M$ groups are at *higher* field when

(9) Eaborn, C.; Jackson, R. A; Pearce, R. *J. Chem. Soc., Perkin Trans. 1*, **1975**, 475.

Table I[a]

system	rel retentn time	assignt
	0.98 1.00	trans[2a,6] cis
	0.93 1.00	trans cis
	0.93 1.00	trans cis
	0.96 1.00	trans[2a,6] cis

a The stereochemistry of the germanium compounds has been established[2a,6] unequivocally.

equatorial (or *pseudoequatorial*) than when *axial* (or *pseudoaxial*) for both (cyclohexyl)- and (cyclohex-2-enyl)$M(CH_3)_3$ systems.[6,10] On this basis, fraction 10 would be predominantly trans and no. 17 predominantly cis.

At this point, it is instructive to introduce a similar system for the appropriate comparisons, viz., (4-*tert*-butylcyclohex-2-enyl)trimethylsilane, which was obtained as shown in eq 7. Capillary VPC of the total product dem-

$$+ \text{ other products} \quad (7)$$
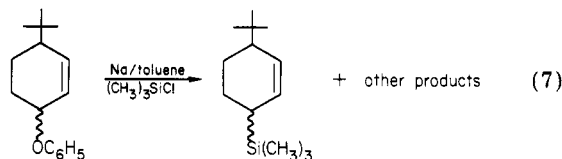
onstrated the presence of five components, with the three of shortest retention time (together $\sim$11%) being vinylic silanes on the basis of their negative ^{29}Si shifts (-6.42, -6.24, and -5.43 ppm).[11] The major components (89%) (^{29}Si at +2.15 and +2.69 ppm) were formed in a ratio of 44:56. Trifluoroacetolysis of this mixture produced only 4-*tert*-butylcyclohexene and, on the basis of regiospecific γ cleavage,[1,2] requires the major components to be the (*cis*-4-*tert*-butylcyclohex-2-enyl)- and (*trans*-4-*tert*-butylcyclohex-2-enyl)trimethylsilanes. The ^{13}C shifts of $(CH_3)_3Si$ groups requires the major component (56%) to be cis as shown below. These conclusions are supported
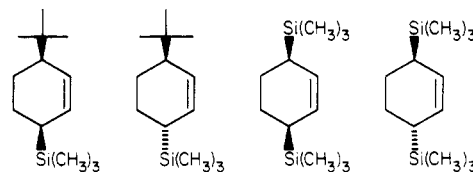
^{13}C shift $\quad \delta$ -2.10 $\quad \delta$ -3.56 $\quad \delta$ -2.71 $\quad \delta$ -3.37

by considerations of VPC behavior (stationary phase

(10) Kitching, W.; Olszowy, H. A.; Waugh, J.; Doddrell, D. *J. Org. Chem.* **1978**, *43*, 898. Kitching, W.; Harvey, K.; Olszowy, H. A. *Ibid.* **1982**, *47*, 1893.

(11) The vinyl silane, 1-(trimethylsilyl)-4-methylcyclohexene has $\delta^{29}Si$ of -6.24 (relative to $(CH_3)_4^{29}Si$), while vinyltrimethylsilane itself has $\delta^{29}Si$ of -6.8 ppm.

OV101 (nonpolar)) given that relative retention times on such columns generally reflect boiling points. These comparisons indicate the cis isomer has the higher boiling point, a conclusion opposite to that of Dunogues,[5] who assumed the trans isomer to have the greater retention time on the nonpolar SE-30 25%/Celite phase (see Table I).

Trifluoroacetolysis Reactions: (a) 3,6-Bis(trimethylsilyl)cyclohexene. Reaction of the isomer mixture with CF_3COOH (chloroform solvent) proceeded readily to provide cyclohex-3-enyltrimethylsilane, the ^{13}C shifts (in δ) of which agreed with those (provided by Prof. R. Benkeser)[7] of an authentic sample. ((CH_3)$_3$SiOCOCF$_3$ and ((CH_3)$_3$Si)$_2$O were also formed.) Use of CF_3COOD provided the 2-deuterio analogue, and the assignments shown in eq 8 were arrived at by considering the effects of ^{2}H substitution on the spectra. The cleavage is regiospecific.

$$(8)$$
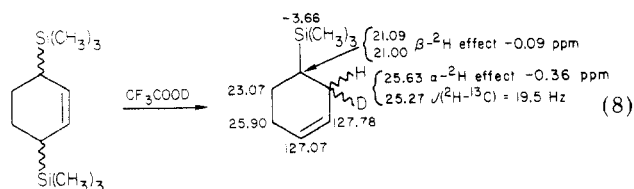
The ^{2}H NMR spectrum of the cleavage product from a mixture of the isomers shows signals for the *cis-* and *trans-*[2]H isomers at δ 1.85 and 1.97. For assignment of those signals, we employed the bromination procedure[2] (such addition to the double bond being very predominantly (~90%) trans diaxial) and complete ^{1}H (300-MHz) and ^{13}C NMR analyses of the resulting dibromides.[2] The 300-MHz ^{1}H NMR spectra of the dibromides of (trimethylsilyl)-, *tert*-butyl-, and methylcyclohexenes were fully assigned by extensive decoupling experiments, and the shifts (in δ) are shown below. Full details can be found elsewhere.[2]
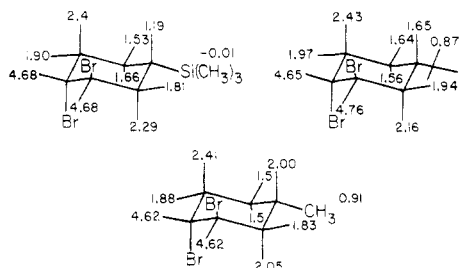
The key assignments are H_{ax} (δ 2.29) and H_e (δ 1.81) in the (CH_3)$_3$Si derivative, with H_{ax} suffering deshielding by both 1,2- and 1,3-bromo interactions. The ^{2}H NMR spectrum of the dibromide of the (2-deuteriocyclohex-3-enyl)trimethylsilane showed signals at δ 2.28 and 1.81, which can be related to the signals of the precursor cyclohexene. Thus, the δ 1.85 signal is associated with the (*cis*-2-deuteriocyclohex-3-enyl)trimethylsilane and δ 1.97 signal with the (*trans*-2-deuteriocyclohex-3-enyl)trimethylsilane resulting from cleavage. With these secure, the stereochemistry of cleavage of the allylic silanes can now be determined directly by ^{2}H NMR spectroscopy. These are shown in Table II.

A superficial examination of these results shows a predominance of trans product alkene irrespective of the starting cis/trans ratio. In view of the regiospecific nature of these cleavages, this means the incoming electrophile approaches so as to avoid the bulky ((CH_3)$_3$C or (CH_3)$_3$Si) substituent. Our previous demonstration that anti trifluoroacetolysis is strongly preferred when steric problems

Table II

system	cis	trans	product		
	38	62		30	70[a]
				33	67[a]
				33	67[b]
	42	58		29	71[a]
	60	40		23	77[a]
				25	75[a]
	62	38		20	80[b]
	54	46		22	78[a]

[a] ^{2}H NMR at 15.24 MHz. [b] ^{2}H NMR at 46.05 MHz.

are absent[2] suggests that the cis isomer could suffer anti cleavage (as the electrophile would be approaching trans to the substituent) but the trans isomer would manifest substantial steric problems as shown.
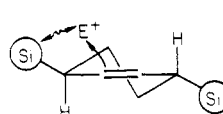
steric hindrance to approach   more favored approach
in trans isomer   in cis isomer

If we assume[12] that the cis isomer experiences stereospecific anti cleavage, it is possible to calculate the anti/syn ratio for the trans isomer for one starting ratio and then (hopefully) reproduce the data for another. Thus for fraction no. 10 we have the data shown in eq 9 and 10.

$$(9)$$

$$(10)$$
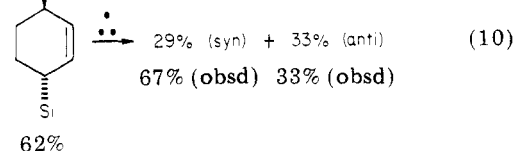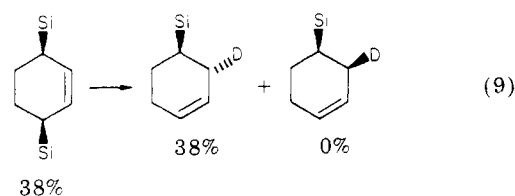
Thus an anti/syn ratio of 1.14 is required for trifluoroacetolysis of the trans isomer on the basis of this analysis. Application of this result to the cis/trans = 62/38 (i.e., opposite ratio) starting material almost precisely reproduces the observed ratio of cis/trans = 20/80 in the product alkene. With respect to the *tert*-butyl compound, the same approach is very satisfactory. Thus the 54/46 (cis/trans) starting material would provide a 22/78 (cis/trans) product if the cis isomer is cleaved in the anti mode, but both syn and anti modes were equally favored for the trans isomer.

(12) This proposition, besides providing a very attractive explanation of the stereochemistry of the trifluoroacetolysis, is completely consistent with our demonstrations that trifluoroacetolysis of (4-methylcyclohex-2-enyl)trimethylgermanes and -stannanes and (4-*tert*-butylcyclohex-2-enyl)trimethylgermanes and -stannanes are stereospecifically anti for the cis isomer, but not so for the trans isomers. (Young, D., unpublished results).

Scheme I

both ^{2}H allylic   one ^{2}H allylic
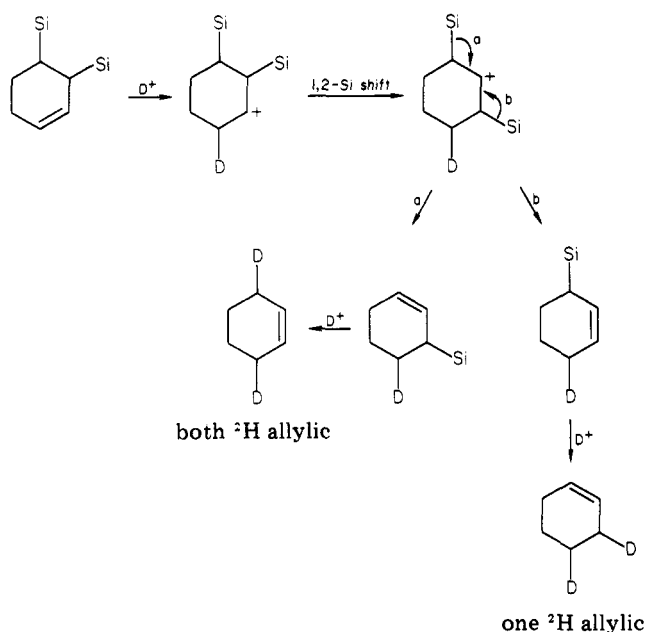
Trifluoroacetolysis of a mixture of cis-3,4- (30%), trans-3,6- (36%), and cis-3,6-disilylcyclohexenes demonstrated that the 3,4-isomer reacts considerably faster than either of the 3,6-isomers with $k_{cis}/k_{trans} \approx 1.6$ for the latter pair, on the basis of ^{13}C NMR monitoring of the (resolved) $(CH_3)_3Si$ signals.

(b) cis-3,4-Bis(trimethylsilyl)cyclohexene. Trifluoroacetolysis with at least 2 equiv of acid produced cyclohexene (together with $(CH_3)_3SiX$). However, if this cleavage proceeded by two sequential S_E' reactions, then use of CF_3COOD should provide the dideuteriocyclohexene in eq 11. Hence, two ^{2}H signals of *equal* intensity should

                                              (11)
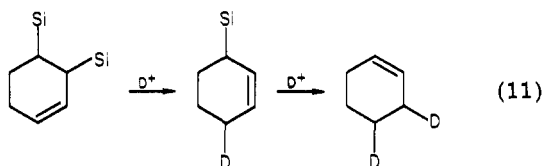
be observed at δ 1.58 and 1.95. However, the observed ^{2}H spectrum was quite different, with signals at δ 1.97 and 1.59 in the ratio of *3.0* (integration). This is completely supported by the ^{13}C NMR spectrum of the product cyclohexene that shows quite clearly a greater abundance of allylic ^{2}H (compare signals at δ 24.90 and 22.27). The reaction then has not proceeded in the presumed uncomplicated way, but a mechanism providing ^{2}H enrichment at the allylic position is shown in Scheme I.

The ratio of allylic ^{2}H/nonallylic ^{2}H (3/1) requires the two dideuterated species be present in equal amounts, consistent with the formation of the symmetrical 2,6-disilylcyclohex-1-yl cation, enjoying stabilization by two flanking β-$Si(CH_3)_3$ groups.[1,13] This analysis requires the 1,2-$Si(CH_3)_3$ shift,[14] if it is not concerted with γ-^{2}H$^+$ attack, to compete very favorably with any loss of $Si(CH_3)_3$ from the initially formed ion. The details of timing in these processes are not clear.

To provide further insight into the above proposal, we conducted an experiment with 0.95 molar equiv of CF_3C-OOD, and the product mixture on the basis of the ^{13}C NMR spectrum was *approximately*

~20%   ~67%   ~13%

                                                (12)

with the other signal (δ 1.70) assigned to $((CH_3)_3Si)_2O$. The ^{29}Si NMR spectrum showed signals for starting material, the cyclohex-2-enylsilane, and $((CH_3)_3Si)_2O$, but no others. Assignments of both the ^{13}C and ^{29}Si NMR spectra were based on the shifts of authentic samples, and hence the starting disilyl isomer suffered no structural change. The product cyclohexene was carefully removed and the ^{2}H NMR spectrum of this consisted of two signals (allylic ^{2}H/nonallylic ^{2}H = 3/1) as found for the cyclohexene product when an excess (3 equiv of CF_3COOD) of acid was employed, viz., a 1:1 mixture of 3,6-dideuteriocyclohexene and 3,4-dideuteriocyclohexene.

The less volatile residue, consisting of starting disilyl compound and cyclohex-2-enyltrimethylsilane, was also examined by ^{13}C and ^{2}H NMR spectroscopy. The details of the ^{13}C spectrum (shifts in δ) of the ^{2}H-substituted cyclohex-2-enylsilane are shown below and compare well with those of authentic sample. In addition to confirming
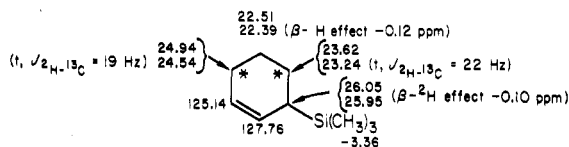
CHCl$_3$ solvent, ^{13}CHCl$_3$ at 77.00 ppm

the dual sites of ^{2}H incorporation (as deduced from the ^{2}H spectrum) the ^{13}C spectrum revealed the triplets (asterisk) at δ 23.24 and 24.54 to be of equal intensity, a result in accord with the proposed rearrangement pathway providing equal amounts of (4-deuteriocyclohex-2-enyl)trimethylsilane and (6-deuteriocyclohex-2-enyl)trimethylsilane on $^+Si(CH_3)_3$ loss from the rearranged disilyl cation.

The ^{2}H NMR spectrum consisted of four major signals at δ 1.46, 1.80, 1.94, and 1.99 with minor signals at δ 1.60 and 5.67. Regarding the major signals, it was clear that the combined intensity of the former two (δ 1.46, 1.80) was equal to that of the latter two (δ 1.94, 1.99), with the intensity ratio within each pair also approximately the same. These aspects and assignments are summarized below. Thus initial anti approach by D$^+$ is slightly favored (ca. 60%). The full scheme is shown in Scheme II.

$\delta(^2$H)   1.99   1.94   1.46   1.80

                    40/60   36/64

                    50%   50%
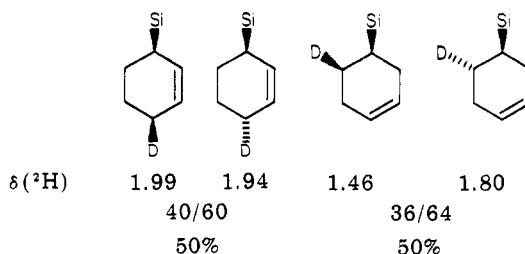
The minor ^{2}H NMR signals at δ 1.60 and 5.67 (vinylic ^{2}H) are accountable by the competitive loss of $^+$H from the disilyl cation as outlined in the right side of Scheme II. This would lead, as shown, to vinylic D as well as >C(D)Si

(13) See, for example: Fleming, I.; Langley, J. A. *J. Chem. Soc., Perkin Trans. 1* **1981**, 1421. Lambert, J. B.; Finzel, R. B. *J. Am. Chem. Soc.* **1982**, *104*, 2020.

(14) See: Brook, A. G.; Bassindale, A. R. "Molecular Rearrangements of Organosilicon Compounds" in "Rearrangements in Ground and Excited States"; de Mayo, P., Ed.; Academic Press: New York, 1980; Vol. 2, p 190.
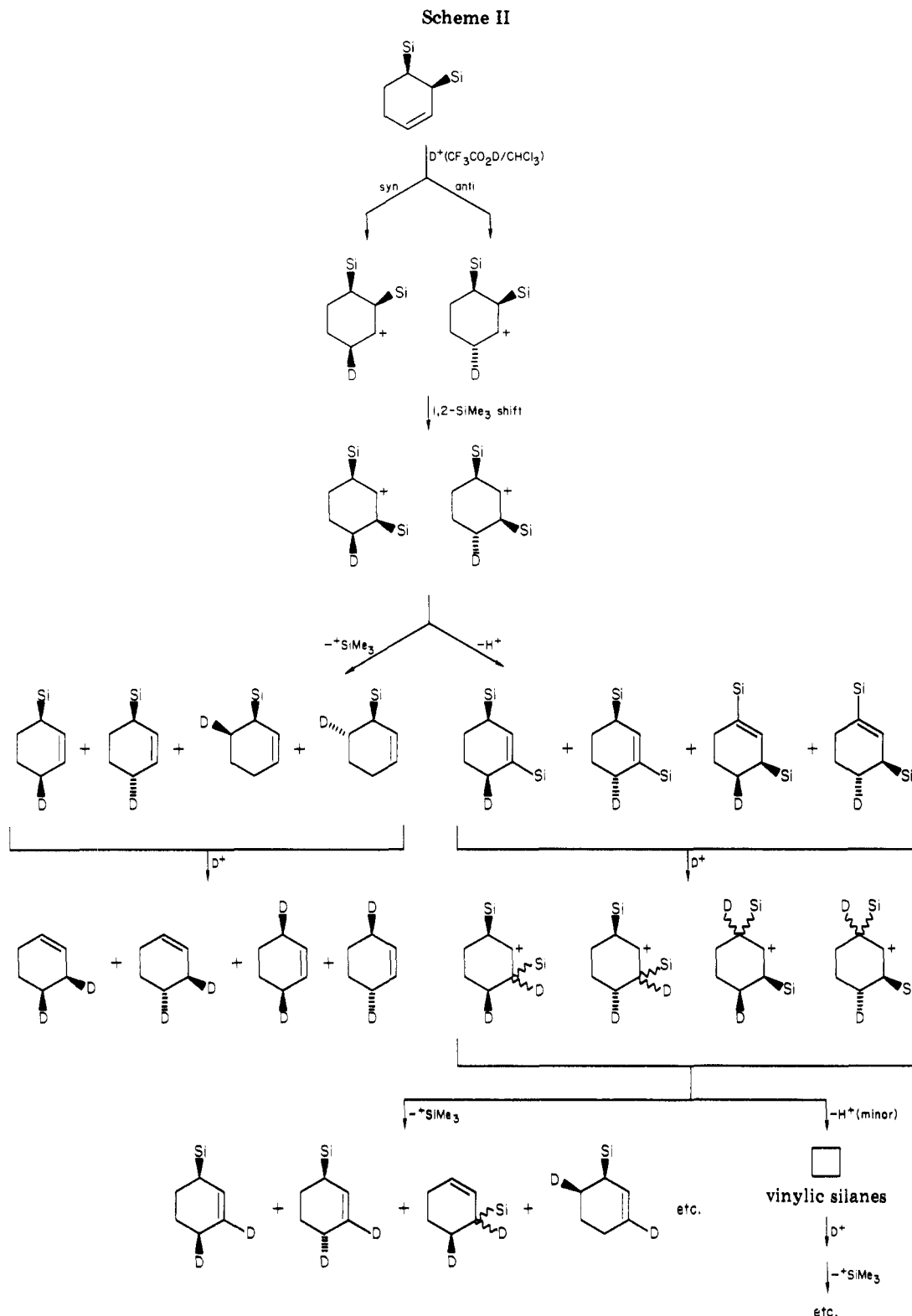
Scheme II

that would reasonably arise at δ 1.60. It is possible to estimate that ⁺H loss is ca. 0.08 as likely as ⁺Si(CH₃)₃ loss. The vinylic silane (Scheme II) resulting from proton loss from the 2,6-disilyl cation was not observed, and this is consistent with its anticipated ready deuteration.

Although these studies of trifluoroacetolysis provide further insight into the reactivity etc. of allylic silanes, they demonstrate further the precarious energy balance between syn and anti modes of electrophilic cleavage of allylic systems. In this respect, a puzzling feature is the only slight preference for anti addition of D⁺ to *cis*-3,4-bis-(trimethylsilyl)cyclohexene as no special features appear

to retard this mode or specially promote syn attack. However, the 1,2-*cis*-Si(CH₃)₃ groups may induce conformational distortions with lowering of the anti preference, which appears to characterize situations for which strong σ–π interactions operate.[2,3] In the absence of such, the normal *axial* electrophilic approach, here leading to syn product, could compete favorably.

Experimental Section

Compounds. (a) Bis(trimethylsilyl)cyclohexenes. To hexamethylphosphoric triamide (HMPA) (~100 mL) freshly distilled from sodium metal were added magnesium powder (3.0

g, 125 mmol), trimethylchlorosilane (55.4 mL, 437 mmol), and 1,3-cyclohexadiene (10.0 g, 125 mmol) under a nitrogen atmosphere. The magnetically stirred solution was gently refluxed (94.5 h) after which the magnesium was consumed and a clear solution resulted. Water was added (to the cooled solution) and the mixture extracted with ether that was then washed thoroughly with water to remove residual HMPA. Drying (MgSO$_4$) and removal of the the ether provided the crude mixture of disilanes (15.3 g, 54%, 100 °C (11 mm)). Separation and characterization have been described in the text. Anal. Calcd for C$_{12}$H$_{26}$Si$_2$: C, 63.63; H, 11.57. Found (3,4-isomer): C, 63.01; H, 11.16. Found (3,6-isomers + 3,4-isomers): C, 63.09; H, 11.32.

(b) 4-*tert*-Butylcyclohex-2-enyltrimethylsilane. Trimethylchlorosilane (2.16 mL, 17.5 mmol) and 4-*tert*-butylcyclohex-2-enyl phenoxide (2.00 g, 8.70 mmol) dissolved in toluene (4 mL) was added dropwise to slivers of sodium metal (0.41 g, 17.8 mmol) in refluxing toluene (5 mL) under N$_2$. After 6–7 h of reflux, the sodium had disappeared and sodium chloride precipitated. After the mixture was cooled, pentane was added and the solution filtered through supercel. The filtrate was washed with water, separated, dried (MgSO$_4$), and evaporated to yield the crude product. A preliminary distillation provided three fractions (1.13 g) of which fraction no. 3 contained mostly the desired allylic silane, with some phenoxytrimethylsilane, which was removed on neutral alumina (pentane eluant). Kugelrohr distillation (oven 120 °C (6 mmHg)) provided 423 mg (23%) of an oil which was >90% pure. The full product analysis is presented in the text: *mass spectrum, m/e* (relative intensities) 212 (0.77), 211 (2.50), 210 (11.54), 195 (3.77), 155 (1.77), 154 (5.88), 153 (28.85), 75 (7.27), 74 (11.54), 73 (100). Anal. Calcd for C$_{13}$H$_{26}$Si: C, 74.22; H, 12.47. Found: C, 74.98; H, 12.49.

Trifluoroacetolysis Experiments. The allylic silane and the appropriate amount of CF$_3$COOH or CF$_3$COOD were mixed in

purified chloroform (CHCl$_3$) and transferred (N$_2$) to a glass ampule and sealed. Reactions were conducted at 20, 30, or 40 °C, but temperature variations had no effect on the results. On completion of the reaction, the contents of the ampule were added to aqueous sodium bicarbonate to destroy any excess acid, and the chloroform layer was separated, dried, and examined directly by ^{13}C, ^{2}H, ^{1}H, and ^{29}Si NMR spectroscopy, as detailed in the text.

NMR Spectra. ^{13}C NMR spectra were obtained at 25.05 or 75.44 MHZ for CHCl$_3$ solutions, and chemical shifts are referenced to ^{13}CHCl$_3$ as 77.00 ppm. Broad-band ^{1}H-decoupled ^{2}H spectra were recorded on a JEOL-FX-100 spectrometer fitted with a 10-mm multinuclear probe, which was tuned to observe ^{2}H at 15.29 MHz. ^{2}H spectra that were accumulated by using 16K data points and a frequency width of 1 KHz (70° pulse, repetition time 4.19 s) refer to CHCl$_3$ solutions, and chemical shifts are referenced to internal CDCl$_3$ (δ 7.24). ^{1}H NMR spectra were recorded for CDCl$_3$ solutions at 100 MHz (JEOL-PS-100) or 300 MHz (Bruker-CXP-300) by using CHCl$_3$ as secondary reference (δ 7.24). Some ^{2}H spectra (at 46.05 MHz) were also obtained on this latter instrument.

Registry No. Trimethylchlorosilane, 75-77-4; 1,3-cyclohexadiene, 592-57-4; 4-*tert*-butylcyclohex-2-enyl phenoxide, 78073-54-8; *cis*-3,4-bis(trimethylsilyl)cyclohexane, 84280-55-7; (*cis*-4-*tert*-butylcyclohex-2-enyl)trimethylsilane, 84280-54-6; (*trans*-4-*tert*-butylcyclohex-2-enyl)trimethylsilane, 84280-58-0; *cis*-3,6-bis(trimethylsilyl)cyclohexane, 84280-56-8; *trans*-3,6-bis-(trimethylsilyl)cyclohexane, 84280-57-9.

Communications

Synthesis and Reactivity of OsH(η²-CH$_2$PMe$_2$)(PMe$_3$)$_3$ and of the Basic Dihydridoosmium Complex *cis*-OsH$_2$(PMe$_3$)$_4$[1]

Helmut Werner* and Josef Gotzig

Institut für Anorganische Chemie der Universität Würzburg Am Hubland, D-8700 Würzburg, B.R.D.
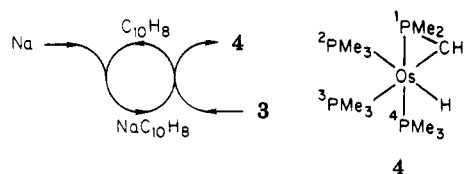
Received July 27, 1982

Summary: The complex OsH(η²-CH$_2$PMe$_2$)(PMe$_3$)$_3$ (**4**) is obtained by reduction of *trans*-OsCl$_2$(PMe$_3$)$_4$ (**3**) with NaC$_{10}$H$_8$ in THF at room temperature. It reacts with electrophiles, e.g., methyl iodide and Brønsted acids, HX, to form OsI(η²-CH$_2$PMe$_2$)(PMe$_3$)$_3$ (**8**) and *cis*-OsX$_2$(PMe$_3$)$_4$ (X = I, Cl, CF$_3$CO$_2$, C$_2$Ph) (**9–12**), respectively. The reaction of **3** with NaC$_{10}$H$_8$ in THF at -78 °C yields *cis*-OsH$_2$(PMe$_3$)$_4$ (**6**) that is also obtained from **4** and methanol. The basic character of **6** is demonstrated by its protonation with NH$_4$PF$_6$ to yield [OsH$_3$(PMe$_3$)$_4$]PF$_6$ (**15**) that reacts with CO to give [OsH(CO)(PMe$_3$)$_4$]PF$_6$ (**16**).

The recent discovery that the reduction of *trans*-RuCl$_2$(PMe$_3$)$_4$ (**1**) with Na/Hg in benzene gives the complex RuH(η²-CH$_2$PMe$_2$)(PMe$_3$)$_3$ (**2**) in nearly quantitative

Scheme I

yield,[2] prompted us to study also the reactivity of the corresponding osmium compound *trans*-OsCl$_2$(PMe$_3$)$_4$ (**3**) toward reducing agents. Complex **3** is formed in 75% yield from OsCl$_2$(PPh$_3$)$_3$[3] and excess PMe$_3$ in hexane and characterized by elemental analysis and mass spectroscopy.[4] It also has been prepared most recently by Wilkinson et al.[5] by a similar route.

In contrast to the ruthenium complex **1**, the osmium analogue **3** does not react with Na/Hg at ambient temperature to form OsH(η²-CH$_2$PMe$_2$)(PMe$_3$)$_3$ (**4**). Also, use of the stronger reducing agents Na/K alloy[6] (benzene, 70 °C, 3 days) and activated Mg[7] (THF, 60 °C, 2 days) does

(1) This work is part of the Diplomarbeit of J. Gotzig, Universität Würzburg, 1982.

(2) Werner, H.; Werner, R. *J. Organomet. Chem.* **1981**, *209*, C 60.

(3) Hoffmann, P. R.; Caulton, K. G. *J. Am. Chem. Soc.* **1975**, *97*, 4221.

(4) Anal. Calcd for OsC$_{12}$H$_{36}$Cl$_2$P$_4$: C, 25.49; H, 6.37; Cl, 12.55. Found: C, 25.33; H, 6.39; Cl, 12.41. Mass spectrum (70 eV), *m/e* (% relative intensity): 566 (M$^+$, 5), 490 (M$^+$ – PMe$_3$, 55), 414 (M$^+$ – 2 PMe$_3$, 100).

(5) Alves, A. S.; Moore, D. S.; Andersen, R. A.; Wilkinson, G. *Polyhedron* **1982**, *1*, 83.

(6) (a) Ellis, J. H.; Flom, E. A. *J. Organomet. Chem.* **1975**, *99*, 263. (b) Werner, H.; Kraus, H.-J. *J. Chem. Soc., Chem. Commun.* **1979**, 814.

g, 125 mmol), trimethylchlorosilane (55.4 mL, 437 mmol), and 1,3-cyclohexadiene (10.0 g, 125 mmol) under a nitrogen atmosphere. The magnetically stirred solution was gently refluxed (94.5 h) after which the magnesium was consumed and a clear solution resulted. Water was added (to the cooled solution) and the mixture extracted with ether that was then washed thoroughly with water to remove residual HMPA. Drying (MgSO₄) and removal of the the ether provided the crude mixture of disilanes (15.3 g, 54%, 100 °C (11 mm)). Separation and characterization have been described in the text. Anal. Calcd for $C_{12}H_{26}Si_2$: C, 63.63; H, 11.57. Found (3,4-isomer): C, 63.01; H, 11.16. Found (3,6-isomers + 3,4-isomers): C, 63.09; H, 11.32.

(b) 4-*tert*-Butylcyclohex-2-enyltrimethylsilane. Trimethylchlorosilane (2.16 mL, 17.5 mmol) and 4-*tert*-butylcyclohex-2-enyl phenoxide (2.00 g, 8.70 mmol) dissolved in toluene (4 mL) was added dropwise to slivers of sodium metal (0.41 g, 17.8 mmol) in refluxing toluene (5 mL) under N₂. After 6–7 h of reflux, the sodium had disappeared and sodium chloride precipitated. After the mixture was cooled, pentane was added and the solution filtered through supercel. The filtrate was washed with water, separated, dried (MgSO₄), and evaporated to yield the crude product. A preliminary distillation provided three fractions (1.13 g) of which fraction no. 3 contained mostly the desired allylic silane, with some phenoxytrimethylsilane, which was removed on neutral alumina (pentane eluant). Kugelrohr distillation (oven 120 °C (6 mmHg)) provided 423 mg (23%) of an oil which was >90% pure. The full product analysis is presented in the text: *mass spectrum, m/e* (relative intensities) 212 (0.77), 211 (2.50), 210 (11.54), 195 (3.77), 155 (1.77), 154 (5.88), 153 (28.85), 75 (7.27), 74 (11.54), 73 (100). Anal. Calcd for $C_{13}H_{26}Si$: C, 74.22; H, 12.47. Found: C, 74.98; H, 12.49.

Trifluoroacetolysis Experiments. The allylic silane and the appropriate amount of CF₃COOH or CF₃COOD were mixed in

purified chloroform (CHCl₃) and transferred (N₂) to a glass ampule and sealed. Reactions were conducted at 20, 30, or 40 °C, but temperature variations had no effect on the results. On completion of the reaction, the contents of the ampule were added to aqueous sodium bicarbonate to destroy any excess acid, and the chloroform layer was separated, dried, and examined directly by ¹³C, ²H, ¹H, and ²⁹Si NMR spectroscopy, as detailed in the text.

NMR Spectra. ¹³C NMR spectra were obtained at 25.05 or 75.44 MHZ for CHCl₃ solutions, and chemical shifts are referenced to ¹³CHCl₃ as 77.00 ppm. Broad-band ¹H-decoupled ²H spectra were recorded on a JEOL-FX-100 spectrometer fitted with a 10-mm multinuclear probe, which was tuned to observe ²H at 15.29 MHz. ²H spectra that were accumulated by using 16K data points and a frequency width of 1 KHz (70° pulse, repetition time 4.19 s) refer to CHCl₃ solutions, and chemical shifts are referenced to internal CDCl₃ (δ 7.24). ¹H NMR spectra were recorded for CDCl₃ solutions at 100 MHz (JEOL-PS-100) or 300 MHz (Bruker-CXP-300) by using CHCl₃ as secondary reference (δ 7.24). Some ²H spectra (at 46.05 MHz) were also obtained on this latter instrument.

Communications

Synthesis and Reactivity of OsH(η²-CH₂PMe₂)(PMe₃)₃ and of the Basic Dihydridoosmium Complex *cis*-OsH₂(PMe₃)₄[1]

Helmut Werner* and Josef Gotzig

Institut für Anorganische Chemie der Universität Würzburg Am Hubland, D-8700 Würzburg, B.R.D.

Received July 27, 1982

Summary: The complex OsH(η²-CH₂PMe₂)(PMe₃)₃ (**4**) is obtained by reduction of *trans*-OsCl₂(PMe₃)₄ (**3**) with NaC₁₀H₈ in THF at room temperature. It reacts with electrophiles, e.g., methyl iodide and Brønsted acids, HX, to form OsI(η²-CH₂PMe₂)(PMe₃)₃ (**8**) and *cis*-OsX₂(PMe₃)₄ (X = I, Cl, CF₃CO₂, C₂Ph) (**9–12**), respectively. The reaction of **3** with NaC₁₀H₈ in THF at −78 °C yields *cis*-OsH₂(PMe₃)₄ (**6**) that is also obtained from **4** and methanol. The basic character of **6** is demonstrated by its protonation with NH₄PF₆ to yield [OsH₃(PMe₃)₄]PF₆ (**15**) that reacts with CO to give [OsH(CO)(PMe₃)₄]PF₆ (**16**).

The recent discovery that the reduction of *trans*-RuCl₂(PMe₃)₄ (**1**) with Na/Hg in benzene gives the complex RuH(η²-CH₂PMe₂)(PMe₃)₃ (**2**) in nearly quantitative

Scheme I

yield,[2] prompted us to study also the reactivity of the corresponding osmium compound *trans*-OsCl₂(PMe₃)₄ (**3**) toward reducing agents. Complex **3** is formed in 75% yield from OsCl₂(PPh₃)₃[3] and excess PMe₃ in hexane and characterized by elemental analysis and mass spectroscopy.[4] It also has been prepared most recently by Wilkinson et al.[5] by a similar route.

In contrast to the ruthenium complex **1**, the osmium analogue **3** does not react with Na/Hg at ambient temperature to form OsH(η²-CH₂PMe₂)(PMe₃)₃ (**4**). Also, use of the stronger reducing agents Na/K alloy[6] (benzene, 70 °C, 3 days) and activated Mg[7] (THF, 60 °C, 2 days) does

(1) This work is part of the Diplomarbeit of J. Gotzig, Universität Würzburg, 1982.

(2) Werner, H.; Werner, R. *J. Organomet. Chem.* **1981**, *209*, C 60.

(3) Hoffmann, P. R.; Caulton, K. G. *J. Am. Chem. Soc.* **1975**, *97*, 4221.

(4) Anal. Calcd for OsC₁₂H₃₆Cl₂P₄: C, 25.49; H, 6.37; Cl, 12.55. Found: C, 25.33; H, 6.39; Cl, 12.41. Mass spectrum (70 eV), *m/e* (% relative intensity): 566 (M⁺, 5), 490 (M⁺ − PMe₃, 55), 414 (M⁺ − 2 PMe₃, 100).

(5) Alves, A. S.; Moore, D. S.; Andersen, R. A.; Wilkinson, G. *Polyhedron* **1982**, *1*, 83.

(6) (a) Ellis, J. H.; Flom, E. A. *J. Organomet. Chem.* **1975**, *99*, 263. (b) Werner, H.; Kraus, H.-J. *J. Chem. Soc., Chem. Commun.* **1979**, 814.

not lead to reduction. The synthesis of **4**, however, could be achieved on reaction of **3** with $NaC_{10}H_8$ in THF. Previously, we had used this route to prepare the (benzene)osmium(0) complexes $C_6H_6OsL_2$ (L = $P(OMe)_3$, PPh_3) and C_6H_6OsLL' (L = PMe_3; L' = C_2H_4, C_3H_6).[8] As it is most difficult to remove quantitatively the naphthalene formed during the reaction of **3** with stoichiometric amounts (2 equiv) of $NaC_{10}H_8$, it is advisable to prepare the compound $NaC_{10}H_8$ in situ and to use only a catalytic quantity of $C_{10}H_8$ according to Scheme I.[9] The NMR data[10] confirm that the product is the hydridoosmium complex **4** analogous to **2**[2] and the well-known iron compound $FeH(\eta^2\text{-}CH_2PMe_2)(PMe_3)_3$ (**5**).[11] A monomeric structure is indicated by the mass spectrum that shows the peak for the molecular ion with high intensity.[9]

If the reaction of **3** with $NaC_{10}H_8$ in THF is carried out at -78 °C instead of at room temperature, the dihydridoosmium complex *cis*-$OsH_2(PMe_3)_4$ (**6**) is obtained.[12] The ^1H NMR hydride resonance is a doublet-of-triplets[13b,c] confirming in accord with the ^{31}P NMR data that the complex is rigid.[12] The cis configuration is even retained on warming to 70 °C (where solutions of **6** in benzene slowly begin to decompose) which proves that **6** is configurationally much more stable than *cis*-$FeH_2(PMe_3)_4$ (**7**).[14] **6** is also formed quantitatively on dissolving **4** in methanol, a procedure which had already been used to

prepare the iron analogue **7**.[7a]

Although complexes **4** and **5** have completely analogous structures, they differ considerably in their dynamic behavior as well as in their reactivity toward electrophilic and nucleophilic substrates. Whereas iron compound **5** is fluxional at room temperature,[11] the osmium complex is configurationally stable on the NMR time scale. The equilibrium between the two isomers $M(PMe_3)_4$ and $MH(CH_2PMe_2)(PMe_3)_3$, which is well established for M = Fe,[7a] is almost completely shifted to the hydride side for M = Os. Accordingly, **4** does not react under normal conditions with CO or $P(OMe)_3$, whereas the reactions of **5** with these ligands yield the iron(0) complexes $Fe(PMe_3)_{5-n}L_n$ (L = CO, $P(OMe)_3$; n = 2 and 3), respectively.[7a]

In contrast to its inertness toward nucleophiles, compound **4** readily reacts with electrophiles such as methyl iodide or protonic acids (Scheme II). Thus treatment of **4** with MeI in benzene gives the corresponding complex $OsI(\eta^2\text{-}CH_2PMe_2)(PMe_3)_3$ (**8**) together with the diiodoosmium(II) compound *cis*-$OsI_2(PMe_3)_4$ (**9**).[15] Complex **8** is probably formed by nucleophilic attack of **4** on the carbon atom of methyl iodide to give $[HOs(CH_2PMe_2)(PMe_3)_3CH_3]^+I^-$ as an intermediate. Elimination of CH_4 (detected by ^1H NMR) and coordination of iodide to the metal would give the observed product. It is seen from preliminary experiments (performed in an NMR tube) that CH_2Br_2 reacts similarly with the hydrido complex **4** to give $OsBr(CH_2PMe_2)(PMe_3)_3$ and *cis*-$OsBr_2(PMe_3)_4$.

The reactions of **4** with HCl, CF_3CO_2H, and PhC_2H follow the same course and lead to the complexes *cis*-$OsX_2(PMe_3)_4$ (**10-12**) in almost quantitative yield.[16] We are presently trying to find out by deuteration experiments whether the fourth PMe_3 ligand in **10-12** is formed *intramolecularly* or via attack of the HX proton on the carbon atom of the three-membered ring. It is interesting to note that the two-step process from **3** to **4** and from **4** to **10** leads to an isomer of the starting compound which is not accessible by a direct route.

Addition of an equimolar amount of $AgPF_6$ to a solution of **3** in methanol leads to an immediate color change from yellow to red and metallic silver precipitates. From the

(7) (a) Karsch, H. H.; Klein, H.-F.; Schmidbaur, H. *Chem. Ber.* **1977**, *110*, 2200. (b) Gausing, W.; Wilke, G. *Angew. Chem., Int. Ed. Engl.* **1981**, *20*, 186.

(8) Werner, H.; Werner, R. *J. Organomet. Chem.* **1980**, *194*, C 7.

(9) **3** (200 mg, 0.35 mmol) was dissolved in 5 mL of THF, and $C_{10}H_8$ (~1 mg) and Na (230 mg, 10.0 mmol) were added. The mixture was stirred at 25 °C for 16 h, and the solvent was removed in vacuo. The residue was dissolved in 5 mL of benzene, and the solution was filtered and the solvent again removed in vacuo. After this procedure was repeated, the residue was cooled to -195 °C and pulverized. It could then be stored under N_2 at room temperature for several days. Anal. Calcd for $OsC_{12}H_{38}P_4$: C, 29.14; H, 7.28; Os, 38.49. Found: C, 28.98; H, 7.15; Os, 38.28. IR (Nujol, cm^{-1}): 1895 (OsH). Mass spectrum (70 eV), m/e (% relative intensity): 496 (M$^+$, 78) 418 (M$^+$ - PMe$_3$ - 2H, 100), 388 (M$^+$ - PMe$_3$ - 2CH$_4$, 60).

(10) ^1H NMR (C_6D_6, 400 MHz, 298 K): δ 1.81 (dd, 3 H, J_{HP} = 10.6 Hz, $J_{HP'}$ = 3.0 Hz, one methyl group of $^1PMe_2$), 1.64 (dd, 18 H, J_{HP} = 7.4 Hz, $J_{HP'}$ = 1.2 Hz, $^{2,3}PMe_3$), 1.42 (dd, 3 H, J_{HP} = 9.0 Hz, $J_{HP'}$ = 2.8 Hz, one methyl group of $^1PMe_2$), 1.34 (d, 9 H, J_{HP} = 6.1 Hz, $^4PMe_3$), 0.45 (m, after ^{31}P decoupling dd, 1 H, J_{HH} = 7.0 and 4.5 Hz, one H of CH$_2$), -0.15 (m, after ^{31}P decoupling dd, 1 H, J_{HH} = 7.0 and 4.5 Hz, one H of CH$_2$), -10.60 (dq, 1 H, $J_{HP(trans)}$ = 65 Hz, $J_{HP(cis)}$ = 20 Hz, OsH). $^{31}P\{^1H\}$ NMR (C_6D_6, 85% H_3PO_4 external, 90 MHz, 298 K): δ -71.43 (ddd, 1 P, J_{1P4P} = 174.2 Hz, J_{1P3P} = 34.2 Hz, J_{1P2P} = 19.3 Hz, $^1PMe_2$), -52.36 (ddd, 1 P, J_{2P3P} = 13.4 Hz, J_{2P1P} = 19.3 Hz, J_{2P4P} = 16.4 Hz, $^2PMe_3$), -46.60 (ddd, 1 P, J_{3P1P} = 34.2 Hz, J_{3P2P} = 13.4 Hz, J_{3P4P} = 8.9 Hz, $^3PMe_3$), -42.85 (ddd, 1 P, J_{4P1P} = 174.2 Hz, J_{4P2P} = 16.4 Hz, J_{4P3P} = 8.9 Hz, $^4PMe_3$).

(11) (a) Rathke, J. W.; Muetterties, E. L. *J. Am. Chem. Soc.* **1975**, *97*, 3272. (b) Karsch, H. H.; Klein, H.-F.; Schmidbaur, H. *Angew. Chem., Int. Ed. Engl.* **1975**, *14*, 637.

(12) **3** (500 mg, 0.88 mmol) was dissolved in 6 mL of THF, and the solution was cooled at -78 °C. After addition of 5.5 mL of cooled 0.4 M solution of $NaC_{10}H_8$ in THF, the mixture was stirred at -78 °C for 5 min and then warmed to room temperature. The solvent was removed in vacuo, and the oily residue was dissolved in 15 mL of benzene. The solution was filtered and concentrated in vacuo and naphthalene removed by sublimation at 60 °C (10^{-2} mmHg). The residue was dissolved in benzene, and the solution was chromatographed under N_2 on Al_2O_3 (Merck, neutral, activity grade III). The solvent was removed in vacuo, and after sublimation at 80 °C (10^{-2} mmHg), 224 mg of white rather air-stable crystals was collected (51% yield). Anal. Calcd for $OsC_{12}H_{38}P_4$: C, 29.02; H, 7.66; Os, 38.33. Found: C, 28.99; H, 7.43; Os, 38.17. IR (C_6H_6, cm^{-1}): 1895 (OsH). ^1H NMR (C_6H_6, 60 MHz, 298 K): δ 1.76 (vt, 18 H, N = 5.8 Hz, $^{1,4}PMe_3$), 1.60 (vt,[13] 18 H, N = 6.0 Hz, $^{2,3}PMe_3$), -10.70 (dt, 2 H, J_{HP} = 35 Hz, $J_{HP'}$ = 27.5 Hz, OsH$_2$). ^{31}P NMR (C_6D_6, 85% H_3PO_4 external, 90 MHz, 298 K): δ -49.0 (t, 2 P, J_{PP} = 17.9 Hz, $^{1,4}PMe_3$), -54.5 (t, 2 P, J_{PP} = 17.9 Hz, $^{2,3}PMe_3$).
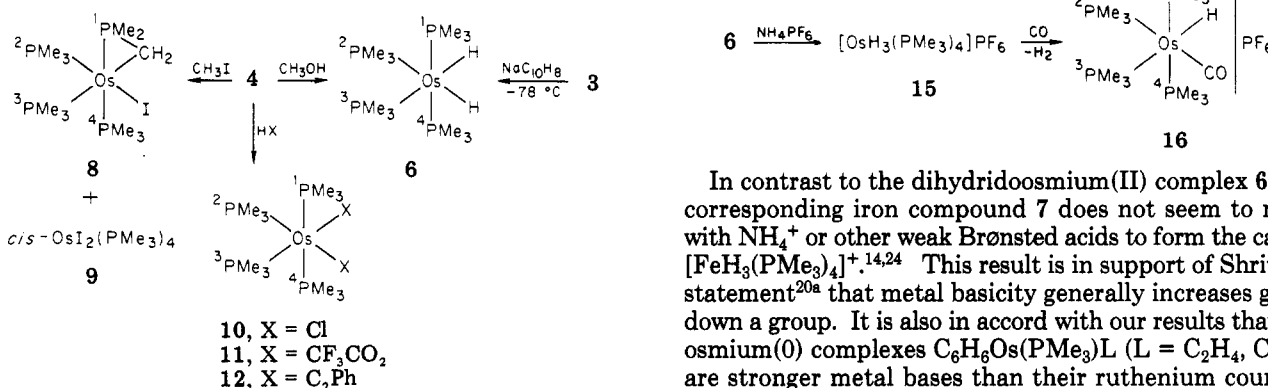
(13) (a) The shape of the virtual triplet consists of two sharp outer lines with a much broader central absorption, the distance of the two outer lines corresponding to N; see: Harris, R. K. *Can. J. Chem.* **1964**, *42*, 2275. (b) Dewhirst, K. C.; Keim, W.; Reilly, C. A. *Inorg. Chem.* **1968**, *7*, 546. (c) Meakin, P.; Muetterties, E. L.; Tebbe, F. N.; Jesson, J. P. *J. Am. Chem. Soc.* **1971**, *93*, 4701.

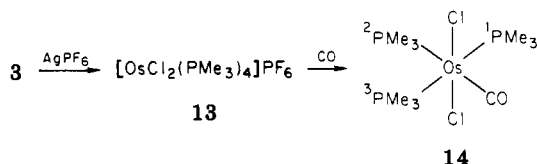(14) Klein, H.-F. *Angew. Chem., Int. Ed. Engl.* **1970**, *9*, 903.

(15) **4** (330 mg, 0.67 mmol) was dissolved in 5 mL of C_6H_6, and CH_3I (8 μL, 1.28 mmol) was added. The solution was stirred at 25 °C for 15 min, and after the slow-gas evolution was finished, hexane (20 mL) was added. The solid precipitate was filtered and recrystallized from CH_2Cl_2/hexane. 200 mg of yellow crystals corresponding to **9** was obtained (40% yield). The filtered benzene/hexane solution was concentrated in vacuo to give 216 mg of **8** as a light brown solid (52% yield), mp 53 °C dec. Anal. Calcd for $OsC_{12}H_{35}IP_4$: C, 23.23; H, 5.65; I, 20.47. Found: C, 23.45; H, 5.61; I, 20.40. Mass spectrum (70 eV), m/e (% relative intensity) 622 (M$^+$, 45), 546 (M$^+$ - PMe$_3$, 100), 470 (M$^+$ - 2PMe$_3$, 41). **9**: mp 239 °C dec. Anal. Calcd for $OsC_{12}H_{36}I_2P_4$: C, 19.25; H, 4.81; I, 33.93. Found: C, 19.46; H, 4.96; I, 33.69.

(16) **4** (120 mg, 0.25 mmol) was dissolved in 5 mL of ether, and an excess of a saturated solution of HCl in ether (1 mL) was added. Accompanied by gas evolution, a bright yellow precipitate was formed, which was filtered and recrystallized from CH_2Cl_2/ether (91% yield). Anal. Calcd for $OsC_{12}H_{36}Cl_2P_4$: C, 25.49; H, 6.37. Found: C, 25.61; H, 6.63. Mass spectrum (70 eV), m/e (% relative intensity): 566 (M$^+$, 10), 490 (M$^+$ - PMe$_3$, 56), 458 (M$^+$ - PMe$_3$ - 2CH$_4$, 46), 414 (M$^+$ - 2PMe$_3$, 100). ^1H NMR (CH_2Cl_2, 60 MHz, 298 K): δ 1.64 (vt,[13] 18 H, N = 8.3 Hz, $^{2,3}PMe_3$), 1.62 (vt, 18 H, N = 6.5 Hz, $^{1,4}PMe_3$). Complexes **11** and **12** were prepared similarly (for **12** with benzene as solvent). **11**: 88% yield. Anal. Calcd for $OsC_{16}H_{36}F_6O_4P_4$: C, 26.66; H, 5.00. Found: C, 26.93; H, 5.04. Mass spectrum (70 eV), m/e (% relative intensity): 722 (M$^+$, 2), 646 (M$^+$ - PMe$_3$, 66), 570 (M$^+$ - 2PMe$_3$, 58), 533 (M$^+$ - PMe$_3$ - CF_3CO_2, 85), 496 (M$^+$ - 2CF$_3$CO$_2$, 5), 457 (M$^+$ - 2PMe$_3$ - CF_3CO_2, 100). ^1H NMR (CH_2Cl_2, 60 MHz, 298 K): δ 1.60 (vt,[13] 18 H, N = 8.8 Hz, $^{2,3}PMe_3$), 1.55 (vt, 18 H, N = 7.1 Hz, $^{1,4}PMe_3$). **12**: 78% yield. Anal. Calcd for $OsC_{28}H_{46}P_4$: C, 48.26; H, 6.61; Os, 27.32. Found: C, 48.22; H, 6.89; Os, 27.33. IR (Nujol, cm^{-1}): 2070 (C≡C). Mass spectrum (70 eV), m/e (% relative intensity) 698 (M$^+$, 30), 622 (M$^+$ - PMe$_3$, 100), 546 (M$^+$ - 2PMe$_3$, 28), 520 (M$^+$ - PMe$_3$ - HC$_2$Ph, 18), 444 (M$^+$ - 2PMe$_3$ - HC$_2$Ph, 14), 418 (M$^+$ - PMe$_3$ - 2HC$_2$Ph, 12). ^1H NMR (C_6H_6, 60 MHz, 298 K): δ 1.83 (vt, 18 H, N = 6.6 Hz, $^{1,4}PMe_3$), 1.53 (vt,[13] 18 H, N = 6.6 Hz, $^{2,3}PMe_3$).

Scheme II

solution, the paramagnetic osmium(III) complex [OsCl₂(PMe₃)₄]PF₆ (13) is obtained in 95% yield.[17] In benzene suspension, it reacts with CO under refluxing conditions to form the carbonylosmium compound *trans*-OsCl₂(CO)(PMe₃)₃ (14) which indicates that even weak reducing agents such as CO or PMe₃[18] are capable of reducing osmium(III) to osmium(II) complexes. Under similar conditions, compound 3 is completely inert toward carbon monoxide.

Like the well-known (C₅H₅)₂WH₂,[19] the dihydridoosmium(II) compound *cis*-OsH₂(PMe₃)₄ (6) also behaves as a metal base.[20] This is demonstrated by the smooth reaction of 6 with NH₄PF₆ that yields quantitatively the PF₆ salt of the trihydridoosmium(IV) cation [OsH₃(PMe₃)₄]⁺ (15).[21] According to the ¹H NMR data, the cation seems to be fluxional at room temperature. In (CD₃)₂CO, a 1:4:6:4:1 quintet is observed for the hydride resonance that broadens below 0 °C, indicating that the dynamic process is slowed down at low temperatures. Experiments are in progress to study the intramolecular rearrangement in more detail and to compare the kinetic parameters with those of the reactions of the hexacoordinated complexes MH₂L₄.[22] In methanolic solution, complex 15 reacts with CO to give [OsH(CO)(PMe₃)₄]PF₆ (16), which is configurationally stable on the NMR time scale.[23]

In contrast to the dihydridoosmium(II) complex 6, the corresponding iron compound 7 does not seem to react with NH₄⁺ or other weak Brønsted acids to form the cation [FeH₃(PMe₃)₄]⁺.[14,24] This result is in support of Shriver's statement[20a] that metal basicity generally increases going down a group. It is also in accord with our results that the osmium(0) complexes C₆H₆Os(PMe₃)L (L = C₂H₄, C₃H₆) are stronger metal bases than their ruthenium counterparts.[25]

(23) 15 (90 mg, 0.14 mmol) was dissolved in 5 mL of methanol, and the solution was stirred at 50 °C for 4 h under a CO atmosphere. The cooled solution was concentrated in vacuo (∼2 mL), and ether (10 mL) was added. After the solution was left standing for 30 min, the white precipitate was filtered and recrystallized from CH₂Cl₂/ether to give 85 mg of 16 (92% yield). Anal. Calcd for OsC₁₃H₃₇F₆OP₅: C, 23.35; H, 5.54; P, 23.18. Found: C, 23.19; H, 5.81; P, 22.96. IR (Nujol, cm⁻¹): 1940 (CO). ¹H NMR (CDCl₃, 60 MHz, 298 K): δ 1.79 (vt, 18 H, N = 6.8 Hz, ¹·⁴PMe₃), 1.58 (d, 9 H, J_{HP} = 7.6 Hz, ²PMe₃), 1.53 (dd, 9 H, J_{HP} = 7.2 Hz, J_{HH} = 0.6 Hz, ³PMe₃), −10.30 (m, after ³¹P decoupling s).

(24) Karsch, H. H. *Chem. Ber.* **1977**, *110*, 2222.

(25) (a) Werner, H.; Werner, R. *J. Organomet. Chem.* **1979**, *174*, C 63. (b) Werner, R. Dissertation Universität Würzburg, 1982.

A Direct Broadly Applicable Approach to the Synthesis of Aromatic Molecular and Supramolecular Selenium and Tellurium Compounds[1]

D. J. Sandman,* J. C. Stark,[2] L. A. Acampora, and P. Gagne[3]

GTE Laboratories, Inc.
Waltham, Massachusetts 02254

Summary: The alkali metals sodium and potassium react directly with elemental Se or Te in dipolar aprotic solvents such as *N,N*-dimethylformamide (DMF), *N*-methylpyrrolidinone (NMP), and hexamethylphosphoramide (HMPA) to give reagents M₂X and M₂X₂ (X = Se, Te),

(17) 13. Anal. Calcd for OsC₁₂H₃₆Cl₂F₆P₅: C, 20.28; H, 5.07; Os, 26.78. Found: C, 20.40; H, 4.86; Os, 26.44. Magnetic moment (determined by NMR method): μ = 1.68 μ_B. 14. IR (Nujol, cm⁻¹): 1930 (CO). ¹H NMR (C₆H₆, 60 MHz, 298 K): δ 1.61 (vt, 18 H, N = 6.8 Hz, ¹·³PMe₃), 1.35 (d, 9 H, J_{HP} = 7.8 Hz, ²PMe₃).

(18) Addition of PMe₃ to a benzene suspension of 13 leads after 3 days under refluxing conditions to the formation of 3.

(19) Green, M. L. H.; McCleverty, J. A.; Pratt, L.; Wilkinson, G. *J. Chem. Soc.* **1961**, 4854.

(20) (a) Shriver, D. F. *Acc. Chem. Res.* **1970**, *3*, 231. (b) Werner, H. *Pure Appl. Chem.* **1982**, *54*, 177.

(21) 6 (214 mg, 0.43 mmol) was dissolved in 3 mL of methanol, and NH₄PF₆ (150 mg, 0.92 mmol) was added. The solution was stirred at 25 °C for 15 min, and ether (15 mL) was added. After the mixture was left standing for 1 h, the gray precipitate was filtered and repeatedly washed with ether. Recrystallization from acetone/ether gives 251 mg of a white crystalline solid (91% yield). Anal. Calcd for OsC₁₂H₃₉F₆P₅: C, 22.42; H, 6.07; Os, 29.62; P, 24.14. Found: C, 22.70; H, 5.68; Os, 29.45; P, 23.98. IR (KBr, cm⁻¹): 2040 (OsH₃). Conductivity (CH₃NO₂, 298 K): Λ = 84.1 cm² Ω⁻¹ mol⁻¹. ¹H NMR ((CD₃)₂CO, 60 MHz, 298 K): δ 1.68 (m, 36 H, after ³¹P decoupling s), −9.63 (qui, 3 H, J_{HP} = 4.9, OsH₃). ³¹P NMR ((CD₃)₂CO, 90 MHz, 298 K): δ −56.0 (s).

(22) Jesson, J. P.; Muetterties, E. L. In "Dynamic Nuclear Magnetic Resonance Spectroscopy"; Jackman, L. M., Cotton, F. A., Ed.; Academic Press: New York, 1975; p 253.

(1) (a) Portions of this work were presented at the 12th Northeast Regional Meeting of the American Chemical Society, Burlington, VT, June 27–30, 1982, Abstract 158 and (b) the 6th International Conference on the Chemistry of the Organic Solid State, Freiburg, German Federal Republic, October 4–8, 1982; *Mol. Cryst. Liq. Cryst.*, to be submitted for publication.

(2) On sabbatical leave at GTE Laboratories, 1980–1981. This work was supported in part by the National Science Foundation, Grant SP1-8160202. Present address: Department of Chemistry, Eastern Nazarene College, Quincy, MA 02170.

(3) 1981 National Science Foundation Industrial Undergraduate Research Participant at GTE Laboratories; College of the Holy Cross, Worcester, MA.

A direct broadly applicable approach to the synthesis of aromatic molecular and supramolecular selenium and tellurium compounds

D. J. Sandman, J. C. Stark, L. A. Acampora, and P. Gagne

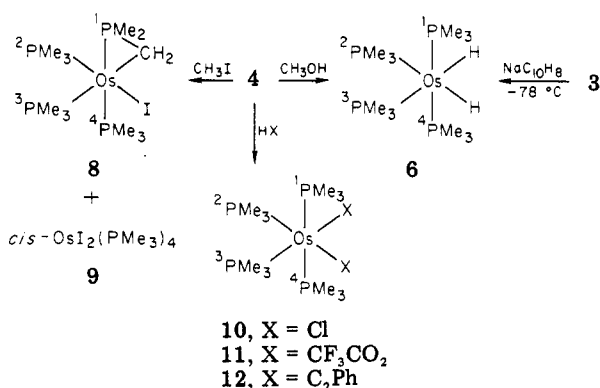## More About This Article

The permalink http://dx.doi.org/10.1021/om00076a014 provides access to:

- Links to articles and content related to this article
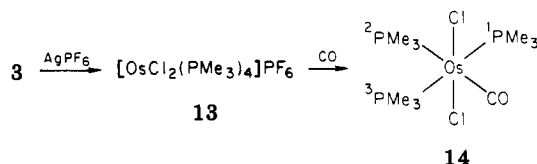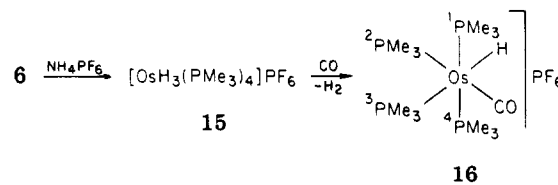- Copyright permission to reproduce figures and/or text from this article

Scheme II

10, X = Cl
11, X = CF₃CO₂
12, X = C₂Ph

solution, the paramagnetic osmium(III) complex [OsCl₂-(PMe₃)₄]PF₆ (13) is obtained in 95% yield.[17] In benzene suspension, it reacts with CO under refluxing conditions to form the carbonylosmium compound *trans*-OsCl₂-(CO)(PMe₃)₃ (14) which indicates that even weak reducing agents such as CO or PMe₃[18] are capable of reducing osmium(III) to osmium(II) complexes. Under similar conditions, compound 3 is completely inert toward carbon monoxide.

Like the well-known (C₅H₅)₂WH₂,[19] the dihydrido-osmium(II) compound *cis*-OsH₂(PMe₃)₄ (6) also behaves as a metal base.[20] This is demonstrated by the smooth reaction of 6 with NH₄PF₆ that yields quantitatively the PF₆ salt of the trihydridoosmium(IV) cation [OsH₃-(PMe₃)₄]⁺ (15).[21] According to the ¹H NMR data, the cation seems to be fluxional at room temperature. In (CD₃)₂CO, a 1:4:6:4:1 quintet is observed for the hydride resonance that broadens below 0 °C, indicating that the dynamic process is slowed down at low temperatures. Experiments are in progress to study the intramolecular rearrangement in more detail and to compare the kinetic parameters with those of the reactions of the hexa-coordinated complexes MH₂L₄.[22] In methanolic solution, complex 15 reacts with CO to give [OsH(CO)(PMe₃)₄]PF₆ (16), which is configurationally stable on the NMR time scale.[23]

In contrast to the dihydridoosmium(II) complex 6, the corresponding iron compound 7 does not seem to react with NH₄⁺ or other weak Brønsted acids to form the cation [FeH₃(PMe₃)₄]⁺.[14,24] This result is in support of Shriver's statement[20a] that metal basicity generally increases going down a group. It is also in accord with our results that the osmium(0) complexes C₆H₆Os(PMe₃)L (L = C₂H₄, C₃H₆) are stronger metal bases than their ruthenium counterparts.[25]

(17) 13. Anal. Calcd for OsC₁₂H₃₆Cl₂F₆P₅: C, 20.28; H, 5.07; Os, 26.78. Found: C, 20.40; H, 4.86; Os, 26.44. Magnetic moment (determined by NMR method): μ = 1.68 μ_B. 14. IR (Nujol, cm⁻¹): 1930 (CO). ¹H NMR (C₆H₆, 60 MHz, 298 K): δ 1.61 (vt, 18 H, N = 6.8 Hz, ¹,³PMe₃), 1.35 (d, 9 H, J_HP = 7.8 Hz, ²PMe₃).

(18) Addition of PMe₃ to a benzene suspension of 13 leads after 3 days under refluxing conditions to the formation of 3.

(19) Green, M. L. H.; McCleverty, J. A.; Pratt, L.; Wilkinson, G. *J. Chem. Soc.* 1961, 4854.

(20) (a) Shriver, D. F. *Acc. Chem. Res.* 1970, 3, 231. (b) Werner, H. *Pure Appl. Chem.* 1982, 54, 177.

(21) 6 (214 mg, 0.43 mmol) was dissolved in 3 mL of methanol, and NH₄PF₆ (150 mg, 0.92 mmol) was added. The solution was stirred at 25 °C for 15 min, and ether (15 mL) was added. After the mixture was left standing for 1 h, the gray precipitate was filtered and repeatedly washed with ether. Recrystallization from acetone/ether gives 251 mg of a white crystalline solid (91% yield). Anal. Calcd for OsC₁₂H₃₉F₆P₅: C, 22.42; H, 6.07; Os, 29.62; P, 24.14. Found: C, 22.70; H, 5.68; Os, 29.45; P, 23.98. IR (KBr, cm⁻¹): 2040 (OsH₃). Conductivity (CH₃NO₂, 298 K): Λ = 84.1 cm² Ω⁻¹ mol⁻¹. ¹H NMR ((CD₃)₂CO, 60 MHz, 298 K): δ 1.68 (m, 36 H, after ³¹P decoupling s), -9.63 (qui, 3 H, J_HP = 4.9, OsH₃). ³¹P NMR ((CD₃)₂CO, 90 MHz, 298 K): δ -56.0 (s).

(22) Jesson, J. P.; Muetterties, E. L. In "Dynamic Nuclear Magnetic Resonance Spectroscopy"; Jackman, L. M., Cotton, F. A., Ed.; Academic Press: New York, 1975; p 253.

(23) 15 (90 mg, 0.14 mmol) was dissolved in 5 mL of methanol, and the solution was stirred at 50 °C for 4 h under a CO atmosphere. The cooled solution was concentrated in vacuo (~2 mL), and ether (10 mL) was added. After the solution was left standing for 30 min, the white precipitate was filtered and recrystallized from CH₂Cl₂/ether to give 85 mg of 16 (92% yield). Anal. Calcd for OsC₁₃H₃₇F₆OP₅: C, 23.35; H, 5.54; P, 23.18. Found: C, 23.19; H, 5.81; P, 22.96. IR (Nujol, cm⁻¹): 1940 (CO). ¹H NMR (CDCl₃, 60 MHz, 298 K): δ 1.79 (vt, 18 H, N = 6.8 Hz, ¹,⁴PMe₃), 1.58 (d, 9 H, J_HP = 7.6 Hz, ²PMe₃), 1.53 (dd, 9 H, J_HP = 7.2 Hz, J_HH = 0.6 Hz, ³PMe₃), -10.30 (m, after ³¹P decoupling s).

(24) Karsch, H. H. *Chem. Ber.* 1977, 110, 2222.

(25) (a) Werner, H.; Werner, R. *J. Organomet. Chem.* 1979, 174, C 63. (b) Werner, R. Dissertation Universität Würzburg, 1982.

A Direct Broadly Applicable Approach to the Synthesis of Aromatic Molecular and Supramolecular Selenium and Tellurium Compounds[1]

D. J. Sandman,* J. C. Stark,[2] L. A. Acampora, and P. Gagne[3]

GTE Laboratories, Inc.
Waltham, Massachusetts 02254

Summary: The alkali metals sodium and potassium react directly with elemental Se or Te in dipolar aprotic solvents such as *N,N*-dimethylformamide (DMF), *N*-methyl-pyrrolidinone (NMP), and hexamethylphosphoramide (HMPA) to give reagents M₂X and M₂X₂ (X = Se, Te),

(1) (a) Portions of this work were presented at the 12th Northeast Regional Meeting of the American Chemical Society, Burlington, VT, June 27–30, 1982, Abstract 158 and (b) the 6th International Conference on the Chemistry of the Organic Solid State, Freiburg, German Federal Republic, October 4–8, 1982; *Mol. Cryst. Liq. Cryst.*, to be submitted for publication.

(2) On sabbatical leave at GTE Laboratories, 1980–1981. This work was supported in part by the National Science Foundation, Grant SP1-8160202. Present address: Department of Chemistry, Eastern Nazarene College, Quincy, MA 02170.

(3) 1981 National Science Foundation Industrial Undergraduate Research Participant at GTE Laboratories; College of the Holy Cross, Worcester, MA.

Table I. Synthesis of Molecular Compounds[a,b]

entry	aromatic halide	nucleo-phile	isolated yield, %
1	9-bromoanthracene	Na₂Te₂	40[c,d]
2	2-chloronaphthalene	Na₂Te₂	20
3	1-chloronaphthalene	Na₂Te₂	7
4	iodobenzene	Na₂Te₂	5[e]
5	bromobenzene	Na₂Te₂	1
6	2-bromonaphthalene	Na₂Te	30
7	iodobenzene	Na₂Te	35
8	2-bromonaphthalene	K₂Se	30[c,f]

[a] All reactions were carried out by using a molar ratio of 2 for the aromatic halide: nucleophile in hexamethyl phosphoramide (HMPA) at 130–170 °C for 16–24 h except for entry 1 which was carried out in N,N-dimethylformamide (DMF) at 110 °C. [b] Known compounds were identified by melting point or boiling point (entry 7); for the case of entry 2, see text. [c] New compounds gave satisfactory elemental analysis. [d] New compound, red-brown needles, mp 190–191 °C. [e] In addition to diphenyl ditelluride, diphenyl telluride is formed in this experiment in ca. 10% yield. [f] New compound, white solid, mp 132–133 °C.

avoiding the use of liquid NH₃. These species undergo direct thermal reaction at 130–170 °C with representative unactivated aryl halides, and examples of both new and previously reported molecular and polymeric ditellurides, tellurides, and selenides are given.

Outlets for the considerable current interest in selenium and tellurium materials, as well as new reagents for their preparation, include natural products synthesis, biological and medicinal applications, imaging systems, and new ion radical solids with metallic and superconducting properties.[4] We have recently[5] reported that a new sodium ditelluride reagent[6] reacts with 5,6,11,12-tetrachlorotetracene (1) in dipolar aprotic solvents to give the novel

1
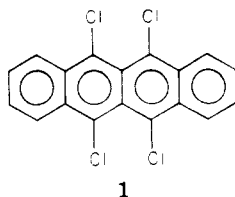
π-donor tetratellurotetracene (TTeT). In view of speculation[7] that Na₂Te₂ might find application in the synthesis of aromatic ditellurides and of a brief patent[9] reporting synthesis of aromatic molecular and polymeric diselenides from Na₂Se₂, we were particularly interested in a study of thermal reactions of aromatic halides less easily reduced

(less "activated") than 1[5] with these nucleophiles.[10] Moreover, we now report that, analogously to the cases of Na₂Te₂[5] and Na₂Se₂,[6] alkali metals react with selenium and tellurium in a 2:1 atomic ratio in dipolar aprotic solvents to give metal selenides and tellurides, respectively, thus avoiding the use of liquid ammonia, which is widely used[7,11] for the preparation of these materials. Further, we find that these new nucleophilic reagents react with unactivated aryl halides to give previously unreported materials as well as more direct preparations of known materials.[12]

Table I summarizes the results on the synthesis of molecular chalcogenides. The reaction products are not decomposed by excess nucleophile under reaction conditions. We observed that monosubstitued aromatics are reactive with the order of reactivity for C₆H₅X with Na₂Te₂ being I > Br > Cl. We note that di-2-naphthyl telluride (2), previously prepared via a three step route,[13] is directly obtained in modest yield in the present work (entry 6).
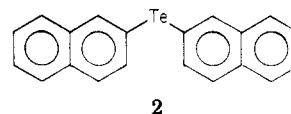
2

In our initial isolation of di-2-naphthyl ditelluride (3), the sample crystallized from mixed hexane isomers (Fisher) exhibited a melting point of 118 °C. The cooled melt of
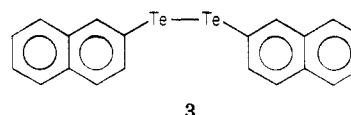
3

this sample remelted at 120–122 °C, in good agreement with literature[14] reports of the melting point of 3. Subsequently, samples of 3 with a melting point of 122–124 °C were obtained by crystallization from 5:1 (v/v) mixed hexane isomers–benzene. The samples of 3 with melting points 116–118 °C and 122–124 °C exhibit markedly different X-ray powder diffraction patterns, indicating polymorphism.[15] Both forms of 3 exhibit broad maxima in their solid-state spectra of 400–410 nm; the higher melting form exhibits a shoulder at ca. 500 nm not observed in the form with lower mp.

While our initial expectation was that reactions of p-dihalobenzenes would lead to molecular products, we observed facile polymerization. The previously unknown[16] selenium analogue of the thermoplastic poly(p-phenylene

(4) (a) Cagniant, D., Kirsch, G., Eds. "Proceedings of the 3rd International Symposium on Organic Selenium and Tellurium Compounds" July 9–12, 1979, Metz, France. (b) Irgolic, K. J. *J. Organomet. Chem.* **1980**, *203*, 367–414; (c) Bechgaard, K.; Jerome, D., *Sci. Am.* **1982**, *246*, (7) 52–61.

(5) Sandman, D. J.; Stark, J. C.; Foxman, B. M. *Organometallics* **1982**, *1*, 739–742.

(6) Balodis, K. A.; Livdane, A. D.; Medne, R. S.; Neiland, O. Y. *J. Org. Chem. USSR (Engl. Transl.)* **1979**, *15*, 343, report the analogous use of a sodium diselenide reagent. We have observed byproducts analogous to those noted in ref 5 in repeating the work of Balodis et al.

(7) Irgolic, K. J. "The Organic Chemistry of Tellurium"; Gordon and Breach: New York, 1974, p 97. It is also noted on p 107 of this book that reactions of sodium telluride prepared in liquid ammonia with aromatic halides had not been carried out. Subsequently, *photostimulated* reactions of Na₂Te and Na₂Se in liquid ammonia with aryl halides to give modest yields of diaryl chalcogenides have been reported.[8]

(8) Rossi, R. A.; Penenory, A. B. *J. Org. Chem.* **1981**, *46*, 4580–4582.

(9) Grushkin, B.; Salzman, M. N. U.S. Patent 3 965 049; cf. *Chem. Abstr.* **1976**, *85*, 124606.

(10) Recent examples of aromatic activated by nitrosubstituents reacting, respectively, with tellurium and selenium nucleophiles include: (a) Suzuki, H.; Abe, H.; Ohmasa, N.; Osuka, A., *Chem. Lett.* **1981**, 1115–1116. (b) Battistoni, P.; Bompadre, S.; Brui, P.; Fava, G. *Gazz. Chim. Ital.* **1981**, *111*, 505–507.

(11) Gunther, W. H. H. In "Organic Selenium Compounds: Their Chemistry and Biology"; Klayman, D. L., Gunther, W. H. H., Eds. Wiley-Interscience: New York, 1973, Chapter III.

(12) This communication will focus on new reactions of ditelluride, telluride, and selenide nucleophiles, as we have reproduced the experiments of ref 9 with the Na₂Se₂ reagents and used them to make other new compounds: Sandman, D. J.; Stark, J. C.; Reed, R.; Allen, G., unpublished experiments. The latter reagent has recently been used by others: Endres, H.; Keller, H. J.; Queckborner, J., Veigel, J.; Schweitzer, D. *Mol. Cryst. Liq. Cryst.* **1982**, *86*, 111–122. Ohnishi, S.; Nogami, T.; Mikawa, H. *Chem. Lett.* **1982**, 1841–1842.

(13) Rheinboldt, H.; Vicentini, G. *Chem. Ber.* **1956**, *89*, 624–631.

(14) Reference 7, p 96.

(15) The crystal structures of both forms of 2 have been solved by Professor B. Foxman and conformational polymorphism has been observed.[1b] The form of 2 with a melting point of 116–118 °C is monoclinic with a = 8.406 Å, b = 6.304 Å, c = 31.960 Å, β = 95.08°, and Z = 4 and the form with melting point of 122–124 °C is also monoclinic with a = 36.654 Å, b = 7.840 Å, c = 12.084 Å, β = 104.56°, and Z = 8. The powder patterns of both forms are completely indexed to the above unit cells.

(16) Okamoto, Y.; Yano, T.; Homsany, R. *Ann. N.Y. Acad. Sci.* **1972**, 60–71, report an unsuccessful attempt to make PPSe.

sulfide) (PPS), i.e., poly(p-phenylene selenide)[17] (PPSe), is readily prepared from either p-dichloro- (4) or p-dibromobenzene (5) and either sodium or potassium selenide in either DMF or N-methylpyrrolidinone (NMP). Our best results are observed on reaction of 5 with Na_2Se in DMF at 120–140 °C for 20 h, where we isolate PPSe free of low molecular weight contaminants in 80% yield as a light yellow powder, mp 220 °C. While both 4 and 5 react with Na_2Te in NMP or DMF to give materials that are at least oligomeric,[18] our best approach to poly(p-phenylene telluride) (PPTe) was obtained via p-diiodobenzene and Na_2Te in DMF at 110–120 °C to give a partially crystalline[19] tan solid, mp 162–170 °C, in 70% yield free of low molecular weight contaminants. The infrared spectra of PPSe and PPTe as prepared herein are superimposable on that of PPS between 4000 and 600 cm^{-1}, while bands at 550 and 475 cm^{-1} in PPS are observed at 500 and 475 cm^{-1} in PPSe and 489 and 465 cm^{-1} in PPTe. The solid-state absorption spectra of PPSe and PPTe exhibit maxima at 300 and 310 nm, respectively, with long tails into the visible. At 140–150 °C, 5 reacts with Na_2Te_2 in DMF to give in 10% yields bis(p-bromophenyl) ditelluride and black amorphous polymer, mp 230–250 °C dec, whose solid-state absorption spectrum shows a maximum at 310 nm tailing into the visible.

Although we have not as yet made a detailed mechanistic study of the experiments reported herein, our observation of products derived from reduction of halogen to hydrogen in reactions of 1,[5] 9-bromoanthracene, and 2-bromonaphthalene (6) suggest involvement of electron-transfer processes. In fact, using electron-transfer initiation with sodium naphthalenide (1.0 M in THF), we have been able to isolate 3 in yields up to 22% from either 6 or 2-chloronaphthalene and Na_2Te_2 in HMPA at temperatures as low as 25 °C. The order of reactivity of C_6H_5X with Na_2Te_2 noted above, the greater reactivity of 4 vs. 5 in reactions with Na_2Se, and the depression of PPSe yield from 80% noted above to 15% by addition of benzophenone[21] equimolar to 5 in the reaction mixture are consistent with a mechanistic pattern of the $S_{RN}1$[21] type. In addition to entry 4 in Table I, another anomalous reaction in molecular compounds has been noted. In HMPA at 170 °C, Na_2Te_2 reacts with 6 to give an isolated 9% yield of 2 as the only organotellurium product. Fragmentation of an intermediate anion radical[22] may be involved in these experiments.

Summarizing, we have used new alkali chalcogenide reagents to prepare both new and previously known selenium and tellurium materials. In some cases, it is apparent that the routes described herein are the methods of choice for laboratory synthesis. We expect that further development of this chemistry will result in additional new materials with interesting chemical, physical, and structural properties.

(17) The structural and electrical properties of PPSe are separately detailed: Sandman, D. J.; Rubner, M., Samuelson, L. *J. Chem. Soc., Chem. Commun.* 1982, 1133–1134.

(18) Isolated molecular products of reaction 3 at 180–190 °C in NMP include 4,4-dichlorobiphenyl and bis(p-chlorophenyl) ditelluride in combined yield of ca. 25%, while bis(p-bromophenyl) ditelluride was isolated in 4% yield from reaction of 4 in DMF at 130–140 °C.

(19) X-ray diffraction of PPTe reveals the prescence of small amounts of elemental tellurium, also observed in the other organotellurium polymers we have isolated, and reflections at d = 5.09, 4.27, 3.57, and 3.04 Å. These reflections indicate that PPTe is not crystallographically similar to PPSe, which was found to be isomorphous to PPS.[17] PPTe has a flotation density of 2.46 g/cm[1].

(20) Scamehorn, R. G.; Bunnett, J. F. *J. Org. Chem.* 1977, 42, 1449–1457.

(21) Bunnett, J. F. *Acc. Chem. Res.* 1978, 11, 413–420.

(22) Rossi, R. A. *Acc. Chem. Res.* 1982, 15, 164–170.

Polypyridyl Hydrido Complexes of Osmium(II) and Ruthenium(II)

Jonathan V. Caspar,* B. Patrick Sullivan,* and Thomas J. Meyer

Department of Chemistry, University of North Carolina Chapel Hill, North Carolina 27514

Summary: A series of polypyridyl hydrido complexes of Os(II) and Ru(II) has been prepared, e.g., *cis*-[M(bpy)$_2$-(CO)H]$^{2+}$ (bpy is 2,2'-bipyridine; M = Ru, Os) and [Os-(phen)(1,2-(Ph$_2$P)$_2$C$_6$H$_4$)(PPh$_3$)H]$^{2+}$ (phen is 1,10-phenanthroline), utilizing three different synthetic routes. The complexes have been characterized by NMR (^{1}H and ^{31}P) and by infrared spectroscopy. Initial results are reported on these photochemical and photophysical properties. The complexes of Os(II) represent rare examples of luminescent metal hydride complexes in fluid solution at room temperature.

In recent work we have reported on the photophysical properties of two series of polypyridyl complexes of Os-(II)—(phen)Os^{II}L$_4$$^{2+}$ and (bpy)Os^{II}L$_4$$^{2+}$ (phen is 1,10-phenanthroline; bpy is 2,2'-bipyridine; L is py, 0.5bpy, 0.5phen, MeCN, PR$_3$, AsR$_3$, CO).[1] The complexes are strong visible light absorbers, and their excited state properties are of note because of the following. (1) They are dictated by metal to ligand charge-transfer (MLCT) excited states, e.g., (bpy$^-$·)Os^{III}L$_4$$^{2+*}$, which are largely triplet in character.[2] (2) Emission energies and excited-state redox potentials can be varied systematically with changes in L. (3) Variations in radiative (k_r) and nonradiative (k_{nr}) rate constants, which determine excited-state lifetimes ($\tau_0 = (k_r + k_{nr})^{-1}$) and emission quantum yields ($\phi_r = k_r(k_r + k_{nr})^{-1}$), can be accounted for *quantitatively* on the basis of existing theories.[3] (4) The excited states undergo facile oxidation or reduction and have provided the basis for an excited-state photoelectrochemical cell for the production of H$_2$O$_2$ and Br$_2$.[4] The excited-state

(1) Kober, E. M.; Sullivan, B. P.; Dressick, W. J.; Caspar, J. V. *J. Am. Chem. Soc.* 1980, 102, 7383.

(2) Kober, E. M.; Meyer, T. J. *Inorg. Chem.* 1982, 21, 3967 and references therein.

(3) Caspar, J. V.; Kober, E. M.; Sullivan, B. P.; Meyer, T. J. *J. Am. Chem. Soc.* 1982, 104, 630. Caspar, J. V.; Meyer, T. J. *J. Phys. Chem.*, in press. Caspar, J. V., Ph.D. Thesis, University of North Carolina, 1982.

sulfide) (PPS), i.e., poly(p-phenylene selenide)[17] (PPSe), is readily prepared from either p-dichloro- (4) or p-dibromobenzene (5) and either sodium or potassium selenide in either DMF or N-methylpyrrolidinone (NMP). Our best results are observed on reaction of 5 with Na_2Se in DMF at 120–140 °C for 20 h, where we isolate PPSe free of low molecular weight contaminants in 80% yield as a light yellow powder, mp 220 °C. While both 4 and 5 react with Na_2Te in NMP or DMF to give materials that are at least oligomeric,[18] our best approach to poly(p-phenylene telluride) (PPTe) was obtained via p-diiodobenzene and Na_2Te in DMF at 110–120 °C to give a partially crystalline[19] tan solid, mp 162–170 °C, in 70% yield free of low molecular weight contaminants. The infrared spectra of PPSe and PPTe as prepared herein are superimposable on that of PPS between 4000 and 600 cm^{-1}, while bands at 550 and 475 cm^{-1} in PPS are observed at 500 and 475 cm^{-1} in PPSe and 489 and 465 cm^{-1} in PPTe. The solid-state absorption spectra of PPSe and PPTe exhibit maxima at 300 and 310 nm, respectively, with long tails into the visible. At 140–150 °C, 5 reacts with Na_2Te_2 in DMF to give in 10% yields bis(p-bromophenyl) ditelluride and black amorphous polymer, mp 230–250 °C dec, whose solid-state absorption spectrum shows a maximum at 310 nm tailing into the visible.

Although we have not as yet made a detailed mechanistic study of the experiments reported herein, our observation of products derived from reduction of halogen to hydrogen in reactions of 1,[5] 9-bromoanthracene, and 2-bromonaphthalene (6) suggest involvement of electron-transfer processes. In fact, using electron-transfer initiation with sodium naphthalenide (1.0 M in THF), we have been able to isolate 3 in yields up to 22% from either 6 or 2-chloronaphthalene and Na_2Te_2 in HMPA at temperatures as low as 25 °C. The order of reactivity of C_6H_5X with Na_2Te_2 noted above, the greater reactivity of 4 vs. 5 in reactions with Na_2Se, and the depression of PPSe yield from 80% noted above to 15% by addition of benzophenone[21] equimolar to 5 in the reaction mixture are consistent with a mechanistic pattern of the $S_{RN}1$[21] type. In addition to entry 4 in Table I, another anomalous reaction in molecular compounds has been noted. In HMPA at 170 °C, Na_2Te_2 reacts with 6 to give an isolated 9% yield of 2 as the only organotellurium product. Fragmentation of an intermediate anion radical[22] may be involved in these experiments.

Summarizing, we have used new alkali chalcogenide reagents to prepare both new and previously known selenium and tellurium materials. In some cases, it is apparent that the routes described herein are the methods of choice for laboratory synthesis. We expect that further development of this chemistry will result in additional new materials with interesting chemical, physical, and structural properties.

(17) The structural and electrical properties of PPSe are separately detailed: Sandman, D. J.; Rubner, M., Samuelson, L. *J. Chem. Soc.*, *Chem. Commun.* **1982**, 1133–1134.

(18) Isolated molecular products of reaction 3 at 180–190 °C in NMP include 4,4-dichlorobiphenyl and bis(p-chlorophenyl) ditelluride in combined yield of ca. 25%, while bis(p-bromophenyl) ditelluride was isolated in 4% yield from reaction of 4 in DMF at 130–140 °C.

(19) X-ray diffraction of PPTe reveals the prescence of small amounts of elemental tellurium, also observed in the other organotellurium polymers we have isolated, and reflections at d = 5.09, 4.27, 3.57, and 3.04 Å. These reflections indicate that PPTe is not crystallographically similar to PPSe, which was found to be isomorphous to PPS.[17] PPTe has a flotation density of 2.46 g/cm^3.

(20) Scamehorn, R. G.; Bunnett, J. F. *J. Org. Chem.* **1977**, *42*, 1449–1457.

(21) Bunnett, J. F. *Acc. Chem. Res.* **1978**, *11*, 413–420.

(22) Rossi, R. A. *Acc. Chem. Res.* **1982**, *15*, 164–170.

Polypyridyl Hydrido Complexes of Osmium(II) and Ruthenium(II)

Jonathan V. Caspar,* B. Patrick Sullivan,* and Thomas J. Meyer

Department of Chemistry, University of North Carolina Chapel Hill, North Carolina 27514

Summary: A series of polypyridyl hydrido complexes of Os(II) and Ru(II) has been prepared, e.g., cis-[M(bpy)$_2$(CO)H]$^{2+}$ (bpy is 2,2'-bipyridine; M = Ru, Os) and [Os(phen)(1,2-(Ph$_2$P)$_2$C$_6$H$_4$)(PPh$_3$)H]$^{2+}$ (phen is 1,10-phenanthroline), utilizing three different synthetic routes. The complexes have been characterized by NMR (^{1}H and ^{31}P) and by infrared spectroscopy. Initial results are reported on these photochemical and photophysical properties. The complexes of Os(II) represent rare examples of luminescent metal hydride complexes in fluid solution at room temperature.

In recent work we have reported on the photophysical properties of two series of polypyridyl complexes of Os-(II)—(phen)Os^{II}L$_4^{2+}$ and (bpy)Os^{II}L$_4^{2+}$ (phen is 1,10-phenanthroline; bpy is 2,2'-bipyridine; L is py, 0.5bpy, 0.5phen, MeCN, PR$_3$, AsR$_3$, CO).[1] The complexes are strong visible light absorbers, and their excited state properties are of note because of the following. (1) They are dictated by metal to ligand charge-transfer (MLCT) excited states, e.g., (bpy$^-$·)Os^{III}L$_4^{2+}$*, which are largely triplet in character.[2] (2) Emission energies and excited-state redox potentials can be varied systematically with changes in L. (3) Variations in radiative (k_r) and nonradiative (k_{nr}) rate constants, which determine excited-state lifetimes ($\tau_0 = (k_r + k_{nr})^{-1}$) and emission quantum yields ($\phi_r = k_r(k_r + k_{nr})^{-1}$), can be accounted for *quantitatively* on the basis of existing theories.[3] (4) The excited states undergo facile oxidation or reduction and have provided the basis for an excited-state photoelectrochemical cell for the production of H_2O_2 and Br_2.[4] The excited-state

(1) Kober, E. M.; Sullivan, B. P.; Dressick, W. J.; Caspar, J. V. *J. Am. Chem. Soc.* **1980**, *102*, 7383.

(2) Kober, E. M.; Meyer, T. J. *Inorg. Chem.* **1982**, *21*, 3967 and references therein.

(3) Caspar, J. V.; Kober, E. M.; Sullivan, B. P.; Meyer, T. J. *J. Am. Chem. Soc.* **1982**, *104*, 630. Caspar, J. V.; Meyer, T. J. *J. Phys. Chem.*, in press. Caspar, J. V., Ph.D. Thesis, University of North Carolina, 1982.

Table I. Spectroscopic and Excited-State Data for Metal Hydride and Related Complexes
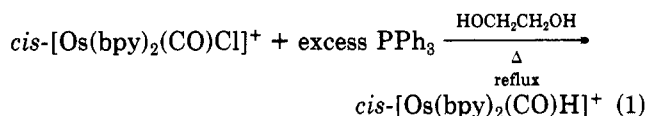
complex	ν_{CO},[a] cm⁻¹	ν_H,[a] cm⁻¹	¹H NMR δ [b]	$E_p(M^{III}/M^{II})$,[c] V	E_{em},[d] cm⁻¹	k_{nr},[e] s⁻¹
[Os(phen)(1,2-(Ph₂P)₂C₆H₄)(PPh₃)H](PF₆)		2075 (w)	−14.6 (d of t)	0.83	14 300	≥1 × 10⁸
[Os(phen)(cis-Ph₂PCH=CHPPh₂)(PEt₃)H](PF₆)	g		−15.5 (d of t)	0.74	13 700	4.8 × 10⁷
cis-[Os(phen)₂(CO)H](PF₆)	1913 (s)	2006 (m)	−11.5 (s)	0.90	13 700	5.1 × 10⁶
cis-[Os(bpy)₂(CO)H](PF₆)	1911 (s)	2005 (m)	−11.4 (s)	0.88	13 500	2.4 × 10⁷
cis-[Ru(bpy)₂(CO)H](PF₆)	1941 (br)	g	−11.3 (s)	1.14	g	
cis-[Os(bpy)₂(CO)Cl](PF₆)	1965 (s)			1.18[f]	14 660	1.09 × 10⁷ (2.3 × 10⁶)[h]
cis-[Ru(bpy)₂(CO)Cl](PF₆)	1984 (s)			1.50[f]	g	
trans-[Os(bpy)(PPh₃)₂(CO)H](PF₆)	1931 (s)	2060 (w)	−12.2 (t)	1.54	16 580	

[a] In CH₂Cl₂ solution.   [b] Taken in (CD₃)₂CO solution for the hydride resonance with Me₄Si as internal standard. s stands for singlet; t stands for triplet; for the first two entries in the column, the resonance is a doublet of triplets.   [c] Peak potential values for the irreversible oxidation of M(II) to M(III) in CH₃CN solution with 0.1 M [NEt₄](ClO₄) as supporting electrolyte vs. the saturated calomel electrode (SCE) using a Pt bead working electrode. The scan rate was 200 mV/s.   [d] In acetonitrile solution; corrected for phototube response.   [e] In acetonitrile from lifetime measurements using laser flash photolysis.   [f] $E_{1/2}$ values for the M(III)/(M(II) couples which are reversible on the cyclic voltammetry timescale, scan rate = 200 mV/s.   [g] Not observed.   [h] k_{nr} for the 1,10-phenanthroline analogue cis-[Os(phen)₂(CO)Cl](PF₆).

properties of related polypyridyl complexes of Ru(II) are similar but are complicated by the presence of low-lying dd states which can provide an efficient pathway for excited-state decay or even can lead to photochemical decomposition by loss of ligands.[5]

We are attempting to develop more sophisticated photochemical systems in which complex photochemical pathways, e.g., multiple-electron-transfer reactions, are induced by initial excitation of polypyridyl-M^{II} (M = Ru, Os) MLCT chromophores. Of considerable interest to us in this context are the photochemical and photophysical properties of metal hydride complexes, in part because of their possible use as photocatalysts.[6] We describe here the preparation of a series of polypyridyl hydrido complexes of Ru(II) and Os(II) and some initial observations concerning their photochemical and photophysical properties.

Three basic synthetic strategies were used to obtain the hydrido complexes; the first, which is a well-known procedure, involves the reaction between a carbonyl halide precursor in alcoholic base with either PPh₃ or 2,6-lutidine as base and ethylene glycol as the alcohol. For example, the reaction shown in eq 1 gives the related carbonyl hydride complex in ~50% yield. In some cases the use of

$$cis\text{-}[Os(bpy)_2(CO)Cl]^+ + \text{excess PPh}_3 \xrightarrow[\substack{\Delta \\ reflux}]{HOCH_2CH_2OH}$$

$$cis\text{-}[Os(bpy)_2(CO)H]^+ \quad (1)$$

PPh₃ resulted in carbonyl displacement (e.g., eq 2, where dppb is bis(1,2-diphenylphosphino)benzene). A poten-

$$[Os(phen)(dppb)(CO)Cl]^+ + \text{excess PPh}_3 \xrightarrow[\substack{\Delta \\ reflux}]{HOCH_2CH_2OH}$$

$$[Os(phen)(dppb)(PPh_3)H]^+ \quad (2)$$

tially general route to metal hydride complexes, although one that has yet to be exploited extensively for chemical synthesis, is the thermolysis of monodentate formate complexes. The complexes cis-[M(bpy)₂(CO)(O₂CH)](PF₆)

(M = Ru, Os) can be heated either in 2-methoxyethanol or ethylene glycol or in the solid state to give the corresponding hydrido carbonyls (eq 3).[7,8] Reaction 3 proceeds

$$cis\text{-}[Ru(bpy)_2(CO)(OC(=O)H)]^+ \xrightarrow[\Delta]{HOCH_2CH_2OCH_3}$$

$$cis\text{-}[Ru(bpy)_2(CO)H]^+ + CO_2 \quad (3)$$

to give 45% isolated yield after purification. A third route that gives exclusively monobipyridyl or phenanthroline complexes involves ligand substitution by the added polypyridine as shown in eq 4. The reaction of eq 4 proceeds in 85% yield as written and appears to be general for many different chelating polypyridyl ligands.

$$mer\text{-}Os(PPh_3)_3(CO)(Cl)H + \text{bpy} \xrightarrow[\substack{\Delta \\ 10\ min}]{HOCH_2CH_2OH}$$

$$trans\text{-}[Os(bpy)(PPh_3)_2(CO)H]^+ + Cl^- + PPh_3 \quad (4)$$

The complexes were purified as hexafluorophosphate salts by chromatography on alumina using toluene–acetonitrile mixtures as eluant in a manner that has been described previously.[9,10] The complexes are all water- and air-stable crystalline solids that are extensively soluble in polar solvents like CH₂Cl₂, acetone, and CH₃CN. Characterization of the complexes was achieved by elemental analysis, ¹H NMR spectroscopy, infrared spectroscopy, cyclic voltammetry, and, where appropriate, ³¹P NMR spectroscopy. Table I shows typical characterization data for the products.

As shown in the table the M–H stretch occurs between 2000 and 2100 cm⁻¹ for all the osmium complexes and is medium to weak in intensity compared to the carbonyl stretch that occurs below 2000 cm⁻¹ in all cases. It is interesting to note that for the complexes cis-[M(bpy)₂(CO)X]⁺ (M = Ru, Os; X = H, Cl) lower energy CO stretches occur for the hydrido complexes (Table I) apparently because of enhanced electron density at the metal center relative to Cl⁻ as the cis ligand.

The structures of the hydride complexes are readily assignable by use of NMR spectroscopy. For example, for

(4) Neyhart, G. A.; Marshall, J. A.; Dressick, W. J.; Sullivan, B. P.; Watkins, P. A.; Meyer, T. *J. J. Chem. Soc., Chem. Commun.* **1982**, 915.

(5) (a) van Houten, J.; Watts, R. J. *Inorg. Chem.* **1978**, 17, 3381. (b) Durham, B.; Caspar, J. V.; Nagle, J. K.; Meyer, T. J. *J. Am. Chem. Soc.* **1982**, 104, 4803.

(6) (a) Cole-Hamilton, D. J. *J. Chem. Soc., Chem. Commun.* **1980**, 1213. (b) Chou, M.; Creutz, C.; Mahajon, D.; Sutin, N.; Zipp, A. P. *Inorg. Chem.* **1982**, 21, 3989.
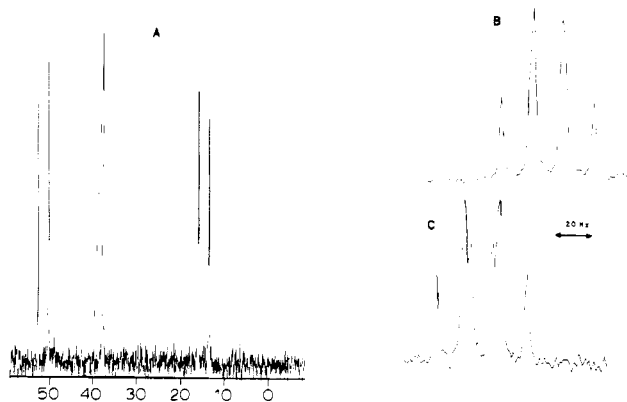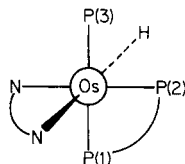
(7) See, for example: Darensbourg, D. J.; Rokicki, A.; Darensbourg, M. Y. *J. Am. Chem. Soc.* **1981**, 103, 3223.

(8) After this paper was submitted, a report appeared concerning the synthesis of cis-Ru(bpy)₂(CO)H⁺. See: Kelley, J. M.; Vos, J. G. *Angew. Chem., Int. Ed. Engl.* **1982**, 21, 628.

(9) Sullivan, B. P.; Salmon, D. J.; Meyer, T. J. *Inorg. Chem.* **1978**, 17, 3334.

(10) Connor, J. A.; Meyer, T. J.; Sullivan, B. P. *Inorg. Chem.* **1979**, 18, 1388.

Figure 1. (A) $^{31}P\{^1H\}$ NMR spectrum of [Os(phen)(1,2-$(Ph_2P)_2C_6H_4)(PPh_3)H](PF_6)$ in CH_3CN (see text). (B) ^1H NMR spectrum of [Os(phen)(1,2-$(Ph_2P)_2C_6H_4)(PPh_3)H](PF_6)$ in acetone in the hydride region. The apparent quartet is a doublet of triplets that is more easily seen for the analogous salt [Os(phen)(*cis*-Ph_2PCH=$CHPPh_2)(PPh_3)H](PF_6)$ in Figure 1C. (C) ^1H NMR spectrum of [Os(phen)(cis-Ph_2PCH=$CHPPh_2)(PPh_3)H](PF_6)$ in acetone solution.

the complexes [Os(phen)$_2$(CO)H]$^+$, [Os(bpy)$_2$(CO)H]$^+$, and [Ru(bpy)$_2$(CO)H]$^+$ the lack of symmetry in the ^1H NMR spectra for the polypyridyl ligand is consistent with the cis geometry. For *trans*-[Os(bpy)(PPh$_3$)$_2$(CO)H]$^+$ (where the PPh$_3$ groups are trans) the ^1H NMR spectrum also shows no symmetry, that is, four doublets and four triplets in first order. The hydride resonance is a triplet centered at -12.2 ppm (Me$_4$Si internal standard in δ units) with J_{P-H} = 20.8 Hz. The $^{31}P\{^1H\}$ NMR spectrum exhibits a single resonance at +19.4 ppm (85% H$_3$PO$_4$ as external standard, CH$_3$CN solution) that is consistent with magnetically equivalent phosphorus nuclei.

Of the three possible isomers for [Os(phen)(1,2-$(Ph_2P)_2C_6H_4)(PPh_3)(CO)H]^+$ the structure shown below is suggested on the basis of the following: (1) The lack

$$
\begin{array}{c}
\text{P(3)} \\
| \quad \diagup \text{H} \\
\text{N---(Os)---P(2)} \\
\diagdown \text{N} \quad | \\
\text{P(1)}
\end{array}
$$

of magnetic symmetry for the phen ligand by ^1H NMR spectroscopy; (2) the appearance of the hydride ligand resonance as two overlapping triplet patterns (Table I and Figure 1A); (3) the existence of three $^{31}P\{^1H\}$ NMR resonances in CH$_3$CN solution due to PPh$_3$ appearing as a doublet centered at +51.5 ppm ($J_{P_3-Os-P_1}$ = 247 Hz) while the dppb chelate phosphine resonances are found centered at +37.8 ppm (d, $J_{P_2-Os-P_1}$ = 13 Hz) and at +14.8 ppm (d of d, $J_{P_1-Os-P_3}$ = 247 Hz, $J_{P_1-Os-P_2}$ = 15 Hz) (Figure 1B). The isomer suggested by the NMR study is the least sterically crowded of the three possible isomers.

Cyclic voltammetry studies on the hydrido complexes in CH$_3$CN with tetraethylammonium perchlorate as supporting electrolyte vs. the saturated calomel reference electrode (SCE) show an irreversible oxidative process that is presumably a metal-based Os^{II} → Os^{III} or Ru^{II} → Ru^{III} oxidation followed by a rapid, irreversible chemical step. There are few examples of well-defined electrochemical studies on metal hydride complexes and the new complexes reported here provide an opportunity for such a study. Although irreversible in nature, the peak potential values (E_p) presumably provide at least a rough measure of the relative ability of the hydride ligand to stabilize the M(III) state over the M(II) state by enhanced σ donation. For

VOLTS (ssce)

Figure 2. Cyclic voltammograms of [Ru(bpy)$_2$(CO)X]PF$_6$ in 0.1 M tetraethylammonium perchlorate/CH$_3$CN medium taken at a Pt bead electrode. The potential for oxidation becomes less positive in the order X = Cl (A), X = H (B), and X = CH$_2$Ph (C). The cathodic processes are stepwise one-electron reductions of the coordinated bpy ligands. All potentials are reported vs. the saturated calomel electrode at a scan rate of 200 mV/s.

the series [Ru(bpy)$_2$(CO)X]$^+$, where X = PhCH$_2$,[11] H, OC(=O)H, or Cl, E_p or $E_{1/2}$ values are +0.76, +1.14, 1.44, and 1.50 V, respectively (Figure 2). Apparently the relative stabilization of Ru^{III} over Ru^{II} is more important for the benzyl group than for hydride, but hydride is in turn a better stabilizing ligand for Ru^{III} than either formate or chloride.

We are just beginning to investigate the thermal reactivity of the hydride ligand in these complexes; however, several interesting points have begun to emerge. For most of the complexes in Table I, addition of HPF$_6$ in CH$_3$CN solution at room temperature results in the rapid appearance of the acetonitrile complex by eq 5. For

$$[Os(bpy)_2(CO)H]^+ + H^+ \xrightarrow{CH_3CN}$$
$$[Os(bpy)_2(CO)CH_3CN]^{2+} + H_2 \quad (5)$$

trans-[Os(bpy)(PPh$_3$)$_2$(CO)H]$^+$ the reaction with acid does not occur even with prolonged heating. From the relative magnitudes of the E_p and ν(CO) values in Table I, the metal center in the latter complex appears to be relatively electron deficient and the metal–H bond less "hydridic" in character. The observation is significant since it suggests that the reactivity of the M–H bond in the ground state of these complexes can be tuned by making systematic variations in the remaining ligands.

The results of our initial photochemical and photophysical studies are revealing. The complexes absorb light

(11) Sullivan, B. P.; Smythe, R. S.; Kober, E. M.; Meyer, T. J. *J. Am. Chem. Soc.* **1982**, *104*, 1701.

strongly in the visible. For example, in acetonitrile λ_{max} for the lowest energy visible MLCT band in CH_3CN occurs at 445 nm for $[Ru(bpy)_2(CO)H](PF_6)$ (ϵ 3170) and at 499 nm for $[Os(phen)_2(CO)H](PF_6)$ (ϵ 5320). As can be seen from the data in Table I, the Os complexes represent rare examples of metal hydride complexes which luminesce in fluid solution at room temperature.[12] However, the complexes are weak emitters, ϕ_r for $[Os(bpy)_2(CO)H](PF_6)$ is 3.8×10^{-4} in CH_3CN at room temperature, and excited-state decay is dominated by nonradiative processes, $1/\tau_0 \simeq k_{nr}$. In this context the values of k_{nr} in Table I are worthy of note. Especially striking are the values for the non-CO-containing hydrides, $[Os(phen)(1,2-(Ph_2P)_2C_6H_4)(PPh_3)H]^+$ and $[Os(phen)(cis-Ph_2PCH=CHPPh_2)(PEt_3)H]^+$. Compared to our earlier results based on the series $(phen)OsL_4^{2+}$, values for k_{nr} are <35 and 10 times greater in magnitude than would have otherwise been predicted by the energy gap law.[3] The shortened lifetimes may have their origin in the intervention of ν-(Os–H) modes as acceptor vibrations for excited-state decay or, perhaps, in new decay channels involving chemical reactions based on the Os–H bond. We have observed that the complex $[Os(phen)_2(CO)H]^{2+}$ does undergo visible photolysis in oxygenated CH_3CN to give $[Os(phen)_2(CO)(CH_3CN)]^{2+}$ and that, when photolyzed in deoxygenated CH_3CN in the presence of the known electron acceptor, paraquat, 1,1'-dimethyl-4,4'-bipyridine(2+) (PQ^{2+}), both $Os(phen)_2(CO)(CH_3CN)]^{2+}$ and the reduced form of paraquat, PQ^+, appear in the solution. The latter reaction presages the appearance of new photochemical pathways for the metal hydride complexes. With related MLCT excited states of Os(II), PQ^{2+} quenching occurs by electron transfer, e.g., $Os(phen)_3^{2+*} + PQ^{2+} \rightarrow Os(phen)_3^{3+} + PQ^+$, and the systems are photochromic because the quenching step is followed by back electron transfer, $Os(phen)_3^{3+} + PQ^+ \rightarrow Os(phen)_3^{2+} + PQ^{2+}$.

(12) Geoffroy, G. L.; Wrighton, M. S. "Organometallic Photochemistry"; Academic Press: New York, 1979.

β-Hydride Elimination: Significance of the Temperature Dependence of the Kinetic Isotope Effect Associated with the Thermal Decomposition of n-Octyllithium[1a]

Ming-Yang Li[1b] **and Joseph San Filippo, Jr.***

Department of Chemistry, Rutgers University
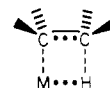*New Brunswick, New Jersey 08903*

Summary: The kinetic and kinetic isotope parameters associated with β-hydride elimination in n-octyllithium are

reported. The latter parameters are not perceptibly different—to a first approximation—from those generally associated with linear or near-linear transition states, indicating that four-center, cyclic hydrogen-transfer processes are not necessarily distinguished by uniquely characteristic kinetic isotope effect parameters.

The focus of much of modern chemical reaction dynamics is the transition state. We report here the results of our efforts to probe the nature of the transition state associated with β-hydride elimination, an important and fundamental process in organometallic chemistry.

Stereochemical and isotopic labeling studies of metal-alkyl decompositions and olefin rearrangements indicate that β-hydride elimination—together with its microscopic reverse, olefin insertion—is a stereospecific process, a fact which places rather severe restrictions on the structure of the associated transition state.[2] The transition-state geometry most consistent with the weight of these and related kinetic findings is the four-center, cyclic arrangement shown

In principle, the influence of temperature on the kinetic isotope effect (KIE) can provide insight into the geometry and nature of the transition state affiliated with a rate-determining, irreversible hydrogen transfer.[3] We have sought to apply this technique to characterize the geometry of the transition state generally ascribed to β-hydride elimination.

The thermal decomposition of n-butyllithium has been extensively studied and is generally recognized as proceeding through an irreversible, unimolecular β-hydride elimination.[4] As the results in Table I show, the corresponding decomposition of n-octyllithium exhibits a completely parallel behavior. Kinetically, the reaction is rigorously first-order, suggesting that the rate-determining step involves β-hydride elimination from a fully associated (probably hexameric)[5a] unit of n-octyllithium. Thus, prior dissociation of the dominant equilibrium structure into a more reactive, less associated intermediate species does not appear to be required.[5b] Also, the corresponding activation parameters are indistinguishable from those observed for n-butyllithium[6] which, in turn, are similar to those re-

(1) (a) Supported by the NSF, Grant CHE 80-17045, and the DOE, Contract No. DE-AS05-80ER10662. (b) Jilin University, Changchun, People's Republic of China.

(2) For a discussion, see: Collman, J. P.; Hegedus, L. S. "Principles and Applications of Organotransition Metal Chemistry"; University Science Books: Mill Valley, Calif., 1980; Chapter 5.

(3) (a) Melander, L.; Saunders, W. H., Jr. " Reaction Rates of Isotopic Molecules"; Wiley: New York, 1900. (b) More O'Ferrall, R. A. In "Proton-Transfer Reactions"; Caldin, E., Gold, V., Eds.; Wiley (Halsted Press): New York, 1900; Chapter 8.

(4) (a) Finnegan, R. A.; Kutta, H. W. *J. Org. Chem.* 1965, 30, 4139. (b) See also: Glaze, W. H.; Lin, J.; Felton, E. G. *Ibid.* 1966, 2643.

(5) (a) n-Butyllithium is hexameric in hexane [Brown, T. L. *Adv. Organomet. Chem.* 1965, 3, 365]. By extension we assume n-octyllithium is hexameric in decane. (b) In instances where the dissociation of an associated organolithium reagent into less associated but kinetically more reactive intermediate species take place, kinetic studies have shown that a fractional order generally obtains with respect to the organolithium reagent and that this order is usually the reciprocal of the degree of association of the organolithium compound; see: Wakefield, B. J. "The Chemistry of Organolithium Compounds"; Pergamon Press: New York, 1974; pp 98–100.

strongly in the visible. For example, in acetonitrile λ_{max} for the lowest energy visible MLCT band in CH_3CN occurs at 445 nm for $[Ru(bpy)_2(CO)H](PF_6)$ (ϵ 3170) and at 499 nm for $[Os(phen)_2(CO)H](PF_6)$ (ϵ 5320). As can be seen from the data in Table I, the Os complexes represent rare examples of metal hydride complexes which luminesce in fluid solution at room temperature.[12] However, the complexes are weak emitters, ϕ_r for $[Os(bpy)_2(CO)H](PF_6)$ is 3.8×10^{-4} in CH_3CN at room temperature, and excited-state decay is dominated by nonradiative processes, $1/\tau_0 \simeq k_{nr}$. In this context the values of k_{nr} in Table I are worthy of note. Especially striking are the values for the non-CO-containing hydrides, $[Os(phen)(1,2-(Ph_2P)_2C_6H_4)(PPh_3)H]^+$ and $[Os(phen)(cis-Ph_2PCH=CHPPh_2)(PEt_3)H]^+$. Compared to our earlier results based on the series $(phen)OsL_4^{2+}$, values for k_{nr} are <35 and 10 times greater in magnitude than would have otherwise been predicted by the energy gap law.[3] The shortened lifetimes may have their origin in the intervention of ν-(Os–H) modes as acceptor vibrations for excited-state decay or, perhaps, in new decay channels involving chemical reactions based on the Os–H bond. We have observed that the complex $[Os(phen)_2(CO)H]^{2+}$ does undergo visible photolysis in oxygenated CH_3CN to give $[Os(phen)_2(CO)(CH_3CN)]^{2+}$ and that, when photolyzed in deoxygenated CH_3CN in the presence of the known electron acceptor, paraquat, 1,1'-dimethyl-4,4'-bipyridine(2+) (PQ^{2+}), both $Os(phen)_2(CO)(CH_3CN)]^{2+}$ and the reduced form of paraquat, PQ^+, appear in the solution. The latter reaction presages the appearance of new photochemical pathways for the metal hydride complexes. With related MLCT excited states of Os(II), PQ^{2+} quenching occurs by electron transfer, e.g., $Os(phen)_3^{2+*} + PQ^{2+} \rightarrow Os(phen)_3^{3+} + PQ^+$, and the systems are photochromic because the quenching step is followed by back electron transfer, $Os(phen)_3^{3+} + PQ^+ \rightarrow Os(phen)_3^{2+} + PQ^{2+}$.

(12) Geoffroy, G. L.; Wrighton, M. S. "Organometallic Photochemistry"; Academic Press: New York, 1979.

β-Hydride Elimination: Significance of the Temperature Dependence of the Kinetic Isotope Effect Associated with the Thermal Decomposition of n-Octyllithium[1a]

Ming-Yang Li[1b] **and Joseph San Filippo, Jr.**[*]

Department of Chemistry, Rutgers University
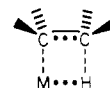*New Brunswick, New Jersey 08903*

Received October 12, 1982

Summary: The kinetic and kinetic isotope parameters associated with β-hydride elimination in n-octyllithium are

reported. The latter parameters are not perceptibly different—to a first approximation—from those generally associated with linear or near-linear transition states, indicating that four-center, cyclic hydrogen-transfer processes are not necessarily distinguished by uniquely characteristic kinetic isotope effect parameters.

The focus of much of modern chemical reaction dynamics is the transition state. We report here the results of our efforts to probe the nature of the transition state associated with β-hydride elimination, an important and fundamental process in organometallic chemistry.

Stereochemical and isotopic labeling studies of metal-alkyl decompositions and olefin rearrangements indicate that β-hydride elimination—together with its microscopic reverse, olefin insertion—is a stereospecific process, a fact which places rather severe restrictions on the structure of the associated transition state.[2] The transition-state geometry most consistent with the weight of these and related kinetic findings is the four-center, cyclic arrangement shown

In principle, the influence of temperature on the kinetic isotope effect (KIE) can provide insight into the geometry and nature of the transition state affiliated with a rate-determining, irreversible hydrogen transfer.[3] We have sought to apply this technique to characterize the geometry of the transition state generally ascribed to β-hydride elimination.

The thermal decomposition of n-butyllithium has been extensively studied and is generally recognized as proceeding through an irreversible, unimolecular β-hydride elimination.[4] As the results in Table I show, the corresponding decomposition of n-octyllithium exhibits a completely parallel behavior. Kinetically, the reaction is rigorously first-order, suggesting that the rate-determining step involves β-hydride elimination from a fully associated (probably hexameric)[5a] unit of n-octyllithium. Thus, prior dissociation of the dominant equilibrium structure into a more reactive, less associated intermediate species does not appear to be required.[5b] Also, the corresponding activation parameters are indistinguishable from those observed for n-butyllithium[6] which, in turn, are similar to those re-
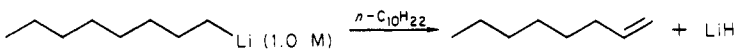
(1) (a) Supported by the NSF, Grant CHE 80-17045, and the DOE, Contract No. DE-AS05-80ER10662. (b) Jilin University, Changchun, People's Republic of China.

(2) For a discussion, see: Collman, J. P.; Hegedus, L. S. "Principles and Applications of Organotransition Metal Chemistry"; University Science Books: Mill Valley, Calif., 1980; Chapter 5.

(3) (a) Melander, L.; Saunders, W. H., Jr. " Reaction Rates of Isotopic Molecules"; Wiley: New York, 1900. (b) More O'Ferrall, R. A. In "Proton-Transfer Reactions"; Caldin, E., Gold, V., Eds.; Wiley (Halsted Press): New York, 1900; Chapter 8.
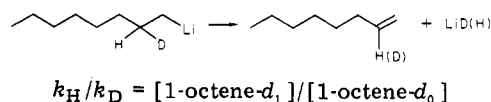
(4) (a) Finnegan, R. A.; Kutta, H. W. *J. Org. Chem.* 1965, *30*, 4139. (b) See also: Glaze, W. H.; Lin, J.; Felton, E. G. *Ibid.* 1966, 2643.

(5) (a) n-Butyllithium is hexameric in hexane [Brown, T. L. *Adv. Organomet. Chem.* 1965, *3*, 365]. By extension we assume n-octyllithium is hexameric in decane. (b) In instances where the dissociation of an associated organolithium reagent into less associated but kinetically more reactive intermediate species take place, kinetic studies have shown that a fractional order generally obtains with respect to the organolithium reagent and that this order is usually the reciprocal of the degree of association of the organolithium compound; see: Wakefield, B. J. "The Chemistry of Organolithium Compounds"; Pergamon Press: New York, 1974; pp 98–100.

Table I. Kinetic Parameters Associated with the Thermal Decomposition of *n*-Octyllithium[a]

T,[b] °C	$10^5 k_H$,[c] s^{-1}	k_H/k_D[d]	Arrhenius parameters
120.0	5.00	3.658$_2$	$E_H = 30.34 \pm 0.30$ kcal/mol
130.0	12.8	3.520$_3$	$A_H = 5.94 \times 10^{12}$
140.0	34.2	3.361$_6$	$\Delta S^\ddagger = -1.6$ eu
150.0	79.3	3.270$_7$	$r = 0.999$
			$[\Delta E]^H{}_D = 1.25 \pm 0.05$ kcal/mol
			$A_H/A_D = 0.724$
			$r = 0.996$

[a] Prepared by the reaction of di-*n*-octylmercury with excess lithium dispersion in *n*-decane. The concentration of *n*-octyllithium was determined by the Gilman double-titration procedure. Residual base level was ≤5% of the total base content. [b] A constant (±0.02 °C) temperature bath was employed. [c] Absolute rate constants were determined from plots of 1-octene vs. reaction time. [d] Relative rate constants were determined under competitive conditions employing (*n*-octyl-2-*d*₁)lithium. Values of k_H/k_D were determined by high-precision, whole-molecule mass spectrometry;[13] monitoring mass 112, 113, and 114 ions of the 1-octene-*d*₀ and -*d*₁ product mixture at 70 eV. Ratios were invariant with the extent of reaction.

$$k_H/k_D = [1\text{-octene-}d_1]/[1\text{-octene-}d_0]$$

ported for other processes for which a four-center, cyclic transition state has been proposed.[7]

However, the most telling of the kinetic parameters related to this process are those associated with the kinetic isotope effect. Thus, the magnitude of the zero-point-energy difference, $[\Delta E]^H{}_D = 1.25 \pm 0.05$ kcal/mol, is essentially equal to the standard zero-point-energy difference for a typical C–H/C–D bond, i.e., $[\Delta E_0]^H{}_D = 1.1 - 1.2$ kcal/mol, suggesting that β-elimination in this instance involves an essentially symmetrical H transfer.[8] Moreover, the value of the preexponential quantity, $A_H/A_D = 0.724$, falls within the range (~0.7–1.2) which generally suggests (but does not require) that hydrogen tunneling is insignificant.[9]

The magnitude of these parameters are noteworthy in at least one additional respect. They confirm the earlier conclusion[10] that a significanly nonlinear hydrogen transfer is *not* necessarily characterized, as has been suggested,[11] by (1) a KIE that is temperature-independent and (2) an Arrhenius preexponential factor that is significantly greater than $2^{1/2}$. Whether Arrhenius parameters of a characteristic magnitude are associated with four-center, cyclic hydrogen-transfer processes remains to be determined by additional experimental and theoretical modeling studies. However, on the basis of the results from the two available studies that have focused on reasonably unequivocal four-center, cyclic hydrogen-transfer processes, it is apparent that the temperature dependence of the KIE in these instances does not provide a ready means of distinguishing four-center, cyclic transition-state geometries from

those associated with linear or near-linear hydrogen transfers.[12]

(12) Such distinctions may prove possible, however, with appropriate computational modeling studies (cf. Stern, M. J.; Wolfsberg, M. *J. Pharm. Sci.* 1965, *54*, 84). We are currently exploring this approach.

(13) Cf. Rosenberg, S.; Kirsch, J. F. *Anal. Chem.* 1975, *51*, 1375.

A General Route to Chiral Clusters SCo₃(CO)₇LX. Synthesis, X-ray Structure, and Electrochemical Behavior of the New Cluster (μ₃-S)Co₃(CO)₇[μ-1,3-η²-NHC(CH₃)S]

Alain Benoit,† André Darchen,‡

Jean-Yves Le Marouille,† Christian Mahé,§ and

Henri Patin*§

Laboratoire de Chimie du Solide et Inorganique Moléculaire, L.A. CNRS No. 254
Laboratoire d'Electrochimie, E.R.A. CNRS No. 896
Laboratoire de Chimie des Organométalliques E.R.A. CNRS No. 477
Université de Rennes, Campus de Beaulieu
35042 Rennes Cedex, France

Summary: Reaction of R–C(S)NH₂ with Co₂(CO)₈ provides a one-step synthesis of the chiral clusters SCo₃-(CO)₇LX where LX is a three-electron bidentate ligand linked by nitrogen and sulfur to two cobalt atoms as shown by X-ray structure analysis. Two molecules of thioamide are consumed in the cluster formation process. One of them is desulfurized to give the corresponding nitrile while the other is retained in the complex to form the bidentate ligand after loss of one hydrogen atom. Electrochemical studies of the titled cluster and of parent compounds show that they can be reversibly reduced to paramagnetic species.

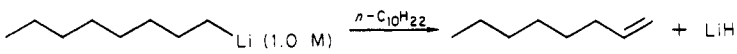(6) $E_a^H = 31$ kcal/mol; $10^5 k$ (140 °C) = 11.5 s^{-1}; $\Delta S_H^\ddagger = -1$ eu.

(7) (a) Maltman, K. R.; Tschuikow-Roux, Jung, K.-H. *J. Phys. Chem.* 1974, *78*, 1035. (b) Egger, K. W. *Int. J. Chem. Kinet.* 1969, *1*, 459.

(8) The term "symmetrical" and "unsymmetrical" hydrogen transfer refers solely to the restoring force constants in the transition-state molecule [A···H···B]*. Thus, a symmetrical (linear) transition state (which is also concerted in the Woodward–Hoffmann sense) is defined by the fact that $F_{A-H} = F_{B-H}$ while an unsymmetrical (linear) transition state is defined by F_{A-H} less than or greater than F_{B-H}.

(9) Bell, R. P. "The Tunnel Effect in Chemistry"; Chapman and Hall: New York, 1980; Chapter 3. It should be noted that the extention of this criterion to processes proceeding through significantly nonlinear transition states remains to be firmly established.
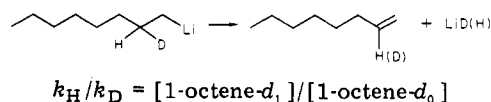
(10) Vitale, A. A.; San Filippo, J., Jr. *J. Am. Chem. Soc.* 1982, *104*, 7341.

(11) Kwart, H.; Brechbiel, M. *J. Am. Chem. Soc.* 1978, *100*, 635 and references therein. (b) Kwart, H.; Brechbiel, M.; Achenson, R. M.; Ward, D. C. *Ibid.* 1982, *104*, 4671. (c) Kwart, H.; Brechbiel, M. *J. Org. Chem.* 1982, *47*, 3353.

†Laboratoire de Chimie du Solide Inorganique Moléculaire.
‡Laboratoire d'Electrochimie.
§Laboratoire de Chimie des Organométalliques.

Table I. Kinetic Parameters Associated with the Thermal Decomposition of *n*-Octyllithium[a]

$T,$[b] °C	$10^5 k_H,$[c] s^{-1}	k_H/k_D[d]	Arrhenius parameters
120.0	5.00	3.658$_2$	E_H = 30.34 ± 0.30 kcal/mol
130.0	12.8	3.520$_3$	A_H = 5.94 × 10^{12}
140.0	34.2	3.361$_6$	$\Delta S^{\ddagger}$ = −1.6 eu
150.0	79.3	3.270$_7$	r = 0.999
			$[\Delta E]^H{}_D$ = 1.25 ± 0.05 kcal/mol
			A_H/A_D = 0.724
			r = 0.996

[a] Prepared by the reaction of di-*n*-octylmercury with excess lithium dispersion in *n*-decane. The concentration of *n*-octyllithium was determined by the Gilman double-titration procedure. Residual base level was ≤5% of the total base content. [b] A constant (±0.02 °C) temperature bath was employed. [c] Absolute rate constants were determined from plots of 1-octene vs. reaction time. [d] Relative rate constants were determined under competitive conditions employing (*n*-octyl-2-d_1)lithium. Values of k_H/k_D were determined by high-precision, whole-molecule mass spectrometry;[13] monitoring mass 112, 113, and 114 ions of the 1-octene-d_0 and -d_1 product mixture at 70 eV. Ratios were invariant with the extent of reaction.

$$k_H/k_D = [\text{1-octene-}d_1]/[\text{1-octene-}d_0]$$

ported for other processes for which a four-center, cyclic transition state has been proposed.[7]

However, the most telling of the kinetic parameters related to this process are those associated with the kinetic isotope effect. Thus, the magnitude of the zero-point-energy difference, $[\Delta E]^H{}_D$ = 1.25 ± 0.05 kcal/mol, is essentially equal to the standard zero-point-energy difference for a typical C–H/C–D bond, i.e., $[\Delta E_0]^H{}_D$ = 1.1 – 1.2 kcal/mol, suggesting that β-elimination in this instance involves an essentially symmetrical H transfer.[8] Moreover, the value of the preexponential quantity, A_H/A_D = 0.724, falls within the range (~0.7–1.2) which generally suggests (but does not require) that hydrogen tunneling is insignificant.[9]

The magnitude of these parameters are noteworthy in at least one additional respect. They confirm the earlier conclusion[10] that a significanly nonlinear hydrogen transfer is *not* necessarily characterized, as has been suggested,[11] by (1) a KIE that is temperature-independent and (2) an Arrhenius preexponential factor that is significantly greater than 2$^{1/2}$. Whether Arrhenius parameters of a characteristic magnitude are associated with four-center, cyclic hydrogen-transfer processes remains to be determined by additional experimental and theoretical modeling studies. However, on the basis of the results from the two available studies that have focused on reasonably unequivocal four-center, cyclic hydrogen-transfer processes, it is apparent that the temperature dependence of the KIE in these instances does not provide a ready means of distinguishing four-center, cyclic transition-state geometries from

those associated with linear or near-linear hydrogen transfers.[12]

(12) Such distinctions may prove possible, however, with appropriate computational modeling studies (cf. Stern, M. J.; Wolfsberg, M. *J. Pharm. Sci.* 1965, *54*, 84). We are currently exploring this approach.

(13) Cf. Rosenberg, S.; Kirsch, J. F. *Anal. Chem.* 1975, *51*, 1375.

A General Route to Chiral Clusters SCo$_3$(CO)$_7$LX. Synthesis, X-ray Structure, and Electrochemical Behavior of the New Cluster (μ_3-S)Co$_3$(CO)$_7$[μ-1,3-η^2-NHC(CH$_3$)S]

Alain Benoît,[†] André Darchen,[‡] Jean-Yves Le Marouille,[†] Christian Mahé,[§] and Henri Patin*[§]

Laboratoire de Chimie du Solide et Inorganique Moléculaire, L.A. CNRS No. 254
Laboratoire d'Electrochimie, E.R.A. CNRS No. 896
Laboratoire de Chimie des Organométalliques E.R.A. CNRS No. 477
Université de Rennes, Campus de Beaulieu
35042 Rennes Cedex, France

Summary: Reaction of R–C(S)NH$_2$ with Co$_2$(CO)$_8$ provides a one-step synthesis of the chiral clusters SCo$_3$-(CO)$_7$LX where LX is a three-electron bidentate ligand linked by nitrogen and sulfur to two cobalt atoms as shown by X-ray structure analysis. Two molecules of thioamide are consumed in the cluster formation process. One of them is desulfurized to give the corresponding nitrile while the other is retained in the complex to form the bidentate ligand after loss of one hydrogen atom. Electrochemical studies of the titled cluster and of parent compounds show that they can be reversibly reduced to paramagnetic species.

(6) $E_a{}^H$ = 31 kcal/mol; $10^5 k$ (140 °C) = 11.5 s^{-1}; $\Delta S_H{}^\ddagger$ = −1 eu.

(7) (a) Maltman, K. R.; Tschuikow-Roux, Jung, K.-H. *J. Phys. Chem.* 1974, *78*, 1035. (b) Egger, K. W. *Int. J. Chem. Kinet.* 1969, *1*, 459.

(8) The term "symmetrical" and "unsymmetrical" hydrogen transfer refers solely to the restoring force constants in the transition-state molecule [A⋯H⋯B]‡. Thus, a symmetrical (linear) transition state (which is also concerted in the Woodward–Hoffmann sense) is defined by the fact that F_{A-H} = F_{B-H} while an unsymmetrical (linear) transition state is defined by F_{A-H} less than or greater than F_{B-H}.

(9) Bell, R. P. "The Tunnel Effect in Chemistry"; Chapman and Hall: New York, 1980; Chapter 3. It should be noted that the extention of this criterion to processes proceeding through significantly nonlinear transition states remains to be firmly established.

(10) Vitale, A. A.; San Filippo, J., Jr. *J. Am. Chem. Soc.* 1982, *104*, 7341.

(11) Kwart, H.; Brechbiel, M. *J. Am. Chem. Soc.* 1978, *100*, 635 and references therein. (b) Kwart, H.; Brechbiel, M.; Achenson, R. M.; Ward, D. C. *Ibid.* 1982, *104*, 4671. (c) Kwart, H.; Brechbiel, M. *J. Org. Chem.* 1982, *47*, 3353.

[†]Laboratoire de Chimie du Solide Inorganique Moléculaire.
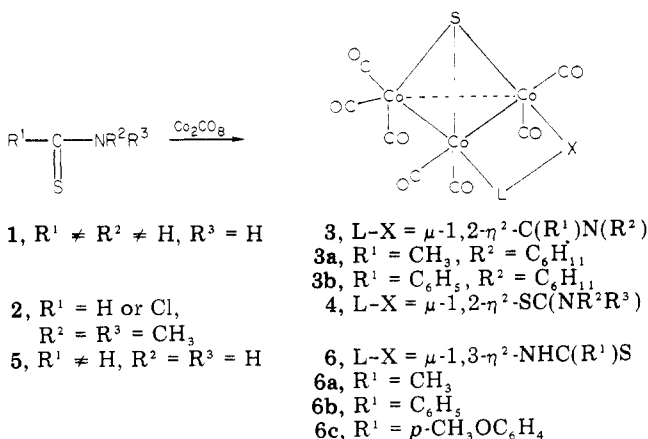[‡]Laboratoire d'Electrochimie.
[§]Laboratoire de Chimie des Organométalliques.

Table I. Most Relevant Bond Lengths (Å) and Angles (deg) with Their Esds

Bond Lengths

S(1)-Co(1)	2.152 (1)	S(2)-C(8)	1.700 (4)	Co(1)-Co(2)	2.480 (1)
S(1)-Co(2)	2.147 (1)	N(1)-C(8)	1.286 (6)	Co(2)-Co(3)	2.525 (1)
S(1)-Co(3)	2.173 (1)	N(1)-Co(2)	1.955 (4)	Co(1)-Co(3)	2.509 (1)
S(2)-Co(1)	2.265 (1)				

Bond Angles

S(2)-C(8)-N(1)	123.8 (3)	C(8)-N(1)-Co(2)	127.6 (3)	Co(1)-Co(2)-Co(3)	60.2 (2)
S(2)-C(8)-C(9)	115.6 (3)	Co(1)-S(1)-Co(2)	70.5 (4)	Co(2)-Co(3)-Co(1)	59.0 (2)
C(9)-C(8)-N(1)	120.5 (4)	Co(2)-S(1)-Co(3)	71.5 (4)	Co(2)-Co(1)-Co(3)	60.8 (2)
Co(1)-S(2)-C(8)	104.7 (2)	Co(1)-S(1)-Co(3)	70.9 (4)		

Metal cluster chemistry is a rapidly developing area in inorganic and organometallic chemistry,[1] and among clusters the family of tricobalt carbonyl complexes has been widely studied[2] with some emphasis on their potential application in homogeneous catalysis.[3] This has led to the development of new synthetic methods to obtain chiral clusters that would be suitable species to examine the process of chiral synthesis in cluster-catalyzed reactions.[4]

The reactions of dicobalt octacarbonyl with either elemental sulfur or sulfur-containing molecules [e.g., H_2S, RSH, R_2S, CS_2, $R^1OC(S)SR^2$, $R^1C(S)SR^2$][5-9] has given rise to a large variety of polynuclear cobalt complexes that contain either sulfur, sulfur and the organic residue, or only the desulfurized starting material. Recently, we have reported that substrates such as 1 or 2, on reaction with $Co_2(CO)_8$, give new tricobalt heptacarbonyl sulfide complexes 3 or 4 that contain a bridging (μ-1,2-η^2-LX) ligand.[10,11]

1, $R^1 \neq R^2 \neq$ H, R^3 = H

2, R^1 = H or Cl,
   $R^2 = R^3 = CH_3$

5, $R^1 \neq$ H, $R^2 = R^3 = H$

3, L-X = μ-1,2-η^2-C(R^1)N(R^2)
3a, $R^1 = CH_3$, $R^2 = C_6H_{11}$
3b, $R^1 = C_6H_5$, $R^2 = C_6H_{11}$
4, L-X = μ-1,2-η^2-SC(NR^2R^3)

6, L-X = μ-1,3-η^2-NHC(R^1)S
6a, $R^1 = CH_3$
6b, $R^1 = C_6H_5$
6c, $R^1 = p$-CH$_3$OC$_6$H$_4$

These results are in contrast with the case of xanthates[7] and dithioesters[8] in that a nitrogen atom α to a thiocarbonyl group is not removed but plays the role of a donor center. Obviously, an elimination step is necessary, as

Figure 1. ORTEP drawing of (μ_3-S)Co$_3$(CO)$_7$[μ-1,3-η^2-NHC(CH$_3$)S]. Probability ellipsoids are at the 50% level.

shown by the removal of hydrogen[10] or chlorine,[11] and we have found that compounds of type R^1-C(S)NR$_2$ ($R^1 \neq R^2 \neq$ H) do not produce clusters. We have examined the case of primary thioamides 5, which in principle should behave like compounds of type 1, but we find that they react in a different manner. As found for 1, one hydrogen atom is removed, but as in the case of compound 2, two molecules of thioamide are required. One of these is converted to the corresponding nitrile, while the second is retained in the cluster where it plays the role of a bidentate, triatomic ligand coordinated to two cobalt atoms by nitrogen and sulfur.

We report in this paper that clusters of type 6, obtained by reaction of R-C(S)NH$_2$ with Co$_2$(CO)$_8$, are of general formula (μ_3-S)Co$_3$(CO)$_7$[μ-1,3-η^2-NHC(R)S]. Like clusters 3 and 4, clusters of type 6 are intrinsically chiral as a result of the dissymmetry of the bridging ligands LX.

Reaction of 5 (R^1 = Me, Ph, p-MeOPh) with Co$_2$(CO)$_8$ in THF for 18 h at room temperature under argon gave complexes 6 and the corresponding nitriles.[12] Spectroscopic characterization of the products showed strong infrared absorptions (1990-2110 cm^{-1}) in the terminal carbonyl region and at 3300 cm^{-1} (NH vibration). ^{1}H and ^{13}C NMR, mass spectral and analytical data are in agreement with the incorporation of 1 mol of ligand 5 minus one hydrogen atom per mole of cluster.

In order to obtain complete information on these clusters, a single-crystal X-ray diffraction study of complex

(1) E. L. Muetterties, *J. Organomet. Chem.*, **200**, 177 (1980).

(2) D. Seyferth, *Adv. Organomet. Chem.*, **14**, 97 (1976).

(3) C. U. Pittman and R. C. Ryan, *CHEM. TECH.*, **8**, 170 (1978).

(4) H. Beurich and H. Vahrenkamp, *Angew. Chem., Int. Ed. Engl.*, **20**, 98 (1981).

(5) L. Markó, G. Bor, E. Klumpp, B. Markó, and G. Almasy, *Chem. Ber.*, **96**, 955 (1963).

(6) C. H. Wei and L. F. Dahl, *Inorg. Chem.*, **6**, 1229 (1967); D. L. Stevenson, V. R. Magnuson, and L. F. Dahl, *J. Am. Chem. Soc.*, **89**, 3727 (1967) and references cited.

(7) G. Mignani, H. Patin, and R. Dabard, *J. Organomet. Chem.*, **169**, C19 (1979).

(8) H. Patin, G. Mignani, and M. T. Van Hulle, *Tetrahedron Lett.*, 2441 (1979).

(9) L. Stanghellini, G. Gervasio, R. Rossetti, and G. Bor, *J. Organomet. Chem.*, **187**, C37 (1980).

(10) H. Patin, G. Mignani, C. Mahé, J. Y. Le Marouille, A. Benoit, D. Grandjean, and G. Levesque, *J. Organomet. Chem.*, **208**, C39 (1981).

(11) C. Mahé, H. Patin, A. Benoit, and J. Y. Le Marouille, *J. Organomet. Chem.*, **216**, C15 (1981).
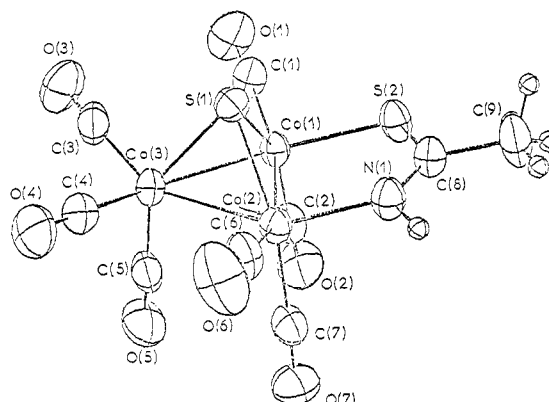
(12) Co$_2$(CO)$_8$ (8 mmol), thio amide 5 (5 mmol), and anhydrous THF (10 mL). The products were purified by TLC on silica gel using hexane-ether (3/2), and clusters 6 were crystallized from CH$_2$Cl$_2$-pentane. Benzonitrile and p-methoxybenzonitrile also were recovered from the plates and characterized by IR and ^{1}H NMR spectroscopy; acetonitrile, PhCN, and p-MeOC$_6$H$_4$CN also were identified by GLC analysis of the reaction mixture. **6a** (R^1 = Me): 62%; C$_9$H$_4$NO$_7$S$_2$Co$_3$; mp 110-112 °C dec. **6b** (R^1 = Ph): 48%; C$_{14}$H$_6$NO$_7$S$_2$Co$_3$; mp 144-146 °C dec. **6c** (R^1 = p-MeOPh): 58%; C$_{15}$H$_8$NO$_8$S$_2$Co$_3$; mp 125-130 °C dec. Elemental analyses were performed by "Le Service Central d'Analyse", CNRS, Vernaison. Satisfactory analytical data (±0.4%) for the elements C, H, Co, N, and S were obtained for all new compounds.

Chart I

$$3 \qquad 4 \qquad 6$$

6a was performed.[13] An ORTEP plot of the cluster is shown on Figure 1, and selected bond distances and angles are presented in Table I. The molecular geometry, as far as the tricobalt sulfide pyramid is concerned, closely resembles those reported before.[6,10,11] The ligand occupies two equatorial positions and is linked to Co(1) and Co(2), respectively, by S(2) and N(1). The plane formed by S(2), N(1), and C(8) makes a dihedral angle of 13° with the metallic triangle. The interatomic distance C(8)–N(1) (in the range of carbon–nitrogen double bonds) and the values of the angles around C(8) agree with a sp^2 hybridization for this carbon atom.[15] The C(8)–S(2) bond length [1.700 (4) Å] is closer to the value of a carbon–sulfur single bond than to that of a carbon–sulfur double bond [1.741 (2) vs. 1.634 (3) Å, respectively].[16] Although these characteristics of the ligand seem to favor a canonical formula such as 7, the small difference found between the S(1)–Co(1) and S(1)–Co(2) bond lengths [2.152 (1) and 2.147 (1) Å, respectively], which are both significantly shorter than S(1)–Co(3) [2.173 (1) Å], lead us to prefer an alternative valence bond formulation such as 8 in which there is electron delocalization over the six atoms concerned.

$$7 \qquad 8$$
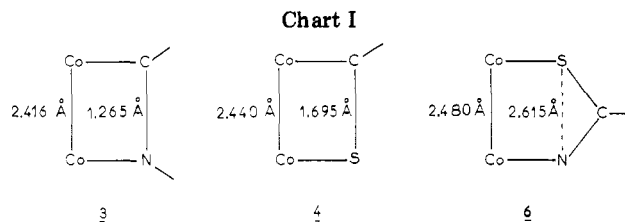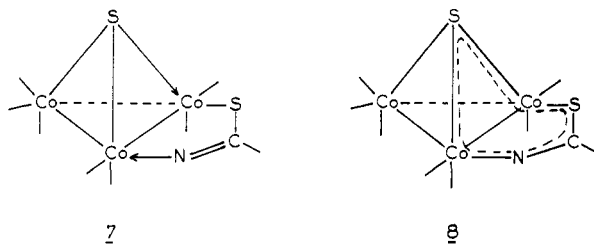
Clusters 3, 4, and 6, which possess the same skeleton as the paramagnetic parent complex SCo$_3$(CO)$_9$, previously described,[6] are diamagnetic, in agreement with the replacement of two molecules of carbon monoxide by a three-electron bidentate ligand which in every case introduces significant modifications on the SCo$_3$ framework. Comparison with the paramagnetic symmetrical cluster SCo$_3$(CO)$_9$ [mean value of the metal–metal bond length 2.637 (3) Å][6] shows that in our case the metallic triangle is never equilateral and that the metal–metal bond distances are always shorter. This lengthening of the metal–metal bonds and the concomitant shortening of the metal–sulfur bonds in the paramagnetic species [with respect to the heteronuclear diamagnetic cluster SFeCo$_2$-

(CO)$_9$] has been interpreted by Dahl[17] to be the result of the delocalization of the unpaired electron into antibonding orbitals of high metallic character.

Our results on these diamagnetic tricobalt sulfur clusters are in agreement with the latter interpretation, but, moreover, we can see that the bridging ligand influences dramatically the opposite metal–metal bond length. As shown on Chart I, modification of the geometrical constraint imposed by the bridge results in the progressive lengthening of the metal–metal bond. This "decompression effect", well documented in dinuclear complexes, does not seem to have been noted before in trinuclear clusters.

Owing to the identity of the metallic framework of 3, 4, and 6 with that of SCo$_3$(CO)$_9$, it was of interest to study their electrochemical behavior and to compare the relative stabilities of the various redox species. As shown by Dahl,[17] any electron in excess of the closed-shell electronic configuration for each metal atom in a triangular metal cluster system will occupy primarily an antibonding metal σ orbital localized in the plane of the metal atoms whose energy level will have only little dependence on the nature of the ligands, provided that the same metallic framework is concerned. Following these conclusions, the energy levels of the LUMO can be correlated with the values of standard potentials, and for a family of clusters one can expect a reversible electron transfer in the same potential range. In order to avoid decomposition of the clusters (especially 6) in dimethyl formamide, we have carried out the measurements also in dichloromethane. The basic electrode processes are similar in both solvents, and we have found that clusters 3, 4, and 6 show the expected reversible one-electron reduction in the relatively narrow range of potentials –0.4 to –0.8 V vs. SCE (see Table II). The cluster radical anions are stable enough under an inert atmosphere to allow a full reversible voltammetric behavior at scan rates as low as 10 mV·s^{-1} (except for 4). The small difference between the redox potentials may be interpreted by taking into account the electronegativities or the electronic effects of the bridging ligands LX. The presence of additional waves on the reverse scan of the voltammogram suggest that fragmentation occurs during the irreversible four-electron oxidation of clusters (near + 1.2 V SCE) or during the irreversible addition of a second electron to the cluster radical anion. It is noteworthy that (alkylidyne)tricobalt nonacarbonyl clusters which have the same metallic framework as 3, 4, and 6 show similar electrochemical behavior under the same conditions.[18,19]

Table II. Electrochemical Data Obtained by Cyclic Voltammetry at a Platinum Electrode for the Process: Cluster + 1e$^-$ ⇄ Cluster$^-$.

	$E°,^a$ V	
cluster	in DMF^b	in CH$_2$Cl$_2^c$
3a	–0.67	
3b	–0.63	–0.80
4	–0.67	–0.82
6a	–0.44	–0.52
6b		–0.49

^{a} Without correction vs. aqueous SCE scan rate 0.1 V· s^{-1} at room temperature; concentration of cluster 2 × 10^{-3} M. ^{b} 0.1 M Bu$_4$N$^+$BF$_4^-$ in dimethylformamide; $|E_{p_a}| - |E_{p_c}| = 60$ mV; $i_{p_a}/i_{p_c} = 1.0$. ^{c} 0.2 M Bu$_4$N$^+$BF$_4^-$; $|E_{p_a}| - |E_{p_c}| = 100$ mV; $i_{p_a}/i_{p_c} = 1.0$.

(13) Crystal data for complex 6a: space group $P2_1/n$, a = 9.298 (7) Å, b = 22.913 (4) Å; c = 7.928 (7) Å, α = 90.0°, β = 112.85 (2)°, γ = 90.0 (0)°; Z = 4; ρ(calcd) = 2.04 g·cm^{-3}. The structure was solved by Patterson and difference Fourier techniques and refined by full-matrix least-squares procedures: R = 0.033 and R_ω = 0.047 using reflections with $I > 2\sigma(I)$. All the structural calculations were performed on a PDP 11/60 computer with the SDP package.[14]

(14) B. A. Frenz, 1978, in M. Schenk and R. Olthof-Hazekamp (Eds.), Enraf-Nonius CAD4-SDP, a real-time system for concurrent X-ray data collection and crystal structure determination. Computing in Crystallography.

(15) In ^{13}C NMR the chemical shift corresponding to C(8) is δ 206 vs. δ 199 in the ligand (CDCl$_3$, Me$_4$Si, 20.115 MHz).

(16) H. Patin, G. Mignani, C. Mahé, J. Y. Le Marouille, A. Benoit, and D. Grandjean, *J. Organomet. Chem.*, **193**, 93 (1980).

(17) C. E. Strouse and L. F. Dahl, *Discuss. Faraday Soc.*, **47**, 93 (1969); *J. Am. Chem. Soc.*, **93**, 6032 (1969).

(18) J. C. Kotz, J. V. Petersen, and R. C. Reed, *J. Organomet. Chem.*, **120**, 433 (1976).

Considering the large interest in single electron-transfer processes that are regarded as important pathways in organic chemistry[20,21] and biochemistry, the study of such radical species may shed light on questions such as electron transfer and adsorption at metal surfaces. Connected to the latter point is the replacement of carbon monoxide by a phosphorus ligand promoted by the temporary addition of one electron. This reaction can be regarded as a model for adsorption on an electrode surface: $L_nM_{n'}(CO)_x + L' \rightarrow L_nM_{n'}(CO)_{x-1}L' + CO$. Whether the supplementary electron favors the departure of a ligand to offer a vacant coordination site or gives rise to the rupture of a metal–metal bond remains a subject of discussion, although this may well depend on the cluster and/or the type of reaction.[22,23]

These questions, as well as the synthesis of optically active clusters, are currently under investigation.

Supplementary Material Available: Listings of positional and thermal atomic parameters and experimental and calculated structure factors (21 pages). Ordering information is given on any current masthead page.

(19) A. M. Bond, B. M. Peake, B. A. Robinson, J. Simpson, and D. J. Watson, *Inorg. Chem.*, 16, 410 (1977).

(20) K. A. Bilevitch and O. Yu. Okhlobystin, *Russ. Chem. Rev. (Engl. Transl.)* 37, 954 (1968).

(21) M. Chanon and M. L. Tobe, *Angew. Chem., Int. Ed. Engl.*, 21, 1 (1982).

(22) G. J. Bezems, P. H. Rieger, and S. Visco, *J. Chem. Soc., Chem. Commun.*, 265 (1981).

(23) A. Darchen, C. Mahé, and H. Patin, *J. Chem. Soc., Chem. Commun.*, 243 (1982).

η⁵-C₅H₅Fe(CO)₂(η¹-C₅H₅). A Synthetic Equivalent of 5-Carbomethoxycyclopentadiene in Cycloaddition Reactions

Michael E. Wright

Department of Chemistry, University of Arizona
Tucson, Arizona 85721

Received November 1, 1982

Summary: Reaction of η⁵-C₅H₅Fe(CO)₂(η¹-C₅H₅) (1) with maleic anhydride, dimethyl fumarate, dimethyl acetylene-dicarboxylate, and 2-chloroacrylonitrile resulted in the formation of the expected *syn*-7-[η⁵-C₅H₅Fe(CO)₂]-bicyclo[2.2.1]hept-5-ene derivatives. Treatment of the latter three adducts with 6 equiv of ammonium cerium(IV) nitrate in CO-saturated methanol produced the *syn*-7-carbomethoxynorbornene compounds in good yields. The molecular and crystal structure of *syn*-7-[η⁵-C₅H₅Fe-(CO)₂]-bicyclo[2.2.1]hept-5-ene-2,3-*endo*-dicarboxylic anhydride (2) was determined by X-ray diffraction. Complex 2 crystallizes in the space group $P2_1/c$ with $a =$ 15.626 (3) Å, $b =$ 6.596 (3) Å, $c =$ 14.239 (5) Å, and $\beta =$ 99.05 (2)° with $Z = 4$. The structure was refined to $R_1 = 0.041$ and $R_2 = 0.045$ for 1737 independent reflections having $I > 3.0\sigma(I)$.
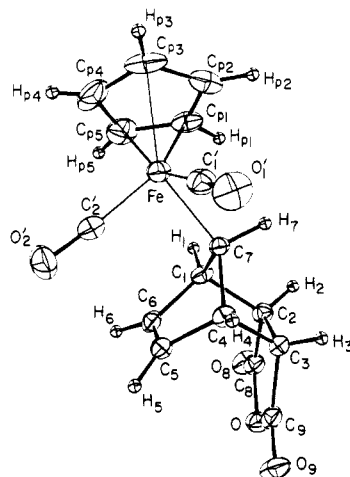

Figure 1. A perspective ORTEP drawing of *syn*-7-[η⁵-C₅H₅Fe-(CO)₂]-bicyclo[2.2.1]hept-5-ene-2,3-*endo*-dicarboxylic anhydride (2) with non-hydrogen atoms represented by thermal vibration ellipsoids drawn to encompass 30% of the electron density. Hydrogen atoms are represented by arbitrarily small spheres for clarity.

Table I. Selected Geometric Parameters in Crystalline *syn*-7-[η⁵-C₅H₅Fe(CO)₂]-bicyclo[2.2.1]hept-5-ene-2,3-*endo*-dicarboxylic Anhydride (2)^a

atom type ^{b}	bond length, Å	atom type ^{b}	bond angle, deg
Fe–C₇	2.061 (4)	C₇–Fe–C₁'	86.2 (2)
Fe–C₁'	1.758 (5)	C₇–Fe–C₂'	94.4 (2)
Fe–C₂'	1.757 (6)	C₇–C₁–C₂	97.9 (3)
C₁–C₂	1.580 (6)	C₇–C₁–C₆	102.0 (3)
C₁–C₇	1.547 (6)	C₂–C₁–C₆	106.5 (3)
C₁–C₆	1.507 (6)	C₁–C₂–C₃	102.8 (3)
C₂–C₃	1.532 (6)	C₂–C₃–C₄	103.2 (3)
C₃–C₄	1.580 (6)	C₇–C₄–C₃	99.2 (3)
C₄–C₅	1.516 (6)	C₇–C₄–C₅	101.8 (3)
C₄–C₇	1.544 (6)	C₃–C₄–C₅	104.2 (3)
C₅–C₆	1.320 (7)	C₄–C₅–C₆	107.7 (3)
		C₁–C₆–C₅	108.0 (3)
		Fe–C₇–C₁	119.6 (3)
		Fe–C₇–C₄	119.5 (3)
		C₁–C₇–C₄	93.2 (3)

^{a} The numbers in parentheses are the estimated standard deviations in the last significant digit. ^{b} Atoms are labeled in agreement with Figure 1.

Although 5-substituted cyclopentadienes are attractive synthetic reagents in cycloaddition reactions,[1] they are thermally unstable[2] and require highly reactive dienophiles. A compound that is thermally stable, but reactive in cycloadditions, and could function as an equivalent of 5-substituted cyclopentadienes would consequently provide a valuable synthetic tool. We report here the use of the Fp(η¹-C₅H₅) [Fp = η⁵-C₅H₅Fe(CO)₂] (1) complex[3] as a new synthetic equivalent for 5-carbomethoxycyclopentadiene. This method allows the regio- and stereoselective synthesis of some new *syn*-7-carbomethoxynorbornenes.

(1) Ranganathan, S.; Ranganathan, D.; Mehrotra, A. K. *Synthesis* 1977, 295.

(2) 5-Substituted cyclopentadienes readily undergo tautomerization into the thermodynamically stable 1- and 2-substituted cyclopentadienes. Mironov, V. A.; Sobolev, E. V.; Elizarova, A. N. *Tetrahedron* 1963, 19, 1939. Mclean, S.; Haynes, P. *Ibid.* 1965, 21, 2329.

(3) Complex 1 was prepared by the method of: Wilkinson, G.; Piper, T. S. *J. Inorg. Nucl. Chem.* 1956, 2, 32. In our hands 1 was obtained with contamination by ferrocene (~20%) after column chromatography (alumina III, petroleum ether). We found it most suitable to use this mixture in the cycloaddition reactions since removal of the ferrocene from the adducts was easily accomplished by column chromatography.

Considering the large interest in single electron-transfer processes that are regarded as important pathways in organic chemistry[20,21] and biochemistry, the study of such radical species may shed light on questions such as electron transfer and adsorption at metal surfaces. Connected to the latter point is the replacement of carbon monoxide by a phosphorus ligand promoted by the temporary addition of one electron. This reaction can be regarded as a model for adsorption on an electrode surface: $L_nM_{n'}(CO)_x + L'$ → $L_nM_{n'}(CO)_{x-1}L' + CO$. Whether the supplementary electron favors the departure of a ligand to offer a vacant coordination site or gives rise to the rupture of a metal-metal bond remains a subject of discussion, although this may well depend on the cluster and/or the type of reaction.[22,23]

These questions, as well as the synthesis of optically active clusters, are currently under investigation.

Supplementary Material Available: Listings of positional and thermal atomic parameters and experimental and calculated structure factors (21 pages). Ordering information is given on any current masthead page.

(19) A. M. Bond, B. M. Peake, B. A. Robinson, J. Simpson, and D. J. Watson, *Inorg. Chem.*, 16, 410 (1977).

(20) K. A. Bilevitch and O. Yu. Okhlobystin, *Russ. Chem. Rev. (Engl. Transl.)* 37, 954 (1968).

(21) M. Chanon and M. L. Tobe, *Angew. Chem., Int. Ed. Engl.*, 21, 1 (1982).

(22) G. J. Bezems, P. H. Rieger, and S. Visco, *J. Chem. Soc., Chem. Commun.*, 265 (1981).

(23) A. Darchen, C. Mahé, and H. Patin, *J. Chem. Soc., Chem. Commun.*, 243 (1982).

η5-C5H5Fe(CO)2(η1-C5H5). A Synthetic Equivalent of 5-Carbomethoxycyclopentadiene in Cycloaddition Reactions

Michael E. Wright

Department of Chemistry, University of Arizona
Tucson, Arizona 85721

Received November 1, 1982

Summary: Reaction of η5-C5H5Fe(CO)2(η1-C5H5) (1) with maleic anhydride, dimethyl fumarate, dimethyl acetylenedicarboxylate, and 2-chloroacrylonitrile resulted in the formation of the expected syn-7-[η5-C5H5Fe(CO)2]-bicyclo[2.2.1]hept-5-ene derivatives. Treatment of the latter three adducts with 6 equiv of ammonium cerium(IV) nitrate in CO-saturated methanol produced the syn-7-carbomethoxynorbornene compounds in good yields. The molecular and crystal structure of syn-7-[η5-C5H5Fe-(CO)2]-bicyclo[2.2.1]hept-5-ene-2,3-endo-dicarboxylic anhydride (2) was determined by X-ray diffraction. Complex 2 crystallizes in the space group $P2_1/c$ with a = 15.626 (3) Å, b = 6.596 (3) Å, c = 14.239 (5) Å, and β = 99.05 (2)° with Z = 4. The structure was refined to R_1 = 0.041 and R_2 = 0.045 for 1737 independent reflections having $I > 3.0\sigma(I)$.
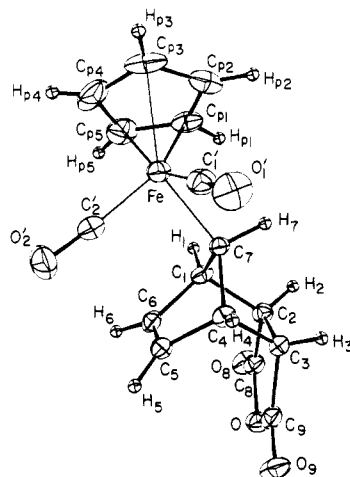

Figure 1. A perspective ORTEP drawing of syn-7-[η5-C5H5Fe-(CO)2]-bicyclo[2.2.1]hept-5-ene-2,3-endo-dicarboxylic anhydride (2) with non-hydrogen atoms represented by thermal vibration ellipsoids drawn to encompass 30% of the electron density. Hydrogen atoms are represented by arbitrarily small spheres for clarity.

Table I. Selected Geometric Parameters in Crystalline syn-7-[η5-C5H5Fe(CO)2]-bicyclo[2.2.1]hept-5-ene-2,3-endo-dicarboxylic Anhydride (2)[a]

atom type[b]	bond length, Å	atom type[b]	bond angle, deg
Fe-C7	2.061 (4)	C7-Fe-C1'	86.2 (2)
Fe-C1'	1.758 (5)	C7-Fe-C2'	94.4 (2)
Fe-C2'	1.757 (6)	C7-C1-C2	97.9 (3)
C1-C2	1.580 (6)	C7-C1-C6	102.0 (3)
C1-C7	1.547 (6)	C2-C1-C6	106.5 (3)
C1-C6	1.507 (6)	C1-C2-C3	102.8 (3)
C2-C3	1.532 (6)	C2-C3-C4	103.2 (3)
C3-C4	1.580 (6)	C7-C4-C3	99.2 (3)
C4-C5	1.516 (6)	C7-C4-C5	101.8 (3)
C4-C7	1.544 (6)	C3-C4-C5	104.2 (3)
C5-C6	1.320 (7)	C4-C5-C6	107.7 (3)
		C1-C6-C5	108.0 (3)
		Fe-C7-C1	119.6 (3)
		Fe-C7-C4	119.5 (3)
		C1-C7-C4	93.2 (3)

[a] The numbers in parentheses are the estimated standard deviations in the last significant digit. [b] Atoms are labeled in agreement with Figure 1.

Although 5-substituted cyclopentadienes are attractive synthetic reagents in cycloaddition reactions,[1] they are thermally unstable[2] and require highly reactive dienophiles. A compound that is thermally stable, but reactive in cycloadditions, and could function as an equivalent of 5-substituted cyclopentadienes would consequently provide a valuable synthetic tool. We report here the use of the Fp(η1-C5H5) [Fp = η5-C5H5Fe(CO)2] (1) complex[3] as a new synthetic equivalent for 5-carbomethoxycyclopentadiene. This method allows the regio- and stereoselective synthesis of some new syn-7-carbomethoxynorbornenes.

(1) Ranganathan, S.; Ranganathan, D.; Mehrotra, A. K. *Synthesis* 1977, 295.

(2) 5-Substituted cyclopentadienes readily undergo tautomerization into the thermodynamically stable 1- and 2-substituted cyclopentadienes. Mironov, V. A.; Sobolev, E. V.; Elizarova, A. N. *Tetrahedron* 1963, 19, 1939. Mclean, S.; Haynes, P. *Ibid.* 1965, 21, 2329.

(3) Complex 1 was prepared by the method of: Wilkinson, G.; Piper, T. S. *J. Inorg. Nucl. Chem.* 1956, 2, 32. In our hands 1 was obtained with contamination by ferrocene (~20%) after column chromatography (alumina III, petroleum ether). We found it most suitable to use this mixture in the cycloaddition reactions since removal of the ferrocene from the adducts was easily accomplished by column chromatography.

Scheme I
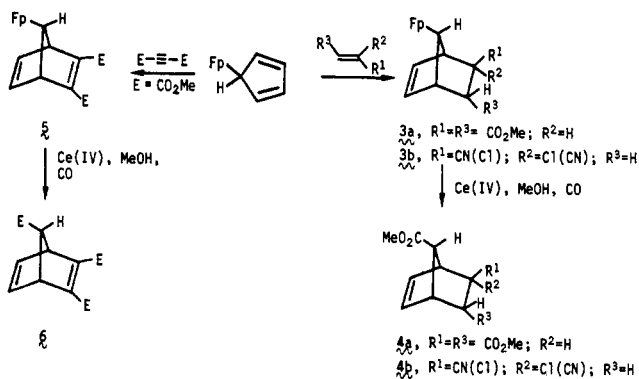
Complex 1 is recognized to react with electrophilic olefins and alkynes to give cycloadducts in a regio- and stereoselective manner on the basis of spectroscopic data.[4] To verify the stereochemistry in these adducts, we undertook a single-crystal X-ray study[5] of the new cycloadduct 2 that is obtained from the reaction of 1 in CH_2Cl_2 at 0 °C with maleic anhydride (eq 1).[6] The structure of 2 is displayed in Figure 1, and selected geometric parameters are given in Table I.
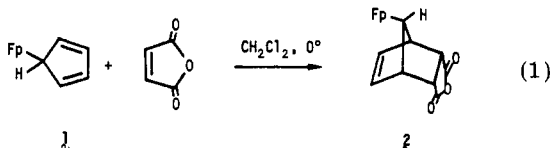
The molecular and crystal structure of 2 indicate how the geometry of the bicyclo[2.2.1]hept-5-ene unit is adjusted to accommodate the steric requirement of the iron moiety. Expansion of the $C_1–C_7$–Fe and $C_4–C_7$–Fe angles is clearly a result of the bulky metal group and is also seen in other related (bicyclo[2.2.1]heptene)metal complexes.[7] However, the remainder of geometry in both the carbon skeleton and the coordination geometry about the iron are similar to previously reported examples of bicyclo[2.2.1]-hept-5-enes[8] and Fp(η^1-alkyl) systems.[9]

The utilization of 1 as a synthetic equivalent for 5-carbomethoxycyclopentadiene is illustrated in Scheme I. Reaction of dimethyl fumarate in CH_2Cl_2 at 25 °C with 1 for 4 h gives the product 3a as a yellow solid (90%) consisting of a single stereoisomer.[10] Treatment of 3a with 6 equiv of ammonium cerium(IV) nitrate in a CO-saturated MeOH solution[11] affords the triester 4a as a white crystalline product (75%).[12] Since the oxidative cleavage of Fp–alkyl compounds to alkyl esters is established to occur with retention of configuration at the carbon bonded to iron,[13] the stereochemistry of the 7-carbomethoxy group in 4a is assigned *syn* with respect to the double bond. This assumption is supported by the ^1H and ^{13}C NMR data where resonances are observed for three distinct methyl esters.

Compound 1 also reacts efficiently with dimethyl acetylenedicarboxylate (CH_2Cl_2, 25 °C, 0.5 h) to give the expected adduct 5 in 85% isolated yield.[14] Subsequent treatment of 5 with ammonium cerium(IV) nitrate (MeOH, CO, 25 °C, 5 h) produces 6 in 70% yield.[15] Thus, the above sequence permits the isolation of these novel *syn*-7-carbomethoxy-5-norbornenes in good overall yields and as a single stereoisomer. Complex 1 does not react with methyl acrylate or dimethyl maleate at 25 °C even after several days. Slight heating of the solution containing 1 and methyl acrylate to 50 °C only causes 1 to convert to ferrocene without concomitant formation of the desired product (eq 2). However, 1 does react smoothly with 2-chloroacrylonitrile in CH_2Cl_2 at 25 °C to give 3b in 87% isolated yield.[16] Complex 3b is then transformed into 4b using ammonium cerium(IV) nitrate (MeOH, CO, 5 h) in good yield.[17]

(4) Compound 1 has previously been reported to give cycloadducts upon reaction with *trans*-NCCH=CHCN, *trans*- and Cis-$F_3C(CN)C$=$C(CN)CF_3$, NCC=CCN, and F_3CC=CCF_3: Williams, J. P.; Wojcicki, A. *Inorg. Chem.* 1977, *16*, 3116. $(CN)_2C$=$C(CN)_2$: Cutler, A.; Ehntholt, D.; Gierinin, W. P.; Lennon, P.; Raghu, S.; Rosan, A.; Rosenblum, M.; Tancrede, J.; Wells, D. *J. Am. Chem. Soc.* 1976, *98*, 3495.
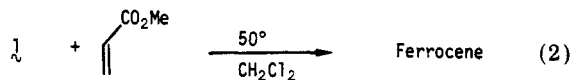
(5) X-ray quality crystals of 2 were obtained by slow diffusion of Et_2O into a $CHCl_3$ solution containing 2. Single crystals of 2 were monoclinic of space group $P2_1/c$ (No. 14) with a = 15.626 (3) Å, b = 6.596 (3) Å, c = 14.239 (5) A, β = 99.05 (2)°, and Z = 4. Complete details of the structure determination can be found in Table G (Crystallographic Report) of the supplementary material. Three-dimensional X-ray diffraction data were collected for the 2897 independent reflections having 4° < 2θ < 50° on a computer-controlled four-circle Syntex P2$_1$ autodiffractometer using graphite-monochromated Mo Kα radiation and 2θ–θ scanning technique. The structure was initially solved by using direct methods (MULTAN), and the remaining non-hydrogen atoms were located by standard difference Fourier techniques. Hydrogen atoms were located by standard difference Fourier techniques or placed in their calculated positions by using idealized sp^2 geometry and a C–H bond length of 0.95 Å. The resulting structural parameters for 2 have been refined to convergence [R_1 = 0.041 and R_2 = 0.045 for 1737 reflections having $I \geq 3\sigma(I)$] by using counter-weighted full-matrix least-squares techniques with anisotropic thermal parameters for all non-hydrogen atoms and isotropic thermal parameters for the hydrogen atoms. A complete listing of final atomic coordinates, thermal parameters, bond lengths, and bond angles can be found in Tables A–F, respectively, of the supplementary material.

(6) 2: ^1H NMR (CDCl$_3$, 250 MHz) δ 6.20 (m, 2, CH=), 4.73 (s, 5, C_5H_5), 3.54 (m, 2, H$_2$, H$_3$), 3.34 (m, 2, H$_1$, H$_4$), 2.59 (t, 1, J = 0.8 Hz, H$_7$); ^{13}C (CDCl$_3$, 62.9 MHz) δ 216.51 (C=O), 170.97 (C=O), 135,47 (C$_5$, C$_6$), 85.59 (C$_5$H$_5$), 56.83 (C$_1$, C$_4$), 50.77 (C$_7$), 48.25 (C$_2$, C$_3$); IR (cm^{-1} in CH$_2$Cl$_2$) ν(CO) 2011, 1955, 1776.

(7) Ibbott, D. G.; Payne, N. C.; Shaver, A. *Inorg. Chem.* 1981, *20*, 2193.

(8) Pfluger, C. E.; Harlow, R. L.; Simonsen, S. H. *J. Cryst. Mol. Struct.* 1973, *3*, 277.

(9) Churchill, M. R.; Ni Chang, S. W. Y. *J. Am. Chem .Soc.* 1973, *95*, 5931.

(10) Column chromatography (alumina III) of the reaction mixture with hexane/benzene (4/1, v/v) removed the ferrocene leaving a yellow band near the top portion of the column. Elution with hexane/ethyl acetate (3/2, v/v) produced 3a: ^1H NMR (CDCl$_3$) δ 6.18 (m, 1, CH=), 5.86 (m, 1, CH=), 4.71 (s, 5, C_5H_5), 3.71 (s, 3, CH$_3$), 3.62 (s, 3, CH$_3$), 3.26, 3.12, 3.01, 2.78 (m's, 4, CH), 2.74 (s, 1, CH); ^{13}C NMR (CDCl$_3$) δ 217.20, 217.05 (C=O), 175.40, 173.22 (C=O), 137.47, 134.80 (CH=), 85.61 (C$_5$H$_5$), 57.98, 55.96 (CH), 51.69, 51.46 (CH$_3$), 48.78, 47.81, 45.21 (CH); IR (cm^{-1} in CH$_2$Cl$_2$) ν(CO) 2005, 1949, 1728.

(11) Lennon, P.; Rosan, A. M.; Rosenblum, M. *J. Am. Chem. Soc.* 1977, *99*, 8426.

(12) 4a: ^1H NMR (CDCl$_3$) δ 6.14 (dd, 2, J = 5.7, 3.1 Hz, CH=), 3.70 (s, 3, CH$_3$), 3.62 (s, 3, CH$_3$), 3.57 (s, 3, CH$_3$), 3.42, 3.38, 2.91 (m's, 3, CH's), 2.70 (d, 1, J = 4.6 Hz, CH); ^{13}C NMR (CDCl$_3$) δ 174.21, 172.57, 171.18 (C=O), 135.58, 133.46 (CH=), 61.08 (CH), 52.26, 51.93, 51.62 (CH$_3$), 49.27, 47.51, 47.13, 46.91 (CH); IR (cm^{-1} in CH$_2$Cl$_2$) ν(CO) 1731. Anal. Calcd for C$_{13}$H$_{16}$O$_6$: C, 58.21; H, 6.01. Found: C, 58.54; H, 6.07.

(13) Bock, P. L.; Baschetto, D. J.; Rasmussen, J. R.; Demers, J. P.; Whitesides, G. M. *J. Am. Chem. Soc.* 1974, *96*, 2814.

(14) 5: ^1H NMR (CDCl$_3$) δ 6.78 (t, 2, J = 2.0 Hz, CH=), 4.70 (s, 5, C_5H_5), 3.77 (m, 3, CH), 3.76 (s, 6, CH$_3$); ^{13}C NMR (CDCl$_3$) δ 216.89 (C=O), 165.96 (C=O), 155.45 (=CCO$_2$Me), 141.66 (CH=), 85.70 (C$_5$H$_5$), 64.62 (CH), 51.78 (CH$_3$); IR (cm^{-1} in CH$_2$Cl$_2$) ν(CO) 2007, 1951, 1729, 1709.

(15) 6: ^1H NMR (CDCl$_3$) δ 6.87 (t, 2, J = 2.0 Hz, CH=), 4.23 (m, 2, CH), 3.80 (s, 6, CH$_3$), 3.62 (s, 3, CH$_3$), 3.36 (t, 1, J = 1.6 Hz, CH); IR (cm^{-1} in CH$_2$Cl$_2$) ν(C=O) 1732, 1712.

(16) 3b (major isomer): ^1H NMR (CDCl$_3$) δ 6.29 (m, 1, CH=), 6.01 (m, 1, CH=), 4.74 (s, 5 C_5H_5), 3.28 (m, 1, CH), 2.88 (m, 1, CH), 2.83 (s, 1, CH), 2.68 (dd, 1, J = 3.7, 12.8 Hz, CH$_2$), 1.74 (d, 1, J = 12.8 Hz, CH$_2$); ^{13}C NMR (CDCl$_3$) δ 216.66, 216.51 (C=O), 139.44, 131.96 (CH=), 123.90 (CN), 85.69 (C$_5$H$_5$), 65.75 (CH), 55.11 (C(Cl)CN), 53.07 (CH), 47.23 (CH$_2$), 44.56 (CH). 3b (minor isomer): ^1H NMR (CDCl$_3$) δ 6.31 (m, 1, CH=), 6.11 (m, 1, CH=), 4.74 (s, 5, C_5H_5), 3.12 (m, 1, CH), 3.05 (s, 1, CH), 2.88 (1, CH), 2.29 (s, d, 2, J = 2.6 Hz); ^{13}C NMR (CDCl$_3$) δ 216.66, 216.51 (C=O), 142.20, 132.78 (CH=), 121.22 (CN), 85.69 (C$_5$H$_5$), 66.48 (CH), 55.11 (C(Cl)CN), 53.07 (CH), 47.97 (CH$_2$), 42.37 (CH); IR (both isomers, cm^{-1} in CH$_2$Cl$_2$) ν(CO) 2009, 1960.

That these Fp-norbornene complexes can be useful in the stereoselective synthesis of various *syn*-7-carbomethoxynorbornene derivatives is demonstrated since the Fp moiety can be cleaved in good yield. Because the iron-containing starting material for this chemistry, 1, is inexpensive, stable, and easy to prepare on a large scale, the reactions outlined here represent a new and potentially powerful method for stereoselectively synthesizing new substituted bicyclo[2.2.1]hept-5-ene systems.

(17) **4b** (major isomer): ^{13}C NMR (CDCl$_3$) δ 169.33 (C=O), 137.46, 130.02 (CH=), 120.41 (CN), 62.05, 56.59 (CH), 55.12 (*C*(Cl)CN), 51.92 (CH$_3$), 45.36 (CH$_2$), 44.81 (CH). **4b** (minor isomer): ^{13}C NMR (CDCl$_3$) δ 169.85 (C=O), 140.11, 130.55 (CH=), 119.10 (CN), 61.15, 57.50 (CH), 55.12 (*C*(Cl)CN), 51.92 (CH$_3$), 46.45, 44.43; ^{1}H NMR (CDCl$_3$, both isomers) δ 6.40, 6.36, 6.15, 6.05 (m's, 2, CH=), 3.75 (CH), 3.56 (s, 3, CH$_3$), 3.34 (b s, CH), 3.13 (m, CH), 2.93 (s, 1, CH), 2.76 (dd, *J* = 3.6, 13.6 Hz, CH$_2$), 1.71 (d, *J* = 13.6 Hz, CH$_2$); IR (cm^{-1} in CH$_2$Cl$_2$) ν(C=O) 1737.

Reductive Cleavage of the N=N Bond of 1,2,3-Thiadiazoles by Iron Carbonyl[1a]

Keith H. Pannell,*[1b] Armin J. Mayr,[1b] and Don VanDerveer[1c]

*Departments of Chemistry, University of Texas at El Paso El Paso, Texas 79968
and Georgia Institute of Technology
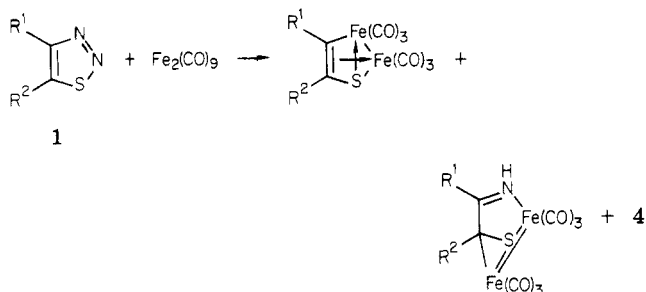Atlanta, Georgia 30332*

Received October 6, 1982

Summary: A series of new thioketo imine complexes of diiron hexacarbonyl have been synthesized from the reaction of Fe$_2$(CO)$_9$ with 1,2,3-thiadiazoles that result from the reductive cleavage of the N=N bond of the starting diazole.

The chemical reactions of α-diazo ketones with transition metals have been extensively studied by Herrmann and co-workers. The resulting products include carbene complexes (from N$_2$ elimination),[2,3] ketene complexes (N$_2$ elimination followed by CO insertion),[4] imine complexes

(reductive elimination of "N"),[4,5] and complexation of the unfragmented ligand.[6]

The related thioketo and selenoketo diazo compounds do not exist in the same open form as the α-diazo ketones but rather as the cyclic isomers 1,2,3-thia- and 1,2,3-selenadiazoles. Rees[7] and Schrauzer[8] have previously reported that such diazoles react with iron carbonyl to form diiron thioketocarbene hexacarbonyl and diiron selenoketocarbene hexacarbonyl complexes via N$_2$ elimination. We recently observed that the reactions of the 1,2,3-selenadiazoles with Fe$_2$(CO)$_9$ also led to high yields of diiron selenoketoketene hexacarbonyl complexes in addition to the selenoketocarbene complexes.[9] We also noted that both the thia- and selenadiazoles reacted with group 6 carbonyls to form complexes in which the ligands have remained intact.[9–11] In the light of the discovery of this new mode of reactivity for the selenadiazoles we have reinvestigated the reactions of thiadiazoles with Fe$_2$(CO)$_9$ and wish to report the formation of hitherto unknown α-thioketo imine complexes in addition to the reported thioketocarbene complexes.

A typical reaction involves stirring 1.0 g of 4-methyl-1,2,3-thiadiazole (**1d**) with 8.0 g of Fe$_2$(CO)$_9$ for 12 h in 100 mL of hexane at ambient temperature. Upon removal of the solvent under reduced pressure the reaction mixture is purified on an alumina column. Elution with hexane leads to the isolation of the corresponding thioketocarbene complex **2d** as an orange oil (20%). Further elution with hexane/dichloromethane (1:1) leads to the isolation of the new imine complex **3d** as brown-red crystals (30%). Final elution with pure dichloromethane yields an unknown complex (**4d**) as orange crystals. All of the thiadiazoles investigated, **1a–e**, gave similar yields.

1

a, R^1, R^2 = -(CH$_2$)$_4$-
b, R^1, R^2 = -(CH$_2$)$_6$-
c, R^1 = *p-t*-BuC$_6$H$_4$, R^2 = C$_6$H$_5$
d, R^1 = CH$_3$, R^2 = H
e, R^1 = *t*-Bu, R^2 = H

The various thioketocarbene complexes were identified by comparison of their spectral properties with those S and Se complexes described in the literature[7,8,12] and by elemental analysis.

(1) (a) Part 6. "Transition Metal Heterocyclic Chemistry". For part 5 see ref 10. (b) University of Texas at El Paso. (c) Georgia Institute of Technology.
(2) Herrmann, W. A. *Angew. Chem., Int. Ed. Engl.* **1974**, *13*, 599.
(3) Herrmann, W. A. *Chem. Ber.* **1975**, *108*, 486.
(4) Ziegler, M. L.; Weidenhammer, K.; Herrmann, W. A. *Angew. Chem., Int. Ed. Engl.* **1977**, *16*, 555.
(5) Herrmann, W. A. *Chem. Ber.* **1974**, *107*, 2899.
(6) Herrmann, W. A. *J. Organomet. Chem.* **1975**, *84*, C25.
(7) Gilchrist, T. L.; Menthe, P. G.; Rees, C. W. *J. Chem. Soc., Perkin Trans. 1* **1972**, 2165.
(8) Schrauzer, G. N.; Kisch, H. J. *J. Am. Chem. Soc.* **1973**, *95*, 2501.
(9) Pannell, K. H.; Mayr, A. J.; Hoggard, R.; Pettersen, R. C. *Angew. Chem., Int. Ed. Engl.* **1980**, *19*, 632.
(10) Pannell, K. H.; Mayr, A. J.; Hoggard, R.; McKennis, J.; Dawson, J. *Chem. Ber.*, in press.
(11) Baetzel, V.; Boese, R. *Z. Naturforsch., B: Anorg. Chem., Org. Chem.* **1981**, *36B*, 172.
(12) Pettersen, R. C.; Pannell, K. H.; Mayr, A. J. *Cryst. Struct. Commun.* **1980**, *9*, 643.

That these Fp-norbornene complexes can be useful in the stereoselective synthesis of various *syn*-7-carbomethoxynorbornene derivatives is demonstrated since the Fp moiety can be cleaved in good yield. Because the iron-containing starting material for this chemistry, 1, is inexpensive, stable, and easy to prepare on a large scale, the reactions outlined here represent a new and potentially powerful method for stereoselectively synthesizing new substituted bicyclo[2.2.1]hept-5-ene systems.

Registry No. 1, 12247-96-0; 2, 84500-50-5; **3a**, 84500-51-6; **3b** (isomer 1), 84581-02-2; **3b** (isomer 2), 84500-53-8; **4a**, 84500-54-9; **4b** (isomer 1), 84500-56-1; **4b** (isomer 2), 84500-57-2; 5, 84500-52-7; 6, 84500-55-0; maleic anhydride, 108-31-6; dimethyl fumarate, 624-49-7; dimethyl acetylenedicarboxylate, 762-42-5; 2-chloroacrylonitrile, 920-37-6.
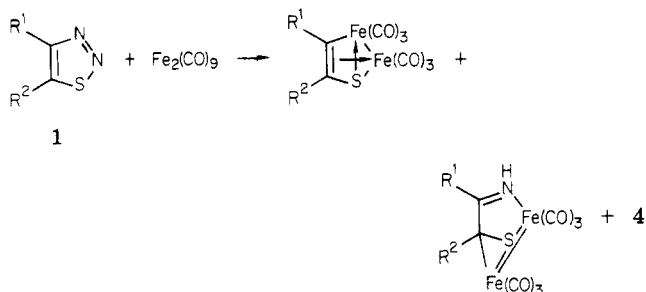
Supplementary Material Available: Tables of final atomic coordinates, anisotropic thermal parameters, hydrogen final positions and isotropic thermal parameters, bond lengths and angles, and comparison of selected bond angles and lengths to related systems and also a crystallographic report and a listing of structure factor amplitudes (20 pages). Ordering information is given on any current masthead page.

---

(17) **4b** (major isomer): ^{13}C NMR (CDCl$_3$) δ 169.33 (C=O), 137.46, 130.02 (CH=), 120.41 (CN), 62.05, 56.59 (CH), 55.12 (*C*(Cl)CN), 51.92 (CH$_3$), 45.36 (CH$_2$), 44.81 (CH). **4b** (minor isomer): ^{13}C NMR (CDCl$_3$) δ 169.85 (C=O), 140.11, 130.55 (CH=), 119.10 (CN), 61.15, 57.50 (CH), 55.12 (*C*(Cl)CN), 51.92 (CH$_3$), 46.45, 44.43; ^{1}H NMR (CDCl$_3$, both isomers) δ 6.40, 6.36, 6.15, 6.05 (m's, 2, CH=), 3.75 (CH), 3.56 (s, 3, CH$_3$), 3.34 (b s, CH), 3.13 (m, CH), 2.93 (s, 1, CH), 2.76 (dd, *J* = 3.6, 13.6 Hz, CH$_2$), 1.71 (d, *J* = 13.6 Hz, CH$_2$); IR (cm^{-1} in CH$_2$Cl$_2$) ν(C=O) 1737.

Reductive Cleavage of the N=N Bond of 1,2,3-Thiadiazoles by Iron Carbonyl[1a]

Keith H. Pannell,*[1b] Armin J. Mayr,[1b] and Don VanDerveer[1c]

Departments of Chemistry, University of Texas at El Paso El Paso, Texas 79968 and Georgia Institute of Technology Atlanta, Georgia 30332

Summary: A series of new thioketo imine complexes of diiron hexacarbonyl have been synthesized from the reaction of Fe$_2$(CO)$_9$ with 1,2,3-thiadiazoles that result from the reductive cleavage of the N=N bond of the starting diazole.

The chemical reactions of α-diazo ketones with transition metals have been extensively studied by Herrmann and co-workers. The resulting products include carbene complexes (from N$_2$ elimination),[2,3] ketene complexes (N$_2$ elimination followed by CO insertion),[4] imine complexes

(reductive elimination of "N"),[4,5] and complexation of the unfragmented ligand.[6]

The related thioketo and selenoketo diazo compounds do not exist in the same open form as the α-diazo ketones but rather as the cyclic isomers 1,2,3-thia- and 1,2,3-selenadiazoles. Rees[7] and Schrauzer[8] have previously reported that such diazoles react with iron carbonyl to form diiron thioketocarbene hexacarbonyl and diiron selenoketocarbene hexacarbonyl complexes via N$_2$ elimination. We recently observed that the reactions of the 1,2,3-selenadiazoles with Fe$_2$(CO)$_9$ also led to high yields of diiron selenoketoketene hexacarbonyl complexes in addition to the selenoketocarbene complexes.[9] We also noted that both the thia- and selenadiazoles reacted with group 6 carbonyls to form complexes in which the ligands have remained intact.[9-11] In the light of the discovery of this new mode of reactivity for the selenadiazoles we have reinvestigated the reactions of thiadiazoles with Fe$_2$(CO)$_9$ and wish to report the formation of hitherto unknown α-thioketo imine complexes in addition to the reported thioketocarbene complexes.

A typical reaction involves stirring 1.0 g of 4-methyl-1,2,3-thiadiazole (**1d**) with 8.0 g of Fe$_2$(CO)$_9$ for 12 h in 100 mL of hexane at ambient temperature. Upon removal of the solvent under reduced pressure the reaction mixture is purified on an alumina column. Elution with hexane leads to the isolation of the corresponding thioketocarbene complex **2d** as an orange oil (20%). Further elution with hexane/dichloromethane (1:1) leads to the isolation of the new imine complex **3d** as brown-red crystals (30%). Final elution with pure dichloromethane yields an unknown complex (**4d**) as orange crystals. All of the thiadiazoles investigated, **1a–e**, gave similar yields.

a, R^1, R^2 = -(CH$_2$)$_4$-
b, R^1, R^2 = -(CH$_2$)$_6$-
c, R^1 = *p-t*-BuC$_6$H$_4$, R^2 = C$_6$H$_5$
d, R^1 = CH$_3$, R^2 = H
e, R^1 = *t*-Bu, R^2 = H

The various thioketocarbene complexes were identified by comparison of their spectral properties with those S and Se complexes described in the literature[7,8,12] and by elemental analysis.

---

(1) (a) Part 6. "Transition Metal Heterocyclic Chemistry". For part 5 see ref 10. (b) University of Texas at El Paso. (c) Georgia Institute of Technology.
(2) Herrmann, W. A. *Angew. Chem., Int. Ed. Engl.* **1974**, *13*, 599.
(3) Herrmann, W. A. *Chem. Ber.* **1975**, *108*, 486.

(4) Ziegler, M. L.; Weidenhammer, K.; Herrmann, W. A. *Angew. Chem., Int. Ed. Engl.* **1977**, *16*, 555.
(5) Herrmann, W. A. *Chem. Ber.* **1974**, *107*, 2899.
(6) Herrmann, W. A. *J. Organomet. Chem.* **1975**, *84*, C25.
(7) Gilchrist, T. L.; Menthe, P. G.; Rees, C. W. *J. Chem. Soc., Perkin Trans. 1* **1972**, 2165.
(8) Schrauzer, G. N.; Kisch, H. J. *J. Am. Chem. Soc.* **1973**, *95*, 2501.
(9) Pannell, K. H.; Mayr, A. J.; Hoggard, R.; Pettersen, R. C. *Angew. Chem., Int. Ed. Engl.* **1980**, *19*, 632.
(10) Pannell, K. H.; Mayr, A. J.; Hoggard, R.; McKennis, J.; Dawson, J. *Chem. Ber.*, in press.
(11) Baetzel, V.; Boese, R. *Z. Naturforsch., B: Anorg. Chem., Org. Chem.* **1981**, *36B*, 172.
(12) Pettersen, R. C.; Pannell, K. H.; Mayr, A. J. *Cryst. Struct. Commun.* **1980**, *9*, 643.

Table I. IR Spectroscopic and Analytical Data for the New Complexes 2a–e and 3a–e[a]

complex	$\nu(CO)$,[b] cm^{-1}	$\nu(NH)$,[c] cm^{-1}	emp form	% C	% H	mp, °C
2a	2070, 2030, 2005, 1996, 1980		$C_{12}H_8Fe_2O_6S$	36.4 (36.8)	2.02 (2.06)	oil
2b	2070, 2028, 2000, 1990, 1970		$C_{14}H_{12}Fe_2O_6S$	40.1 (40.0)	3.01 (2.88)	38–40
2c	ref 7					
2d	2078, 2038, 2005, 1999, 1983		$C_9H_4Fe_2O_6S$	30.8 (30.7)	1.25 (1.15)	oil
2e	2076, 2036, 2005, 1996, 1979		$C_{12}H_{10}Fe_2O_6S$	36.8 (36.6)	2.70 (2.56)	oil
3a	2075, 2015, 1996, 1988, 1965, 1955	3350	$C_{12}H_9Fe_2NO_6S$	35.5 (35.4) % N 3.39 (3.44)	2.12 (2.29)	138–140
3b	2074, 2020, 2000, 1990, 1970, 1960	3346	$C_{14}H_{13}Fe_2NO_6S$	38.9 (38.7) % N 3.35 (3.22)	3.24 (3.01)	34–36
3c	2066, 2022, 1997, 1990, 1969, 1956	3345	$C_{24}H_{19}Fe_2NO_6S$	51.7 (51.4) % N 2.54 (2.50)	3.51 (3.41)	154–156
3d	2079, 2021, 1999, 1990, 1960	3353	$C_9H_5Fe_2NO_6S$	29.5 (29.5) % N 3.67 (3.82)	1.31 (1.37)	64–66
3e	2078, 2020, 1998, 1989, 1966	3354	$C_{12}H_{11}Fe_2NO_6S$	35.3 (35.2) % N 3.31 (3.42)	2.60 (2.71)	128–130

[a] Analyses performed by Galbraith Laboratories, Inc., Knoxville, TN. Figures in parentheses are calculated values. [b] In hexane. [c] In CH_2Cl_2.
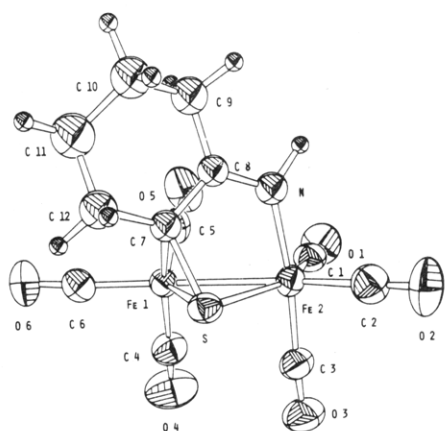

Figure 1. Crystal structure of (μ-imino-1-sulfidocyclohexyl-*N,S*)bis(tricarbonyliron)(Fe–Fe) **3a**, crystallized in the orthorhombic space group *Pna*2$_1$ with $a = 17.346$ (4) Å, $b = 9.787$ (2) Å, $c = 9.030$ (2) Å, and $Z = 4$. Data was collected on a Syntex P2$_1$ diffractometer by using θ–2θ scans. Full-matrix least-squares refinement using SHELX-76 gave a final R of 0.036. Selected bond lengths (Å): Fe–Fe 2.689 (1); Fe2–S 2.257 (2); Fe1–S 2.173 (2); Fe2–N 1.952 (6); N=C8 1.292 (9). Ellipsoids are shown for the 50% probability level.

The structure of complex **3a** was determined by single-crystal X-ray analysis and is representitive of this new class of complex. The result (Figure 1) illustrates the complex to be a diiron hexacarbonyl derivative of the previously unknown thioketo imine fragment. Full spectroscopic and analytical data for the new complexes are recorded in Tables I and II.

The new complexes apparently result from a chemical reaction not reported for the starting thiadiazoles, i.e., reductive cleavage of the N=N bond. Given the moderate to good yields of the thioketo imine complexes and their oxidative and thermal stability, it is surprising that they were not observed in either of the previous studies on the interactions of the thiadiazoles with iron carbonyl.

Our results thus establish that each of the various modes of chemical reactivity observed by Herrmann and his co-workers for the α-diazo ketones is also exhibited by the related thia- and selenadiazoles. However, it is striking that the thia- and selenadiazoles do not behave the same; both yield the corresponding ketocarbene complexes, but the major products from the respective reactions with

Table II. ^{1}H NMR Spectroscopic Data for the New Complexes[a]

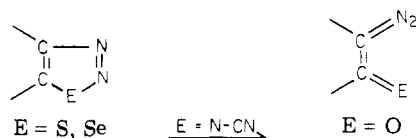| complex	δ
2a	α-H 2.70 (b m, 2 H), α'-H 2.42 (b m, 2 H), β,β'-H 1.80 (b m, 4 H)
2b	α,α'-H 2.60 (b m, 4 H), β,β', γ,γ'-H 1.92 (b m, 8 H)
2c	ref 7
2d	R = CH_3 2.37 (s, 3 H), R' = 7.51 (s, 1 H)
2e	R = $C(CH_3)_3$ 1.32 (s, 9 H), R' = H 7.42 (s, 1 H)
3a	α-H 2.20 (b m, 4 H), α'-H 1.85 (b m, 2 H), $\beta,\beta'\gamma,\gamma'$-H 1.60 (b m, 4 H), NH 5.50 (b s, 1 H)
3b	α,α'-H 2.20 (b m, 4 H), $\beta,\beta',\gamma,\gamma'$-H 1.62 (b m, 8 H), NH 5.90 (b s, 1 H)
3c	C_6H_5 7.02 (s, 5 H), C_6H_4 6.92 (AB qt, 4 H), $C(CH_3)_3$ 1.11 (s, 9 H), NH 6.18 (b s, 1 H)
3d	R = CH_3 2.08 (s, 3 H), R' = H 2.92 (d,[b] 1 H), NH 5.80 (b s, 1 H)
3e	R = $C(CH_3)_3$ 1.18 (s, 9 H), R' = H 3.13 (d,[b] 1 H), NH 6.00 (b s, 1 H)

[a] Spectra were recorded in CDCl$_3$ by using Me$_4$Si as external standard. Values are in ppm. Abbreviations: b = broad, s = singlet, d = doublet, m = multiplet. α, β, and γ designations are as noted:
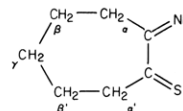
[b] $J = 2$ Hz. The origin of this splitting is unclear. Perhaps a long-range CH···NH interaction.

Fe$_2$(CO)$_9$ are the thioketo imine and selenoketoketene complexes. We have been unable to observe either selenoketo imine or thioketoketene complexes from the various reactions we have performed. It is possible to speculate upon this behavior. As noted above, the thia- and selenadiazoles are the cyclic isomers of α-diazo ketones, which themselves do not exist in the cyclic form. The related 1-cyano-1,2,3-triazole does exist in both the open and ring-closed forms.[13]

As noted in the above scheme, the stability of the open form seems to be directly related to the ability of the hetero

(13) Hermes, M. E.; Marsh, F. D. *J. Am. Chem. Soc.* **1967**, *89*, 4760.

E = S, Se   E = N-CN   E = O

atom to form a double bond to carbon. Thus the first-row elements O and N can exist in the open form, while the second- and third-row elements S and Se cannot.

We suggest that the initial effect of the iron carbonyl is to cause a ring opening by cleavage of the S(Se)–N bond, thus forming the diazoketo form of the ligand possibly stabilized by a metal carbonyl fragment. Given the greater capacity of the second-row S to form a C=S grouping compared to the C=Se group, a longer lifetime might be expected for the ring-opened α-diazo thioketone. This would permit the thioketone to exhibit chemistry more reminiscent of the α-diazo ketones as observed by Herrmann, i.e., imine formation. The selenium analogue would immediately exhibit loss of N_2 with resulting carbene formation. The inability to observe thioketoketene complexes is probably related to the more facile decarbonylation of such complexes or, conversely, the inability of thioketocarbenes to insert carbon monoxide.

The complete reaction mechanism leading to the formation of 3, and the imine complexes of Herrmann, is unclear. A possibility is the intermediacy of dimerized diazo ketones, i.e. tetrazenes, which are known to eliminate N_2 with concurrent formation of amines.[14]

Registry No. 1a, 56382-72-0; 1b, 56382-70-8; 1c, 38010-76-3; 1d, 18212-62-9; 1e, 40753-16-0; 2a, 84642-31-9; 2b, 84624-06-6; 2d, 84642-32-0; 2e, 84624-07-7; 3a, 84624-08-8; 3b, 84624-09-9; 3c, 84624-10-2; 3d, 84624-11-3; 3e, 84624-12-4; $Fe_2(CO)_9$, 15321-51-4; Fe, 7439-89-6.

Supplementary Material Available: Tables of interatomic distances and angles, fractional coordinates and thermal parameters, and crystal data and a listing of structure factor amplitudes for 3 (10 pages). Ordering information is given on any current masthead page.

(14) Hube, J.; Shine, H. *J. Am. Chem. Soc.* 1973, *95*, 2501.

Alkane Carbon–Hydrogen Bond Activation by Homogeneous Rhodium(I) Compounds

William D. Jones* and **Frank J. Feher**

*Department of Chemistry, University of Rochester
Rochester, New York 14627*

Summary: The complex $[C_5(CH_3)_5]Rh[P(CH_3)_3](CH_3)Cl$ was prepared by reaction of methyllithium with the corresponding dichloride. Removal of the chloride ligand with Ag^+ followed by addition of $Na^+[H_2Al(OCH_2CH_2OCH_3)_2]^-$ at –40 °C produces thermally unstable $[C_5(CH_3)_5]Rh[P(CH_3)_3](CH_3)(H)$, which undergoes first-order reductive elimination at –17 °C ($k = 6.5 \times 10^{-5}$ s^{-1}). Irradiation of $[C_5(CH_3)_5]Rh[P(CH_3)_3]H_2$ in liquid propane at –55 °C produces $[C_5(CH_3)_5]Rh[P(CH_3)_3](H)(n$-propyl), which can be converted into $[C_5(CH_5)]Rh[P(CH_3)_3](n$-propyl)Br by reaction with $CHBr_3$.

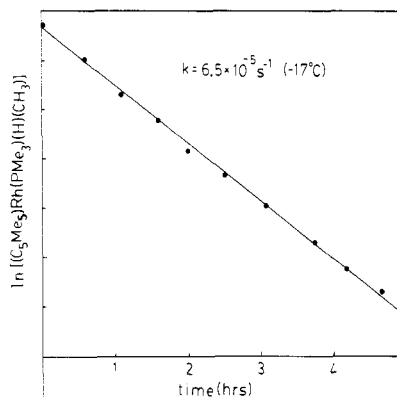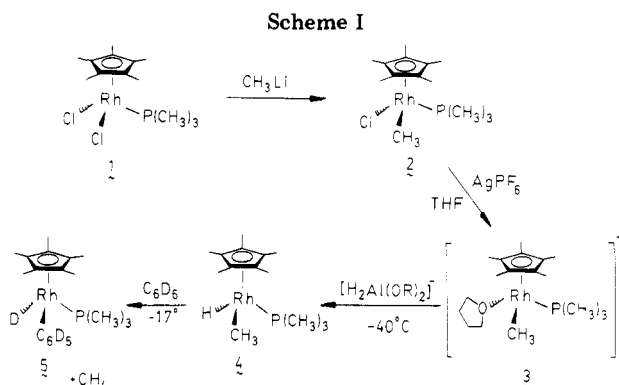**Figure 1.** First-order plot of the disappearance of the methyl ¹H NMR resonance of 4 at –17 °C in 25% C_6D_6/75% THF-d_8.

Scheme I

The activation of carbon–hydrogen bonds for catalysis by transition-metal complexes is an area of rapidly increasing interest.[1,2] Recent observations of alkane C–H bond activation have brought into reach even more attractive possibilities for potential substrates.[2] We have recently reported the activation of arene C–H bonds by a (permethylcyclopentadienyl)rhodium complex[3] and now report the activation of alkane C–H bonds by this molecule.

Most known transition-metal alkyl hydrides have been reported to be unstable toward facile elimination of R–H.[4] The stability of alkyl hydrides of the formula $[C_5(CH_3)_5]Rh[P(CH_3)_3](R)(H)$ was initially determined by preparing the methyl derivative 4. A solution of 76 mg of $[C_5(CH_3)_5]Rh[P(CH_3)_3]Cl_2$,[5] 1, in 5 mL of THF was treated with 1.1 equiv of methyllithium at –40 °C under a nitrogen atmosphere. After the mixture was slowly warmed to 25 °C over a period of 25 min, the solvent was removed (0.01
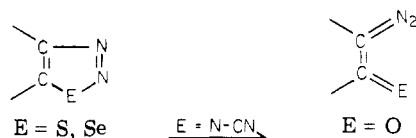
(1) (a) Green, M. L. H. *Pure Appl. Chem.* 1978, *50*, 27–35. (b) Rausch, M. D.; Gastinger, R. G.; Gardner, S. A.; Brown, R. K.; Wood, J. S. *J. Am. Chem. Soc.* 1977, *99*, 7870–7876. (c) Grebenik, P. D.; Green, M. L. H.; Izquierdo, A. *J. Chem. Soc., Chem. Commun.* 1981, 186–187. (d) Gell, K. I.; Schwartz, J. *J. Am. Chem. Soc.* 1981, *103*, 2687–2695. (e) Bradley, M. G.; Roberts, D. A.; Geoffrey, G. L. *Ibid.* 1981, *103*, 379–384. (f) Gustavson, W. A.; Epstein, P. S.; Curtis, M. D. *Organometallics* 1982, *1*, 884–885. (g) Diamond, S. E.; Szalkiewicz, A.; Mares, F. *J. Am. Chem. Soc.* 1979, *101*, 490–491. (h) Horino, H.; Inoue, N. *Tetrahedron Lett.* 1979, *26*, 2403–2406. (i) Fujiwara, Y.; Kawauchi, T.; Taniguchi, H. *J. Chem. Soc., Chem. Commun.* 1980, 220–221.

(2) (a) Janowicz, A. H.; Bergman, R. G. *J. Am. Chem. Soc.* 1982, *104*, 352. (b) Hoyano, J. K.; Graham, W. A. G. *J. Am. Chem. Soc.* 1982, *104*, 3723–3725. (c) Crabtree, R. H.; Mellea, M. F.; Mihelcic, J. M.; Quirk, J. M. *Ibid.* 1982, *104*, 107–113. (d) Baudry, D.; Ephritikhine, M.; Felkin, H. *J. Chem. Soc., Chem. Commun.* 1980, 1243–1244.

(3) Jones, W. D.; Feher, F. J. *J. Am. Chem. Soc.* 1982, *104*, 4240–4242.

(4) See, for recent examples: Abis, L.; Sen, A.; Halpern, J. *J. Am. Chem. Soc.* 1978, *100*, 2915–2916. Suggs, J. W. *Ibid.* 1978, *100*, 640–641. Okrasinski, S. J.; Norton, J. R. *Ibid.* 1977, *99*, 295–297. Muetterties, E. L.; Watson, P. L. *Ibid.* 1976, *98*, 4665–4667. Gell, K. I.; Schwartz, J. *Ibid.* 1978, *100*, 3246–3248.

(5) Isobe, K.; Bailey, P. M.; Maitlis, P. M. *J. Chem. Soc., Dalton Trans.* 1981, 2003–2008.

E = S, Se   E = N-CN   E = O

atom to form a double bond to carbon. Thus the first-row elements O and N can exist in the open form, while the second- and third-row elements S and Se cannot.

We suggest that the initial effect of the iron carbonyl is to cause a ring opening by cleavage of the S(Se)–N bond, thus forming the diazoketo form of the ligand possibly stabilized by a metal carbonyl fragment. Given the greater capacity of the second-row S to form a C=S grouping compared to the C=Se group, a longer lifetime might be expected for the ring-opened α-diazo thioketone. This would permit the thioketone to exhibit chemistry more reminiscent of the α-diazo ketones as observed by Herrmann, i.e., imine formation. The selenium analogue would immediately exhibit loss of N_2 with resulting carbene formation. The inability to observe thioketoketene complexes is probably related to the more facile decarbonylation of such complexes or, conversely, the inability of thioketocarbenes to insert carbon monoxide.

The complete reaction mechanism leading to the formation of 3, and the imine complexes of Herrmann, is unclear. A possibility is the intermediacy of dimerized diazo ketones, i.e. tetrazenes, which are known to eliminate N_2 with concurrent formation of amines.[14]

Registry No. 1a, 56382-72-0; 1b, 56382-70-8; 1c, 38010-76-3; 1d, 18212-62-9; 1e, 40753-16-0; 2a, 84642-31-9; 2b, 84624-06-6; 2d, 84642-32-0; 2e, 84624-07-7; 3a, 84624-08-8; 3b, 84624-09-9; 3c, 84624-10-2; 3d, 84624-11-3; 3e, 84624-12-4; $Fe_2(CO)_9$, 15321-51-4; Fe, 7439-89-6.

Supplementary Material Available: Tables of interatomic distances and angles, fractional coordinates and thermal parameters, and crystal data and a listing of structure factor amplitudes for 3 (10 pages). Ordering information is given on any current masthead page.

(14) Hube, J.; Shine, H. *J. Am. Chem. Soc.* 1973, 95, 2501.

Alkane Carbon–Hydrogen Bond Activation by Homogeneous Rhodium(I) Compounds

William D. Jones* and Frank J. Feher

*Department of Chemistry, University of Rochester
Rochester, New York 14627*

Summary: The complex [$C_5(CH_3)_5$]Rh[P(CH_3)$_3$](CH_3)Cl was prepared by reaction of methyllithium with the corresponding dichloride. Removal of the chloride ligand with Ag^+ followed by addition of Na^+[$H_2Al(OCH_2CH_2OCH_3)_2$]$^-$ at –40 °C produces thermally unstable [$C_5(CH_3)_5$]Rh[P-(CH_3)$_3$](CH_3)(H), which undergoes first-order reductive elimination at –17 °C ($k = 6.5 \times 10^{-5}$ s^{-1}). Irradiation of [$C_5(CH_3)_5$]Rh[P(CH_3)$_3$]H_2 in liquid propane at –55 °C produces [$C_5(CH_3)_5$]Rh[P(CH_3)$_3$](H)(n-propyl), which can be converted into [$C_5(CH_5)$]Rh[P(CH_3)$_3$](n-propyl)Br by reaction with CHBr$_3$.

Figure 1. First-order plot of the disappearance of the methyl ^{1}H NMR resonance of 4 at –17 °C in 25% C_6D_6/75% THF-d_8.

Scheme I

The activation of carbon–hydrogen bonds for catalysis by transition-metal complexes is an area of rapidly increasing interest.[1,2] Recent observations of alkane C–H bond activation have brought into reach even more attractive possibilities for potential substrates.[2] We have recently reported the activation of arene C–H bonds by a (permethylcyclopentadienyl)rhodium complex[3] and now report the activation of alkane C–H bonds by this molecule.

Most known transition-metal alkyl hydrides have been reported to be unstable toward facile elimination of R–H.[4] The stability of alkyl hydrides of the formula [C_5-(CH_3)$_5$]Rh[P(CH_3)$_3$](R)(H) was initially determined by preparing the methyl derivative 4. A solution of 76 mg of [$C_5(CH_3)_5$]Rh[P(CH_3)$_3$]Cl$_2$,[5] 1, in 5 mL of THF was treated with 1.1 equiv of methyllithium at –40 °C under a nitrogen atmosphere. After the mixture was slowly warmed to 25 °C over a period of 25 min, the solvent was removed (0.01

(1) (a) Green, M. L. H. *Pure Appl. Chem.* 1978, 50, 27–35. (b) Rausch, M. D.; Gastinger, R. G.; Gardner, S. A.; Brown, R. K.; Wood, J. S. *J. Am. Chem. Soc.* 1977, 99, 7870–7876. (c) Grebenik, P. D.; Green, M. L. H.; Izquierdo, A. *J. Chem. Soc., Chem. Commun.* 1981, 186–187. (d) Gell, K. I.; Schwartz, J. *J. Am. Chem. Soc.* 1981, 103, 2687–2695. (e) Bradley, M. G.; Roberts, D. A.; Geoffrey, G. L. *Ibid.* 1981, 103, 379–384. (f) Gustavson, W. A.; Epstein, P. S.; Curtis, M. D. *Organometallics* 1982, 1, 884–885. (g) Diamond, S. E.; Szalkiewicz, A.; Mares, F. *J. Am. Chem. Soc.* 1979, 101, 490–491. (h) Horino, H.; Inoue, N. *Tetrahedron Lett.* 1979, 26, 2403–2406. (i) Fujiwara, Y.; Kawauchi, T.; Taniguchi, H. *J. Chem. Soc., Chem. Commun.* 1980, 220–221.

(2) (a) Janowicz, A. H.; Bergman, R. G. *J. Am. Chem. Soc.* 1982, 104, 352. (b) Hoyano, J. K.; Graham, W. A. G. *J. Am. Chem. Soc.* 1982, 104, 3723–3725. (c) Crabtree, R. H.; Mellea, M. F.; Mihelcic, J. M.; Quirk, J. M. *Ibid.* 1982, 104, 107–113. (d) Baudry, D.; Ephritikhine, M.; Felkin, H. *J. Chem. Soc., Chem. Commun.* 1980, 1243–1244.

(3) Jones, W. D.; Feher, F. J. *J. Am. Chem. Soc.* 1982, 104, 4240–4242.

(4) See, for recent examples: Abis, L.; Sen, A.; Halpern, J. *J. Am. Chem. Soc.* 1978, 100, 2915–2916. Suggs, J. W. *Ibid.* 1978, 100, 640–641. Okrasinski, S. J.; Norton, J. R. *Ibid.* 1977, 99, 295–297. Muetterties, E. L.; Watson, P. L. *Ibid.* 1976, 98, 4665–4667. Gell, K. I.; Schwartz, J. *Ibid.* 1978, 100, 3246–3248.

(5) Isobe, K.; Bailey, P. M.; Maitlis, P. M. *J. Chem. Soc., Dalton Trans.* 1981, 2003–2008.

mm at 25 °C) and the products were chromatographed on silica gel by using 4% THF/CH$_2$Cl$_2$ as eluent. An orange band (R_f 0.5) was collected and evaporated to yield [C$_5$-(CH$_3$)$_5$]Rh[P(CH$_3$)$_3$](CH$_3$)Cl, 2, in 71% isolated yield.[6] Addition of 1 equiv of AgPF$_6$ to a 0.05 M THF-d_8/C$_6$D$_6$ solution (73:27) of 2 produces a solution whose ^{1}H NMR spectrum (~70 °C)[7] can be assigned to the complex {[C$_5$-(CH$_3$)$_5$]Rh[P(CH$_3$)$_3$](CH$_3$)(THF-d_8)}$^+$(PF$_6$)$^-$, 3. One equivalent of Na$^+$[H$_2$Al(OCH$_2$CH$_2$OCH$_3$)$_2$]$^-$ (70% solution in toluene) was then introduced by syringe at –70 °C. When the mixture was warmed to –40 °C, a new species was observed in 80% (NMR) yield. The ^{1}H NMR spectrum of this new compound displays resonances consistent with the formula [C$_5$(CH$_3$)$_5$]Rh[P(CH$_3$)$_3$](CH$_3$)(H),[8] 4. When the solution was warmed to –17 °C in the probe of the NMR spectrometer, a slow first-order disappearance of the resonances attributable to 4 is observed (k = 6.5 × 10^{-5} s^{-1}, Figure 1) with a concomitant increase in resonances attributable to methane (δ 0.171) and [C$_5$(CH$_3$)$_5$]-Rh[P(CH$_3$)$_3$](D)(C$_6$D$_5$),[3] 5 (Scheme I). If the same reaction sequence is performed in pure THF-d_8, no identifiable products are observed upon warming above –20 °C.

The reverse of this reaction, the oxidative addition of alkane to the coordinatively unsaturated rhodium center in [C$_5$(CH$_3$)$_5$]Rh[P(CH$_3$)$_3$] can therefore only be expected to be observed below –20 °C. Generation of this 16-electron species in an alkane with a boiling point below –20 °C would permit removal of the excess alkane without decomposition of the oxidative-addition product. Accordingly, we chose to irradiate [C$_5$(CH$_3$)$_5$]Rh[P(CH$_3$)$_3$]H$_2$,[5] 6, in liquid propane (bp –40 °C) at –55 °C in an NMR tube attached to a vacuum line. Warming to –40 °C under vacuum (10^{-4} mm) removed unreacted propane. THF-d_8 was then condensed into the tube at –78 °C, the tube sealed, and a ^{1}H NMR spectrum recorded at –40 °C. Aside from unreacted 6, new resonances appeared at δ –14.963 (dd, J = 50, 32 Hz, 1 H), 0.840 (t, J = 7 Hz, 3 H), 1.278 (d, J = 9 Hz, 9 H), and 1.820 (d, J = 1.8 Hz, 15 H). The complex is assigned as [C$_5$(CH$_3$)$_5$]Rh[P(CH$_3$)$_3$](H)(n-propyl), 7, on the basis of this spectral data[9] and from the fact that propane (δ 0.892 (t, J = 7 Hz), 1.317 (sept, J = 7 Hz)) is produced as a decomposition product when the sample is warmed to –15 °C (eq 1).

Additional support for the formulation of 7 as the n-propyl derivative arises from its derivatization with a halocarbon. Addition of a five fold excess of CHBr$_3$ in THF to the solution containing 7 at –78 °C results in an

instantaneous reaction producing a red solution. Removal of solvent (25 °C (10 mm)) followed by addition of CDCl$_3$ allows identification of [C$_5$(CH$_3$)$_5$]Rh[P(CH$_3$)$_3$](n-propyl)(Br), 8, by ^{1}H NMR and ^{13}C NMR spectroscopy.[10]

These results demonstrate the oxidative addition and reductive elimination of alkane C–H bonds at a reactive rhodium center. Alkane reductive elimination from 4 occurs at about the same temperature (–17 °C) as reductive elimination of arene from 5 (–10 °C).[3] The difference in overall stability between 4 and 5 can be attributed to the capability for η^2-arene coordination following reductive elimination in 5, whereas reductive elimination of alkane from 4 results in the formation of two distinct species, free to separate in solution. These rhodium complexes are much less stable than the iridium analogues reported by Janowicz and Bergman,[2a] suggesting that stable oxidative-addition products with alkanes will be found predominantly in the third row. The kinetic and thermodynamic factors influencing alkane vs. arene C–H bond activation are under further investigation.

Note Added in Proof. Prof. Robert G. Bergman and Roy A. Periana–Pillai of the University of California at Berkeley have recently informed us of the isolation of alkyl derivatives similar to 8 in analytically pure form and of similar results with alkane activation.

(10) An authentic sample of [C$_5$(CH$_3$)$_5$]Rh[P(CH$_3$)$_3$](n-propyl)(Br) was prepared by addition of 1 equiv of n-propyllithium to [C$_5$(CH$_3$)$_5$]Rh[P-(CH$_3$)$_3$]Br$_2$[11] at –40 °C in THF. Removal of solvent (25 °C (10 mm)) followed by extraction of the residue with hexane separates the n-propyl derivative from unreacted starting material and LiBr. Removal of hexane (25 °C (10^{-4} mm)) provides pure 8. For 8: ^{1}H NMR (CDCl$_3$) δ 1.601 (d, J = 2.6 Hz, 15 H), 1.472 (d, J = 10.1 Hz, 9 H), 0.958 (t, J = 7.2 Hz, 3 H), 1.20, m, 2 H), 1.85 (m, 2 H); ^{13}C NMR (CDCl$_3$) δ 98.016 (d, J = 4.5 Hz, C$_5$(CH$_3$)$_5$), 29.051 (t of d, J = 122.6, 5.7 Hz, CH$_2$CH$_2$CH$_3$), 23.183 (t of d of d, J = 136.0, 22.7, 13.6 Hz, CH$_2$CH$_2$CH$_3$), 19.754 (q, J = 124.3 Hz, C$_5$(CH$_3$)$_5$), 15.844 (q of d, J = 126.6, 30.2 Hz, P(CH$_3$)$_3$), 9.360 (q, J = 127.0 Hz, CH$_2$CH$_2$CH$_3$).
(11) Gill, D. S.; Maitlis, P. M. *J. Organomet. Chem.* 1975, 87, 359.

Controlled Carbometalation.[1] 15. Zirconium-Promoted Carbozincation of Alkynes

Ei-Ichi Negishi,[*†] **David E. Van Horn, Tadao Yoshida, and Cynthia L. Rand**

Departments of Chemistry, Syracuse University
Syracuse, New York 13210
and Purdue University
West Lafayette, Indiana 47907

Summary: The reaction of alkynes with an alkylzinc derivative and X$_2$ZrCp$_2$ (X = I, Br, or Cl) can produce the corresponding alkenylzinc derivatives 2 in high yields, the stereoselectivity and regioselectivity being ≥98% and 70–95%, respectively. The reaction appears to involve

(6) 2 was further purified by recrystallization from CH$_2$Cl$_2$/hexane: ^{1}H NMR (CDCl$_3$) δ 1.632 (d, J = 2.8 Hz, 15 H), 1.413 (d, J = 10.2 Hz, 9 H), 0.574 (dd, J = 7.1, 2.2 Hz, 3 H); ^{13}C NMR (CDCl$_3$) δ 97.322 (s, C$_5$(CH$_3$)$_5$), 14.829 (q of d, J = 129.2, 30.6 Hz, P(CH$_3$)$_3$), 9.120 (q, J = 127.3 Hz, C$_5$(CH$_3$)$_5$), –1.693 (q of d of d, J = 133.4, 24.2, 16.8 Hz, RhCH$_3$); mass spectrum (7 eV), (M – 15)$^+$. Anal. Calcd for C$_{14}$H$_{27}$ClPRh: C, 46.11; H, 7.46. Found: C, 45.98; H, 7.49.
(7) For 3: ^{1}H NMR (–70 °C) δ 1.437 (d, J = 2.7 Hz, 15 H), 1.333 (d, J = 10.2 Hz, 9 H), 0.616 (d, J = 7.5 Hz, 3 H).
(8) For 4: ^{1}H NMR (–60 °C) δ 1.790 (d, J = 2.1 Hz, 15 H), 1.178 (d, J = 9.6 Hz, 9 H), –0.130 (dd, J = 5.1, 2.5 Hz, 3 H), –14.424 (dd, J = 48.3, 30.3 Hz, 1 H). A 10% (NMR) yield of [C$_5$(CH$_3$)$_5$]Rh[P(CH$_3$)$_3$]H$_2$ is also observed.
(9) The methylene groups, being both diasteriotopic and coupled to several nuclei, were not observed directly but are believed to fall partially under the PMe$_3$ resonances. Irradiation of the δ 1.20–1.45 region causes the triplet at δ 0.840 to collapse to a singlet.

†Purdue University.

(1) Selective Carbon-Carbon Bond Formation via Transition Metal Catalysis. 31. Part 30: Negishi, E.; Boardman, L. D. *Tetrahedron Lett.* 1982, 23, 3327.

mm at 25 °C) and the products were chromatographed on silica gel by using 4% THF/CH$_2$Cl$_2$ as eluent. An orange band (R_f 0.5) was collected and evaporated to yield [C$_5$-(CH$_3$)$_5$]Rh[P(CH$_3$)$_3$](CH$_3$)Cl, **2**, in 71% isolated yield.[6] Addition of 1 equiv of AgPF$_6$ to a 0.05 M THF-d_8/C$_6$D$_6$ solution (73:27) of **2** produces a solution whose ^{1}H NMR spectrum (~70 °C)[7] can be assigned to the complex {[C$_5$-(CH$_3$)$_5$]Rh[P(CH$_3$)$_3$](CH$_3$)(THF-d_8)}$^+$(PF$_6$)$^-$, **3**. One equivalent of Na$^+$[H$_2$Al(OCH$_2$CH$_2$OCH$_3$)$_2$]$^-$ (70% solution in toluene) was then introduced by syringe at ~70 °C. When the mixture was warmed to ~40 °C, a new species was observed in 80% (NMR) yield. The ^{1}H NMR spectrum of this new compound displays resonances consistent with the formula [C$_5$(CH$_3$)$_5$]Rh[P(CH$_3$)$_3$](CH$_3$)(H),[8] **4**. When the solution was warmed to ~17 °C in the probe of the NMR spectrometer, a slow first-order disappearance of the resonances attributable to **4** is observed (k = 6.5 × 10^{-5} s^{-1}, Figure 1) with a concomitant increase in resonances attributable to methane (δ 0.171) and [C$_5$(CH$_3$)$_5$]-Rh[P(CH$_3$)$_3$](D)(C$_6$D$_5$),[3] **5** (Scheme I). If the same reaction sequence is performed in pure THF-d_8, no identifiable products are observed upon warming above ~20 °C.

The reverse of this reaction, the oxidative addition of alkane to the coordinatively unsaturated rhodium center in [C$_5$(CH$_3$)$_5$]Rh[P(CH$_3$)$_3$] can therefore only be expected to be observed below ~20 °C. Generation of this 16-electron species in an alkane with a boiling point below ~20 °C would permit removal of the excess alkane without decomposition of the oxidative-addition product. Accordingly, we chose to irradiate [C$_5$(CH$_3$)$_5$]Rh[P(CH$_3$)$_3$]H$_2$,[5] **6**, in liquid propane (bp ~40 °C) at ~55 °C in an NMR tube attached to a vacuum line. Warming to ~40 °C under vacuum (10^{-4} mm) removed unreacted propane. THF-d_8 was then condensed into the tube at ~78 °C, the tube sealed, and a ^{1}H NMR spectrum recorded at ~40 °C. Aside from unreacted **6**, new resonances appeared at δ ~14.963 (dd, J = 50, 32 Hz, 1 H), 0.840 (t, J = 7 Hz, 3 H), 1.278 (d, J = 9 Hz, 9 H), and 1.820 (d, J = 1.8 Hz, 15 H). The complex is assigned as [C$_5$(CH$_3$)$_5$]Rh[P(CH$_3$)$_3$](H)(n-propyl), **7**, on the basis of this spectral data[9] and from the fact that propane (δ 0.892 (t, J = 7 Hz), 1.317 (sept, J = 7 Hz)) is produced as a decomposition product when the sample is warmed to ~15 °C (eq 1).

Additional support for the formulation of **7** as the n-propyl derivative arises from its derivatization with a halocarbon. Addition of a five fold excess of CHBr$_3$ in THF to the solution containing **7** at ~78 °C results in an

instantaneous reaction producing a red solution. Removal of solvent (25 °C (10 mm)) followed by addition of CDCl$_3$ allows identification of [C$_5$(CH$_3$)$_5$]Rh[P(CH$_3$)$_3$](n-propyl)(Br), **8**, by ^{1}H NMR and ^{13}C NMR spectroscopy.[10]

These results demonstrate the oxidative addition and reductive elimination of alkane C–H bonds at a reactive rhodium center. Alkane reductive elimination from **4** occurs at about the same temperature (~17 °C) as reductive elimination of arene from **5** (~10 °C).[3] The difference in overall stability between **4** and **5** can be attributed to the capability for η^2-arene coordination following reductive elimination in **5**, whereas reductive elimination of alkane from **4** results in the formation of two distinct species, free to separate in solution. These rhodium complexes are much less stable than the iridium analogues reported by Janowicz and Bergman,[2a] suggesting that stable oxidative-addition products with alkanes will be found predominantly in the third row. The kinetic and thermodynamic factors influencing alkane vs. arene C–H bond activation are under further investigation.

Note Added in Proof. Prof. Robert G. Bergman and Roy A. Periana–Pillai of the University of California at Berkeley have recently informed us of the isolation of alkyl derivatives similar to **8** in analytically pure form and of similar results with alkane activation.

(10) An authentic sample of [C$_5$(CH$_3$)$_5$]Rh[P(CH$_3$)$_3$](n-propyl)(Br) was prepared by addition of 1 equiv of n-propyllithium to [C$_5$(CH$_3$)$_5$]Rh[P(CH$_3$)$_3$]Br$_2$[11] at ~40 °C in THF. Removal of solvent (25 °C (10 mm)) followed by extraction of the residue with hexane separates the n-propyl derivative from unreacted starting material and LiBr. Removal of hexane (25 °C (10^{-4} mm)) provides pure **8**. For **8**: ^{1}H NMR (CDCl$_3$) δ 1.601 (d, J = 2.6 Hz, 15 H), 1.472 (d, J = 10.1 Hz, 9 H), 0.958 (t, J = 7.2 Hz, 3 H), 1.20, m, 2 H), 1.85 (m, 2 H); ^{13}C NMR (CDCl$_3$) δ 98.016 (d, J = 4.5 Hz, C$_5$(CH$_3$)$_5$), 29.051 (t of d, J = 122.6, 5.7 Hz, CH$_2$CH$_2$CH$_3$), 23.183 (t of d of d, J = 136.0, 22.7, 13.6 Hz, CH$_2$CH$_2$CH$_3$), 19.754 (q, J = 124.3 Hz, C$_5$(CH$_3$)$_5$), 15.844 (q of d, J = 126.6, 30.2 Hz, P(CH$_3$)$_3$), 9.360 (q, J = 127.0 Hz, CH$_2$CH$_2$CH$_3$).
(11) Gill, D. S.; Maitlis, P. M. *J. Organomet. Chem.* **1975**, *87*, 359.

Controlled Carbometalation.[1] 15.
Zirconium-Promoted Carbozincation of Alkynes

Ei-Ichi Negishi,[*†] **David E. Van Horn, Tadao Yoshida, and Cynthia L. Rand**
Departments of Chemistry, Syracuse University
Syracuse, New York 13210
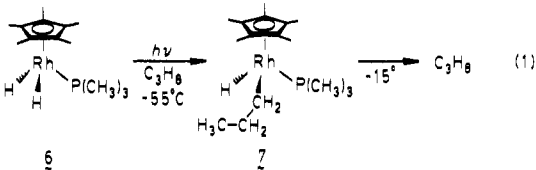*and Purdue University*
West Lafayette, Indiana 47907

Summary: The reaction of alkynes with an alkylzinc derivative and X$_2$ZrCp$_2$ (X = I, Br, or Cl) can produce the corresponding alkenylzinc derivatives **2** in high yields, the stereoselectivity and regioselectivity being ≥98% and 70–95%, respectively. The reaction appears to involve

(6) **2** was further purified by recrystallization from CH$_2$Cl$_2$/hexane: ^{1}H NMR (CDCl$_3$) δ 1.632 (d, J = 2.8 Hz, 15 H), 1.413 (d, J = 10.2 Hz, 9 H), 0.574 (dd, J = 7.1, 2.2 Hz, 3 H); ^{13}C NMR (CDCl$_3$) δ 97.322 (s, C$_5$(CH$_3$)$_5$), 14.829 (q of d, J = 129.2, 30.6 Hz, P(CH$_3$)$_3$), 9.120 (q, J = 127.3 Hz, C$_5$(CH$_3$)$_5$), ~1.693 (q of d of d, J = 133.4, 24.2, 16.8 Hz, RhCH$_3$); mass spectrum (7 eV), (M – 15)$^+$. Anal. Calcd for C$_{14}$H$_{27}$ClPRh: C, 46.11; H, 7.46. Found: C, 45.98; H, 7.49.
(7) For **3**: ^{1}H NMR (~70 °C) δ 1.437 (d, J = 2.7 Hz, 15 H), 1.333 (d, J = 10.2 Hz, 9 H), 0.616 (d, J = 7.5 Hz, 3 H).
(8) For **4**: ^{1}H NMR (~60 °C) δ 1.790 (d, J = 2.1 Hz, 15 H), 1.178 (d, J = 9.6 Hz, 9 H), ~0.130 (dd, J = 5.1, 2.5 Hz, 3 H), ~14.424 (dd, J = 48.3, 30.3 Hz, 1 H). A 10% (NMR) yield of [C$_5$(CH$_3$)$_5$]Rh[P(CH$_3$)$_3$]H$_2$ is also observed.
(9) The methylene groups, being both diastereotopic and coupled to several nuclei, were not observed directly but are believed to fall partially under the PMe$_3$ resonances. Irradiation of the δ 1.20–1.45 region causes the triplet at δ 0.840 to collapse to a singlet.

†Purdue University.

(1) Selective Carbon-Carbon Bond Formation via Transition Metal Catalysis. 31. Part 30: Negishi, E.; Boardman, L. D. *Tetrahedron Lett.* **1982**, *23*, 3327.

a direct C–Zn addition assisted by X₂ZrCp₂.

We have recently reported the reaction of alkynes with Me_3Al and X_2ZrCp_2 (X = Cl, I, or alkyl; Cp = η^5-C_5H_5) to produce ((E)-β-methylalkenyl)alanes[2] **1**. When higher alkylalanes were employed, however, the reaction was complicated by (a) competitive β elimination leading to hydrometalation of the alkynes and (b) a noticeable decrease (by 15–25%) in regioselectivity. In fact, an exclusive hydroalumination catalyzed by Cl_2ZrCp_2 was observed with *i*-Bu_3Al–Cl_2ZrCp_2.[3] The above-mentioned difficulties prompted us to seek alternative carbometalation reactions.

We now report that the reaction of a dialkylzinc and X_2ZrCp_2 (X = I, Br, or Cl) with alkynes can produce the corresonding alkenylzinc derivatives **2** in high yields and that, as in the Al–Zr reaction,[2] the Zn–Zr reaction herein described appears to involve a direct C–Zn addition.

$$ (1) $$
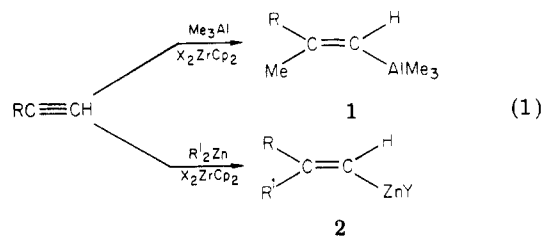
X = I, Br, Cl, or alkyl; Y = R¹ or X

Typically, treatment of 1-octyne with Et_2Zn (2 equiv) and I_2ZrCp_2, either preformed from Cl_2ZrCp_2 and BI_3[4] or generated in situ by treating Cl_2ZrCp_2 with NaI in acetone,[5] for 3 h at 20–22 °C provides, after hydrolysis, a 76:24 mixture of **3** and **4** in 100% combined yield. That the carbometalation products are indeed alkenylmetal species has been established by converting them into a 75:25 mixture of **5** and **6** in quantitative combined yield via iodinolysis.
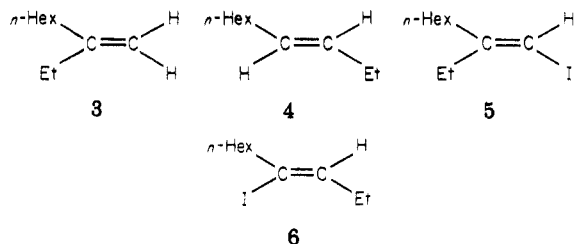
Although Cl_2ZrCp_2 and Br_2ZrCp_2 also induce this carbometalation, their reactions are slower than that induced by I_2ZrCp_2. Thus, the reaction of 1-octyne with 2 equiv of Et_2Zn and 1 equiv of Cl_2ZrCp_2 for 48 h at 50 °C gives, after hydrolysis, a 96:4 mixture of **3** and **4** in only 56% combined yield. The favorable regioselectivity turned out to be a consequence of a competitive alkyne proton abstraction leading to the formation of a 1-octynylzinc derivative that, in turn, undergoes a highly regioselective carbometalation,[6] indicating that the acetylenic proton abstraction can be a serious side reaction in a slow carbometalation reaction with an organozinc reagent. For-

tunately, there was little or no indication for proton abstraction in the reaction of 1-octyne with Et_2Zn and I_2ZrCp_2.

Although the scope of the carbometalation with Zn–Zr reagents has not yet been delineated, the following observations indicate that the reaction may be of reasonable scope. Ethylzinc chloride can replace Et_2Zn without noticeable adverse effects in the carbometalation of 1-octyne. Equally satisfactory are other di-*n*-alkylzincs, e.g., *n*-Bu_2Zn. Little or no β elimination occurs with these reagents. The regioselectivity for terminal metalation observed with *n*-alkylzinc reagents ranged from 70 to 80%.[7] On the other hand, the reaction of 1-octyne with Me_2Zn[8] (2 equiv) and I_2ZrCp_2 (1 equiv) for 6 h at room temperature produced a 95:5 mixture of 2-methyl-1-octene and 2-nonene in quantitative combined yield. Internal alkynes also react satisfactorily. Thus, the reaction of 5-decyne with Et_2Zn (1 equiv) and I_2ZrCp_2 (1 equiv) at room temperature is essentially complete within 6 h, producing, after iodinolysis, an 88% yield of 5-iodo-6-ethyl-5-decene as a single stereoisomer.

That the Zr-promoted carbozincation involves an exclusive cis addition of a carbon–metal bond has been established for the methylmetalation of 1-octyne described above by spectral and chromatographic comparison of the iodinated product with that obtained by the reaction with Me_3Al and Cl_2ZrCp_2.[2] The stereochemical assignments in the other cases are less definitive. In all cases reported here, however, did we observe the formation of single (≥98%) stereoisomers, as judged by ¹H and ¹³C NMR spectroscopy as well as by GLC analysis.

To probe if the carbometalation reported here involves the addition of C–Zn and/or C–Zr bond to acetylenes, we resorted to the same technique as that used to probe the mechanism of the Zr-catalyzed carboalumination.[9] Thus, the reaction of 1-octyne with Et_2Zn and $I(Me)ZrCp_2$, prepared by mixing I_2ZrCp_2 with Me_2ZrCp_2 in a 1:1 ratio,[10] gave, after protonolysis, 2-ethyl-1-octene in ca. 40% yield along with other minor products. However, only a trace, if any, of 2-methyl-1-octene was formed. These results are consistent with a mechanism involving the addition of C–Zn bond to acetylenes.

Although the reaction of alkynes with Me_2Zn and I_2ZrCp_2 does not require 1 equiv of I_2ZrCp_2, it is very sluggish with less then 1 equiv of I_2ZrCp_2. Whereas the reaction of 1-octyne with Me_2Zn was ≥97% complete in 6 h with 1 equiv of I_2ZrCp_2 at room temperature, it was only 62 and 9% complete with 0.5 and 0.1 equiv of I_2ZrCp_2, respectively. The carbometalation yield realized with 0.5 equiv of I_2ZrCp_2 went up to 85% after 48 h, indicating that the reaction is catalytic in I_2ZrCp_2 but that satisfactory results may be obtained with at least 1 equiv of I_2ZrCp_2.

Although a nonstereoselective addition of *t*-Bu_2Zn with conjugated enynes[11] and the reaction of allylic or propargylic organozinc derivatives with alkynes[12] are known,

(2) Van Horn, D. E.; Negishi, E. *J. Am. Chem. Soc.* **1978**, *100*, 2252.

(3) Negishi, E.; Yoshida, T. *Tetrahedron Lett.* **1980**, *21*, 1501.

(4) Aylett, B. J.; Campbell, J. M.; Walton, A. *J. Chem. Soc. A* **1969**, 2106.

(5) Reid, A. F.; Wailes, P. C. *J. Organomet. Chem.* **1964**, *2*, 329.

(6) Although the extent of the alkynyl proton abstraction in this case was not determined, the reaction of preformed 1-octynylzinc chloride with Et_2Zn and Cl_2ZrCp_2 cleanly produced, after treatment with D_2O, 1,1-dideuterio-2-methyl-1-octene in 60% yield. Treatment of 1-phenyl-2-deuterioethyne with *n*-Bu_2Zn in 1,2-dichloroethane for 1 day at ca. 20 °C gave, after hydrolysis, a 46:54 mixture of terminally protonated and deuterated phenylethynes.

(7) Our attempts to improve the regioselectivity by using a sterically more demanding zirconium compound, i.e., I_2ZrInd_2, where Ind = indenyl, resulted in a reduced regioselectivity of ca. 60%.

(8) Gray, A. P.; Callear, A. B.; Edgecomb, I. H. C. *Can. J. Chem.* **1963**, *41*, 1502.

(9) Yoshida, T.; Negishi, E. *J. Am. Chem. Soc.* **1981**, *103*, 4985.

(10) The 1:1 reaction of I_2ZrCp_2 with Me_2ZrCp_2 for 3 h at room temperature in 1,2-dichloroethane gives a clear, pale yellow solution showing a Cp proton NMR signal at δ 6.22 along with two minor signals at δ 6.52 and 5.84 for the Cp protons of the starting compounds. This mixture was used without further purification.

(11) Courtois, G.; Miginiac, L. *J. Organomet. Chem.* **1980**, *195*, 13.

(12) (a) Bernadou, F.; Miginiac, L. *C. R. Hebd. Seances Acad. Sci., Ser. C* **1975**, *280*, 1473. (b) Frangin, Y.; Gaudemar, M. *Bull. Soc. Chim. Fr.* **1976**, 1173. (c) Bellassoued, M.; Frangin, Y.; Gaudemar, M. *J. Organomet. Chem.* **1979**, *166*, 1.

stereoselective carbozincation of simple alkynes, e.g., 1-octyne, with alkylzinc derivatives appears to be unprecedented. Delineation of its scope and limitations is currently underway.

Cyclooctatetraenyllanthanide Complexes. 1. Alkyl- and Arylmonocyclooctatetraenyllutetium Derivatives

Andrea L. Wayda

Bell Laboratories
Murray Hill, New Jersey 07974

Summary: The class of monocyclooctatetraenyllanthanide complexes $(C_8H_8)LnCl(THF)_x$, previously known only for the early lanthanides (Ln = Ce, Pr, Nd, Sm), has been extended to include lanthanum and the late lanthanides erbium and lutetium. This synthetic extension provides an opportunity to systematically investigate the metathetical derivative chemistry of an inclusive homologous organolanthanide series. Such a study, aimed at the alkyl derivatization of $(C_8H_8)LnCl(THF)_x$ has resulted in the isolation and characterization of $(C_8H_8)Lu[CH_2Si(CH_3)_3](THF)_2$ (1) and $(C_8H_8)Lu[o-C_6H_4CH_2N(CH_3)_2](THF)$ (2). Attempted derivatization of the analogous lanthanum and samarium complexes has failed to yield characterizable alkyl complexes.

Concomitant with the recent renewed interest in organolanthanide chemistry,[1] concerted effort has recently been directed toward the development of the synthesis and reaction chemistry of cyclopentadienyl derivatives of the lanthanide elements.[2] In sharp contrast, little or no interest has been shown in the development of the chemistry of the monocyclooctatetraenyl complexes of the same elements.[3,4] This is surprising since these derivatives,

$(C_8H_8)LnCl(THF)_x$, previously described only for the early lanthanides (Ln = Ce, Pr, Nd, Sm),[3] should readily lend themselves to facile metathetical derivatization. Furthermore, the extension of this homologous series to include the late lanthanides would provide only the second complete series of precursor organolanthanide complexes.[5] The existence of such homologous series is critically important to a systematic study of the derivative chemistry of organolanthanide complexes. In particular, only through such studies can important observations relating the reactivity of organolanthanide complexes (and their derivatives) to their position in the lanthanide series be made. "Reactivity tailoring" or "fine tuning" of the relevant chemistry of these complexes should directly accrue from such fundamental studies.

Therefore, we have investigated the extension of the known $(C_8H_8)LnCl(THF)_x$ derivatives to include lanthanum and the later lanthanides erbium and lutetium. As noted, the completion of this homologous series provides an opportunity to systematically investigate the metathetical derivative chemistry of an organolanthanide compound class. In this regard, as an initial and obvious synthetic goal, we have addressed the synthesis and characterization of cyclooctatetraenyllanthanide alkyl complexes. The synthesis of such derivatives should allow a rich reaction chemistry to be explored. (cf. the use of bis(cyclopentadienyl)lanthanide alkyls as precursors to heteroleptic alkynides,[6] hydrides,[7] carbon monoxide insertion products,[8] and Ziegler–Natta polymerization catalysts[9]). We therefore also report at this time the synthesis and characterization of the first cyclooctatetraenyllanthanide alkyl and aryl derivatives $(C_8H_8)Lu[CH_2Si(CH_3)_3](THF)_2$ (1) and $(C_8H_8)Lu[o-C_6H_4CH_2N(CH_3)_2](THF)$ (2).

The new $(C_8H_8)LnCl(THF)_x$ complexes are synthesized by using the methodology of Streitwieser et al. with minor modification.[3] Slow ambient-temperature addition of a freshly prepared THF solution of $K_2(C_8H_8)$ to an equimolar amount of LnCl$_3$ suspended in THF yields, after a reaction time of 24 h, characteristically colored slurries (pink for erbium, off-white for lutetium, and pale yellow for lanthanum). The crude products are isolated and initially purified by removal of solvent in vacuo followed by THF extraction to remove soluble by-products (such as K[Ln(C$_8$H$_8$)$_2$]).[3] Final purification is achieved by Soxhlet extraction of the residue with THF for 24 h. Vacuum filtration of the Soxhlet receiver solution allows the isolation of pure, microcrystalline $(C_8H_8)LnCl(THF)_x$ in 50% (Er, Lu) to 80% yield (La).

These extremely air- and moisture-sensitive materials are only marginally soluble in THF. They are characterized by X-ray fluorescence (Ln and Cl present in ~1:1 ratios; no K), infrared [bands are observed that are assignable to coordinated THF (1020 cm^{-1})[10] and C$_8$H$_8$$^{-2}$ (890, 700 cm^{-1})[11], and ^{1}H NMR [THF-d_8, La, δ 6.18 (s), Lu, δ 6.33 (s)] spectroscopy and complexometric metal and

(1) (a) Evans, W. J. "The Chemistry of the Metal-Carbon Bond"; Hartley, F. R., Patai, S., Eds.; Wiley-Interscience: New York, 1982; Chapter 12. (b) Marks, T. J. *Prog. Inorg. Chem.* **1978**, *24*, 51.

(2) (a) Wayda, A. L.; Evans, W. J. *Inorg. Chem.* **1980**, *19*, 2190. Tilley, T. D.; Andersen, R. A. *Ibid.* **1981**, *20*, 3267. Watson, P. L.; Whitney, J. F.; Harlow, R. L. *Ibid.* **1981**, *20*, 3271. (b) John, J. N.; Tsutsui, M. *Ibid.* **1981**, *20*, 1602. Tsutsui, M.; Chen, Li-Ban; Bergbreiter, D. E.; Miyamoto, T. K. *J. Am. Chem. Soc.* **1982**, *104*, 855. (c) Lappert, M. F.; Singh, A.; Atwood, J. L.; Hunter, W. E. *J. Chem. Soc., Chem. Commun.* **1981**, 1190.

(3) Mares, F.; Hodgson, K. O.; Streitwieser, A., Jr. *J. Organomet. Chem.* **1971**, *28*, C24. Hodgson, K. O.; Mares, F.; Starks, D. F.; Streitwieser, A., Jr. *J. Am. Chem. Soc.* **1973**, *95*, 8650.

(4) Only one derivative of these complexes, (C$_8$H$_8$)Ln(C$_5$H$_5$)(THF) has been reported. See: Jamerson, J. D.; Masino, A. P.; Takats, J. *J. Organomet. Chem.* **1974**, *65*, C33.

(5) The first well-characterized inclusive homologous precursor series was recently reported by Lappert and co-workers. See ref 2c.

(6) Evans, W. J.; Wayda, A. L. *J. Organomet. Chem.* **1980**, *202*, C6. Atwood, J. L.; Hunter, W. E.; Wayda, A. L.; Evans, W. J. *Inorg. Chem.* **1981**, *20*, 4115.

(7) Evans, W. J.; Meadows, J. H.; Wayda, A. L.; Hunter, W. E.; Atwood, J. L. *J. Am. Chem. Soc.* **1982**, *104*, 2008, 2015. Schumann, H.; Genthe, W. *J. Organomet. Chem.* **1981**, *213*, C7.

(8) Evans, W. J.; Wayda, A. L.; Hunter, W. E.; Atwood, J. L. *J. Chem. Soc., Chem. Commun.* **1981**, 706.

(9) Watson, P. L. *J. Am. Chem. Soc.* **1982**, *104*, 337.

(10) Clark, R. J. H.; Lewis, J.; Machin, D. J.; Nyholm, R. S. *J. Chem. Soc.* **1963**, 379.

(11) Fritz, H. P.; Keller, H. *Z. Naturforsch., B: Anorg. Chem., Org. Chem., Biochem., Biophys.* **1961**, *16B*, 231.

Cyclooctatetraenyllanthanide complexes. 1. Alkyl- and arylmonocyclooctatetraenyllutetium derivatives

Andrea L. Wayda

More About This Article

The permalink http://dx.doi.org/10.1021/om00076a022 provides access to:

- Links to articles and content related to this article
- Copyright permission to reproduce figures and/or text from this article

stereoselective carbozincation of simple alkynes, e.g., 1-octyne, with alkylzinc derivatives appears to be unprecedented. Delineation of its scope and limitations is currently underway.

Registry No. 3, 51655-64-2; 4, 19150-21-1; 5, 77161-69-4; 6, 84695-55-6; I$_2$ZrCp$_2$, 1298-41-5; Br$_2$ZrCp$_2$, 1294-67-3; Cl$_2$ZrCp$_2$, 1291-32-3; EtaZn, 557-20-0; n-Bu$_2$Zn, 1119-90-0; Me$_2$Zn, 544-97-8; I(Me)ZrCp$_2$, 63643-49-2; u-octyne, 629-05-0; ethylzinc chloride, 2633-75-2; 2-methyl-1-octene, 4588-18-5; 2-nonene, 2216-38-8; 5-decyne, 1942-46-7; 5-iodo-6-ethyl-5-decene, 84695-56-7; 2-ethyl-1-octene, 51655-64-2; 1-octynylzinc chloride, 68113-72-4; 1,1-dideuterio-2-methyl-1-octene, 84695-57-8; 1-phenyl-2-deuterioethyne, 3240-11-7; phenylethyne, 536-74-3.

Cyclooctatetraenyllanthanide Complexes. 1. Alkyl- and Arylmonocyclooctatetraenyllutetium Derivatives

Andrea L. Wayda

Bell Laboratories
Murray Hill, New Jersey 07974

Summary: The class of monocyclooctatetrenyllanthanide complexes (C$_8$H$_8$)LnCl(THF)$_x$, previously known only for the early lanthanides (Ln = Ce, Pr, Nd, Sm), has been extended to include lanthanum and the late lanthanides erbium and lutetium. This synthetic extension provides an opportunity to systematically investigate the metathetical derivative chemistry of an inclusive homologous organolanthanide series. Such a study, aimed at the alkyl derivatization of (C$_8$H$_8$)LnCl(THF)$_x$ has resulted in the isolation and characterization of (C$_8$H$_8$)Lu[CH$_2$Si(CH$_3$)$_3$](THF)$_2$ (1) and (C$_8$H$_8$)Lu[o-C$_6$H$_4$CH$_2$N(CH$_3$)$_2$](THF) (2). Attempted derivatization of the analogous lanthanum and samarium complexes has failed to yield characterizable alkyl complexes.

Concomitant with the recent renewed interest in organolanthanide chemistry,[1] concerted effort has recently been directed toward the development of the synthesis and reaction chemistry of cyclopentadienyl derivatives of the lanthanide elements.[2] In sharp contrast, little or no interest has been shown in the development of the chemistry of the monocyclooctatetraenyl complexes of the same elements.[3,4] This is surprising since these derivatives,

(C$_8$H$_8$)LnCl(THF)$_x$, previously described only for the early lanthanides (Ln = Ce, Pr, Nd, Sm),[3] should readily lend themselves to facile metathetical derivatization. Furthermore, the extension of this homologous series to include the late lanthanides would provide only the second complete series of precursor organolanthanide complexes.[5] The existence of such homologous series is critically important to a systematic study of the derivative chemistry of organolanthanide complexes. In particular, only through such studies can important observations relating the reactivity of organolanthanide complexes (and their derivatives) to their position in the lanthanide series be made. "Reactivity tailoring" or "fine tuning" of the relevant chemistry of these complexes should directly accrue from such fundamental studies.

Therefore, we have investigated the extension of the known (C$_8$H$_8$)LnCl(THF)$_x$ derivatives to include lanthanum and the later lanthanides erbium and lutetium. As noted, the completion of this homologous series provides an opportunity to systematically investigate the metathetical derivative chemistry of an organolanthanide compound class. In this regard, as an initial and obvious synthetic goal, we have addressed the synthesis and characterization of cyclooctatetraenyllanthanide alkyl complexes. The synthesis of such derivatives should allow a rich reaction chemistry to be explored. (cf. the use of bis(cyclopentadienyl)lanthanide alkyls as precursors to heteroleptic alkynides,[6] hydrides,[7] carbon monoxide insertion products,[8] and Ziegler–Natta polymerization catalysts[9]). We therefore also report at this time the synthesis and characterization of the first cyclooctatetraenyllanthanide alkyl and aryl derivatives (C$_8$H$_8$)Lu[CH$_2$Si(CH$_3$)$_3$](THF)$_2$ (1) and (C$_8$H$_8$)Lu[o-C$_6$H$_4$CH$_2$N(CH$_3$)$_2$](THF) (2).

The new (C$_8$H$_8$)LnCl(THF)$_x$ complexes are synthesized by using the methodology of Streitwieser et al. with minor modification.[3] Slow ambient-temperature addition of a freshly prepared THF solution of K$_2$(C$_8$H$_8$) to an equimolar amount of LnCl$_3$ suspended in THF yields, after a reaction time of 24 h, characteristically colored slurries (pink for erbium, off-white for lutetium, and pale yellow for lanthanum). The crude products are isolated and initially purified by removal of solvent in vacuo followed by THF extraction to remove soluble by-products (such as K[Ln(C$_8$H$_8$)$_2$]).[3] Final purification is achieved by Soxhlet extraction of the residue with THF for 24 h. Vacuum filtration of the Soxhlet receiver solution allows the isolation of pure, microcrystalline (C$_8$H$_8$)LnCl(THF)$_x$ in 50% (Er, Lu) to 80% yield (La).

These extremely air- and moisture-sensitive materials are only marginally soluble in THF. They are characterized by X-ray fluorescence (Ln and Cl present in ~1:1 ratios; no K), infrared [bands are observed that are assignable to coordinated THF (1020 cm^{-1})[10] and C$_8$H$_8^{-2}$ (890, 700 cm^{-1})[11]], and ^{1}H NMR [THF-d_8, La, δ 6.18 (s), Lu, δ 6.33 (s)] spectroscopy and complexometric metal and

(1) (a) Evans, W. J. "The Chemistry of the Metal-Carbon Bond"; Hartley, F. R., Patai, S., Eds.; Wiley-Interscience: New York, 1982; Chapter 12. (b) Marks, T. J. *Prog. Inorg. Chem.* **1978**, *24*, 51.

(2) (a) Wayda, A. L.; Evans, W. J. *Inorg. Chem.* **1980**, *19*, 2190. Tilley, T. D.; Andersen, R. A. *Ibid.* **1981**, *20*, 3267. Watson, P. L.; Whitney, J. F.; Harlow, R. L. *Ibid.* **1981**, *20*, 3271. (b) John, J. N.; Tsutsui, M. *Ibid.* **1981**, *20*, 1602. Tsutsui, M.; Chen, Li-Ban; Bergbreiter, D. E.; Miyamoto, T. K. *J. Am. Chem. Soc.* **1982**, *104*, 855. (c) Lappert, M. F.; Singh, A.; Atwood, J. L.; Hunter, W. E. *J. Chem. Soc., Chem. Commun.* **1981**, 1190.

(3) Mares, F.; Hodgson, K. O.; Streitwieser, A., Jr. *J. Organomet. Chem.* **1971**, *28*, C24. Hodgson, K. O.; Mares, F.; Starks, D. F.; Streitwieser, A., Jr. *J. Am. Chem. Soc.* **1973**, *95*, 8650.

(4) Only one derivative of these complexes, (C$_8$H$_8$)Ln(C$_5$H$_5$)(THF) has been reported. See: Jamerson, J. D.; Masino, A. P.; Takats, J. *J. Organomet. Chem.* **1974**, *65*, C33.

(5) The first well-characterized inclusive homologous precursor series was recently reported by Lappert and co-workers. See ref 2c.

(6) Evans, W. J.; Wayda, A. L. *J. Organomet. Chem.* **1980**, *202*, C6. Atwood, J. L.; Hunter, W. E.; Wayda, A. L.; Evans, W. J. *Inorg. Chem.* **1981**, *20*, 4115.

(7) Evans, W. J.; Meadows, J. H.; Wayda, A. L.; Hunter, W. E.; Atwood, J. L. *J. Am. Chem. Soc.* **1982**, *104*, 2008, 2015. Schumann, H.; Genthe, W. *J. Organomet. Chem.* **1981**, *213*, C7.

(8) Evans, W. J.; Wayda, A. L.; Hunter, W. E.; Atwood, J. L. *J. Chem. Soc., Chem. Commun.* **1981**, 706.
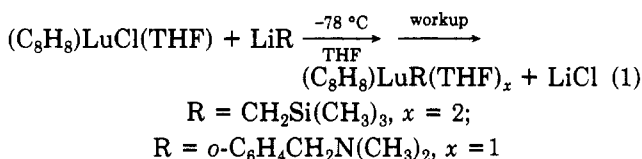
(9) Watson, P. L. *J. Am. Chem. Soc.* **1982**, *104*, 337.

(10) Clark, R. J. H.; Lewis, J.; Machin, D. J.; Nyholm, R. S. *J. Chem. Soc.* **1963**, 379.

(11) Fritz, H. P.; Keller, H. *Z. Naturforsch., B: Anorg. Chem., Org. Chem., Biochem., Biophys.* **1961**, *16B*, 231.

complete elemental analysis.[12] As analyzed the lanthanum derivative contains two molecules of THF while the erbium and lutetium derivatives contain one molecule of THF. The complexes are not sufficiently soluble in THF for ^{13}C NMR spectroscopy or isopiestic molecular weight measurement.

Attempted alkyl derivatization of the $(C_8H_8)LnCl(THF)_x$ series has been initially confined to Ln = La, Sm, and Lu due to the ease of characterization of these complexes and their reaction products by ^{1}H and ^{13}C NMR spectroscopy. Accordingly, we have synthesized the first cyclooctatetraenyllanthanide alkyl and aryl complexes $(C_8H_8)Lu[CH_2Si(CH_3)_3](THF)_2$ (1) and $(C_8H_8)Lu[o\text{-}C_6H_4CH_2N(CH_3)_2](THF)$ (2) by reaction of $(C_8H_8)LuCl(THF)$ and the appropriate lithium reagent.[13] The reactions are conducted in THF at –78 °C, and the reaction mixture is then allowed to slowly warm to ambient temperature with stirring. Solvent is removed in vacuo, and the resulting oils are triturated with pentane or hexane to yield off-white/beige powders. After the mixture was washed with additional alkane solvent, the powders are extracted with toluene, and the solvent is removed in vacuo to yield spectroscopically pure 1 and 2 in 50–55% yield (eq 1).

$$(C_8H_8)LuCl(THF) + LiR \xrightarrow[\text{THF}]{-78\ ^\circ C} \xrightarrow{\text{workup}}$$
$$(C_8H_8)LuR(THF)_x + LiCl \quad (1)$$
$$R = CH_2Si(CH_3)_3,\ x = 2;$$
$$R = o\text{-}C_6H_4CH_2N(CH_3)_2,\ x = 1$$

1 is marginally stable in toluene at ambient temperature and cannot be readily crystallized. However, it can be satisfactorily characterized by infrared (bands characteristic of $CH_2Si(CH_3)_3$[14] at 1240, 1230, 1225, and 855 cm^{-1}, coordinated THF at 1015 cm^{-1}, and $C_8H_8{}^{2-}$ at 890 and 705 cm^{-1} are observed) and ^{1}H NMR spectroscopy[15] [benzene-d_6, δ 6.69 (s, CH_8), 3.31 (m, α-THF), 1.18 (m, β-THF), 0.45 (s, CH$_2$Si(CH_3)$_3$), –1.72 (s, CH_2Si(CH$_3$)$_3$)], complexometric metal analysis [% Lu(calcd) 32.10; % Lu (found) 33.16], and X-ray fluorescence (Lu and Si; no Cl). The marginal stability of 1 precludes complete elemental analysis.

Compound 2 is more stable than 1 presumably due to the stability conferred by chelation of the integral Lewis base, –N(CH$_3$)$_2$. Unlike 1, it can be purified further by crystallization from a mixture of toluene and hexane maintained at –30 °C. Unfortunately, X-ray quality crystals have not yet been obtained. However, satisfactory characterization of the complex is provided by infrared [bands characteristic of $C_6H_4CH_2N(CH_3)_2$[14] (1420, 1380, 1360, 1305, 1235, 1170, 1095, 1040, 1010, 990, 940, 855, 750 cm^{-1}), and $C_8H_8{}^{2-}$ (890, 700 cm^{-1}) are observed] and ^{1}H NMR spectroscopy[15] [benzene-d_6, δ 8.15, 7.01 (m, C$_6$$H_4CH_2$N(CH$_3$)$_2$), 6.71 (s, C$_8$$H_8$), 3.01, 1.00 (m, α- and β-THF, respectively), 2.79 (s, C$_6$H$_4$CH_2N(CH$_3$)$_2$), 1.82 (s,

$C_6H_4CH_2N(CH_3)_2$], X-ray fluorescence (Lu; no Cl), and complete elemental analysis. (Anal. Calcd for LuC$_{21}$H$_{28}$NO: Lu, 36.04; C, 51.96; H, 5.81; N, 2.88; O, 3.29. Found: Lu, 36.45; C, 51.62; H, 5.68; N, 2.78; O, 3.47 (by difference)).

Unfortunately, analogous alkyl and aryl derivatives cannot be isolated for La and Sm. When R = CH$_2$Si(CH$_3$)$_3$, no characterizable product can be obtained for Sm. For La, only the THF-soluble [(C$_8$H$_8$)$_2$La][Li(THF)$_x$] can be isolated (identified by infrared and ^{1}H NMR spectroscopy and complexometric metal analysis),[16] suggesting that the desired alkyl or alkyl intermediate has formed but is unstable with respect to ligand redistribution. In this context, it should be noted that [(C$_8$H$_8$)$_2$Lu][Li(THF)$_x$][17] is an isolated byproduct in the synthesis of 1, indicating that, even at the end of the lanthanide series, ligand redistribution is a concern when R = CH$_2$Si(CH$_3$)$_3$. When R = C$_6$H$_4$CH$_2$N(CH$_3$)$_2$, no characterizable product is obtained for either La or Sm.

Despite these synthetic difficulties, this work clearly demonstrates that (1) an easily prepared homologous monocyclooctatetraenyl-based organolanthanide series exists and is available for systematic study and derivatization and (2) alkyl- and arylmonocyclooctatetraenyllutetium derivatives can be synthesized and characterized. Studies aimed at broadening the scope and number of these derivative complexes along with an investigation of their reaction chemistry are currently being conducted.

(16) IR (Nujol mull, cm^{-1}): 1045 (THF coordinated to lithium), 895, 695 (C$_8$H$_8{}^{2-}$). ^{1}H NMR (THF-d_8): δ 5.75 (s).

(17) IR (Nujol mull, cm^{-1}) identical with that of [Li(THF)$_x$][La-(C$_8$H$_8$)$_2$]. ^{1}H NMR (THF-d_8) δ 5.62 (s).

Surface and Catalytic Chemistry of Organoactinides. Evidence for Surface-Stabilized Alkylidenes

Ming-Yuan He, Robert L. Burwell, Jr.,* and Tobin J. Marks*

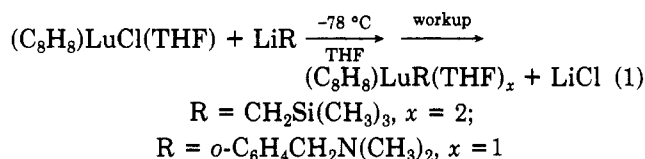*Department of Chemistry, Northwestern University
Evanston, Illinois 60201*

Summary: The reaction of M[η^5-(CH$_3$)$_5$C$_5$]$_2$(CH$_3$)$_2$ and M[η^5-(CH$_3$)$_5$C$_5$]$_2$(CD$_3$)$_2$ compounds, M = Th and U, with partially dehydroxylated and nearly completely dehydroxylated alumina yields methane via protolysis by surface OH, ring H atom abstraction, and elimination within the M(CH$_3$)$_2$ groups. The latter pathway is proposed on the basis of chemical evidence to result in alumina-stabilized actinide alkylidenes.

We have previously shown that bis(pentamethylcyclopentadienyl)thorium and bis(pentamethylcyclopentadienyl)uranium dialkyls, when supported upon high surface area metal oxides such as γ-alumina, are precursors for highly active olefin hydrogenation and polymerization catalysts.[1] In an effort better to delineate the nature of

(12) Anal. Calcd for LaC$_{16}$H$_{24}$ClO$_2$: La, 32.86; C, 45.46; H, 5.72; Cl, 8.38; O, 7.56. Found: La, 33.20; C, 45.17; H, 5.48; Cl, 7.80; O, 8.35 (by difference). Anal. Calcd for ErC$_{12}$H$_{16}$ClO: Er, 44.13; C, 38.03; H, 4.25; Cl, 9.35; O, 4.22. Found: Er, 44.40; C, 37.78; H, 4.13; Cl, 9.20; O, 4.49 (by difference). Anal. Calcd for LuC$_{12}$H$_{16}$ClO: Lu, 45.25. Found: Lu, 45.61 (complexometric); Lu:Cl ratio = 1.01. Complete elemental analyses and determination of Lu:Cl ratio were performed by Analytische Laboratorien, Engelskirchen, West Germany.

(13) LiCH$_2$Si(CH$_3$)$_3$ is prepared using the method described by Lewis and Brown (Lewis, H. L.; Brown, T. L. *J. Am. Chem. Soc.* 1970, 92, 4664). Li[o-C$_6$H$_4$CH$_2$N(CH$_3$)$_2$] is prepared by following the procedure described by Cope and Gourley (Cope, A. C.; Gourley, R. N. *J. Organomet. Chem.* 1967, 8, 527).

(14) Band assignments are made by comparison with the infrared spectra of the lithium salts LiCH$_2$Si(CH$_3$)$_3$ and Li[o-C$_6$H$_4$CH$_2$N(CH$_3$)$_2$].

(15) Integrated ratios are as expected.

complete elemental analysis.[12] As analyzed the lanthanum derivative contains two molecules of THF while the erbium and lutetium derivatives contain one molecule of THF. The complexes are not sufficiently soluble in THF for ^{13}C NMR spectroscopy or isopiestic molecular weight measurement.

Attempted alkyl derivatization of the $(C_8H_8)LnCl(THF)_x$ series has been initially confined to Ln = La, Sm, and Lu due to the ease of characterization of these complexes and their reaction products by ^1H and ^{13}C NMR spectroscopy. Accordingly, we have synthesized the first cyclooctatetraenyllanthanide alkyl and aryl complexes $(C_8H_8)Lu[C-H_2Si(CH_3)_3](THF)_2$ (1) and $(C_8H_8)Lu[o\text{-}C_6H_4CH_2N-(CH_3)_2](THF)$ (2) by reaction of $(C_8H_8)LuCl(THF)$ and the appropriate lithium reagent.[13] The reactions are conducted in THF at -78 °C, and the reaction mixture is then allowed to slowly warm to ambient temperature with stirring. Solvent is removed in vacuo, and the resulting oils are triturated with pentane or hexane to yield off-white/beige powders. After the mixture was washed with additional alkane solvent, the powders are extracted with toluene, and the solvent is removed in vacuo to yield spectroscopically pure 1 and 2 in 50–55% yield (eq 1).

$$(C_8H_8)LuCl(THF) + LiR \xrightarrow[\text{THF}]{-78\,°C} \xrightarrow{\text{workup}}$$
$$(C_8H_8)LuR(THF)_x + LiCl \quad (1)$$
$$R = CH_2Si(CH_3)_3, \; x = 2;$$
$$R = o\text{-}C_6H_4CH_2N(CH_3)_2, \; x = 1$$

1 is marginally stable in toluene at ambient temperature and cannot be readily crystallized. However, it can be satisfactorily characterized by infrared (bands characteristic of $CH_2Si(CH_3)_3$[14] at 1240, 1230, 1225, and 855 cm^{-1}, coordinated THF at 1015 cm^{-1}, and $C_8H_8{}^{2-}$ at 890 and 705 cm^{-1} are observed) and ^1H NMR spectroscopy[15] [benzene-d_6, δ 6.69 (s, CH_8), 3.31 (m, α-THF), 1.18 (m, β-THF), 0.45 (s, CH$_2$Si(CH_3)$_3$), -1.72 (s, CH_2Si(CH$_3$)$_3$)], complexometric metal analysis [% Lu(calcd) 32.10; % Lu (found) 33.16], and X-ray fluorescence (Lu and Si; no Cl). The marginal stability of 1 precludes complete elemental analysis.

Compound 2 is more stable than 1 presumably due to the stability conferred by chelation of the integral Lewis base, -N(CH$_3$)$_2$. Unlike 1, it can be purified further by crystallization from a mixture of toluene and hexane maintained at -30 °C. Unfortunately, X-ray quality crystals have not yet been obtained. However, satisfactory characterization of the complex is provided by infrared [bands characteristic of C$_6$H$_4$CH$_2$N(CH$_3$)$_2$[14] (1420, 1380, 1360, 1305, 1235, 1170, 1095, 1040, 1010, 990, 940, 855, 750 cm^{-1}), and C$_8$H$_8{}^{2-}$ (890, 700 cm^{-1}) are observed] and ^1H NMR spectroscopy[15] [benzene-d_6, δ 8.15, 7.01 (m, C$_6$$H_4CH_2$N(CH$_3$)$_2$), 6.71 (s, C$_8$$H_8$), 3.01, 1.00 (m, α- and β-THF, respectively), 2.79 (s, C$_6$H$_4$CH_2N(CH$_3$)$_2$), 1.82 (s,

$C_6H_4CH_2N(CH_3)_2$], X-ray fluorescence (Lu; no Cl), and complete elemental analysis. (Anal. Calcd for LuC$_{21}$H$_{28}$NO: Lu, 36.04; C, 51.96; H, 5.81; N, 2.88; O, 3.29. Found: Lu, 36.45; C, 51.62; H, 5.68; N, 2.78; O, 3.47 (by difference)).

Unfortunately, analogous alkyl and aryl derivatives cannot be isolated for La and Sm. When R = CH$_2$Si(C-H$_3$)$_3$, no characterizable product can be obtained for Sm. For La, only the THF-soluble [(C$_8$H$_8$)$_2$La][Li(THF)$_x$] can be isolated (identified by infrared and ^1H NMR spectroscopy and complexometric metal analysis),[16] suggesting that the desired alkyl or alkyl intermediate has formed but is unstable with respect to ligand redistribution. In this context, it should be noted that [(C$_8$H$_8$)$_2$Lu][Li(THF)$_x$][17] is an isolated byproduct in the synthesis of 1, indicating that, even at the end of the lanthanide series, ligand redistribution is a concern when R = CH$_2$Si(CH$_3$)$_3$. When R = C$_6$H$_4$CH$_2$N(CH$_3$)$_2$, no characterizable product is obtained for either La or Sm.

Despite these synthetic difficulties, this work clearly demonstrates that (1) an easily prepared homologous monocyclooctatetraenyl-based organolanthanide series exists and is available for systematic study and derivatization and (2) alkyl- and arylmonocyclooctatetraenyl-lutetium derivatives can be synthesized and characterized. Studies aimed at broadening the scope and number of these derivative complexes along with an investigation of their reaction chemistry are currently being conducted.

(16) IR (Nujol mull, cm^{-1}): 1045 (THF coordinated to lithium), 895, 695 (C$_8$H$_8{}^{2-}$). ^1H NMR (THF-d_8): δ 5.75 (s).

(17) IR (Nujol mull, cm^{-1}) identical with that of [Li(THF)$_x$][La-(C$_8$H$_8$)$_2$]. ^1H NMR (THF-d_8) δ 5.62 (s).

Surface and Catalytic Chemistry of Organoactinides. Evidence for Surface-Stabilized Alkylidenes

Ming-Yuan He, Robert L. Burwell, Jr.,* and Tobin J. Marks*

Department of Chemistry, Northwestern University Evanston, Illinois 60201

Summary: The reaction of M[η^5-(CH$_3$)$_5$C$_5$]$_2$(CH$_3$)$_2$ and M[η^5-(CH$_3$)$_5$C$_5$]$_2$(CD$_3$)$_2$ compounds, M = Th and U, with partially dehydroxylated and nearly completely dehydroxylated alumina yields methane via protolysis by surface OH, ring H atom abstraction, and elimination within the M(CH$_3$)$_2$ groups. The latter pathway is proposed on the basis of chemical evidence to result in alumina-stabilized actinide alkylidenes.

We have previously shown that bis(pentamethylcyclopentadienyl)thorium and bis(pentamethylcyclopentadienyl)uranium dialkyls, when supported upon high surface area metal oxides such as γ-alumina, are precursors for highly active olefin hydrogenation and polymerization catalysts.[1] In an effort better to delineate the nature of

(12) Anal. Calcd for LaC$_{18}$H$_{24}$ClO$_2$: La, 32.86; C, 45.46; H, 5.72; Cl, 8.38; O, 7.56. Found: La, 33.20; C, 45.17; H, 5.48; Cl, 7.80; O, 8.35 (by difference). Anal. Calcd for ErC$_{12}$H$_{16}$ClO: Er, 44.13; C, 38.03; H, 4.25; Cl, 9.35; O, 4.22. Found: Er, 44.40; C, 37.78; H, 4.13; Cl, 9.20; O, 4.49 (by difference). Anal. Calcd for LuC$_{12}$H$_{16}$ClO: Lu, 45.25. Found: Lu, 45.61 (complexometric); Lu:Cl ratio = 1.01. Complete elemental analyses and determination of Lu:Cl ratio were performed by Analytische Laboratorien, Engelskirchen, West Germany.

(13) LiCH$_2$Si(CH$_3$)$_3$ is prepared using the method described by Lewis and Brown (Lewis, H. L.; Brown, T. L. *J. Am. Chem. Soc.* 1970, *92*, 4664). Li[o-C$_6$H$_4$CH$_2$N(CH$_3$)$_2$] is prepared by following the procedure described by Cope and Gourley (Cope, A. C.; Gourley, R. N. *J. Organomet. Chem.* 1967, *8*, 527).

(14) Band assignments are made by comparison with the infrared spectra of the lithium salts LiCH$_2$Si(CH$_3$)$_3$ and Li[o-C$_6$H$_4$CH$_2$N(CH$_3$)$_2$].

(15) Integrated ratios are as expected.

the organoactinide species present on the surface and to provide information concerning how, in general, such surfaces afford organometal-derived catalysts,[2] we have undertaken a mechanistic investigation of the reaction of $M[\eta^5\text{-}(CH_3)_5C_5]_2(CH_3)_2$ complexes (M = Th, U) with partially dehydroxylated (or dedeuteroxylated) alumina (PDA or PDA-d) and nearly completely dehydroxylated (or dedeuteroxylated) alumina (DA or DA-d). PDA (American Cyanamid PHF γ-alumina, 99.99% purity) contains ca. 4 surface OH (OD) groups (weak Brønsted acid), 5.5 surface O^{2-} (strong Lewis base), and 5.5 exposed Al^{3+} (strong Lewis acid) sites/100 Å^2, while DA, although mainly composed of O^{2-} and exposed Al^{3+} ions, also contains ca. 0.12 residual OH unit/per 100 Å^2.[3] In this communication we report several reaction pathways that have been identified; perhaps most significant is the observation that alumina surfaces may stabilize reactive metal alkylidenes in a manner analogous to recently documented solution chemistry.

PDA and DA were prepared in flowing helium (475 °C and 950–1000 °C, respectively) and were deuterated (PDA-d, DA-d) as described elsewhere.[1,3a,4] The compounds $M[(CH_3)_5C_5]_2(CH_3)_2$ and $M[(CH_3)_5C_5](CD_3)_2$ (M = Th, U) were synthesized from CH$_3$Li or CD$_3$Li as reported previously.[5] The CD$_3$ groups in the latter complexes were shown to be >98% trideuterated by ^{1}H NMR (integrating vs. the $(CH_3)_5C_5$ resonance) and mass spectrometry. Measured quantities (18–47 μmol) of the organometallics were dissolved in pentane and slurried with 0.25 g of alumina under rigorously anaerobic conditions in a previously described flow reaction/analysis system.[6] These loadings correspond to 0.3–0.7 actinide molecule/100 Å^2 of surface area.[3f] The samples were then subjected to the following sequence of reaction conditions: flowing helium for 1 h at 0 °C (pentane evaporation), for 1 h at 25 °C, and for 1 h at 100 °C (abbreviated as follows: He, 0 °C, 1; He, 25 °C, 1; He, 100 °C, 1). Gases evolved during these time intervals were measured gas chromatographically and were collected for mass spectrometric analysis.

Labeling experiments were designed to probe three distinct methane-evolving pathways: H abstraction from a surface OH group;[5a] H abstraction from the $(CH_3)_5C_5$ rings; H abstraction from another methyl group. These

Scheme I. Labeling Experiment

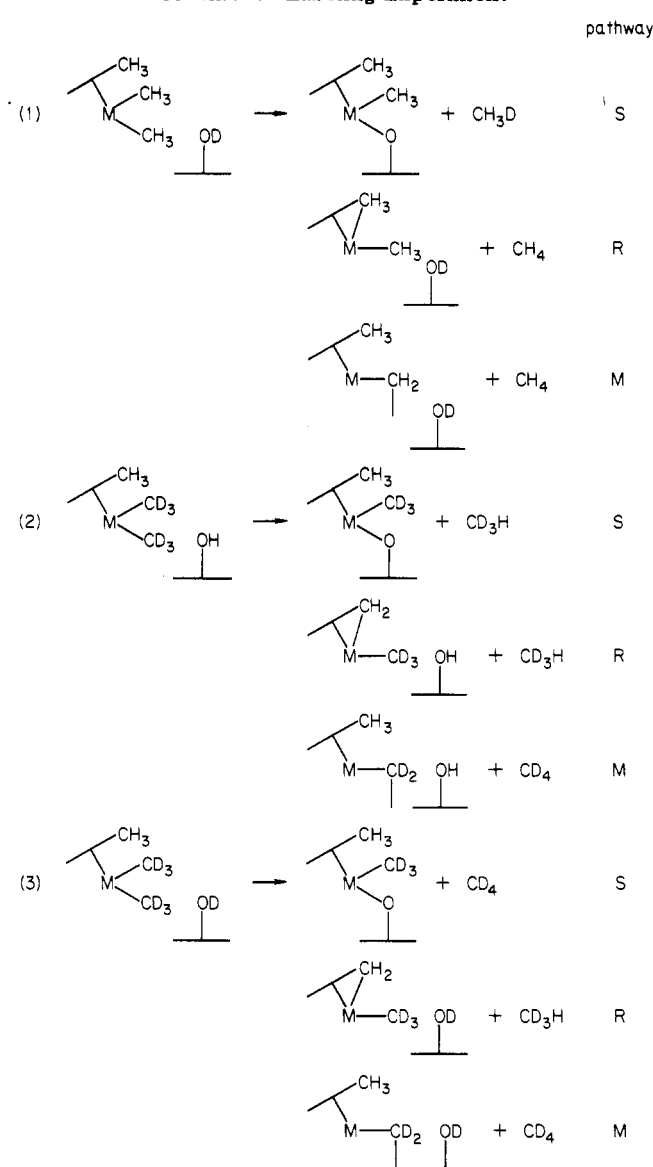(1) (a) Bowman, R. G.; Nakamura, R.; Fagan, P. J.; Burwell, R. L., Jr.; Marks, T. J. *J. Chem. Soc., Chem. Commun.* 1981, 257–258. (b) Bowman, R. G.; Fagan, P. J.; He, M.-Y.; Nakamura, R.; Stecher, H. A.; Burwell, R. L., Jr.; Marks, T. J. "Abstracts of Papers", 182nd National Meeting of the American Chemical Society, New York, Aug 1981; American Chemical Society: Washington, DC, 1981; INOR 4. (c) He, M.-Y.; Stecher, H. A.; Burwell, R. L., Jr.; Marks, T. J., manuscript in preparation. (d) For example, turnover frequencies comparable to supported platinum and rhodium catalysts have been measured for propylene hydrogenation.

(2) (a) Boor, J., Jr. "Ziegler-Natta Catalysts and Polymerizations"; Academic Press: New York, 1979; Chapters 6, 22. (b) Zakharov, V. A.; Yermakov, Yu. I. *Catal. Rev.—Sci. Eng.* 1979, *19*, 67–103. (c) Hartley, F. R.; Vezry, P. N. *Adv. Organomet. Chem.* 1978, *15*, 189–234. (d) Yermakov, Yu. I. *Catal. Rev.—Sci. Eng.* 1976, *13*, 77–120. (e) Ballard, D. G. H. *J. Polym. Sci.* 1975, *13*, 2191–2212. (f) Ballard, D. G. H. *Adv. Catal.* 1973, *23*, 263–325.

(3) (a) Bowman, R. G.; Burwell, R. L., Jr. *J. Catal.* 1980, *63*, 463–475. (b) Beránek, L.; Kraus, M. In "Comprehensive Chemical Kinetics"; Bamford, C. H., Tipper, C. F. H.; Eds.; Elsevier: Amsterdam, 1978; pp 263–398. (c) Benesi, H. A.; Winquist, B. H. C. *Adv. Catal.* 1978, *27*, 97–182. (d) Knözinger, H.; Ratnasamy, P. *Catal. Rev.—Sci. Eng.* 1978, *17*, 31–70. (e) Lippens, B. C.; Steggerda, J. J. In "Physical and Chemical Aspects of Adsorbents and Catalysts"; Linsen, B. G., ed.; Academic Press: London, 1970; Chapter 4. (f) The surface areas of PDA and DA are comparable, 160 m^2/g by BET measurements.[3a]

(4) (a) Laniecki, M.; Burwell, R. L., Jr. *J. Catal.* 1980, *75*, 95–104. (b) Hall, W. K.; Leftin, H. P.; Cheselske, F. J.; O'Reilly, D. E. *Ibid* 1963, *2*, 506–517.

(5) (a) Fagan, P. J.; Manriquez, J. M.; Maatta, E. A.; Seyam, A. M.; Marks, T. J. *J. Am. Chem. Soc.* 1981, *103*, 6650–6667. (b) LiCD$_3$ was prepared from CD$_3$I and lithium metal in diethyl ether.

(6) Brenner, A.; Burwell, R. L., Jr. *J. Catal.* 1978, *52*, 353–363.

Table I. Surface Reaction Pathway Partitioning for $U[(CH_3)_5C_5]_2(CH_3)_2$[a]

pathway	He, 0 °C, 1 (%)	He, 25 °C, 1 (%)	He, 100 °C, 1 (%)
	PDA		
S	81	72	70
R	12	23	29
M	1.6	2.3	1.2
(S + R + M)	95[b]	97[b]	100[b]
methane[c]	60[c]	4[c]	12[c]
	DA		
S	45	25[d]	19
R	45	63[d]	73
M	7	12[d]	11
(S + R + M)	97[b]	100[b,d]	103[b]
methane[c]	6.0[c]	1[c,d]	9.5[c]

[a] Given as percentages of the reaction pathway. [b] Sum of reaction pathways from three experiments. [c] Yield of methane as a percentage of total available methyl groups. [d] Low methane yield limits accuracy.

processes are illustrated schematically in Scheme I without specification as to structure or reaction molecularity (several bimolecular processes can be excluded—vide infra). It can be seen that labeling experiments 1, 2, and 3

Table II. Surface Reaction Pathway Partitioning
for $Th[(CH_3)_5C_5]_2(CH_3)_2$ [a]

| pathway	He, 0 °C 1 (%)	He, 25 °C 1 (%)	He, 100 °C 1 (%)
	DA		
S	69	58[d]	23
R	31	39[d]	52
M	3.0	24[d]	29
(S + R + M)	103[b]	121[b,d]	104[b]
methane[c]	8.0[c]	1[c,d]	4.0[c]

[a] Given as percentages of the reaction pathway. [b] Sum of reaction pathways from three experiments. [c] Yield of methane as a percentage of total available methyl groups. [d] Low methane yield limits accuracy.

uniquely assay the pathways S (surface), M (methyl), and R (ring), respectively. A possible complication is isotopic exchange prior to and/or following methane formation. If extensive, this would be evidenced by lack of self-consistency in the yield data, i.e., the sum of the three pathways deduced from the three separate labeling experiments would not equal 100%. Furthermore, we find in control experiments that, under the reaction conditions, added methane does not undergo significant isotopic exchange with PDA-*d* or DA-*d*.[7] It is also conceivable, but at this time not established, that the quantitative reaction channel analysis might be biased somewhat by kinetic isotope effects. This question is presently under investigation. In other work we have shown that U(IV) does not undergo detectable oxidation (evolve H_2) under the reaction conditions,[1b,c] nor is it likely[1b,5a] that significant $(CH_3)_5C_5H$ displacement occurs.

The results of the labeling experiments are shown in Tables I and II. It can be seen in Table I that PDA with a high coverage of surface OH (OD) functionalities is far more reactive for methane evolution than DA, and under all conditions on PDA, pathway S dominates. It can also be seen in Table I that there is good self-consistency in the data ($\sum(S + R + M) \approx 100\%$). Pathway S is considerably less important on DA, and although pathways R and M take on greater relative importance, the $U[(CH_3)_5C_5]_2(CH_3)_2$ data show that the absolute yields through He, 100 °C, via R and M are roughly the same on PDA and DA. The amount of methane produced via S in heating the uranium complex on DA through He, 100 °C, represents approximately one-eighth of the surface OH content (ca. 8 μmol/0.25 g). Table II shows that on DA, $Th[(CH_3)_5C_5]_2(CH_3)_2$, and $U[(CH_3)_5C_5]_2(CH_3)_2$ give comparable yields of methane and, furthermore, that the total methane yield via pathway M is nearly the same for the two metals. Again $\sum(S + R + M) \approx 100\%$ except in cases where the quantities of methane approach the detection limits. The molecularity of pathway M was investigated in a cross-over experiment whereby a 1:1 mixture of $Th[(CH_3)_5C_5]_2(CH_3)_2$ and $Th[(CH_3)_5C_5]_2(CD_3)_2$ was subjected to the standard activation conditions on DA. It was found in all three activation periods that the methane isotopic distribution was identical with the sum of the distributions from the separate $Th[(CH_3)_5C_5]_2(CH_3)_2$ and $Th[(CH_3)_5C_5]_2(CD_3)_2$ experiments. From these results it is possible to estimate that the percentage of pathway M which is intramolecular is greater than 95%.

The course of and the environment in which pathway M occurs strongly suggest an analogy to the group 4B aluminum-stabilized alkylidenes of Tebbe, Grubbs, and

co-workers (A).[8,9] Further support for a formulation such

A

B
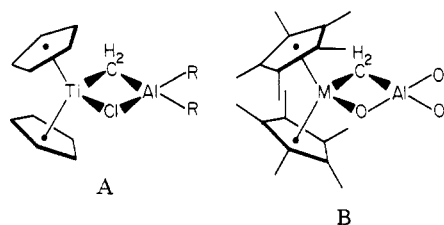
as B in which an exposed Al^{3+} site on the surface stabilizes[10] an actinide alkylidene[11] is provided by the following chemical evidence. When pulses of acetone were passed at 25 °C over $M[(CH_3)_5C_5]_2(CH_3)_2$/DA that had been activated at He, 100 °C, 1, the major (70–90%) hydrocarbon product was isobutylene. For a large excess of acetone, (360 μmol), yields of isobutylene were ~20% (M = U) and ~38% (M = Th) on the basis of available surface methylene calculated from the data in Tables I and II. Also produced in these reactions were traces (totalling <5% of the isobutylene yield) of ethylene, propane, propylene, *cis*- and *trans*-2-butene, and five isomeric pentenes. Blank experiments indicated that only propane and propylene are primary reaction products of acetone and DA. When the above methylene assay was conducted with $Th[(CH_3)_5C_5]_2(CD_3)_2$, the evolved isobutylene was found to be >99% isobutylene-d_2 ($(CH_3)_2C=CD_2$) by mass spectrometry. The isobutylene formation can be interpreted in terms of the known methylene-transfer chemistry of species such as A[8,9,12] (eq 1 and 2). As for the trace, non-C_3
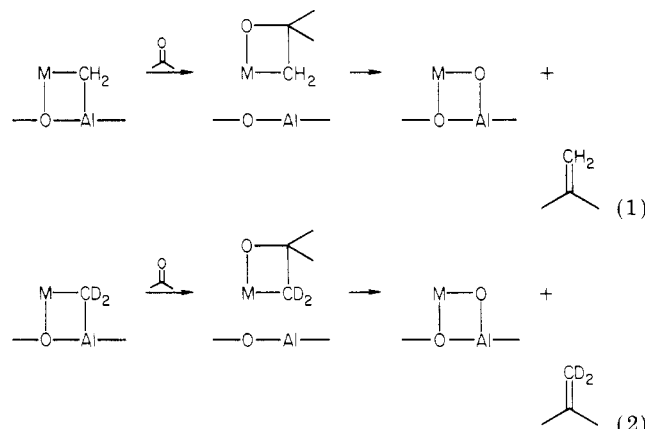
olefins, the known olefin metathesis activity of A[8,9] suggests that they might arise from propylene and/or isobutylene metathesis. This question is under further investigation.

In identifying three discrete, methane-evolving reaction pathways between $M[(CH_3)_5C_5]_2(CH_3)_2$ compounds and alumina surfaces, this study initiates a description of the chemistry that ultimately leads to supported organo-

(7) Exchange is observed at longer contact times: Larson, J. G.; Hall, W. K. *J. Phys. Chem.* **1965**, *69*, 3080–3089.

(8) (a) Tebbe, F. N.; Harlow, R. L. *J. Am. Chem. Soc.* **1980**, *102*, 6149–6151. (b) Tebbe, F. N.; Parshall, G. W.; Reddy, G. S. *Ibid.* **1978**, *100*, 3611–3613.

(9) (a) Ott, K. C.; Lee, J. B.; Grubbs, R. H. *J. Am. Chem. Soc.* **1982**, *104*, 2942–2944. (b) Lee, J. B.; Gajda, G. L.; Schaefer, W. P.; Howard, T. R.; Ikariya, T.; Straus, D. A.; Grubbs, R. H. *Ibid.* **1981**, *103*, 7358–7361. (c) Howard, T. F.; Lee, J. B.; Grubbs, R. H. *Ibid.* **1980**, *102*, 6876–6878.

(10) For an AlX_3/Al_2O_3 analogy in metal carbonyl chemistry, see: Correa, F.; Nakamura, R.; Stimson R. E.; Burwell, R. L., Jr.; Shriver, D. F. *J. Am. Chem. Soc.* **1980**, *102*, 5112–5114.

(11) (a) Considering the evidence[12b,c] for the instability of divalent thorium and uranium organometallics, an unstabilized, formally divalent $M[(CH_3)_5C_5]_2CH_2$ species seems far less likely. (b) Marks, T. J.; Ernst, R. D. In "Comprehensive Organometallic Chemistry"; Wilkinson, G., Stone, F. G. A., Abel, E. W., Eds.; Pergamon Press: Oxford, in press. (c) Marks, T. J. *Prog. Inorg. Chem.* **1979**, *25*, 223–333.

(12) Pine, S. H.; Zahler, R.; Evans, D. A.; Grubbs, R. H. *J. Am. Chem. Soc.* **1980**, *102*, 3270–3272.

actinide catalysts.[1] Interestingly, the measured molar yields via pathway M during activation are roughly the same as the moles of active sites for hydrogenation of propylene measured by poisoning with carbon monoxide.[1] No effort has been made to optimize any of the reaction pathways, and indeed, actinide ions are not likely to be optimum for any one particular pathway. However, on a more general level and with specific reference to metal alkylidene stabilization by electron-deficient supports, it is not difficult to visualize how such species might play roles in heterogeneous catalytic olefin polymerization, olefin metathesis, and CO reduction chemistry.

High Yield Multiple Hydroboration of the Polyhedral Thiaborane 6-SB$_9$H$_{11}$

N. Canter, C. G. Overberger,* and R. W. Rudolph†

*Department of Chemistry, University of Michigan
Ann Arbor, Michigan 48109*

Summary: Monohexylthiaborane 1, derived from *cis*-3-hexene and 6-SB$_9$H$_{11}$, reacted with additional *cis*-3-hexene at elevated temperatures to produce monohexylthiaborane 2, dihexylthiaborane 3, and trihexylthiaborane 4 in a process called multiple hydroboration. Pyrolysis and displacement experiments with monohexylthiaborane 1 and monooctylthiaborane 5, respectively, suggested that multiple hydroboration was reversible.

Hydroboration has proven to be an effective means for generating organoboranes that have wide utility in synthetic organic chemistry.[1] In most cases, only monomeric boron hydrides participate in the reaction. Previous attempts to treat unsaturated organic substrates with polyhedral boranes resulted in complex product mixtures and/or low overall yields.[2] We recently demonstrated that the borane cluster 6-SB$_9$H$_{11}$ will add to olefins.[3] In our continuing examination of this novel hydroboration agent, we wish to report that additional borons on 6-SB$_9$H$_{11}$ engage in multiple hydroboration with olefins at elevated temperatures to yield di- and trialkylthiaboranes in high yields. This result suggests the possibility of employing 6-SB$_9$H$_{11}$ for cross-linking olefinic polymers.
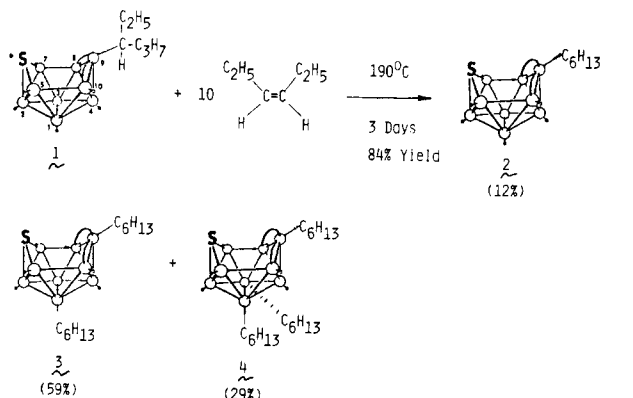

Figure 1. The boron cage numbering scheme and the proposed structure of the products (monohexylthiaborane 2, dihexylthiaborane 3, and trihexylthiaborane 4) are depicted.

Monohexylthiaborane 1[4] (Figure 1) and a 10-fold excess of *cis*-3-hexene were placed in a pyrolysis tube, which was sealed under vacuum conditions and heated at 190 °C for 3 days. After removal of excess substrate, sublimation produced monohexylthiaborane 2, dihexylthiaborane 3,[5] and trihexylthiaborane 4[6] in 84% total yield. Preparative gas chromatography was then used to separate dihexylthiaborane 3 from the other species.

GC/MS and proton-coupled ^{11}B NMR data suggest that a second *cis*-3-hexene molecule adds to the thiaborane cage at boron 1. Assignment of the second hydroboration site was made by comparing the ^{11}B NMR spectra of monohexylthiaborane 1 and dihexylthiaborane 3 (Figure 2). The presence of a second singlet and nine signals in the dihexylthiaborane 3 spectrum indicated that a reaction took place at an asymmetric boron. Attachment of a second alkyl group induces a dramatic shift of the boron 1 signal, as was observed with the initial monohydroboration at boron 9.[7]

Nearly exclusive formation of trihexylthiaborane 4 was attained by heating monohexylthiaborane 1, a 10-fold excess of *cis*-3-hexene, and tetralin in a sealed tube for 3 days at 200 °C. GC/MS and ^{11}B NMR showed that trihexylthiaborane 4 and dihexylthiaborane 3 were present in the ratio 98:2, respectively, in 75% yield.[8]

The proton-coupled ^{11}B NMR spectrum of trihexylthiaborane 4 is consistent with addition of a third olefin molecule onto the thiaborane cage. In contrast to dihexylthiaborane 3 (Figure 2), the downfield shift of an additional boron signal combined with restoration of symmetry means that hydroboration occurs at boron 3. Extensive broadening obscures B–H coupling in trihexylthiaborane 4 at room temperature because of the quadrupolar nature of the ^{11}B nucleus.[9] The spectrum shown in Figure 2 was taken at 100 °C and displays no-

---

†Deceased May 11, 1981.

(1) (a) Brown, H. C. "Hydroboration"; W. A. Benjamin: New York, 1962. (b) Cragg, G. M. L. "Organoboranes in Organic Synthesis"; Marcel Dekker: New York, 1973.

(2) (a) Ryschkewitsch, G. E.; Mezey, E. J.; Altwicker, E. R.; Sisler, H.; Garret, A. B. *Inorg. Chem.* 1963, 2, 893. (b) Vance, R. L.; Bramlett, C. L.; Grimes, R. N. *Ibid.* 1968, 7, 1066. (c) Maguire, R. G.; Solomon, I. J.; Klein, M. J. *Ibid.* 1963, 2, 1133. (d) Venzel, J.; Becker, S. D.; Mizusawa, E.; Tolpin, E. I. *Ibid.* 1980, 19, 1182.

(3) (a) Meneghelli, B. J.; Bower, M.; Canter, N.; Rudolph, R. W. *J. Am. Chem. Soc.* 1980, 102, 4355. (b) Meneghelli, B. J.; Rudolph, R. W. *Ibid.* 1978, 100, 4626.

(4) Treatment of equimolar amounts of *cis*-3-hexene and 6-SB$_9$H$_{11}$ in toluene for 4 h at room temperature produced monohexylthiaborane 1 in 96% yield. Alkaline peroxide oxidation yielded 3-hexanol. Anal. Calcd for C$_6$H$_{23}$B$_9$S: C, 32.08; H, 10.32; B, 43.32; S, 14.28. Found: C, 31.77; H, 10.24; B, 42.96; S, 14.04.

(5) The high-resolution mass spectrum of dihexylthiaborane 3 contained a parent ion peak at *m/e* 310.3306 corresponding to ^{12}C$_{12}$^{1}H$_{36}$^{11}B$_9$^{32}S$^+$ ion (calcd 310.3298).

(6) Anal. Calcd for C$_{18}$H$_{47}$B$_9$S: C, 55.02; H, 12.06; B, 24.76; S, 8.16. Found: C, 55.33; H, 11.70; B, 24.43; S, 8.29. The high-resolution mass spectrum of trihexylthiaborane 4 contained a parent ion peak at *m/e* 394.4219 corresponding to ^{12}C$_{18}$^{1}H$_{47}$^{11}B$_9$^{32}S$^+$ ion (calcd 394.4236).

(7) Meneghelli, B. J.; Bower, M.; Canter, N.; Rudolph, R. W. *J. Am. Chem. Soc.* 1980, 102, 4355.

(8) During the workup procedure, the removal of tetralin by distillation also provides a separation of monohexylthiaborane 2 and dihexylthiaborane 3 from trihexylthiaborane 4.

(9) Brice, V. T.; Shore, S. G. *Inorg. Chem.* 1973, 12, 309.

actinide catalysts.[1] Interestingly, the measured molar yields via pathway M during activation are roughly the same as the moles of active sites for hydrogenation of propylene measured by poisoning with carbon monoxide.[1] No effort has been made to optimize any of the reaction pathways, and indeed, actinide ions are not likely to be optimum for any one particular pathway. However, on a more general level and with specific reference to metal alkylidene stabilization by electron-deficient supports, it is not difficult to visualize how such species might play roles in heterogeneous catalytic olefin polymerization, olefin metathesis, and CO reduction chemistry.

High Yield Multiple Hydroboration of the Polyhedral Thiaborane 6-SB₉H₁₁

N. Canter, C. G. Overberger,* and R. W. Rudolph†

*Department of Chemistry, University of Michigan
Ann Arbor, Michigan 48109*

Summary: Monohexylthiaborane **1**, derived from *cis*-3-hexene and 6-SB₉H₁₁, reacted with additional *cis*-3-hexene at elevated temperatures to produce monohexylthiaborane **2**, dihexylthiaborane **3**, and trihexylthiaborane **4** in a process called multiple hydroboration. Pyrolysis and displacement experiments with monohexylthiaborane **1** and monooctylthiaborane **5**, respectively, suggested that multiple hydroboration was reversible.

Hydroboration has proven to be an effective means for generating organoboranes that have wide utility in synthetic organic chemistry.[1] In most cases, only monomeric boron hydrides participate in the reaction. Previous attempts to treat unsaturated organic substrates with polyhedral boranes resulted in complex product mixtures and/or low overall yields.[2] We recently demonstrated that the borane cluster 6-SB₉H₁₁ will add to olefins.[3] In our continuing examination of this novel hydroboration agent, we wish to report that additional borons on 6-SB₉H₁₁ engage in multiple hydroboration with olefins at elevated temperatures to yield di- and trialkylthiaboranes in high yields. This result suggests the possibility of employing 6-SB₉H₁₁ for cross-linking olefinic polymers.
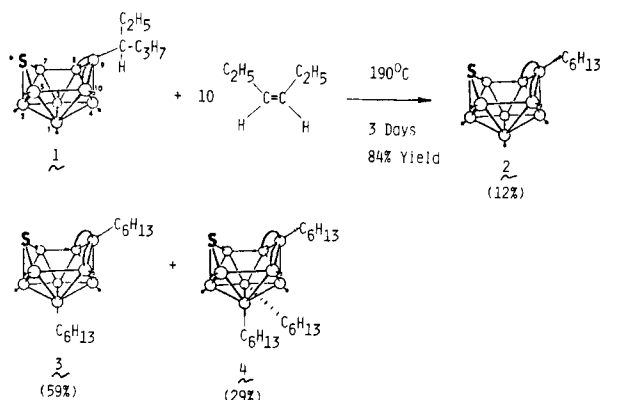

Figure 1. The boron cage numbering scheme and the proposed structure of the products (monohexylthiaborane **2**, dihexylthiaborane **3**, and trihexylthiaborane **4**) are depicted.

Monohexylthiaborane **1**[4] (Figure 1) and a 10-fold excess of *cis*-3-hexene were placed in a pyrolysis tube, which was sealed under vacuum conditions and heated at 190 °C for 3 days. After removal of excess substrate, sublimation produced monohexylthiaborane **2**, dihexylthiaborane **3**,[5] and trihexylthiaborane **4**[6] in 84% total yield. Preparative gas chromatography was then used to separate dihexylthiaborane **3** from the other species.

GC/MS and proton-coupled ¹¹B NMR data suggest that a second *cis*-3-hexene molecule adds to the thiaborane cage at boron 1. Assignment of the second hydroboration site was made by comparing the ¹¹B NMR spectra of monohexylthiaborane **1** and dihexylthiaborane **3** (Figure 2). The presence of a second singlet and nine signals in the dihexylthiaborane **3** spectrum indicated that a reaction took place at an asymmetric boron. Attachment of a second alkyl group induces a dramatic shift of the boron 1 signal, as was observed with the initial monohydroboration at boron 9.[7]

Nearly exclusive formation of trihexylthiaborane **4** was attained by heating monohexylthiaborane **1**, a 10-fold excess of *cis*-3-hexene, and tetralin in a sealed tube for 3 days at 200 °C. GC/MS and ¹¹B NMR showed that trihexylthiaborane **4** and dihexylthiaborane **3** were present in the ratio 98:2, respectively, in 75% yield.[8]

The proton-coupled ¹¹B NMR spectrum of trihexylthiaborane **4** is consistent with addition of a third olefin molecule onto the thiaborane cage. In contrast to dihexylthiaborane **3** (Figure 2), the downfield shift of an additional boron signal combined with restoration of symmetry means that hydroboration occurs at boron 3. Extensive broadening obscures B–H coupling in trihexylthiaborane **4** at room temperature because of the quadrupolar nature of the ¹¹B nucleus.[9] The spectrum shown in Figure 2 was taken at 100 °C and displays no-

---

†Deceased May 11, 1981.

(1) (a) Brown, H. C. "Hydroboration"; W. A. Benjamin: New York, 1962. (b) Cragg, G. M. L. "Organoboranes in Organic Synthesis"; Marcel Dekker: New York, 1973.

(2) (a) Ryschkewitsch, G. E.; Mezey, E. J.; Altwicker, E. R.; Sisler, H.; Garret, A. B. *Inorg. Chem.* **1963**, *2*, 893. (b) Vance, R. L.; Bramlett, C. L.; Grimes, R. N. *Ibid.* **1968**, *7*, 1066. (c) Maguire, R. G.; Solomon, I. J.; Klein, M. J. *Ibid.* **1963**, *2*, 1133. (d) Venzel, J.; Becker, S. D.; Mizusawa, E.; Tolpin, E. I. *Ibid.* **1980**, *19*, 1182.

(3) (a) Meneghelli, B. J.; Bower, M.; Canter, N.; Rudolph, R. W. *J. Am. Chem. Soc.* **1980**, *102*, 4355. (b) Meneghelli, B. J.; Rudolph, R. W. *Ibid.* **1978**, *100*, 4626.

(4) Treatment of equimolar amounts of *cis*-3-hexene and 6-SB₉H₁₁ in toluene for 4 h at room temperature produced monohexylthiaborane **1** in 96% yield. Alkaline peroxide oxidation yielded 3-hexanol. Anal. Calcd for C₆H₂₃B₉S: C, 32.08; H, 10.32; B, 43.32; S, 14.28. Found: C, 31.77; H, 10.24; B, 42.96; S, 14.04.

(5) The high-resolution mass spectrum of dihexylthiaborane **3** contained a parent ion peak at *m/e* 310.3306 corresponding to ¹²C₁₂¹H₃₆¹¹B₉³²S⁺ ion (calcd 310.3298).

(6) Anal. Calcd for C₁₈H₄₇B₉S: C, 55.02; H, 12.06; B, 24.76; S, 8.16. Found: C, 55.33; H, 11.70; B, 24.43; S, 8.29. The high-resolution mass spectrum of trihexylthiaborane **4** contained a parent ion peak at *m/e* 394.4219 corresponding to ¹²C₁₈¹H₄₇¹¹B₉³²S⁺ ion (calcd 394.4236).

(7) Meneghelli, B. J.; Bower, M.; Canter, N.; Rudolph, R. W. *J. Am. Chem. Soc.* **1980**, *102*, 4355.

(8) During the workup procedure, the removal of tetralin by distillation also provides a separation of monohexylthiaborane **2** and dihexylthiaborane **3** from trihexylthiaborane **4**.

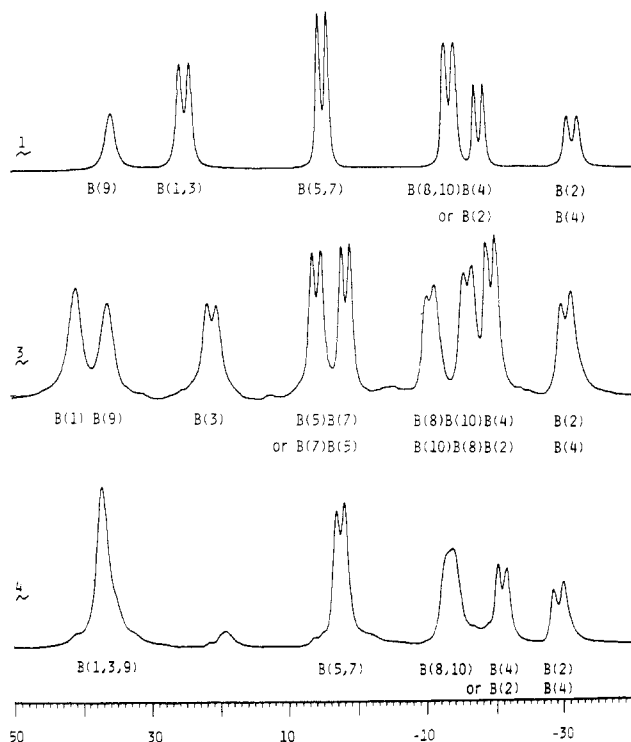(9) Brice, V. T.; Shore, S. G. *Inorg. Chem.* **1973**, *12*, 309.

Figure 2. The 115-MHz ^{11}B proton-coupled NMR of monohexylthiaborane 1 (25 °C), dihexylthiaborane 3 (25 °C), and trihexylthiaborane 4 (100 °C). All samples were dissolved in toluene-d_8 and referenced to $BF_3\cdot O(C_2H_5)_2$ (δ 0.0).

ticeable sharpening of all signals except for the boron 8, 10 doublet. Attempts at producing discernible exo B–H coupling in the boron 8, 10 signal by selectively decoupling the bridge hydrogens failed. The exact nature of this phenomenon is unknown and is currently under further investigation.

A sealed tube containing dihexylthiaborane 3, a 10-fold excess of cis-3-hexene, and tetralin produced trihexylthiaborane 4 after being heated at 200 °C for 2 days. This establishes dihexylthiaborane 3 as a reaction intermediate in the multiple hydroboration pathway.

The position of the boron atoms on the alkyl chains was determined by alkaline peroxide oxidation. Oxidation of trihexylthiaborane 4 yielded a 61:36:3 ratio of 2-hexanol, 3-hexanol, and 1-hexanol, respectively, by GC/MS data. Formation of 2-hexanol and 1-hexanol indicated that the

substituted borons migrate toward the terminal carbon.[10] There is no evidence that borons 1, 3, and 9 bond to a specific carbon which means that trihexylthiaborane 4 actually could represent many carbon chain isomers.

The results of two additional experiments suggest that multiple hydroboration is reversible. Small amounts of two unsubstituted thiaboranes, closo-1-SB$_9$H$_9$[11] and closo-1-SB$_{11}$H$_{11}$,[12] were obtained by pyrolyzing neat, monohexylthiaborane 1 in a sealed tube for ten hours at 200 °C. Cleavage of the boron–carbon bond is a logical step in the transformation of monohexylthiaborane 1 to these closo thiaboranes. In another sealed tube procedure, treatment of monooctylthiaborane 5[13] (synthesized from 1-octene and 6-SB$_9$H$_{11}$) with 10 equiv of cis-3-hexene in tetralin for 3 days at 200 °C produced a mixture containing dihexylthiaborane 3 and trihexylthiaborane 4. This displacement reaction demonstrates that the bond between boron 9 and the octyl side chain in monooctylthiaborane 5 is broken and new bonds are formed between borons 1, 3, and 9 and cis-3-hexene.

Preliminary examination of the reaction between 6-SB$_9$H$_{11}$ and polybutadiene reveals that a cross-linked polymer is formed when the reactants are heated in a sealed tube for 4 h at 165 °C. The potential reversibility of this cure could yield a material with thermoset capabilities at room temperature and thermoplastic properties at elevated temperatures.

(10) (a) Similar reactivity was reported for other organoboranes.[10b] (b) Zweifel, G.; Brown, H. C. *J. Am. Chem. Soc.* **1966**, *88*, 1433.

(11) Pretzer, W. R.; Rudolph, R. W. *J. Am. Chem. Soc.* **1973**, *95*, 931.

(12) Plesek, J.; Hermanek, S. *J. Chem. Soc., Chem. Commun.* **1975**, 127.

(13) Meneghelli, B. J.; Bower, M.; Canter, N.; Rudolph, R. W. *J. Am. Chem. Soc.* **1980**, *102*, 4355.